Plant Biochemistry

Fourth edition

Plant Biochemistry

Hans-Walter Heldt

Birgit Piechulla

in cooperation with Fiona Heldt

Translation of the 4th German edition

ELSEVIER

AMSTERDAM • BOSTON • HEIDELBERG • LONDON
NEW YORK • OXFORD • PARIS • SAN DIEGO
SAN FRANCISCO • SINGAPORE • SYDNEY • TOKYO

Academic Press is an imprint of Elsevier

Academic Press is an imprint of Elsevier
32 Jamestown Road, London NW1 7BY, UK
30 Corporate Drive, Suite 400, Burlington, MA 01803, USA
525 B Street, Suite 1800, San Diego, CA 92101-4495, USA

Fourth edition 2011

British Library Cataloguing-in-Publication Data
A catalogue record for this book is available from the British Library

Library of Congress Cataloging-in-Publication Data
A catalog record for this book is available from the Library of Congress

ISBN : 978-0-12-384986-1

For information on all Academic Press publications visit our website at elsevierdirect.com

Typeset by MPS Limited, a Macmillan Company, Chennai, India
www.macmillansolutions.com

Printed and bound in United States of America

10 11 12 13 14 15 10 9 8 7 6 5 4 3 2 1

Dedicated to my teacher, Martin Klingenberg
Hans–Walter Heldt

Preface

The present textbook is written for students and is the product of more than three decades of teaching experience. It intends to give a broad but concise overview of the various aspects of plant biochemistry including molecular biology. We attached importance to an easily understood description of the principles of metabolism but also restricted the content in such a way that a student is not distracted by unnecessary details. In view of the importance of plant biotechnology, industrial applications of plant biochemistry have been pointed out, wherever it was appropriate. Thus special attention was given to the generation and utilization of transgenic plants.

Since there are many excellent textbooks on general biochemistry, we have deliberately omitted dealing with elements such as the structure and function of amino acids, carbohydrates and nucleotides, the function of nucleic acids as carriers of genetic information and the structure and function of proteins and the basis of enzyme catalysis. We have dealt with topics of general biochemistry only when it seemed necessary for enhancing understanding of the problem in hand. Thus, this book is in the end a compromise between a general and a specialized textbook.

To ensure the continuity of the textbook in the future, Birgit Piechulla is the second author of this edition. We have both gone over all the chapters in the fourth edition, HWH concentrating especially on Chapters 1–15 and BP on the Chapters 16–22. All the chapters of the book have been thoroughly revised and incorporate the latest scientific knowledge. Here are just a few examples: the descriptions of the metabolite transport and the ATP synthase were revised and starch metabolism and glycolysis were dealt with intensively. The descriptions of the sulfate assimilation and various aspects of secondary assimilation, especially the isoprenoid synthesis, have been expanded. Because of the rapid advance in the field of phytohormones and light sensors it was necessary to expand and bring this chapter up to date. The chapter on gene technology takes into account the great advance in this field. The literature references for the various chapters have been brought up to date. They relate mostly to reviews accessible via data banks, for example PubMed, and should enable the reader to attain more detailed information about the often rather compact explanations in the

textbook. In future years these references should facilitate opening links to the latest literature in data banks.

I (HWH) would like to express my thanks to Prof. Ivo Feussner, director of the biochemistry division – as emeritus, I had the infrastructure of the division at my disposal, an important precondition for producing this edition.

Our special thanks go to the Spektrum team, particularly to Mrs. Merlet Behncke-Braunbeck who encouraged us to work on this new edition and gave us many valuable suggestions. We also thank Fiona Heldt for her assistance.

We are very grateful to the Elsevier team for their friendly and very fruitful cooperation. Our thanks go in particular to Kristi Gomez for the vast effort she invested in advancing the publication of our translation. We also thank Pat Gonzalez and Caroline Johnson for their thoughtful support for our ideas about the layout of this book and their excellent work on its production.

Once again many colleagues have given us valuable suggestions for the latest edition. Our special thanks go to the colleagues listed below for critical reading of parts of the text and for information, material and figures.

Prof. Erwin Grill, Weihenstephan-München
Prof. Bernhard Grimm, Berlin
Steven Huber, Illinois, USA
Wolfgang Junge, Osnabrück
Prof. Klaus Lendzian, Weihenstephan-München
Prof. Gertrud Lohaus, Wuppertal
Prof. Katharina Pawlowski, Stockholm
Prof. Sigrun Reumann, Stavanger
Prof. David. G. Robinson, Heidelberg
Prof. Matthias Rögner, Bochum
Prof. Norbert Sauer, Erlangen
Prof. Renate Scheibe, Osnabrück
Prof. Martin Steup, Potsdam
Dr. Olga Voitsekhovskaja, St. Petersburg

We have tried to eradicate as many mistakes as possible but probably not with complete success. We are therefore grateful for any suggestions and comments.

Hans-Walter Heldt
Birgit Piechulla
Göttingen and Rostock, May 2008 (German edition)
July 2010 (Translation)

Introduction

Plant biochemistry examines the molecular mechanisms of plant life. One of the main topics is photosynthesis, which in higher plants takes place mainly in the leaves. Photosynthesis utilizes the energy of the sun to synthesize carbohydrates and amino acids from water, carbon dioxide, nitrate and sulfate. Via the vascular system a major part of these products is transported from the leaves through the stem into other regions of the plant, where they are required, for example, to build up the roots and supply them with energy. Hence the leaves have been given the name "source," and the roots the name "sink." The reservoirs in seeds are also an important group of the sink tissues, and, depending on the species, act as a store for many agricultural products such as carbohydrates, proteins and fat.

In contrast to animals, plants have a very large surface, often with very thin leaves in order to keep the diffusion pathway for CO_2 as short as possible and to catch as much light as possible. In the finely branched root hairs the plant has an efficient system for extracting water and inorganic nutrients from the soil. This large surface, however, exposes plants to all the changes in their environment. They must be able to withstand extreme conditions such as drought, heat, cold or even frost as well as an excess of radiated light energy. Day to day the leaves have to contend with the change between photosynthetic metabolism during the day and oxidative metabolism during the night. Plants encounter these extreme changes in external conditions with an astonishingly flexible metabolism, in which a variety of regulatory processes take part. Since plants cannot run away from their enemies, they have developed a whole arsenal of defense substances to protect themselves from being eaten.

Plant agricultural production is the basis for human nutrition. Plant gene technology, which can be regarded as a section of plant biochemistry, makes a contribution to combat the impending global food shortage due to the enormous growth of the world population. The use of environmentally compatible herbicides and protection against viral or fungal infestation by means of gene technology is of great economic importance. Plant biochemistry is also instrumental in breeding productive varieties of crop plants.

Plants are the source of important industrial raw material such as fat and starch but they are also the basis for the production of pharmaceutics. It is to be expected that in future gene technology will lead to the extensive use of plants as a means of producing sustainable raw material for industrial purposes.

The aim of this short list is to show that plant biochemistry is not only an important field of basic science explaining the molecular function of a plant, but is also an applied science which, now at a revolutionary phase of its development, is in a position to contribute to the solution of important economic problems.

To reach this goal it is necessary that sectors of plant biochemistry such as bioenergetics, the biochemistry of intermediary metabolism and the secondary plant compounds, as well as molecular biology and other sections of plant sciences such as plant physiology and the cell biology of plants, co-operate closely with one another. Only the integration of the results and methods of working with the different sectors of plant sciences can help us to understand how a plant functions and to put this knowledge to economic use. This book will try to describe how this could be achieved.

Since there are already very many good general textbooks on biochemistry, the elements of general biochemistry will not be dealt with here and it is presumed that the reader will obtain the knowledge of general biochemistry from other textbooks.

1

A leaf cell consists of several metabolic compartments

In higher plants photosynthesis occurs mainly in the **mesophyll,** the chloroplast-rich tissue of leaves. Figure 1.1 shows an electron micrograph of a mesophyll cell and Figure 1.2 shows a schematic presentation of the cell structure. The cellular contents are surrounded by a **plasma membrane**

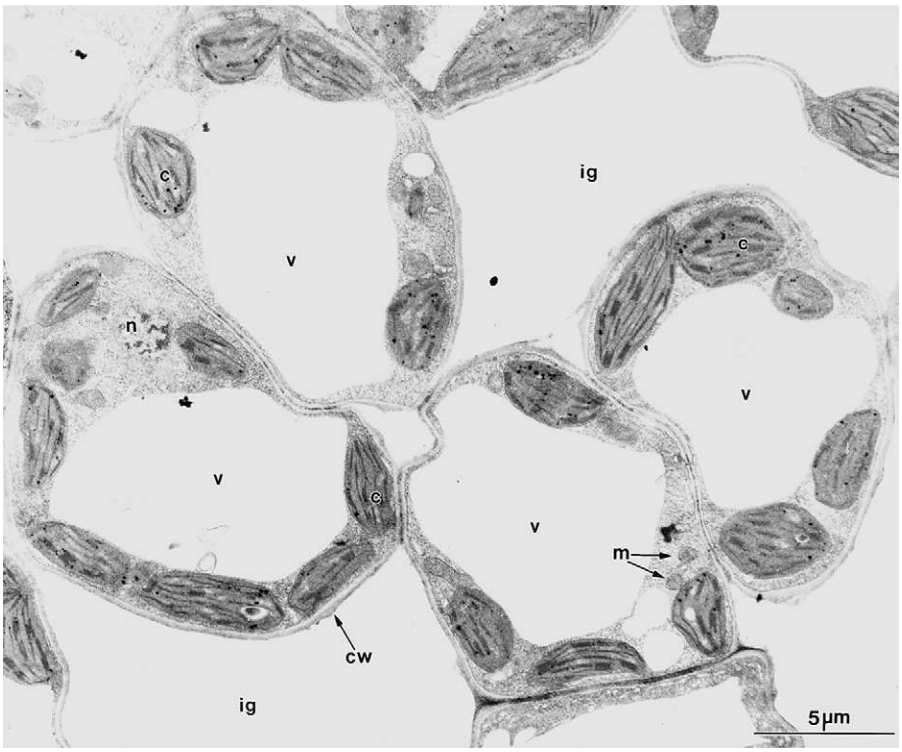

Figure 1.1 Electron micrograph of mesophyll tissue from tobacco. In most cells the large central vacuole is to be seen (v). Between the cells are the intercellular gas spaces (ig), which are somewhat enlarged by the fixation process. c: chloroplast; cw: cell wall; n: nucleus; m: mitochondrion. (By D. G. Robinson, Heidelberg.)

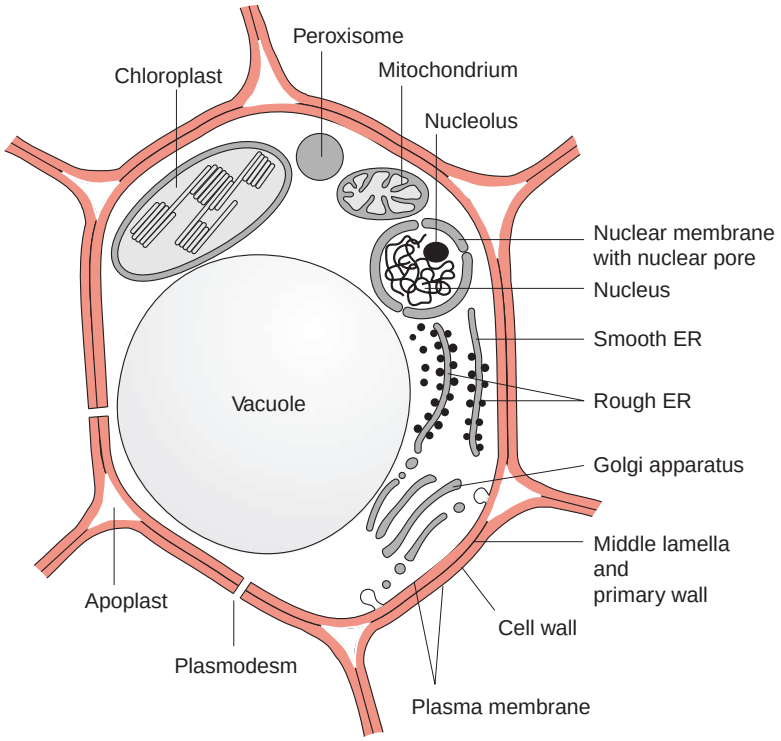

Figure 1.2 Schematic presentation of a mesophyll cell. The black lines between the red cell walls represent the regions where adjacent cell walls are glued together by pectins.

called the plasmalemma and are enclosed by a **cell wall**. The cell contains organelles, each with its own characteristic shape, which divide the cell into various compartments (subcellular compartments). Each compartment has specialized metabolic functions, which will be discussed in detail in the following chapters (Table 1.1). The largest organelle, the vacuole, usually fills about 80% of the total cell volume. Chloroplasts represent the next largest compartment, and the rest of the cell volume is filled with mitochondria, peroxisomes, the nucleus, the endoplasmic reticulum, the Golgi bodies, and, outside these organelles, the cell plasma, called **cytosol**. In addition, there are oil bodies derived from the endoplasmic reticulum. These oil bodies, which occur in seeds and some other tissues (e.g., root nodules), are storage organelles for triglycerides (see Chapter 15).

The **nucleus** is surrounded by the **nuclear envelope**, which consists of the two membranes of the endoplasmic reticulum. The space between the two membranes is known as the **perinuclear space**. The nuclear envelope is interrupted by **nuclear pores** with a diameter of about 50 nm. The nucleus contains **chromatin**, consisting of DNA double strands that are stabilized

Table 1.1: Subcellular compartments in a mesophyll cell* and some of their functions

	Percent of the total cell volume	Functions (incomplete)
Vacuole	79	Maintenance of cell turgor.
		Store of, e.g., nitrate, glucose and storage proteins, intermediary store for secretory proteins, reaction site of lytic enzymes and waste depository
Chloroplasts	16	Photosynthesis, synthesis of starch and lipids
Cytosol	3	General metabolic compartment, synthesis of sucrose
Mitochondria	0.5	Cell respiration
Nucleus	0.3	Contains the genome of the cell. Reaction site of replication and transcription
Peroxisomes		Reaction site for processes in which toxic intermediates, such as H_2O_2 and glyoxylate, are formed and eliminated
Endoplasmic reticulum		Storage of Ca^{++} ions, participation in the export of proteins from the cell and in the transport of newly synthesized proteins into the vacuole and their secretion from the cell
Oil bodies (oleosomes)		Storage of triacylglycerols
Golgi bodies		Processing and sorting of proteins destined for export from the cells or transport into the vacuole

* Mesophyll cells of spinach; data by Winter, Robinson, and Heldt (1994).

by being bound to basic proteins (**histones**). The genes of the nucleus are collectively referred to as the **nuclear genome**. Within the nucleus, usually off-center, lies the nucleolus, where ribosomal subunits are formed. These ribosomal subunits and the messenger RNA formed by transcription of the DNA in the nucleus migrate through the nuclear pores to the ribosomes in the cytosol, the site of protein biosynthesis. The synthesized proteins are distributed between the different cell compartments according to their final destination.

The cell contains in its interior the **cytoskeleton**, which is a three-dimensional network of fiber proteins**.** Important elements of the cytoskeleton are the **microtubuli** and the **microfilaments**, both macromolecules formed by the aggregation of soluble (globular) proteins. Microtubuli are tubular structures composed of α and β **tubuline** monomers. The microtubuli are connected to a large number of different motor proteins that transport bound organelles along the microtubuli at the expense of ATP. Microfilaments are chains of polymerized **actin** that interact with **myosin** to achieve movement.

Actin and myosin are the main constituents of the animal muscle. The cytoskeleton has many important cellular functions. It is involved in the spatial organization of the organelles within the cell, enables thermal stability, plays an important role in cell division, and has a function in cell-to-cell communication.

1.1 The cell wall gives the plant cell mechanical stability

The difference between plant cells and animal cells is that plant cells have a cell wall. This wall limits the volume of the plant cell. The water taken up into the cell by osmosis presses the plasma membrane against the inside of the cell wall, thus giving the cell mechanical stability. The cell walls are very complex structures; in *Arabidopsis* about 1,000 genes were found to be involved in its synthesis. Cell walls also protect against infections.

The cell wall consists mainly of carbohydrates and proteins

The cell wall of a higher plant is made up of about 90% carbohydrates and 10% proteins. The main carbohydrate constituent is **cellulose**. Cellulose is an unbranched polymer consisting of D-glucose molecules, which are connected to each other by β-1,4 glycosidic linkages (Fig. 1.3A). Each glucose unit is rotated by 180° from its neighbor, so that very long straight chains can be formed with a chain length of 2,000 to 25,000 glucose residues. About 36 cellulose chains are associated by interchain hydrogen bonds to a crystalline lattice structure known as a **microfibril**. These crystalline regions are impermeable to water. The microfibrils have an unusually high tensile strength, are very resistant to chemical and biological degradations, and are in fact so stable that they are very difficult to hydrolyze. However, many bacteria and fungi have cellulose-hydrolyzing enzymes (cellulases). These bacteria can be found in the digestive tract of some animals (e.g., ruminants), thus enabling them to digest grass and straw. It is interesting to note that cellulose is the most abundant organic substance on earth, representing about half of the total organically bound carbon.

Hemicelluloses are also important constituents of the cell wall. They are defined as those polysaccharides that can be extracted by alkaline solutions. The name is derived from an initial belief, which later turned out to be incorrect, that hemicelluloses are precursors of cellulose. Hemicelluloses consist of a variety of polysaccharides that contain, in addition to D-glucose,

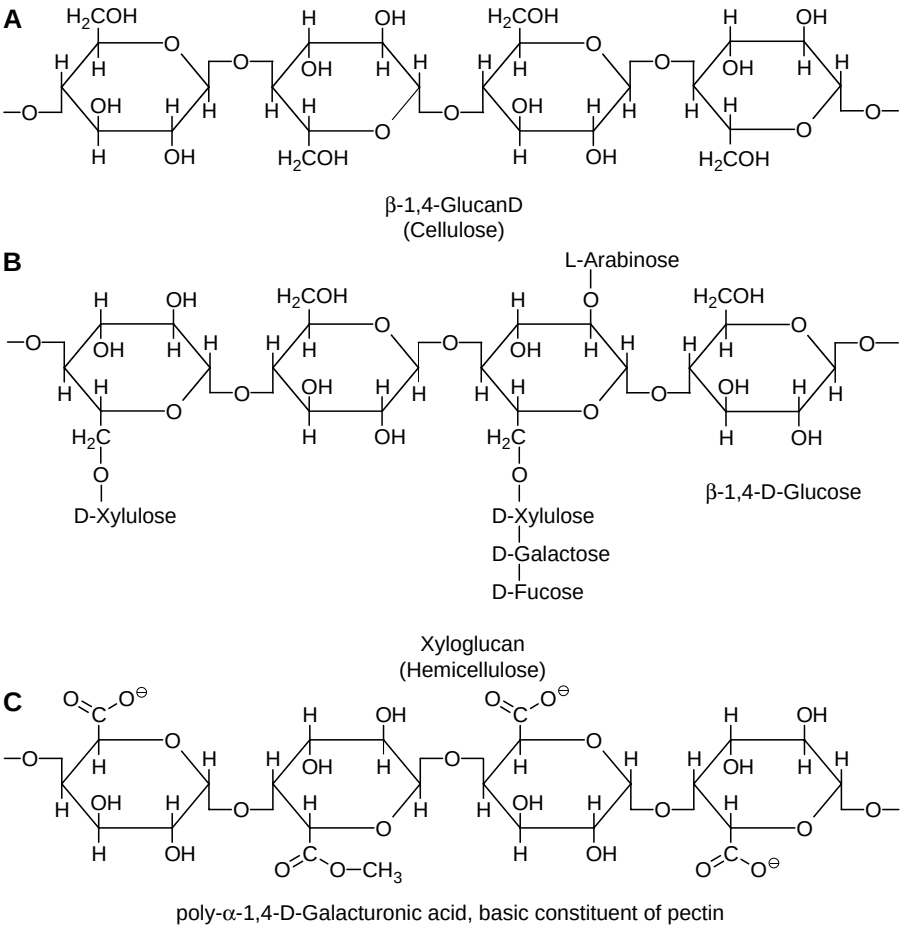

Figure 1.3 Main constituents of the cell wall. A. Cellulose; B. A hemicellulose; C. Constituent of pectin

other carbohydrates such as the hexoses D-mannose, D-galactose, D-fucose, and the pentoses D-xylose and L-arabinose. Figure 1.3B shows xyloglycan as an example of a hemicellulose. The basic structure is a β-1,4-glucan chain to which xylose residues are bound via α-1,6 glycosidic linkages, which in part are linked to D-galactose and D-fucose. In addition to this, L-arabinose residues are linked to the 2′OH group of the glucose.

Another major constituent of the cell wall is **pectin**, a mixture of polymers from sugar acids, such as D-galacturonic acid, which are connected by α-1,4 glycosidic links (Fig. 1.3C). Some of the carboxyl groups are esterified by methyl groups. The free carboxyl groups of adjacent chains are linked by Ca^{++} and Mg^{++} ions (Fig. 1.4). When Mg^{++} and Ca^{++} ions are absent, pectin is a soluble compound. The Ca^{++}/Mg^{++} salt of pectin forms an amorphous, deformable gel that is able to swell. Pectins function like

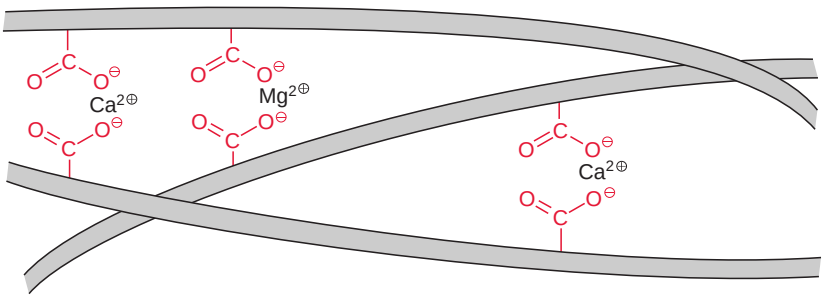

Figure 1.4 Ca^{++} and Mg^{++} ions mediate electrostatic interactions between pectin strands.

glue in sticking neighboring cells together, but these cells can be detached again during plant growth. The food industry makes use of this property of pectin when preparing jellies and jams.

The structural proteins of the cell wall are connected by glycosidic linkages to the branched polysaccharide chains and belong to the class of proteins known as **glycoproteins**. The carbohydrate portion of these glycoproteins varies from 50% to over 90%.

For a plant cell to grow, the very rigid cell wall has to be loosened in a precisely controlled way. This is facilitated by the protein **expansin**, which occurs in growing tissues of all flowering plants. It probably functions by breaking hydrogen bonds between cellulose microfibrils and cross-linking polysaccharides. Cell walls also contain **waxes** (Chapter 15), **cutin**, and **suberin** (Chapter 18).

In a monocot plant, the **primary wall** (i.e., the wall initially formed after the growth of the cell) consists of 20% to 30% cellulose, 25% hemicellulose, 30% pectin, and 5% to 10% glycoprotein. It is permeable for water. Pectin makes the wall elastic and, together with the glycoproteins and the hemicellulose, forms the matrix in which the cellulose microfibrils are embedded. When the cell has reached its final size and shape, another layer, the **secondary wall**, which consists mainly of cellulose, is added to the primary wall. The microfibrils in the secondary wall are arranged in a **layered structure** like plywood (Fig. 1.5).

The incorporation of **lignin** in the secondary wall causes the lignification of plant parts and the corresponding cells die, leaving the dead cells with only a supporting function (e.g., forming the branches and twigs of trees or the stems of herbaceous plants). Lignin is formed by the polymerization of the **phenylpropane derivatives** cumaryl alcohol, coniferyl alcohol, and sinapyl alcohol, resulting in a very solid structure (section 18.3). Dry wood consists of about 30% lignin, 40% cellulose, and 30% hemicellulose. After cellulose, lignin is the most abundant natural compound on earth.

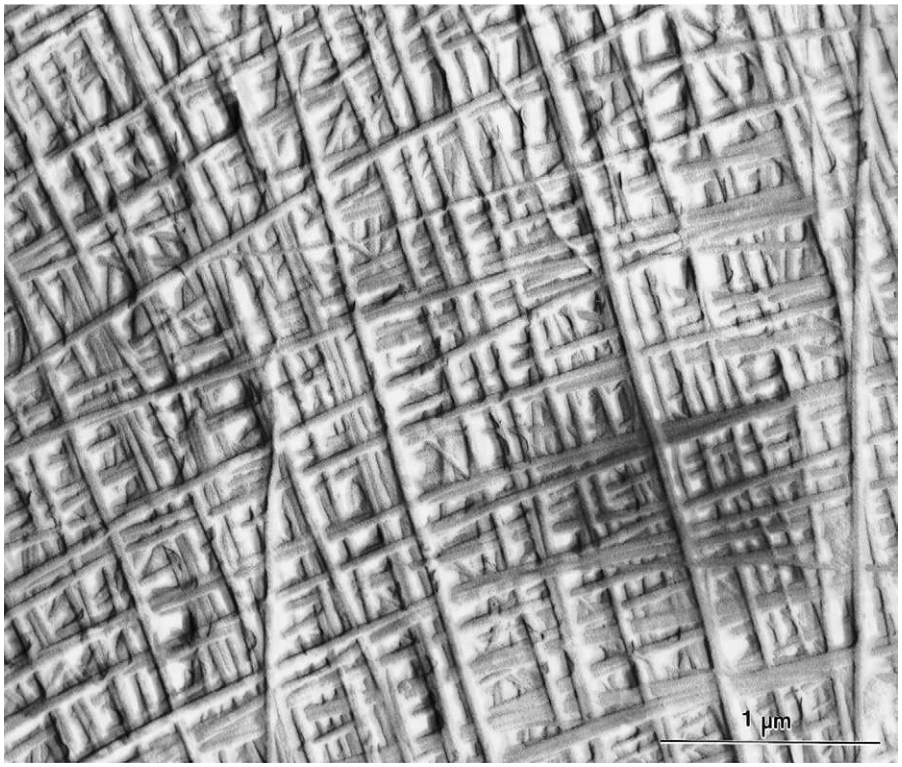

Figure 1.5 Cell wall of the green alga *Oocystis solitaria*. The cellulose microfibrils are arranged in a pattern, in which parallel layers are arranged one above the other. Freeze etching microscopy. (By D. G. Robinson, Heidelberg.)

Plasmodesmata connect neighboring cells

Neighboring cells are normally connected by **plasmodesmata** thrusting through the cell walls. Plant cells often contain 1,000–10,000 plasmodesmata. In its basic structure plasmodesmata allow the passage of molecules up to a molecular mass of 800 to 1,200 Dalton, but, by mechanisms to be discussed in the following, plasmodesmata can be widened to allow the passage of much larger molecules. Plasmodesmata connect many plant cells to form a single large metabolic compartment where the metabolites in the cytosol can move between the various cells by diffusion. This continuous compartment formed by different plant cells (Fig. 1.6) is called the **symplast**. In contrast, the spaces between cells, which are often continuous, are termed the extracellular space or the **apoplast** (Figs. 1.2, 1.6).

Figure 1.7 shows a schematic presentation of a plasmodesm. The tube like opening through the cell wall is lined by the plasma membrane, which is continuous between the neighboring cells. In the interior of this tube there is another tube-like membrane structure, which is part of the endoplasmatic

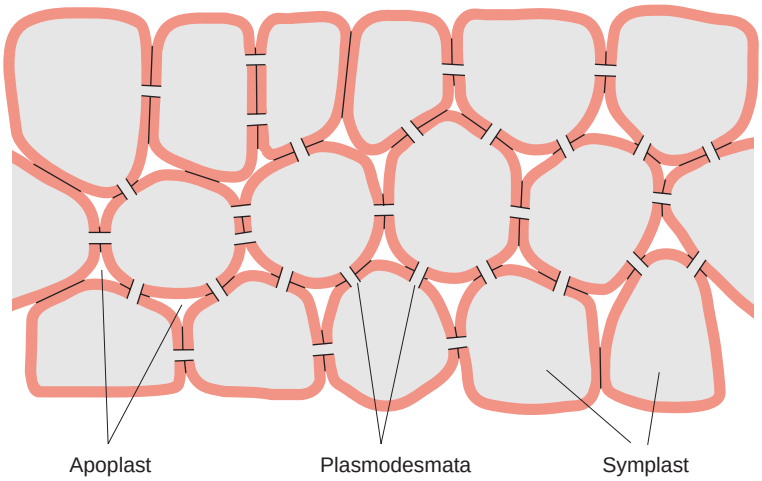

Figure 1.6 Schematic presentation of symplast and apoplast. Plasmodesmata connect neighboring cells to form a symplast. The extracellular spaces between the cell walls form the apoplast. Each of the connections actually consists of very many neighboring plasmodesmata.

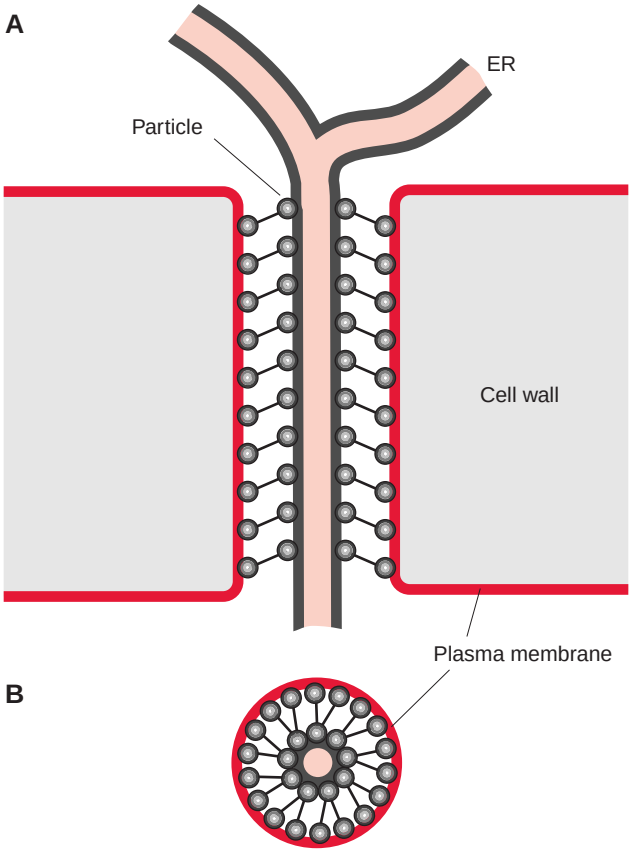

Figure 1.7 Schematic presentation of a plasmodesm. The plasma membrane of the neighboring cells is connected by a tube-like membrane invagination. Inside this tube is a continuation of the endoplasmatic reticulum (ER). Embedded in the ER membrane and plasma membrane are protein complexes that are connected to each other. The spaces between the protein complexes form the diffusion path of the plasmodesm. A. Cross-sectional view of the cell wall; B. vertical view of a plasmodesm.

reticulum (ER) of the neighboring cells. In this way the ER system of the entire symplast represents a continuous compartment. The space between the plasma membrane and the ER membrane forms the diffusion pathway between the cytosol of neighboring cells. There are probably two mechanisms for increasing this opening of the plasmodesmata. A **gated pathway** widens the plasmodesmata to allow the unspecific passage of molecules with a mass of up to 20,000 Dalton. The details of the regulation of this gated pathway remain to be elucidated. In the **selective trafficking** the widening is caused by helper proteins, which are able to bind specifically macromolecules such as RNAs in order to guide these through the plasmodesm. This was first observed with **virus movement proteins** encoded by viruses, which form complexes with virus RNAs to facilitate their passage across the plasmodesm and in this way enable the spreading of the viruses over the entire symplast. By now many of these virus movement proteins have been identified, and it was also observed that plants produce movement proteins that guide macromolecules through plasmodesmata. Apparently this represents a general transport process of which the viruses take advantage. It is presumed that the cell's own movement proteins, upon the consumption of ATP, facilitate the transfer of macromolecules, such as RNA and proteins, from one cell to the next via the plasmodesmata. In this way transcription factors may be distributed in a regulated mode as signals via the symplast, which might play an important role during defense reactions against pathogen infections.

The plant cell wall, which is very rigid and resistant, can be lysed by cellulose and pectin hydrolyzing enzymes obtained from microorganisms. When leaf pieces are incubated with these enzymes, plant cells can be obtained without the cell wall. These naked cells are called **protoplasts**. Protoplasts, however, are stable only in an **isotonic medium** in which the osmotic pressure corresponds to the osmotic pressure of the cell fluid. In pure water the protoplasts, as they have no cell wall, swell so much that they burst. In appropriate media, the protoplasts of many plants are viable, they can be propagated in cell culture, and they can be stimulated to form a cell wall and even to regenerate a whole new plant.

1.2 Vacuoles have multiple functions

The vacuole is enclosed by a membrane, called a **tonoplast**. The number and size of the vacuoles in different plant cells vary greatly. Young cells contain a larger number of smaller vacuoles but, taken as a whole, occupy only a

minor part of the cell volume. When cells mature, the individual vacuoles amalgamate to form a **central vacuole** (Figs. 1.1 and 1.2). The increased volume of the mature cell is due primarily to the enlargement of the vacuole. In cells of storage or epidermal tissues, the vacuole often takes up almost the entire cellular space.

An important function of the vacuole is to maintain **cell turgor**. For this purpose, salts, mainly from inorganic and organic acids, are accumulated in the vacuole. The accumulation of these osmotically active substances draws water into the vacuole, which in turn causes the tonoplast to press the protoplasm of the cell against the surrounding cell wall. Plant turgor is responsible for the rigidity of nonwoody plant parts. The plant wilts when the turgor decreases due to lack of water.

Vacuoles have an important function in **recycling** those cellular constituents that are defective or no longer required. Vacuoles contain hydrolytic enzymes for degrading various macromolecules such as proteins, nucleic acids, and many polysaccharides. Structures, such as mitochondria, can be transferred by endocytosis to the vacuole and are digested there. For this reason one speaks of **lytic vacuoles**. The resulting degradation products, such as amino acids and carbohydrates, are made available to the cell. This is especially important during **senescence** (see section 19.5) when prior to abscission, part of the constituents of the leaves are mobilized to support the propagation and growth of seeds.

Last, but not least, vacuoles also function as **waste deposits**. With the exception of gaseous substances, leaves are unable to rid themselves of waste products or xenobiotics such as herbicides. These are ultimately deposited in the vacuole (Chapter 12).

In addition, vacuoles also have a **storage function**. Many plants use the vacuole to store reserves of nitrate and phosphate. Some plants store malic acid temporarily in the vacuoles in a diurnal cycle (see section 8.5). Vacuoles of storage tissues contain carbohydrates (section 13.3) and storage proteins (Chapter 14). Many plant cells contain different types of vacuoles (e.g., lytic vacuoles and protein storage vacuoles next to each other).

The storage function of vacuoles plays a role when utilizing plants as natural protein factories. Genetic engineering now makes it possible to express economically important proteins (e.g., antibodies) in plants, where the vacuole storage system functions as a cellular storage compartment for accumulating high amounts of these proteins. Since normal techniques could be used for the cultivation and harvest of the plants, this method has the advantage that large amounts of proteins can be produced at low costs.

1.3 Plastids have evolved from cyanobacteria

Plastids are cell organelles which occur only in plant cells. They multiply by division and in most cases are **maternally** inherited. This means that all the plastids in a plant usually have descended from the **proplastids** in the egg cell. During cell differentiation, the proplastids can differentiate into green **chloroplasts**, colored **chromoplasts**, and colorless **leucoplasts**. Plastids possess their own genome, of which many copies are present in each plastid. The plastid genome (**plastome**) has properties similar to that of the prokaryotic genome, e.g., of cyanobacteria, but encodes only a minor part of the plastid proteins; most of the chloroplast proteins are encoded in the nucleus and are subsequently transported into the plastids. The proteins encoded by the plastome comprise enzymes for replication, gene expression, and protein synthesis, and part of the proteins of the photosynthetic electron transport chain and of the ATP synthase.

As early as 1883 the botanist Andreas Schimper postulated that plastids are evolutionary descendants of intracellular symbionts, thus founding the basis for the **endosymbiont hypothesis**. According to this hypothesis, the plastids descend from cyanobacteria, which were taken up by phagocytosis into a host cell (Fig. 1.8) and lived there in a symbiotic relationship. Through time these endosymbionts lost the ability to live independently because a large portion of the genetic information of the plastid genome was transferred to the nucleus. Comparative DNA sequence analyses of proteins from chloroplasts and from early forms of cyanobacteria allow the conclusion that all chloroplasts of the plant kingdom derive from a symbiotic event. Therefore it is justified to speak of the **endosymbiotic theory**.

Proplastids (Fig. 1.9A) are very small organelles (diameter 1 to 1.5 μm). They are undifferentiated plastids found in the meristematic cells of the shoot

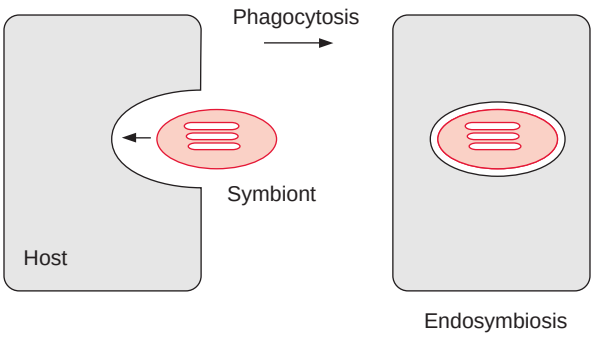

Figure 1.8 A cyanobacterium forms a symbiosis with a host cell.

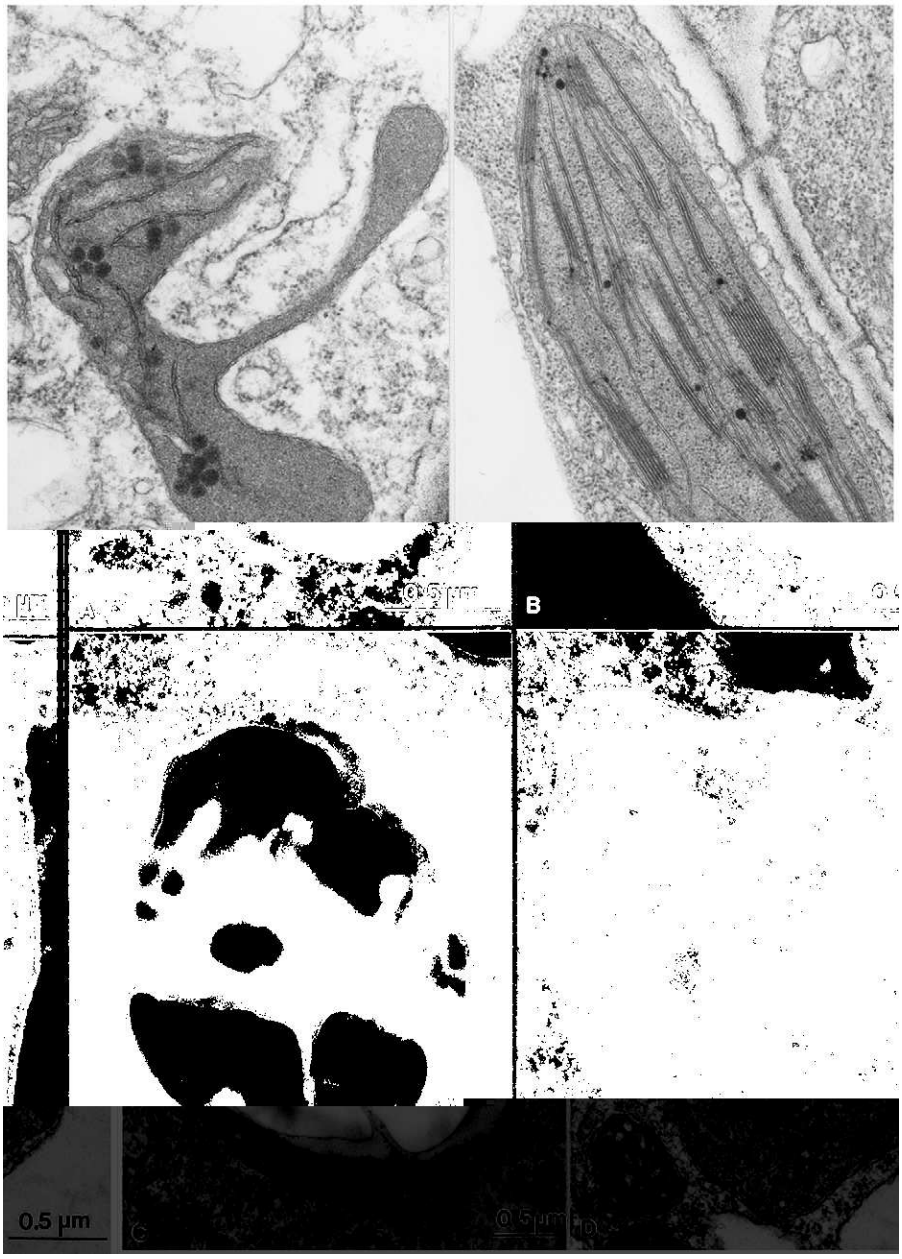

Figure 1.9 Plastids occur in various differentiated forms. A. Proplastid from young primary leaves of *Cucurbita pepo* (courgette); B. Chloroplast from a mesophyll cell of a tobacco leaf at the end of the dark period; C. Leucoplast: Amyloplast from the root of *Cestrum auranticum*; D. Chromoplast from petals of *C. auranticum*. (By D. G. Robinson, Heidelberg.)

and the root. They, like all other plastids, are enclosed by two membranes forming an envelope. According to the endosymbiont theory, the inner envelope membrane derives from the plasma membrane of the protochlorophyte and the outer envelope membrane from plasma membrane of the host cell.

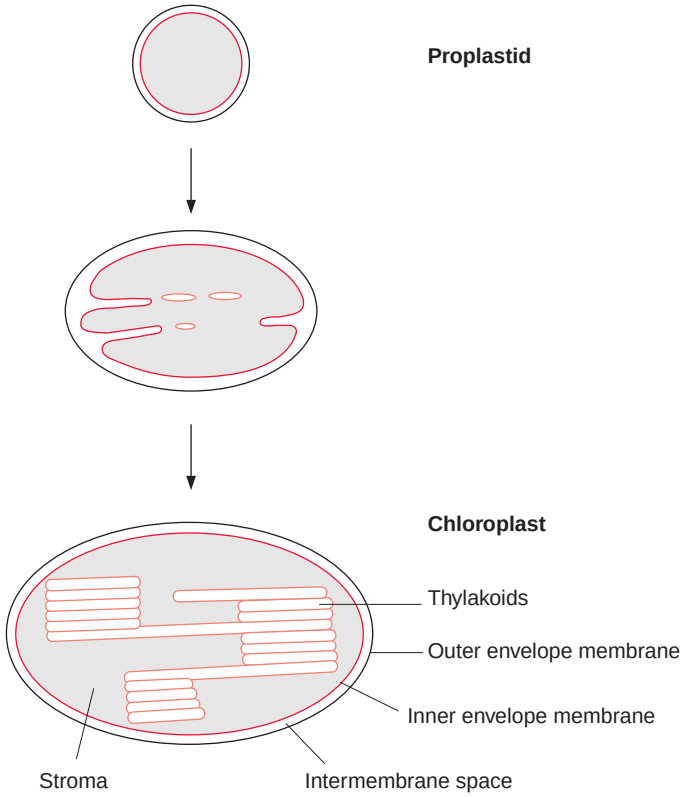

Figure 1.10 Schematic presentation of the differentiation of a proplastid to a chloroplast.

Chloroplasts (Fig. 1.9B) are formed by differentiation of the proplastids (Fig. 1.10). In greening leaves **etioplasts** are formed as intermediates during this differentiation. A mature mesophyll cell contains about 50 to 100 chloroplasts. By definition chloroplasts contain chlorophyll. However, they are not always green. In blue and brown algae, other pigments mask the green color of the chlorophyll. Chloroplasts are lens-shaped and can adjust their position within the cell to receive an optimal amount of light. In higher plants their length is 3 to 10 μm. The two **envelope membranes** enclose the **stroma**. The stroma contains a system of membranes arranged as flattened sacks (Fig. 1.11), which were given the name **thylakoids** (in Greek, sac-like) by Wilhelm Menke in 1960. During differentiation of the chloroplasts, the inner envelope membrane invaginates to form thylakoids, which are subsequently sealed off. In this way a large membrane area is provided for the photosynthesis apparatus (Chapter 3). The thylakoids are connected to each other by tube-like structures, forming a continuous compartment. Many of the thylakoid membranes are squeezed very closely together; they

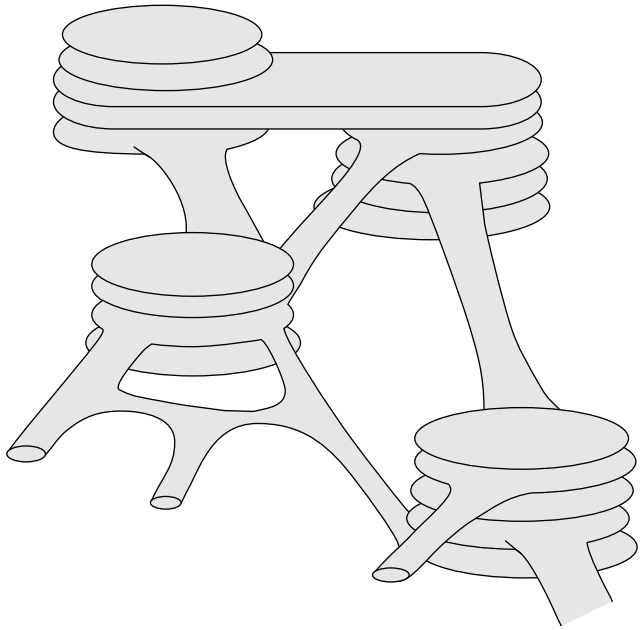

Figure 1.11 The grana stacks of the thylakoid membranes are connected by tubes, forming a continuous thylakoid space (thylakoid lumen). (After Weier and Stocking, 1963.)

are said to be stacked. These stacks can be seen by light microscopy as small particles within the chloroplasts and have been named **grana**.

There are three different compartments in chloroplasts: the **intermembrane space** between the outer and inner envelope membrane (Fig. 1.10); the **stroma space** between the inner envelope membrane and the thylakoid membrane; and the **thylakoid lumen**, which is the space within the thylakoid membranes. The **inner envelope membrane** is a permeability barrier for metabolites and nucleotides, which can pass through only with the help of specific translocators (section 1.9). In contrast, the **outer envelope membrane** is permeable to metabolites and nucleotides (but not to macromolecules such as proteins or nucleic acids). This permeability is due to the presence of specific membrane proteins called **porins**, which form pores permeable to substances with a molecular mass below 10,000 Dalton (section 1.11). Thus, the inner envelope membrane is the selective membrane of the metabolic compartment of the chloroplasts. The chloroplast stroma can be regarded as the "protoplasm" of the plastids. In comparison, the thylakoid lumen represents an external space that functions primarily as a compartment for partitioning protons to form a proton gradient (Chapter 3).

The stroma of chloroplasts contains **starch grains**. This starch serves mainly as a diurnal carbohydrate stock, the starch formed during the day being a reserve for the following night (section 9.1). Therefore at the end of the day the starch grains in the chloroplasts are usually very large and their

sizes decrease during the following night. The formation of starch in plants always takes place in plastids.

Often structures that are not surrounded by a membrane are found inside the stroma. They are known as **plastoglobuli** and contain, among other substances, lipids and plastoquinone. A particularly high amount of plastoglobuli is found in the plastids of senescent leaves, containing degraded products of the thylakoid membrane. About 10 to 100 identical plastid genomes are localized in a special region of the stroma known as the **nucleoide**. The ribosomes present in the chloroplasts are either free in the stroma or bound to the surface of the thylakoid membranes.

In leaves grown in the dark (etiolation), e.g., developing in the soil, the plastids are yellow and are termed **etioplasts**. These etioplasts contain some, but not all, of the chloroplast proteins. The lipids and membranes form **prolammelar bodies** (**PLB**) which exhibit pseudo crystalline structures. The PLB function as precursors for the synthesis of thylakoid membranes and grana stacks. Carotenoides give the etioplasts the yellow color. Illumination induces the conversion from etioplasts to chloroplasts; chlorophyll is synthesized from precursor molecules (**protochlorophyllide**) and thylakoids are formed.

Leucoplasts (Fig. 1.9C) are a group of plastids that include many differentiated colorless organelles with very different functions (e.g., the **amyloplasts**), which act as a store for starch in non-green tissues such as roots, tubers, or seeds (Chapter 9). Leucoplasts are also the site of lipid biosynthesis in non-green tissues. Lipid synthesis in plants is generally located in plastids. The reduction of nitrite to ammonia, a partial step of nitrate assimilation (Chapter 10), is also always located in plastids. When nitrate assimilation takes place in the roots, leucoplasts are the site of nitrite reduction.

Chromoplasts (Fig. 1.9D) are plastids that, due to their high carotenoid content (Fig. 2.9), are colored red, orange, or yellow. In addition to the cytosol, chromoplasts are the site of isoprenoid biosynthesis, including the synthesis of carotenoids (Chapter 17). Lycopene, for instance, gives tomatoes their red color.

1.4 Mitochondria also result from endosymbionts

Mitochondria are the site of cellular respiration where substrates are oxidized for generating ATP (Chapter 5). Mitochondria, like plastids, multiply

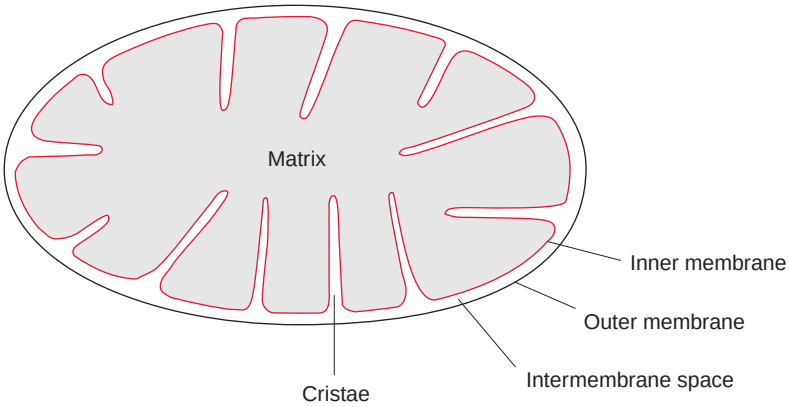

Figure 1.12 Schematic presentation of the structure of a mitochondrion.

by division and are maternally inherited. They also have their own genome (in plants consisting typically of a large circular DNA and several small circular DNAs, so-called "minicircles") and their own machinery for replication, gene expression, and protein synthesis. The mitochondrial genome encodes only a small number of the mitochondrial proteins (Table 20.6); most of the mitochondrial proteins are encoded in the nucleus. Mitochondria are of **endosymbiotic origin**. Phylogenetic experiments based on the comparison of DNA sequences led to the conclusion that all mitochondria derive from a single event in which a precursor **proteobacterium** entered an anaerobic bacterium (probably an **archaebacterium**).

The endosymbiotic origin (Fig. 1.8) explains why the mitochondria are enclosed by two membranes (Fig. 1.12). Similar to chloroplasts, the **mitochondrial outer membrane** contains **porins** (section 1.11) that render this membrane permeable to molecules below a mass of 4,000 to 6,000 Dalton, such as metabolites and nucleotides. The permeability barrier for these compounds and the site of specific translocators (section 5.8) is the **mitochondrial inner membrane**. Therefore the **intermembrane space** between the inner and the outer membrane has to be considered as an external compartment. The "protoplasm" of the mitochondria, which is surrounded by the inner membrane, is called the **mitochondrial matrix**. The mitochondrial inner membrane contains the proteins of the respiratory chain (section 5.5). In order to enlarge the surface area of the inner membrane, it is invaginated in folds (**cristae mitochondriales**) or **tubuli** (Fig. 1.13) into the matrix. The membrane invaginations correspond to the thylakoid membranes, the only difference is that in the mitochondria these invaginations are not separated from the inner membrane to form a distinct compartment. Similar to chloroplasts, the mitochondrial inner membrane is the site for the formation of a **proton gradient**. Therefore the mitochondrial intermembrane space and the chloroplastic thylakoid lumen correspond functionally.

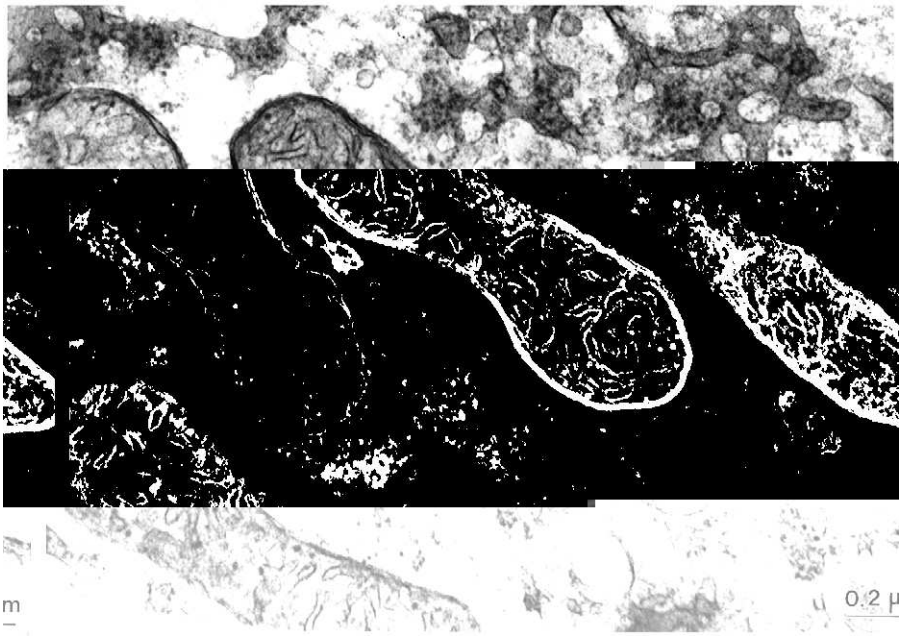

Figure 1.13 Invaginations of the inner mitochondrial membrane result in an enlargement of the membrane surface. Mitochondria of a barley aleurone cell. (By D.G. Robinson, Heidelberg.)

1.5 Peroxisomes are the site of reactions in which toxic intermediates are formed

Peroxisomes, also termed microbodies, are small, spherical organelles with a diameter of 0.5 to 1.5 µm (Fig. 1.14), which, in contrast to plastids and mitochondria, are enclosed by only a single membrane. The peroxisomal matrix represents a specialized compartment for reactions in which toxic intermediates are formed. Thus peroxisomes contain enzymes catalyzing the oxidation of substances accompanied by the formation of $\mathbf{H_2O_2}$, and also contain **catalase**, which immediately degrades H_2O_2 (section 7.4). Peroxisomes are a common constituent of eukaryotic cells. In plants peroxisomes occur in two important differentiated organelle types: the **leaf peroxisomes** (Fig. 1.14A), which participate in photorespiration (Chapter 7); and the **glyoxysomes** (Fig. 1.14B), which are present in seeds containing oils (triacylglycerols) and play a role in the conversion of triacylglycerols to carbohydrates (section 15.6). They contain all the enzymes for fatty acid β-oxidation. Peroxisomes multiply by division, but it has also been observed that they can be generated *de novo* from vesicles of the endoplasmic reticulum. Since peroxisomes do not have a genome of their own, it seems rather improbable that they descend from a prokaryotic endosymbiont like

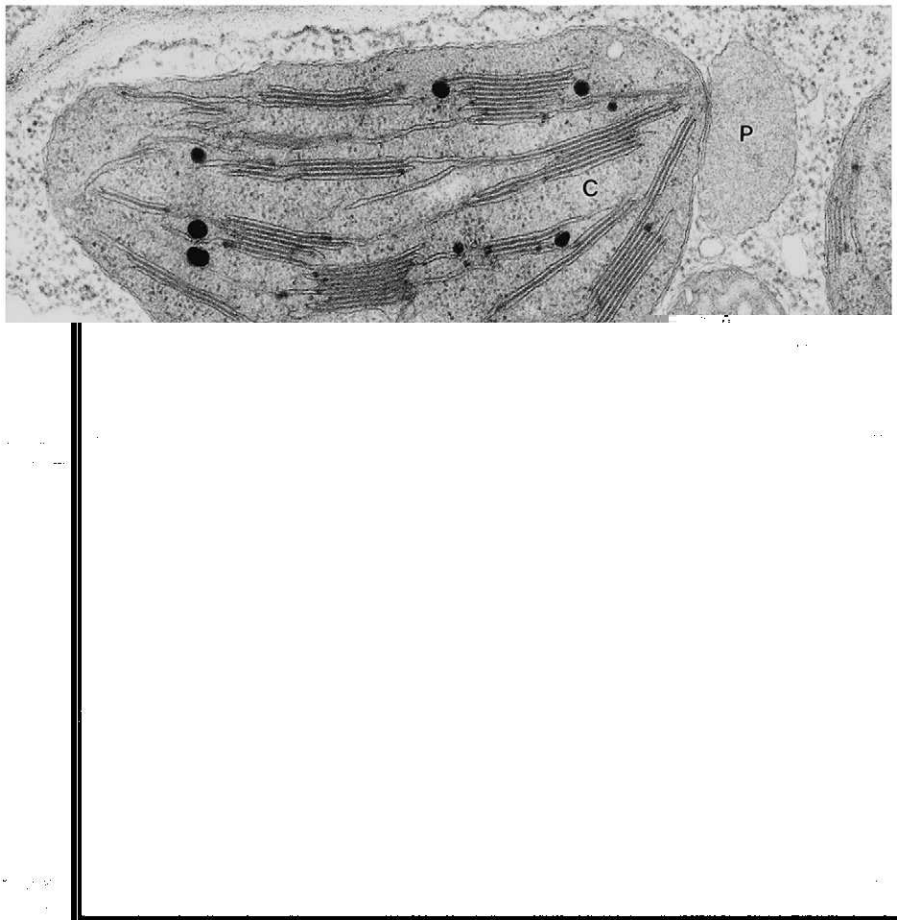

Figure 1.14 Peroxisomes. A. Peroxisome from the mesophyll cell of tobacco. The proximity of the peroxisome (P), mitochondrion (M), and chloroplast (C) reflects the rapid metabolite exchange between these organelles in the course of photorespiration (discussed in Chapter 7). B. Glyoxysomes from germinating cotyledons of *Cucurbita pepo* (courgette). The lipid degradation (section 15.6) and the accompanying gluconeogenesis require a close contact between lipid droplets (L), glyoxysome (G), and mitochondrion (M). (By D. G. Robinson, Heidelberg.)

mitochondria and chloroplasts. Phylogenetic analyses suggest that peroxisomes are derived from the endoplasmic reticulum of an early eukaryote.

1.6 The endoplasmic reticulum and Golgi apparatus form a network for the distribution of biosynthesis products

In an electron micrograph, the **endoplasmic reticulum** (**ER**) appears as a labyrinth traversing the cell (Fig. 1.15). Two structural types of ER can be differentiated: the rough and the smooth forms. The **rough ER** consists

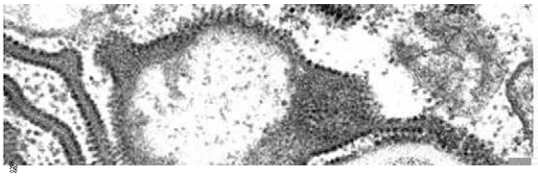

Figure 1.15 Rough endoplasmic reticulum (ER) in the geminating pollen of *Lilium longiflorum*. The surface of the ER is densely occupied with ribosomes. Between the lipid monolayers is a triacylglyceride containing lipid body (see also Fig. 15.6). (By D. G. Robinson, Heidelberg.)

of flattened sacs that are sometimes arranged in loose stacks of which the outer side of the membranes is occupied by **ribosomes**. The **smooth ER** consists primarily of branched tubes without ribosomes. Despite these morphological differences, the rough ER and the smooth ER are constituents of a continuous membrane system.

The presence of ribosomes on the outer surface of the ER is temporary. Ribosomes are attached to the ER membrane only when the protein that they synthesize is destined for the ER itself, for the vacuoles, or for export from the cell. These proteins contain an amino acid sequence (**signal sequence**) that causes the peptide chain in the initial phase of its synthesis to enter the lumen of the ER (section 14.5). A snapshot of the ribosome complement of the ER only shows those ribosomes that at the moment of tissue fixation are involved in the synthesis of proteins destined for import into the ER lumen. Membranes of the ER are also the site of membrane lipid synthesis, for which the necessary fatty acids are provided by the plastids.

In seeds and other tissues, **oil bodies** (also called **oleosomes**) are present. These are derived from the ER membrane. The oil bodies store triacylglycerides and are of great economic importance for oil fruits, such as rape seed or olives. The oil bodies are only enclosed by half of a biomembrane (monolayer), of which the hydrophobic fatty acid residues of the membrane lipids project into the oil and the hydrophilic parts of the lipid layer protrude into the cytosol (section 15.2).

In addition, the ER is a suitable storage site for the production of transgene proteins in genetically engineered plants. Native as well as transgene proteins are equipped with a signal sequence and the amino terminal ER-retention signal KDEL (Lys Asp Glu Leu). The ER of leaves is capable of accumulating large amounts of such extraneous proteins (up to 2.5 to 5% of the total leaf protein) without affecting the function of the ER. In the ER lumen, proteins are often modified by N-glycosylation (attachment of hexose chains to amino acid residues, e.g., asparagin (section 17.7)).

The transport of proteins into the vacuoles proceeds in different ways. There exists a **direct transport** via vesicles between the ER and the vacuoles. Most proteins, however, are at first channeled via vesicles to the *cis*-side of the **Golgi apparatus** (Fig. 1.16), and only after having been processed in the Golgi apparatus are further transferred into the vacuoles or are excreted from the cell as secretory proteins. Two mechanisms for transporting proteins through the Golgi apparatus are under discussion. (1) According to the **vesicle shuttle** model (Fig. 1.16), the proteins pass through the different cisternae by enbudding and vesicle transfer, while each cisterna has its fixed position. (2) According to the **cisternae progression** model, cisternae are constantly being newly formed by vesicle fusion at the *cis*-side, and they then decompose to vesicles at the *trans*-side. Present results show that both systems probably function in parallel. The budding of the protein loaded

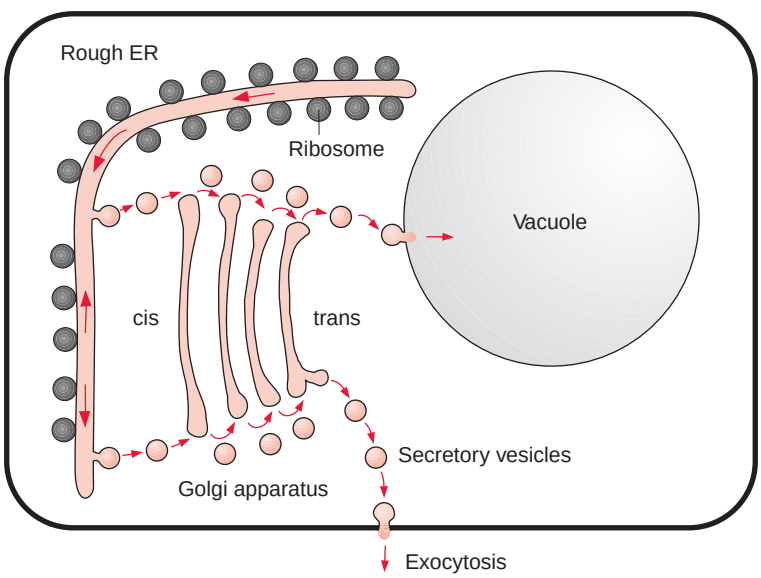

Figure 1.16 Schematic presentation of the interplay between the endoplasmic reticulum and the Golgi apparatus during the transfer of proteins from the ER to the vacuoles and the secretion of proteins from the cell.

vesicles from the Golgi apparatus occurs at certain regions of the ER membrane called **ERES** (ER export sites). The vesicles are covered at the outer surface of the surrounding membrane with a coat protein (**COP II**). The fusion of the vesicles with the membrane of the Golgi apparatus is facilitated by so-called **SNARE-proteins** (soluble N-ethylmaleinimide sensitive attachment protein receptors). For the backflow of the emptied vesicles to the ER, the vesicles are covered with another coat protein (**COP I**) and the fusion with the ER again requires a SNARE protein. In *Arabidopsis* altogether 15 genes encoding for SNARE proteins have been identified.

The Golgi apparatus was discovered in 1898 by the Italian Camillo Golgi by using a light microscope. The Golgi system consists of up to 20 curved discs arranged in parallel, the so-called **Golgi cisternae** or dictyosomes, which are surrounded by smooth membranes (not occupied by ribosomes) (Fig. 1.17). At both sides of the discs, vesicles of various sizes can be seen to bud off. The Golgi apparatus consists of the *cis*-compartment, the middle compartment, and the *trans*-compartment. During transport through the Golgi apparatus, proteins are often modified by O-glycosylation (attachment of hexose chains to serine and threonine residues).

In the Golgi apparatus, proteins are selected either to be removed from the cell by exocytosis (secretion) or to be transferred to lytic vacuoles or to storage vacuoles (section 1.2). Signal sequences of proteins act as sorting signals to direct proteins into the vacuolar compartment; the proteins destined for the lytic vacuoles are transferred in **clathrin-coated vesicles**.

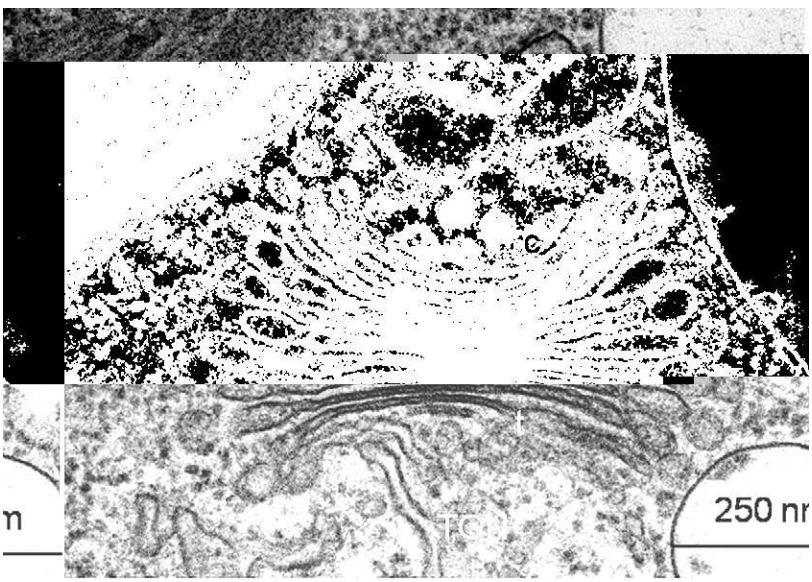

Figure 1.17 Golgi apparatus (dictyosome) in the green alga *Chlamydomonas noctigama*. C = *cis*-side, t = *trans*-side. In the neighborhood of the *cis*-side is a segment of the endoplasmatic reticulum (ER). The membranes extending from the *trans*-side are part of the trans-Golgi network (TGN). (By D. G. Robinson, Heidelberg.)

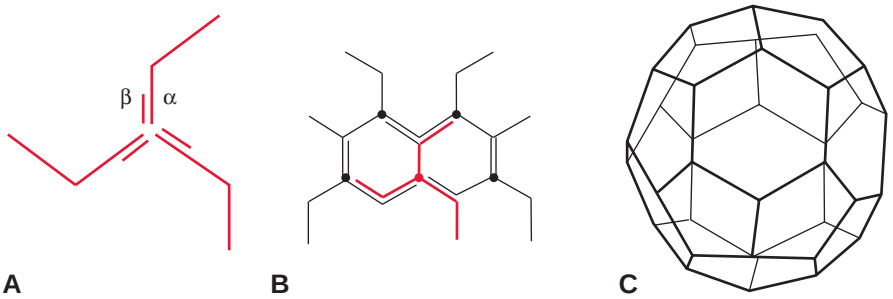

Figure 1.18 Model of the structure of clathrin-coated vesicles. A. Three α- and three β-subunits of clathrin form a complex with three arms. B. From this a hexagonal and pentagonal lattice (the latter not shown here) is formed by polymerization. This forms the coat (C). (From Kleinig and Sitte.)

Clathrin is a protein consisting of two different subunits (α-UE 180,000 Dalton, β-UE 35,000 to 40,000 Dalton). Three α- and three β-subunits form a complex with three arms (triskelion), which polymerizes to a hexagonal latticed structure surrounding the vesicle (Fig. 1.18). The transport into the storage vacuoles proceeds via other vesicles without clathrin. Secretion proteins, containing only the signal sequence for entry into the ER, reach the plasma membrane via **secretion vesicles** without a protein coat and are secreted by **exocytosis**.

The ER membrane, the membranes of the Golgi apparatus (derived from the ER), the transfer vesicles, and the nuclear envelope are collectively called the **endomembrane system**.

1.7 Functionally intact cell organelles can be isolated from plant cells

In order to isolate cell organelles, the cell has to be disrupted only to such an extent that its intact organelles are released into the isolation medium, resulting in a **cell homogenate**. To prevent the liberated organelles from swelling and disruption, the isolation medium must be isotonic. The presence of an **osmotic compound** (e.g., sucrose) generates an osmotic pressure in the medium, which should correspond to the osmotic pressure of the aqueous phase within the organelle. Media containing 0.3 mol/L sucrose or sorbitol usually are used for such cell homogenizations.

Figure 1.19 shows the protocol of the isolation scheme for chloroplasts. Small leaf pieces are homogenized by cutting them up within seconds using blades rotating at high speed, such as in a food mixer. It is important that the homogenization time is short; otherwise the cell organelles released into the isolation medium would also be destroyed. Such homogenization is

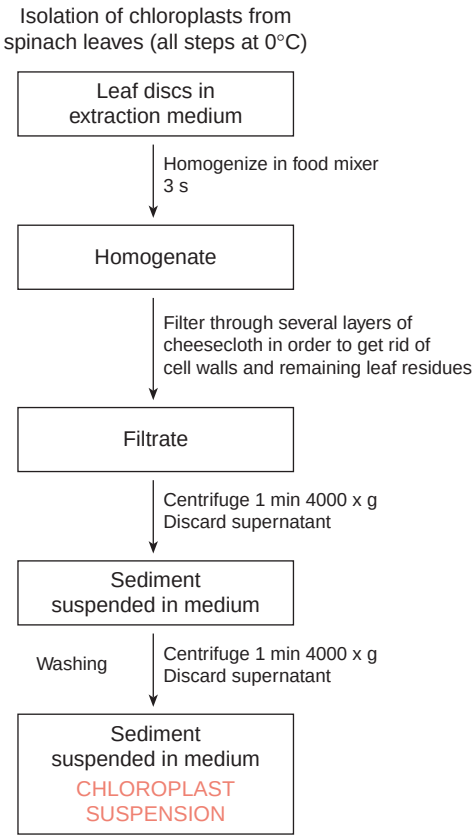

Figure 1.19 Protocol for the isolation of functionally intact chloroplasts.

only applicable for leaves that have soft cell walls, e.g., spinach. In the case of leaves with more rigid cell walls (e.g., cereal plants), protoplasts are first prepared from leaf pieces as described in section 1.1. These protoplasts are then ruptured by forcing the protoplast suspension through a net with a mesh smaller than the size of the protoplasts.

The desired organelles can be separated and purified from the rest of the cell homogenate by differential or density gradient centrifugation. In the case of **differential centrifugation**, the homogenate is suspended in a medium with a density much lower than that of the cell organelles. In the gravitational field of the centrifuge, the sedimentation velocity of the particles depends primarily on the **particle size** (the large particles sediment faster than the small particles). As shown in Figure 1.19, taking the isolation of chloroplasts as an example, relatively pure organelle preparations can be obtained within a short time by a sequence of centrifugation steps at increasing speeds.

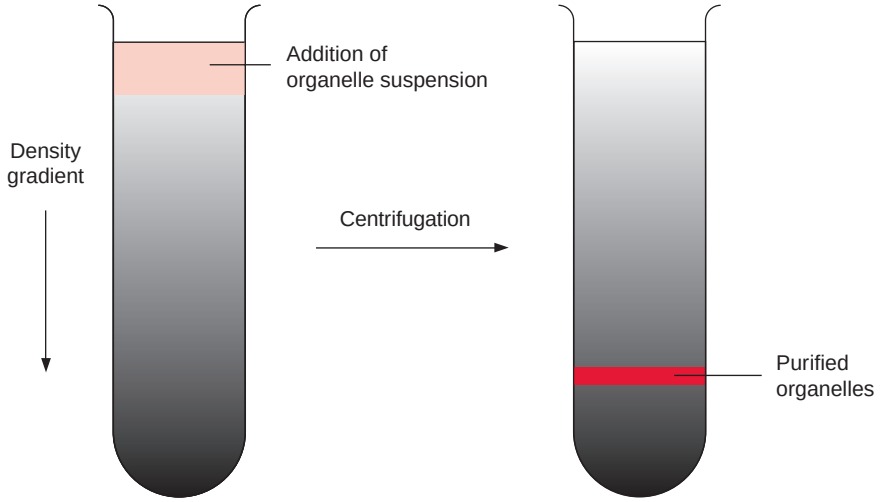

Figure 1.20 Organelles and particles are separated by density gradient centrifugation according to their different densities.

In the case of **density gradient centrifugation** (Fig. 1.20), the organelles are separated according to their **density**. Media of differing densities are assembled in a centrifuge tube so that the density increases from top to bottom. To prevent alterations of the osmolarity of the medium, heavy macromolecules (e.g., Percoll = silica gel) are used to achieve a high density. The cell homogenate is layered on the density gradient prepared in the centrifuge tube and centrifuged until all the particles of the homogenate have reached their zone of equal density in the gradient. As this density gradient centrifugation requires high centrifugation speed and long running times, it is often used as the final purification step after preliminary separation by differential centrifugation.

By using these techniques it is possible to obtain functionally intact chloroplasts, mitochondria, peroxisomes, and vacuoles of high purity with the option to study their metabolic properties thereafter in the test tube.

1.8 Various transport processes facilitate the exchange of metabolites between different compartments

Each of the cell organelles mentioned in the preceding section has a specific function in cell metabolism. The interplay of the metabolic processes in the various compartments requires a transfer of substances across the membranes of these cell organelles as well as between the different cells. This

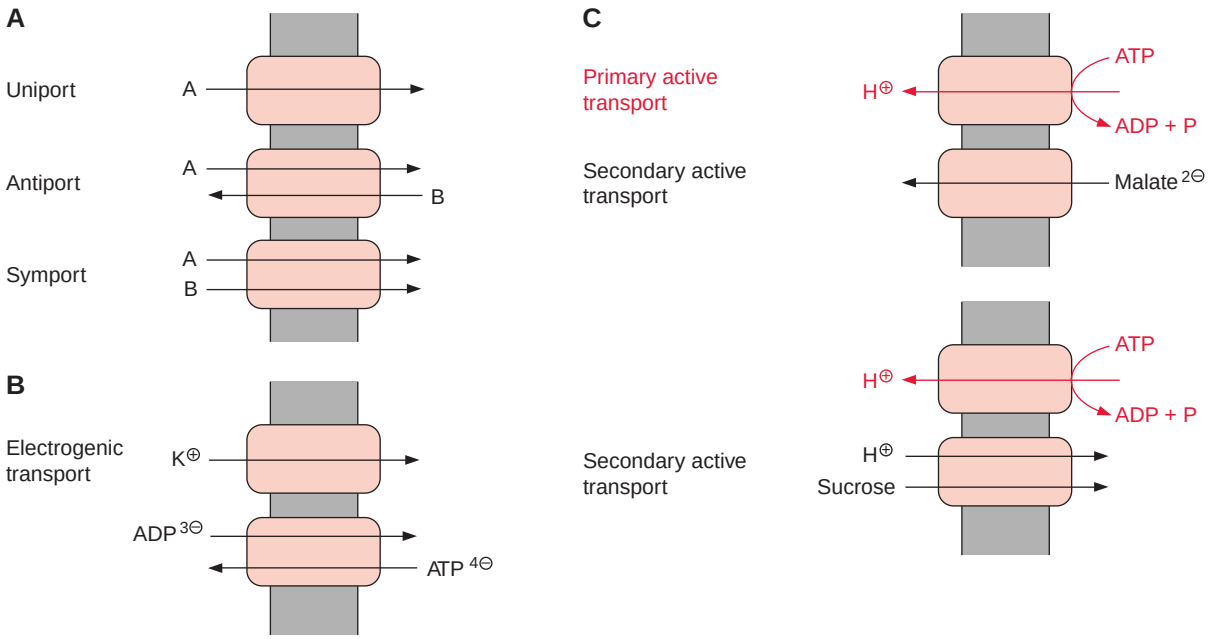

Figure 1.21 Classification of membrane transport processes.

transfer of compounds takes place in various ways: by specific translocators, channels, pores, via vesicle transport, and in a few cases (e.g., CO_2 or O_2) by non-specific diffusion through membranes. The vesicle transport and the function of the plasmodesmata have already been described (section 1.6).

Figure 1.21 illustrates various types of transport processes according to formal criteria. When a molecule moves across a membrane independent of the transport of other molecules, the process is called **uniport**, and when counter-exchange of molecules is involved, it is called **antiport**. The mandatory simultaneous transport of two substances in the same direction is called **symport**. A transport via uniport, antiport, or symport, in which a charge is simultaneously moved, is termed **electrogenic transport**. A vectorial transport, which is coupled to a chemical or photochemical reaction, is named **active** or **primary active transport**. Examples of active transport are the transport of protons driven by the electron transfer of the photosynthetic electron transport chain (Chapter 3) or the respiratory chain (Chapter 5) or by the consumption of ATP (Fig. 1.21C). Such proton transport is electrogenic; the transfer of a positive charge results in the formation of a membrane potential. Another example of primary active transport is the ATP-dependent transport of glutathione conjugates into vacuoles (section 12.2).

In a **secondary active transport**, the only driving force is an electrochemical potential across the membrane. In the case of an electrogenic uniport, the membrane potential can be the driving force by which a substrate is

transported across the membrane against the concentration gradient. An example of this is the accumulation of malate in the vacuole (Figure 1.21C; see also Chapter 8). Another example of secondary active transport is the transport of sucrose via an H^+-sucrose symport in which a proton gradient, formed by primary active transport, drives the accumulation of sucrose (Figure 1.21C). This transport plays an important role in loading sieve tubes with sucrose (Chapter 13).

1.9 Translocators catalyze the specific transport of metabolic substrates and products

Specialized membrane proteins catalyze a specific transport across membranes. In the past these proteins were called carriers, as it was assumed that after binding the substrate at one side of the membrane, they would diffuse through the membrane to release the substrate on the other side. We now know that this simple picture does not apply. Instead, transport can be visualized as a process by which a molecule moves through a specific pore. The proteins catalyzing such a transport are termed **translocators** or **transporters**. The triose phosphate-phosphate translocator of chloroplasts will be used as an example to describe the structure and function of such a translocator. This translocator enables the export of photoassimilates from the chloroplasts by catalyzing a counter-exchange of phosphate with triose phosphate (dihydroxyacetone phosphate or glyceraldehyde-3-phosphate) (Fig. 9.12). Quantitatively it is the most abundant transport protein in plants.

Silicone layer filtering centrifugation is a very useful tool (Fig. 1.22) for measuring the uptake of substrates into chloroplasts or other cell organelles. To start measurement of transport, the corresponding substrate is added to a suspension of isolated chloroplasts and is terminated by separating the chloroplasts from the surrounding medium by centrifugation through a silicone layer. The amount of substrate taken up into the separated chloroplasts is then quantitatively analyzed.

A hyperbolic curve is observed (Fig. 1.23) when this method is used to measure the uptake of phosphate into chloroplasts at various external concentrations of phosphate. At very low phosphate concentrations the rate of uptake rises proportionally to the external concentration, whereas at higher phosphate concentrations the curve levels off until a **maximal velocity** is reached (V_{max}). These are the same characteristics as seen in enzyme catalysis.

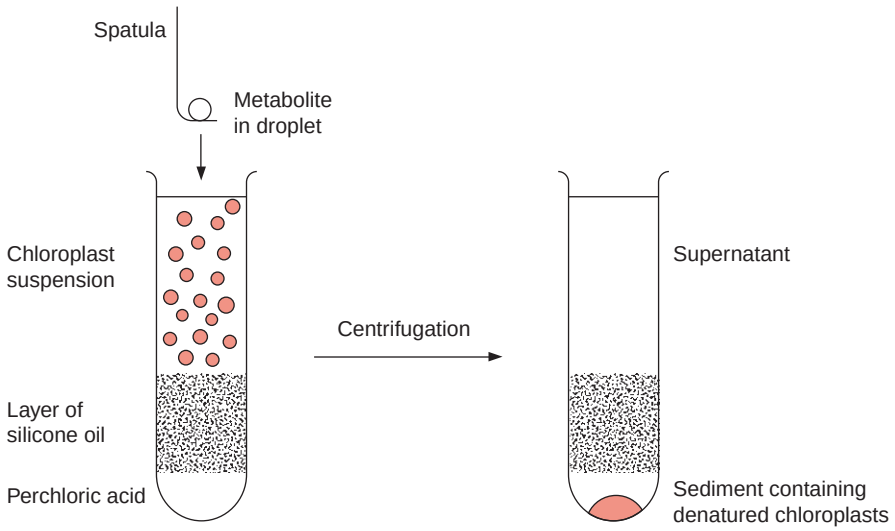

Figure 1.22 Silicone oil filtering centrifugation: measurement of the uptake of compounds into isolated chloroplasts. For the measurement, the bottom of a centrifuge tube was filled with perchloric acid on which silicone oil is layered. The compound/metabolite to be transported is added to the chloroplast suspension above the silicone layer using a small spatula. To simplify detection, metabolites labeled with radio isotopes (e.g., ^{32}P or ^{14}C) are usually used. The uptake of metabolites into the chloroplasts is terminated by centrifugation in a rapidly accelerating centrifuge. Upon centrifugation the chloroplasts migrate within a few seconds through the silicone layer into the perchloric phase, where they are denatured. That portion of the metabolite, which has not been taken up, remains in the supernatant. The amount of metabolite that has been taken up into the chloroplasts is determined by measurement of the radioactivity in the sedimented fraction. The amount of metabolite carried nonspecifically through the silicone layer, either by adhering to the outer surface of the plastid or present in the space between the inner and the outer envelope membranes, can be evaluated in a control experiment in which a compound is added (e.g., sucrose) that is known not to permeate the inner envelope membrane.

During enzyme catalysis the substrate (S) is first bound to the enzyme (E). The product (P) formed on the enzyme surface is then released:

$$E + S \rightarrow ES \xrightarrow{Catalysis} EP \rightarrow E + P$$

The transport by a specific translocator can be depicted in a similar way:

$$S + T \rightarrow ST \xrightarrow{Transport} TS \rightarrow T + S$$

The substrate is bound to a specific binding site of the translocator protein (T), transported through the membrane, and then released from the

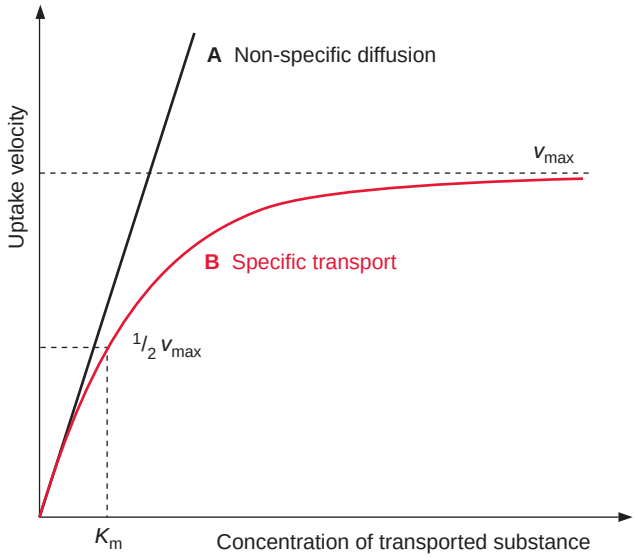

Figure 1.23 Determination of the concentration dependence of the uptake of a compound distinguishes whether the uptake occurs by nonspecific diffusion through the membrane (A) or by specific transport (B).

translocator. The maximal velocity V_{max} corresponds to a state in which all the binding sites of the translocators are saturated with substrate. As is the case for enzymes, the K_m for a translocator corresponds to the substrate concentration at which transport occurs at half maximum velocity. Also in analogy to enzyme catalysis, the translocators usually show high **specificity** for the transported substrates. For instance, the chloroplast triose phosphate-phosphate translocator (trioseP-P translocator) of C_3 plants (section 9.1) transports orthophosphate, dihydroxyacetone phosphate, glyceraldehyde-3-phosphate, and 3-phosphoglycerate, but not 2-phosphoglycerate. The various substrates compete for the binding site. Therefore, one substrate such as phosphate will be a **competitive inhibitor** for the transport of another substrate such as 3-phosphoglycerate. The trioseP-P translocator of chloroplasts is an antiporter, so that for each molecule transported inward (e.g., phosphate), another molecule (e.g., dihydroxyacetone phosphate) must be transported out of the chloroplasts. Another example for an antiporter is the mitochondrial ATP-ADP translocator (section 5.6) which transports ADP and ATP, but not AMP, phosphate or other nucleotides.

Metabolite transport is achieved by a conformational change of the translocator

Translocators are, as **integral membrane proteins**, part of a membrane. Due to their high hydrophobicity they are not soluble in water, which made

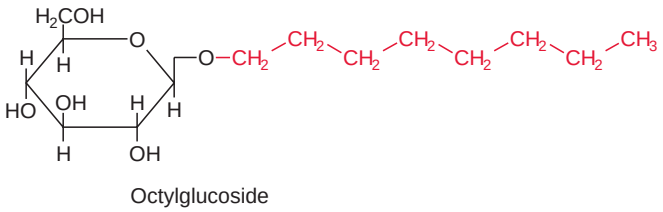

Figure 1.24
Octylglucoside, a glycoside composed from α-D-glucose and octyl alcohol, is a mild non-ionic detergent that allows membrane proteins to be solubilized from the membranes without being denatured.

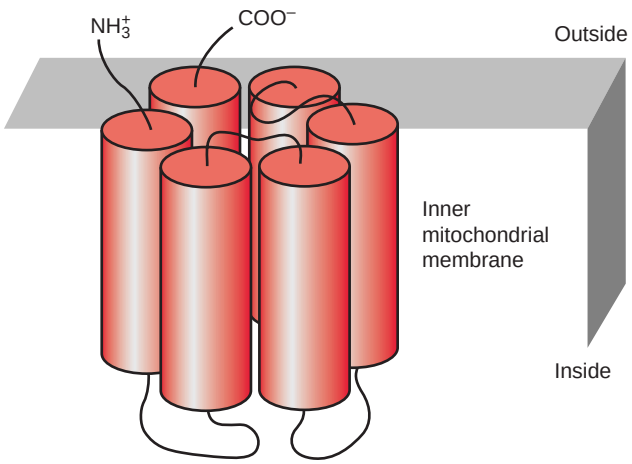

Figure 1.25 Structural model of the mitochondrial ATP-ADP translocator. Six transmembrane α-helices traverse the inner mitochondrial membrane.

studies of their protein structure difficult. In order to isolate these proteins from the membranes by solubilization, mild nonionic detergents, such as octylglucoside (Fig. 1.24), are employed. The hydrophobic hydrocarbon chain of the detergent associates with the hydrophobic protein. Because of the glucose residue of octylglucoside, the formed micelle is water soluble. A removal of the detergent would turn the membrane protein into a sticky mass, which could not be solubilized again.

Translocators traverse the lipid bilayer of a membrane via **α-helices**, of which the outside directed amino acid side chains are hydrophobic. The transmembrane helices contain predominantly hydrophobic amino acids such as alanine, valine, leucine, isoleucine or phenylalanine. Figure 1.25 shows a structural model of the monomer of the mitochondrial ATP-ADP translocator. Six transmembrane helices span the inner mitochondrial membrane, and loops directed to the inside cause the specificity of the transport. The mitochondrial ATP-ADP translocator occurs in the membrane

as a dimer of identical monomers (**homodimer**). The X-ray structure analysis (section 3.3) of the mitochondrial ATP/ADP translocator revealed for the first time the three-dimensional structure of a eukaryotic metabolite translocator. It appeared that the six transmembrane helices of the monomer form a barrel-like structure functioning as a translocation pore. Consequently, the homodimer consists of **two adjacent identical pores**. Similarly, the chloroplast trioseP-P translocator occurs in the membrane as a homodimer, but it is not yet certain how many transmembrane helices the monomer consists of.

As discussed earlier, the translocation pores are gated, each containing only one substrate binding site, accessible either from the outside or from the inside, whereas the accessibility is governed by the conformation of the translocator protein (Fig. 1.26). The transport process resembles a gate. The binding of a substrate (A) to a binding site directed to the outside

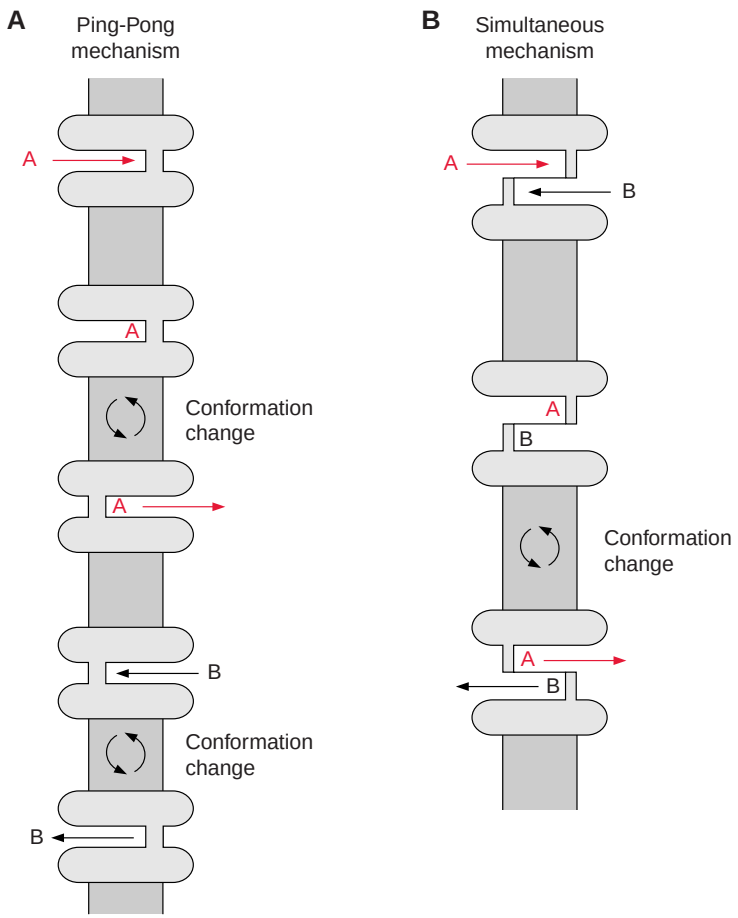

Figure 1.26 Schematic presentation of antiport transports. Two possibilities for the counter-exchange of two substrate molecules (A, B). A. Ping-pong mechanism: a translocator molecule catalyzes the transport of A and B sequentially. B. Simultaneous mechanism: A and B are transported simultaneously by two translocator molecules tightly coupled to each other. See text for further explanations.

induces a **conformational change** of the translocator by which the substrate binding site is shifted to the inside, enabling the release of the substrate. The now empty binding site at the inside can bind another substrate (B), inducing a conformational change for B to be transported to the outside. An obligatory counter-exchange can be explained in terms of the opening of the gate by shifting the binding sites via conformational change being possible only when the substrate binding site is occupied. This principle of an antiport has been termed **ping-pong mechanism** (Fig. 1.26A)**,** and probably describes the action of the chloroplast trioseP-P translocator. In many cases, e.g., the mitochondrial ATP-ADP translocator, the counter-exchange follows a **simultaneous mechanism** (Fig. 1.26B), where the substrate binding sites of the adjacent pores of the dimer are oppositely directed; one pore is accessible from the inside and the other from the outside, and a simultaneous conformational change occurs only when both binding sites are occupied.

A plant contains a large number of such metabolite translocators. The analysis of the *Arabidopsis* genome suggests that altogether about 150 plastidic and 60 mitochondrial translocator genes exist.

Aquaporins make cell membranes permeable for water

The water permeability of a pure lipid bilayer is relatively low. Peter Agre from the Johns Hopkins University in Baltimore isolated from kidney and blood cells proteins that form **membrane channels for water**, which he termed **aquaporins**. In 2003 he was awarded the Nobel Prize in Chemistry for this important discovery. It turned out that these aquaporins also occur in plants (e.g., in plasma membranes and membranes of the vacuole). Notably both types of membranes play a major role in the hydrodynamic response of a plant cell. A plant contains many aquaporin isoforms. Thus in the model plant *Arabidopsis thaliana* (section 20.1) about 35 different genes of the aquaporin family have been found, which are specifically expressed in the various plant organs.

X-ray structure analysis by electron cryomicroscopy showed that the subunits of the aquaporins each have six transmembrane helices (section 3.3). In the membranes the subunits of the aquaporins are present as tetramers, of which each monomer forms a channel, transporting 10^9 to 10^{11} water molecules per second. The **water channel** consists of a very narrow primarily **hydrophobic pore** with binding sites for only seven H_2O molecules. These binding sites act as a **selection filter** for a specific water transport. It can be deduced from the structure that, for energetic reasons, these water channels are relatively impermeable for protons. It was also observed that an aquaporin from the plasma membrane of tobacco also

transports CO_2. This finding suggests that aquaporins may play a role as CO_2 transporters in plants.

By regulating the opening of the aquaporins, the water conductivity of the plasma membrane can be adjusted to the environmental conditions. The aquaporins of plants possess a peptide loop which is able to close the water channel like a lid via conformational change. In this way the water channels can be closed upon drought stress or flooding. During drought stress the closure of the water channel is caused by dephosphorylation of two highly conserved serine residues. In the case of flooding or waterlogging the accompanying oxygen deficiency (anoxy) results in a decrease of the pH in the cytosol, causing the protonation of a histidine residue, which in turn induces a conformational change of the channel protein closing the lid of the water channel.

The now commonly used term *aquaporin* is rather unfortunate, since aquaporins have an entirely different structure from the porins. Whereas the aquaporins, the translocators and ion channels are formed of transmembrane helices (sections 1.9 and 1.10), the porins consist of β-sheets (section 1.11).

1.10 Ion channels have a very high transport capacity

The chloroplast trioseP-P translocator mentioned previously has a turnover number of $80\,s^{-1}$ at 25°C, which means that it transports 80 substrate molecules per second. The turnover numbers of other translocators are in the range of 10 to $1{,}000\,s^{-1}$. Membranes also contain proteins which form **ion channels** that transport various ions at least three orders of magnitude faster than translocators (10^6 to 10^8 ions per second). They differ from the translocators in having a pore open to both sides at the same time. The flux of ions through the ion channel is so large that it is possible to determine the transport capacity of a single channel from the measurement of electrical conductivity.

The procedure for such single channel measurements, called the **patch clamp technique**, was developed by two German scientists, Erwin Neher and Bert Sakmann, who were awarded the Nobel Prize in Medicine and Physiology in 1991 for this research. The set-up for this measurement (Fig. 1.27) consists of a glass pipette that contains an electrode filled with an electrolyte fluid. The very thin tip of this pipette (diameter about 1 μm) is sealed tightly by a membrane patch. The number of ions transported through this patch per unit time can be determined by measuring the electrical

current (usually expressed as conductivity in Siemens (S)). Figure 1.28 shows an example of the measurement of the single channel currents with the plasma membrane of broad bean guard cells. As shown from the recording of the current, the channel opens for various lengths of time and then closes. This principle of **stochastic switching** between a **non-conductive state** and a defined **conductive state** is a typical property of ion channels. In the open state various channels have different conductivities, which can

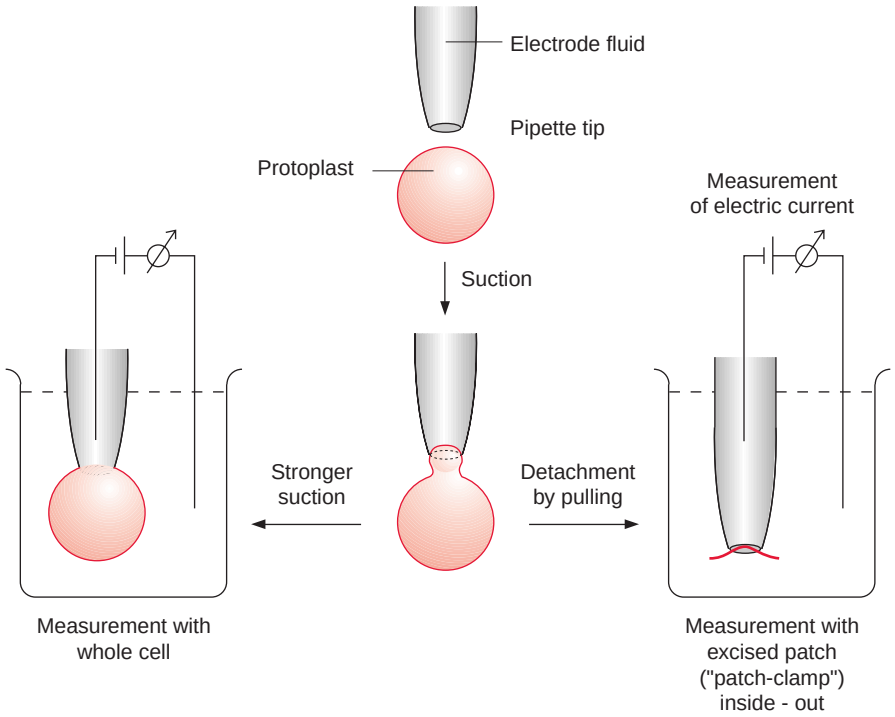

Figure 1.27 Measurement of ion channel currents by the "patch clamp" technique. A glass pipette with a diameter of about 1 μm at the tip, containing an electrode and electrode fluid, is brought into contact with the membrane of a protoplast or organelle (e.g., vacuole). By applying slight suction, the opening of the pipette tip is sealed by the membrane. By applying stronger suction, the membrane surface over the pipette opening disrupts, and the electrode within the pipette is now in direct electrical connection with the cytosol of the cell. In this way the channel currents can be measured for all the channels present in the membrane (whole cell configuration). Alternatively, by slight pulling, the pipette tip can be removed from the protoplast or the organelle with a remaining membrane patch, which is sealed to the tip, being torn from the rest of the cell/organelle. In this way the currents are measured only for those channels that are present in the membrane patch. A voltage is applied to determine the channel current. Since the currents are in the range of μA and pA they need to be amplified.

range from between a few pS and several hundred pS. Moreover, various channels have characteristic mean open and close times, which, depending on the channel, can last from a few milliseconds to seconds. The transport capacity of the channel per unit time therefore depends on the conductivity of the opened channel as well as on the mean duration of the open state.

Many ion channels have been characterized that are more or less specific for certain ions. Plants contain highly selective cation channels for H^+, K^+, Na^+ and Ca^{++} and also selective anion channels for Cl^- and dicarboxylates, such as malate. The opening of many ion channels is regulated by the electric **membrane potential**. This means that membranes have a very important function in the electrical regulation of ion fluxes. Thus, in guard cells (section 8.1) the hyperpolarization of the plasma membrane (>100 mV) opens a channel that allows potassium ions to flow into the cell (**K^+ inward channel**), whereas depolarization opens another channel by which potassium ions can leave the cell (**K^+ outward channel**). In addition, the opening of many ion channels is controlled by ligands such as Ca^{++} ions, protons, or by phosphorylation of the channel protein. This enables regulation of the channel activity by metabolic processes and by messenger substances (Chapter 19).

Up to now the amino acid sequences of many channel proteins have been determined. It emerged that certain channels (e.g., those for K^+ ions in bacteria, animals, and plants) are very similar. Roderick MacKinnon and coworkers from the Rockefeller University in New York resolved the three-dimensional structure of the K^+ channel for the bacterium *Streptomyces lividans* using X-ray structure analysis (section 3.3). These pioneering results, for which Roderick MacKinnon was awarded the Nobel Prize in Chemistry in 2003, have made it possible to recognize for the first time the molecular function of an ion channel. It has long been known that the channel protein is built from two identical subunits, each of which has two trans-

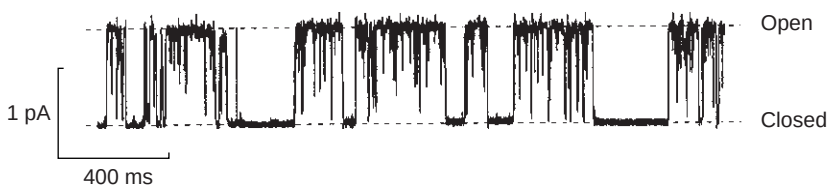

Figure 1.28 Measurement of single channel current of the K^+ outward channel in a patch (Fig. 1.27) of the plasma membrane of guard cells from *Vicia faba*. (Outer medium 50 mM K^+, cytoplasmic side 200 mM K^+, voltage +35 mV.) (Data from G. Thiel, Darmstadt.)

membrane helices connected by a **sequence of about 30 amino acids (loop)** (Fig. 1.29A). This loop is responsible for the ion selectivity of the channel. Structure analysis showed that a K^+ channel is built of four of these subunits (Fig. 1.29B, C). One helix of each subunit (the inner one) lines the channel while the other (outer) helix is directed towards the lipid membrane. The pore's interior consists of a channel filled with water, which is separated from the outside by a selectivity filter. This filter is formed from the loops of the four subunits. The channel has such a small pore that the K^+ ions first have to **strip off their hydrate coat** before they can pass through. In order to compensate for the large amount of energy required to dehydrate the K^+ ions, the pore is lined with a circular array of oxygen atoms that act as a "**water substitute**" and form a complex with the K^+ ions. The pore is also negatively charged to bind the cations. The new K^+ ions that enter the pore push those ions that are already bound through the pore to the other side of the filter. Na^+ ions are too small to be complexed in the pore's selection filter; they are unable to strip off their hydrate coat and therefore their passage through the filter is blocked. This explains the K^+ channel's ion selectivity. The aforementioned loops between the transmembrane helices acting as a selectivity filter appear to be a common characteristic of K^+ ion channels in microorganisms, animals and plants. Studies with K^+ channels from plants revealed that a decisive factor in the K^+ selectivity is the presence of glycine residues in the four loops of the selectivity filter. Analogous results were obtained from the analysis of the three-dimensional structure of chloride channels from the bacteria *Salmonella* and *E. coli* (belonging to a large family of anion channels from prokaryotic and eukaryotic organisms). These channels, formed from transmembrane helices, also contain in their interior loops, which function as selectivity filters by electrostatic interaction and coordinated binding of the chloride anion. It appears now that the features the K^+ channel of *Streptomyces* reveals a general mechanistic principle by which specific ion channels function.

There are similarities between the basic structure of ion channels and translocators. Translocators, such as the mitochondrial aspartate-glutamate translocator, can be converted by the action of chemical agents (e.g., organic mercury compounds reacting with -SH groups) into a channel, which is simultaneously open to both sides, and has an ion conductivity similar to the ion channels discussed above. The functional differences between translocators and ion channels can be explained by differences in the outfit of the pore by peptide chains. In metabolite translocators the substrate binding site is at a given time only accessible from one side, and the transport involves a conformational change configurating the channel as a gate, whereas in open ion channels the aqueous pore is simultaneously open to both sides.

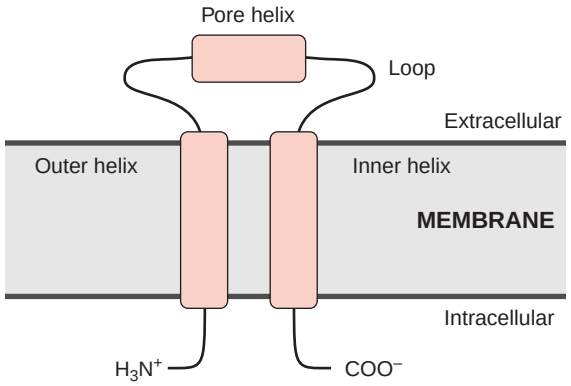
Pore helix
Loop
Extracellular
Outer helix
Inner helix
MEMBRANE
Intracellular
H_3N^+
COO^-

A

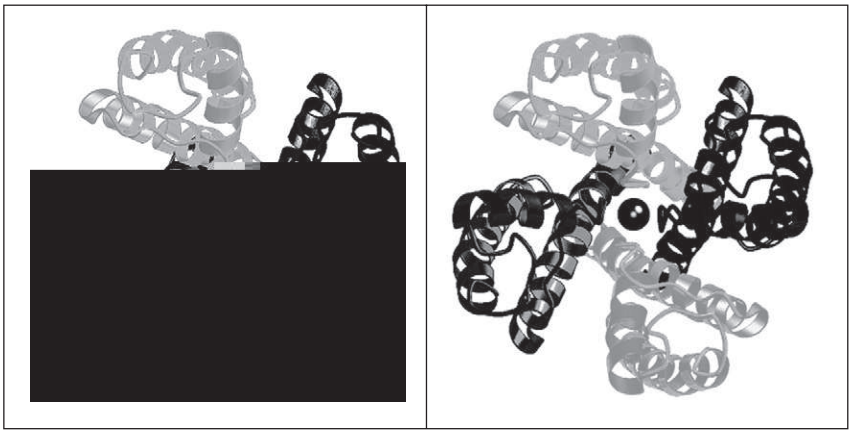

B

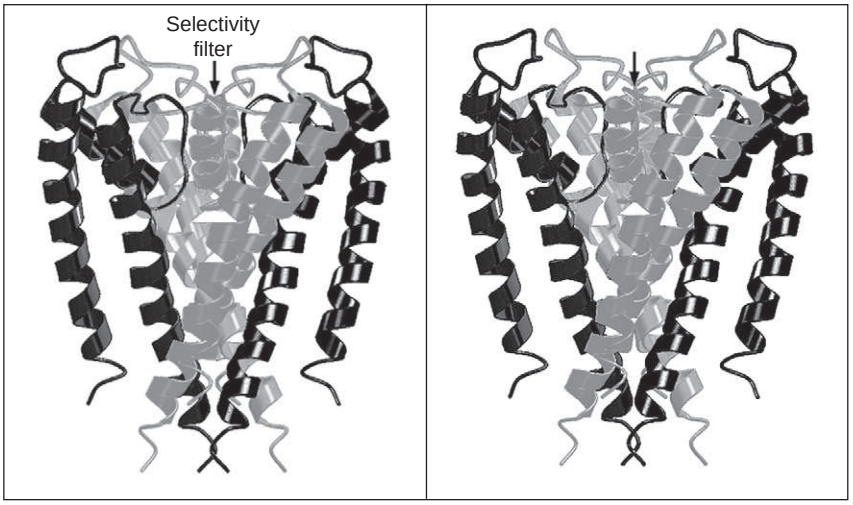
Selectivity
filter

C

1.11 Porins consist of β-sheet structures

As already mentioned, the outer membranes of chloroplasts and mitochondria appear to be unspecifically permeable to metabolites such as, for instance, nucleotides and sugar phosphates. This relatively unspecific permeability is due to pore-forming proteins named **porins**. These porins represent a family of proteins which are entirely different from the channel and translocator proteins.

The size of the aperture of the pore formed by a porin can be determined by incorporating porins into an artificial lipid membrane that separates two chambers filled with an electrolyte (Fig. 1.30). Membrane proteins, which have been solubilized in a detergent, are added to one of the two chambers. Because of their hydrophobicity, the porin molecules incorporate, one after another, into the artificial lipid membrane. Each time a new channel is formed, a stepwise increase of conductivity is observed. Each step in conductivity corresponds to the conductivity of a single pore. Therefore it is possible to evaluate the size of the aperture of the pore from the conductivity of the electrolyte fluid. Thus the size of the aperture for the porin pore of mitochondria has been estimated to be 1.7 nm and that of chloroplasts about 3 nm.

Porins have been first identified in the outer membrane of Gram negative bacteria, such as *Escherichia coli*. In the meantime, several types of porins, differing in their properties, have been characterized. **General porins** form unspecific diffusion pores, consisting of a channel containing water, allowing the diffusion of substrate molecules. These porins consist of subunits with a

Figure 1.29 Structural model of the K^+ channel from *Streptomyces lividans*. A. Schematic presentation of the amino acid sequence of a channel protein monomer. The protein forms two transmembrane helices that are connected by a loop. There is another helix within this loop, which, however, does not protrude through the membrane. B. Stereo pair of a view of the K^+ channel from the extracellular side of the membrane. The channel is formed by four subunits (marked black and red alternately), from which one transmembrane helix lines the channel (inner helix). The ball symbolizes a K^+ ion. C. Stereo pair of a side view of the K^+ ion channel. The eight transmembrane helices form a spherical channel, which is connected to the wide opening by a selection filter. Results of X-ray structure analysis by Doyle et al. (1998) with kind permission. How to look properly at a stereo picture: sit at a window and look into the distance. Push the picture quickly in front of your eyes without changing the focus. At first you will see three pictures unclearly. Focus your eyes so that the middle picture is the same size as those at either side of it. Now focus sharply on the middle picture. Suddenly you will see a very plastic picture of the spherical arrangement of the molecules.

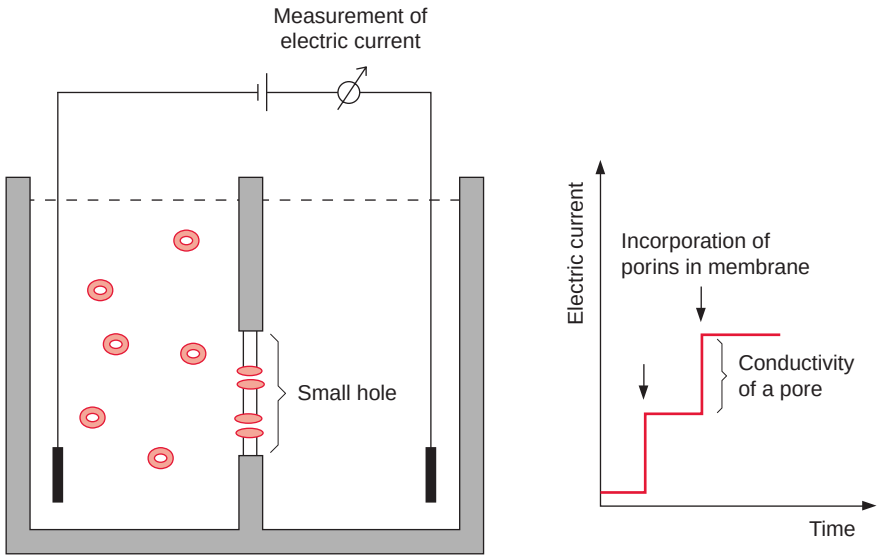

Figure 1.30 Measurement of the size of a porin aperture. Two chambers, each provided with an electrode and filled with electrolyte fluid, are separated from each other by a divider containing a small hole. A small drop containing membrane lipids is brushed across this hole. The solvent is taken up into the aqueous phase and the remaining lipid forms a double layer, an artificial membrane. Upon the addition of a porin, which has been isolated from a membrane, spontaneous incorporation of the single porin molecule into the artificial membrane occurs. The aqueous channel through the lipid membrane is formed. With each incorporation of a porin protein into the artificial membrane a stepwise increase of conductivity, measurable as electric current, occurs.

molecular mass of about 30 kDa. Porins in the membrane often occur as **trimers**, in which each of the three subunits forms a pore. Porins differ distinctly from the translocator proteins in that they have no exclusively hydrophobic regions in their amino acid sequence, a requirement for forming transmembrane helices. Analysis of the three-dimensional structure of a bacterial porin by X-ray structure analysis (section 3.3) revealed that the walls of the pore are formed by **β-sheet** structures (Fig. 1.31). Altogether, 16 β-sheets, each consisting of about 13 amino acids, connected to each other by hydrogen bonds, form a pore (Fig. 1.32A). This structure resembles a **barrel** in which the β-sheets represent the barrel staves. Hydrophilic and hydrophobic amino acids alternate in the amino acid sequences of the β-sheets. One side of the β-sheet, occupied by hydrophobic residues, is directed towards the lipid membrane phase. The other side, with the hydrophilic residues, is directed towards the aqueous phase inside the pore (Fig. 1.32B). Compared with the ion channel proteins, the porins have an economical structure in the

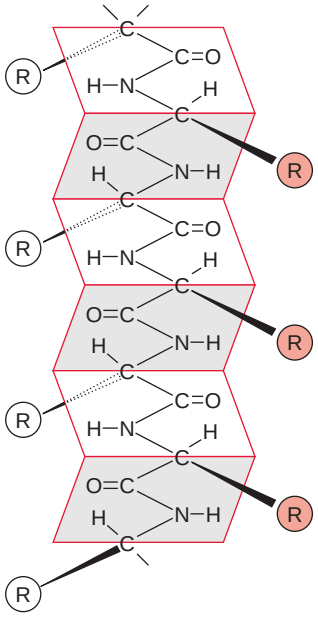

Figure 1.31 In a β-sheet conformation the amino acid residues of a peptide chain are arranged alternately in front and behind the surface of the sheet.

sense that a much larger channel is formed by one porin molecule than by a channel protein that has a two times higher molecular mass.

Another type of porin forms **selective pores**, which contain binding sites for ionic and non-ionic substrates (e.g., carbohydrates). In *E. coli* a maltodextrin-binding porin was found to consist of 16 β-sheets, with loops in between, which protrude into the aqueous channel of the pore and contain the corresponding substrate binding sites.

The **mitochondrial porin** resembles in its structure the bacterial general porin. It also consists of 16 β-sheets. The measurement of porin activity in artificial lipid bilayer membranes (Fig. 1.30) revealed that the open pore had slight anion selectivity. Applying a voltage of 30 mV closes the pore to a large extent and renders it cation specific. For this reason the mitochondrial porin has been named voltage-dependent anion selective channel (**VDAC**). The physiological function of this voltage-dependent regulation of the pore opening remains to be elucidated.

In **chloroplasts** the outer envelope membrane was found to contain a porin with a molecular mass of 24 kDa (outer envelope protein, **OEP24**), forming an unspecific diffusion pore. OEP24 resembles in its function the mitochondrial VDAC, although there is no sequence homology between them. OEP24, in its open state, allows the diffusion of various metabolites.

Moreover, the outer envelope membrane of chloroplasts contains another porin (**OEP21**) forming an **anion selective channel**. OEP21 especially enables the diffusion of phosphorylated metabolites such as

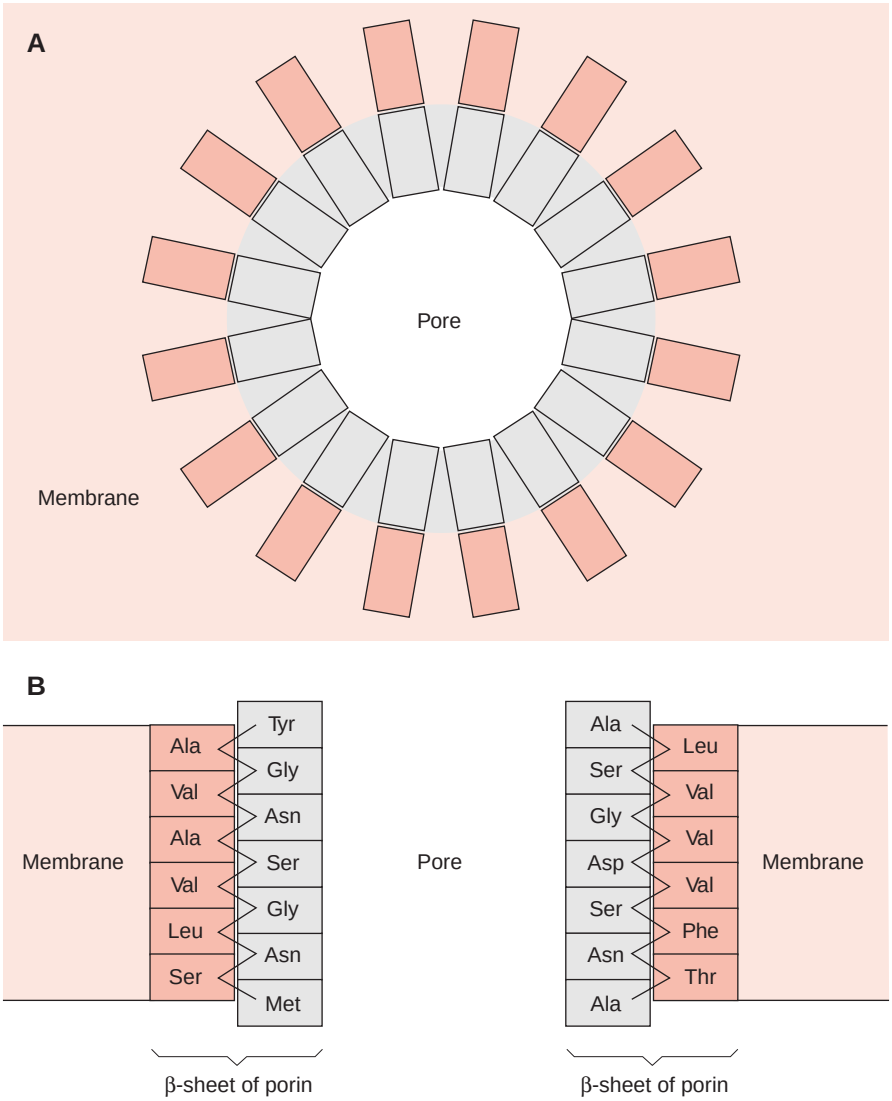

Figure 1.32 Schematic presentation of the structure of a membrane pore formed by a porin. A. View from above. B. Cross-section through the membrane. Sixteen β-sheets of the porin molecules, each 13 amino acids long, form the pore. The amino acid residues directed towards the membrane side of the pore have hydrophobic character; those directed to the aqueous pore are hydrophilic. The amino acid sequence of the porin shown in the cross-section is from a porin of maize amyloplasts. (Data by Fischer et al., 1994.)

dihydroxyacetone phosphate and 3-phosphoglycerate. The opening of this pore is regulated by the binding of substrates. Another pore forming protein is located in the membrane of peroxisomes (section 7.4).

Further reading

Block, M. A., Douce, R., Joyard, J., Rolland, N. Chloroplast envelope membranes: A dynamic interface between plastids and the cytosol. Photosynthesis Research 92, 225–244 (2007).

Choi, D., Lee, Yi., Cho, H.-T., Kende, H. Regulation of expansin gene expression affects growth and development in transgenic rice plants. The Plant Cell 15386–1398 (2003).

Doyle, D. A., Cabrai, J. M., Pfuetzner, R. A., Kuo, A., Gulbis, J. M., Cohen, S. L., Chait, B. T., Mackinnon, R. The structure of the potassium channel: Molecular basis of K^+ conduction and selectivity. Science 280, 69–77 (1998).

Dutzler, R., Campbell, E. B., Cadene, M., Chait, B. T., MacKinnon, R. X-ray structure of a CIC chloride channel at 3.0 Å reveals the molecular basis of anion selectivity. Nature 415, 287–294 (2002).

Gabaldón, T., Snel, B., van Zimmeren, F., Hemrika, W., Tabak, H., Huynen, M. A. Origin and evolution of the peroxisomal proteome. Biology Direct 1, 8–28 (2006).

Hanton, S. L., Matheson, L. A., Brandizzi, F. Seeking a way out: Export of proteins from the plant endoplasmatic reticulum. Trends in Plant Science 11, 335–343 (2006).

Herman, E., Schmidt, M. Endoplasmatic reticulum to vacuole trafficking of endoplasmic reticulum bodies provides an alternative pathway for protein transfer to the vacuole. Plant Physiology 136, 3440–3446 (2004).

Horie, T., Schroeder, J. I. Sodium transporters in plants. Diverse genes and physiological functions. Plant Physiology 136, 2457–2462 (2004).

Kaldenhoff, R., Bertl, A., Otto, B., Moshelion, M., Uehlein, N. Characterization of plant aquaporins. Methods Enzymology 428, 505–531 (2007).

Kuo, A., Gulbis, J. M., Antcliff, J. F., Rahman, T., Lowe, E. D., Zimmer, J., Cuthbertson, J., Ashcroft, F. M., Ezaki, T., Doyle, D. A. Crystal structure of the potassium channel KirBac1.1 in the closed state. Science 300, 1922–1926 (2003).

López-Juez, E. Plastid biogenesis, between light and shadows. Journal Experimental Botany 58, 11–26 (2007).

Lucas, W. J., Lee, J.-Y. Plasmodesmata as a supracellular control network in plants. Nature reviews. Molecular Cell Biology 5, 712–726 (2004).

Lunn, J. E. Compartmentation in plant metabolism. Journal Experimental Botany 58, 35–47 (2007).

Maple, J., Moeller, S. G. An emerging picture of plastid division in higher plants. Planta 223, 1–4 (2005).

Martinez-Ballesta, M. C., Silva, C., Lopez-Berenguer, C., Cabanero, F. J., Carvajal, M. Plant aquaporins: New perspectives on water and nutrient uptake in saline environment. Plant Biology 8, 535–546 (2006).

Mullen, R. T., Trelease, R. N. The ER-peroxisome connection in plants: Development of the "ER semiautonomous peroxisome maturation and replication" model for plant peroxisome biogenesis. Biochimica Biophysica Acta 1763, 1655–1668 (2006).

Pebay-Peyroula, E., Dahout-Gonzalez, C., Kahn, R., Trezeguet, V., Lauquin, G. J.-M., Brandolin, G. Structure of mitochondrial ATP/ADP carrier in complex with atractyloside. Nature 426, 39–44 (2003).

Picault, N., Hodges, M., Palmieri, L., Palmieri, F. The growing family of mitochondrial carriers in *Arabidopsis*. Trends in Plant Science 9, 138–146 (2004).

Robinson, D. G. (Ed.). The Golgi apparatus and the plant secretory pathway. Oxford UK: Blackwell. (2003)

Robinson, D. G., Herranz, M.-C., Bubeck, J., Pepperkok, R., Ritzenthaler, C. Membrane dynamics in the early secretory pathway. Critical Reviews in Plant Science 26, 199–225 (2007).

Schlueter, A., Fourcade, S., Ripp, R., Mandel, J. L., Poch, O., Pujol, A. The evolutionary origin of peroxisomes: An ER-peroxisome connection. Molecular Biology Evolution 23, 838–845 (2006).

Somerville, C., et al. Toward a systems approach to understanding plant cell walls. Science 306, 2206–2211 (2004).

Toernroth- Horsefield, S., et al. Structural mechanisms of plant aquaporin gating. Nature 439, 688–694 (2006).

Visser, W. F., Roermund, C. W. T., Ijlst, L., Waterham, H. R., Wanders, J. A. Metabolite transport across the peroxisomal membrane. Biochemical Journal 401, 365–375 (2007).

Weber, A. P. M., Schwacke, R., Fluegge, U.-I. Solute transporters of the plastid envelope membrane. Annual Reviews Plant Biology 56, 133–164 (2005).

Weber, A. P. M., Fischer, K. Making the connections—the crucial role of metabolite transporters at the interface between chloroplast and cytosol. FEBS Letters 581, 2215–2222 (2007).

Winter, H., Robinson, D. G., Heldt, H. W. Subcellular volumes and metabolite concentrations in spinach leaves. Planta 193, 530–535 (1994).

2

The use of energy from sunlight by photosynthesis is the basis of life on earth

Plants and cyanobacteria capture the light of the sun and utilize its energy to synthesize organic compounds from inorganic substances such as CO_2, nitrate, and sulfate to synthesize their cellular material; they are photoautotrophic. In photosynthesis photon energy splits water into oxygen and hydrogen, the latter bound as NADPH. This process, termed the *light reaction*, takes place in the photosynthetic reaction centers embedded in membranes. It involves the transport of electrons, which is coupled to the synthesis of ATP. NADPH and ATP are consumed in a so-called dark reaction to synthesize carbohydrates from CO_2 (Fig. 2.1). The photosynthesis of plants and cyanobacteria created the biomass on earth, including the deposits of fossil fuels and atmospheric oxygen. Animals are dependent on the supply of carbohydrates and other organic compounds as food; they are heterotrophic. They generate the energy required for their life processes by oxidizing the biomass, which has first been produced by plants. When oxygen is consumed, CO_2 is formed. Thus light energy captured by plants is the source of energy for the life processes of animals.

2.1 How did photosynthesis start?

Measurements of the distribution of radioisotopes led to the conclusion that the earth was formed about 4.6 billion years ago. The earliest indicators of life on earth are fossils of bacteria-like structures, estimated to be 3.5 billion years old. There was no oxygen in the atmosphere when life on

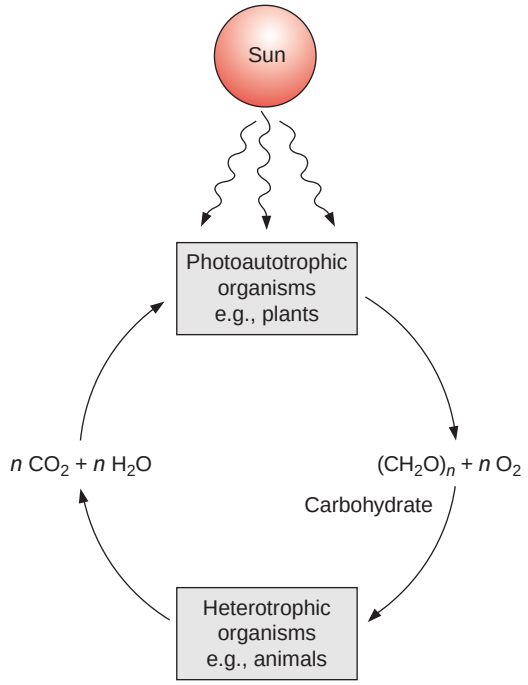

Figure 2.1 Life on earth involves a CO_2 cycle.

earth commenced. This is concluded from the fact that in very early sediment rocks iron is present as Fe^{2+}. Mineral iron is oxidized to Fe^{3+} in the presence of oxygen. According to our present knowledge, the earth's atmosphere initially contained components such as carbon dioxide, molecular hydrogen, methane, ammonia, prussic acid, and water.

In 1922 the Russian scientist Alexander Oparin presented the interesting hypothesis that organic compounds were formed spontaneously in the early atmosphere by the input of energy (e.g., in the form of ultraviolet radiation (there was no protective ozone layer), electrical discharges (lightning), or volcanic heat). It was further postulated that these organic compounds accumulated in ancient seas and became the constituents of early forms of life. In 1953 the American scientists Stanley Miller and Harold Urey substantiated this hypothesis by simulating the postulated **prebiotic synthesis** of organic substances. They exposed a gaseous mixture of components present in the early atmosphere, consisting of H_2O, CH_4, NH_3 and H_2 to electrical discharges for about a week at 80°C. Amino acids (such as glycine and alanine) and other carboxylic acids (such as formic, acetic, lactic, and succinic acid) were found in the condensate of this experiment. Other investigators added substances such as CO_2, HCN, and formaldehyde to the gaseous mixture, and these experiments showed that many components

of living cells (e.g., carbohydrates, fatty acids, tetrapyrroles, and the nucleobases adenine, guanine, cytosine, and uracil) were formed spontaneously by exposing a postulated early atmosphere to electric or thermal energy.

It is assumed that the organic substances formed by the abiotic processes accumulated in the ancient seas, lakes, and pools over a long period of time prior to the emergence of life on earth. There was no oxygen to oxidize the compounds that had accumulated and no bacteria or other organisms to degrade them. Alexander Oparin speculated that a **"primordial" soup** was formed in this way, providing the building material for the origin of life. Since oxygen was not yet present, the first organisms must have been **anaerobes**.

It is widely assumed now that early organisms on this planet generated the energy for their subsistence by **chemolithotrophic metabolism**, for example, by the reaction:

$$FeS + H_2S \rightarrow FeS_2 + H_2 \quad (\Delta G^{\circ\prime} = -42\ \text{kJ/mol})$$

It seems likely that already at a very early stage of evolution the catalysis of this reaction was coupled to the generation of a proton motive force (section 4.1) across the cellular membrane, yielding the energy for the synthesis of ATP by a primitive ATP synthase (section 4.3). **Archaebacteria**, which are able to live anaerobically under extreme environmental conditions (e.g., near hot springs in the deep sea), and which are regarded as the closest relatives of the earliest organisms on earth, are able to produce ATP via the preceding reaction. It was probably a breakthrough for the propagation of life on earth when organisms evolved that were able to utilize the energy of the sun as a source for biomolecule synthesis, which occurred at a very early stage in evolution. The now widely distributed **purple bacteria** and **green sulfur bacteria** may be regarded as relics from an early period in the evolution of photosynthesis.

Prior to the description of photosynthesis in Chapter 3, the present chapter will discuss how plants capture sunlight and how the light energy is conducted into the photosynthesis apparatus.

2.2 Pigments capture energy from sunlight

The energy content of light depends on its wavelength

In Berlin at the beginning of the twentieth century Max Planck and Albert Einstein, two Nobel Prize winners, carried out the epoch-making studies proving

that light has a dual nature. It can be regarded as an electromagnetic wave as well as an emission of particles, which are termed **light quanta** or **photons**.

The energy of the photon is proportional to its frequency v:

$$E = h \cdot v = h \cdot \frac{c}{\lambda} \tag{2.1}$$

where h is the Planck constant ($6.6 \cdot 10^{-34}\,\mathrm{J\,s}$) and c the velocity of the light ($3 \cdot 10^{8}\,\mathrm{m\,s^{-1}}$). λ is the wavelength of light.

The mole (abbreviated to mol) is used as a chemical measure for the amount of molecules and the amount of photons corresponding to $6 \cdot 10^{23}$ molecules or photons (Avogadro number N_A). The energy of one mol photons amounts to:

$$E = h \cdot \frac{c}{\lambda} \cdot N_A \tag{2.2}$$

In order to utilize the energy of a photon in a thermodynamic sense, this energy must be at least as high as the Gibbs free energy of the photochemical reaction involved. (In fact much energy is lost during energy conversion (section 3.4), with the consequence that the energy of the photon must be higher than the Gibbs free energy of the corresponding reaction.) We can equate the Gibbs free energy ΔG with the energy of the absorbed light:

$$\Delta G = E = h \cdot \frac{c}{\lambda} \cdot N_A \tag{2.3}$$

The introduction of numerical values of the constants h, c, and N_A yields:

$$\Delta G = 6.6 \cdot 10^{-34} \cdot (\mathrm{J \cdot s}) \cdot \frac{3 \cdot 10^{8}(\mathrm{m})}{(\mathrm{s})} \cdot \frac{1}{\lambda(\mathrm{m})} \cdot \frac{6 \cdot 10^{23}}{(\mathrm{mol})} \tag{2.4}$$

$$\Delta G = \frac{119000}{\lambda\,(\mathrm{nm})} \quad \left[\mathrm{kJ/mol\,photons}\right] \tag{2.5}$$

It is often useful to state the electrical potential (ΔE) of the irradiation instead of energy when comparing photosynthetic reactions with redox reactions, which will be discussed in Chapter 3:

$$\Delta E = -\frac{\Delta G}{F} \tag{2.6}$$

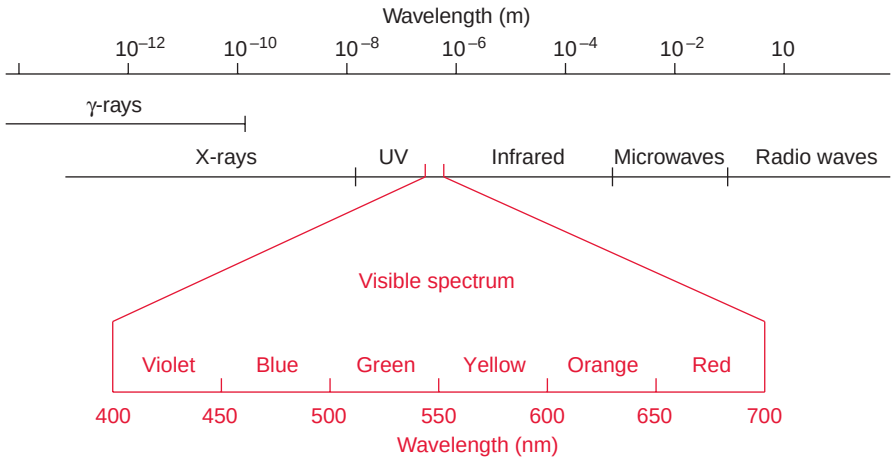

Figure 2.2 Spectrum of the electromagnetic radiation. The enlargement in red illustrates the visible spectrum.

where F = number of charges per mol = 96,485 Amp·s·mol^{-1}. The introduction of this value yields:

$$\Delta E = -\frac{N_A \cdot h \cdot c}{F \cdot \lambda(\text{nm})} = \frac{1231}{\lambda(\text{nm})} \quad [\text{Volt}] \tag{2.7}$$

The human eye perceives only the small range between about 400 and 700 nm of the broad spectrum of electromagnetic waves (Fig. 2.2). The light in this range, where the intensity of solar radiation is especially high, is utilized in plant photosynthesis. Bacterial photosynthesis, however, is able to utilize light in the infrared range.

According to equation 2.3 the energy of irradiated light is inversely proportional to the wavelength. Table 2.1 shows the light energy per mol photons for light of different colors. Consequently, violet light has an energy of about 300 kJ/mol photons. Dark blue light, with the highest wavelength (700 nm) that can still be utilized by plant photosynthesis, contains 170 kJ/mol photons. This is only about half the energy content of violet light.

Chlorophyll is the main photosynthetic pigment

In photosynthesis of a green plant, light is collected primarily by **chlorophylls**, pigments that absorb light at a wavelength below 480 nm and between 550 and 700 nm (Fig. 2.3). When white sunlight falls on a chlorophyll layer, the green light with a wavelength between 480 and 550 nm is not absorbed, but is reflected. This is why plant chlorophylls and whole leaves appear green.

Experiments carried out between 1905 and 1913 in Zurich and Berlin by Richard Willstätter and his collaborators led to the discovery of the

Table 2.1: The energy content and the electrochemical potential difference of photons of different wavelengths

Wavelengths (nm)	Light color	Energy content kJ/mol photons	ΔE e volt
700	Red	170	1.76
650	Bright red	183	1.90
600	Yellow	199	2.06
500	Blue green	238	2.47
440	Blue	271	2.80
400	Violet	298	3.09

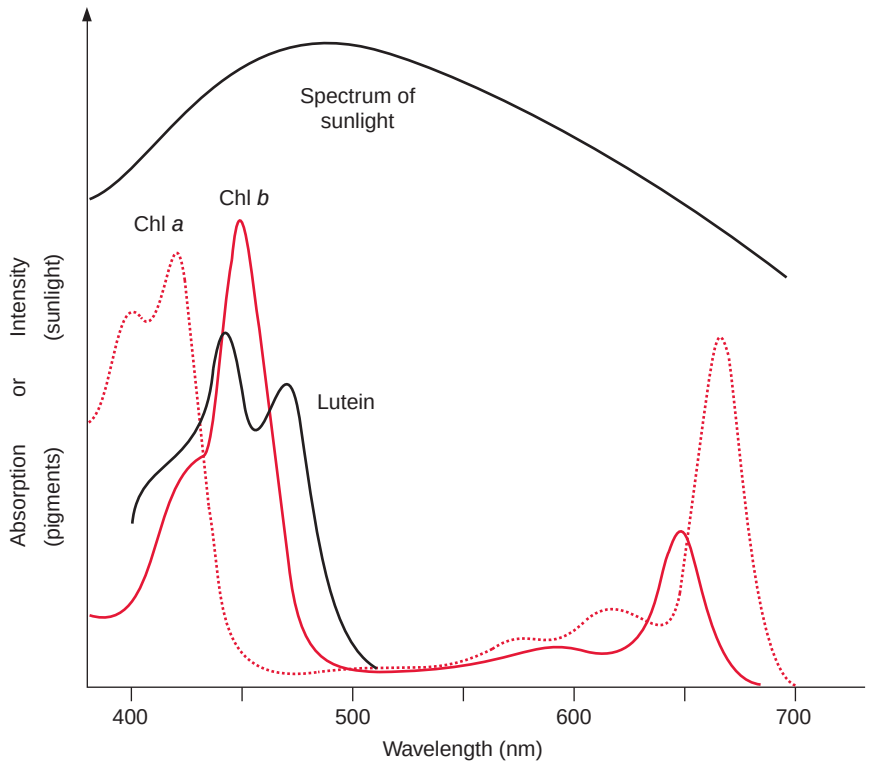

Figure 2.3 Absorption spectrum of chlorophyll-*a* (chl-*a*), chlorophyll-*b* (chl-*b*) and of the xanthophyll lutein dissolved in acetone. The intensity of the sun's radiation at different wavelengths is given as a comparison.

structural formula of the green leaf pigment chlorophyll, a milestone in the history of chemistry. This discovery made such an impact that Richard Willstätter was awarded the Nobel Prize in Chemistry as early as 1915. There are different classes of chlorophylls. Figure 2.4 shows the structural

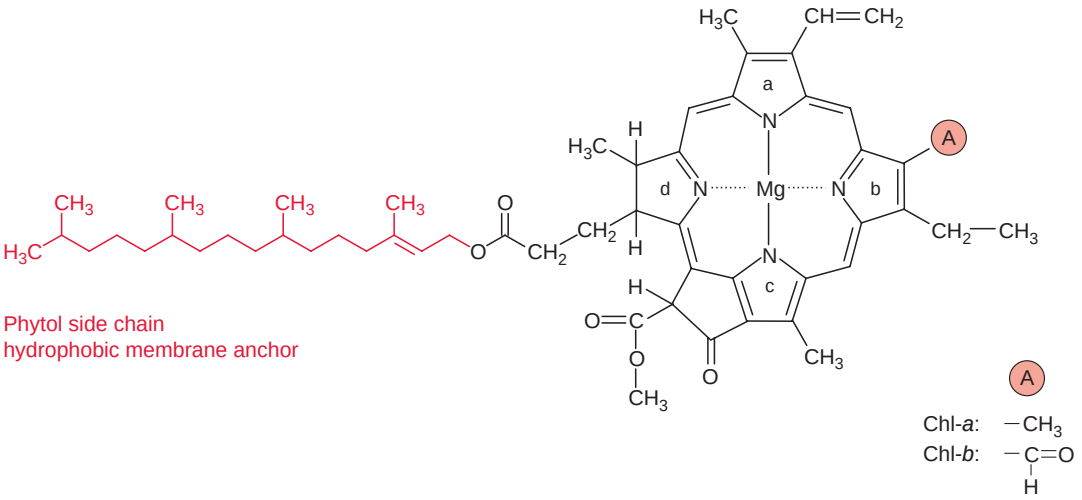

Figure 2.4 Structural formula of chlorophyll-*a*. In chlorophyll-*b* the methyl group in ring b is replaced by a formyl group (A). The phytol side chain in red gives chlorophyll a lipid character.

formulas of chlorophyll-*a* and chlorophyll-*b* (**chl-*a***, **chl-*b***). The basic structure is a ring made of four pyrroles, a **tetrapyrrole**, which is also named **porphyrin**. **Mg^{++}** is present in the center of the ring as the central atom. Mg^{++} is covalently bound with two N atoms and coordinately bound to the other two atoms of the tetrapyrrole ring. A cyclopentanone is attached to ring c. At ring d a propionic acid group forms an ester with the alcohol **phytol**. Phytol consists of a long branched hydrocarbon chain with one C-C double bond. It is derived from an isoprenoid, formed from four isoprene units (section 17.7). This long hydrophobic hydrocarbon tail renders the chlorophyll highly soluble in lipids and therefore promotes its presence in the membrane phase. Chlorophyll always occurs bound to proteins. Chl-*b* contains a formyl residue in ring b instead of the methyl residue as in chl-*a*. This small difference has a large influence on light absorption. Figure 2.3 shows that the absorption spectra of chl-*a* and chl-*b* differ markedly.

In plants, the ratio chl-*a* to chl-*b* is about three to one. Only chl-*a* is a constituent of the photosynthetic reaction centers (sections 3.6 and 3.8) and therefore it can be regarded as the central photosynthesis pigment. In a wide range of the visible spectrum, however, chl-*a* does not absorb light (Fig. 2.3). This non-absorbing region is named the "**green window**." The absorption gap is narrowed by the light absorption of chl-*b*, with its first maximum at a higher wavelength than chl-*a* and the second maximum at a lower wavelength. As shown in section 2.4, the light energy absorbed by chl-*b* can be transferred very efficiently to chl-*a*. In this way, chl-*b* enhances the plant's efficiency for utilizing sunlight energy.

The structure of chlorophylls has remained remarkably constant during the course of evolution. Purple bacteria, probably formed more than 3 billion

years ago, contain as photosynthetic pigment a bacteriochlorophyll-*a*, which differs from the chl-*a* shown in Fig. 2.4 only by the alteration of one side chain and by the lack of one double bond. This, however, influences light absorption; both absorption maxima are shifted outwards and the non-absorbing spectral region in the middle is broadened. This shift allows purple bacteria to utilize light in the infrared region.

The tetrapyrrole ring not only is a constituent of chlorophyll but also has attained a variety of other functions during evolution. It is involved in methane formation by bacteria with Ni^{++} as the central atom. With Co^{++} it forms **cobalamin** (vitamin B_{12}), which participates as a cofactor in reactions in which hydrogen and organic groups change their position. With Fe^{++} instead of Mg^{++} as the central atom, the tetrapyrrole ring forms the basic structure of **hemes** (Fig. 3.24), which as cytochromes function as redox carriers in electron transport processes (sections 3.7 and 5.5) and as myoglobin or hemoglobin stores or transports oxygen in aerobic organisms. The tetrapyrrole ring in animal hemoglobin differs only slightly from the tetrapyrrole ring of chl-*a* (Fig. 2.4).

It seems remarkable that a substance that attained a certain function during evolution is being utilized after only minor changes for completely different functions. The reason for this functional variability is that the reactivity of compounds such as chlorophyll or heme is governed to a great extent by the proteins to which they are bound.

Chlorophyll molecules are bound to chlorophyll-binding proteins. In a complex with proteins the absorption spectrum of the bound chlorophyll differs considerably from the absorption spectrum of the free chlorophyll. The same applies for other light-absorbing compounds, such as carotenoids, xanthophylls, and phycobilins, which also occur bound to proteins. These complexes will be discussed in the following sections. For better discrimination in this text book, free absorbing compounds are called **chromophore** (Greek, carrier of color) and the chromophore-protein complexes are called **pigments**. Pigments are further characterized by the wavelength of their absorption maximum. Chlorophyll-a_{700} describes a pigment of protein-chl-*a* complex with an absorption maximum of 700 nm. Another common designation is P_{700}; this nomination leaves the nature of the chromophore open.

2.3 Light absorption excites the chlorophyll molecule

What happens when a chromophore absorbs a photon? When a photon with a certain wavelength hits a chromophore molecule that absorbs light

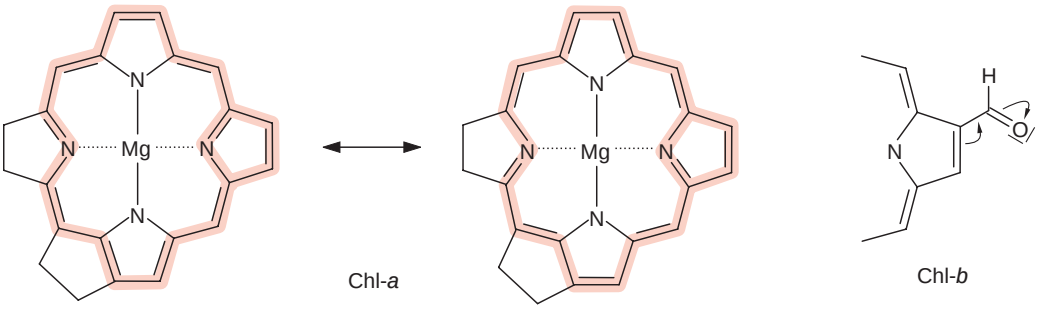

Figure 2.5 Resonance structures of chlorophyll-*a*. In the region marked red, the double bonds are not localized; the π electrons are distributed over the entire conjugated system. The formyl residue of chlorophyll-*b* attracts electrons and thus affects the π electrons of the conjugated system.

of this wavelength, the energy of the photon excites electrons and transfers them to a higher energy level. This occurs as an "all or nothing" process. According to the principle of energy conservation expressed by the first law of thermodynamics, the energy of the chromophore is increased by the energy of the photon, which results in an **excited state** of the chromophore molecule. The energy is absorbed only in discrete quanta, resulting in discrete excitation states. The energy required to excite a chromophore molecule depends on the chromophore structure. A general property of chromophores is that they contain many **conjugated double bonds**, 10 in the case of the tetrapyrrole ring of chl-*a*. These double bonds are delocalized. Figure 2.5 shows two possible resonance forms.

After absorption of energy, an electron of the conjugated system is elevated to a higher orbit. This excitation state is termed **singlet**. Figure 2.6 shows a scheme of the excitation process. As a rule, the higher the number of double bonds in the conjugated system, the lower the amount of energy required to produce a first singlet state. For the excitation of chlorophyll, dark red light is sufficient, whereas butadiene, with only two conjugated double bonds, requires energy-rich ultraviolet light for excitation. The light absorption of the conjugated system of the tetrapyrrole ring is influenced by the side chains. Thus, the differences in the absorption maxima of chl-*a* and chl-*b* mentioned previously can be explained by an electron attracting effect of the carbonyl side chain in ring b of chl-*b* (Fig. 2.5).

The spectra of chl-*a* and chl-*b* (Fig. 2.3) each have two main absorption maxima, showing that each chlorophyll has two main excitation states. In addition, chlorophylls have minor absorption maxima, which for the sake of simplicity will not be discussed here. The two main excitation states of chlorophyll are known as the first and second singlet (Fig. 2.6). The absorption

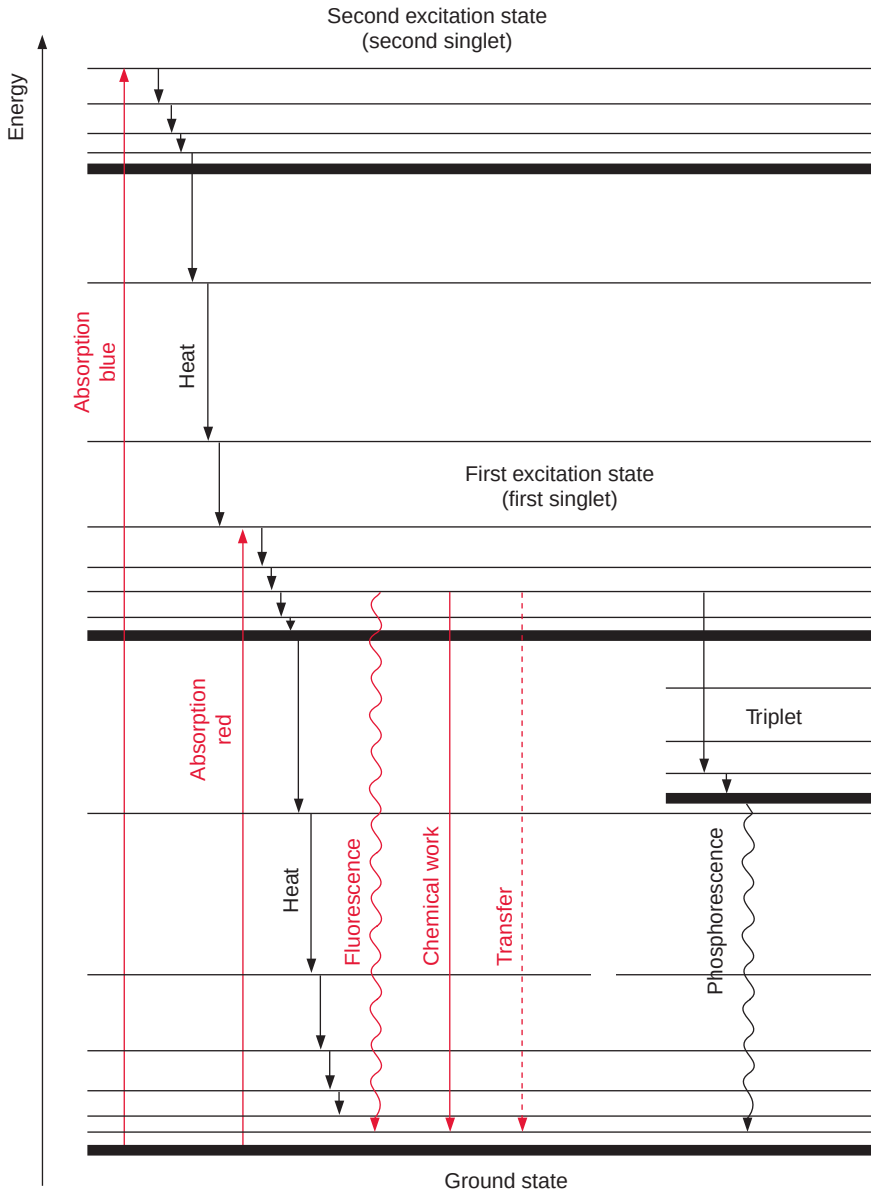

Figure 2.6 Schematic presentation of the excitation states of chlorophyll-*a* and their return to the ground state. The released excitation energy is converted to photochemical work, fluorescent or phosphorescent light, or dissipated into heat. This simplified scheme shows only the excitation states of the two main absorbing maxima of the chlorophylls.

maxima in the spectra are relatively broad. At a higher resolution the spectra can be shown to consist of many separate absorption lines. This fine structure of the absorption spectra is due to chlorophyll molecules that are in the ground and in the singlet states as well in **rotation** and **vibration**. In the energy scheme the various rotation and vibration energy levels are drawn as fine lines and the corresponding ground states as solid lines (Fig. 2.6).

The energy levels of the various rotation and vibration states of the ground state overlap with the lowest energy levels of the **first singlet**. Analogously, the energy levels of the first and the second singlet also overlap. If a chlorophyll molecule absorbs light in the region of its absorption maximum (blue light), one of its electrons is elevated to the **second singlet** state. This second singlet state with a half-life of only 10^{12} s is too unstable to use its energy for chemical work. The excited molecules lose energy as heat by rotations and vibrations until the first singlet state is reached. This first singlet state can also be attained by absorption of a photon of red light, which contains less energy. The first singlet state is much more stable than the second one; its half-life time is $4 \cdot 10^9$ s.

The return of the chlorophyll molecule from the first singlet state to the ground state can proceed in different ways:

1. The most important path for the conversion of the energy released upon the return of the first singlet state to the ground state is its utilization for **chemical work**. The chlorophyll molecule transfers the excited electron from the first singlet state to an electron acceptor and a positively charged chlorophyll radical $chl^{+\bullet}$ remains. This is possible since the excited electron is bound less strongly to the chromophore molecule than in the ground state. Section 3.5 describes in detail how the electron can be transferred back from the acceptor to the $chl^{+\bullet}$ radical via an electron transport chain. When the chlorophyll molecule returns to the ground state, the free energy derived from this process is conserved for chemical work. As an alternative, the electron deficit in the $chl^{+\bullet}$ radical may be replenished by another electron donor (e.g., water (section 3.6)).
2. The excited chlorophyll can return to the ground state by releasing excitation energy as light; this emitted light is named **fluorescence**. Due to vibrations and rotations, part of the excitation energy is usually lost as heat, with the result that the fluorescence light has less energy (corresponding to a longer wavelength) than the energy of the excitation light, which was required for attaining the first singlet state (Fig. 2.7).

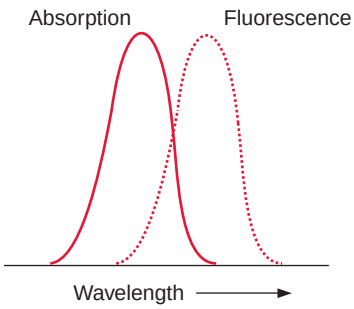

Figure 2.7 Fluorescent light has a longer wavelength than excitation light.

3. It is also possible that the return from the first singlet to the ground state proceeds in a stepwise fashion via the various levels of vibration and rotation energy, by which the energy difference is completely converted into heat.
4. By releasing part of the excitation energy as heat, the chlorophyll molecule can attain a lower energy excitation state, called the first **triplet state**. This triplet state cannot be reached directly from the ground state by excitation, since the spin of the excited electrons has been reversed. Since the probability of a reversal spin is low, the triplet state does not occur frequently. In the case of a very high excitation, however, some of the electrons of the chlorophyll molecules can reach this state. By emitting so-called **phosphorescent light**, the molecule can return from the triplet state to the ground state. Phosphorescent light is lower in energy than the light required to attain the first singlet state. The return from the triplet state to the ground state requires a reversal of the **electron spin**. As this is rather improbable, the triplet state, in comparison to the first singlet state, has a relatively long half-life time (10^{-4} to 10^{-2} s). The triplet state of the chlorophyll has no function in photosynthesis *per se*. In its triplet state, however, the chlorophyll can excite oxygen to a singlet state, whereby the oxygen becomes very reactive (reactive oxygen species, ROS, section 5.7) with a damaging effect on cell constituents. Section 3.10 describes how the plant manages to protect itself from the **harmful singlet oxygen**.
5. The return to the ground state can be coupled with the excitation of a neighboring chromophore molecule. This transfer is important for the function of the antennae and will be described in the following section.

2.4 An antenna is required to capture light

In order to excite a photosynthetic reaction center, a photon with defined energy content has to react with a chlorophyll molecule in the reaction center. The probability is very low that a photon not only has the proper energy, but also hits the pigment exactly at the site of the chlorophyll molecule. Therefore efficient photosynthesis is possible only when the energy of photons of various wavelengths is captured over a certain surface by a so-called **antenna** (Fig. 2.8). Similarly, radio and television sets could not work without an antenna.

The antennae of plants consist of a large number of protein-bound chlorophyll molecules that absorb photons and transfer their energy to the

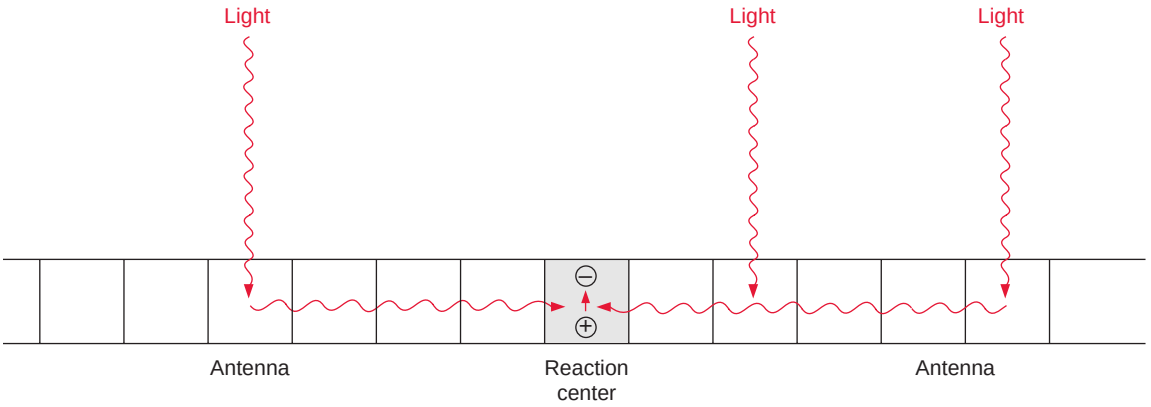

Figure 2.8 Photons are collected by an antenna and their energy is transferred to the reaction center. In this scheme the squares represent chlorophyll molecules. The excitons conducted to the reaction center cause a charge separation (section 3.4).

reaction center. Only a few thousandths of the chlorophyll molecules in the leaf are constituents of the actual reaction centers; the remainder are contained in the antennae. Observations made as early as 1932 by Robert Emerson and William Arnold in the United States indicated that the large majority of chlorophyll molecules are not part of the reaction centers. The two researchers illuminated a suspension of the green alga *Chlorella* with light pulses of 10 μs duration, interrupted by dark intervals of 20 ms. Evolution of oxygen was used as a measure for photosynthesis. The light pulses were made so short that chlorophyll could undergo only one photosynthetic excitation cycle and a high light intensity was chosen in order to achieve maximum oxygen evolution. Apparently the photosynthetic apparatus was thus saturated with photons. Analysis of the chlorophyll content of the algae suspension showed that under saturating conditions only one molecule of O_2 was formed per 2,400 chlorophyll molecules.

In the following years Robert Emerson refined these experiments and was able to show when pulses were applied at very low light intensity, the amount of oxygen formed increased proportionally with the light intensity. From this it was calculated that the release of one molecule of oxygen had a minimum quantum requirement of about **eight photons**. These results settled a long scientific dispute with Otto Warburg, who had concluded from his experiments that only four photons are required for the evolution of one molecule of O_2. Later it was recognized that each of the two reaction centers requires four photons for the formation of O_2. Moreover, the results of Emerson and Arnold allowed the calculation that about **300 chlorophyll molecules** are associated with one reaction center. These are constituents of the **antennae**.

The antennae contain additional accessory pigments to utilize those photons where the wavelength corresponds to the "**green window**" between the absorption maxima of the chlorophylls. In higher plants these pigments

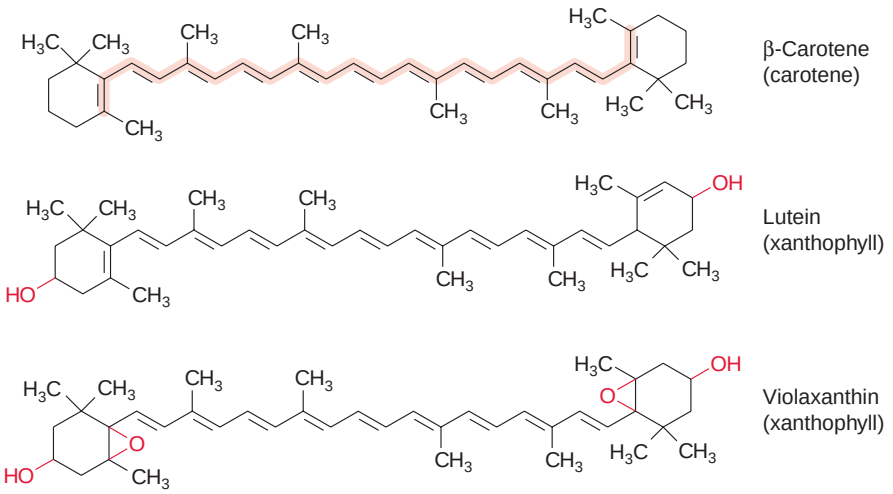

Figure 2.9 Structural formula of β-carotene and of two xanthophylls (lutein and violaxanthin). Due to the conjugated double bounds of the isoprenoid chain, these molecules absorb light and also have lipid character.

are carotenoids, mainly **xanthophylls**, including lutein and the related violaxanthin as well as **carotenes** such as β-carotene to name the major compound (Fig. 2.9). Moreover, an important function of these carotenoids in the antennae is to prevent the formation of the harmful triplet state of the chlorophylls (section 3.10). Important constituents of the antennae in cyanobacteria are **phycobilins**, which will be discussed at the end of this chapter.

How is the excitation energy of the photons captured in the antennae and transferred to the reaction centers?

The transfer of energy in the antennae via electron transport from chromophore to chromophore in a sequence of redox processes, as in the electron transport chains of photosynthesis or of mitochondrial respiration (Chapters 3 and 5), could be excluded, since such an electron transport would need considerable activation energy. This is not the case, since a flux of excitation energy can be measured in the antennae at temperatures as low as 1 K. At these low temperatures light absorption and fluorescence still occur, whereas chemical processes catalyzed by enzymes are completely inactive. Under these conditions the energy transfer in the antennae proceeds according to a mechanism that is related to those of light absorption and fluorescence.

When chromophores are positioned very close to each other, the quantum energy of an irradiated photon is transferred from one chromophore to the next. One quantum of light energy is named a **photon**, one quantum of excitation energy transferred from one molecule to the next is termed

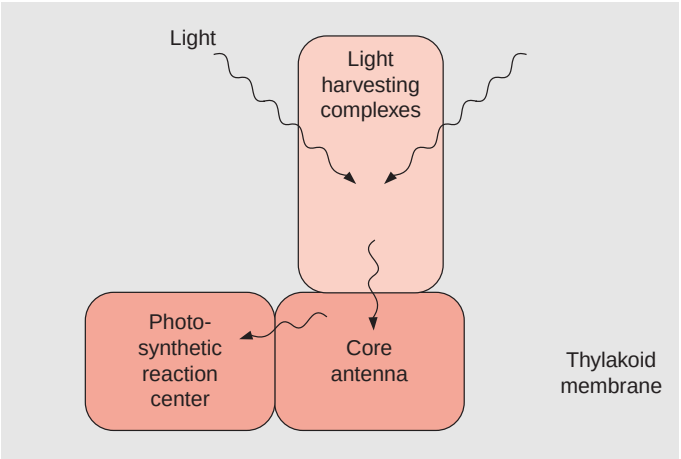

Figure 2.10 Schematic presentation of a higher plant antenna.

an **exciton**. A prerequisite for the transfer of excitons is a specific positioning of the chromophores. This is arranged by proteins, and therefore the chromophores of the antennae always occur as protein complexes.

The antennae of plants consist of an inner part and an outer part (Fig. 2.10). The outer antenna, formed by the **light harvesting complexes** (**LHC**s), collects the light. The inner antenna, consisting of the **core complexes**, is an integral constituent of the reaction centers; it also collects light and conducts the excitons that were collected in the outer antenna to the photosynthetic reaction centers.

The LHCs are composed of polypeptides, which bind chl-*a*, chl-*b*, xanthophylls, and carotenes. These proteins, termed **LHC polypeptides**, are encoded in the nucleus. A plant contains many different LHC polypeptides. In a tomato, for instance, at least 19 different genes for LHC polypeptides have been found, which are very similar to each other and are members of a multigene family. They are homologous, as they have all evolved from a common ancestor.

Plants contain two reaction centers, which are arranged in sequence: a reaction center of photosystem II (**PS II**), which has an absorption maximum at 680 nm, and a photosystem I (**PS I**) with an absorption maximum at 700 nm. The function of these reaction centers will be described in sections 3.6 and 3.8. Both photosystems are composed of different LHCs.

The function of an antenna is illustrated by the antenna of photosystem II

The antenna of the PS II reaction center contains primarily four LHCs termed LHC-II*a–d*. The main component is **LHC-II*b***; it represents 67% of

Table 2.2: Composition of the LHC-II*b*-monomer

Peptide:	232 amino acids
Lipids:	1 phosphatidylglycerol, 1 digalactosyldiacylglycerol
Chromophores:	8 chl-***a***, 6 chl-***b***, 2 lutein, 1 violaxanthin, 1 neoxanthin

the total chlorophyll of the PS II antenna and is the most abundant membrane protein of the thylakoid membrane, and has therefore been particularly thoroughly investigated. LHC-II*b* occurs in the membrane, most probably as a trimer. The monomer consists of a polypeptide to which four xanthophyll molecules are bound (Table 2.2). The polypeptide contains one threonine residue, which can be phosphorylated by ATP via a protein kinase. Phosphorylation regulates the activity of LHC-II (section 3.10).

There has been a breakthrough in establishing the three-dimensional structure of LHC-II*b* by electron cryomicroscopy at a temperature of 4 K of crystalline layers of LHC-II*b*-trimers (Fig. 2.11). The LHC-II*b*-peptide forms three transmembrane helices. The two lutein molecules span the membrane crosswise. The other two molecules are not visible in the isolated LHC complex. The chl-*b*-molecules, where the absorption maximum in the red spectral region lies at a shorter wavelength than that of chl-*a*, are positioned in the outer region of the complexes. Only one of the chl-*a*-molecules is positioned in the outer region; the others are all present in the center. Figure 2.12 shows a vertical projection of the arrangement of the monomers to form a trimer. The chl-*a* positioned in the outer region mediates the transfer of energy to the neighboring trimers or to the reaction center. The trimers are arranged in the membrane as oligomers forming the antenna for the conductance of the absorbed excitons. The chl-*a*/chl-*b* ratio is much higher in LHC-II*a* and LHC-II*c* than in LHC-II*b*. Most likely LHC-II*a* and LHC-II*c* are positioned between LHC-II*b* and the reaction center.

Figure 2.13 shows a hypothetical scheme of the array of the PS II antenna. The outer complexes, consisting of LHC-II*b*, are present at the periphery of the antenna. The excitons captured by chl-*b* in LHC-II*b* are transferred to chl-*a* in the center of the LHC-II*b* monomers and are then transferred further by chl-*a* contacts between the trimers to the inner antennae complexes. The inner complexes are connected by small chlorophyll containing subunits to the core complex. This consists of the antennae proteins CP 43 and CP 47, which are closely attached to the reaction center (Fig. 3.22), and each containing about 15 chl-*a* molecules. Since the absorption maximum of chl-*b* is at a lower wavelength than that of chl-*a*, the

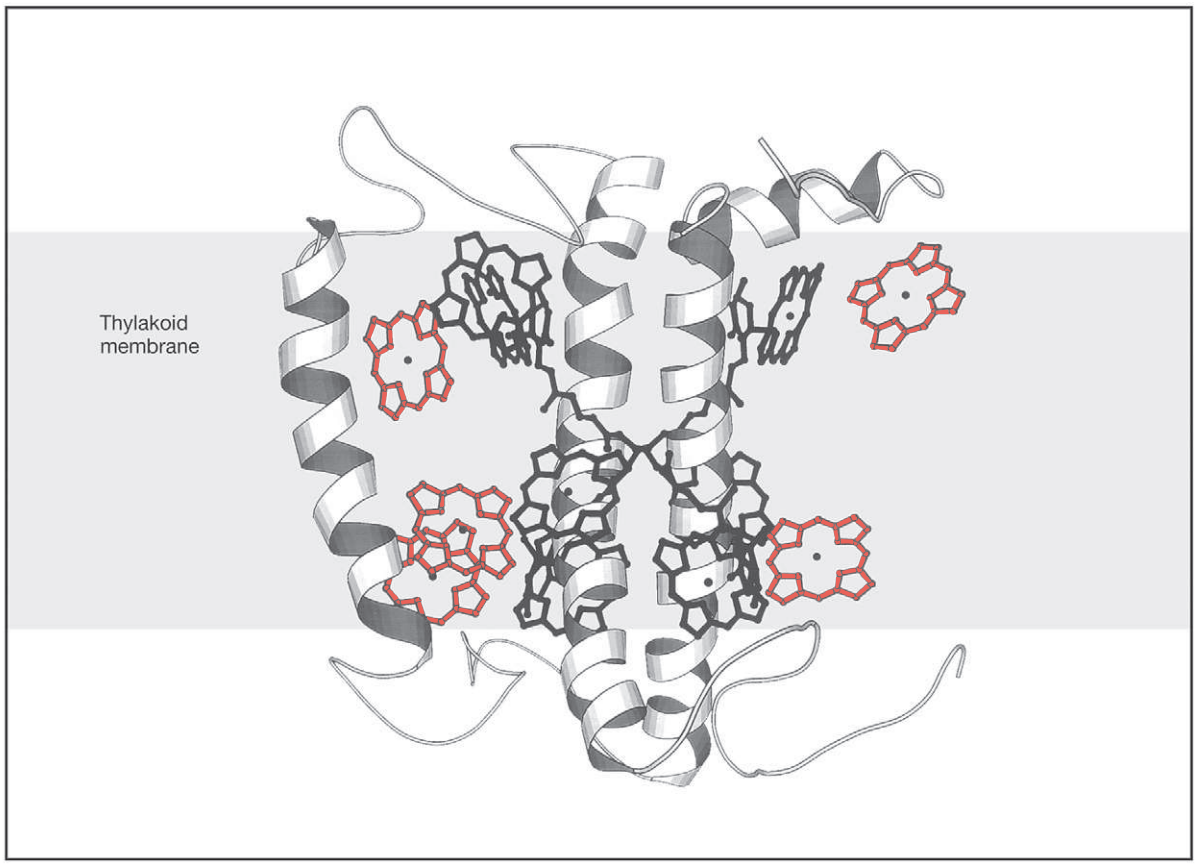

transfer of excitons from chl-*b* to chl-*a* is accompanied by loss of energy as heat. This promotes the flux of excitons from the periphery to the reaction center. The connection between the outer LHCs (LHC-II*b*) and the PS II can be interrupted by phosphorylation. In this way the actual size of the antenna can be adjusted to the intensity of illumination (section 3.10).

Photosystem I contains fewer LHCs than photosystem II (section 3.8) since its core antenna is larger than in PS II. The LHCs of PS I are similar to those of PS II. Sequence analysis shows that LHC-I and LHC-II stem from a common ancestor. It has been suggested that in the phosphorylated state LHC-II*b* can also function as an antenna of PS I (section 3.10).

There are two mechanisms for the movement of excitons. The excitons may be delocalized by distribution over the whole chromophore molecules. On the other hand, excitons may also initially be present in a certain chromophore molecule and subsequently transferred to a more distant chromophore. This process of exciton transfer has been termed the **Förster mechanism**. The transfer of excitons between closely neighboring chlorophyll

Figure 2.11 Sterical arrangement of the LHC-II*b* monomer in the thylakoid membrane, viewed from the side. Three α-helices of the protein span the membrane. Chlorophyll-*a* (black tetrapyrrole ring) and chlorophyll-*b* (red tetrapyrrol ring) are oriented almost perpendicularly to the membrane surface. Two lutein molecules (black carbon chain) in the center of the complex act as an internal cross brace. (By courtesy of W. Kühlbrandt, Heidelberg.)

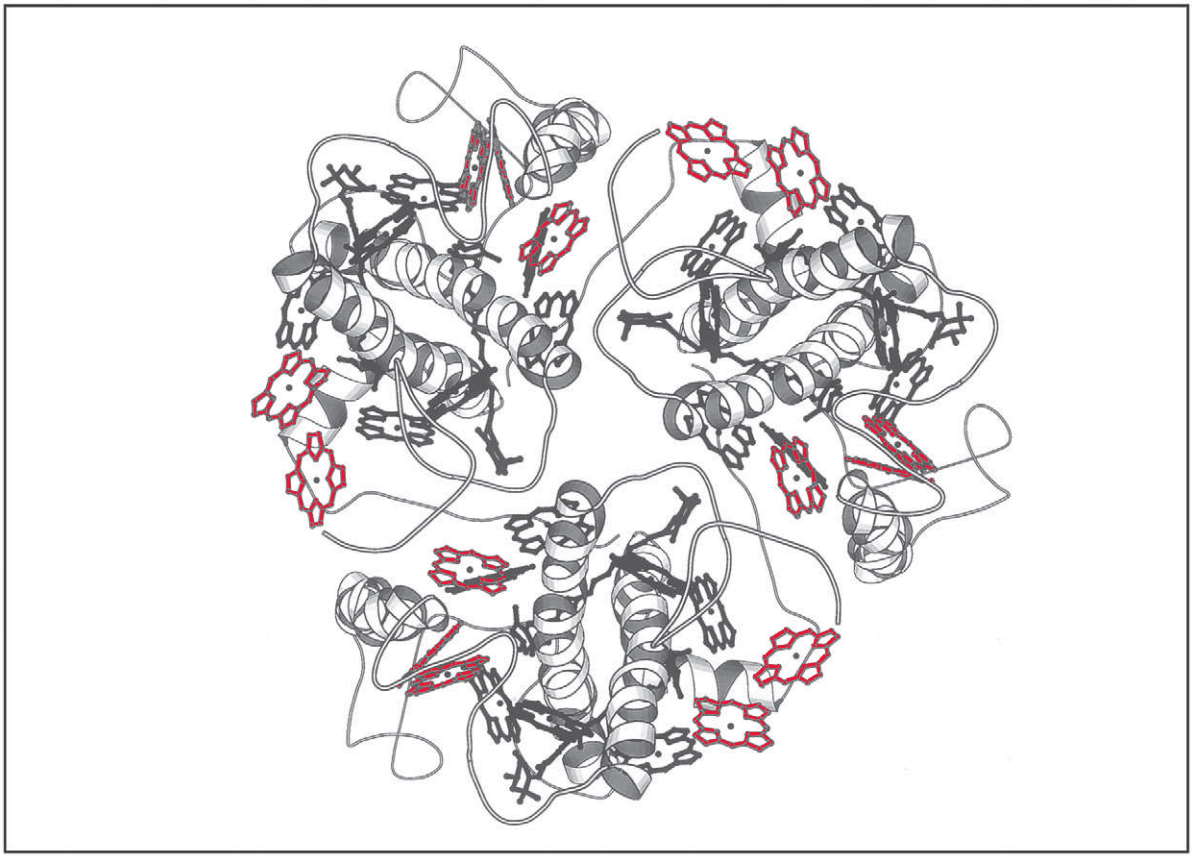

Figure 2.12 The LHC-II-trimer viewed from above from the stroma side. Within each monomer the central pair of helices forms a left-handed super coil, which is surrounded by chlorophyll molecules. The chl-*b* molecules (red) are positioned at the side of the monomers. (By courtesy of W. Kühlbrandt, Heidelberg.)

molecules within an LHC complex probably proceeds via **delocalized electrons**, and the transfer between the LHCs and the reaction center occurs via the Förster mechanism. Absorption measurements with ultrafast laser technique have shown that the exciton transfer between two chlorophyll molecules proceeds within 0.1 ps (10^{-13} s). Thus the velocity of the exciton transfer in the antennae is much faster than the charge separation in the reaction center (≈3.5 ps) (section 3.4). The reaction center functions as an **energy trap** for excitons present in the antenna.

Phycobilisomes enable cyanobacteria and red algae to carry out photosynthesis even in dim light

Cyanobacteria and red algae possess antennae structures that can collect light of very low intensity. These antennae are arranged as complexes on top of the membrane near the reaction centers of photosystem II (Fig. 2.14).

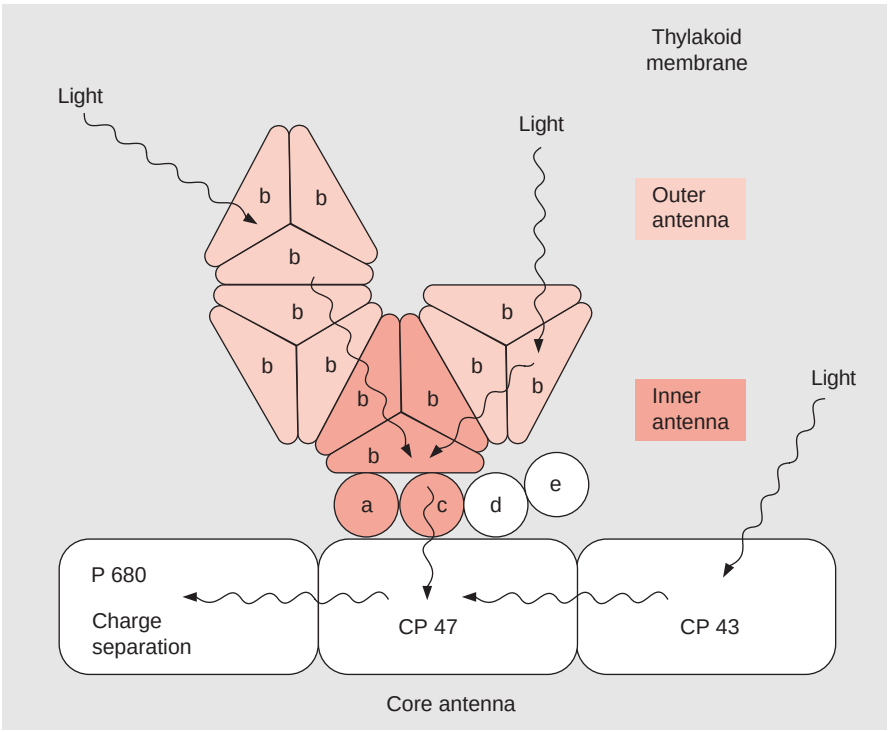

Figure 2.13 Schematic presentation of the light harvesting complexes in the antenna of photosystem II in a plant viewed from above (after Thornber); (a) LHC-II*a*, (b) LHC-II*b*. The inner antenna complexes are linked to the core complex by LHC-II*a* and LHC-II*c* (c) monomers. The function of the LHC-II*d* (d) and LHC-II*e* (e) monomers is not entirely known.

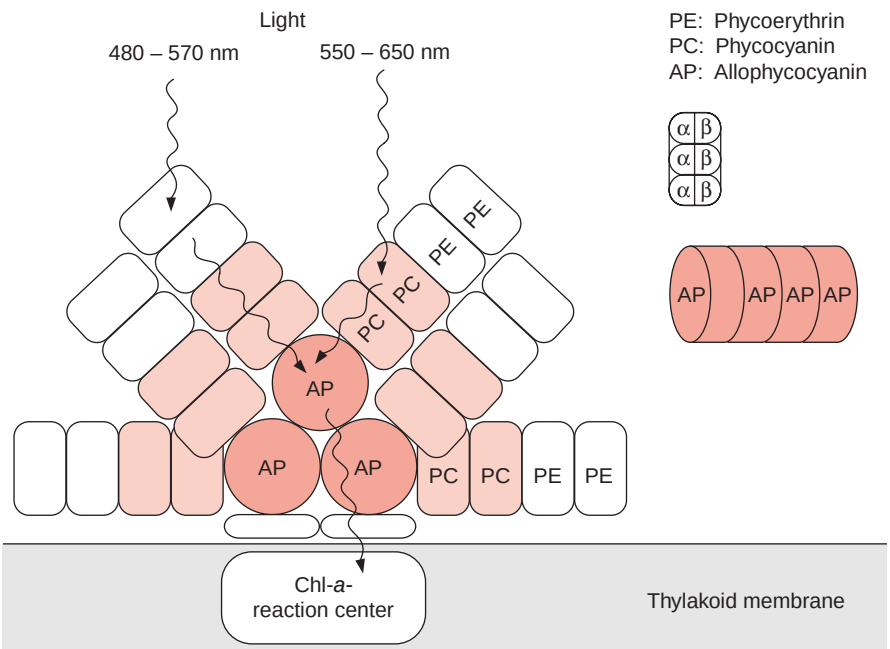

Figure 2.14 Schematic presentation of a side view of the structure of a phycobilisome. Each of the units shown consists of three α- and three β-subunits. (After Bryanth.)

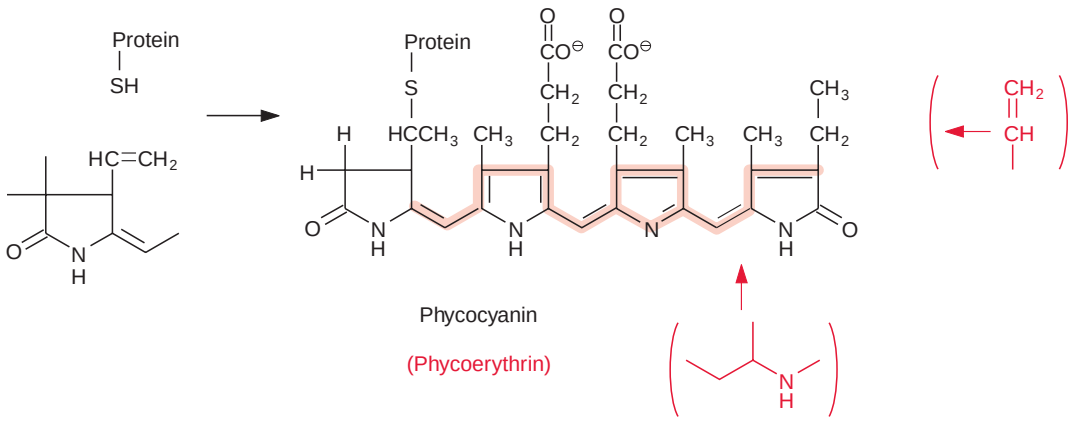

Figure 2.15 Structural formula of the biliproteins that are present in the phycobilisomes, phycocyanin (black), and phycoerythrin (structural differences from phycocyanin are shown in red). The corresponding chromophores, phycocyanobilin and phycoerythrobilin are covalently bound to proteins via thioether linkages between the SH group of a cysteine residue of the protein and the vinyl group of the chromophore. The conjugated double bonds (red) show molecules with pigment-like character.

These complexes, termed **phycobilisomes**, consist of proteins (**phycobiliproteins**), which are covalently linked with phycobilins. **Phycobilins** are open-chained tetrapyrroles and therefore are structurally related to the chlorophylls. Open-chained tetrapyrroles are also contained in bile, which explains the name -*bilin*. The phycobilins are linked to the protein by a thioether bond between an SH-group of the protein and the vinyl side chain of the phycobilin. The protein **phycoerythrin** is linked to the chromophore **phycoerythrobilin,** and the proteins **phycocyanin** and **allophycocyanin** to the chromophore **phycocyanobilin** (Fig. 2.15). The basic structure in the phycobiliproteins consists of a heterodimer composed of α- and β-subunits. Each of these protein subunits binds one to four phycobilins as a chromophore. Three of these heterodimers aggregate to a trimer $(\alpha,\beta)_3$ and thus form the actual building block of a phycobilisome. Specific linker polypeptides function as "mortar" between the building blocks.

Figure 2.14 shows the structure of a phycobilisome. The phycobilisome is attached to the membrane by anchor proteins. Three aggregates of four to five $(\alpha,\beta)_3$ units form the core. This core contains the chromophore allophycocyanin (AP) to which cylindrical rod like structures are attached, each with four to six building blocks. The inner units contain mainly phycocyanine (PC) and the outer ones phycoerythrin (PE). The function of this structural organization is illustrated by the absorption spectra of

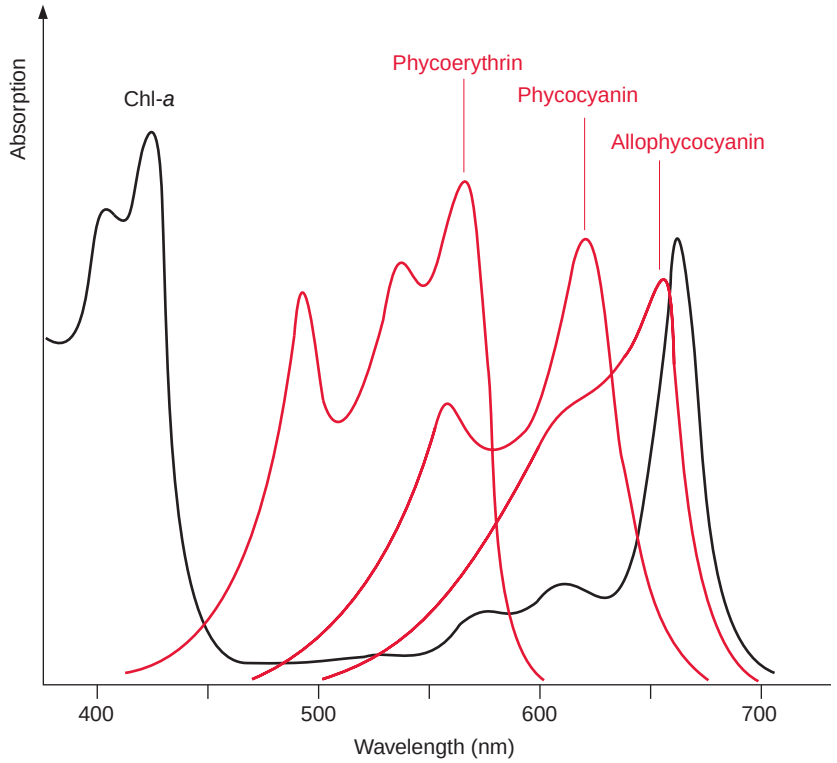

Figure 2.16
Absorption spectra of the phycobiliproteins phycoerythrin, phycocyanin, and allophycocyanin. For the sake of comparison chlorophyll-*a* is shown.

the various biliproteins shown in Figure 2.16. The light of shorter wavelength is absorbed in the periphery of the rods by phycoerythrin and the light of longer wavelength in the inner regions of the rods by phycocyanin. The core transfers the excitons to the reaction center. The principle of spatial distribution between the short wavelength absorbing pigments at the periphery and the long wavelength absorbing pigments in the center is also implemented for the PS II antennae of higher plants (Fig. 2.10).

Due to the phycobiliproteins, phycobilisomes are able to absorb green light very efficiently (Fig. 2.16), thus allowing cyanobacteria and red algae to survive in deep waters with low light intensities. At these depths, due to the "green window" of photosynthesis (Fig. 2.3), only green light is available, as the light of the other wavelengths is absorbed by green algae living in the upper regions of the water column. The algae in the deeper regions are obliged to invest a large portion of their cellular matter in phycobilisomes in order to carry out photosynthesis at this very low light intensity and at distinct wavelengths. Biliproteins can amount to 40% of the total cellular protein of the algae. These organisms undertake an extraordinary expenditure to collect enough light for survival.

Further reading

Adir, N. Elucidation of the molecular structures of components of the phycobilisome: Restructuring a giant. Photosynthesis Research 85, 15–32 (2005).

Bada, J. L., Lazcano, A. Prebiotic soup—revisiting the Miller experiment. Science 300, 745–746 (2003).

Cerullo, G., Polli, D., Lanzani, G., De Silverstri, S., Hashimoto, H., Cogdell, R. J. Photosynthetic light harvesting by carotenoids: Detection of an intermediate excited state. Science 298, 2395–2398 (2002).

Emerson, R. The quantum yield of photosynthesis. Annual Review Plant Physiology 9, 1–24 (1958).

Horton, P., Ruban, A. Molecular design of the photosystem II light harvesting antenna: Photosynthesis and photoprotection. Journal Experimental Botany 56, 365–373 (2005).

Kühlbrandt, W. Structure and function of the plant light harvesting complex LHC-II. Current Biology 4, 519–528 (1994).

Minagawa, J., Takahashi, Y. Structure, function and assembly of photosystem II and its light-harvesting proteins. Photosynthesis Research 82, 241–263 (2004).

Vogelmann, T. C., Nishio, J. N., Smith, W. K. Leaves and light capture light propagation and gradients of carbon fixation in leaves. Trends in Plant Science 1, 6570 (1996).

Wormit, M., Dreuw, A. Quantum chemical insights in energy dissipation and carotenoid radical cation formation in light harvesting complexes. Physical Chemistry, Chemical Physics 9, 2917–2931 (2007).

Xiong, J., Fischer, W. M., Inoue, K., Nakahara, M., Bauer, C. E. Molecular evidence for the early evolution of photosynthesis. Science 289, 1724–1730 (2000).

3

Photosynthesis is an electron transport process

The previous chapter described how photons are captured by an antenna and conducted as excitons to the reaction centers. This chapter deals with the function of these reaction centers and describes how photon energy is converted to chemical energy to be utilized by the cell. As mentioned in Chapter 2, plant photosynthesis probably evolved from bacterial photosynthesis, so that the basic mechanisms of the photosynthetic reactions are alike in bacteria and plants. Bacteria have proved to be very suitable objects for studying the principles of photosynthesis since their reaction centers are more simply structured than those of plants and they are more easily isolated. For this reason, first bacterial photosynthesis and then plant photosynthesis will be described.

3.1 The photosynthetic machinery is constructed from modules

The photosynthetic machinery of bacteria is constructed from defined complexes, which also appear as components of the photosynthetic machinery in plants. As will be described in Chapter 5, some of these complexes are also components of mitochondrial electron transport. These complexes can be thought of as modules that developed at an early stage of evolution and have been combined in various ways for different purposes. For easier understanding, the functions of these modules in photosynthesis will be treated first as **black boxes** and a detailed description of their structure and function will be given later.

Purple bacteria have only one reaction center (Fig. 3.1). In this reaction center the energy of the absorbed photon excites an electron, which will be elevated to a negative redox state. The excited electron is transferred back to the ground state by an electron transport chain, called the **cytochrome-*b*/*c*$_1$ complex**, and the released energy is transformed to a chemical compound (NADH), which is then used for the synthesis of biomass (e.g., proteins and carbohydrates). Generation of energy is based on coupling the electron transport with the transport of protons across the membrane. In this way the energy of the excited electron is conserved as an electrochemical H^+-potential across the membrane. The photosynthetic reaction centers and the main components of the electron transport chain are always located in a membrane.

Via ATP-synthase the energy of the H^+-potential is used to synthesize ATP from ADP and phosphate. Since the excited electrons in purple bacteria return to the ground state of the reaction center, this electron transport is called **cyclic electron transport**. In purple bacteria the proton gradient is also used to reduce NAD^+ via an additional electron transport chain named the **NADH dehydrogenase complex** (Fig. 3.1). By consuming the energy of the H^+-potential, electrons are transferred from a reduced compound (e.g., organic acids or hydrogen sulfide) to NAD^+. The ATP and NADH formed by bacterial photosynthesis are used for the synthesis of organic matter; especially important is the synthesis of carbohydrates from CO_2 via the Calvin cycle (see Chapter 6).

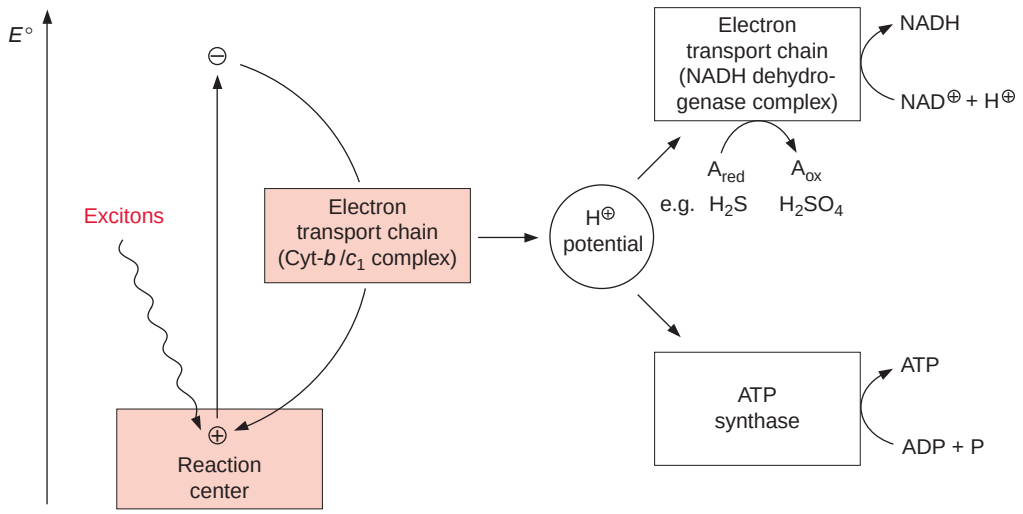

Figure 3.1 Schematic presentation of the photosynthetic apparatus of purple bacteria. The energy of a captured exciton in the reaction center elevates an electron to a negative redox state. The electron is transferred to the ground state via an electron transport chain including the cytochrome-*b*/*c*$_1$ complex and cytochrome-*c* (the latter is not shown). Free energy of this process is conserved by formation of a proton potential which is used partly for synthesis of ATP and partly to enable an electron flow for the formation of NADH from electron donors such as H_2S.

The reaction center of **green sulfur bacteria** (Fig. 3.2) is homologous to that of purple bacteria, indicating that they have both evolved from a common ancestor. ATP is also formed in green sulfur bacteria by cyclic electron transport. The electron transport chain (cytochrome-b/c_1 complex) and the ATP-synthase involved here are very similar to those in purple bacteria. However, in contrast to purple bacteria, green sulfur bacteria are able to synthesize NADH by a **noncyclic electron transport process**. In this case, the excited electrons are transferred to the **ferredoxin-NAD-reductase complex**, which reduces NAD^+ to NADH. Since the excited electrons in this noncyclic pathway do not return to the ground state, an electron deficit remains in the reaction center and is replenished by electron donors such as H_2S, ultimately being oxidized to sulfate.

Cyanobacteria and plants use water as an electron donor in photosynthesis (Fig. 3.3). As oxygen is liberated, this process is called **oxygenic photosynthesis**. Two photosystems designated II and I are arranged in tandem. The machinery of oxygenic photosynthesis is built by modules that have already been described in bacterial photosynthesis. The structure of the reaction center of photosystem II corresponds to that of the reaction center of purple bacteria, and that of photosystem I corresponds to the reaction center of green sulfur bacteria. The enzymes ATP synthase and ferredoxin-NADP-reductase are very similar to those of photosynthetic bacteria. The

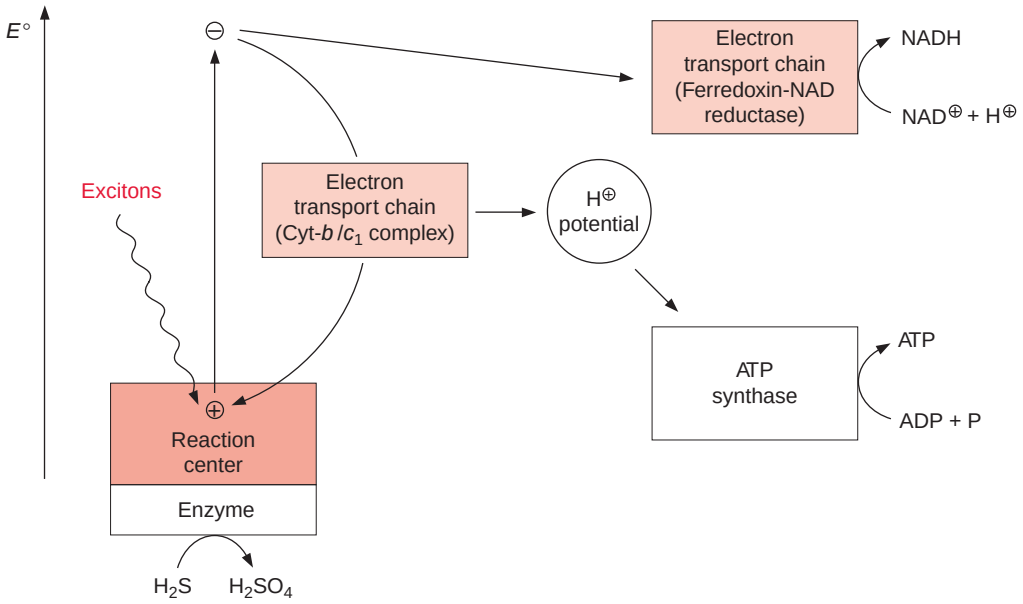

Figure 3.2 Schematic presentation of the photosynthetic apparatus in green sulfur bacteria. In contrast to the scheme in Figure 3.1, part of the electrons elevated to a negative redox state is transferred via an electron transport chain (ferredoxin-NAD reductase) to NAD^+, yielding NADH. The electron deficit arising in the reaction center is compensated by electron donors such as H_2S (see also Fig. 3.1).

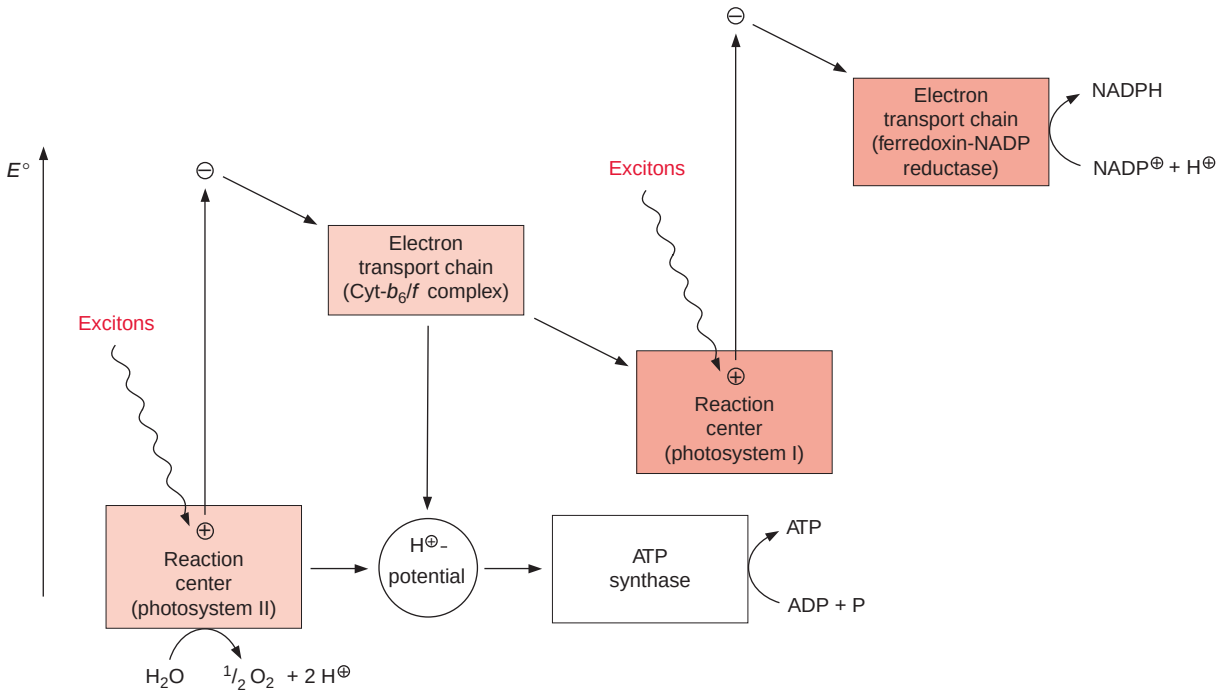

Figure 3.3 Schematic presentation of the photosynthetic apparatus of cyanobacteria and plants. The two sequentially arranged reaction centers correspond in their function to the photosynthetic reaction centers of purple bacteria and green sulfur bacteria (shown in Figs. 3.1 and 3.2).

electron transport chain of the **cytochrome-*b*$_6$*f* complex** has the same basic structure as the cytochrome-*b*/*c*$_1$ complex in bacteria.

Four excitons are required in oxygenic photosynthesis to split one molecule of water:

$$H_2O + NADP^+ + 4 \text{ excitons} \rightarrow 1/2\, O_2 + NADPH + H^+$$

In this noncyclic electron transport, electrons are transferred to $NADP^+$ and protons are transported across the membrane to generate a proton gradient that drives the synthesis of ATP. Thus, for each mol of NADPH formed by oxygenic photosynthesis, about 1.5 molecules of ATP are generated simultaneously (section 4.4). Most of this ATP and NADPH are used for CO_2 and nitrate assimilation to synthesize carbohydrates and amino acids. Oxygenic photosynthesis in plants takes place in the chloroplasts, a cell organelle of the plastid family (section 1.3).

3.2 A reductant and an oxidant are formed during photosynthesis

In the 1920s Otto Warburg (Berlin) postulated that the energy of light is transferred to CO_2 and that the CO_2, activated in this way, reacts with water to form a carbohydrate, accompanied by the release of oxygen. According to this hypothesis, the oxygen released by photosynthesis was derived from the CO_2. In 1931 this hypothesis was opposed by Cornelis van Niel (USA) by postulating that during photosynthesis a **reductant** is formed, which then reacts with CO_2. The so-called van Niel equation describes photosynthesis in the following way:

$$CO_2 + 2\,H_2A \xrightarrow{Light} [CH_2O] + H_2O + 2\,A$$
$$([CH_2O] = \text{carbohydrate})$$

He proposed that a compound H_2A is split by light energy into a reducing compound (2H) and an oxidizing compound (A). For oxygenic photosynthesis of cyanobacteria or plants, it can be rewritten as:

$$CO_2 + 2\,H_2O \xrightarrow{Light} [CH_2O] + H_2O + O_2$$

In this equation the oxygen released during photosynthesis is derived from water.

In 1937 Robert Hill (Cambridge, UK) proved that a reductant is actually formed in the course of photosynthesis. He was the first to succeed in isolating chloroplasts with photosynthetic activity, which, however, had no intact envelope membranes and consisted only of thylakoid membranes. When these chloroplasts were illuminated in the presence of Fe^{3+} compounds (initially ferrioxalate, later ferricyanide ($[Fe\ (CN)_6]^{3-}$)), Robert Hill observed an evolution of oxygen accompanied by the reduction of the **Fe^{3+}**-compounds to the **Fe^{2+}** form.

$$H_2O + 2\,Fe^{+++} \xrightarrow{Light} 2\,H^+ + 1/2\,O_2 + 2\,Fe^{++}$$

This "**Hill reaction**" proved that the photochemical splitting of water can be separated from the reduction of the CO_2. Therefore the complete reaction of photosynthetic CO_2 assimilation can be divided into two reactions:

1. The so-called **light reaction**, in which water is split by photon energy to yield reductive power (NADPH) and chemical energy (ATP); and

2. the so-called **dark reaction** (Chapter 6), in which CO_2 is assimilated at the expense of the reductive power and of ATP.

In 1952 the Dutchman Louis Duysens made a very important observation that helped explain the mechanism of photosynthesis. When illuminating isolated membranes of the purple bacterium *Rhodospirillum rubrum* with short light pulses, he found a decrease in light absorption at 890 nm, which was immediately reversed when the bacteria were darkened again. The same "**bleaching**" effect was found at 870 nm in the purple bacterium *Rhodobacter sphaeroides*. Later, Bessil Kok (USA) and Horst Witt (Germany) also found similar pigment bleaching at 700 nm and 680 nm in chloroplasts. This bleaching was attributed to the **primary reaction of photosynthesis**, and the corresponding pigments of the reaction centers were named P_{870} (*Rb. sphaeroides*) and P_{680} and P_{700} (chloroplasts). When an oxidant (e.g., $[Fe(CN)_6]^{3-}$) was added, this bleaching effect could also be achieved in the dark. These results indicated that these absorption changes of the pigments were due to a **redox reaction**. This was the first indication that chlorophyll can be oxidized. Electron spin resonance measurements revealed that **radicals** are formed during this "bleaching." "Bleaching" could also be observed at the very low temperature of 1 K. This showed that in the electron transfer leading to the formation of radicals, the reaction partners are located so close to each other that thermal oscillation of the reaction partners (normally the precondition for a chemical reaction) is not required for this redox reaction. Spectroscopic measurements indicated that the reaction partner of this primary redox reaction are two closely adjacent chlorophyll molecules arranged as a pair, called a "**special pair**."

3.3 The basic structure of a photosynthetic reaction center has been resolved by X-ray structure analysis

The reaction centers of purple bacteria proved to be especially suitable objects for explaining the structure and function of the photosynthetic machinery. It was a great step forward when in 1970 Roderick Clayton (USA) developed a method for isolating reaction centers from purple bacteria. Analysis of the components of the reaction centers of the different purple bacteria (shown in Table 3.1 for the reaction center of *Rhodobacter sphaeroides* as an example) revealed that the reaction centers had the same basic structure in all the purple bacteria investigated. The minimum structure

Table 3.1: Composition of the reaction center from *Rhodobacter sphaeroides* (P870)

	Molecular mass
1 subunit L	21 kDa
1 subunit M	24 kDa
1 subunit H	28 kDa
4 bacteriochlorophyll-*a*	
2 bacteriopheophytin-*a*	
2 ubiquinone	
1 non-heme-Fe-protein	
1 carotenoid	

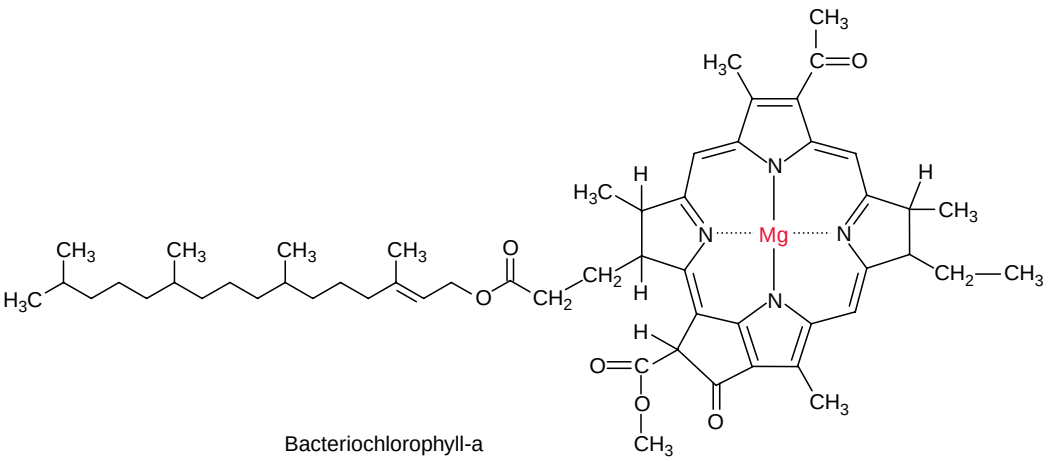

Figure 3.4
Bacteriochlorophyll-*a*.

consists of the three subunits L, M, and H (light, medium, and heavy). Subunits L and M are peptides with a similar amino acid sequence. They are homologous. The reaction center of *Rb. sphaeroides* contains four bacteriochlorophyll-*a* (Bchl-*a*, Fig. 3.4) and two bacteriopheophytin-*a* (Bphe-*a*). Pheophytins differ from chlorophylls in that they lack magnesium as the central atom. In addition, the reaction center contains an iron atom that is not part of a heme. It is therefore called a *non-heme iron*. Furthermore, the reaction center is comprised of two molecules of ubiquinone (Fig. 3.5), which are designated as Q_A and Q_B. Q_A is tightly bound to the reaction center, whereas Q_B is only loosely associated with it.

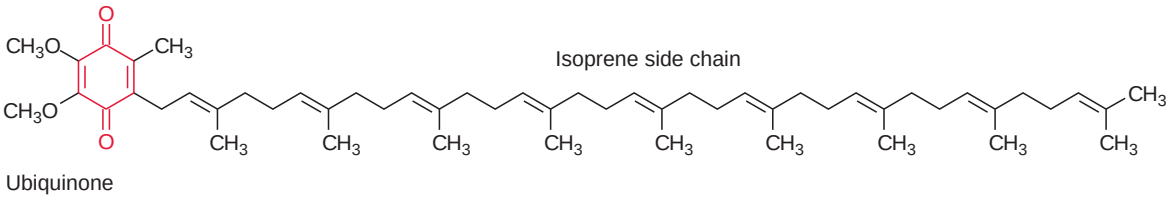

Figure 3.5 Ubiquinone. The long isoprenoid side chain mediates the lipophilic character and membrane anchorage.

X-ray structure analysis of the photosynthetic reaction center

If ordered crystals can be prepared from a protein, it is possible to analyze the spherical structure of the protein molecule by **X-ray structure analysis**. In this method a protein crystal is exposed to X-ray irradiation. The electrons of the atoms in the molecule cause a scattering of X-rays. Diffraction is observed when the irradiation passes through a regular repeating structure. The corresponding diffraction pattern, consisting of many single reflections, is measured by an X-ray film positioned behind the crystal or by an alternative detector. The principle is demonstrated in Figure 3.6. To obtain as many reflections as possible, the crystal, mounted in a capillary, is rotated. From a few dozen to up to several hundred exposures are required for one set of data, depending on the form of the crystal and the size of the crystal lattice. To evaluate a new protein structure, several sets of data are required in which the protein has been changed by the incorporation or binding of a heavy metal ion. With the help of elaborate computer programs, it is possible to reconstruct the spherical structure of the exposed protein molecules by applying the rules for scattering X-rays by atoms of various electron densities.

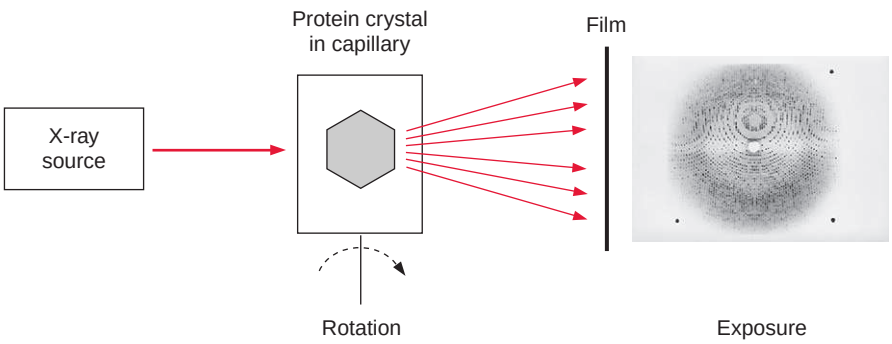

Figure 3.6 Schematic presentation of X-ray structural analysis of a protein crystal. A capillary containing the crystal rotates slowly and the diffraction pattern is monitored on an X-ray film. Nowadays much more sensitive detector systems (image platers) are used instead of films. The diffraction pattern shown was obtained by the structural analysis of the reaction center of *Rb. sphaeroides*. (Courtesy of H. Michel, Frankfurt.)

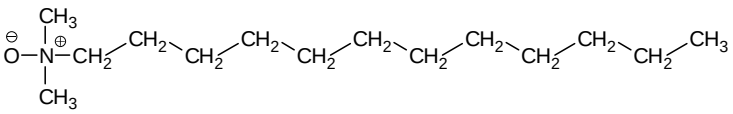

N,*N*-Dimethyldodecylamin-*N*-oxide

Figure 3.7 The detergent *N*,*N*′-dimethyldodecylamine-*N*-oxide.

X-ray structure analysis requires a highly technical expenditure and is very time-consuming, but the actual limiting factor in the elucidation of a spherical structure is usually the preparation of **suitable single crystals**. Until 1980 it was thought to be impossible to prepare crystals suitable for X-ray structure analysis from hydrophobic membrane proteins. The application of the detergent **N,N′-dimethyldodecylamine-N-oxide** (Fig. 3.7) was a great step forward in helping to solve this problem. This detergent forms water-soluble protein-detergent micelles with membrane proteins. With the addition of ammonium sulfate or polyethylene glycol is was then possible to crystallize membrane proteins. The micelles form a regular lattice in these crystals (Fig. 3.8). The protein in the crystal remains in its native state since the hydrophobic regions of the membrane protein, which normally border on the hydrophobic membrane, are covered by the hydrophobic chains of the detergent.

Using this procedure, Hartmut Michel (Munich) succeeded in obtaining crystals from the reaction center of the purple bacterium *Rhodopseudomonas viridis* and, together with his colleagues Johann Deisenhofer and Robert Huber, performed an X-ray structure analysis of these crystals. The immense amount of time invested in these investigations is illustrated by the fact that the evaluation of the stored data sets alone took two and a half years (nowadays modern computer programs would do it very much faster). The X-ray structure analysis of a photosynthetic reaction center successfully elucidated for the first time the three-dimensional structure of a membrane protein. For this work, Michel, Deisenhofer, and Huber were awarded the Nobel Prize in Chemistry in 1988. Using the same method, the reaction center of *Rb. sphaeroides* was analyzed and it turned out that the basic structures of the two reaction centers are astonishingly similar.

The reaction center of *Rhodopseudomonas viridis* has a symmetric structure

Figure 3.9 shows the three-dimensional structure of the reaction center of the purple bacterium *Rhodopseudomonas viridis*. The molecule has a cylindrical shape and is about 8 nm long. The homologous subunits L (red) and

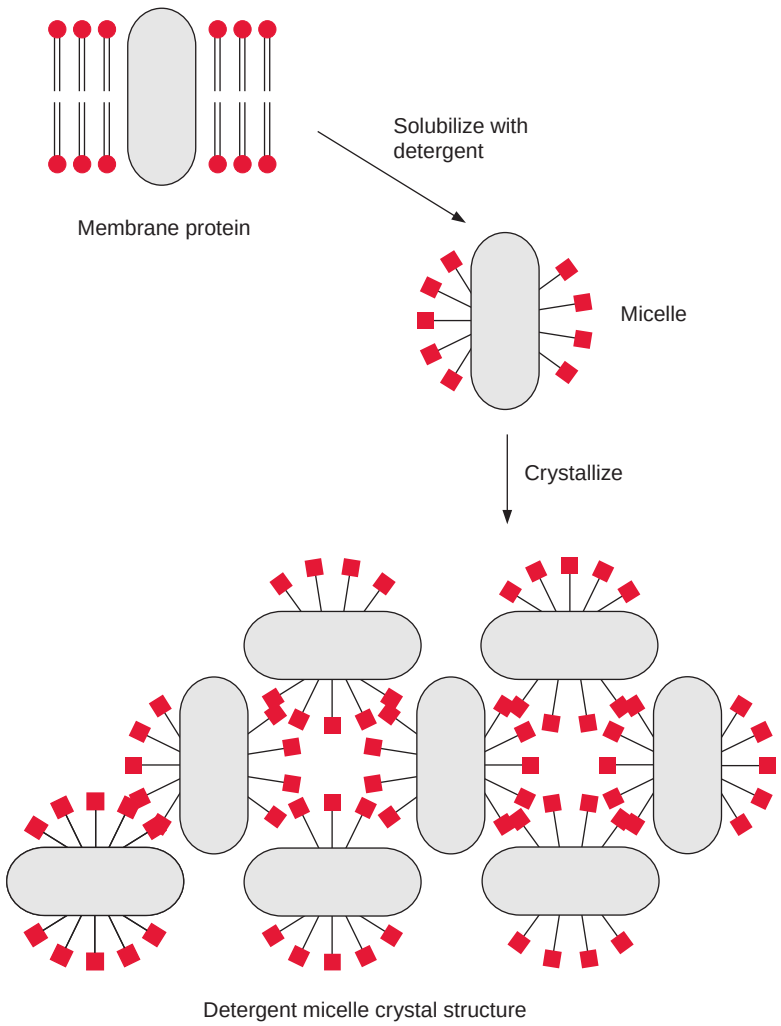

Figure 3.8 A micelle is formed after solubilization of a membrane protein with detergent. The hydrophobic region of the membrane proteins, the membrane lipids, and the detergent are shown in black and the hydrophilic regions in red. Crystal structures can be formed by association of the hydrophilic regions of the detergent micelle.

M (black) are arranged symmetrically and enclose the chlorophyll and pheophytin molecules. The H subunit is attached like a lid to the lower part of the cylinder.

In the same projection as in Figure 3.9, Figure 3.10 shows the location of the chromophores in the protein molecule. All the chromophores are positioned as pairs divided by a symmetry axis. Two Bchl-*a* molecules (D_M, D_L) can be recognized in the upper part of the structure. The two tetrapyrrole rings are so close (0.3 nm) that their orbitals overlap in the excited state. This confirmed the actual existence of the "**special pair**" of chlorophyll molecules, postulated earlier from spectroscopic investigations, as the

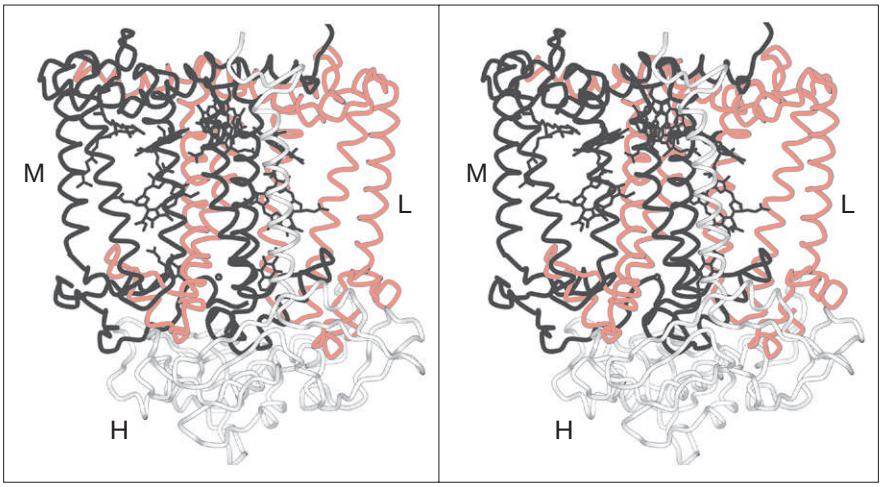

Figure 3.9 Stereo pair of the three-dimensional structure of the reaction center of *Rp. viridis*. The peptide chain of subunit L is marked red and subunit M is black. The polypeptide chains are shown as bands and the chromophores (chlorophylls, pheophytins) and quinones are shown as wire models. The upper part of the reaction center borders the periplasmatic compartment and the lower part the cytoplasm. (By courtesy of H. Michel and R. C. R. D. Lancaster, Frankfurt.) *How to look at a stereo picture, see legend to Figure 1.29.*

site of the primary redox process of photosynthesis. The chromophores are arranged underneath the chlorophyll pair in two nearly identical branches, both comprised of a Bchl-*a* (B_A, B_B) monomer and a bacteriopheophytin (Φ_A, Φ_B). Whereas the chlorophyll pair (D_M, D_L) is bound by both subunits L and M, the chlorophyll B_A and the pheophytin Φ_A are associated with subunit L, and B_B and Φ_B with subunit M. The quinone ring of Q_A is bound via hydrogen bonds and hydrophobic interaction to subunit M, whereas the loosely associated Q_B is bound to subunit L.

3.4 How does a reaction center function?

The analysis of the structure and extensive kinetic investigations allowed a detailed description of the function of the bacterial reaction center. The kinetic investigations included measurements by absorption and fluorescence spectroscopy after light flashes in the range of less than 10^{-13} s, as well as measurements of nuclear spin and electron spin resonance. Although the reaction center shows a symmetry with two almost identical branches of chromophores, electron transfer proceeds only along the right branch (the L side, Fig. 3.10). The chlorophyll monomer (B_B) on the M side is in close contact with a **carotenoid molecule**, which abolishes a harmful **triplet state** of chlorophylls in the reaction center (sections 2.3 and 3.7). The function of the pheophytin (Φ_B) on the M side and of the non-heme iron is not yet fully understood.

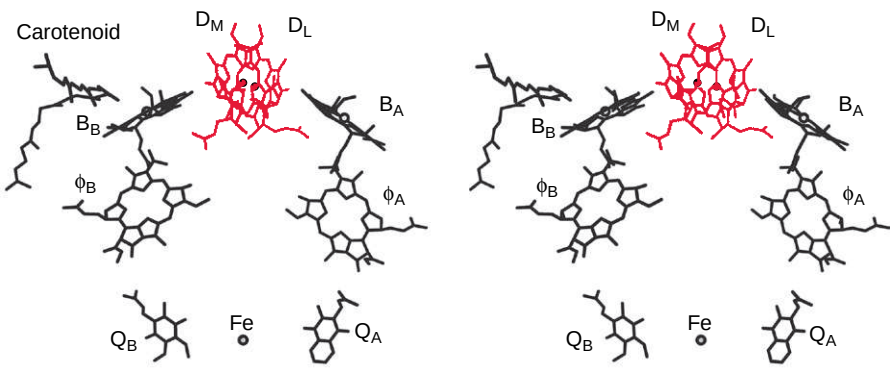

Figure 3.10 Stereo pair of the three-dimensional array of chromophores and quinones in the reaction center of *Rp. viridis.* The projection corresponds to the structure shown in Figure 3.9. The Bchl-*a*-pair D_MD_L (see text) is shown in red. (By courtesy of H. Michel and R. C. R. D. Lancaster, Frankfurt. Figures 3.9 and 3.10 were produced by P. Kraulis, Uppsala, with the program MOLSCRIPT.)

Figure 3.11 presents a scheme of the reaction center with the reaction partners arranged according to their electrochemical potential. The exciton of the primary reaction is provided by the antenna (section 2.4) which then excites the chlorophyll pair. This primary excitation state has only a very short half-life time, then a charge separation occurs, and, as a result of the large potential difference, an electron is removed within picoseconds to reduce bacteriopheophytin (Bphe).

$$(\text{Bchl})_2 + 1\,\text{Exciton} \rightarrow (\text{Bchl})_2^*$$

$$(\text{Bchl})_2^* + \text{Bphe} \rightarrow (\text{Bchl})_2^{\bullet+} + \text{Bphe}^{\bullet-}$$

The electron is probably transferred first to the Bchl-monomer (B_A) and then to the pheophytin molecule (Φ_A). The second electron transfer proceeds with a half-time of 0.9 picoseconds, about four times as fast as the electron transfer to B_A. The **pheophytin radical** has a tendency to return to the ground state by a return of the translocated electron to the Bchl-monomer (B_A). To prevent this, within 200 picoseconds a high potential difference withdraws the electron from the pheophytin radical to a quinone (Q_A) (Fig. 3.11). The **semiquinone radical** thus formed, in response to a further potential difference, transfers its electron to the loosely bound ubiquinone Q_B. After a second electron transfer, first **ubisemiquinone** and then **ubihydroquinone** are formed (Fig. 3.12). In contrast to the very labile radical intermediates of the pathway, ubihydroquinone is a **stable reductant**. However, this stability has its price. For the formation of ubihydroquinone as a first stable product from the primary excitation state of the chlorophyll, more than half of the exciton energy is dissipated as **heat**.

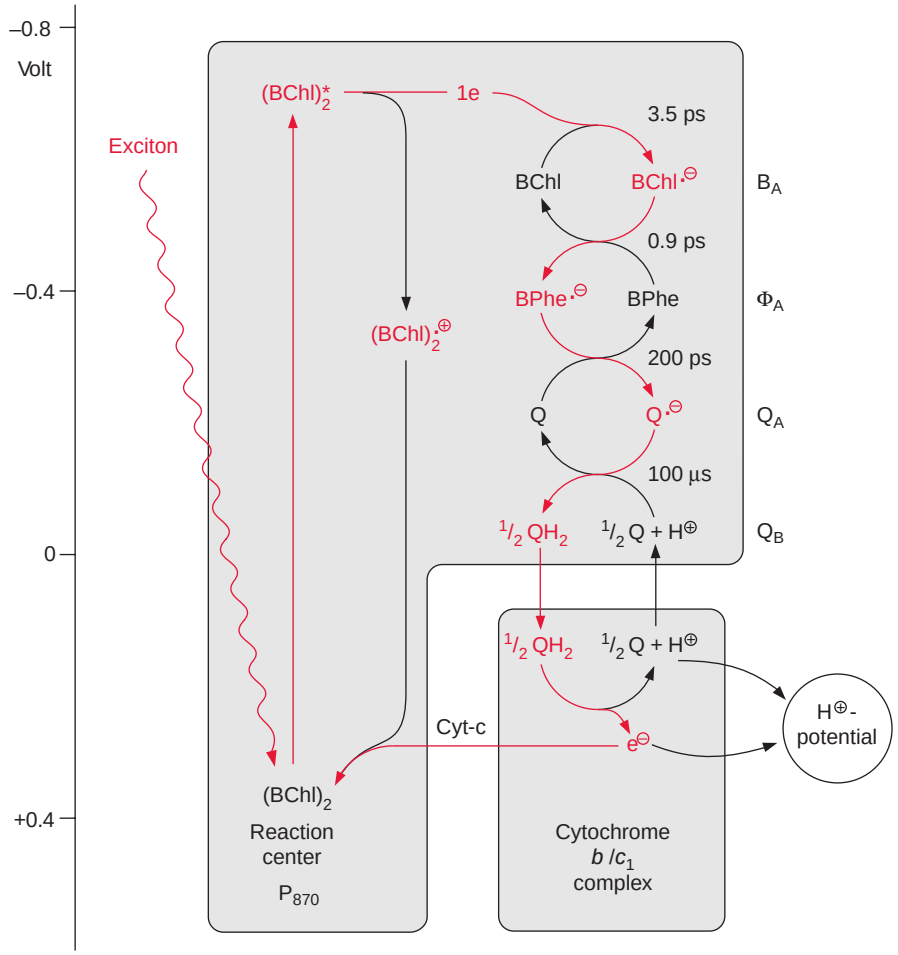

Figure 3.11 Schematic presentation of cyclic electron transport in photosynthesis of *Rb. sphaeroides*. The excited state symbolized by a star results in a charge separation; an electron is transferred via pheophytin, the quinones Q_A, Q_B, and the cyt-*b*/*c* complex to the positively charged chlorophyll radical. Q: quinone, $Q^{\bullet}_{-}$: semiquinone radical, QH_2: hydroquinone.

Ubiquinone (Fig. 3.5) contains a hydrophobic isoprenoid side chain, by which it is soluble in the lipid phase of the photosynthetic membrane. The same function of an isoprenoid side chain has already been discussed in the case of chlorophyll (section 2.2). In contrast to chlorophyll, pheophytin, and Q_A, which are all tightly bound to proteins, ubihydroquinone Q_B is only loosely associated with the reaction center and can be exchanged by another ubiquinone. Ubihydroquinone remains in the membrane phase, is able to diffuse rapidly along the membrane, and functions as a transport metabolite for reducing equivalents in the membrane phase. It feeds the electrons into the **cytochrome-b/c$_1$ complex**, also located in the membrane. The electrons are then transferred back to the reaction center through the cytochrome-b/c$_1$

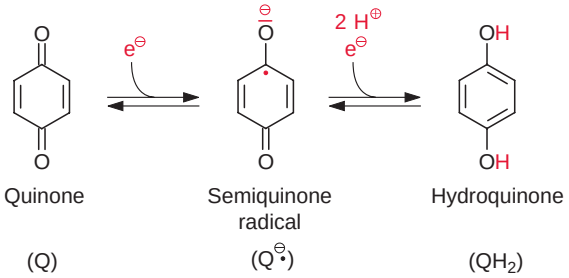

Figure 3.12 Reduction of a quinone by one electron results in a semiquinone radical and further reduction to hydroquinone. Q: quinone, $Q^{\bullet}_{-}$: semiquinone radical, QH_2: hydroquinone.

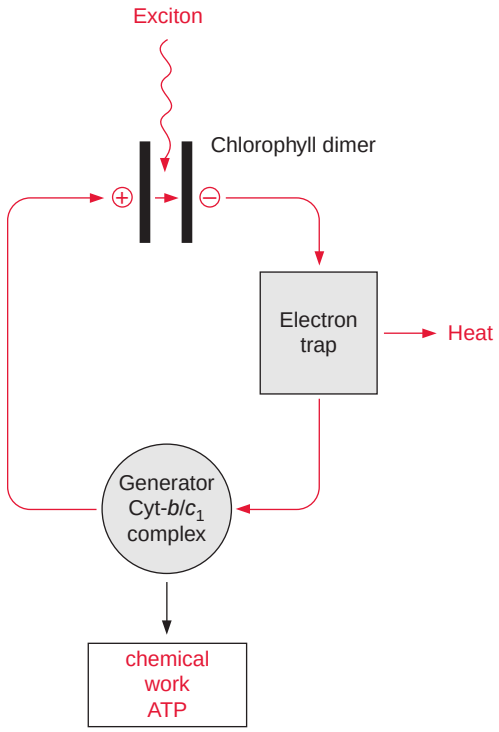

Figure 3.13 Cyclic electron transport of photosynthesis drawn as an electrical circuit.

complex and via cytochrome-*c*. Energy is conserved during this electron transport as a proton potential (section 4.1), which is used for ATP-synthesis. The structure and mechanism of the cytochrome-b/c_1 complex and of ATP-synthase will be described in section 3.7 and Chapter 4, respectively.

In summary, the cyclic electron transport of the purple bacteria resembles a simple electric circuit (Fig. 3.13). The two pairs of chlorophyll and pheophytin, between which an electron is transferred by light energy, may be regarded as the two plates of a capacitor between which a voltage is generated, driving a flux of electrons, a current. Voltage drops via a resistor and a large amount of the electron energy is dissipated as heat. This resistor functions

as an electron trap, and withdraws the electrons rapidly from the capacitor. A generator utilizes the remaining voltage to produce chemical energy.

3.5 Two photosynthetic reaction centers are arranged in tandem in photosynthesis of algae and plants

In green algae about eight photons are required (**quantum requirement**: photons absorbed per molecule O_2 produced) for the photosynthetic water splitting (section 2.4). Instead of the term quantum requirement, one often uses the reciprocal term **quantum yield** (molecules of O_2 produced per photon absorbed). According to the color of irradiated light (action spectrum) the quantum yield dropped very sharply when algae were illuminated with red light above a wavelength of 680 nm (Fig. 3.14). This effect, named "**red drop**," remained unexplained since algae contain chlorophyll, which absorbs light at 700 nm. Robert Emerson and coworkers (USA) solved this problem in 1957 when they observed that the quantum yield in the spectral range above 680 nm increased dramatically when algae were illuminated with orange light (650 nm) and red light simultaneously. Then the quantum yield was higher than the sum of both yields when irradiated separately with the light of each wavelength. This **Emerson effect** led to the conclusion that two different reaction centers are involved in photosynthesis of green algae (and also of cyanobacteria and higher plants). In 1960 Robert Hill (Cambridge, UK) postulated a reaction scheme (Fig. 3.15) in which **two reaction centers are**

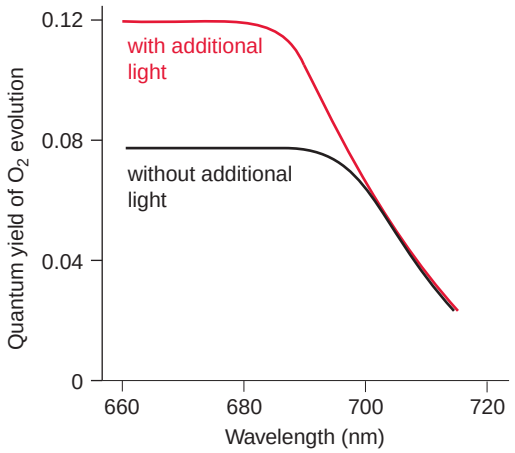

Figure 3.14 The quantum yield of O_2 release in green algae (*Chlorella*) depends on the wavelength of irradiated light. The upper curve shows the result of supplementary irradiation of 650 nm light. (After Emerson and Rabinowitch.)

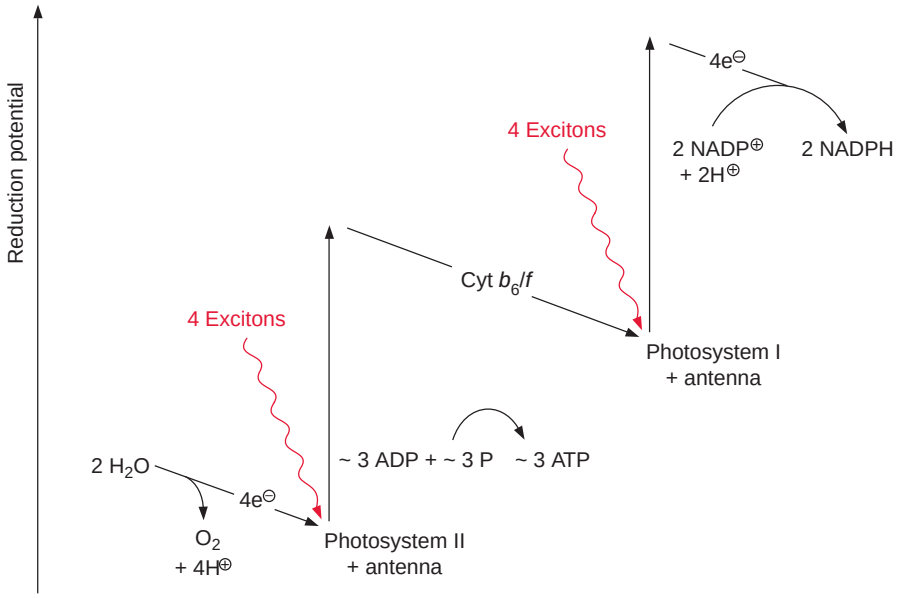

Figure 3.15 The Z scheme of photosynthesis in plants. Electrons are transferred via two tandemly arranged photosystems from water to $NADP^+$ with the synthesis of ATP. The amount of ATP formed is not known but is probably between two and three per four excitons captured at each reaction center (section 4.4).

arranged in tandem and connected by an electron transport chain containing cytochrome-b_6 and cytochrome-*f* (cytochrome-*f* is a cytochrome of the c type; see section 3.7). Light energy of 700 nm was sufficient for the excitation of reaction center I, whereas excitation of the other reaction center II required light of higher energy with a wavelength of 680 nm. The electron flow according to the redox potentials of the intermediates shows a zigzag, leading to the name **Z scheme**. The numbering of the two photosystems corresponds to the sequence of their discovery. **Photosystem II** (PS II) can use light up to a wavelength of **680 nm**, whereas **photosystem I** (PS I) can utilize light with a wavelength up to **700 nm**. The sequence of the two photosystems makes it possible that at PS II a very **strong oxidant** is generated for the oxidation of water and at PS I a very **strong reductant** is produced for the reduction of $NADP^+$ (see also Fig. 3.3).

Figure 3.16 gives an overview of electron transport through the photosynthetic complexes; the carriers of electron transport are drawn according to their electric potential (see also Fig. 3.11). Figure 3.17 shows how the photosynthetic complexes are arranged in the thylakoid membrane. There is a potential difference of about 1.2 volt between the process of water oxidation and $NADP^+$ reduction. The absorbed photons of 680 and 700 nm together correspond to a total potential difference of 3.45 volt (see section 2.2, equation 2.7). Thus, only about one-third of the energy of the photons absorbed by the two photosystems is used to transfer electrons from

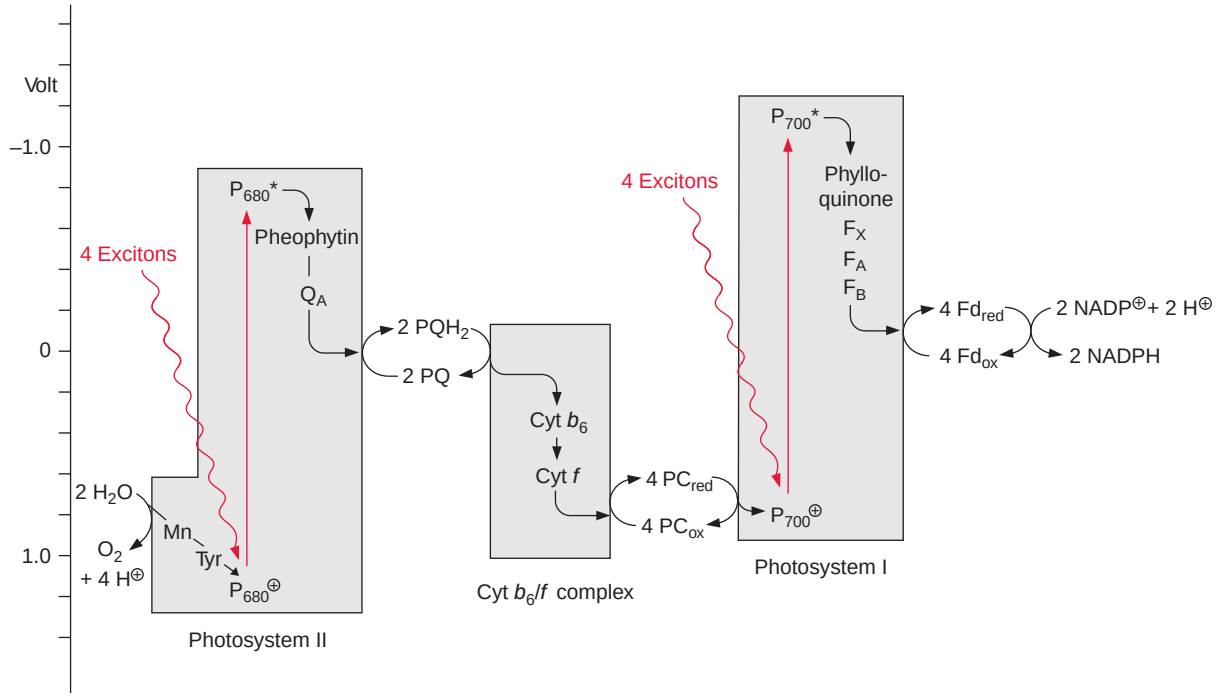

Figure 3.16 Schematic presentation of noncyclic electron transport in plants. The redox components are placed according to their midpoint redox potential and their association with the three complexes involved in the electron transport. A star symbolizes an excited state. The electron transport between the photosystem II complex and the cyt-b_6/f complex occurs by plastohydroquinone (PQH_2), which is oxidized by the cyt-b_6/f complex to plastoquinone (PQ). The electrons are transferred from the cyt-b_6/f complex to photosystem I by plastocyanin (PC). This reaction scheme is also valid for cyanobacteria with the exception that instead of plastocyanin, cytochrome-*c* is involved in the second electron transfer. For details see Figures 3.18 and 3.31.

water to $NADP^+$. In addition to this, about one-eighth of the light energy absorbed by the two photosystems is conserved by pumping protons into the lumen of the thylakoids via PS II and the cytochrome-b_6/f complex (Fig. 3.17). This proton transport leads to the formation of a proton gradient between the lumen and the stroma space. An H^+-ATP synthase, also located in the thylakoid membrane, uses the energy of the proton gradient to synthesize ATP.

Thus about half the absorbed light energy of the two photosystems is not used for chemical work but is dissipated as heat. The significance of the loss of energy as heat during photosynthetic electron transport has been discussed in section 2.3.

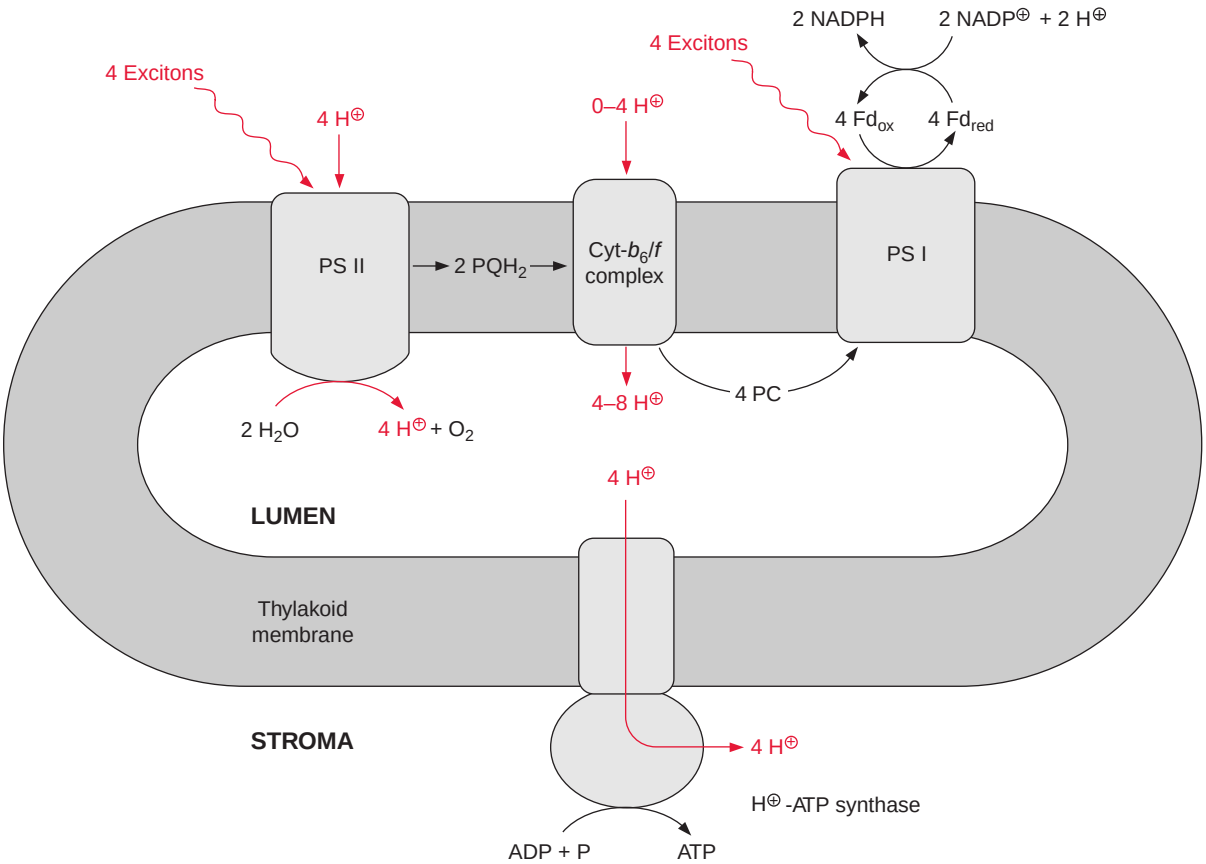

Figure 3.17 Schematic presentation of the localization of the photosynthetic complexes and the H^+-ATP synthase in the thylakoid membrane. Transport of electrons between PS II and the cytochrome-b_6/f complex is mediated by plastohydroquinone (PQH_2), and that between the cytochrome-b_6/f complex and PS I by plastocyanin (PC). Water splitting occurs on the luminal side of the membrane, and the formation of NADPH and ATP on the stromal side. The electrochemical gradient of protons pumped into the lumen drives ATP synthesis. The number of protons transported to the lumen during electron transport and the proton requirement of ATP synthesis is not known (section 4.4).

3.6 Water is split by photosystem II

The groups of Horst Witt and Wolfgang Saenger (both in Berlin) resolved the three-dimensional structure of **PS II** by X-ray structure analysis of crystals from the PS II of the thermophilic cyanobacteria *Thermosynechococcus elongatis*. The subsequent X-ray structure analysis of **PS I** revealed that PS II and PS I are constructed after the same basic principles as the reaction

centers of purple bacteria (section 3.4). This, and sequence analyses, clearly demonstrate that all **these photosystems have a common origin**. Thus PS II also has a chl-*a* pair in the center, although the distance between the two molecules is so large that probably only one of the two chl-*a* molecules reacts with the exciton. Two arms, each with one chl-*a* and one pheophytin molecule, are connected with this central pair as in the purple bacteria shown in Figure 3.10. Also in the cyanobacteria, only one of these arms appears to be involved in the electron transport.

In contrast to the bacterial reaction center the excitation of the reaction center results in an electron transfer via the chl-*a* monomer to pheophytin (Phe), and from there to a tightly bound plastoquinone (Q_A), thus forming a semiquinone radical (Fig. 3.18). The electron is then further transferred

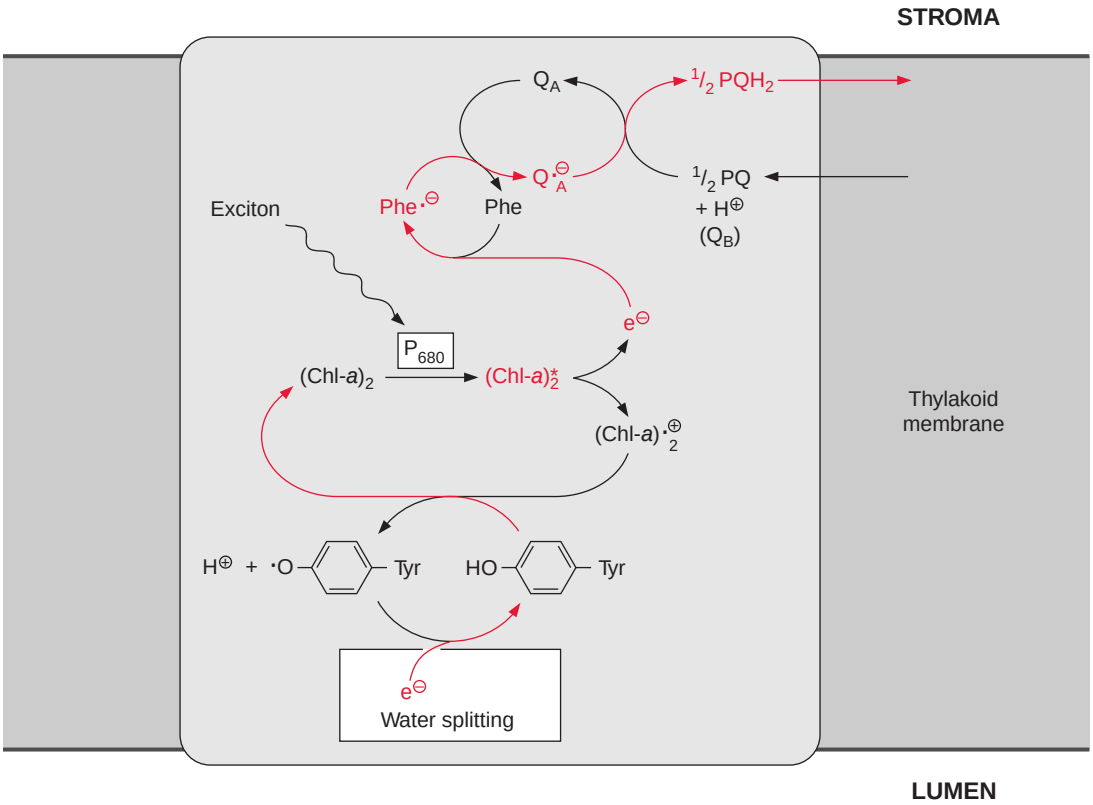

Figure 3.18 Reaction scheme of photosynthetic electron transport in the photosystem II complex. Excitation by a photon results in the release of one electron. The remaining positively charged chlorophyll radical is reduced by a tyrosine residue and the latter by a cluster of probably four manganese atoms involved in the oxidation of water (Fig. 3.20). The negatively charged chlorophyll radical transfers its electron via chl-*a* (not shown) and pheophytin and a quinone Q, of which the entire structure is not yet known, finally to plastoquinone.

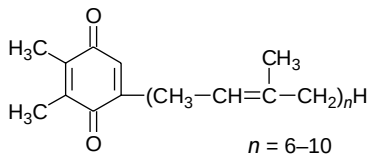

Plastoquinone

Figure 3.19
Plastoquinone.

to a loosely bound plastoquinone (Q_B). This plastoquinone (PQ) (Fig. 3.19) accepts two electrons and two protons one after the other and is thus reduced to hydroquinone (PQH_2). The hydroquinone is released from the photosynthesis complex and may be regarded as the final product of photosystem II. This sequence, consisting of a transfer of a single electron between (chl-*a*)$_2$ and Q_A and the transfer of two electrons between Q_A and Q_B, corresponds to the reaction sequence shown for *Rb. sphaeroides* (Fig. 3.11). The only difference is that the quinones are ubiquinone or menaquinone in bacteria and plastoquinone in photosystem II.

However, the similarity between the reaction sequence in PS II and the photosystem of the purple bacteria applies only to the electron acceptor region. The electron donor function in PS II of plants is completely different from that in purple bacteria. The electron deficit in $(\text{chl-}a)_2^{+\bullet}$ caused by non-cyclic electron transport is compensated for by electrons derived from the oxidation of water. In the transport of electrons from water to chlorophyll **manganese cations** and a **tyrosine** residue are involved. The $(\text{chl-}a)_2^{+\bullet}$ radical with a redox potential of about +1.1 volt is such a strong oxidant that it can withdraw an electron from a tyrosine residue in the protein of the reaction center and a tyrosine radical remains. This reactive tyrosine residue is often designated as Z. The electron deficit in the tyrosine radical is restored by oxidation of a manganese ion (Fig. 3.20). The PS II complex contains several manganese ions, probably four, which are close to each other. This arrangement of Mn ions is called the **Mn cluster**. The Mn cluster depicts a redox system that can take up and release four electrons. During this process the Mn ions probably change between the oxidation state Mn^{3+} and Mn^{4+}.

To liberate one molecule of O_2 from water, the reaction center must withdraw four electrons and thus capture four excitons. The time differences between the capture of the single exciton in the reaction center depends on the intensity of illumination. If oxidation of water were to proceed stepwise, **oxygen radicals** could be formed as intermediary products, especially at low light intensities. Oxygen radicals have a destructive effect on biomolecules such as lipids and proteins (section 3.10). The water splitting machinery of the Mn clusters minimizes the formation of oxygen radical intermediates by

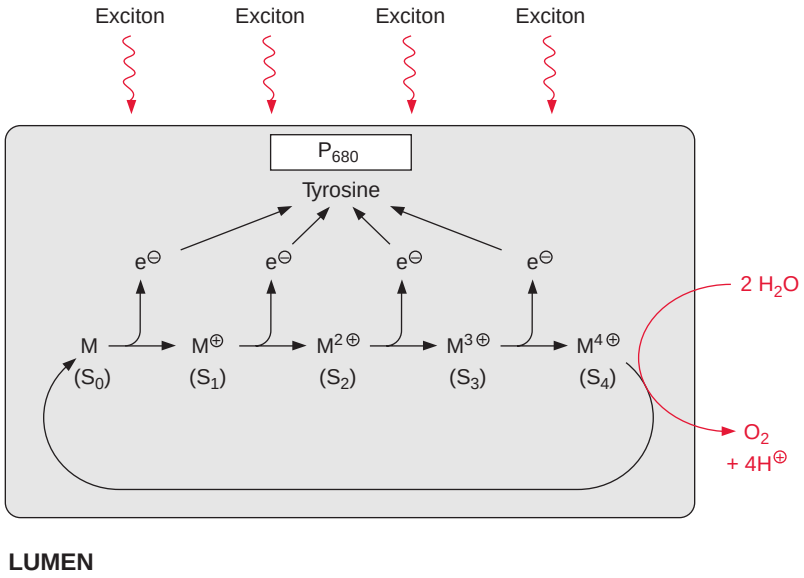

Figure 3.20 A schematic presentation of the mechanism of water splitting by photosystem II. M stands for a cluster of probably four manganese atoms. The different manganese atoms are present in different oxidation states. The cluster functions as a redox unit and feeds a total of four electrons, one after the other, into the reaction center of PS II. The deficit of these four electrons is compensated by splitting of $2H_2O$ into O_2 and $4H^+$. M stands for $(4Mn)^{n+}$, M^+ stands for $(4Mn)^{(n+1)+}$, and so on.

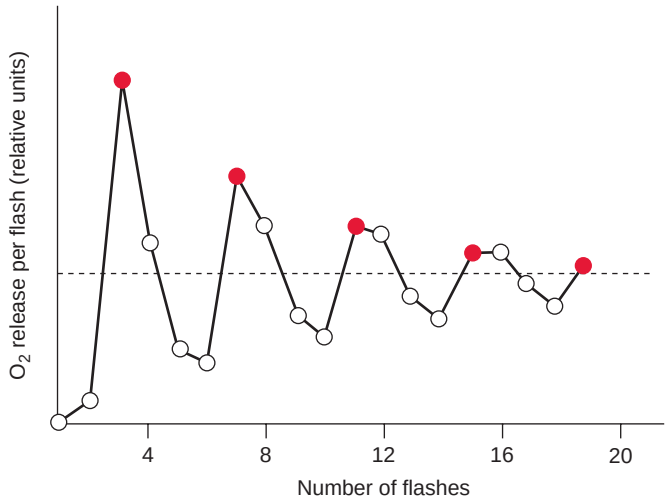

Figure 3.21 Yield of the oxygen released by chloroplasts as a function of the number of light pulses. The chloroplasts, previously kept in the dark, were illuminated by light pulses of 2 μs duration, interrupted by pauses of 0.3 s. (After Forbush, Kok, and McGoild, 1971.)

supplying the reaction center via tyrosine with four electrons one after the other (Fig. 3.20). The Mn cluster is transformed during this transfer from the ground oxidation state stepwise to four different oxidation states (these have been designated as S_0 and S_1–S_4).

Experiments by Pierre Joliot (France) and Bessel Kok (USA) presented evidence that the water splitting apparatus can be in five different oxidation states (Fig. 3.21). When chloroplasts that were kept in the dark were

then illuminated by a series of light pulses, an oscillation of the oxygen release was observed. Whereas after the first two light pulses almost no O_2 was released, the O_2 release was maximal after three pulses and then after a further four pulses, and so on. An increasing number of light pulses, however, dampened the oscillation. This can be explained by pulses that do not cause excitation of PS II and thus desynchronize the oscillation. In darkened chloroplasts the water splitting apparatus is in the S_1 state. After the fourth oxidation state (S_4) has been reached, O_2 is released in one reaction and the Mn cluster returns to its ground oxidation state (S_0). During this reaction, protons from water are released to the lumen of the thylakoids. The formal description of this reaction is:

$$2\,H_2O \rightarrow 4\,H^+ + 2\,O^{2-}$$

$$2\,O^{2-} + M^{4+} \rightarrow O_2 + M$$

Figuratively speaking, the four electrons needed in the reaction center are loaned in advance by the Mn cluster and then repaid at one stroke by oxidizing water to synthesize one oxygen molecule. In this way the Mn cluster minimizes the formation of oxygen radicals in photosystem II. Despite this safety device, still some oxygen radicals are formed in the PS II complex which damage the proteins of the complex. The consequences will be discussed in section 3.10.

Photosystem II complex is very similar to the reaction center in purple bacteria

Photosystem II is a complex consisting of at least 20 different subunits (Table 3.2), only two of which are involved in the actual reaction center. For the sake of simplicity the scheme of the PS II complex shown in Fig. 3.22 contains only some of these subunits. The PS II complex is surrounded by an antenna consisting of light harvesting complexes (Fig. 2.13).

The center of the PS II complex is a heterodimer consisting of the subunits **D_1** and **D_2** with six chl-*a*, two pheophytin, two plastoquinone, and one to two carotenoid molecules bound to it. The D_1 and D_2 proteins are homologous to each other and also to the L proteins and M proteins from the reaction center of the purple bacteria (section 3.4). As in purple bacteria, only the pheophytin molecule bound to the D_1 protein of PS II is involved in electron transport. Q_A is bound to the D_2 protein, whereas Q_B is bound to the D_1 protein. The Mn cluster is probably enclosed by both the D_1 and D_2 proteins. The tyrosine that is reactive in electron transfer is a constituent

Table 3.2: Protein components of photosystem II (list not complete)

Protein	Molecular mass (kDa)	Localization	Encoded in	Function
D_1	32	In membrane	Chloroplast	Binding of P_{680}, Pheo, Q_B, Tyr, Mn-cluster
D_2	34	"	"	Binding of P_{680}, Pheo, Q_A, Mn-cluster
CP_{47}	47	"	"	Core-antenna, binds peripheral antennae LHC
CP_{43}	43	"	"	" "
Cyt-$b_{559\alpha}$	9	"	"	Binds heme, protection of PS II against light damage
Cyt-$b_{559\beta}$	4	"	"	"
Manganese-stabilizing protein (MSP)	33	Peripheral: lumen	Nucleus	Stabilization of Mn-cluster
P	23	"	"	?
Q	16	"	"	?

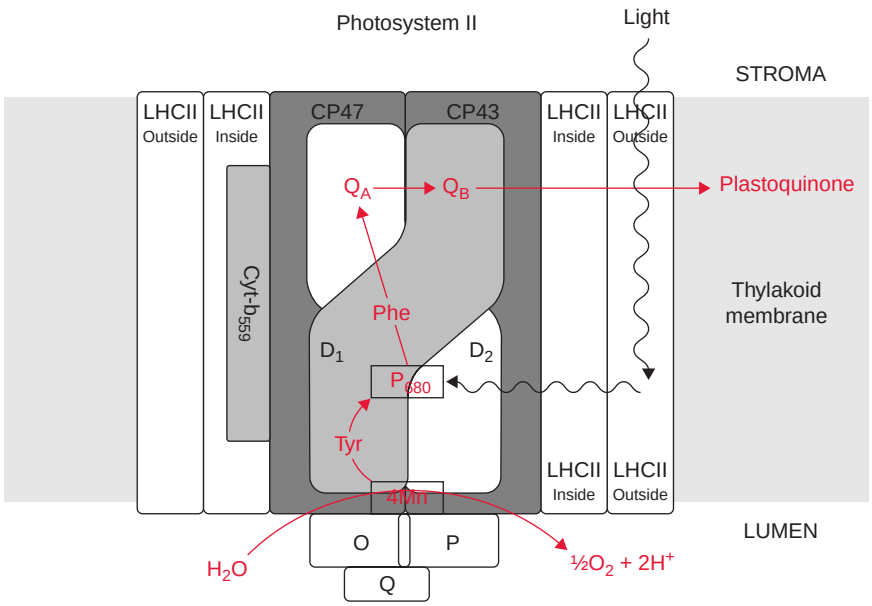

Figure 3.22 Schematic presentation of a simplified structure of the photosystem II complex. Structural analysis was carried out by the collaborating groups of Witt and Saenger (Berlin). The binding of quinone to the subunits D_1 and D_2 is homologous to the subunits L and M in purple bacteria. It appears that the structure of PS II and the structure of the reaction centers in purple bacteria share the same basic features (see also Table 3.2). The two core antennae CP_{43} and CP_{47} flank both sides of the D_1-D_2 complex. Attached to the core reaction center II are the inner and outer antennae (LHC I and LHC II).

of D_1. The subunits O, P, Q stabilize the Mn cluster. The two subunits CP 43 and CP 47 (CP means chlorophyll protein) each bind about 15 chlorophyll molecules and form the **core complex of the antenna** shown in Figure 2.10. CP 43 and CP 47 flank both sides of the D_1-D_2 complex. Cyt-b_{559} does not seem to be involved in the electron transport of PS II; possibly its function is to protect the PS II complex from light damage. The inner and outer light harvesting complexes of LHC II are arranged at the periphery.

The D_1 protein of the PS II complex has a high turnover; it is constantly being resynthesized. It seems that the D_1 protein wears out during its function, perhaps through damage by oxygen radicals, which still occurs despite all the protection mechanisms. It has been estimated that the D_1 protein is replaced after 10^6 to 10^7 catalytic cycles of the PS II reaction center.

A number of compounds that are similar in their structure to plastoquinone can block the plastoquinone binding site at the D_1 protein, causing inhibition of photosynthesis. Such compounds are used as weed killers (herbicides). Before the effect of these compounds is discussed in detail, some general aspects of the application of herbicides shall be introduced.

Mechanized agriculture usually necessitates the use of herbicides

About 50% of the money spent worldwide for plant protection is expended for **herbicides**. The high cost of labor is one of the main reasons for using herbicides in agriculture. It is cheaper and faster to keep a field free of weeds by using herbicides rather than manual labor. Weed control in agriculture is necessary not only to decrease harvest losses by weed competition, but also because weeds hinder the operation of harvesting machineries; fields free of weeds are a prerequisite for a mechanized agriculture. The herbicides usually block a specific reaction of the plant metabolism and have a low toxicity for animals and humans. A large number of herbicides (examples will be given at the end of this section) inhibit photosystem II by being antagonists to plastoquinone. To achieve substantial inhibition the herbicide molecule has to bind to most of the many photosynthetic reaction centers. To be effective, 125 to 4,000 g of these herbicides have to be applied per hectare.

In an attempt to reduce the amount of herbicides applied to the soil, new efficient herbicides have been developed that inhibit key biosynthetic processes such as the synthesis of fatty acids, amino acids (sections 10.1 and 10.4), carotenoids, or chlorophyll. There are also herbicides that act as analogues of phytohormones or mitosis inhibitors. Some of these herbicides are effective with amounts as low as 5 g per hectare.

Some herbicides are taken up only by the roots and others by the leaves. To keep the railway tracks free of weeds, **nonselective herbicides** are employed, which destroy the complete vegetation. Nonselective herbicides are also used in agriculture, e.g., to combat weeds in citrus plantations. In the latter case, herbicides are applied that are only taken up by the leaves to combat herbaceous plants at the ground level. Especially interesting are **selective herbicides** that combat only weeds and effect cultivars as little as possible (sections 12.2 and 15.3). Selectivity can be due to different uptake efficiencies of the herbicide in different plants, different sensitivities of the metabolism towards the herbicide, or different ability of the plants to detoxify the herbicide. Important mechanisms that plants utilize to detoxify herbicides and other foreign compounds (xenobiotics) are the introduction of hydroxyl groups by P-450 monooxygenases (section 18.2) and the formation of glutathione conjugates (section 12.2). Selective herbicides have the advantage that weeds can be destroyed at a later growth stage of the cultivars where the dead weeds form a mulch layer conserving water and preventing erosion.

In some cases, the application of herbicides has led to the evolution of herbicide-resistant plant mutants (section 10.4). Conventional breeding has used such mutated plants to generate herbicide-resistant cultivars. In contrast to the occurrence of herbicide resistance by accidental mutations, nowadays genetic engineering is employed on a very large scale to generate cultivars which are resistant to a certain herbicide, allowing weed control in the presence of the growing cultivar (section 22.6)

A large number of herbicides inhibit photosynthesis: the urea derivative **DCMU** (Diuron, DuPont), the triazine **Atrazine** (earlier Ciba Geigy), **Bentazon** (BASF) (Fig. 3.23), and many similar compounds function as herbicides by binding to the plastoquinone binding site on the D_1 protein and thus blocking the photosynthetic electron transport. Nowadays, DCMU is not often used, as the required dosage is high and its degradation is slow. It is, however, often used in the laboratory to inhibit photosynthesis in an experiment (e.g., of leaves or isolated chloroplasts). Atrazine acts selectively: maize plants are relatively insensitive to this herbicide since they have a particularly efficient mechanism for its detoxification (section 12.2). Because of its relatively slow degradation in the soil, the use of Atrazine has been restricted in some countries, e.g., Germany. In areas where certain herbicides have been used continuously over the years, some weeds have become resistant to these herbicides. In some cases, the resistance can be traced back to mutations resulting in a single amino acid change in the D_1-proteins. These changes do not markedly affect photosynthesis of these weeds, but they do decrease binding of the herbicides to the D_1-protein.

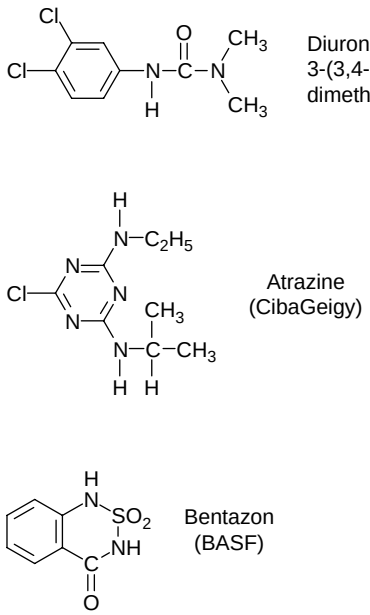

Figure 3.23 Inhibitors of photosystem II used as herbicides.

3.7 The cytochrome-b_6/f complex mediates electron transport between photosystem II and photosystem I

Iron atoms in cytochromes and in iron-sulfur centers have a central function as redox carriers

Cytochromes occur in all organisms except a few obligate anaerobes. These are proteins to which one to two **tetrapyrrole** rings are bound. These tetrapyrroles are very similar to the chromophores of chlorophylls. However, chlorophylls contain Mg^{++} as the central atom in the tetrapyrrole, whereas the cytochromes have an iron atom (Fig. 3.24). The tetrapyrrole ring of the cytochromes with iron as the central atom is called the **heme**. The bound iron atom can change between the oxidation states $\mathbf{Fe^{+++}}$ and $\mathbf{Fe^{++}}$ so that cytochromes function as a one-electron-carrier, in contrast to quinones, NAD(P) and FAD, which transfer two electrons together with protons.

Cytochromes are divided into three main groups, the cytochromes-*a*, -*b*, and -*c*. These correspond to heme-*a*, -*b*, and -*c*. Heme-*b* may be regarded as the basic structure (Fig. 3.24). In heme-*c* the -SH-group of a **cysteine** is added to each of the two vinyl groups of heme-*b*. In this way heme-*c* is

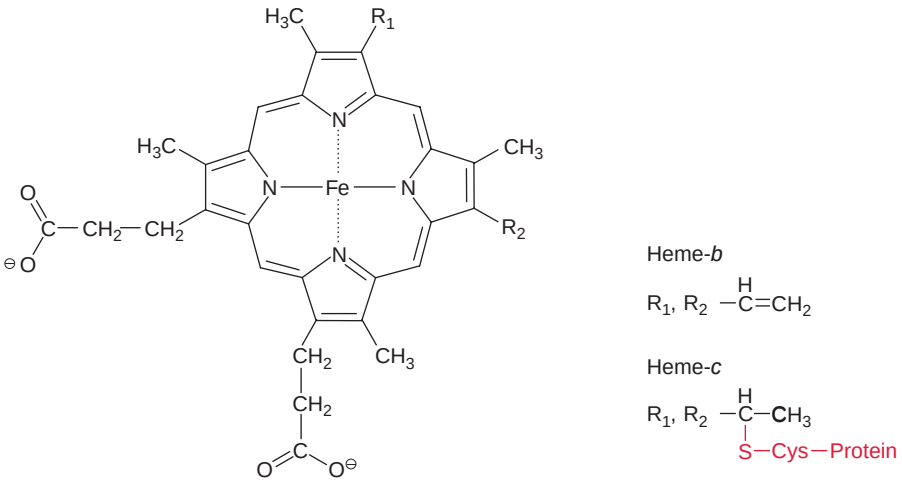

Figure 3.24 Heme-*b* and heme-*c* as prosthetic group of the cytochromes. Heme-*c* is covalently bound to the cytochrome apoprotein by the addition of two cysteine residues of the apoprotein to the two vinyl groups of heme-*b*.

covalently bound by a sulfur bridge to the protein of the cytochrome. Such a mode of covalent binding has already been shown for phycocyanin in Figure 2.15, and there is actually a structural relationship between the corresponding apoproteins. In heme-*a* (not shown) an **isoprenoid side chain** consisting of three isoprene units is attached to one of the vinyl groups of heme-*b*. This side chain functions as a hydrophobic membrane anchor, similar to that found in quinones (Figs. 3.5 and 3.19). Heme-*a* is mentioned here only for the sake of completeness. It plays no role in photosynthesis, but it does have a function in the mitochondrial electron transport chain (section 5.5).

The iron atom in the heme can form up to six coordinative bonds. Four of these bonds are formed with the nitrogen atoms of the tetrapyrrole ring. This ring has a planar structure. The two remaining bonds of the Fe atom coordinate with two histidine residues, which are positioned vertically to the tetrapyrrole plane (Fig. 3.25). Cyt-*f* (*f* = foliar, in leaves) contains, like cyt-*c*, one heme-*c* and therefore belongs to the *c*-type cytochromes. In cyt-*f* one bond of the Fe atom coordinates with the terminal amino group of the protein and the other with a histidine residue.

Iron-sulfur centers are of general importance as electron carriers in electron transport chains and thus also in photosynthetic electron transport. Cysteine residues of proteins within iron-sulfur centers (Fig. 3.26) are coordinatively or covalently bound to Fe atoms. These iron atoms are linked to each other by S-bridges. Upon acidification of the proteins, the sulfur between the Fe atoms is released as H_2S and for this reason it has been called **labile sulfur**. Iron-sulfur centers occur mainly as 2Fe-2S or 4Fe-4S centers. The Fe atoms in these centers are present in the oxidation states

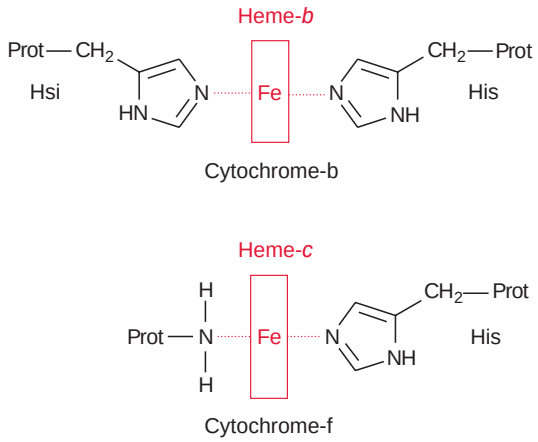

Figure 3.25 Axial ligands of the Fe atoms in the heme groups of cytochrome-*b* and cytochrome-*f*. Of the six possible coordinative bonds of the Fe atom in the heme, four are saturated with the N atoms present in the planar tetrapyrrole ring. The two remaining coordinative bonds are formed either with two histidine residues of the protein, located vertically to the plane of the tetrapyrrole, or with the terminal amino group and one histidine residue of the protein. Prot = protein.

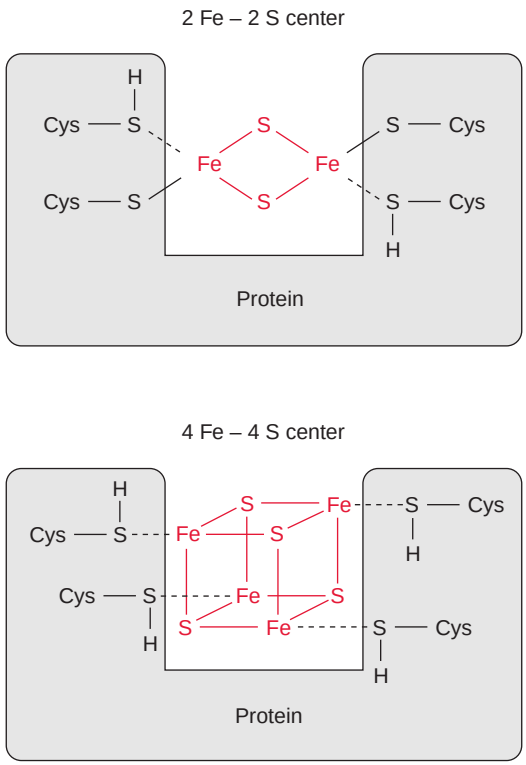

Figure 3.26 Structure of metal clusters of iron-sulfur proteins.

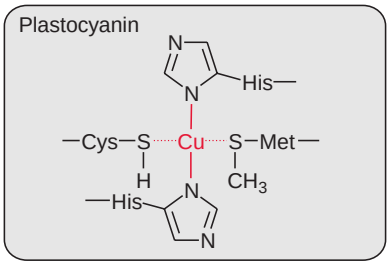

Figure 3.27 Plastocyanin. Two histidine, one methionine, and one cysteine residue of the apoprotein bind one Cu atom, which changes between the redox states Cu^{+} and Cu^{++} by the addition or removal of an electron.

Fe^{++} and Fe^{+++}. Irrespective of the number of Fe atoms in a center, the oxidized and reduced state of the center differs only by a single charge. For this reason, iron-sulfur centers can take up and transfer only one electron. Various iron-sulfur centers have very different redox potentials, depending on the surrounding protein.

The electron transport by the cytochrome-b_6/f complex is coupled to a proton transport

Plastohydroquinone (PQH_2) formed by PS II diffuses through the lipid phase of the thylakoid membrane and transfers its electrons to the cytochrome-b_6/f complex (Fig. 3.17). This complex then transfers the electrons to **plastocyanin**, which is thus reduced. Therefore the cytochrome-b_6/f complex has also been called **plastohydroquinone-plastocyanin oxidoreductase**. Plastocyanin is a protein with a molecular mass of 10.5 kDa, containing a **copper atom**, which is coordinatively bound to one cysteine, one methionine, and two histidine residues of the protein (Fig. 3.27). This copper atom alternates between the oxidation states Cu^{+} and Cu^{++} and thus is able to take up and transfer one electron. Plastocyanin is soluble in water and is located in the thylakoid lumen.

Electron transport through the cyt-b_6/f complex proceeds along a potential difference gradient of about 0.4 V (Fig. 3.16). The energy liberated by the transfer of the electron down this redox gradient is conserved by transporting protons to the thylakoid lumen. The cyt-b_6/f complex is a membrane protein consisting of at least eight subunits. The main components of this complex are four subunits: cyt-b_6, cyt-f, an iron-sulfur protein called **Rieske protein** after its discoverer, and a subunit IV. Additionally, there are some smaller peptides and a chlorophyll and a carotenoid of unknown function. The Rieske protein has a 2Fe-2S center with the very positive redox potential of +0.3 V, untypical of such iron-sulfur centers.

The cyt-b_6/f complex has an **asymmetric structure** (Fig. 3.28). Cyt-b_6 and subunit IV span the membrane. Cyt-b_6 containing two heme-b molecules is almost vertically arranged to the membrane and forms a redox chain across

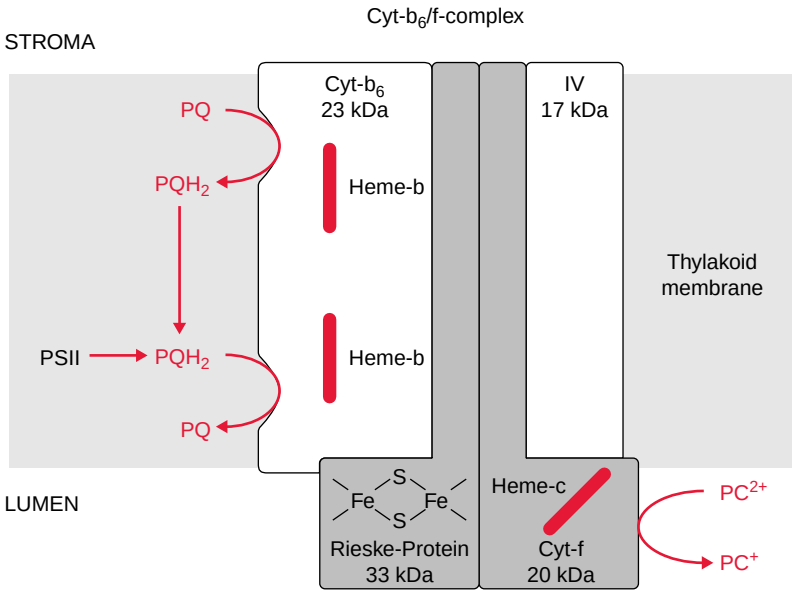

Figure 3.28 Schematic presentation of the structure of the cytochrome-b_6/f complex. The scheme is based on the molecular structures predicted from the amino acid sequences. (After Hauska.)

Table 3.3: Function of cytochrome-*b*/*c* complexes

Purple bacteria	Cyt-b/c_1	Reduction of cyt-*c*	Proton pump
Green sulfur bacteria	Cyt-b/c_1	"	"
Mitochondria	Cyt-b/c_1	"	"
Cyanobacteria	Cyt-b_6/f	"	"
Chloroplasts	Cyt-b_6/f	Reduction of plastocyanin	"

the membrane. Cyt-b_6 also contains a heme-*c*, of which the function has not been fully resolved and is therefore not shown in the figure. Cyt-b_6 has two binding sites for PQH_2/PQ, one in the region of the lumen and one in the region of the stroma. The function of these binding sites will be explained in Figures 3.29 and 3.30. The iron sulfur **Rieske protein** protrudes from the lumen into the membrane. Closely adjacent to it is **cyt-*f*** containing a binding site responsible for the reduction of plastocyanin. The Rieske protein and cyt-*f* are attached to the membrane by a membrane anchor.

The cyt-b_6/f complex resembles in its structure the cyt-b/c_1 complex in bacteria and mitochondria (section 5.5). Table 3.3 summarizes the function of these cyt-b_6/f and cyt-b/c_1 complexes. All these complexes possess

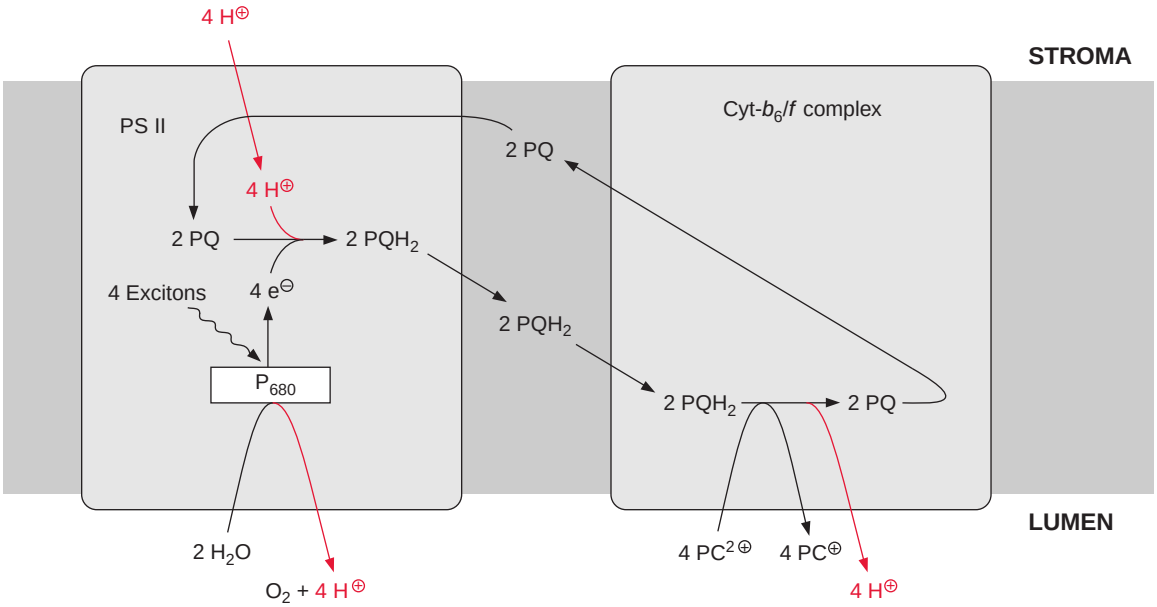

Figure 3.29 Proton transport coupled to electron transport by PS II and the cyt-b_6/f complex in the absence of a Q-cycle The oxidation of water occurs by the reaction center of PS II and the oxidation of plastohydroquinone (PQH_2) by cyt-b_6/f, both at the luminal side of the thylakoid membrane. PQH_2 reacts with a binding site in the lumen region, and PQ and PQH_2 diffuse through the lipid phase of the membrane away from the cyt-b_6/f complex.

one iron-sulfur protein. The amino acid sequence of cyt-*b* in the cyt-b/c_1 complex of bacteria and in mitochondria corresponds to the sum of the sequences of cyt-b_6 and the subunit IV in the cyt-b_6/f complex. Apparently during evolution the cyt-*b* gene was cleaved into two genes, for cyt-b_6 and subunit IV. Whereas in plants the cyt-b_6/f complex reduces plastocyanin, the cyt-b/c_1 complex of bacteria and mitochondria reduces cyt-*c*. Cyt-*c* is a very small cytochrome molecule that is water-soluble and, like plastocyanin, transfers redox equivalents from the cyt-b_6/f complex to the next complex along the aqueous phase. In cyanobacteria, which also possess a cyt-b_6/f complex, the electrons are transferred from this complex to photosystem I via cyt-*c* instead of plastocyanin. The great similarity between the cyt-b_6/f complex in plants and the cyt-b/c_1 complexes in bacteria and mitochondria suggests that these complexes have basically similar functions in photosynthesis and in mitochondrial oxidation: they are proton translocators that are driven by a hydroquinone-plastocyanin (or -cyt-*c*) reductase.

The interplay of PS II and the cyt-b_6/f complex electron transport causes the transport of protons from the stroma space to the thylakoid lumen. The principle of this transport is explained in the schematic presentations

of Figures 3.28 and 3.29. A crucial point is that the reduction and oxidation of the quinone occur at different sides of the thylakoid membrane. The required protons for the reduction of PQ (Q_b) by the PS II complex are taken up from the stroma space. Subsequently PQH_2 diffuses across the lipid phase of the membrane to the binding site in the lumenal region of the cyt-b_6/f complex where it is oxidized by the Rieske protein and cyt-*f* to yield reduced plastocyanin. The protons of this reaction are released into the thylakoid lumen. According to this scheme, the capture of four excitons by the PS II complex transfers four protons from the stroma space to the lumen. In addition four protons produced during water splitting by PS II are released into the lumen as well.

The number of protons pumped through the cyt-b_6/f complex can be doubled by a Q-cycle

Studies with mitochondria indicated that during electron transport through the cyt-b/c_1 complex, the number of protons transferred per transported electron is larger than four (Fig. 3.29). Peter Mitchell (Great Britain), who established the chemiosmotic hypothesis of energy conservation (section 4.1), also postulated a so-called **Q-cycle**, by which the number of transported protons for each electron transferred through the cyt-b/c_1 complex is doubled. It later became apparent that the Q-cycle also has a role in photosynthetic electron transport.

Figure 3.30 shows the principle of Q-cycle operation in the photosynthesis of chloroplasts. The cyt-b_6/f complex contains two different binding sites for conversion of quinones, one located at the stromal side and the other at the luminal side of the thylakoid membrane (Fig. 3.28). The plastohydroquinone (PQH_2) formed in the PS II complex is oxidized by the Rieske iron-sulfur center at the binding site adjacent to the lumen. Due to its very positive redox potential, the Rieske protein tears off one electron from the plastohydroquinone. Because its redox potential is very negative, the remaining semiquinone is unstable and transfers its electron to the first heme-*b* of the cyt-b_6 (b_p) and from there to the other heme-*b* (b_n), thus raising the redox potential of heme b_n to about –0.1 V. In this way a total of four protons are transported to the thylakoid lumen per two molecules of plastohydroquinone oxidized. Of the two plastoquinone molecules (PQ) formed, only one molecule returns to the PS II complex. The other PQ diffuses away from the cyt-b_6/f complex through the lipid phase of the membrane to the stromal binding site of the cyt-b_6/f complex to be reduced via semiquinone to hydroquinone by the high reduction potential of heme-b_n. This is accompanied by the uptake of two protons from the stromal space. The hydroquinone thus regenerated diffuses through the membrane back to

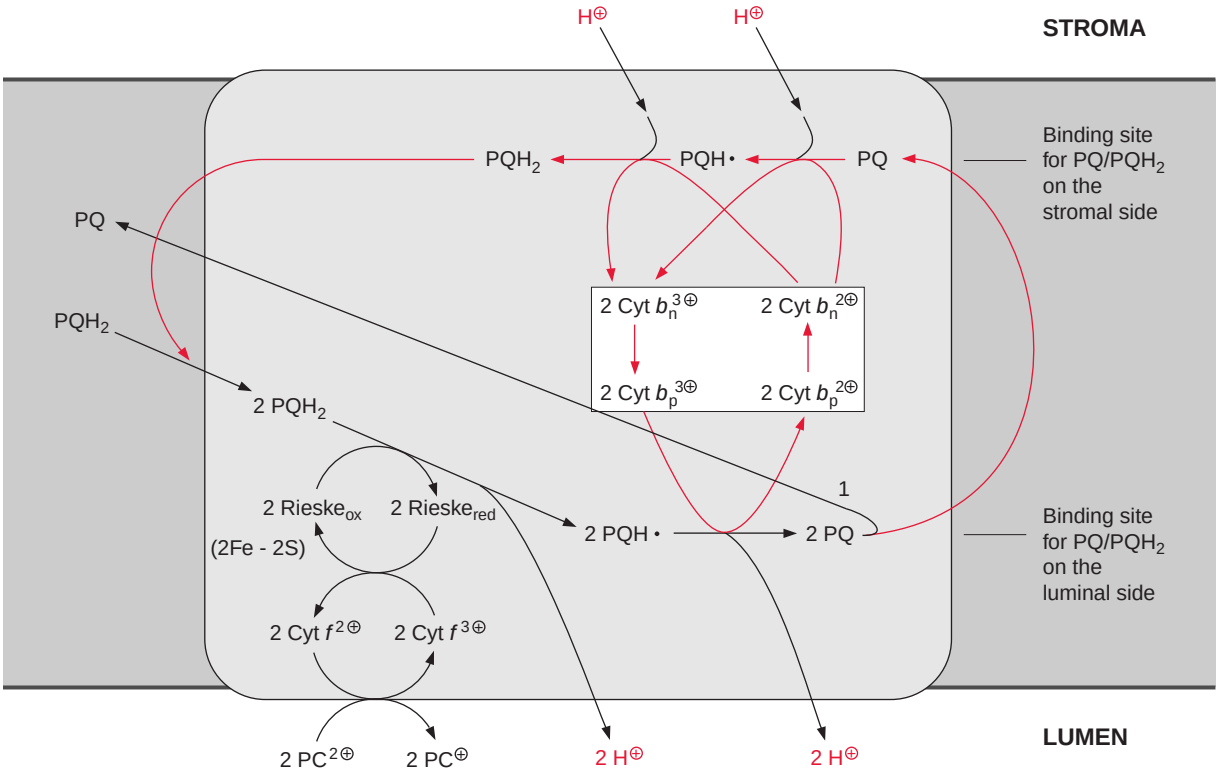

Figure 3.30 The number of protons released by the cyt-b_6/f complex to the lumen is doubled by the Q-cycle. This cycle is based on the finding that the redox reactions of the PQH_2 and PQ occur at two binding sites, one in the lumen and one in the stromal region of the thylakoid membrane (Fig. 3.28). The movement of the quinones between these binding sites occurs by diffusion through the lipid phase of the membrane. The Q-cycle is explained in more detail in the text.

the luminal binding site where it is oxidized in turn by the Rieske protein, and so on. In total, the number of transported protons is doubled by the Q-cycle (1/2 + 1/4 + 1/8 + 1/16… + 1/n = 1). The fully operating Q-cycle transports four electrons through the cyt-b_6/f complex which results in total to the transfer of eight protons from the stroma to the lumen. The function of this Q-cycle in mitochondrial oxidation is now undisputed, while its function in photosynthetic electron transport is still a matter of controversy. The analogy of the cyt-b_6/f complex to the cyt-b/c_1 complex suggests that the Q-cycle also plays an important role in chloroplasts. So far, the operation of a Q-cycle in plants has been observed mainly under low light conditions. The Q-cycle is perhaps suppressed by a high proton gradient generated across the thylakoid membrane, for instance, by irradiation with high light intensity. In this way the flow of electrons through the Q-cycle could be adjusted to the energy demand of the plant cell.

3.8 Photosystem I reduces $NADP^+$

Plastocyanin that has been reduced by the cyt-b_6/f complex diffuses through the lumen of the thylakoids, binds to a positively charged binding site of PS I, transfers its electron, and the resulting oxidized form diffuses back to the cyt-b_6/f complex (Fig. 3.31).

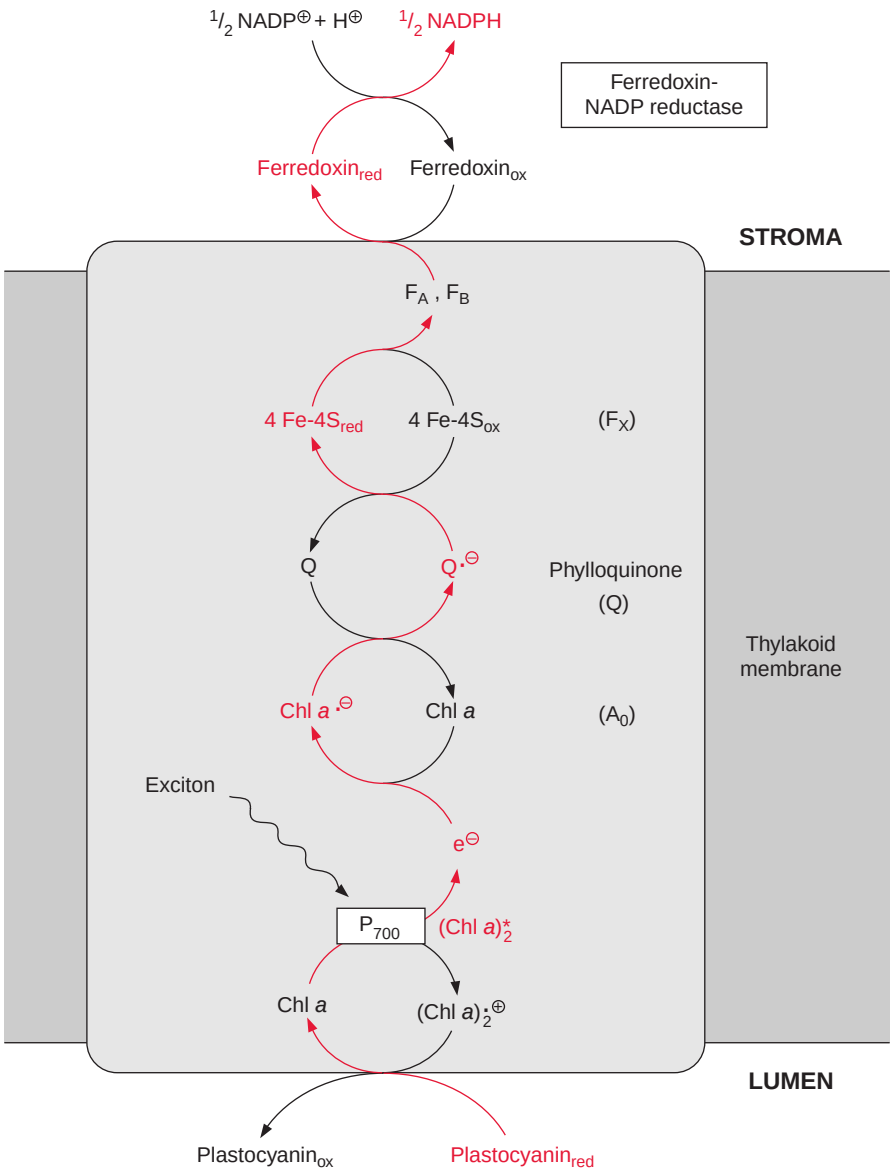

Figure 3.31 Reaction scheme of electron transport in photosystem I. The negatively charged chlorophyll radical formed after excitation of a chlorophyll pair results in reduction of $NADP^+$ via chl-*a*, phylloquinone, and three iron-sulfur proteins. The electron deficit in the positively charged chlorophyll radical is compensated by an electron delivered from plastocyanin.

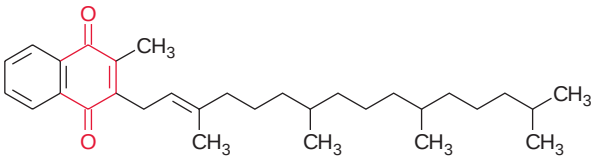

Figure 3.32
Phylloquinone.

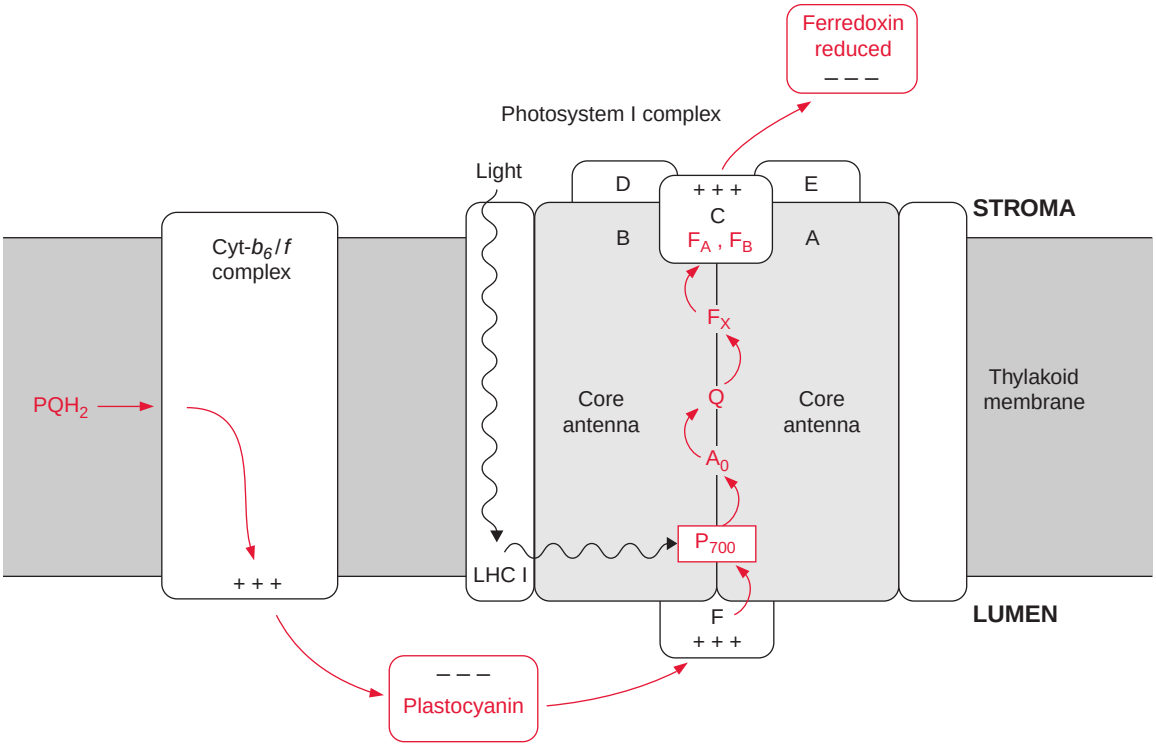

Figure 3.33 Schematic presentation of the structure of the photosystem I complex. This scheme is based on results of X-ray structure analyses. The principal structure of the PSI complex is similar to that of the PSII complex.

Also the reaction center of PS I with an absorption maximum of 700 nm contains a chlorophyll pair (chl-*a*)$_2$ (Fig. 3.31). As in PS II, the excitation caused by a photon reacts probably with only one of the two chlorophyll molecules. The resulting (chl-*a*)$_2^{+\bullet}$ is then reduced by plastocyanin. It is assumed that (chl-*a*)$_2$ transfers its electron to a chl-*a* monomer (A_0), which then transfers the electron to a strongly bound **phylloquinone** (Q) (Fig. 3.32). Phylloquinone contains the same phytol side chain as chl-*a* and its function corresponds to Q_A in PS II. The electron is transferred from the semiphylloquinone to an iron-sulfur center named F_X. F_X is a 4Fe-4S center

Table 3.4: Protein components of photosystem I (list not complete)

Protein	Molecular mass (kDa)	Localization	Encoded in	Function
A	83	In membrane	Chloroplast	Binding of P_{700}, chl-***a***, A_0, A_1, Q F_x, antennae function
B	82	"	"	(as in protein A)
C	9	Peripheral:stroma	"	Binding of F_A, F_B, ferredoxin
D	17	"	Nucleus	"
E	10	"	"	"
F	18	Peripheral:lumen	"	Binding of plastocyanin
H	10	Peripheral:stroma	Nucleus	Binding of LHC II

with a very negative redox potential. It transfers one electron to two other 4Fe-4S centers (F_A, F_B), which in turn reduce **ferredoxin**, a protein with a molecular mass of 11 kDa with a 2Fe-2S center. Ferredoxin also takes up and transfers only one electron. The reduction occurs at the stromal side of the thylakoid membrane. For this purpose, the ferredoxin binds at a positively charged binding site on subunit D of PS I (Fig. 3.33). The reduction of $NADP^+$ by ferredoxin, catalyzed by **ferredoxin-NADP reductase**, yields NADPH as an end product of the photosynthetic electron transport.

The PS I complex consists of at least 17 different subunits, of which some are shown in Table 3.4. The center of the PS I complex is a **heterodimer** (as is the center of PS II) consisting of subunits A and B (Fig. 3.33). The molecular masses of **A** and **B** (each 82–83 kDa) correspond approximately to the sum of the molecular masses of the PS II subunits D_1 and CP_{43}, and D_2 and CP_{47}, respectively (Table 3.2). In fact, both subunits A and B have a double function. Like D_1 and D_2 in PS II, they bind chromophores (chl-*a*) and redox carriers (phylloquinone, FeX) of the reaction center and, additionally, they contain about 100 chl-*a* molecules as antennae pigments. Thus, the heterodimer of A and B represents the reaction center and the core antenna as well. The three-dimensional structure of photosystem I in cyanobacteria, green algae and plants has been resolved. The principal structure of photosystem I, with a central pair of chl-*a* molecules and two branches, each with two chlorophyll molecules, is very similar to photosystem II and to the bacterial photosystem (Fig. 3.10). It has not been definitely clarified whether both or just one of these branches are involved in the electron transport. The Fe-S-centers F_A and F_B are ascribed to subunit C, and subunit F is considered to be the binding site for plastocyanin.

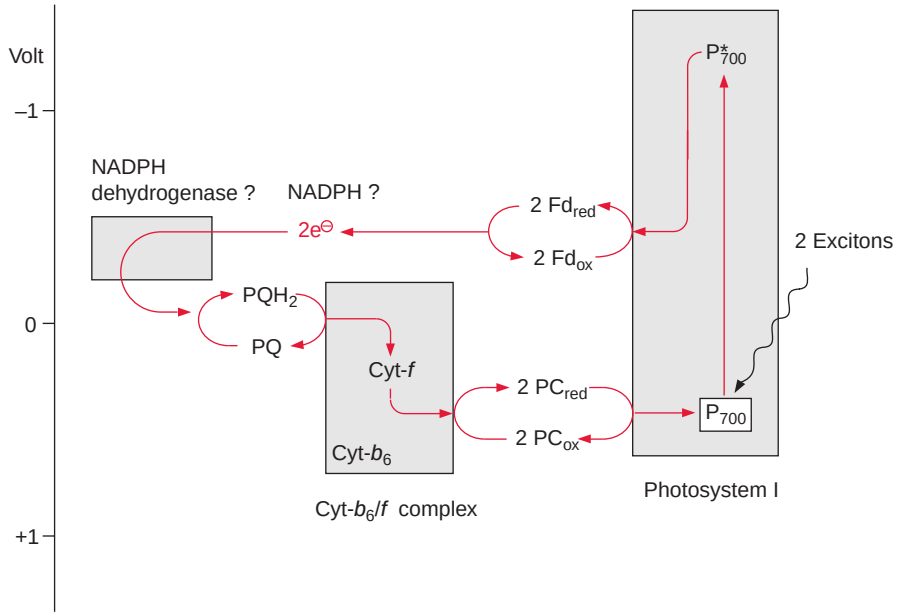

Figure 3.34 Cyclic electron transport between photosystem I and the cyt-b_6/f complex. The path of the electrons from the excited PS I to the cyt-b_6/f complex is still unclear.

The light energy driving the cyclic electron transport of PS I is only utilized for the synthesis of ATP

Besides the noncyclic electron transport discussed so far, cyclic electron transfer can also take place in which the electrons from the excited photosystem I are transferred back to the ground state of PS I, probably via the cyt-b_6/f complex (Fig. 3.34). The energy thus released is used only for the synthesis of ATP, and NADPH is not formed. This electron transport is termed **cyclic photophosphorylation**. In intact leaves, and even in isolated intact chloroplasts, it is quite difficult to differentiate experimentally between cyclic and non-cyclic photophosphorylation. It has been a matter of debate as to whether and to what extent cyclic photophosphorylation occurs in a leaf under normal physiological conditions. Recent evaluations of the proton stoichiometry of photophosphorylation (see section 4.4) suggest that the yield of ATP in noncyclic electron transport is not sufficient for the requirements of CO_2 assimilation, and therefore cyclic photophosphorylation seems to be required to synthesize the lacking ATP. Moreover, cyclic photophosphorylation must operate at very high rates in the bundle sheath chloroplasts of certain C_4 plants (section 8.4). These cells have a high demand for ATP and they contain high PS I activity but very little PS II. Presumably, the cyclic electron flow is governed by the redox state of the acceptor of the photosystem in such a way that by increasing the reduction of the NADP system, and consequently of ferredoxin, the diversion of the

electrons in the cycle is enhanced. The function of cyclic electron transport is probably to adjust the rates of ATP and NADPH formation according to the plant's demand.

Despite intensive investigations, the pathway of electron flow from PS I to the cyt-b_6/f complex in cyclic electron transport remains unresolved. It has been proposed that cyclic electron transport is structurally separated from the linear electron transport chain in a super complex. Most experiments on cyclic electron transport have been carried out with isolated thylakoid membranes that catalyze only cyclic electron transport when redox mediators, such as ferredoxin or flavin adenine mononucleotide (FMN, Fig. 5.16), have been added. Cyclic electron transport is inhibited by the antibiotic **antimycin A**. It is not clear at which site this inhibitor functions. Antimycin A does not inhibit noncyclic electron transport.

Surprisingly, proteins of the NADP dehydrogenase complex of the mitochondrial respiratory chain (section 5.5) have also been identified in the thylakoid membrane of chloroplasts. The function of these proteins in chloroplasts is still not known. The proteins of this complex occur very frequently in chloroplasts from bundle sheath cells of C_4 plants, which have little PS II but a particularly high cyclic photophosphorylation activity (section 8.4). These observations raise the possibility that in cyclic electron transport the flow of electrons from NADPH or ferredoxin to plastoquinone proceeds via a complex similar to the mitochondrial NADH dehydrogenase complex. As will be shown in section 5.5, the mitochondrial NADH dehydrogenase complex transfers electrons from NADH to ubiquinone. Results indicate that an additional pathway for a cyclic electron transport exists in which electrons are directly transferred via a plastoquinone reductase from ferredoxin to plastoquinone.

3.9 In the absence of other acceptors electrons can be transferred from photosystem I to oxygen

When ferredoxin is very highly reduced, it is possible that electrons are transferred from PS I to oxygen to form **superoxide radicals** ($\bullet O_2^-$) (Fig. 3.35). This process is called the **Mehler reaction**. The superoxide radical reduces metal ions present in the cell such as Fe^{3+} and Cu^{2+} (M^{n+}):

$$\bullet O_2^- + M^{n+} \rightarrow O_2 + M^{(n-1)+}$$

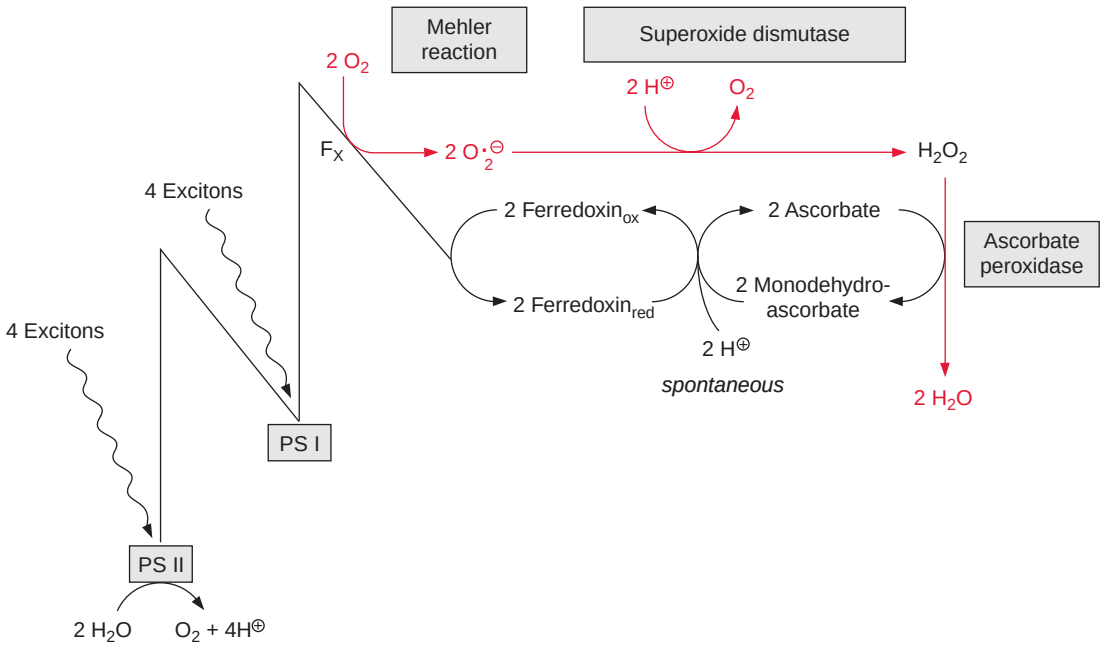

Figure 3.35 A scheme for the Mehler reaction. Upon strong reduction of ferredoxin, electrons are transferred by the Mehler reaction to oxygen and superoxide is formed. The elimination of this highly aggressive superoxide radical involves reactions catalyzed by superoxide dismutase and ascorbate peroxidase.

Superoxide dismutase catalyzes the dismutation of $\bullet\mathbf{O_2^-}$ into H_2O_2 and O_2, accompanied by the uptake of two protons:

$$2 \bullet O_2^- + 2\,H^+ \rightarrow O_2 + H_2O_2$$

$\bullet\mathbf{O_2^-}$, H_2O_2 and •OH are summarized as **ROS** (reactive oxygen species). The metal ions reduced by superoxide react with hydrogen peroxide to form hydroxyl radicals:

$$H_2O_2 + M^{(n-1)+} \rightarrow OH^- + \bullet OH + M^{n+}$$

The hydroxyl radical (**•OH**) is a very aggressive substance and damages enzymes and lipids by oxidation. The plant cell has no protective enzymes against •OH. Therefore it is essential that a reduction of the metal ions be prevented by rapid elimination of $\bullet\mathbf{O_2^-}$ by superoxide dismutase. But hydrogen peroxide ($\mathbf{H_2O_2}$) also has a damaging effect on many enzymes. To prevent such damage, hydrogen peroxide is eliminated by an **ascorbate**

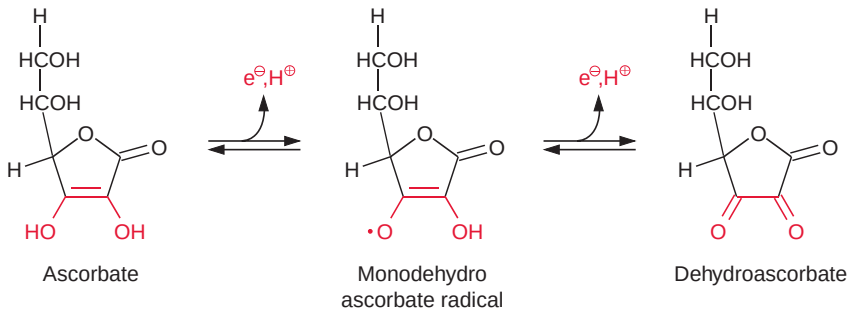

Figure 3.36 The oxidation of ascorbate proceeds via the formation of the monodehydroascorbate radical.

peroxidase located in the thylakoid membrane. **Ascorbate**, an important antioxidant in plant cells (Fig. 3.36), is oxidized by this enzyme and converted to the radical **monodehydroascorbate**, which is spontaneously reconverted by photosystem I to ascorbate via reduced ferredoxin. Monodehydroascorbate can be also reduced to ascorbate by an NAD(P)H-dependent monodehydroascorbate reductase that is present in the chloroplast stroma and the cytosol.

As an alternative to the preceding reaction, two molecules of monodehydroascorbate can dismutate to ascorbate and dehydroascorbate. Dehydroascorbate is reconverted to ascorbate by reduction with glutathione in a reaction catalyzed by **dehydroascorbate reductase** present in the stroma (Fig. 3.37). **Glutathione** (**GSH**) occurs as an antioxidant in all plant

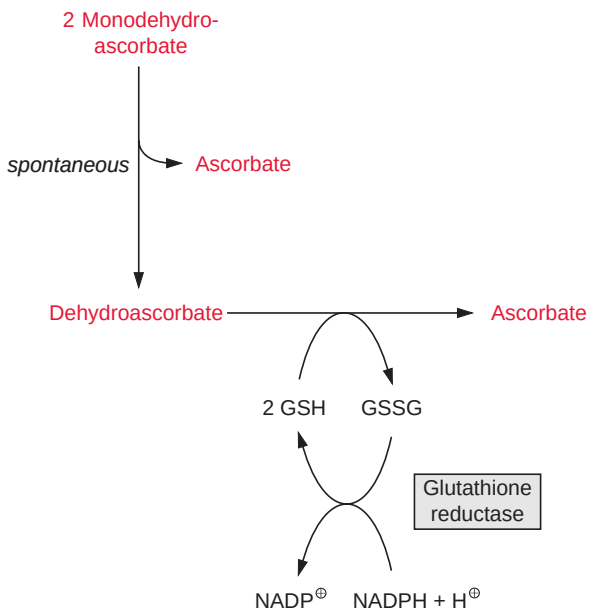

Figure 3.37 Dehydroascorbate can be reduced to form ascorbate by interplay of glutathione and glutathione reductase.

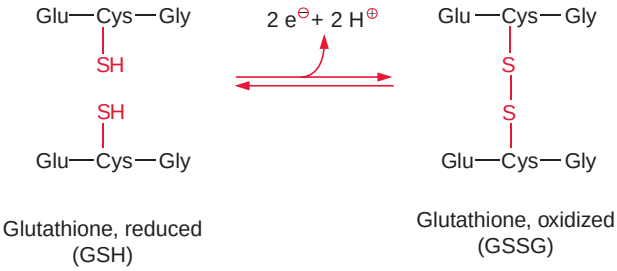

Figure 3.38 Redox reaction of glutathione.

cells (section 12.2). It is a tripeptide composed of the amino acids glutamate, cysteine, and glycine (Fig. 3.38). Oxidation of GSH results in the formation of a disulfide (**GSSG**) between the cysteine residues of two glutathione molecules. Reduction of GSSG is catalyzed by a **glutathione reductase** with NADPH as the reductant (Fig. 3.37).

The major function of the Mehler-ascorbate-peroxidase cycle is to dissipate excessive excitation energy of photosystem I as heat. The absorption of a total of eight excitons via PS I results in the formation of two superoxide radicals and two molecules of reduced ferredoxin, the latter serving as a reductant for eliminating H_2O_2 (Fig. 3.35). The transfer of electrons to oxygen by the Mehler reaction is a reversal of the water splitting of PS II. As will be discussed in the following section, the Mehler reaction occurs when ferredoxin is very highly reduced. The only gain of this reaction is the generation of a proton gradient from electron transport through PS II and the cyt-b_6/f complex. This proton gradient can be used for the synthesis of ATP if ADP is present. But since there is usually a shortage in ADP under the conditions of the Mehler reaction, it mostly results in the formation of a high pH gradient. A feature common to the Mehler reaction and cyclic electron transport is that there is no net production of NADPH. For this reason, electron transport via the Mehler reaction has been termed **pseudocyclic electron transport**.

Yet another group of antioxidants was recently found in plants, the so-called **peroxiredoxins**. These proteins, comprising -SH groups as redox carriers, have been known in the animal world for some time. Ten different peroxiredoxin genes have been identified in the model plant *Arabidopsis*. Peroxiredoxins, being present in chloroplasts as well as in other cell compartments, differ from the aforementioned antioxidants glutathione and ascorbate in that they reduce a remarkably wide spectrum of peroxides, such as **H_2O_2**, **alkylperoxides**, and **peroxinitrites**. In chloroplasts, oxidized peroxiredoxins are reduced by photosynthetic electron transport of photosystem I with ferredoxin and thioredoxin as intermediates.

Instead of ferredoxin, PS I can also reduce methylviologen. Methylviologen, also called **paraquat**, is used commercially as a herbicide

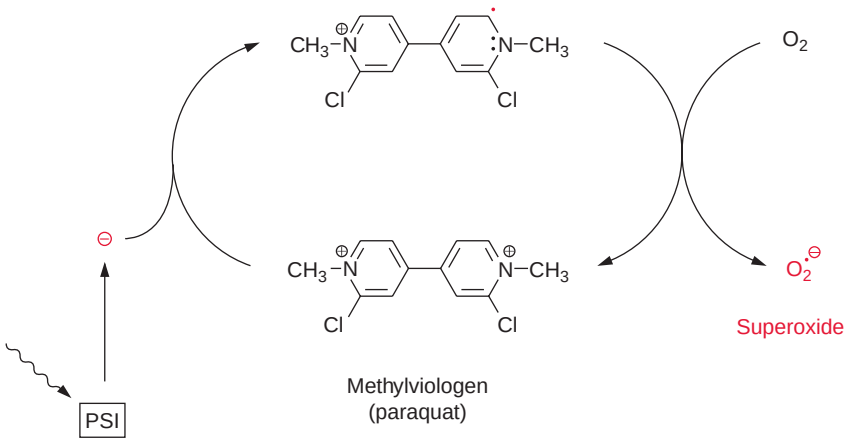

Figure 3.39
Methylviologen is reduced by the transfer of an electron from the excited PS I to form a radical compound. The latter transfers the electron to oxygen and the aggressive superoxide radical is formed. Methylviologen, also called paraquat, is a potent herbicide which is distributed by ICI under the trade name Gramoxone.

(Fig. 3.39). The herbicidal effect is due to the reduction of oxygen to superoxide radicals. Additionally, paraquat competes with dehydroascorbate for the reducing equivalents provided by photosystem I. Therefore, in the presence of paraquat, ascorbate is no longer regenerated from dehydroascorbate and the ascorbate peroxidase reaction can no longer proceed. The increased production of superoxide and decreased detoxification of hydrogen peroxide in the presence of paraquat causes severe oxidative damage to mesophyll cells, noticeable by a bleaching of the leaves. In the past, paraquat has been used to destroy marijuana fields in South America.

3.10 Regulatory processes control the distribution of the captured photons between the two photosystems

Linear photosynthetic electron transport through the two photosystems requires the even distribution of the captured excitons between them. As discussed in section 2.4, the excitons are transferred preferentially to the chromophore which requires the least energy for excitation. Photosystem I (P_{700}) being on a lower energetic level than PS II (Fig. 3.16) requires less energy for excitation than photosystem II (P_{680}). In an unrestricted competition between the two photosystems, excitons would primarily be directed to PS I. Due to this imbalance, the distribution of the excitons between the two photosystems must be regulated. The spatial separation of PS I and PS II and their antennae in the thylakoid membrane plays an important role in this regulation.

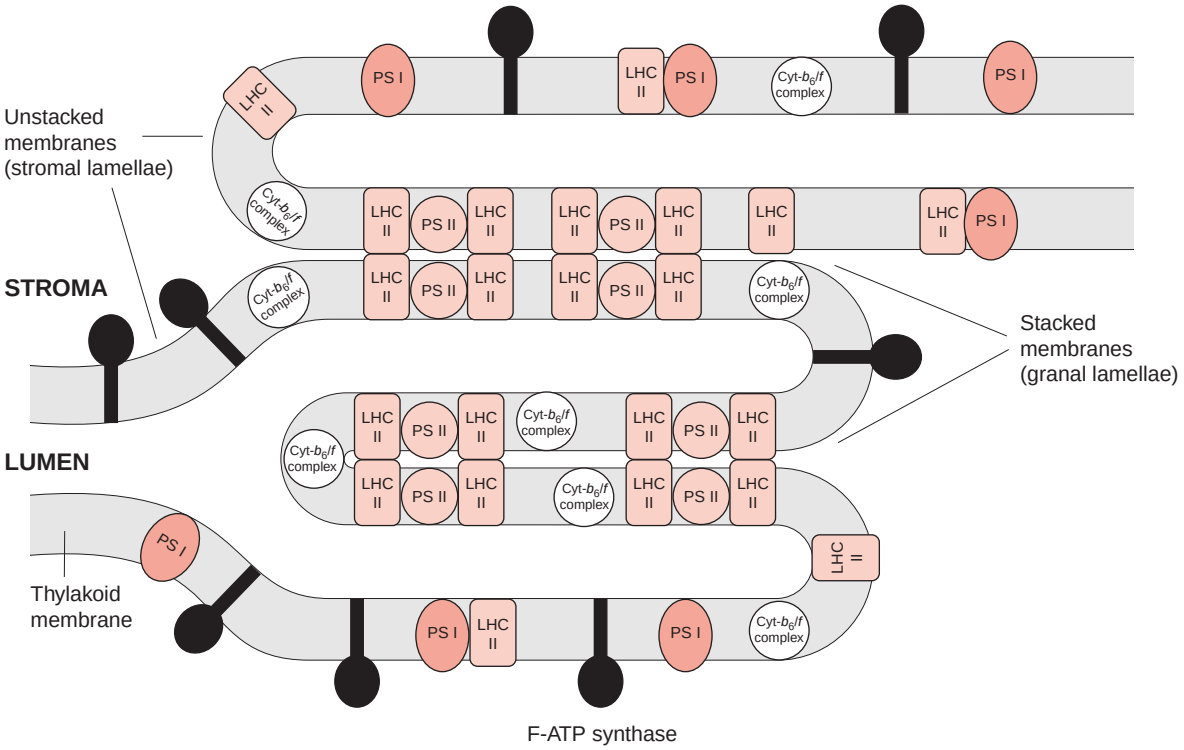

Figure 3.40 Distribution of photosynthetic protein complexes between the stacked and unstacked regions of thylakoid membranes. Stacking is probably caused by light harvesting complexes II (LHC II).

In chloroplasts, the thylakoid membranes are present in two different arrays, as **stacked** and **unstacked membranes**. The outer surface of the unstacked membranes has free access to the stromal space; these membranes are called **stromal lamellae** (Fig. 3.40). In the stacked membranes, the neighboring thylakoid membranes are in direct contact with each other. These membrane stacks can be seen as grains (grana) in light microscopy and are therefore called **granal lamellae**.

ATP synthase and the PS I complex (including its light harvesting complexes, not further discussed here) are located either in the stromal lamellae or in the outer membrane region of the granal lamellae. Therefore, these proteins have free access to ADP and $NADP^+$ in the stroma. The PS II complex, on the other hand, is primarily located in the granal lamellae. Peripheral LHC II subunits attached to the PS II complex (section 2.4) contain a protein chain protruding from the membrane, which can probably interact with the LHC II subunit of the adjacent membrane and thus

cause tight membrane stacking. The cyt-b_6/f complexes are only present in stacked membranes. Since the proteins of PS I and F-ATP-synthase project into the stroma space, they do not fit into the space between the stacked membranes. Thus the PS II complexes in the stacked membranes are separated spatially from the PS I complexes in the unstacked membranes. It is assumed that this prevents an uncontrolled **spillover of excitons** from PS II to PS I.

However, the spatial separation of the two photosystems and thus the spillover of excitons from PS II to PS I can be regulated. For example, if the excitation of PS II is greater than that of PS I, plastohydroquinone accumulates, which cannot be oxidized rapidly enough via the cyt-b_6/f complex by PS I. Under these conditions, a protein kinase is activated, which phosphorylates the hydroxyl groups of threonine residues of peripheral LHC II subunits, causing a conformational change of the LHC protein. As a result of this, the affinity to PS II is decreased and the LHC II subunits dissociate from the PS II complexes. Furthermore, due to the changed conformation, LHC II subunits can now bind to PS I, mediated by the H subunit of PS II. This LHC II-PS I complex purposely increases the spillover of excitons from LHC II to PS I. In this way the accumulation of reduced plastoquinone decreases the excitation of PS II and enhances the excitation of PS I. A protein phosphatase facilitates the reversal of this regulation. This regulatory process, which has been simplified here, enables an optimized distribution of the captured photons between the two photosystems, independent of the spectral quality of the absorbed light.

Excess light energy is eliminated as heat

Plants face the general problem that the energy of irradiated light can be much higher than the demand of photosynthetic metabolites such as NADPH and ATP. This is the case when very high light intensities are present and the metabolism cannot keep pace. Such a situation arises at low temperatures, when the metabolism is slowed down because of decreased enzyme activities (cold stress) or at high temperatures, when stomata close to prevent loss of water. Excess excitation of the photosystems could result in an excessive reduction of the components of the photosynthetic electron transport.

Very high excitation of photosystem II, recognized by the accumulation of plastohydroquinone, results in damage to the photosynthetic apparatus, termed **photoinhibition**. A major cause of this damage is an overexcitation of the reaction center, by which chlorophyll molecules attain a triplet state, resulting in the formation of aggressive singlet oxygen (section 2.3). The damaging effect of triplet chlorophyll can be demonstrated by placing

a small amount of chlorophyll under the human skin, which after illumination causes severe tissue damage. This photodynamic principle is utilized in medicine for the selective therapy of skin cancer.

Carotenoids (e.g., β-carotene, Fig. 2.9) are able to convert the triplet state of chlorophyll and the singlet state of oxygen to the corresponding ground states by forming a triplet carotenoid, which dissipates its energy as heat. In this way carotenoids have an important protective function. If under certain conditions this protective function of carotenoids is unable to cope with excessive excitation of PS II, the remaining singlet oxygen has a damaging effect on the PS II complex. The site of this damage could be the D_1 protein of the photosynthetic reaction center in PS II, which already under normal photosynthetic conditions experiences a high turnover (see section 3.6). When the rate of D_1-protein damage exceeds the rate of its resynthesis, the rate of photosynthesis is decreased, resulting in **photoinhibition**.

Plants have developed several mechanisms to protect the photosynthetic apparatus from light damage. One mechanism is **chloroplast avoidance movement**, in which chloroplasts move under high light conditions from the cell surface to the side walls of the cells. Another way is to dissipate the energy arising from an excess of excitons as heat. This process is termed **nonphotochemical quenching** of exciton energy. Although our knowledge of this quenching process is still incomplete, it is undisputed that **zeaxanthin** plays an important role. Zeaxanthin causes the dissipation of exciton energy to heat by interacting with a chlorophyll-binding protein (CP 22) of photosystem II. Zeaxanthin is formed by the reduction of the diepoxide **violaxanthin**. The reduction proceeds with ascorbate as the reductant and the monoepoxide antheraxanthin is formed as an intermediate. Zeaxanthin can be reconverted to violaxanthin by epoxidation which requires NADPH and O_2 (Fig. 3.41). Formation of zeaxanthin by diepoxidase takes place on the luminal side of the thylakoid membrane at an optimum pH of 5.0, whereas the regeneration of violaxanthin by the epoxidase proceeding at the stromal side of the thylakoid membrane occurs at about pH 7.6. Therefore, the formation of zeaxanthin requires a high pH gradient across the thylakoid membrane. As discussed in connection with the Mehler reaction (section 3.9), a high pH gradient can be an indicator of the high excitation state of photosystem II. When there is too much excitation energy, an increased pH gradient initiates zeaxanthin synthesis, dissipating excess energy of the PS II complex as heat. This mechanism explains how under strong sunlight most plants convert 50% to 70% of all the absorbed photons to heat. The non-photochemical quenching of excitation energy is the primary way for plants to protect themselves from too much light energy. In comparison, the Mehler reaction (section 3.9) and photorespiration (section 7.7) under

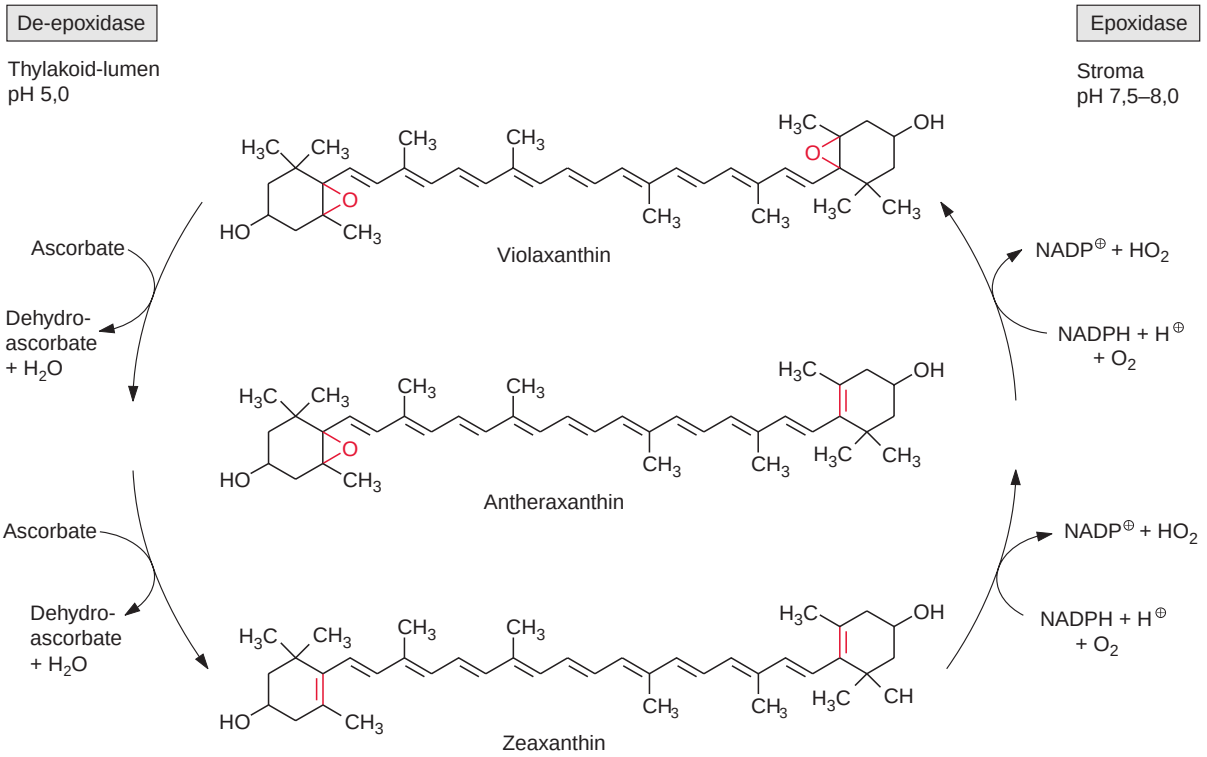

Figure 3.41
The zeaxanthin cycle.
(After Demmig-Adams.)

most conditions play only a minor role in the elimination of excess excitation energy.

Further reading

Allen, J. F. Cyclic, pseudocyclic and non-cyclic photophosphorylation: New links in the chain. Trends in Plant Science 8, 15–19 (2003).

Amunts, A., Drory, O., Nelson, N. The structure of a plant photosystem I supercomplex at 3.4Å resolution. Nature 447, 58–63 (2007).

Asada, K. Production and scavenging of reactive oxygen species in chloroplasts and their function. Plant Physiology 141, 391–396 (2006).

Bonardi, V., Pesaresi, P., Becker, T., Schleiff, E., Wagner, R., Pfannschmidt, T., Jahns, P., Leister, D. Photosystem II core phosphorylation and photosynthetic acclimation require two different protein kinases. Nature 437, 1179–1182 (2005).

Cramer, W. A., Zhang, H., Yan, J., Kurisu, G., Smith, J. L. Transmembrane traffic in the cytochrome b6f complex. Annual Review Biochemistry 75, 769–790 (2006).

Deisenhofer, J., Michel, H. Nobel Lecture: The photosynthetic reaction center from the purple bacterium *Rhodopseudomonas viridis*. EMBO Journal 8, 2149–2169 (1989).

Dietz, K. J. The dual function of plant peroxiredoxins in antioxidant defence and redox signaling. Subcellular Biochemistry 4, 267–294 (2007).

Ermler, U., Fritzsch, G., Buchanan, S. K., Michel, H. Structure of the photosynthetic reaction center from *Rhodobacter sphaeroides* at 2.65Å resolution: Cofactors and protein-cofactor interactions. Structure 2, 925–936 (1994).

Govindjee, Gest, H. (Eds.), (2002). Historical highlights of photosynthesis research I. Photosynthesis Research *73*, 1–308.

Govindjee, Gest, H. (Eds.), (2003). Historical highlights of photosynthesis research II. Photosynthesis Research *79*, 1–450.

Halliwell, B. Reactive species and antioxidants. Redox biology is a fundamental theme of aerobic life. Plant Physiology 141, 312–322 (2006).

Holzwarth, A. R., Müller, M. G., Reus, M., Novaczyk, J., Sander, J., Rögner, M. Kinetics and mechanism of electron transfer in intact photosystem II and in the isolated reaction center: Pheophytin is the primary electron acceptor. Proceedings of the National Academy of Science USA 103, 6895–6900 (2006).

Iverson, T. M. Evolution and unique bioenergetic mechanisms in oxygenic photosynthesis. Current Opinion Chemistry Biology 10, 91–100 (2006).

Jensen, P. E., Bassi, R., Boekema, E. J., Dekker, J. P., Jansson, S., Leister, D., Robinson, C., Scheller, H. V. Structure, function and regulation of plant photosystem I. Biochimica Biophysica Acta 1767, 335–352 (2007).

Joliot, P., Joliot, A. Cyclic electron flow in C3 plants. Biochim Biophysica Acta 1757, 362–368 (2006).

Jordan, P., Fromme, P., Witt, H. T., Klukas, O., Saenger, W., Krauß, N. Three-dimensional structure of cyanobacterial photosystem I at 2.5Å resolution. Nature 411, 909–917 (2001).

Kramer, D. M., Avenson, T. J., Edwards, G. E. Dynamic flexibility in the light reactions of photosynthesis governed by both electron and proton transfer reactions. Trends in Plant Science 9, 349–357 (2004).

Kurisu, G., Zhang, H., Smith, J. L., Cramer, W. A. Structure of the cytochrome b_6f complex of oxygenic photosynthesis: tuning the cavity. Science 302, 1009–1014 (2003).

Loll, B., Kern, J., Saenger, W., Zouni, A., Biesiadka, J. Towards complete cofactor arrangement in the 3.0Å resolution structure of photosystem II. Nature 438, 1040–1044 (2005).

Murray, J. W., Duncan, J., Barber, J. CP43-like chlorophyll binding proteins: Structural and evolutionary implications. Trends in Plant Science 11, 152–158 (2006).

Nelson, N., Yocum, C. F. Structure and function of photosystems I and II. Annual Review of Plant Biology 57, 521–565 (2006).

Nield, J., Barber, J. Refinement of the structural model for the Photosystem II supercomplex of higher plants. Biochimica Biophysica Acta 1757, 53–61 (2006).

Raval, M. K., Biswal, B., Biswal, U. C. The mystery of oxygen evolution: Analysis of structure and function of photosystem II, the water-plastoquinone oxido-reductase. Photosynthesis Research 85, 267–293 (2005).

Renger, G. Oxidative photosynthetic water splitting: Energetics, kinetics and mechanism. Photosynthesis Research 92, 407–425 (2007).

Shikanai, T. Cyclic electron transport around photosystem I: Genetic approaches. Annual Review Plant Biology 58, 199–217 (2007).

Stroebel, D., Choquet, Y., Popot, J.-L., Picot, D. An atypical heme in the cytochrome-b_6f-complex. Nature 426, 413–418 (2003).

Szabo, I., Bergantino, E., Giacometti, G. M. Light and oxygenic photosynthesis: Energy dissipation as a protection mechanism against photooxidation. EMBO Reports 6, 629–634 (2005).

Trebst, A. Inhibitors in the functional dissection of the photosynthetic electron transport system. Photosynthesis Research 92, 217–224 (2007).

Vieira Dos Santos, C., Rey, P. Plant thioredoxins are key actors in the oxidative stress response. Trends in Plant Science 11, 329–334 (2006).

4

ATP is generated by photosynthesis

Chapter 3 discussed the transport of protons across a thylakoid membrane by photosynthetic electron transport and how, in this way, a proton gradient is generated. This chapter describes how this proton gradient is utilized for the synthesis of ATP.

In 1954 Daniel Arnon (Berkeley) discovered that upon illumination suspended thylakoid membranes synthesize ATP from ADP and inorganic phosphate. This process is called **photophosphorylation**. Further experiments showed that photophosphorylation is coupled to the generation of NADPH. This result was unexpected, as at that time it was generally believed that the synthesis of ATP in chloroplasts, as in mitochondria, was driven by an electron transport from NADPH to oxygen. It soon became apparent, however, that the mechanism of photophosphorylation coupled to photosynthetic electron transport was very similar to that of ATP synthesis coupled to electron transport of mitochondria, termed **oxidative phosphorylation** (section 5.6).

In 1961 Peter Mitchell (Edinburgh) postulated in his **chemiosmotic hypothesis** that during electron transport a proton gradient is formed, and that it is the **proton motive force** of this gradient that drives the synthesis of ATP. At first this revolutionary hypothesis was strongly opposed by many workers in the field, but in the course of time, experimental results of many researchers supported the chemiosmotic hypothesis, which is now fully accepted. In 1978 Peter Mitchell was awarded the Nobel Prize in Chemistry for this hypothesis.

4.1 A proton gradient serves as an energy-rich intermediate state during ATP synthesis

Let us first ask: How much energy is actually required in order to synthesize ATP?

The free energy for the synthesis of ATP from ADP and phosphate is calculated from the van't Hoff equation:

$$\Delta G = \Delta G^{0'} + RT \ln \frac{[ATP]}{[ADP] \cdot [P]} \tag{4.1}$$

The standard free energy for the synthesis of ATP is:

$$\Delta G^{0'} = +30.5\,\text{kJ/mol} \tag{4.2}$$

The concentrations of ATP, ADP, and phosphate in the chloroplast stroma are very much dependent on metabolism. Typical concentrations are:

$$\text{ATP} = 2.5 \cdot 10^{-3}\ \text{mol/L};\ \text{ADP} = 0.5 \cdot 10^{-3}\ \text{mol/L};\ \text{P} = 5 \cdot 10^{-3}\ \text{mol/L}$$

When these values are introduced into equation 4.1 ($R = 8.32\,\text{J/mol} \cdot \text{K}$, $T = 298\,\text{K}$), the energy required for synthesis of ATP is evaluated as:

$$\Delta G = +47.8\,\text{kJ/mol} \tag{4.3}$$

This value is, of course, variable because it depends on the metabolic conditions. For further considerations an average value of 50 kJ/mol will be employed for ΔG_{ATP}.

The transport of protons across a membrane can have different effects. If the membrane is permeable to counter ions of the proton (e.g., a chloride ion (Fig. 4.1A)), the charge of the proton will be compensated, since each transported proton will pull a chloride ion across a membrane. This is how a proton concentration gradient can be generated. The free energy for the transport of protons from A to B is:

$$\Delta \text{G} = RT \ln \frac{[H^+]_\text{B}}{[H^+]_\text{A}} \quad [\text{J/mol}] \tag{4.4}$$

If the membrane is impermeable for counter ions (Fig. 4.1B), a charge compensation for the transported proton is not possible. In this case, the

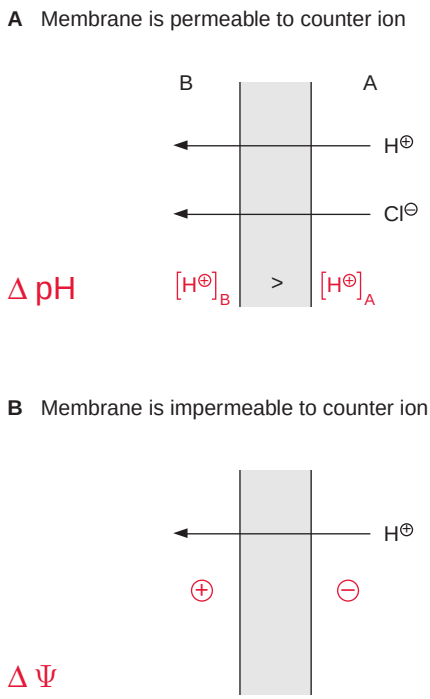

Figure 4.1 A. Transport of protons through a membrane. Permeablity to a counter ion such as chloride results in the formation of a proton gradient. B. When the membrane is impermeable to a counter ion, proton transport results in the formation of a membrane potential.

transfer of only a few protons across the membrane results in the formation of a membrane potential $\Delta\Psi$, measured as the voltage difference across the membrane. By convention, $\Delta\Psi$ is positive when a cation is transferred in the direction of the more positive region. Voltage and free energy are connected by the following equation:

$$\Delta G = mF \cdot \Delta\Psi \tag{4.5}$$

where m is the charge of the ion (in the case of a proton = 1), and F is the Faraday constant, 96,485 A s/mol.

Proton transport across a biological membrane leads to the formation of a proton concentration gradient and a membrane potential. The free energy for the transport of protons from A to B therefore consists of the sum of the free energies for the generation of the H^+ concentration gradient and the membrane potential:

$$\Delta G = RT \ln \bullet \frac{[H^+]_B}{[H^+]_A} + F\Delta\Psi \tag{4.6}$$

In chloroplasts, the energy stored in a proton gradient corresponds to the change of free energy during the flux of protons from the lumen into the stroma.

$$\Delta G = RT \ln \frac{[H^+]_S}{[H^+]_L} + F\Delta\Psi \tag{4.7}$$

where S = stroma, L = lumen, and $\Delta\Psi$ = voltage difference stroma-lumen.

The conversion of the natural logarithm into the decadic logarithm yields:

$$\Delta G = 2.3 \cdot RT \log \frac{[H^+]_S}{[H^+]_L} + F\Delta\Psi \tag{4.8}$$

The logarithmic factor is the negative pH difference between lumen and stroma:

$$\log[H^+]_S - \log[H^+]_L = -\Delta\mathrm{pH} \tag{4.9}$$

A rearrangement yields:

$$\Delta G = -2.3RT \bullet \Delta\mathrm{pH} + F\Delta\Psi \tag{4.10}$$

At 25°C: $2.3 \cdot RT = 5{,}700\,\mathrm{J/mol}$

Thus: $$\Delta G = -5{,}700\Delta\mathrm{pH} + F\Delta\Psi \quad [\mathrm{J/mol}] \tag{4.11}$$

The expression $\frac{\Delta G}{F}$ is called **proton motive force** (PMF) (unit in volts):

$$\frac{\Delta \mathrm{G}}{\mathrm{F}} = PMF = -\frac{2.3\,\mathrm{RT}}{\mathrm{F}} \cdot \Delta pH + \Delta\Psi \quad [\mathrm{V}] \tag{4.12}$$

At 25°C: $\frac{2.3RT}{F} = 0.059\,\mathrm{V}$

Thus: $$\mathrm{PMF} = -0.059 \cdot \Delta\mathrm{pH} + \Delta\Psi \quad [\mathrm{V}] \tag{4.13}$$

Equation 4.13 is of general significance for electron transport-coupled ATP synthesis. In mitochondrial oxidative phosphorylation, the PMF is primarily the result of a membrane potential. In chloroplasts, on the other

hand, the membrane potential does not contribute much to the PMF, since the PMF is almost entirely due to the concentration gradient of protons across the thylakoid membrane. In illuminated chloroplasts, a ΔpH across the thylakoid membrane of about 2.5 can be measured. Introducing this value into equation 4.11 yields:

$$\Delta G = -14.3\,\text{kJ/mol}$$

A comparison of this value with ΔG for the formation of ATP (50 kJ/mol) suggests that at least four protons are required for the ATP synthesis from ADP and phosphate.

4.2 The electron chemical proton gradient can be dissipated by uncouplers to heat

Photosynthetic electron transport from water to $NADP^+$ is coupled with photophosphorylation. Electron transport occurs only if ADP and phosphate are present as precursor substances for ATP synthesis. When an **uncoupler** is added, electron transport proceeds at a high rate in the absence of ADP; electron transport is then uncoupled from ATP synthesis. Therefore, in the presence of an uncoupler, ATP synthesis is abolished.

The chemiosmotic hypothesis explains the effect of uncouplers (Fig. 4.2). Uncouplers are amphiphilic compounds, soluble in both water and lipids. They are able to permeate the lipid phase of a membrane by **diffusion** and in this way to transfer a proton or an alkali ion across the membrane, thus eliminating a proton concentration gradient or a membrane potential, respectively. In the presence of an uncoupler a proton gradient is absent, but protons are transported by ATP synthase from the stroma to the thylakoid lumen. This proton transport costs energy: ATP is hydrolyzed to ADP and phosphate. This is the reason why uncouplers cause an ATP hydrolysis (**ATPase**).

Figure 4.2A shows the effect of the uncoupler carbonylcyanide-*p*-trifluormethoxyphenylhydrazone (**FCCP**), which is a weak acid. FCCP diffuses in the undissociated (protonated) form from the compartment with a high proton concentration (on the left in Fig. 4.2A), through the membrane into the compartment with a low proton concentration, where it finally dissociates into a proton and the FCCP anion**.** The proton remains and the FCCP anion returns by diffusion to the other compartment, where it is protonated again. In this way the presence of FCCP at a concentration of only

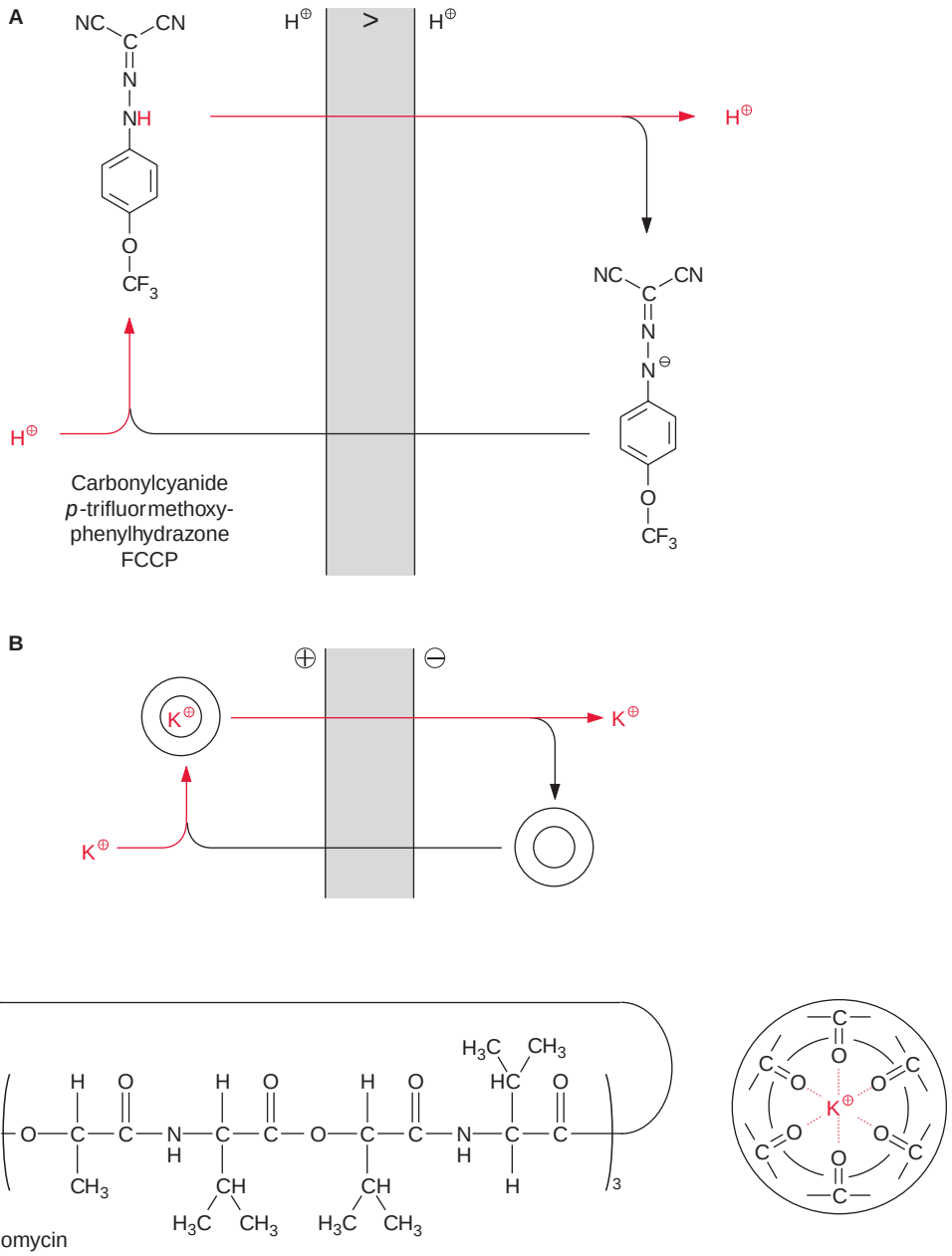

Figure 4.2 The proton motive force of a proton gradient is eliminated by uncouplers. A. The hydrophobicity of FCCP allows the diffusion through a membrane in the protonated form as well as in the deprotonated form. This uncoupler, therefore, eliminates a proton gradient by proton transfer. B. Valinomycin, an antibiotic with a cyclic structure, folds to a hydrophobic spherical molecule, which is able to bind K^+ ions in the interior. Loaded with K^+ ions, valinomycin can diffuse through a membrane. In this way valinomycin can eliminate a membrane potential by transferring K^+ ions across a membrane.

$7 \cdot 10^{-8}$mol/L results in complete dissipation of the proton gradient. The substance **SF 6847** (3.5-Di (*tert*-butyl)-4-hydroxybenzyldimalononitril) (Fig. 4.3) has an even higher uncoupling effect. Uncouplers such as FCCP or SF 6847, which transfer protons across a membrane, are called **protonophores**.

In addition to the protonophores, there is a second class of uncouplers, termed **ionophores**, which are able to transfer alkali cations across a membrane and thus dissipate a membrane potential. **Valinomycin**, an antibiotic from *Streptomyces*, is such an ionophore (Fig. 4.2B). Valinomycin is a cyclic molecule containing the sequence (L-lactate)-(L-valine)-(D-hydroxyisovalerate)-(D-valine) three times. Due to its hydrophobic outer surface, valinomycin is able to diffuse through a membrane. Oxygen atoms directed towards the inside of the valinomycin molecule form the binding site for dehydrated Rb^+ and K^+ ions. Na^+ ions because of their small size are only very loosely bound. When K^+ ions are present, the addition of valinomycin results in the elimination of the membrane potential. The ionophore **gramicidine**, not discussed here in detail, is also a polypeptide antibiotic. Gramicidine incorporates into membranes and forms a transmembrane ion channel by which both alkali cations and protons can diffuse through the membrane.

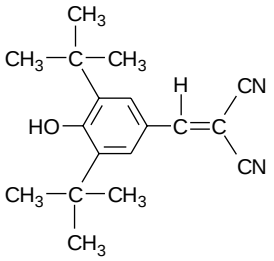

SF 6847

Figure 4.3 Di(*tert*-butyl)-4-hydroxybenzyl malononitrile (SF6847) is an especially effective uncoupler. Only 10^{-9}mol/L of this compound is sufficient to completely dissipate a proton gradient across a membrane. This uncoupling is based on the permeation of the protonated and deprotonated molecule through the membrane, as shown in Figure 4.2A for FCCP.

The chemiosmotic hypothesis was proved experimentally

In 1966 the American scientist André Jagendorf presented conclusive evidence for the validity of the chemiosmotic hypothesis involved in chloroplast photophosphorylation (Fig. 4.4). He incubated thylakoid membranes in an acidic medium of pH 4 in order to acidify the thylakoid lumen by unspecific uptake of protons. In a next step he added inorganic phosphate and ADP to the thylakoid suspension and then increased the pH of the medium to pH 8 by adding an alkaline buffer. This led to the sudden generation of a proton gradient of $\Delta pH = 4$, and for a short time ATP was synthesized. Since this experiment was carried out in the dark, it presented evidence that synthesis of ATP in chloroplasts can be driven without illumination just by a pH gradient across a thylakoid membrane.

4.3 H^+-ATP synthases from bacteria, chloroplasts, and mitochondria have a common basic structure

How is the energy of the proton gradient utilized to synthesize ATP?

A proton coupled ATP synthase (H^+-ATP synthase) is not unique to the chloroplast. It evolved during an early stage of evolution and occurs in

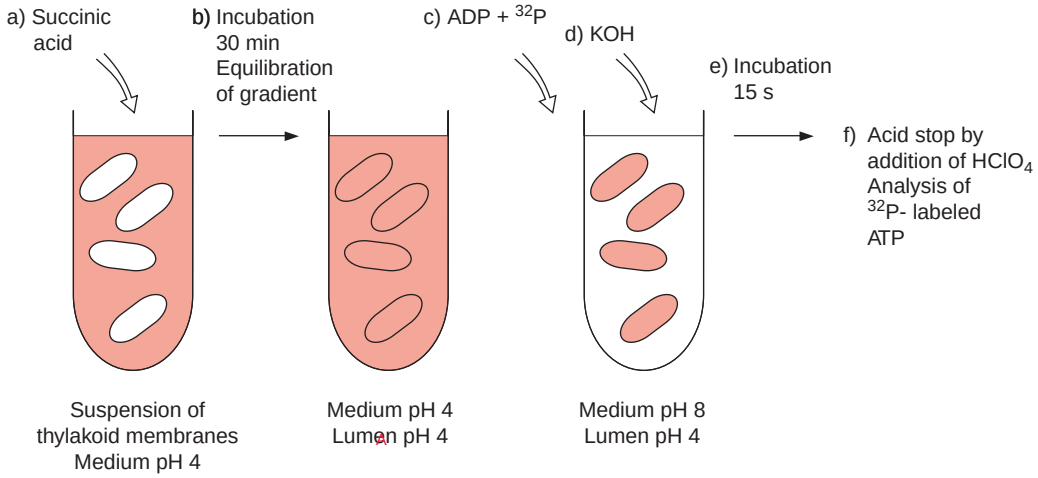

Figure 4.4 Thylakoid membranes can synthesize ATP in the dark by an artificially formed proton gradient. In a suspension of thylakoid membranes, the pH in the medium is lowered to 4.0 by the addition of succinic acid (a). After incubation for about 30 minutes, the pH in the thylakoid lumen is equilibrated with the pH of the medium due to a slow permeation of protons across the membrane (b). The next step is to add ADP and phosphate, the latter being radioactively labeled by the isotope ^{32}P (c). Then the pH in the medium is raised to 8.0 by adding KOH (d). In this way a ΔpH of 4.0 is generated between the thylakoid lumen and the medium, and this gradient drives the synthesis of ATP from ADP and phosphate. After a short time of reaction (e), the mixture is denatured by the addition of perchloric acid, and the amount of radioactively labeled ATP formed in the deproteinized extract is determined. (After Jagendorf, 1966.)

its basic structure in bacteria, chloroplasts, and mitochondria. In bacteria this enzyme catalyzes not only ATP synthesis driven by a proton gradient, but also (in a reversal of this reaction) the transport of protons against the concentration gradient at the expense of ATP. This was probably the original function of the enzyme. In some bacteria an ATPase homologous to the H^+-ATP synthase functions as an ATP-dependent Na^+ transporter.

Our present knowledge about the structure and function of the H^+-ATP synthase derives from investigations of mitochondria, chloroplasts, and bacteria. By 1960 progress in electron microscopy led to the detection of small particles, which were attached by stalks to the inner membranes of mitochondria and the thylakoid membranes of chloroplasts. These particles occur only at the matrix or stromal side of the corresponding membranes. By adding urea, Ephraim Racker and coworkers (Cornell University, USA), succeeded in removing these particles from mitochondrial membranes. The isolated particles catalyzed the hydrolysis of ATP to ADP and phosphate. Racker called them **F1-ATPase**. Mordechai Avron (Rehovot, Israel)

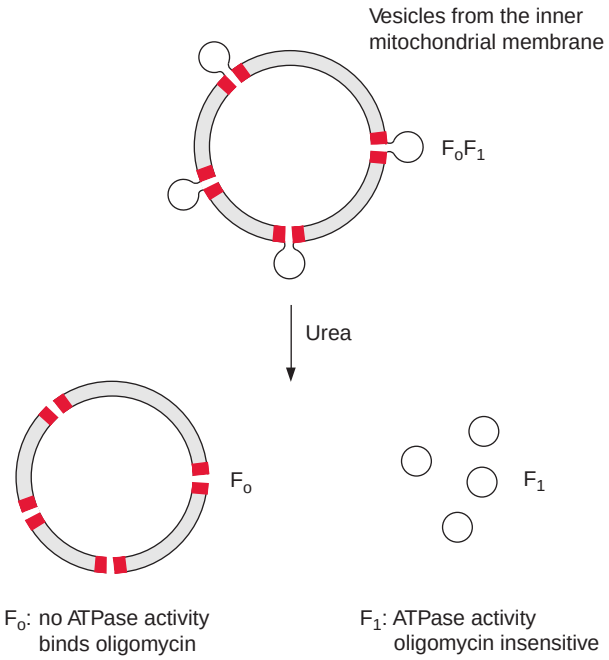

Figure 4.5 Vesicles prepared by ultrasonic treatment of mitochondria contain functionally intact H^+-ATP synthase. The soluble factor F_1 with ATPase function is removed by treatment with urea. The oligomycin binding factor F_o remains in the membrane.

showed that the corresponding particles from chloroplast membranes also have ATPase activity.

Vesicles containing F_1 particles could be prepared from the inner membrane of mitochondria. These membrane vesicles synthesized ATP during respiration, and as in intact mitochondria (section 5.6), the addition of uncouplers resulted in an increased ATPase activity. The uncoupler-induced ATPase activity, as well as ATP synthesis performed by these vesicles, was found to be inhibited by the antibiotic **oligomycin**. Mitochondrial vesicles where the F_1 particles had been removed showed no ATPase activity but were highly permeable for protons. This proton permeability was eliminated by adding oligomycin. In contrast, the ATPase activity of the removed F_1 particles was not affected by oligomycin. These and other experiments showed that the H^+-ATP synthase of the mitochondria consists of two parts:

1. A soluble factor 1 (F_1) that catalyzes the synthesis of ATP; and
2. A membrane-bound factor enabling the flux of protons through the membrane to which oligomycin is bound.

Racker designated this factor **Fo** (O, oligomycin) (Fig. 4.5). Basically the same result was found for H^+-ATP synthases of chloroplasts and bacteria, with the exception that the H^+-ATP synthase of chloroplasts is not

Table 4.1: Compounds of the F-ATP synthase from chloroplasts. Nomenclature as in *E. coli* F-ATP synthase

Subunits	Number in F_oF_1-molecule	Molecular mass (kDa)	Encoded in
F_1:α	3	55	Plastid genome
β	3	54	Plastid genome
γ	1	36	Nuclear genome
δ	1	21	Nuclear genome
ε	1	15	Plastid genome
F_o:a	1	27	Plastid genome
b	1	16	Nuclear genome
b′	1	21	Plastid genome
c	12	8	Plastid genome

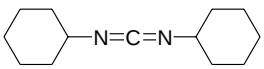

Dicyclohexylcarbodiimide
DCCD

Figure 4.6
Dicyclohexylcarbodiimide (DCCD), an inhibitor of the F_o part of F-ATP synthase.

inhibited by oligomycin. Despite this, the membrane part of the chloroplastic ATP synthase is also designated as F_o. The H^+-ATP synthases of chloroplasts, mitochondria, and bacteria, as well as the corresponding H^+- and Na^+-ATPases of bacteria, are collectively termed **F-ATP synthases** or **F-ATPases**. The terms F_oF_1-ATP synthase and F_oF_1-ATPase are also used.

F_1, after removal from the membrane, is a soluble oligomeric protein with the composition $\alpha_3\beta_3\gamma\delta\varepsilon$ (Table 4.1). This composition has been found in chloroplasts, bacteria, and mitochondria.

F_o is a strongly hydrophobic protein complex that can be removed from the membrane only by detergents. Dicyclohexylcarbodimide (**DCCD**) (Fig. 4.6) binds to the F_o embedded in the membrane, and thus closes the proton channel. In chloroplasts four different subunits have been detected as the main constituents of F_o and are named a, b, b′, and c (Table 4.1, Fig. 4.7). Subunit c, probably occurring in the chloroplastic F_o in 12–14 copies, contains two transmembrane helices and is the binding site for DCCD. The c subunits appear to form a cylinder, which spans the membrane. On the outside of the cylinder spanning the membrane, the subunits a, b, and b′ are arranged, whereby b and b′ are in contact with the F_1 part via subunit δ. Subunits γ and ε form the central connection between F_1 and F_o.

Whereas the structure of the F_o part is still somewhat hypothetical, the structure of the F_1 part has been thoroughly investigated (Fig. 4.7). The F_1

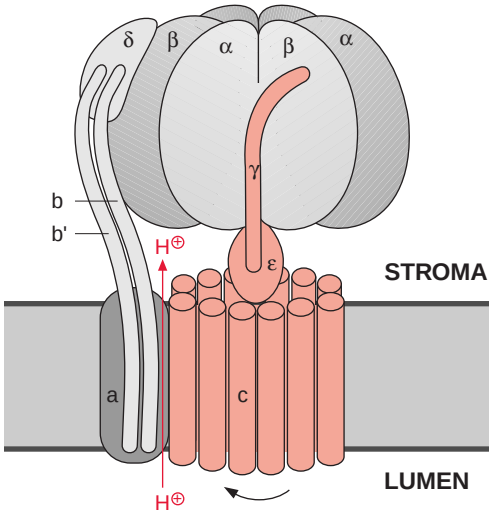

Figure 4.7 Scheme of the structure of an F-ATP synthase. The structure of the F_1 subunit concurs with the results of X-ray analysis discussed in the text. (After Junge.)

particles are so small that details of their structure are not visible on a single electron micrograph. However, details of the structure can be resolved if a very large number of F_1 images obtained by electron microscopy are subjected to a **computer-aided image analysis**. Figure 4.8 shows a delineated image of F-ATP synthase from chloroplasts. In the side projection, the stalk connecting the F_1 part with the membrane can be recognized. Using more refined picture analysis (not shown here), two stems, one thick and the other thin, were found between F_1 and F_o. In the vertical projection, a hexagonal array is to be seen, corresponding to an alternating arrangement of α- and β-subunits. Investigations of the isolated F_1 protein showed that an F_oF_1 protein has three catalytic binding sites for ADP or ATP. One of these binding sites is occupied by very tightly bound ATP, which is released only when energy is supplied from the proton gradient.

X-ray structure analysis of the F_1 part of ATP synthase yields an insight into the machinery of ATP synthesis

In 1994 the group of John Walker in Cambridge (England) succeeded in analyzing the three-dimensional structure of the F_1 part of ATP synthase. Crystals of F_1 from beef heart mitochondria were used for this analysis. Prior to crystallization, the F_1 preparation was loaded with a mixture of ADP and an ATP analogue (5′adenylyl-imidodiphosphate, AMP-PNP). This ATP analogue differs from ATP in that the last two phosphate residues are connected by an N atom. It binds to the ATP binding site as ATP,

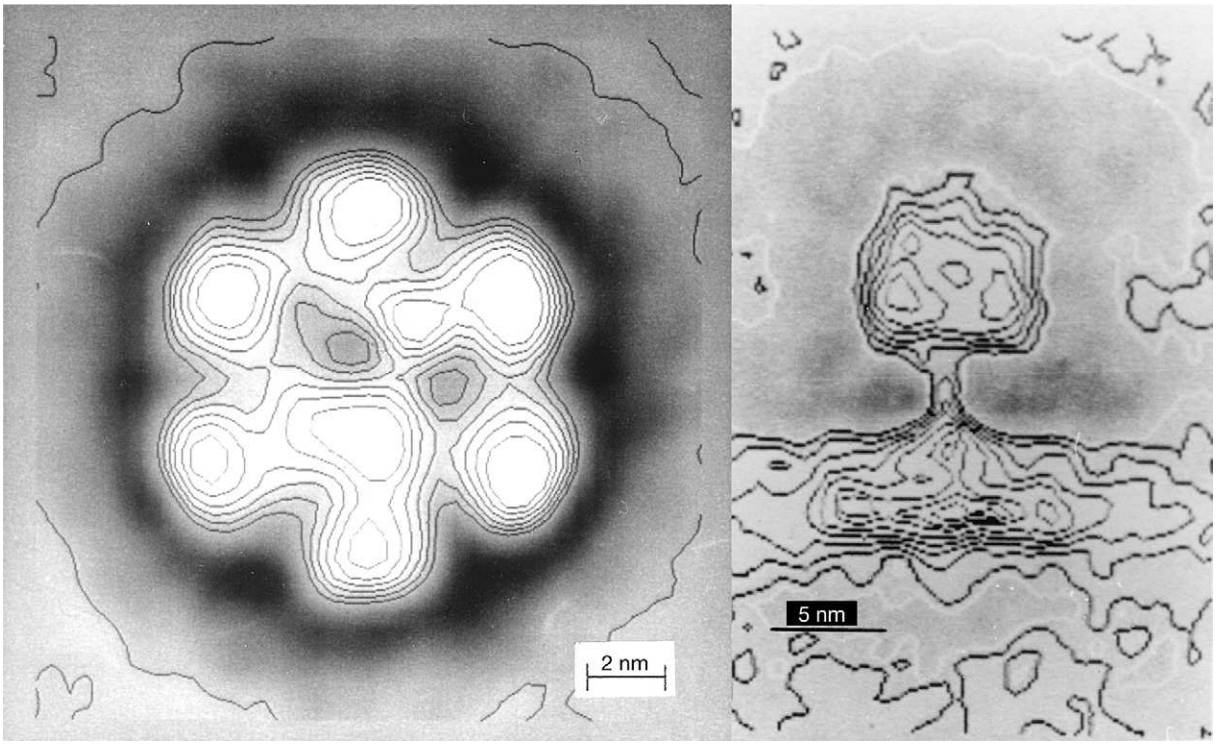

Figure 4.8 Averaged image of 483 electromicrographs of the F-ATP synthase from spinach chloroplasts. A. Vertical projection of the F_1 part. A hexameric structure reflects the alternating ($\alpha\beta$)-subunits. B. Side projection, showing the stalk connecting the F_1 part with the membrane. (By P. Graeber, Stuttgart.)

but cannot be hydrolyzed by the ATPase. The structural analysis confirmed the alternating arrangement of the α- and β-subunits (Figs. 4.7 and 4.9). One α- and one β-subunit form a unit comprising a binding site for one adenine nucleotide. The β-subunit is primarily involved in the synthesis of ATP. In the F_1 crystal investigated, one ($\alpha\beta$)-unit contained one ADP, the second the ATP analogue, whereas the third ($\alpha\beta$)-subunit was empty. These differences in nucleotide binding were accompanied by conformational differences of the three β-subunits (Fig. 4.9). The γ-subunit is arranged **asymmetrically**, protrudes through the center of the F_1 part, and is bent to the side of the ($\alpha\beta$)-unit loaded with ADP (Figs. 4.7 and 4.9). This asymmetry enlightens the function of the F_1 part of ATP synthase. Some general considerations about ATP synthase will be made before the function is explained in more detail.

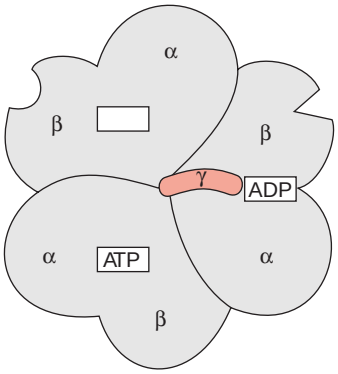

Figure 4.9 Schematic presentation of the vertical projection of the F_1 part of the F-ATP synthase. The enzyme contains three nucleotide binding sites, each consisting of an α-subunit and a β-subunit. Each of the three β-subunits occurs in a different conformation. The γ-subunit in the center, vertical to the viewer, is bent to the α- and β-subunit loaded with ADP. This representation corresponds to the results of X-ray structure analysis by Walker and coworkers mentioned in the text.

4.4 The synthesis of ATP is effected by a conformation change of the protein

For the reaction:

$$ATP + H_2O \rightleftharpoons ADP + Phosphate$$

the standard free energy is:

$$\Delta G^{\circ\prime} = -30.5\,kJ/mol$$

Because of its high free energy of hydrolysis, ATP is regarded as an energy-rich compound. It should be noted, however, that the standard value $\Delta G^{\circ\prime}$ has been determined for an aqueous solution of 1 mol of ATP, ADP, and phosphate per liter, respectively, corresponding to a water concentration of 55 mol/L. If the concentration of water was only 10^{-4} mol/L, the ΔG for ATP hydrolysis would be +2.2 kJ/mol. This means that at very low concentrations of water the reaction proceeds towards the synthesis of ATP. This example demonstrates that **in the absence of water the synthesis of ATP does not require the uptake of energy**.

The catalytic site of an enzyme can form a reaction site where water is excluded. Catalytic sites are often located in a hydrophobic area of the enzyme protein in which the substrates are bound in the absence of water. Thus, with ADP and P tightly bound to the enzyme, the synthesis of ATP could proceed spontaneously without requiring energy (Fig. 4.10). This has been proved for H^+-ATP synthase. Since the step of ATP synthesis itself does proceed without the uptake of energy, the amount of energy required to form ATP from ADP and phosphate in the aqueous phase has to be otherwise consumed, e.g., for the removal of the tightly bound newly synthesized

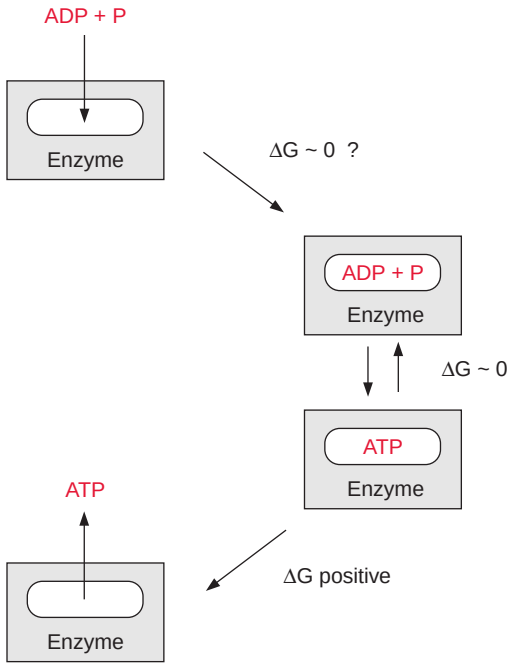

Figure 4.10 In the absence of H_2O, ATP synthesis can occur without the input of energy. In this case, the energy required for ATP synthesis in an aqueous solution has to be spent on binding ADP and P and/or on the release of the newly formed ATP. From available evidence, the latter case is more likely.

ATP from the binding site. This could occur by an energy-dependent conformation change of the protein.

In 1977 Paul Boyer (USA) put forward the hypothesis that the **three identical sites of the F1 protein alternate in their binding properties** (Fig. 4.11). One of the binding sites is present in the L form, which binds ADP and phosphate loosely but is not catalytically active. A second binding site, T, binds ADP and ATP tightly and is catalytically active. The third binding site, O, is open, binds ADP and ATP only very loosely, and is catalytically inactive. According to this ***"binding change" hypothesis***, the synthesis of ATP proceeds in a cycle. First, ADP and phosphate are bound to the loose binding site, L. A conformational change of the F_1 protein converts site L to a binding site T, where ATP is synthesized from ADP and phosphate in the absence of water. The ATP formed remains tightly bound. Another conformational change converts the binding site T to an open binding site O, and the newly formed ATP is released. A crucial point of this hypothesis is that with the conformational change of the F_1 protein, driven by the energy of the proton gradient, the conformation of each of the three catalytic sites is converted simultaneously to the next conformation

$$(L \rightarrow T \qquad T \rightarrow O \qquad O \rightarrow L)$$

The results of X-ray analysis, shown above, support the binding change hypothesis. The evaluated structure clearly shows that the three subunits

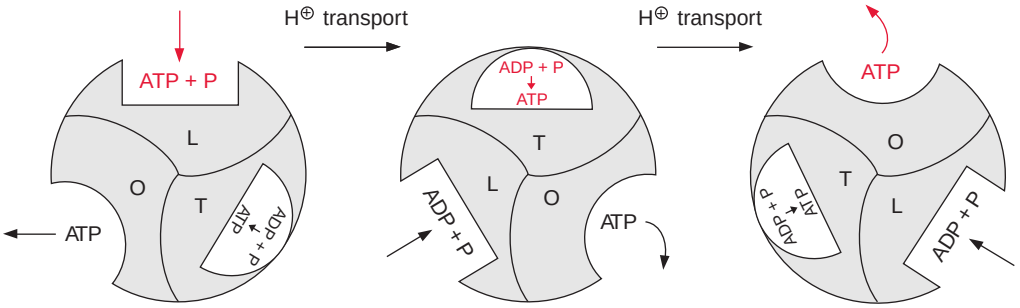

Figure 4.11 ATP synthesis by the binding change mechanism as proposed by Boyer. The central feature of this postulated mechanism is that synthesis of ATP proceeds in the F_1 complex by three nucleotide binding sites, which occur in three different conformations: conformation L binds ADP and P loosely, T binds ADP and P tightly and catalyzes the ATP formation; the ATP thus formed is tightly bound. The open form, O, releases the newly formed ATP. The flux of protons through the F-ATP synthase, as driven by the proton motive force, results in a concerted conformation change of the three binding sites.

of F_1—one free, one loaded with ADP, and one with the ATP analogue AMP-PNP—have different conformations. Paul Boyer and John Walker were awarded the Nobel Prize (1997) for these results. However, the details of this mechanism are still a matter of debate.

Further investigations showed that the central γ-subunit rotates. The γ- and ε-subunits of F_1 together with the 12 c-subunits of F_o (shown in red in Fig. 4.7) form a rotor. This rotor rotates in a stator consisting of subunits-$(\alpha\beta)_3$, δ, a, b, b′, by which the conformations of each of the catalytic centers shown in Fig. 4.11 is changed. This model suggests that three molecules of ATP are formed by one complete revolution.

This model was confirmed by a startling experiment carried out by Masasuka Yoshida and Kazohiko Kinosito in Japan. These researchers attached a fluorescent molecule to the upper end of a γ-subunit contained in an F_o particle present in a membrane. Using a special video microscopy documentation it was possible to make visible that upon the hydrolysis of ATP the γ-subunit did in fact rotate. The F_o part functions as a type of nano motor. The velocity of rotation of the F-ATP-synthase in chloroplasts has been estimated to be up to 160 revolutions per second. To explain how this nano motor is driven by a proton gradient on the basis of known structural data, Wolfgang Junge (Osnabrueck, Germany) developed the model shown in Figure 4.12. In this model the a-subunit of the stator (shown in gray) possesses a channel through which protons can move from the outside of the membrane to a binding site of a c-subunit of the rotor, possibly a glutamate residue. At another site of the stator is a second channel through which the protons bound to the c-subunit can be released to the inside. By Brownian movement this proton-loaded c-subunit can rotate to the other proton channel where the proton is released, facilitating a proton transport driven by the proton gradient from the outside to the inside. But why does the rotation caused by Brownian movement proceed only in one direction? Two factors could be responsible for this: the spacial separation of the two channels and a positively charged arginine residue of the a-subunit of the stator. It is assumed that the positive charge of the arginine repels

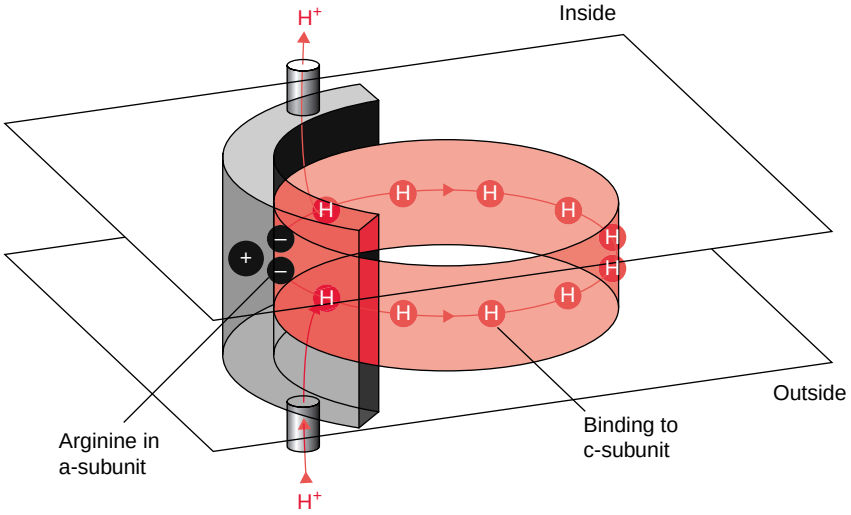

Figure 4.12 Model for the proton driven rotation of the rotor of the F_o part of the ATP synthase consisting of c-subunits. (After Junge et al., 1997.) The mechanism is described in the text.

the proton-loaded subunit and thus prevents a backward movement of the rotor, orientating the Brownian movement into one direction. Driven by a proton gradient that causes the loading and unloading of the proton binding sites at the respective channels, according to this model the nano motor rotates step by step like a ratchet in only one direction. In this way one full revolution causes the conformational change in the F_1-part leading to the formation of three molecules of ATP. Although an experimental verification of this model remains to be done, it gives an idea of how the nano motor of the ATP synthase may be driven by a proton gradient.

As discussed previously, several bacteria contain an **F-ATP synthase** that is driven by an Na^+ gradient. The model of the proton driven rotor allows the assumption that the subunit c of the Na^+ F-ATP synthase binds Na^+ ions and the two partial ion channels conduct Na^+.

It is still unclear how many c-subunits make up the rotor. Investigations of the number of c-subunits per F-ATP synthase molecule yielded values of 12 to 14 (chloroplasts), 10 (yeast mitochondria), and 12 (*E. coli*). Apparently in various organisms the number of c-subunits in the F_o part vary, therefore the number of protons required for one revolution to form three molecules of ATP will vary accordingly.

In photosynthetic electron transport the stoichiometry between the formation of NADPH and ATP is still a matter of debate

According to the model discussed here, chloroplasts with 14 c-subunits per rotor would require 14 protons for a complete rotation. Since three ATP molecules are formed during one rotation, this would correspond to an H^+/ATP

ratio of 4.7. Independent measurements indicated that in chloroplasts at least four protons are necessary for the synthesis of one ATP, which would be similar to the proton stoichiometry calculated for the rotor model. It is still not clear to what extent the Q-cycle plays a role in proton transport. In the linear (noncyclic) electron transport, for each NADPH formed without a Q-cycle, four protons (PS II: $2H^+$, Cyt-b_6/f complex: $2H^+$), and with a Q-cycle (Cyt-b_6/f complex: $4H^+$) six protons, are transported into the lumen (section 3.7). With a H^+/ATP ratio of 4.7, for each NADPH produced 1.3 ATP would be generated with the Q-cycle in operation and just 0.9 ATP without a Q-cycle. If these stoichiometries are correct, noncyclic photophosphorylation would not be sufficient to meet the demands of CO_2 assimilation in the Calvin cycle (ATP/NADPH = 1.5, see Chapter 6) and therefore cyclic photophosphorylation (section 3.8) would be required as well. The question concerning the stoichiometry of photophosphorylation is still not finally answered.

H^+-ATP synthase of chloroplasts is regulated by light

H^+-ATP synthase catalyzes a reaction that is in principle reversible. In chloroplasts, a pH gradient across the thylakoid membrane is generated only during illumination. In darkness, therefore, due to the reversibility of ATP synthesis, one would expect that the ATP synthase then operates in the opposite direction by transporting protons into the thylakoid lumen at the expense of ATP. In order to avoid such a costly reversion, chloroplast ATP synthase is subject to **strict regulation**. This is achieved in two ways. If the pH gradient across the thylakoid membrane decreases below a threshold value, the catalytic sites of the β-subunits are instantaneously switched off, and they are switched on again when the pH gradient is restored upon illumination. The mechanism of this is not yet understood. Furthermore, chloroplast ATP synthase is regulated by **thiol modulation**. By this process, described in detail in section 6.6, a disulfide bond in the γ-subunit of F_1 is reduced in the light by **ferredoxin** to form two -SH groups. This is mediated by reduced **thioredoxin (**section 6.6). The reduction of the γ-subunit causes the activation of the catalytic centers in the β-subunits. In this way illumination switches F-ATP synthase on. Upon darkening, the two -SH groups are oxidized by oxygen from air to form a disulfide, and as a result of this, the catalytic centers in the β-subunits are switched off. The simultaneous action of the two regulatory mechanisms allows an efficient control of ATP synthase in chloroplasts.

V-ATPase is related to the F-ATP synthase

Vacuoles contain a proton which transports V-ATPase and is conserved in all eukaryotes. Some V-ATPases transport Na^+ ions instead of protons. In

plants, V-ATPases are located not only in vacuoles (V = vacuoles), but also in plasma membranes and membranes of the endoplasmic reticulum and the Golgi apparatus. Genes for at least 12 different subunits have been identified in *Arabidopsis thaliana*. Major functions of this pump are to acidify the vacuole and to generate proton gradients across membranes for driving the transport of ions. V-ATPases also play a role in stomatal closure of guard cells. They resemble the F-ATP synthase in its basic structure, but are more complex. They consist of several proteins embedded in the membrane, similar to the F_o part of the F-ATPase, to which a spherical part (e.g., F_1) is attached by a stalk that protrudes into the cytosol. The spherical part consists of 3A- and 3B-subunits, which are arranged alternately like the ($\alpha\beta$)-subunits of F-ATP synthase. F-ATP synthase and V-ATPase are derived from a common ancestor. The exact number of protons transported per ATP depends on how many c-subunits the rotor of the F_o part contains. The V-ATPase is able to generate titratable proton concentrations of up to 1.4 mol/L within the vacuoles (section 8.5).

Vacuolar membranes also contain an **H^+-pyrophosphatase**, which upon the hydrolysis of one molecule of pyrophosphate to phosphate pumps one proton into the vacuole, but it does not reach such high proton gradients as the V-ATPase. H^+-pyrophosphatase probably consists of only a single protein with 16 transmembrane helices. It remains to be elucidated why there are two enzymes transporting H^+ across the vacuolar membrane. Plasma membranes contain a proton transporting **P-ATPase**, which will be discussed in section 8.2.

Further reading

Abrahams, J. P., Leslie, A. G. W., Lutter, R., Walker, J. E. Structure at 2.8 Å resolution of F1-ATPase from bovine heart mitochondria. Nature 370, 621–628 (1994).

Boekema, E. J., Braun, H. P. Supramolecular structure of the mitochondrial oxidative phosphorylation system. Journal Biological Chemistry 282, 1–4 (2007).

Boyer, P. D. The binding change mechanism for ATP synthase—some probabilities and possibilities. Biochimica Biophysica Acta 1149, 215–250 (1993).

Drory, O., Nelson, N. The emerging structure of vacuolar ATPases. Physiology (Bethesda) 21, 317–325 (2006).

Drozdowicz, Y. M., Rea, P. A. Vacuolar H^+ pyrophosphatases: From the evolutionary backwaters into the mainstream. Trends in Plant Science 6, 206–211 (2001).

Gaxiola, R. A., Palmgren, M. G., Schuhmacher, K. Plant proton pumps. FEBS Letters 581, 2204–2214 (2007).

Inoue, T., Wang, Y., Jefferies, K., Qi, J., Hinton, A., Forgac, M. Structure and regulation of the V-ATPases. Journal Bioenergetics Biomembranes 37, 393–398 (2005).

Junge, W., Lill, H., Engelbrecht, S. ATP synthase, an electrochemical transducer with rotary mechanics. Trends in Biochemical Science 22, 420–423 (1997).

Junge, W. Photophosphorylation. In G. Renger, ed. Primary Processes of Photosynthesis: Principles and Applications. Cambridge, UK: Royal Society of Chemistry, (pp. 447–467). (2007)

Kluge, C., Lahr, L., Hanitzsch, L., Bolte, S., Golldack, D., Dietz, K.-J. New insight into the structure and regulation of the plant vacuolar V-ATPase. Journal Bioenergetics Biomembranes 35, 377–388 (2003).

Kramer, D. M., Cruz, J. A., Kanazawa, A. Balancing the central roles of the thylakoid proton gradient. Trends in Plant Science 8, 27–32 (2003).

Noji, H., Yasuda, R., Yoshida, M., Kinosita, Jr., K. Direct observation of the rotation of F1-ATPase. Nature 386, 299–302 (1997).

Sambongi, Y., Iko, Y., Tanabe, M., Omote, H., Iwamoto-Kihara, A., Ueda, I., Yanagida, T., Wada, Y., Futai, M. Mechanical rotation of the c-subunit oligomer in ATP synthase (FoF_1): Direct observation. Science 286, 1722–1724 (1999).

Serrano, A., Pérez-Castiñeira, J. R., Baltscheffsky, M., Baltscheffsky, H. H^+-PPases: Yesterday, today and tomorrow. IUBMB Life 59, 76–83 (2007).

Stock, D., Leslie, A. G. W., Walker, J. E. Molecular architecture of the rotary motor in ATP synthase. Science 286, 1700–1705 (1999).

Sze, H., Schumacher, K., Mueller, M. L., Padmanaban, S., Taiz, L. A simple nomenclature for a complex proton pump: VHA genes encode the vacuolar H^+-ATPase. Trends Plant Science 7, 157–161 (2002).

Walker, J. E., Dickson, V. K. The peripheral stalk of the mitochondrial ATP synthase. Biochimica Biophysica Acta 1757, 286–296 (2006).

5

Mitochondria are the power station of the cell

In the process of biological oxidation, substrates such as carbohydrates are oxidized to form water and CO_2. Biological oxidation can be seen as a reversal of the photosynthesis process. It evolved only after oxygen accumulated in the atmosphere during photosynthesis. Both biological oxidation and photosynthesis serve the purpose of generating energy in the form of ATP. Biological oxidation involves a transport of electrons through a mitochondrial electron transport chain, which is in part similar to the photosynthetic electron transport discussed in Chapter 3. The present chapter will show that the machinery of mitochondrial electron transport is also assembled of three modules. The second complex has the same basic structure as the cytochrome-b_6/f complex of the chloroplasts. As in photosynthesis, the mitochondrial oxidative electron transport and ATP synthesis are coupled to each other via a proton gradient. The synthesis of ATP proceeds by an F-ATP synthase, which was described in Chapter 4.

5.1 Biological oxidation is preceded by a degradation of substrates to form bound hydrogen and CO_2

The overall reaction of biological oxidation is equivalent to a combustion of substrates. In contrast to technical combustion, however, biological oxidation proceeds in a sequence of partial reactions, which allows the utilization of the major part of the free energy for ATP synthesis.

The principle of biological oxidation was formulated in 1932 by the Nobel Prize winner Heinrich Wieland (Germany):

$$XH_2 + 1/2\,O_2 \rightarrow X + H_2O$$

First, hydrogen is removed from substrate XH_2 and afterwards oxidized to water. The oxidation of carbohydrates $[CH_2O]_n$ involves a degradation by reaction with water to form CO_2 and bound hydrogen [H], which is oxidized to water:

$$[CH_2O] + H_2O \rightarrow CO_2 + 4[H]$$

$$4[H] + O_2 \rightarrow 2H_2O$$

In 1934 Otto Warburg (Berlin, winner of the 1931 Nobel Prize in Medicine) showed that the transfer of bound hydrogen from substrates to the site of oxidation occurs in the form of **NADH**. From studies with homogenates from pigeon muscles, Hans Krebs formulated the **citrate cycle** (also called the Krebs cycle) in England in 1937, as a mechanism for substrate degradation yielding NADH for biological oxidation. In 1953 he was awarded the Nobel Prize in Medicine for this discovery. The operation of the citrate cycle will be discussed in detail in section 5.3.

5.2 Mitochondria are the sites of cell respiration

Light microscopic studies of many different cells revealed small granules, with an appearance similar to bacteria. In 1898 the botanist Carl Benda (Berlin) named these granules **mitochondria** ("threadlike bodies"). For a long time, however, the function of these mitochondria remained unclear.

As early as 1913, Otto Warburg realized that cell respiration involves the function of granular cell constituents. He succeeded in isolating a protein from yeast that he termed "**Atmungsferment**" (respiratory ferment), which catalyzes the oxidation by oxygen. He also showed that iron atoms are involved in this catalysis. In 1925 David Keilin from Cambridge (England) discovered the cytochromes and their participation in cell respiration. Using

a manual spectroscope, he identified the cytochromes-*a*, -a_3, -*b*, and -*c* (Fig. 3.24). In 1928 Otto Warburg showed that his "Atmungsferment" contained **cytochrome-a_3**. A further milestone in the clarification of cell respiration was reached in 1937, when Hermann Kalckar (USA) observed that the synthesis of ATP in aerobic systems depends on the consumption of oxygen. The interplay between cell respiration and ATP synthesis, termed **oxidative phosphorylation**, was now apparent. In 1948 Eugene Kennedy and Albert Lehninger (USA) showed that mitochondria contain the enzymes of the citrate cycle and oxidative phosphorylation. These findings demonstrated the function of the mitochondria as the **power station of the cell**.

Mitochondria form a separated metabolic compartment

Like plastids, mitochondria also form a separated metabolic compartment. The structure of the mitochondria is discussed in section 1.4. Figure 5.1 provides an overview of mitochondrial metabolism. The degradation of substrates to CO_2 and hydrogen (the latter bound to the transport metabolite NADH) takes place in the mitochondrial matrix. NADH thus formed diffuses through the matrix to the mitochondrial inner membrane and is oxidized there by the **respiratory chain**. The respiratory chain comprises

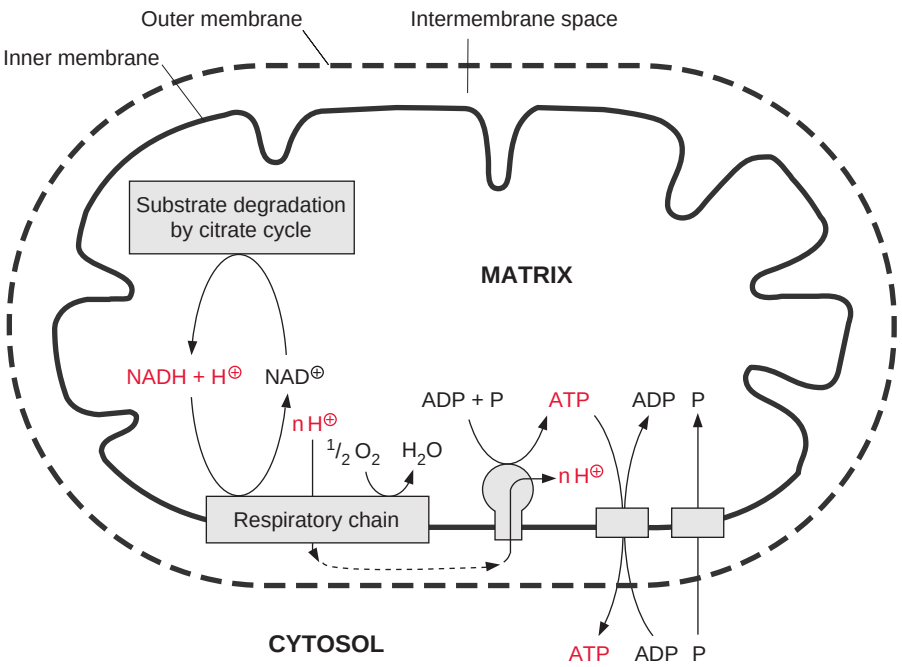

Figure 5.1 Schematic presentation of the mitochondrial energy metabolism.

a sequence of redox reactions by which electrons are transferred from NADH to oxygen. As in the photosynthetic electron transport, the mitochondrial electron transport by the respiratory chain releases free energy which is used to generate a proton gradient. This in turn drives the synthesis of ATP, which is exported from the mitochondria and provides the energy required for cellular metabolism. This process is universal and functions in the mitochondria of all eukaryotic cells.

5.3 Degradation of substrates applicable for biological oxidation takes place in the matrix compartment

Pyruvate, which is synthesized by the glycolytic catabolism of carbohydrates in the cytosol, is the starting compound for substrate degradation by the citrate cycle (Fig. 5.2). Pyruvate is first oxidized to acetate (in the form of acetyl coenzyme A), which is then completely degraded to CO_2 by the citrate cycle, yielding 10 reducing equivalents [H] to be oxidized by the respiratory chain to generate ATP. Figure 5.3 shows the reactions of the citrate cycle.

Pyruvate is oxidized by a multienzyme complex

Pyruvate oxidation is catalyzed by the **pyruvate dehydrogenase complex**, a multienzyme complex located in the mitochondrial matrix. It consists of three different catalytic subunits: **pyruvate dehydrogenase**, **dihydrolipoyl transacetylase**, and **dihydrolipoyl dehydrogenase** (Fig. 5.4). The pyruvate dehydrogenase subunit contains **thiamine pyrophosphate** (**TPP**, Fig. 5.5A) as the prosthetic group. The reactive group of TPP is the thiazole ring. Due to the presence of a positively charged N atom, the thiazole ring contains an acidic C-atom. After dissociation of a proton, a carbanion is formed,

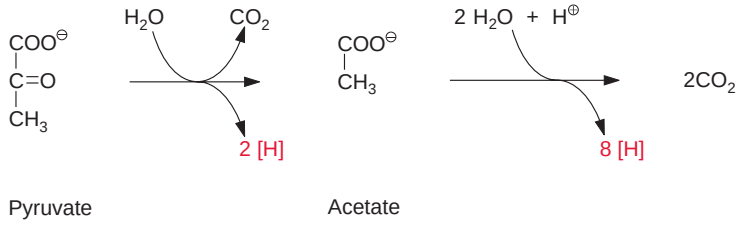

Figure 5.2 Overall reaction of the oxidation of pyruvate by mitochondria. The acetate is formed as acetyl coenzyme A. [H] represents bound hydrogen in NADH and $FADH_2$, respectively.

which binds to the carbonyl group of the pyruvate. The positively charged N atom of the thiazole ring enhances the decarboxylation of the bound pyruvate and hydroxethyl-TPP is formed (Fig. 5.4). The hydroxethyl group is now transferred to lipoic acid.

Lipoic acid is the prosthetic group of the dihydrolipoyl transacetylase subunit. It is covalently bound by its carboxyl group to a lysine residue of the enzyme protein via an amide bond (Fig. 5.5B). The lipoic acid residue is attached to the protein by a long carbon chain and therefore able to react with the various reaction sites of the multienzyme complex. Lipoic acid is equipped with two S atoms linked by a disulfide bond. When the hydroxyethyl residue is transferred to the lipoic acid residue, lipoic acid is

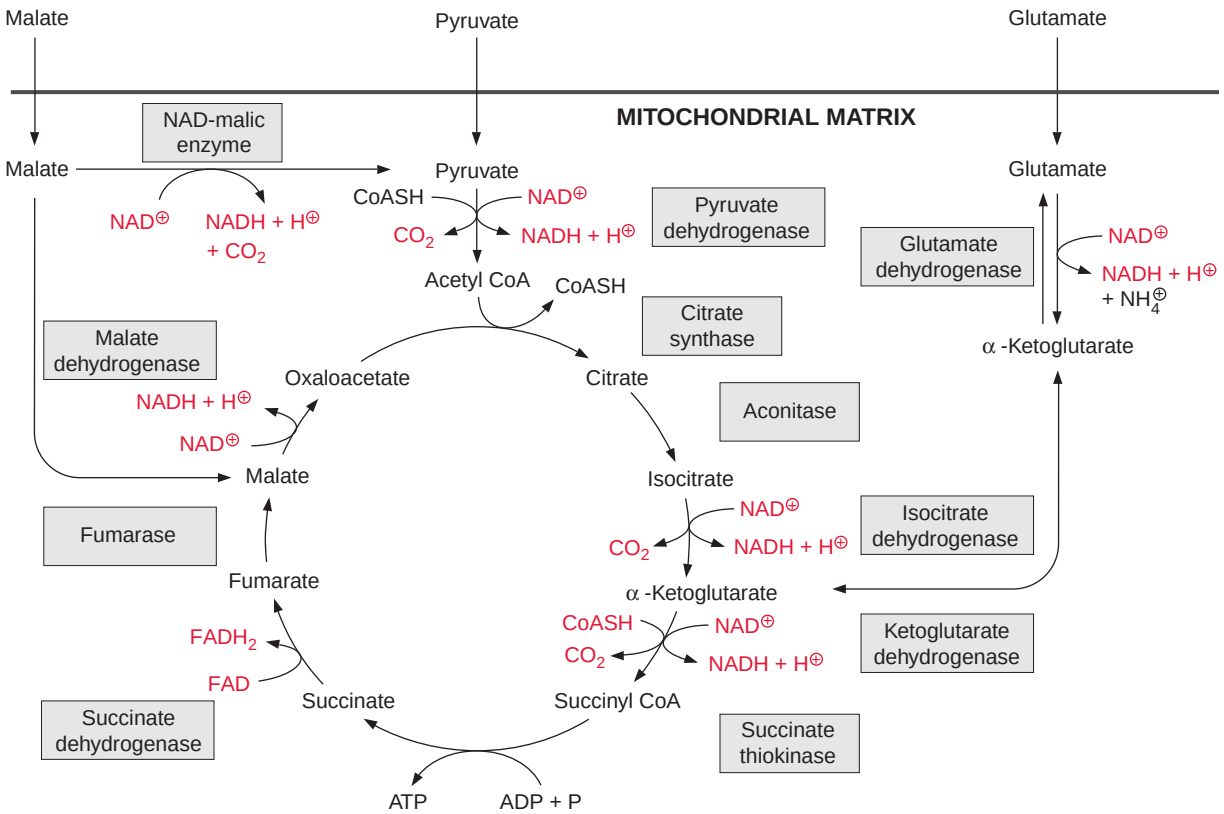

Figure 5.3 Schematic presentation of the citrate cycle. The enzymes are all localized in the mitochondrial matrix, with the exception of succinate dehydrogenase, which is located in the inner mitochondrial membrane. NAD-malic enzyme in the mitochondrial matrix allows plant mitochondria to also oxidize malate via the citrate cycle when no pyruvate is delivered by glycolysis. Glutamate dehydrogenase enables mitochondria to oxidize glutamate.

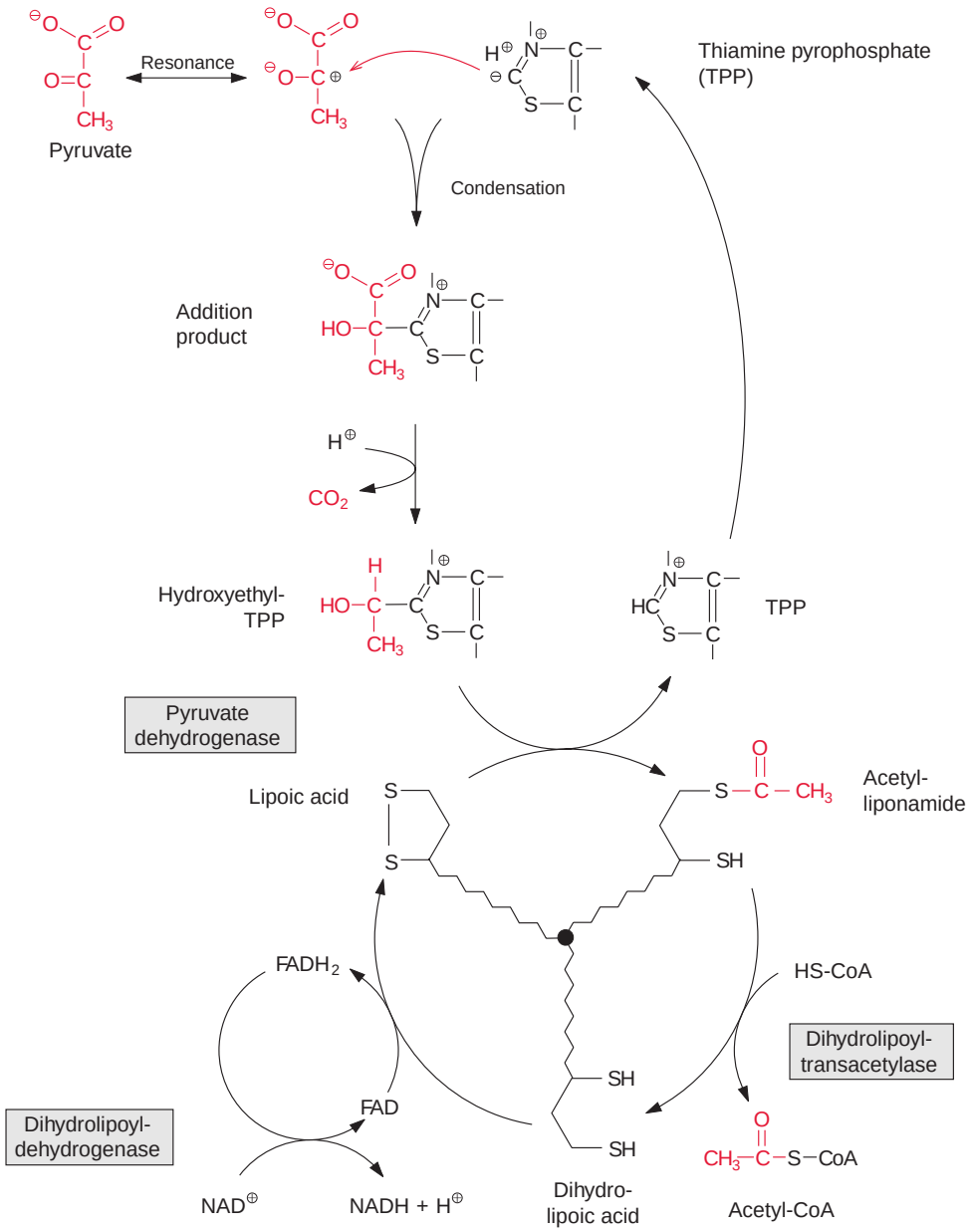

Figure 5.4 Oxidation of pyruvate by the pyruvate dehydrogenase complex, consisting of the subunits pyruvate dehydrogenase (with the prosthetic group thiamine pyrophosphate), dihydrolipoyl transacetylase (prosthetic group lipoic acid), and dihydrolipoyl dehydrogenase (prosthetic group FAD). The reactions of the cycle are described in the text.

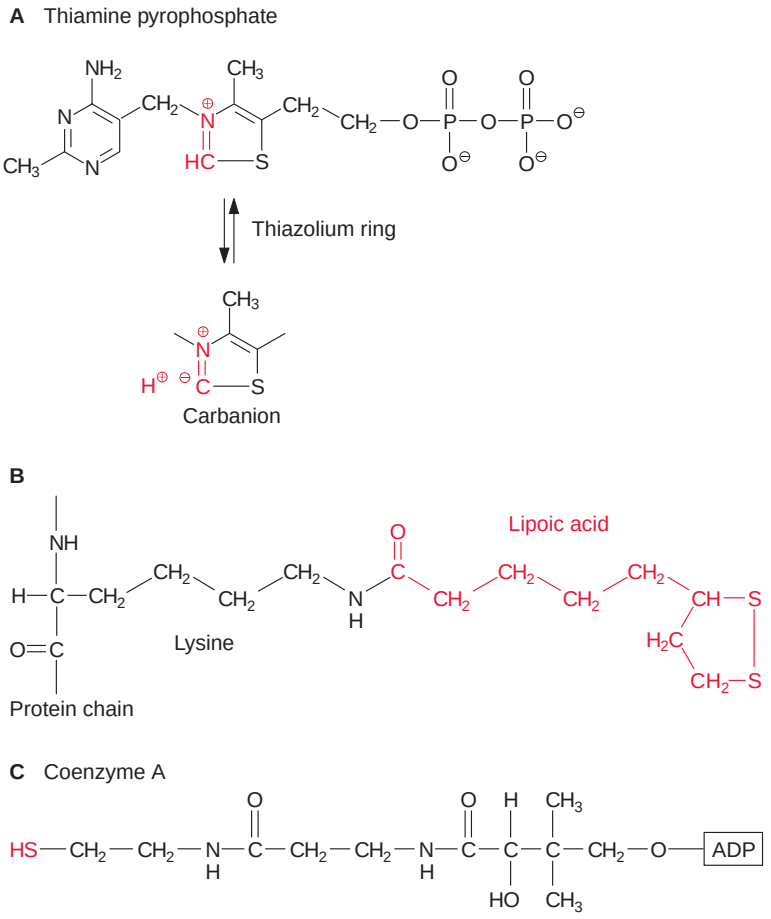

Figure 5.5 Reaction partners of pyruvate oxidation: A. Thiamine pyrophosphate; B. Lipoic amide; C. Coenzyme A.

reduced to dihydrolipoic acid and the hydroxyethyl residue is oxidized to an acetyl residue. The latter is now attached to the dihydrolipoic acid by a thioester bond. Thioester bonds are rich in energy, and store the energy released during oxidation of the carbonyl group. The acetyl residue is then transferred by dihydrolipoyl transacetylase to the sulfhydryl group of coenzyme A (Fig. 5.5C) to synthesize acetyl coenzyme A. **Acetyl CoA**—also called active acetic acid—was discovered by Feodor Lynen from Munich (1984 Nobel Prize in Medicine). Dihydrolipoic acid is reoxidized to lipoic acid by dihydrolipoyl dehydrogenase and NAD^+ is reduced to NADH via **FAD** (see Fig. 5.16). A pyruvate dehydrogenase complex is also present in the chloroplasts and its function in lipid biosynthesis will be discussed in section 15.3.

Acetate is completely oxidized in the citrate cycle

Acetyl coenzyme A enters the citrate cycle and condenses with oxaloacetate to citrate (Fig. 5.6). This reaction is catalyzed by the enzyme **citrate synthase**. The energy of the thioester group promotes the removal of a proton of the acetyl residue, and the carbanion thus formed binds to the carbonyl carbon of oxaloacetate. Subsequent release of CoA-SH makes the reaction irreversible. The enzyme **aconitase** (Fig. 5.7) catalyzes the reversible isomerization of citrate to isocitrate. In this reaction, first water is released, and the *cis*-aconitate thus formed remains bound to the enzyme and is then isomerized to isocitrate by the addition of water. In addition to the mitochondrial aconitase, there is also an isoenzyme of aconitase in the cytosol of plant cells.

Oxidation of isocitrate to α-ketoglutarate by **NAD isocitrate dehydrogenase** (Fig. 5.8) results in the formation of NADH. Oxalosuccinate is formed as intermediate, tightly bound to the enzyme to be decarboxylated to **α-ketoglutarate** (also termed 2-oxo-glutarate). This **oxidative decarboxylation** is an irreversible reaction. Besides the NAD-isocitrate dehydrogenase, mitochondria also contain an NADP-isocitrate dehydrogenase.

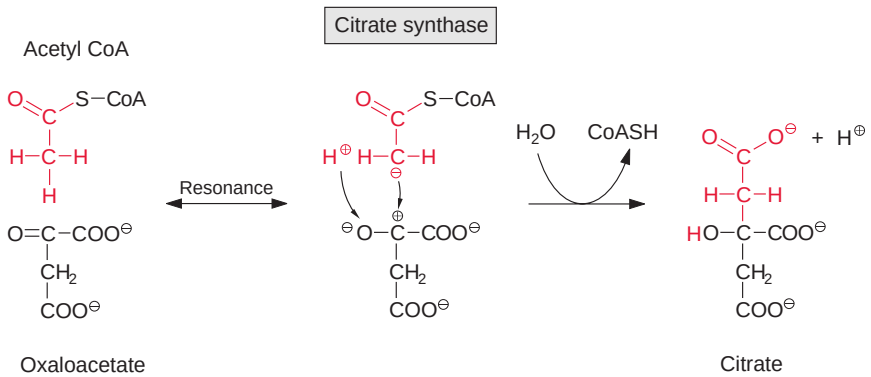

Figure 5.6 Condensation of acetyl CoA with oxaloacetate to synthesize citrate catalyzed by citrate synthase.

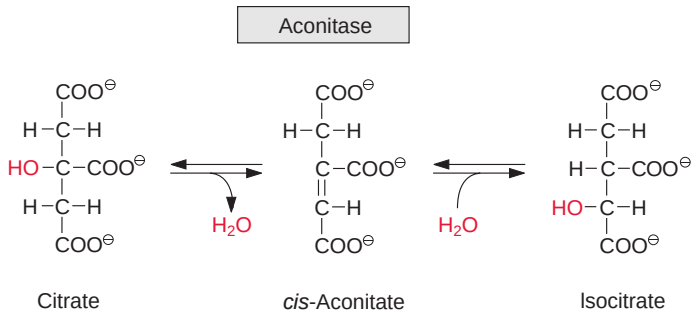

Figure 5.7 Isomerization of citrate to isocitrate catalyzed by aconitase.

NADP-isocitrate dehydrogenases also occur in the chloroplast stroma and in the cytosol. The function of the latter enzyme will be discussed in section 10.4.

Oxidation of α-ketoglutarate to succinyl-CoA (Fig. 5.8) is catalyzed by the **α-ketoglutarate dehydrogenase multienzyme complex**. This complex contains thiamine pyrophosphate, lipoic acid, and FAD, analogously to the pyruvate dehydrogenase multienzyme complex which catalyzes the reaction of pyruvate to acetyl CoA.

The thioester bond of the succinyl CoA is rich in energy. In the **succinate thiokinase** reaction, the free energy released upon the hydrolysis of this thioester is utilized to form ATP (Fig. 5.9). It may be noted that in animal metabolism the mitochondrial succinate thiokinase reaction yields GTP. The succinate formed is oxidized by **succinate dehydrogenase** to synthesize fumarate. Succinate dehydrogenase is the only enzyme of the citrate cycle that is not located in the matrix, but in the mitochondrial inner membrane, with its succinate binding site accessible from the matrix (section 5.5). Reducing equivalents ($FADH_2$) derived from succinate oxidation are transferred to ubiquinone. Catalyzed by **fumarase**, water reacts by *trans*-addition with the C-C double bond of fumarate to form L-malate. This is a reversible reaction (Fig. 5.9). Oxidation of malate by **malate dehydrogenase**, yielding oxaloacetate and NADH, is the final step in the citrate cycle (Fig. 5.9). The reaction equilibrium of this reversible reaction favors strongly the educt malate.

$$\frac{[\mathrm{NADH}] \cdot [\text{oxaloacetate}]}{[\mathrm{NAD^+}] \cdot [\text{malate}]} = 2.8 \cdot 10^{-5} (\text{pH } 7)$$

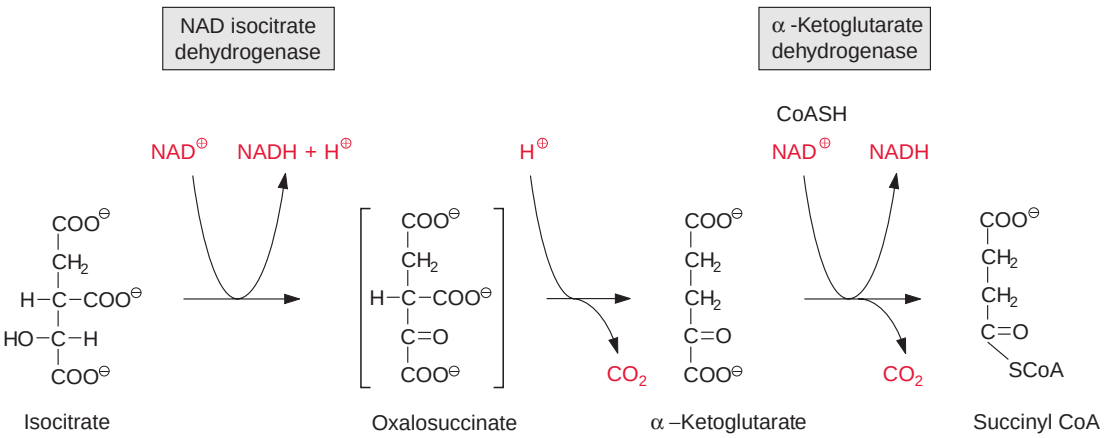

Figure 5.8 Oxidation of isocitrate to synthesize succinyl CoA catalyzed by NAD isocitrate dehydrogenase and α-ketoglutarate dehydrogenase.

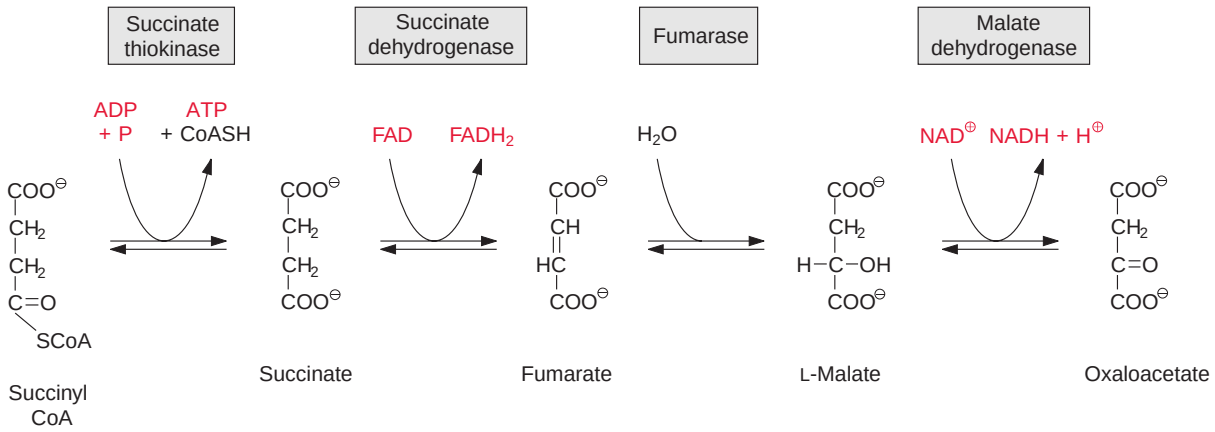

Figure 5.9 Conversion of succinyl CoA to oxaloacetate catalyzed by succinate thiokinase, succinate dehydrogenase, fumarase, and malate dehydrogenase.

Due to this equilibrium reaction, it is essential for an efficient operation of the citrate cycle that the citrate synthase reaction is irreversible. In this way oxaloacetate can be withdrawn from the malate dehydrogenase equilibrium to further support the reactions of the citrate cycle. Isoenzymes of malate dehydrogenase also occur outside the mitochondria. Both the cytosol and the peroxisomal matrix contain NAD-malate dehydrogenases, while an NADP-malate dehydrogenase is present only in the chloroplast stroma. These enzymes will be discussed in Chapter 7.

A loss of intermediates of the citrate cycle is replenished by anaplerotic reactions

The citrate cycle can proceed only when the oxaloacetate required as acceptor for the acetyl residue is fully regenerated. Section 10.4 describes how citrate and α-ketoglutarate are withdrawn from the citrate cycle to synthesize the carbon skeletons of amino acids in the course of nitrate assimilation. It is necessary, therefore, to replenish the loss of citrate cycle intermediates by **anaplerotic reactions**. In contrast to mitochondria from animal tissues, plant mitochondria are able to transport oxaloacetate into the chloroplasts via a specific translocator of the inner membrane (section 5.8). Therefore, the citrate cycle can be replenished by the uptake of oxaloacetate, which has been synthesized by phosphoenolpyruvate carboxylase in the cytosol (section 8.2). Oxaloacetate can also be delivered by oxidation of malate in the mitochondria. Malate is stored in the vacuole (sections 1.2, 8.2, and 8.5)

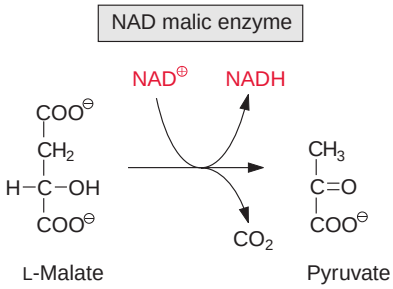

Figure 5.10 Oxidative decarboxylation of malate to synthesize pyruvate catalyzed by NAD-malic enzyme.

and is an important substrate for mitochondrial respiration. A special feature of plant mitochondria is that malate is oxidized in the matrix via **NAD-malic enzyme** to pyruvate with the reduction of NAD^+ and the release of CO_2 (Fig. 5.10). Thus interplay of malate dehydrogenase and NAD-malic enzyme allows citrate to be formed from malate without the operation of the complete citrate cycle (Fig. 5.3). It may be noted that an **NADP-dependent malic enzyme** is present in the chloroplasts, especially in C_4 plants (section 8.4).

Another important substrate of mitochondrial oxidation is **glutamate**, which is one of the main products of nitrate assimilation (section 10.1) and, besides sucrose, the most highly concentrated organic compound in the cytosol of many plant cells. Glutamate oxidation, accompanied by formation of NADH, is catalyzed by **glutamate dehydrogenase** located in the mitochondrial matrix (Fig. 5.11). This enzyme also reacts with $NADP^+$. NADP-glutamate dehydrogenase activity is also present in plastids, although its function is yet not understood.

Glycine is the main substrate of respiration in the mitochondria from mesophyll cells of illuminated leaves. The oxidation of glycine as a partial reaction of the photorespiratory pathway will be discussed in section 7.1.

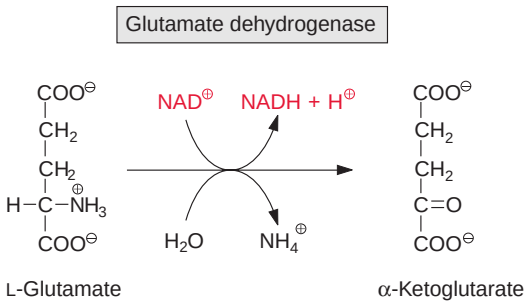

Figure 5.11 Oxidation of glutamate catalyzed by glutamate dehydrogenase.

5.4 How much energy can be gained by the oxidation of NADH?

How much energy is released during mitochondrial respiration or, to be more exact, how large is the difference in free energy in the mitochondrial redox processes? To answer this question the differences of the potentials of the redox pairs are calculated by the Nernst equation:

$$E = E^{0'} + \frac{RT}{nF} \ln \frac{\text{oxidized substance}}{\text{reduced substance}} \tag{5.1}$$

where $E^{0'}$ = standard potential at pH 7, 25°C; R (gas constant) = 8.31 J/K·mol; $T = 298$ K; n is the number of electrons transferred; and F (Faraday constant) = 96,485 A s/mol.

The standard potential for the redox pair NAD^+/NADH is:

$$E^{0'} = -0.320 \text{ V}$$

Under certain metabolic conditions, an NAD^+/NADH ratio was found to be 3 in mitochondria from leaves. The introduction of this value into equation 5.1 yields:

$$E_{NAD^+/NADH} = -0.320 + \frac{RT}{2F} \ln 3 = -0.306 \text{ V} \tag{5.2}$$

The standard potential for the redox pair H_2O/O_2 is:

$$E^{0'} = +0.815 \text{ V} \qquad ([H_2O] \text{ in water } 55 \text{ mol/L})$$

To evaluate the actual potential of $[O_2]$ the partial pressure of the oxygen in the air is introduced:

$$E_{H_2O/O_2} = 0.815 + \frac{RT}{2F} \ln \sqrt{p}\ O_2 \tag{5.3}$$

The partial pressure of the oxygen in the air (pO_2) is 0.2. Introducing this value into equation 5.3 yields:

$$E_{H_2O/O_2} = 0.805 \text{ V}$$

The difference of the potentials amounts to:

$$\Delta E = E_{H_2O/O_2} - E_{NAD^+/NADH} = +1.11\,V \tag{5.4}$$

The free energy (ΔG) is related to ΔE as follows:

$$\Delta G = -nF\Delta E \tag{5.5}$$

Two electrons are transferred in the reaction. The introduction of ΔE into equation 5.5 shows that the change of free energy during the oxidation of NADH by the respiratory chain amounts to:

$$\Delta G = -214\,kJ/mol$$

How much energy is required for the formation of ATP? It has been calculated in section 4.1 that the synthesis of ATP under the metabolic conditions in the chloroplasts requires a change of free energy of $\Delta G \approx +50\,kJ/mol$. This value also applies approximately for the ATP which mitochondria provide for the cytosol.

The calculated free energy released by the oxidation of NADH would therefore be sufficient to generate four molecules of ATP, but in fact the amount of ATP synthesized by NADH oxidation *in vivo* is much lower (section 5.6).

5.5 The mitochondrial respiratory chain shares common features with the photosynthetic electron transport chain

The photosynthesis of cyanobacteria led to the accumulation of oxygen in the early atmosphere, which was the basis for the oxidative metabolism of mitochondria. Many cyanobacteria can satisfy their ATP demand both by photosynthesis and by oxidative metabolism. Cyanobacteria contain a photosynthetic electron transport chain that consists of three modules (complexes), namely, photosystem II, the cyt-b_6/f complex, and photosystem I (Chapter 3, Fig. 5.12). These complexes are located in the inner membrane of cyanobacteria, where the enzymes of the respiratory electron transport chain are also localized. This respiratory chain consists of three modules: an **NADH**

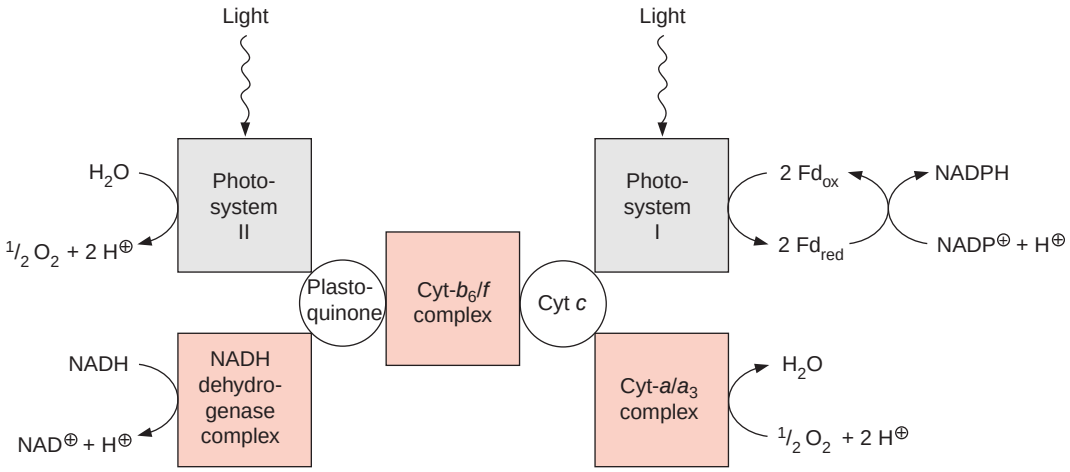

Figure 5.12 Schematic presentation of photosynthetic and oxidative electron transport in cyanobacteria. In both electron transport chains the cytochrome-b_6/f complex functions as the central complex.

dehydrogenase complex, catalyzing the oxidation of NADH; the same **cyt-b_6/f complex** that is also part of the photosynthetic electron transport chain; and a **cyt-a/a_3 complex**, by which oxygen is reduced to water. Plastoquinone feeds the electrons into the cyt-b_6/f complex not only in photosynthesis (section 3.7), but also in the respiratory chain of the cyanobacteria. Likewise, cytochrome-*c* mediates the electron transport from the cyt-b_6/f complex to photosystem I as well as to the cyt-a/a_3 complex. The relationship between photosynthetic and oxidative electron transport in cyanobacteria is obvious; both electron transport chains possess the same module as the middle of the reaction sequence, the cyt-b_6/f complex. Section 3.7 described how the cyt-b_6/f complex released the energy during electron transport to build up a proton gradient. The function of the cyt-b_6/f complex in respiration and photosynthesis shows that the principle of energy conservation in photosynthetic and oxidative electron transport is the same.

The mitochondrial respiratory chain is analogous to the respiratory chain of cyanobacteria (Fig. 5.13), but with ubiquinone instead of plastoquinone as redox carrier and slightly different cytochromes. The mitochondria contain a related cyt-b/c_1 complex instead of a cyt-b_6/f complex, but both cyt-*c* and cyt-*f* contain heme-*c*.

Figure 5.13 shows succinate dehydrogenase, another electron acceptor of the mitochondrial respiratory chain. This enzyme (historically termed complex II) catalyzes the oxidation of succinate to fumarate, a step of the citrate cycle (Fig. 5.9).

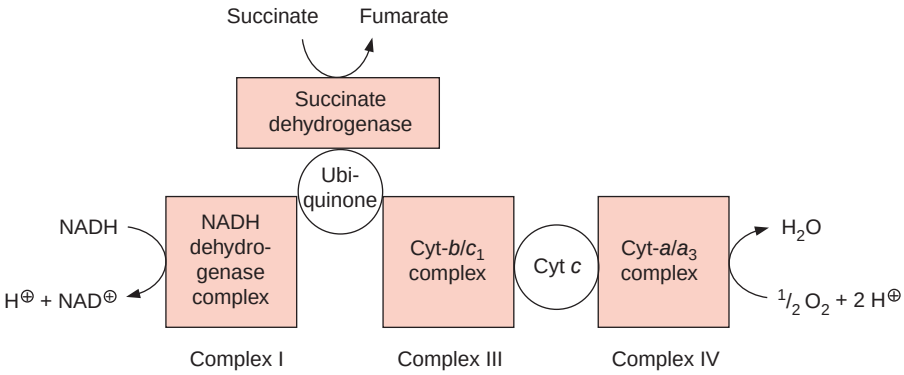

Figure 5.13 Schematic presentation of the mitochondrial electron transport. The respiratory chain consists of four complexes; the central cyt-b/c_1 complex corresponds to the cyt-b_6/f complex of cyanobacteria and chloroplasts.

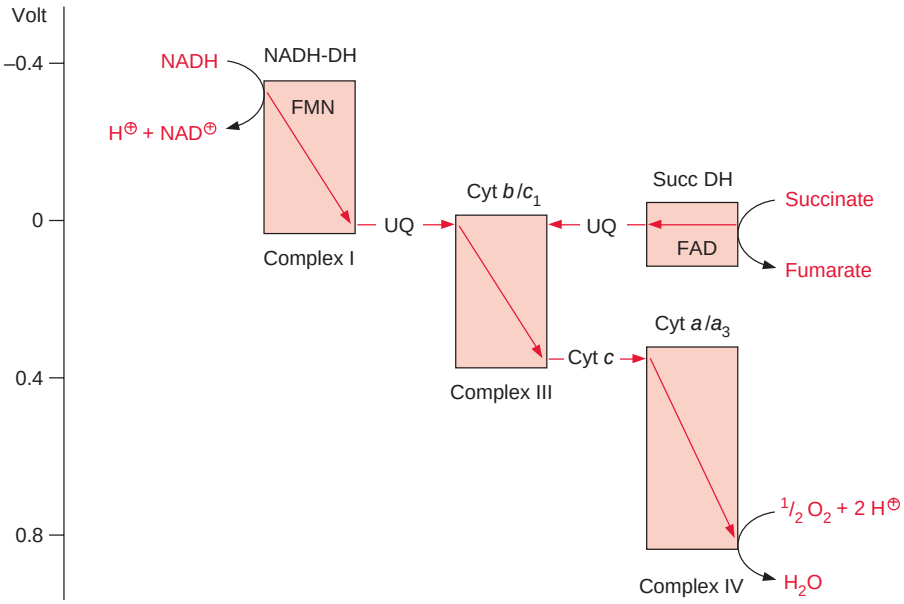

Figure 5.14 Schematic presentation of the complexes of the respiratory chain arranged according to their redox potentials.

The complexes of the mitochondrial respiratory chain

The subdivision of the respiratory chain into several complexes goes back to the work of Youssef Hatefi (USA, 1962), who succeeded in isolating four different complexes, which he termed complexes I–IV, while working with beef heart mitochondria. In the complexes I, III, and IV, the electron transport is accompanied by a decrease in the redox potential (Fig. 5.14); the energy thus released creates a proton gradient.

The **NADH dehydrogenase complex** (complex I) (Fig. 5.15) feeds the respiratory chain with the electrons from NADH formed from the degradation of substrates in the matrix. The electrons are transferred to ubiquinone via a flavin adenine mononucleotide (**FMN**) and several iron-sulfur centers.

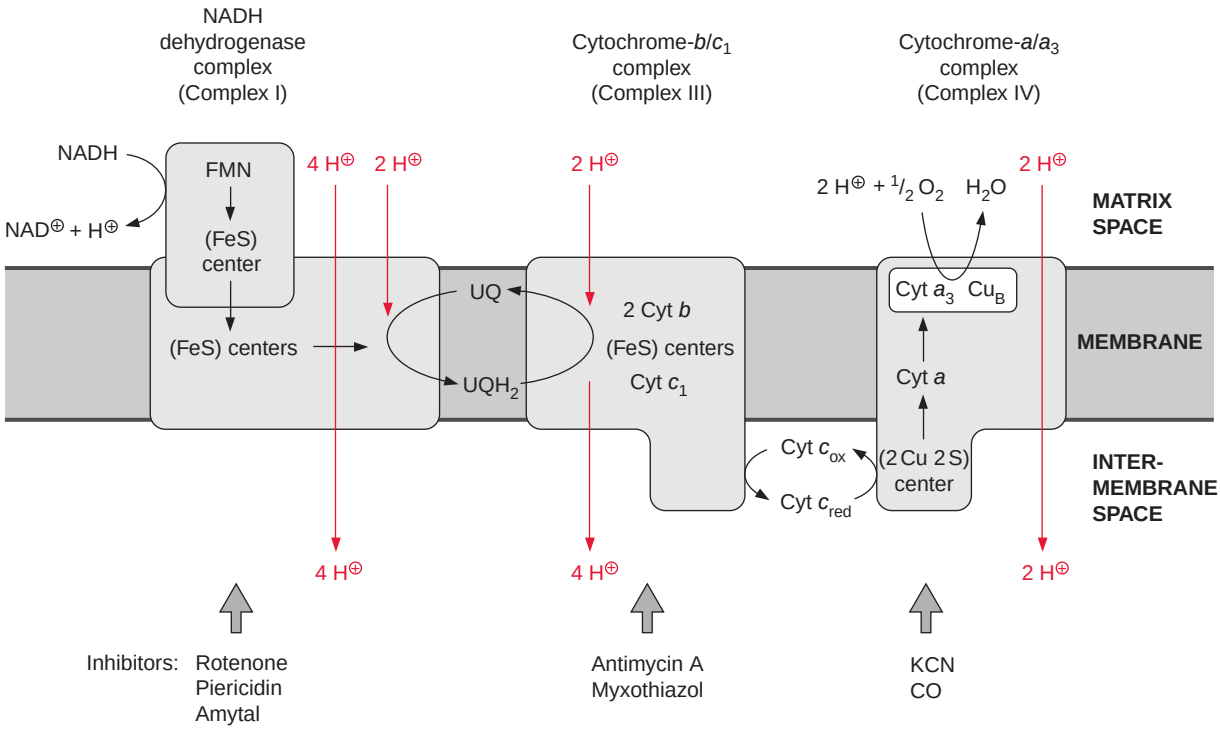

Figure 5.15 Schematic presentation of the location of complexes I, III, and IV in the mitochondrial respiratory chain. Positions of proton transfer are indicated. Antibiotics inhibit the membrane complexes.

Complex I has the most complicated structure of all the mitochondrial electron transport complexes. It consists of more than 40 different subunits (of which, depending on the organism, seven to nine are encoded in the mitochondria). Part of the complex is embedded in the membrane (**membrane part**) and a **peripheral part** protrudes into the matrix space. The peripheral part provides the binding site for NADH and comprises FMN (Fig. 5.16) and at least three Fe-S-centers (Fig. 3.26). The membrane part contains another Fe-S-center, as well as the binding site for ubiquinone. The electron transport can be inhibited by a variety of poisons deriving from plants and bacteria, such as **rotenone** (which protects plants from being eaten by animals); the antibiotic **piericidin A**; and **amytal**, a barbiturate. The electron transport catalyzed by complex I is reversible. It is therefore possible for electrons to be transferred from ubiquinone to NAD^+, driven by the proton motive force of the proton gradient. In this way the NADH dehydrogenase complex can provide purple bacteria with NADH (see Fig. 3.1).

In plants the **succinate dehydrogenase** (complex II) (Fig. 5.9) consists of seven subunits comprising a flavin adenine nucleotide (FAD, Fig. 5.16) as

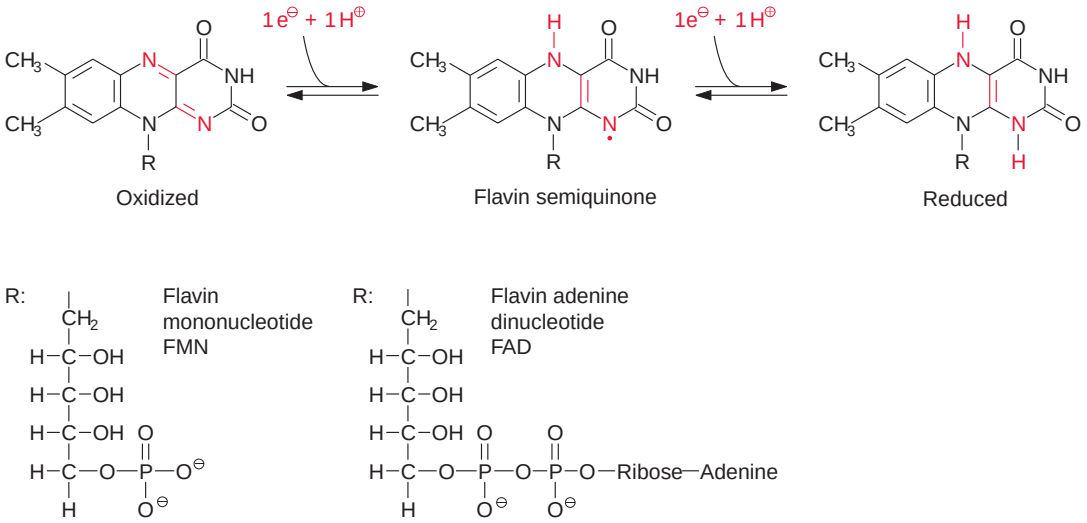

Figure 5.16 Structures of reduced and oxidized FMN and FAD.

the electron acceptor; several Fe-S-centers (Fig. 3.26) as redox carriers; and one cytochrome-*b*, of which the function is not known. Electron transport by succinate dehydrogenase to ubiquinone proceeds with no major decrease in the redox potential, so no energy is gained in the electron transport from succinate to ubiquinone.

Ubiquinone reduced by the NADH dehydrogenase complex or succinate dehydrogenase is oxidized by the **cyt-*b*/*c*$_1$ complex** (complex III) (Fig. 5.15). In mitochondria this complex consists of 11 subunits, only one of which (the cyt-*b* subunit) is encoded in the mitochondria. The cyt-*b*/*c*$_1$ complex is very similar in structure and function to the cyt-b_6/*f* complex of chloroplasts (section 3.7). Electrons are transferred by the cyt-*b*/*c*$_1$ complex to cyt-*c*, which is bound to the outer surface of the inner membrane. Several antibiotics, such as **antimycin A** and **myxothiazol**, inhibit the electron transport by the cyt-*b*/*c*$_1$ complex.

Due to its positive charge, reduced cyt-*c* diffuses along the negatively charged surface of the inner membrane to the **cyt-*a*/*a*$_3$ complex** (Fig. 5.15), also termed **complex IV** or **cytochrome oxidase**. The cyt-*a*/*a*$_3$ complex contains 13 different subunits, three of which are encoded in the mitochondria. The three-dimensional structures of the beef heart mitochondrial and *Paracoccus denitrificans* cyt-*a*/*a*$_3$ complex have been resolved by X-ray crystallography. The complex has a large hydrophilic region that protrudes into the intermembrane space and provides the binding site for cyt-*c*. During the oxidation of cyt-*c* the electrons are transferred to a **copper sulfur cluster** containing two Cu atoms called Cu$_A$. These two Cu atoms are linked by two S-atoms of cysteine side chains (Fig. 5.17). This copper-sulfur cluster

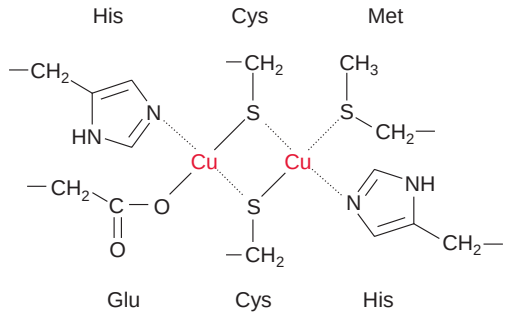

Figure 5.17 A copper-sulfur cluster of the cytochrome-*a*/a_3 complex. Cu_A, a Cu^{2+}- and a Cu^{+}-ion are linked by two cysteine residues, two histidines, one glutamate and one methionine to the protein. Cu_A probably transfers one electron.

probably takes up one electron and transfers it via cyt-*a* to a **binuclear center**, consisting of cyt-a_3 and a Cu atom (Cu_B), bound to histidine. This binuclear center functions as a redox unit in which the Fe atom of the cyt-a_3, together with Cu_B, take up two electrons.

$$[Fe^{+++} \cdot Cu_B^{++}] + 2e^- \rightarrow [Fe^{++} \cdot Cu_B^{+}]$$

In contrast to cyt-*a* and the other cytochromes of the respiratory chain, the sixth coordination position of cyt-a_3 of the heme Fe atom is not saturated by an amino acid of the protein (Fig. 5.18). This free coordination position as well as Cu_B are the binding site for the oxygen molecule, which is reduced to water by the uptake of four electrons:

$$O_2 + 4\,e^- \rightarrow 2\,O^{2-} + 4\,H^+ \rightarrow 2\,H_2O$$

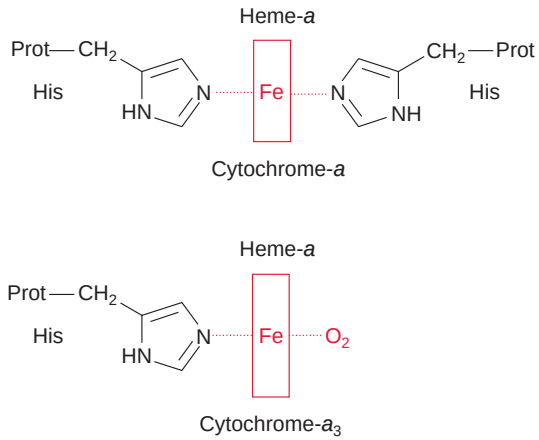

Figure 5.18 Axial ligands of the Fe atoms in the heme groups of cytochrome-*a* and -a_3. Of the six coordinative bonds of the Fe atom in the heme, four are saturated by the N atoms present in the planar tetrapyrrole ring. Whereas in cytochrome-*a* the two remaining coordination positions of the central Fe atom bind to two histidine residues of the protein, positioned at either side vertically to the plane of the tetrapyrrole, in cytochrome-a_3 one of these coordination positions is free and functions as binding site for the O_2 molecule.

Furthermore, Cu_B probably has an important function in electron-driven proton transport, which is discussed in the next section. Instead of O_2, also CO and CN^- can be very tightly bound to the free coordination position of the Cyt-a_3, and efficiently inhibit the respiration. Therefore, both carbon monoxide and prussic acid (HCN) are very potent poisons.

5.6 Electron transport of the respiratory chain is coupled to the synthesis of ATP via proton transport

The electron transport of the respiratory chain is coupled to the formation of ATP. This is illustrated in the experiment of Figure 5.19, in which the velocity of respiration in a mitochondrial suspension was determined by measuring the decrease of the oxygen concentration in the suspension medium. The addition of a substrate alone (e.g., malate) causes only a minor increase in respiration. The subsequent addition of a limited amount of ADP results in a considerable acceleration of respiration. After some time, however, respiration returns to the lower rate prior to the addition of ADP,

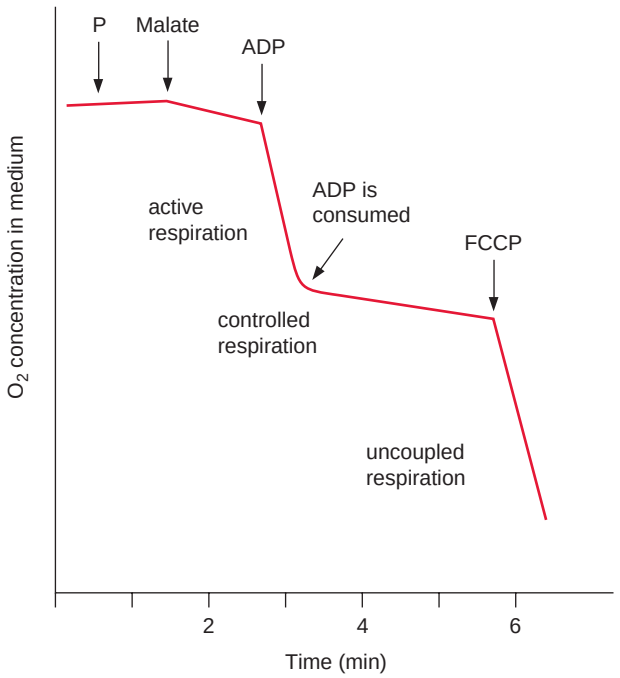

Figure 5.19 Registration of oxygen consumption by isolated mitochondria. Phosphate and malate are added one after the other to mitochondria suspended in a buffered osmotic solution. Addition of ADP results in a high rate of respiration. The subsequent decrease of oxygen consumption indicates that the conversion of the added ADP into ATP is completed. Upon the addition of an uncoupler (e.g., FCCP), a high respiration rate is attained without ADP: respiration is now uncoupled from ATP synthesis.

as the ADP has been completely converted to ATP. Respiration in the presence of ADP is called **active respiration**, whereas that after ADP is consumed is called **controlled respiration**. As the ADP added to the mitochondria is completely converted to ATP, the amount of ATP formed with the oxidation of a certain substrate can be determined from the ratio of ADP added to oxygen consumed (**ADP/O**). An ADP/O of about 2.5 is determined for substrates oxidized in the mitochondria via the formation of NADH (e.g., malate), and of about 1.6 for succinate, from which the redox equivalents are directly transferred via FADH to ubiquinone. The problem of ATP stoichiometry of respiration will be discussed at the end of this section.

Like photosynthetic electron transport (Chapter 4), the electron transport of the respiratory chain is accompanied by the generation of a proton

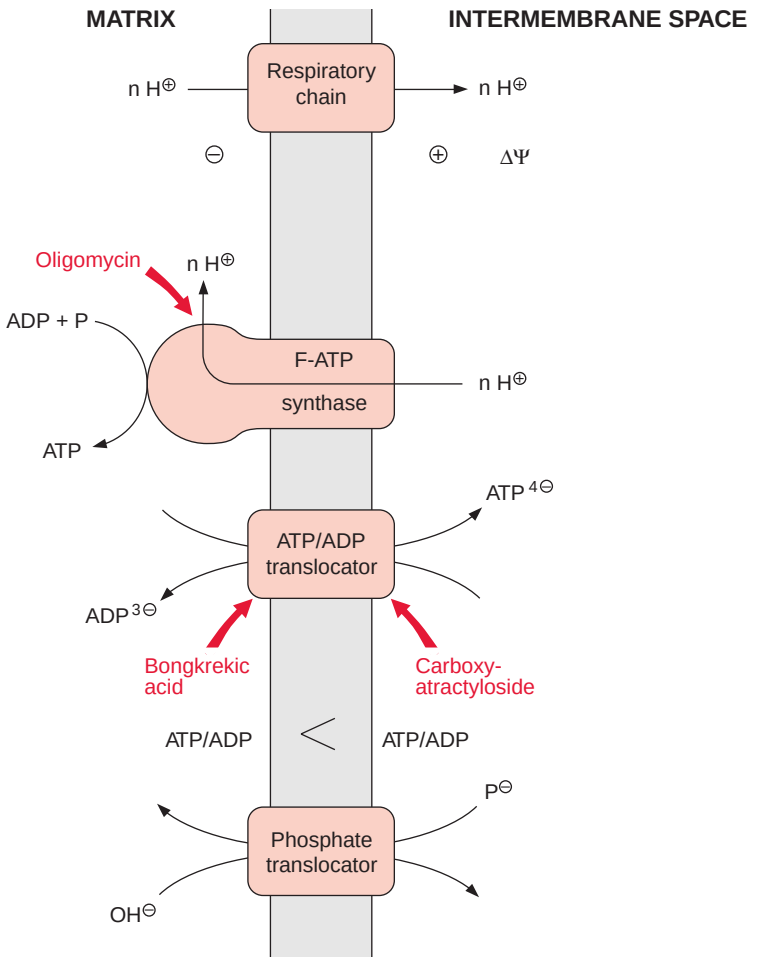

Figure 5.20 ATP synthesis by mitochondria requires an uptake of phosphate by the phosphate translocator in counter-exchange for OH^- ions, and an electrogenic exchange of ATP for ADP, as catalyzed by the ATP/ADP translocator. Due to the membrane potential generated by electron transport of the respiratory chain, ADP is preferentially transported inward and ATP outward. As a result of this the ATP/ADP ratio in the cytosol is higher than in the mitochondrial matrix. ATP/ADP transport is inhibited by carboxyactractyloside (binding from the intermembrane space) and bongkrekic acid (binding from the matrix side). F_1 part of the F-ATP synthase of the mitochondria is inhibited by oligomycin.

motive force (Fig. 5.15), which in turn drives the synthesis of ATP (Fig. 5.20). Therefore substances such as FCCP (Fig. 4.2) function as uncouplers of mitochondrial as well as photosynthetic electron transport. Figure 5.19 shows that the addition of the uncoupler FCCP results in a high stimulation of respiration. As discussed in section 4.2, the uncoupling function of the FCCP is due to a short circuit of protons across a membrane, resulting in the elimination of the proton gradient. The respiration is then uncoupled from ATP synthesis and the energy set free during electron transport is dissipated as heat.

To match respiration to the energy demand of the cell, it is regulated by an overlapping of two different mechanisms. The classic mechanism of **respiratory control** is based on the fact that when the ATP/ADP ratio increases, the proton motive force also increases, which in turn causes a decrease of electron transport by the respiratory chain. Recently it was discovered that ATP also impedes the electron transport by binding to a subunit of cytochrome oxidase, which results in a decrease of its activity.

Mitochondrial proton transport results in the formation of a membrane potential

Mitochondria, in contrast to chloroplasts, have no closed thylakoid space to form a proton gradient. Instead, in mitochondrial electron transport, protons are transported from the matrix to the intermembrane space, which is, however, connected to the cytosol by pores (formed by porines (Fig. 1.30)). In chloroplasts the formation of a proton gradient of $\Delta pH = 2.5$ in the light results in a decrease of pH in the thylakoid lumen from about pH 7.5 to pH 5.0. If during mitochondrial oxidation such a strong acidification were to occur in the cytosol, it would have a grave effect on the activity of the cytosolic enzymes. In fact, during mitochondrial controlled respiration the ΔpH across the inner membrane is only about 0.2, and therefore mitochondrial proton transport leads primarily to the formation of a membrane potential ($\Delta\Psi \approx 200\,mV$). Mitochondria are unable to generate a larger proton gradient, as their inner membrane is impermeable for anions, such as chloride. As shown in Figure 4.1, a proton concentration gradient can be formed only when the charge of the transported protons is compensated by the diffusion of a counter anion.

Despite intensive research for more than 30 years our knowledge of the mechanism of coupling between mitochondrial electron transport and transport of protons is still incomplete. Four protons are probably taken up from the matrix side during the transport of two electrons from the NADH dehydrogenase complex to ubiquinone and released into the intermembrane space by the cyt-b/c_1 complex (Fig. 5.15). It is generally accepted that in

mitochondria the cyt-b/c_1 complex catalyzes a **Q-cycle** (Fig. 3.30) by which, when two electrons are transported, two additional protons are transported out of the matrix space into the intermembrane space. Finally, the cyt-a/a_3 complex transports two protons per two electrons. The three-dimensional structure of the cyt-a/a_3 complex indicates that the binuclear center from cytochrome-a_3 and Cu_B is involved in this proton transport. If these stoichiometries are correct, altogether 10 protons would be transported during the oxidation of NADH and only six during the oxidation of succinate.

Mitochondrial ATP synthesis serves the energy demand of the cytosol

The energy of the proton gradient is used in the mitochondria for ATP synthesis by an F-ATP synthase (Fig. 5.20), which has the same basic structure as the F-ATP synthase of chloroplasts (section 4.3). However, there are differences regarding the inhibition by **oligomycin**, an antibiotic from *Streptomyces*. Whereas the mitochondrial F-ATP synthase is very strongly inhibited by oligomycin, due to the presence of an oligomycin binding protein, the chloroplast enzyme is insensitive to this inhibitor. Although the mechanism of ATP synthesis appears to be identical for both ATP synthases, the proton stoichiometry in mitochondrial ATP synthesis has not been resolved unequivocally. Assuming that the rotor of the F-ATP synthase in mitochondria has 10 c-subunits, 3.3 protons would be required for the synthesis of 1 mol of ATP (according to the mechanism for ATP synthesis discussed in section 4.4). This rate corresponds more or less with previous independent investigations.

In contrast to chloroplasts, which synthesize ATP essentially for their own consumption, the ATP in mitochondria is synthesized mainly for export into the cytosol. This requires the uptake of ADP and phosphate from the cytosol into the mitochondria and vice versa the release of the synthesized ATP. The uptake of phosphate proceeds by the **phosphate translocator** in a counter-exchange for OH^- ions, whereas the uptake of ADP and the release of ATP are mediated by the **ATP/ADP translocator** (Fig. 5.20). The mitochondrial ATP/ADP translocator is inhibited by **carboxyatractyloside**, a glucoside from the thistle *Atractylis gumnifera*, and by **bongkrekic acid**, an antibiotic from the bacterium *Cocovenerans*, growing on coconuts. Both compounds are deadly poisons.

The ATP/ADP translocator catalyzes a strict **counter-exchange**; for each ATP or ADP transported out of the chloroplasts, an ADP or ATP is transported inward. Since the transported ATP contains one negative charge more than the ADP, the transport is electrogenic. Due to the membrane potential generated by the proton transport of the respiratory chain, there

is a preference for ADP to be taken up and ATP to be transported outward. As a result of this asymmetric transport of ADP and ATP the ATP/ADP ratio outside the mitochondria is much higher than in the matrix. In this way mitochondrial ATP synthesis maintains a high ATP/ADP ratio in the cytosol. With the exchange of ADP for ATP, one negative charge is transferred from the matrix to the outside, which requires the transport of a proton in the other direction to compensate this charge difference. This is why protons from the proton gradient are consumed not only for ATP synthesis as such, but also for export of the synthesized ATP from the mitochondria.

Let us return to the stoichiometry between the transported protons and the ATP formation during respiration. It is customary to speak of three coupling sites of the respiratory chain, which correspond to the complexes I, III, and IV. Textbooks often state that during NADH oxidation by the mitochondrial respiratory chain, one molecule of ATP is formed per coupling site, and as a result of this, the ADP/O quotient for oxidation of NADH amounts to three, and that for succinate to two. However, considerably lower values have been determined in experiments with isolated mitochondria. The attempt was made to explain this discrepancy by assuming that owing to a proton leakage of the membrane, the theoretical ADP/O values were not attained in the isolated mitochondria. It appears now that even in theory these whole numbers for ADP/O ratios are incorrect. Probably 10 protons are transported upon the oxidation of NADH. In the event that 3.3 protons are required for the synthesis of ATP and another one for its export from the mitochondria, the resulting ADP/O would be 2.3. With isolated mitochondria, values of about 2.5 have been obtained experimentally.

At the beginning of this chapter, the change in free energy during the oxidation of NADH was evaluated to be $-214\,kJ/mol$ and for the synthesis of ATP as about $+50\,kJ/mol$. An ADP/O of 2.3 for the respiration of NADH-dependent substrates indicates that about 54% of the free energy released during oxidation is used for the synthesis of ATP. However, these values must still be treated with caution.

5.7 Plant mitochondria have special metabolic functions

The function of the mitochondria as being the power station of the cell applies for all mitochondria, from unicellular organisms to animals and

plants. In plant cells which perform photosynthesis, the role of the mitochondria as a supplier of energy is not restricted to the dark phase; the mitochondria provide the cytosol with ATP also during photosynthesis.

Plant mitochondria fulfill additional functions. The mitochondrial matrix contains enzymes for the oxidation of glycine to serine, an important step in the photorespiratory pathway (section 7.1):

$$2\ \text{glycine} + NAD^+ + H_2O \rightarrow \text{serine} + NADH + CO_2 + NH_4^+$$

The NADH generated from glycine oxidation is the main fuel for mitochondrial ATP synthesis during photosynthesis. Another important role of plant mitochondria is the conversion of oxaloacetate and pyruvate to form citrate, a precursor for the synthesis of α-ketoglutarate. This pathway is important for providing the carbon skeletons for amino acid synthesis during nitrate assimilation (Fig. 10.11).

Mitochondria can oxidize surplus NADH without forming ATP

In mitochondrial electron transport, the participation of flavins, ubisemiquinones, and other electron carriers leads to the formation of superoxide radicals, H_2O_2, and hydroxyl radicals (summarized as **ROS**, reactive oxygen species (section 3.9)) as by-products. These by-products cause severe cell damage. Since the formation of ROS is especially high, when the components of the respiratory chain are highly reduced, there is a necessity to avoid an overreduction of the respiratory chain. On the other hand, it is essential for a plant that glycine, formed in large quantities by the photorespiratory cycle (section 7.1), is converted by mitochondrial oxidation even when the cell does not require ATP. Plant mitochondria have several **overflow mechanisms**, which oxidize surplus NADH without synthesizing ATP in order to prevent an overreduction of the respiratory chain (Fig. 5.21). Among those are an alternative NADH-dehydrogenase, an alternative oxidase (Fig. 5.21) and uncoupling proteins. The **alternative NADH dehydrogenase**, located in the inner mitochondrial membrane, transfers electrons from NADH to ubiquinone, without coupling to proton transport. This pathway is not inhibited by rotenone. However, oxidation of NADH via this rotenone-insensitive pathway proceeds only when the NADH/NAD^+ ratio in the matrix is exceptionally high. In addition, the matrix side of the mitochondrial inner membrane contains an alternative NADPH dehydrogenase (not shown in Figure 5.21).

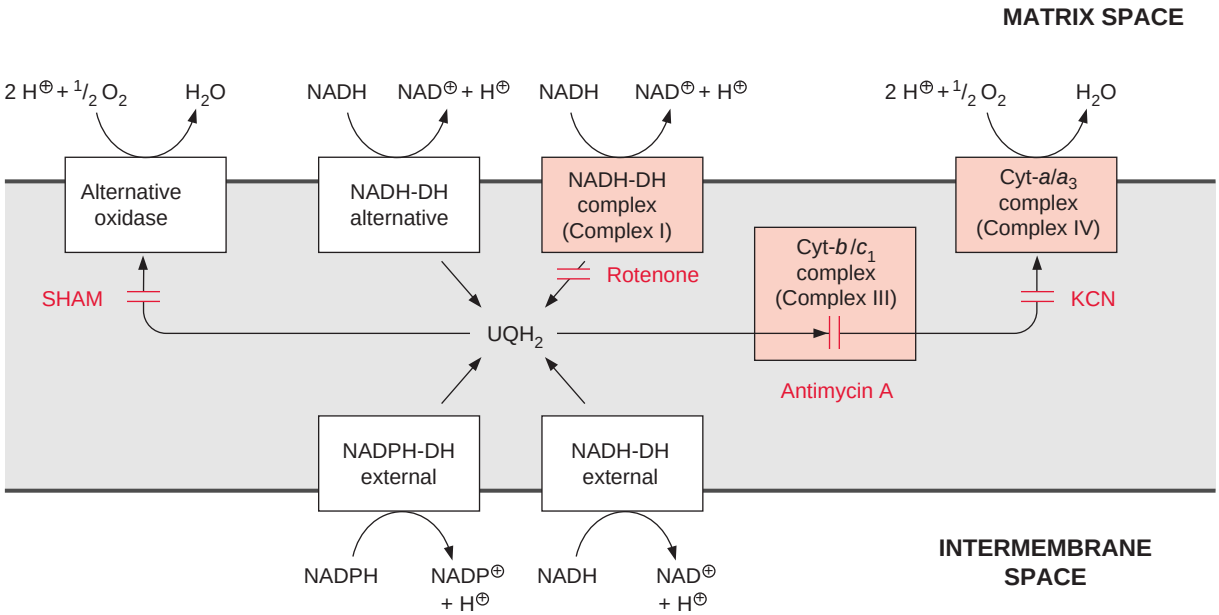

Figure 5.21 Besides the rotenone-sensitive NADH dehydrogenase (NADH DH) of the respiratory chain, there are other dehydrogenases that transfer electrons to ubiquinone without an accompanying proton transport. An alternative NADPH dehydrogenase exists that is directed to the matrix side (not shown). An alternative oxidase enables the oxidation of ubihydroquinone (UQH_2). This pathway is insensitive to the inhibitors antimycin A and KCN, but it is inhibited by salicylic hydroxamate (SHAM).

The **alternative oxidase** transfers electrons directly from ubiquinone to oxygen; this pathway is also not coupled to proton transport. The alternative oxidase is insensitive to **antimycin-A** and **KCN** (inhibitors of complex III and II, respectively), but is inhibited by salicylic hydroxamate (**SHAM**). Recent results show that the alternative oxidase is a membrane protein consisting of two identical subunits (each 36 kDa). From the amino acid sequence it can be predicted that each subunit possesses two transmembrane helices. The two subunits together form a **di-iron oxo-center** (like in the fatty acid desaturase, Fig. 15.16), which catalyzes the oxidation of ubiquinone by oxygen. Electron transport via the alternative oxidase can be understood as a short circuit. It occurs only when the mitochondrial ubiquinone pool is highly reduced. The alternative oxidase is activated by a high concentration of pyruvate which is a signal for an excess of metabolites.

Mitochondrial uncoupling proteins were first detected in animal tissues. These proteins are closely related to the mitochondrial ATP/ADP translocator. They build a channel in the inner mitochondrial membrane which is permeable to protons, resulting in the elimination of the membrane potential,

and therefore in the uncoupling of electron transport from ATP synthesis. Uncoupling proteins are widely distributed in eukaryotes; thus also in plants, where they are called **PUMP**s (plant uncoupling mitochondrial proteins). Their apparent function is the prevention of excessive increase of the mitochondrial membrane potential, in order to minimize the formation of reactive oxygen species (ROS).

When metabolites in the mitochondria are in excess, the interplay of the alternative NADH dehydrogenase, the alternative oxidase and the uncoupling proteins lead to their elimination by oxidation without accompanying ATP synthesis, and the oxidation energy is dissipated as heat. The capacity of the alternative oxidase in the mitochondria from different plant tissues is variable and also depends on the developmental state. Thus one observes a high expression of PUMPs in plants that have been subjected to a cold stress. An especially high alternative oxidase activity has been found in the spadix of the voodoo lily *Sauromatum guttatum*, which uses the alternative oxidase to heat up the spadix by which volatile amine compounds are emitted, which produce a nasty smell like carrion or dung. This strong stench attracts insects from far and wide. The formation of the alternative oxidase is synchronized in these spadices with the beginning of flowering.

NADH and NADPH from the cytosol can be oxidized by the respiratory chain of plant mitochondria

In contrast to mitochondria from animal tissues, plant mitochondria can also oxidize cytosolic NADH and in some cases cytosolic NADPH. Oxidation of this external NADH and NADPH proceeds via two specific dehydrogenases of the inner membrane, of which the substrate binding site is directed towards the intermembrane space. As in the case of succinate dehydrogenase, the electrons from external NADH and NADPH dehydrogenase are fed into the respiratory chain at the site of **ubiquinone**, and therefore this electron transport is not inhibited by rotenone. As oxidation of external NADH and NADPH (like the oxidation of succinate) does not involve a proton transport by complex I (Fig. 5.21), the oxidation of external pyridine nucleotides yields less ATP than the oxidation of NADH provided from the matrix. Oxidation by external NADH dehydrogenase proceeds only when the cytosolic NAD system is reduced excessively. Also, the external NADH dehydrogenase may be regarded as part of an overflow mechanism, which comes into action only when the NADH in the cytosol is overreduced. As discussed in section 3.10, in certain situations photosynthesis may produce a surplus of reducing power, which is hazardous for a cell. The plant cell has the capacity to eliminate excessive reducing power by making use of the uncoupling protein PUMP, the external NADH

dehydrogenase, the alternative dehydrogenase for internal NADH from the matrix, and the alternative oxidase mentioned earlier.

5.8 Compartmentation of mitochondrial metabolism requires specific membrane translocators

The mitochondrial inner membrane is impermeable for metabolites. Specific translocators enable a specific transport of metabolites between the mitochondrial matrix and the cytosol in a counter-exchange mode (Fig. 5.22).

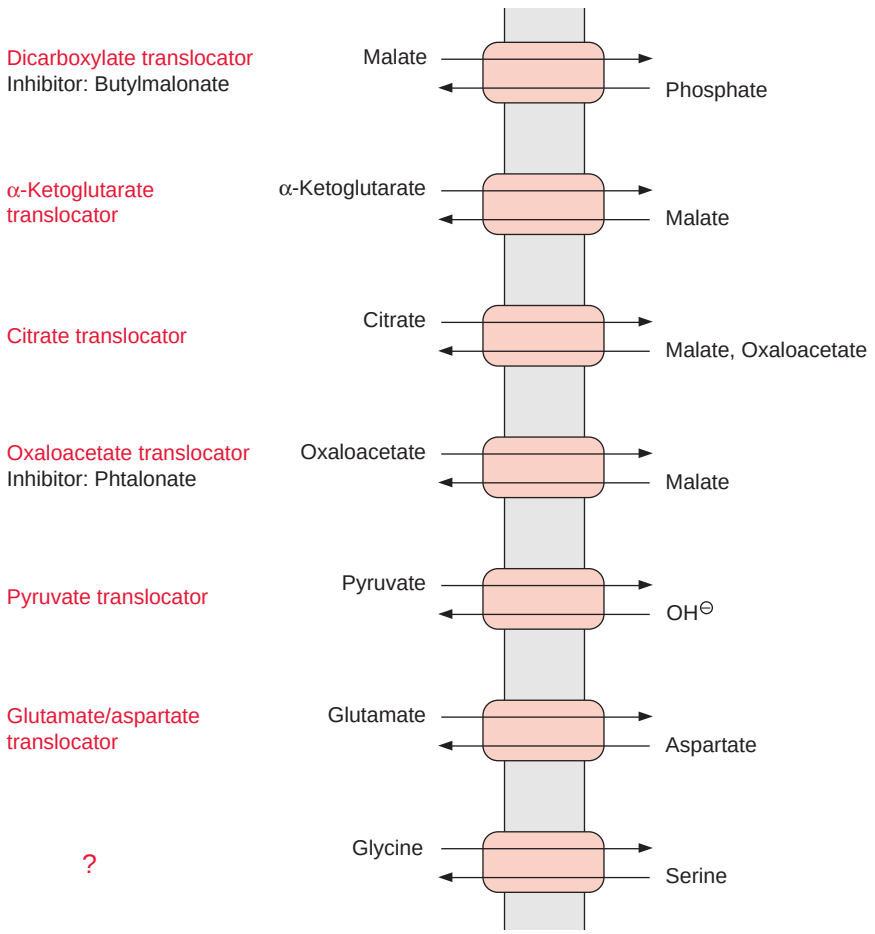

Figure 5.22 Important translocators of the inner mitochondrial membrane. The phosphate- and the ATP/ADP-translocator are shown in Figure 5.20.

The role of the ATP/ADP and the phosphate translocators (Fig. 5.20) has been discussed in section 5.6. Malate and succinate are transported into the mitochondria in counter-exchange for phosphate by a **dicarboxylate translocator**. This transport is inhibited by **butylmalonate**. α-Ketoglutarate, citrate, and oxaloacetate are transported in counter-exchange for malate. By these translocators, substrates can be fed into the citrate cycle. Glutamate is transported in counter-exchange for aspartate, and pyruvate in counter-exchange for OH^- ions. Although these translocators all occur in plant mitochondria, most of our present knowledge about them is based on studies with mitochondria from animal tissues. A comparison of the amino acid sequences known for the ATP/ADP, phosphate, citrate, and glutamate/aspartate translocators shows that they are homologous; the proteins of these translocators represent a family deriving from a common ancestor. As mentioned in section 1.9, all these translocators are composed of 2×6 transmembrane helices.

The malate-oxaloacetate translocator is a special component of plant mitochondria and has an important function in the malate-oxaloacetate cycle described in section 7.3. It also transports citrate and is involved in providing the carbon skeletons for nitrate assimilation (Fig. 10.11). The oxaloacetate translocator and, to a lesser extent, the α-ketoglutarate translocator are inhibited by the dicarboxylate **phthalonate**. The transport of glycine and serine, involved in the photorespiratory pathway (section 7.1), has not yet been characterized. Although final proof is still lacking, it is expected that this transport is mediated by one or two mitochondrial translocators.

Further reading

Clifton, R., Millar, A. H., Whelan, J. Alternative oxidases in *Arabidopsis*: A comparative analysis of differential expression in the gene family provides new insights into function on non-phosphorylating bypasses. Biochimica Biophysica Acta 1757, 730–741 (2006).

Dudkina, N. V., Heinemeyer, J., Sunderhaus, S., Boekma, E. J., Braun, H.-P. Respiratory chain supercomplexes in the plant mitochondrial membrane. Trends in Plant Science 11, 232–240 (2006).

Duy, D., Soll, J., Philippar, K. Solute channels of the outer membrane: From bacteria to chloroplasts. Biological Chemistry 388, 879–889 (2007).

Eubel, H., Jaensch, L., Braun, H.-P. New insights into the respiratory chain of plant mitochondria. Supercomplexes and a unique composition of complex II. Plant Physiology 133, 274–286 (2003).

Iwata, S., Ostermeier, C., Ludwig, B., Michel, H. Structure at 2.8Å resolution of cytochrome C oxidase from *Paracoccus denitrificans*. Nature 376, 660–669 (1995).

Kadenbach, B., Arnold, A. A second mechanism of respiratory control. FEBS Letters 447, 131–134 (1999).

Klingenberg, M. The ADP and ATP transport in mitochondria and its carrier. Biochimica Biophysica Acta 1778, 1978–2021 (2008).
Krömer, S. Respiration during photosynthesis. Annual Reviews of Plant Physiology and Plant Molecular Biology 46, 45–70 (1995).
Logan, D. C. The mitochondrial compartment. Journal Experimental Botany 58, 1225–1243 (2007).
Noctor, G., De Paepe, R., Foyer, C. F. Mitochondrial redox biology and homeostasis in plants. Trends in Plant Science 12, 125–134 (2007).
Pebay-Peyroula, E., Dahout-Gonzalez, C., Kahn, R., Trezeguet, V., Lauquin, G. J.-M., Brandolin, G. Structure of mitochondrial ATP/ADP carrier in complex with carboxyatractyloside. Nature 426, 39–44 (2003).
Plaxton, W. C., Podesta, F. E. The functional organization and control of plant respiration. Critical Reviews in Plant Sciences 25, 159–198 (2006).
Raghavendra, A. S., Padmasree, K. Beneficial interaction of mitochondrial metabolism with photosynthetic carbon assimilation. Trends in Plant Science 8, 546–553 (2003).
Rasmusson, A. G., Geisler, D. A., Møller, I. M. The multiplicity of dehydrogenases in the electron transport chain of plant mitochondria. Mitochondrion 8, 47–60 (2008).
Rhoads, D. M., Umbach, A. L., Subbaiah, C. C., Siedow, J. N. Mitochondrial reactive oxygen species. Contribution to oxidative stress and interorganellar signalling. Plant Physiology 141, 357–366 (2006).
Sweetlove, L. J., Fait, A., Nunes-Nesi, A., Williams, T., Fernie, A. R. The mitochondrion: An integration point of cellular metabolism and signaling. Critical Reviews in Plant Sciences 26, 17–43 (2007).
Vercesi, A. E., Borecky, J., de Godoy Maia, I., Arruda, P., Cuccovia, I. M., Chaimovich, H. Plant uncoupling mitochondrial proteins. Annual Reviews of Plant Biology 57, 383–404 (2006).

6

The Calvin cycle catalyzes photosynthetic CO_2 assimilation

Chapters 3 and 4 showed how the electron transport chain and the ATP synthase of the thylakoid membrane use the energy from light to provide reducing equivalents in the form of NADPH, and chemical energy in the form of ATP. This chapter will describe how NADPH and ATP are used for CO_2 assimilation.

6.1 CO_2 assimilation proceeds via the dark reaction of photosynthesis

It is relatively simple to isolate chloroplasts with intact envelope from leaves (see section 1.7). Upon transfer of these chloroplasts to an isotonic medium containing an osmoticum, a buffer, bicarbonate, and inorganic phosphate, and the light is switched on, the generation of oxygen can be observed. By the action of light water is split and oxygen evolved, and the resulting reducing equivalents are used for CO_2 assimilation (Fig. 6.1, see also Chapter 3). There is no oxygen evolution with intact chloroplasts in the absence of CO_2 or phosphate, demonstrating that the light reaction in the intact chloroplasts is (a) coupled to CO_2 assimilation and (b) the product of this assimilation contains phosphate. The main assimilation product of the chloroplasts is **dihydroxyacetone phosphate**, a **triose phosphate**. Figure 6.2 shows that the synthesis of triose phosphate from CO_2 requires energy as ATP and reducing equivalents as NADPH, which have been provided by the **light reaction of photosynthesis**. The reaction chain for the formation of triose phosphate from CO_2, ATP, and NADPH was formerly called

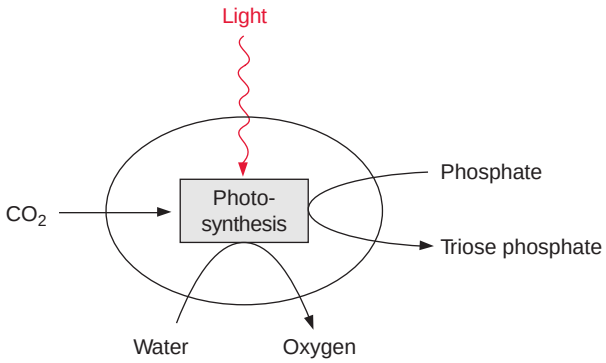

Figure 6.1 Schematic presentation of photosynthesis in a chloroplast.

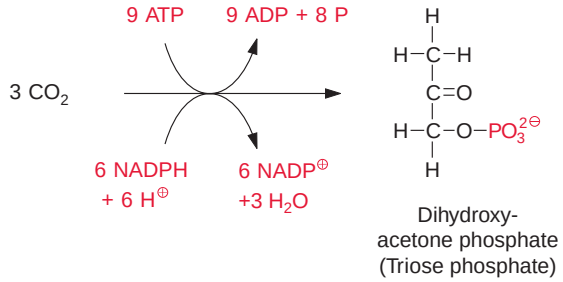

Figure 6.2 Overall reaction of photosynthetic CO_2 fixation.

the **dark reaction of photosynthesis**, as it requires no light *per se* and theoretically it should also be able to proceed in the dark. The fact is, however, that in leaves this reaction does not proceed during darkness, since some of the enzymes of the reaction chain, due to regulatory processes, are active only during illumination (section 6.6).

Between 1946 and 1953 Melvin Calvin and his collaborators Andrew Benson and James Bassham, in Berkeley, California, resolved the mechanism of photosynthetic CO_2 assimilation. In 1961 Calvin was awarded the Nobel Prize in Chemistry for this fundamental discovery. A prerequisite for the elucidation of the CO_2 fixation pathway was the discovery of the radioactive carbon isotope ^{14}C in 1940, which, as a by-product of nuclear reactors, was available in larger amounts in the United States after 1945. Calvin chose the green alga *Chlorella* for his investigations. He added radioactively labeled CO_2 to illuminated algal suspensions, killed the algae after a short incubation period by adding hot ethanol, and used paper chromatography to analyze the radioactively labeled products of the CO_2 fixation. By successively shortening the incubation time, he was able to show that 3-phosphoglycerate was synthesized as the first stable product of CO_2 fixation. More detailed studies revealed that CO_2 fixation proceeds by a cyclic process,

which has been named the **Calvin cycle** after its discoverer. **Reductive pentose phosphate pathway** is another term that will be used in some sections of this book. This name derives from the fact that a reduction occurs and pentoses are formed in the cycle.

The Calvin cycle can be subdivided into three sections:

1. The **carboxylation** of the C_5 sugar ribulose 1,5-bisphosphate leading to the formation of two molecules 3-phosphoglycerate;
2. The **reduction** of the 3-phosphoglycerate to triose phosphate; and
3. The **regeneration** of the CO_2 acceptor ribulose 1,5-bisphosphate from triose phosphate (Fig. 6.3).

As a product of photosynthesis, triose phosphate is exported from the chloroplasts into the cytosol by specific transport. However, most of the triose phosphate remains in the chloroplasts to regenerate ribulose 1,5-bisphosphate. These reactions will be discussed in detail in the following sections.

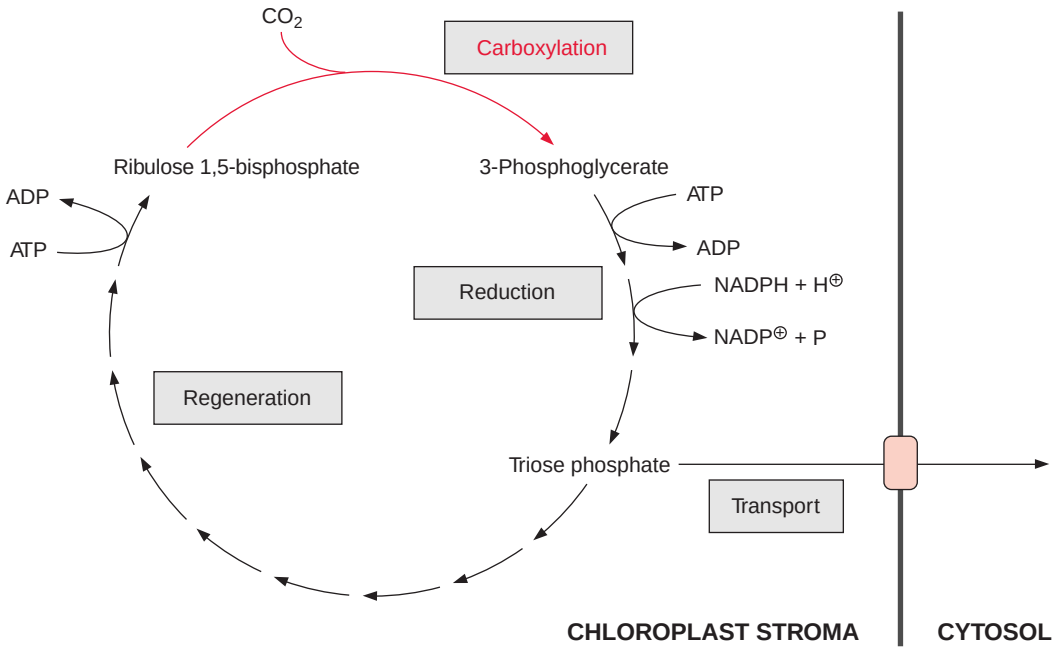

Figure 6.3 Simplified overview of the reactions of the Calvin cycle (without stoichiometries).

6.2 Ribulose bisphosphate carboxylase catalyzes the fixation of CO_2

The key reaction for photosynthetic CO_2 assimilation is the binding of atmospheric CO_2 to the acceptor ribulose 1,5-bisphosphate (RuBP) to synthesize two molecules of 3-phosphoglycerate. The reaction is very exergonic (ΔG^o − 35 kJ/mol) and therefore virtually irreversible. It is catalyzed by the enzyme ribulose bisphosphate carboxylase/oxygenase (abbreviated **RubisCO**). It is also called oxygenase because the same enzyme also catalyzes a side-reaction in which the ribulose bisphosphate reacts with O_2 (Fig. 6.4).

Figure 6.5 shows the reaction sequence of the **carboxylase reaction**. Keto-enol isomerization of RuBP yields an enediol, which reacts with CO_2 to form the intermediate 2-carboxy 3-ketoarabinitol 1,5-bisphosphate, which is cleaved to two molecules of 3-phosphoglycerate. In the **oxygenase reaction**, an unavoidable by-reaction, probably O_2, reacts in a similar way as CO_2 with the enediol to form a peroxide as an intermediate. In a subsequent cleavage of the O_2 adduct, one atom of the O_2 molecule is released in the form of water and the other is incorporated into the carbonyl group of 2-phosphoglycolate (Fig. 6.6). The final products of the oxygenase reaction are 2-phosphoglycolate and 3-phosphoglycerate.

Ribulose bisphosphate-carboxylase/oxygenase **is the only enzyme that enables the fixation of atmospheric CO_2 for the formation of biomass**. This

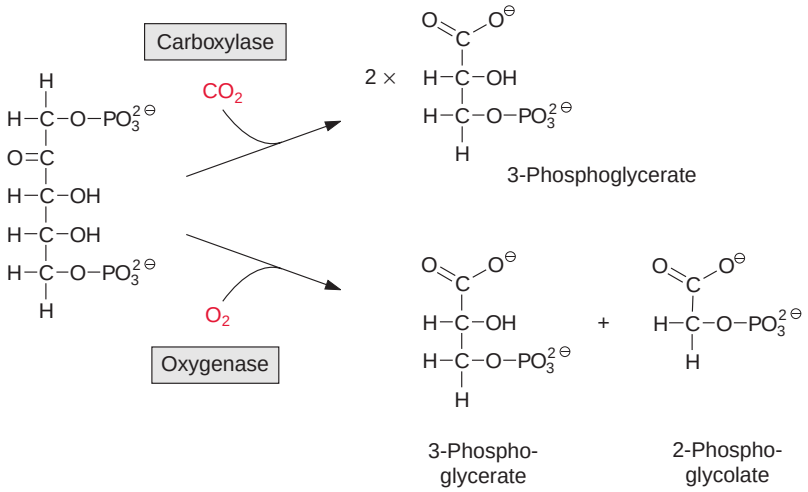

Figure 6.4 Ribulose bisphosphate carboxylase catalyzes two reactions with the substrate RuBP: the carboxylation, which is the actual CO_2 fixation reaction; and the oxygenation, an unavoidable side-reaction.

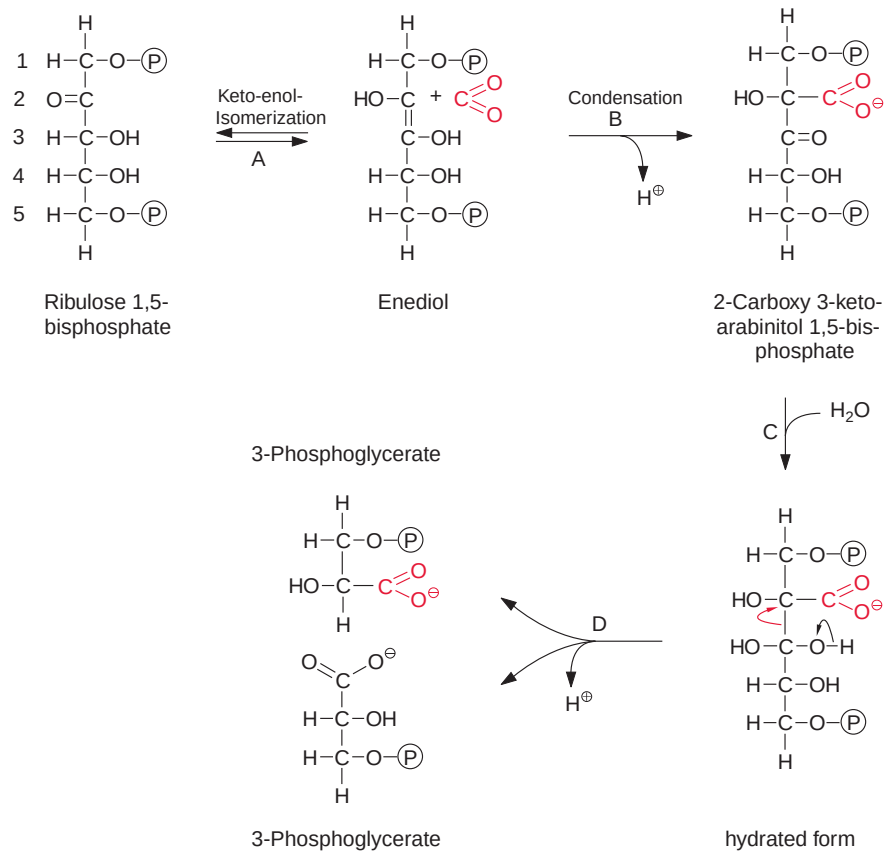

Figure 6.5 Reaction sequence of the carboxylation of RuBP by RubisCO. For the sake of simplicity, -PO_3^{2-} is symbolized as -P. An enediol, formed by keto-enol-isomerization of the carbonyl group of the RuBP (A), allows the nucleophilic reaction of CO_2 with the C-2 atom of RuBP by which 2-carboxy 3-ketoarabinitol 1,5-bisphosphate (B) is synthesized. After hydration (C), the bond between C-2 and C-3 is cleaved and two molecules of 3-phosphoglycerate are released (D).

enzyme is therefore a prerequisite for the existence of the present life on earth. In plants and cyanobacteria it consists of eight identical **large subunits** (depending on the species of a molecular mass of 51–58 kDa) and eight identical **small subunits** (molecular mass 12–18 kDa). **With its 16 subunits, RubisCO is one of the largest enzymes in nature**. In plants the genetic information for the large subunit is encoded in the plastid genome and for the small subunit in the nucleus. Each large subunit contains one catalytic center. The function of the small subunits is not yet fully understood. It has been suggested that the eight small subunits stabilize the complex of the eight large subunits. Apparently the small subunit is not essential for the process of CO_2 fixation *per se*. RubisCO occurs in some phototrophic

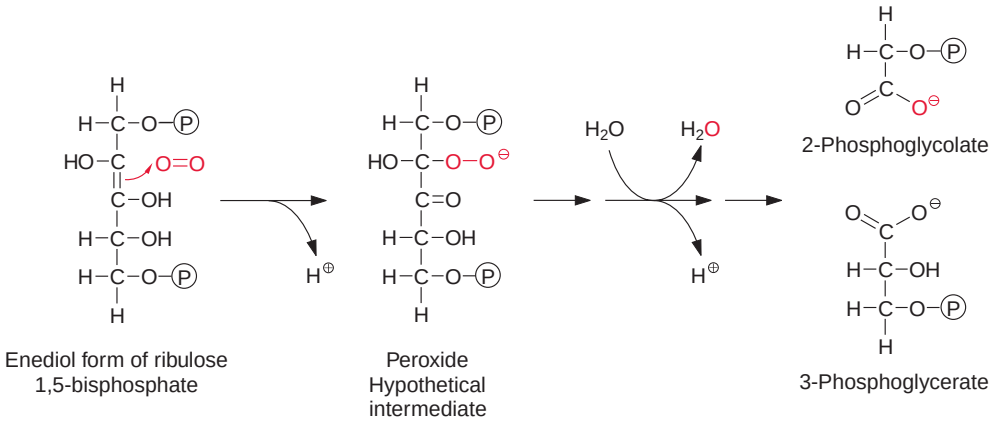

Figure 6.6 Oxygenation reaction of RubisCO with the substrate RuBP. P symbolizes $-PO_3^{2-}$.

purple bacteria as a dimer of only large subunits, but the catalytic properties of the corresponding bacterial enzymes are not basically different from those in plants. The bacterial enzymes consisting of only two large subunits, however, exhibit a higher ratio of oxygenase versus carboxylase activity than the plant enzymes, which consist of eight large and eight small subunits.

The oxygenation of ribulose bisphosphate: a costly side-reaction

Although the CO_2 concentration required for half saturation of the enzyme (K_M [CO_2]) is much lower than that of O_2 (K_M [O_2]) (Table 6.1), the velocity of the oxygenase reaction is very high. This high velocity is a consequence of the different atmospheric concentrations; the concentration of O_2 in air amounts to 21% and that of CO_2 to only 0.035%. Moreover, the CO_2 concentration in the gaseous space of the leaves can be considerably lower than the CO_2 concentration in the atmosphere. For these reasons, the ratio of oxygenation to carboxylation during photosynthesis of a leaf at 25°C is in the range of **1:4** to **1:2**, which implies *that every third to fifth ribulose 1,5-bisphosphate molecule is consumed in the side-reaction*. When the temperature rises, the CO_2/O_2 specificity of the RubisCO (Table 6.1) decreases, and as a consequence, the ratio of oxygenation to carboxylation increases. On the other hand, a rise in the CO_2 concentration in the atmosphere lowers oxygenation, which in many cases leads to higher plant growth. Moreover, the concentration of CO_2 in water (thus also in cellular water) which is in equilibrium with the atmospheric concentration decreases with increasing temperature more strongly than that of O_2. Both effects result in an increase

Table 6.1: Kinetic properties of ribulose bisphosphate carboxylase/oxygenase (RubisCO) at 25°

Substrate concentrations at half saturation of the enzyme

K_M [CO_2] : 9 μmol/L*

K_M [O_2] : 535 μmol/L*

K_M (RuBP) : 28 μmol/L

Maximal turnover (related to one subunit)

Kcat [CO_2] : 3.3 s^{-1}

Kcat [O_2] : 2.4 s^{-1}

$$CO_2/O_2 \text{ specificity} = \left(\frac{K\text{cat}[CO_2]}{K_M[CO_2]} \Big/ \frac{K\text{cat}[O_2]}{K_M[O_2]} \right) = 82$$

* For comparison:

In equilibrium with air (0.035% = 350 ppm CO_2, 21% O_2) the concentrations in water at 25°C amounts to

CO_2 : 11 μmol/L

O_2 : 253 μmol/L

(Data from Woodrow and Berry, 1988)

of the oxygenation/carboxylation ratio due to the increasing temperature. In greenhouses the oxygenation can be decreased by an artificial increase of the atmospheric CO_2 concentration to obtain higher plant growth.

It will be shown in Chapter 7 that recycling of the by-product 2-phosphoglycolate, produced in very large amounts, is a very costly process for plants. This recycling process requires a metabolic chain with more than 10 enzymatic reactions distributed over three different organelles (chloroplasts, peroxisomes, and mitochondria), as well as very high energy consumption. Section 7.5 describes in detail that about a **third of the photons absorbed** during the photosynthesis of a leaf are consumed to reverse the consequences of oxygenation.

Apparently evolution has not been successful in eliminating this costly side-reaction of ribulose bisphosphate carboxylase. The ratio of the carboxylase and oxygenase activities of RubisCO is only increased by a factor of less than two when enzymes of cyanobacteria and of higher plants are compared. It seems as if the evolutionary refinement of a key process of life has reached its limitation due to the chemistry of the reaction. It is speculated that the early evolution of the RubisCO occurred at a time when there was no oxygen in the atmosphere. A comparison of the RubisCO proteins from different organisms leads to the conclusion that this enzyme was already present about three and a half billion years ago, when the first chemolithotrophic bacteria evolved. When more than one and a half billion years later, due to photosynthesis, oxygen appeared in the atmosphere in higher concentrations,

the RubisCO protein probably had reached such a complexity that it was no longer possible to change the catalytic center to eliminate the oxygenase activity. Experimental results support this conception. A large number of experiments, in which genetic engineering was employed to obtain site-specific amino acid exchanges in the region of the active center of RubisCO, were unable to improve the ratio between the activities of carboxylation and oxygenation. The only chance of lowering oxygenation by molecular engineering may lie in simultaneously exchanging several amino acids in the catalytic binding site of RubisCO, which would be an extremely unlikely event in the process of evolution. Section 7.7 will show how plants make a virtue of necessity, and use the energy-consuming oxygenation to eliminate surplus NADPH and ATP produced by the light reaction.

Ribulose bisphosphate carboxylase/oxygenase: special features

The catalysis of the carboxylation of RuBP by RubisCO is very slow (Table 6.1): the turnover number for each subunit amounts to $3.3\,s^{-1}$. This implies that at substrate saturation only about three molecules of CO_2 and RuBP are converted per second at one catalytic site of RubisCO. In comparison, the turnover numbers of dehydrogenases and carbonic anhydrase are in the order of $10^3\,s^{-1}$ and $10^5\,s^{-1}$, respectively. Because of the extremely low turnover number of RubisCO, very large amounts of enzyme protein are required to catalyze the fluxes necessary for photosynthesis. RubisCO can account for **50% of the total soluble proteins** in leaves. The wide distribution of plants makes RubisCO by far the **most abundant protein on earth**. The concentration of the catalytic large subunits in the chloroplast stroma is as high as $4–10 \times 10^{-3}$ mol/L. A comparison of this value with the aqueous concentration of CO_2 in equilibrium with air (at 25°C about 11×10^{-6} mol/L) shows the abnormal situation in which the concentration of an enzyme is up to 1,000 times higher than the concentration of its substrate CO_2 and at a similar concentration as its substrate RuBP.

Activation of ribulose bisphosphate carboxylase/oxygenase

All the large subunits of RubisCO contain a lysine in position 201 of their 470 amino acid long sequence. RubisCO is active only when the ε-amino group of this lysine reacts with CO_2 to form a **carbamate** (carbonic acid amide), to which an Mg^{++} ion is bound (Fig. 6.7). The activation is due to a change in the conformation of the protein of the large subunit. The active conformation is stabilized by the complex formation with Mg^{++}. This carbamylation is a prerequisite for the activity of all known RubisCO proteins.

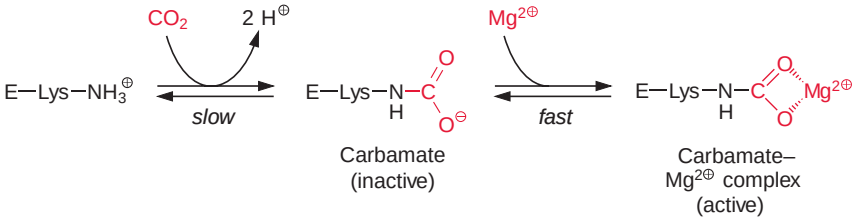

Figure 6.7 RubisCO is activated by the carbamylation of a lysine residue.

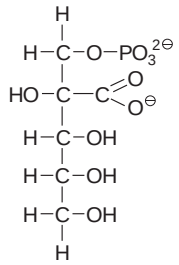

2-Carboxyarabinitol
1-phosphate

Figure 6.8
2-Carboxyarabinitol 1-phosphate is an inhibitor of RubisCO.

It should be noted that the CO_2 bound as carbamate is different from the CO_2 that is a substrate of the carboxylation reaction of RubisCO.

The activation of RubisCO requires ATP and is catalyzed by the enzyme **RubisCO activase**. The noncarbamylated, inactive form of RubisCO binds RuBP very tightly, resulting in the inhibition of the enzyme. Upon the consumption of ATP, the activase releases the tightly bound RuBP and thus enables the carbamylation of the free enzyme. The regulation of RubisCO activase is discussed in section 6.6.

RubisCO is inhibited by several hexose phosphates and by 3-phosphoglycerate, which all bind to the active site instead of RuBP. A very strong inhibitor is **2-carboxyarabinitol 1-phosphate** (CA1P) (Fig. 6.8). This compound has a structure very similar to that of 2-carboxy 3-ketoarabinitol 1,5-bisphosphate (Fig. 6.5), which is an intermediate of the carboxylation reaction. CA1P has a 1,000-fold higher affinity to the RuBP binding site of RubisCO than RuBP. In a number of species, CA1P accumulates in the leaves during the night, blocking a large number of the binding sites of RubisCO and thus inactivating the enzyme. During the day, CA1P is released by RubisCO activase and is degraded by a specific phosphatase, which hydrolyzes the phosphate residue from CA1P and thus eliminates the effect of the RubisCO inhibitor. CA1P is synthesized from fructose 1.6-bisphosphate with the intermediates hexosephosphates hamamelose bisphosphate and hamamelose monophosphate. Since CA1P is not formed in all plants, its role in the regulation of RubisCO is still a matter of debate.

6.3 The reduction of 3-phosphoglycerate yields triose phosphate

For the synthesis of dihydroxyacetone phosphate the carboxylation product 3-phosphoglycerate is phosphorylated to 1,3-bisphosphoglycerate by the enzyme **phosphoglycerate kinase**. In this reaction, with the consumption of ATP, a mixed anhydride is formed between the new phosphate residue and the carboxyl group (Fig. 6.9). As the free energy for the hydrolysis of this anhydride is similarly high to that of the phosphate anhydride in ATP, the phosphoglycerate kinase reaction is reversible. An isoenzyme of the chloroplast phosphoglycerate kinase is also involved in the glycolytic pathway proceeding in the cytosol, where it catalyzes the formation of ATP from ADP and 1,3-bisphosphoglycerate (section 13.3).

The reduction of 1,3-bisphosphoglycerate to D-glyceraldehyde 3-phosphate is catalyzed by the enzyme **glyceraldehyde phosphate dehydrogenase** (Fig. 6.9). The carboxylic acid phosphoanhydride reacts with an SH-group of a cysteine residue in the active center of the enzyme to form a thioester intermediate with the release of the phosphate group (Fig. 6.10). The free energy for the hydrolysis of the thioester so formed is similarly high to that of the anhydride ("energy-rich bond"). When a thioester is reduced, a thiosemiacetal is formed which has low free energy.

Through the catalysis of phosphoglycerate kinase and glyceraldehyde phosphate dehydrogenase, the large difference in redox potentials between the carboxylate and the aldehyde in the course of the reduction of 3-phosphoglycerate to glyceraldehyde phosphate is overcome by the consumption

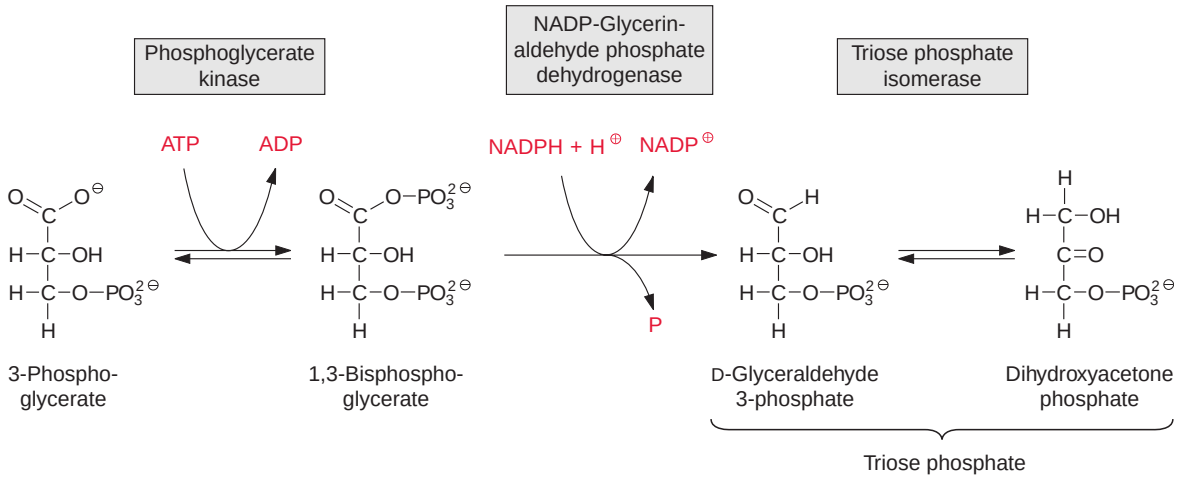

Figure 6.9 Conversion of 3-phosphoglycerate into triose phosphate.

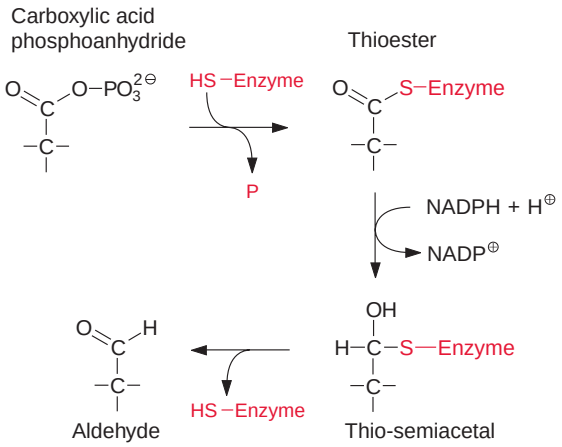

Figure 6.10 Reaction sequence catalyzed by glyceraldehyde phosphate dehydrogenase. HS-enzyme symbolizes the sulfhydryl group of a cysteine residue in the active center of the enzyme.

of ATP. It is therefore a reversible reaction. A glyceraldehyde phosphate dehydrogenase in the cytosol catalyzes the conversion of glyceraldehyde phosphate to 1,3-bisphosphoglycerate as part of the glycolytic pathway (section 13.3). In contrast to the cytosolic enzyme, which catalyzes mainly the oxidation of glyceraldehyde phosphate using NAD^+ as hydrogen acceptor, the chloroplast enzyme uses NADPH as a hydrogen donor.

This is an example of the different roles that the NADH/NAD^+ and NADPH/$NADP^+$ systems play in the metabolism of eukaryotic cells. Whereas the NADH system is specialized in collecting reducing equivalents to be oxidized for the synthesis of ATP, the NADPH system mainly gathers reducing equivalents to be donated to synthetic processes. Figuratively speaking, the NADH system has been compared with a **hydrogen low pressure line** through which reducing equivalents are pumped off for oxidation to generate energy, while the NADPH system is a **hydrogen high pressure line** through which reducing equivalents are pressed into synthesis processes. Usually the reduced/oxidized ratio is about 100 times higher for the NADPH system than for the NADH system. The relatively high degree of reduction of the NADPH system in chloroplasts (about 50–60% reduced) allows the very efficient reduction of 1,3-bisphosphoglycerate to glyceraldehyde-3-phosphate.

Triose phosphate isomerase catalyzes the isomerization of glyceraldehyde phosphate to dihydroxyacetone phosphate. This conversion of an aldose into a ketose proceeds via a 1,2-enediol as intermediate and is basically similar to the reaction catalyzed by ribose phosphate isomerase. The equilibrium of the reaction lies towards the ketone. Triose phosphates, as a collective term, comprise about 96% dihydroxyacetone phosphate and only 4% glyceraldehyde phosphate.

6.4 Ribulose bisphosphate is regenerated from triose phosphate

The fixation of three molecules of CO_2 in the Calvin cycle results in the synthesis of six molecules of phosphoglycerate which are converted to six molecules of triose phosphate (Fig. 6.11). Of these, only one molecule of triose phosphate is the actual gain, which is provided to the cell for various biosynthetic processes. The remaining five triose phosphates are needed to regenerate three molecules of ribulose bisphosphate so that the Calvin cycle can continue. Figure 6.12 shows the metabolic pathway of the conversion of the five triose phosphates (white boxes) to three pentose phosphates (red boxes).

The two trioses dihydroxyacetone phosphate and glyceraldehyde phosphate are condensed in a reversible reaction to fructose 1,6-bisphosphate, as catalyzed by the enzyme **aldolase** (Fig. 6.13). Figure 6.14 shows the reaction mechanism. As an intermediate of this reaction, a protonated Schiff base is formed between a lysine residue of the active center of the enzyme and the keto group of dihydroxyacetone phosphate. This Schiff base enhances the release of a proton from the C-3 position and enables a nucleophilic reaction with the C atom of the aldehyde group of glyceraldehyde phosphate. Fructose 1,6-bisphosphate is hydrolyzed by **fructose 1,6-bisphosphatase** in an irreversible reaction to fructose 6-phosphate (Fig. 6.15).

The enzyme **transketolase** transfers a carbohydrate residue with two carbon atoms from fructose 6-phosphate to glyceraldehyde 3-phosphate yielding xylulose 5-phosphate, and erythrose 4-phosphate in a reversible

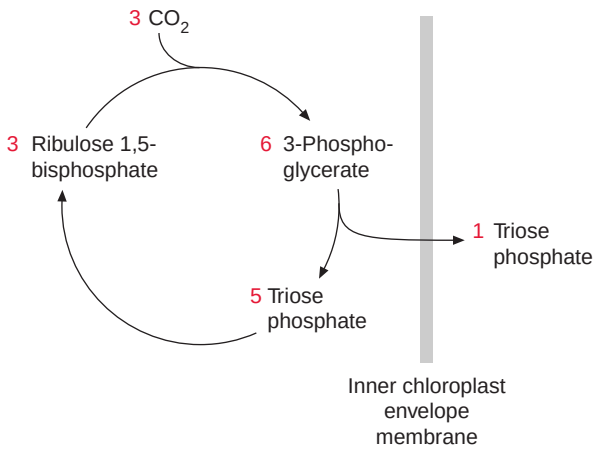

Figure 6.11 Five of the six triose phosphates formed by photosynthesis are required for the regeneration of ribulose 1,5-bisphosphate. One molecule of triose phosphate represents the net product and can be utilized by the chloroplast for biosynthesis or be exported.

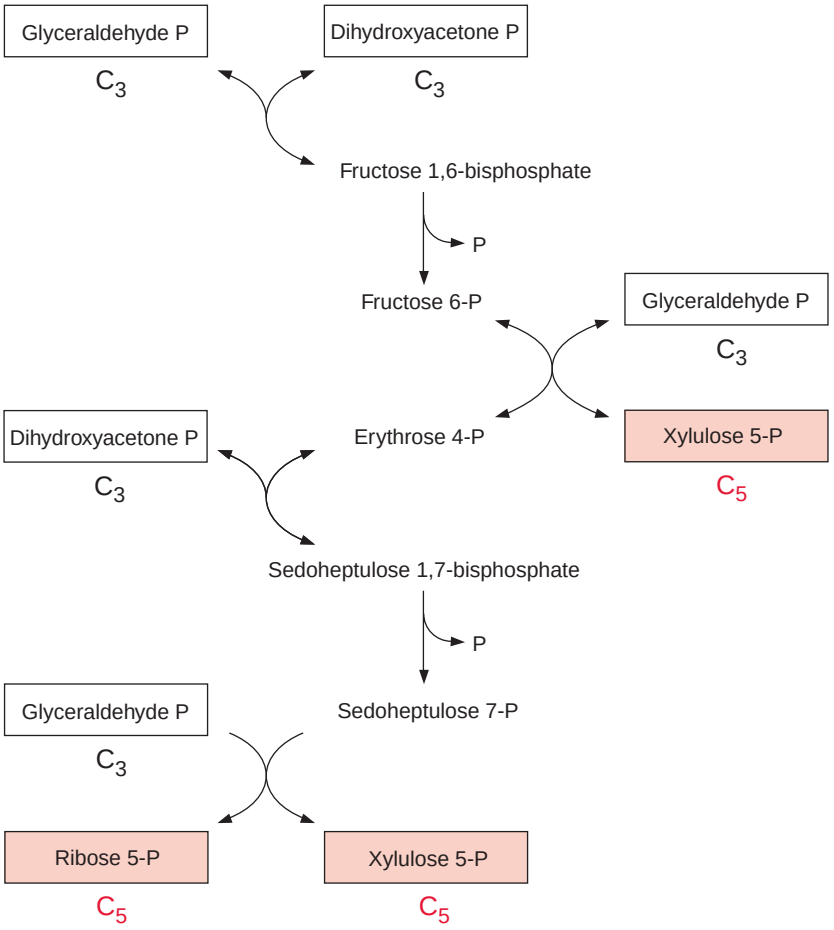

Figure 6.12 Reaction chain for the conversion of five molecules of triose phosphate into three molecules of pentose phosphate. P symbolizes $-PO_3^{2-}$.

reaction (Fig. 6.16). Thiamine pyrophosphate (Fig. 5.5), already discussed as a reaction partner of pyruvate oxidation (section 5.3), is involved as the prosthetic group in this reaction (Fig. 6.17).

Once more an **aldolase** (Fig. 6.13) catalyzes a condensation reaction; erythrose 4-phosphate is combined with dihydroxyacetone phosphate to form sedoheptulose 1,7-bisphosphate. Subsequently, the enzyme **sedoheptulose 1,7-bisphosphatase** catalyzes the irreversible hydrolysis of sedoheptulose 1,7-bisphosphate. This reaction is similar to the hydrolysis of fructose 1,6-bisphosphate, despite the fact that both reactions are catalyzed by different enzymes. Again, a carbohydrate residue of two C atoms is transferred by **transketolase** from sedoheptulose 7-phosphate to dihydroxyacetone phosphate to form ribose 5-phosphate and xylulose 5-phosphate (Fig. 6.16).

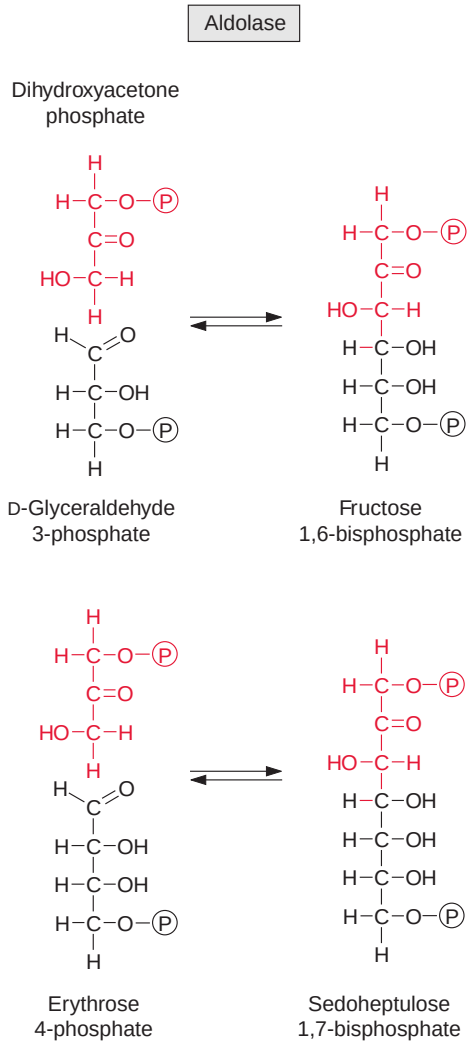

Figure 6.13 Aldolase catalyzes the condensation of dihydroxyacetone phosphate with the aldoses glyceraldehyde 3-phosphate or erythrose 4-phosphate. Ⓟ symbolizes $-PO_3^{2-}$.

The three pentose phosphates synthesized are then converted to ribulose 5-phosphate (Fig. 6.18). The conversion of xylulose 5-phosphate is catalyzed by **ribulose phosphate epimerase**; this reaction proceeds via a keto-enol isomerization and a 2,3-enediol intermediate. The conversion of the aldose ribose 5-phosphate to the ketose ribulose 5-phosphate is catalyzed by **ribose phosphate isomerase**, again via an enediol as intermediate, although in the 1,2-position. The three molecules of ribulose 5-phosphate formed in this way are converted to the CO_2 acceptor ribulose 1,5-bisphosphate upon consumption of ATP by **ribulose phosphate kinase** (Fig. 6.19).

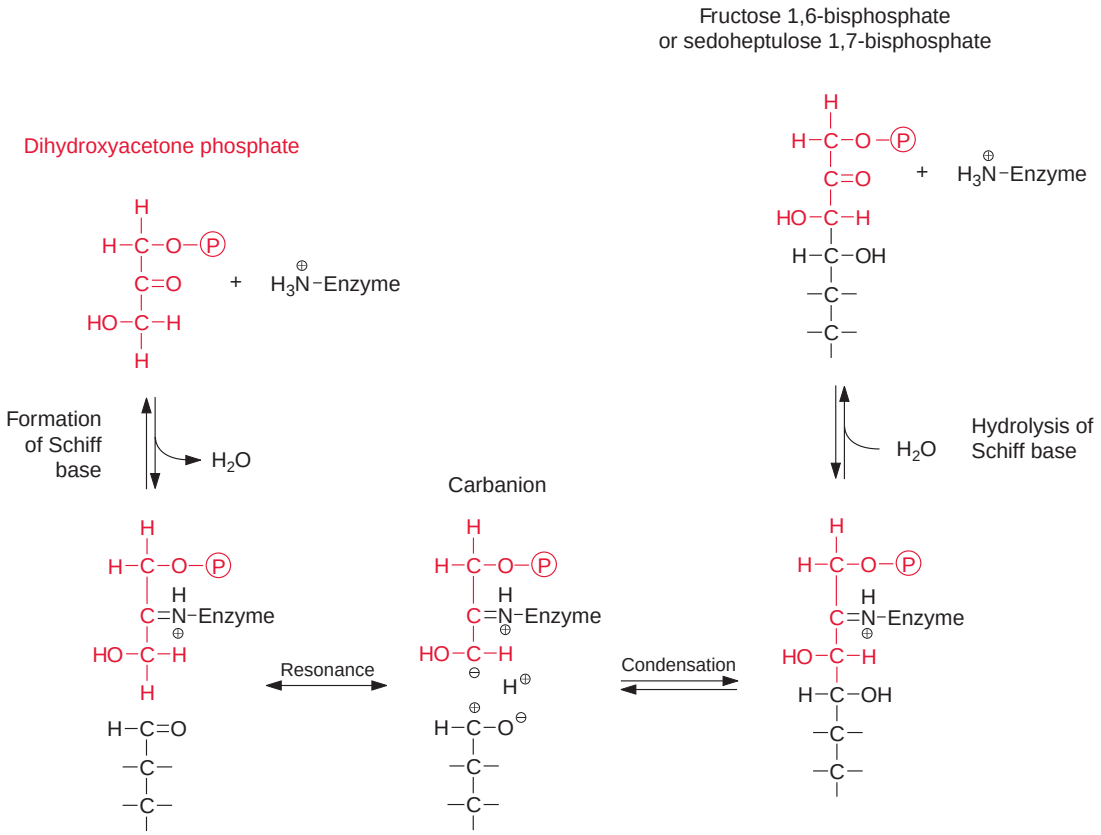

Figure 6.14 Pathway of the aldolase reaction. Dihydroxyacetone phosphate forms a Schiff base with the terminal amino group of a lysine residue of the enzyme protein. The positive charge at the nitrogen atom favors the release of a proton at C-3, and thus a carbanion is formed. In one mesomeric form of the glyceraldehyde phosphate, the C atom of the aldehyde group is positively charged. This enables condensation between this C atom and the negatively charged C-3 of the dihydroxyacetone phosphate. After condensation, the Schiff base is cleaved again and fructose 1,6-bisphosphate is released. Sedoheptulose 1,7-bisphosphate is synthesized by the same enzyme which catalyzes the reaction with erythrose 4-phosphate. The aldolase reaction is reversible. P symbolizes $-PO_3^{2-}$.

This kinase reaction is irreversible, since a phosphate of the "energy-rich" anhydride in the ATP is converted to a phosphate ester with a low free energy of hydrolysis.

The scheme in Figure 6.20 presents a summary of the various reactions of the Calvin cycle. Four irreversible steps are indicated in the cycle (bold arrows): carboxylation, hydrolysis of fructose- and sedoheptulose bisphosphate,

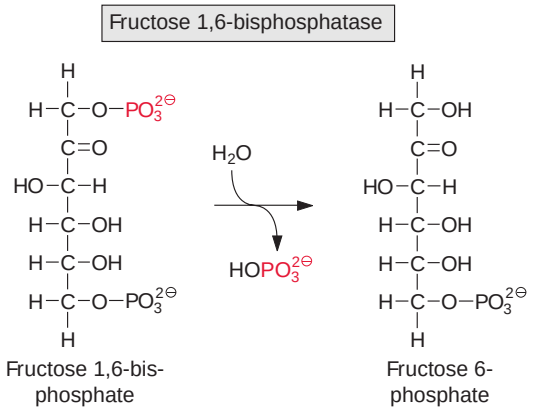

Figure 6.15 Hydrolysis of fructose 1,6-bisphosphate by fructose 1,6-bisphosphatase.

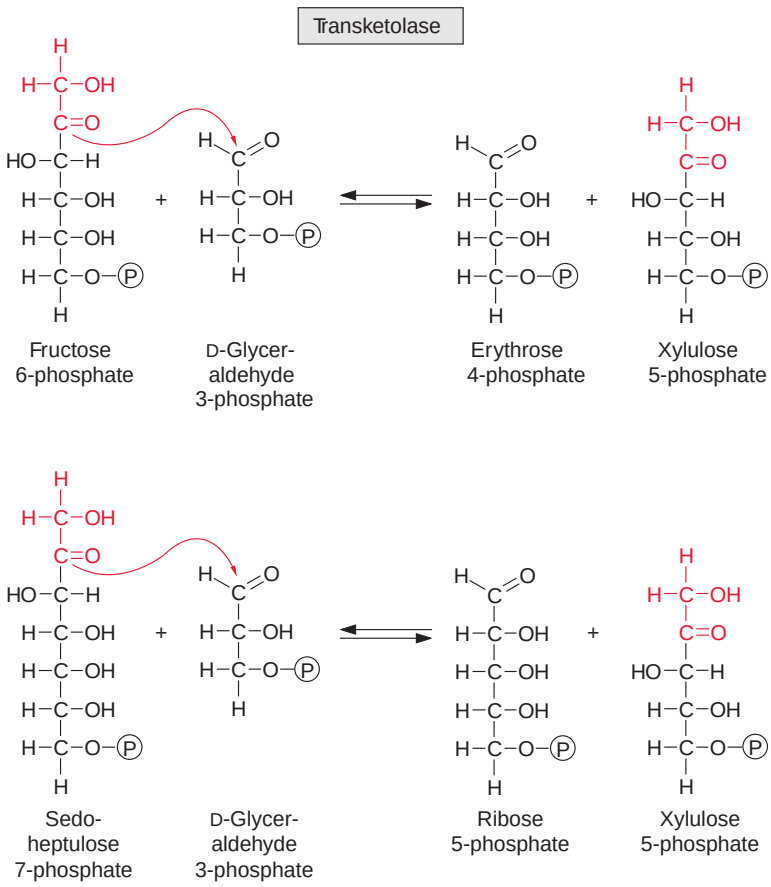

Figure 6.16 Transketolase catalyzes the transfer of a C_2 moiety from ketoses to aldoses. P symbolizes $-PO_3^{2-}$.

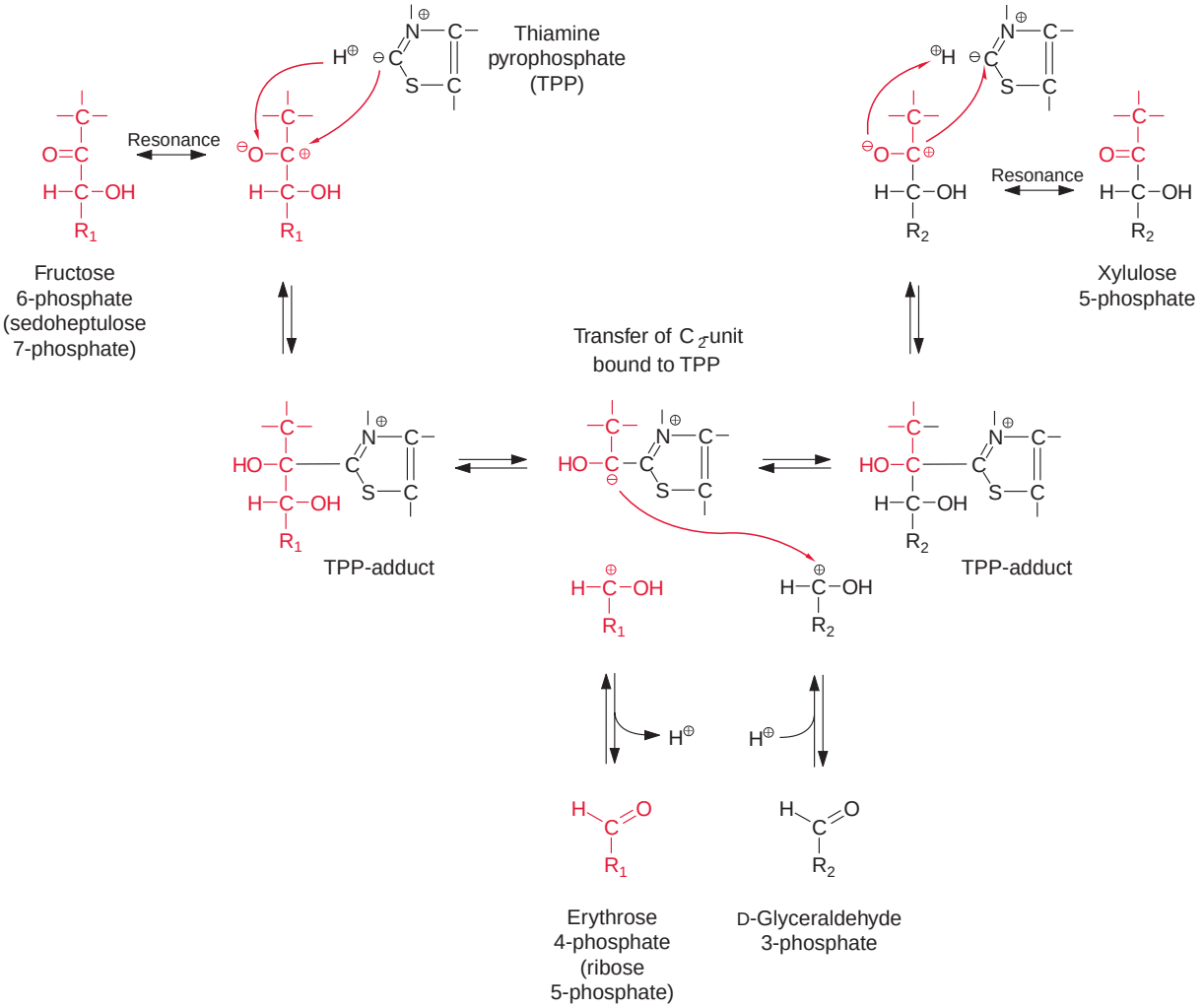

Figure 6.17 Mechanism of the transketolase reaction. The enzyme contains thiamine pyrophosphate as a prosthetic group, the thiazole ring is the reactive component. The positive charge of the N atom in this ring enhances the release of a proton at the neighboring C atom, resulting in a negatively charged C atom (carbanion). The partially positively charged C atom of the keto group binds the substrate. The positively charged N atom of the thiazole favors the cleavage of the carbon chain, resulting in an carbanion at the carbon atom in position 2. The reaction mechanism is basically the same as that of the aldolase reaction in Figure 6.14. The C_2 carbohydrate moiety bound to the thiazole is transferred to the C-1 position of the glyceraldehyde 3-phosphate.

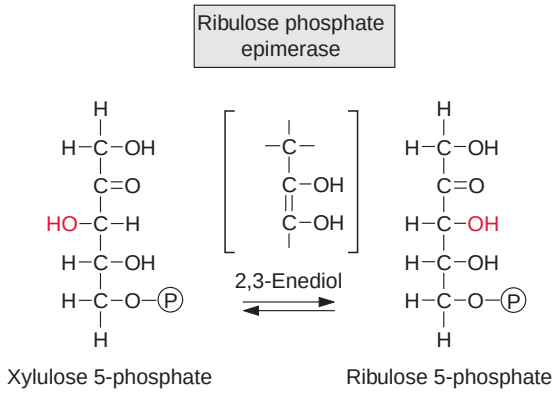

Figure 6.18 The conversion of xylulose 5-phosphate and ribose 5-phosphate to ribulose 5-phosphate. In both reactions a *cis*-enediol is formed as intermediate. Ⓟ symbolizes $-PO_3^{2-}$.

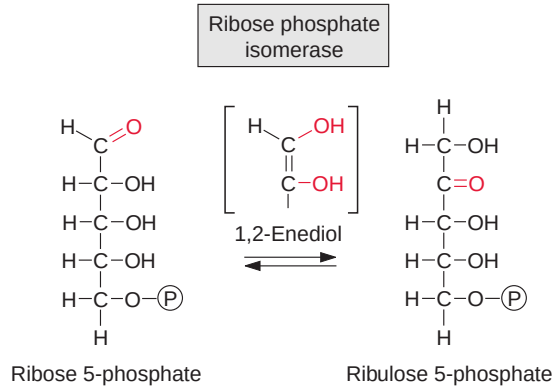

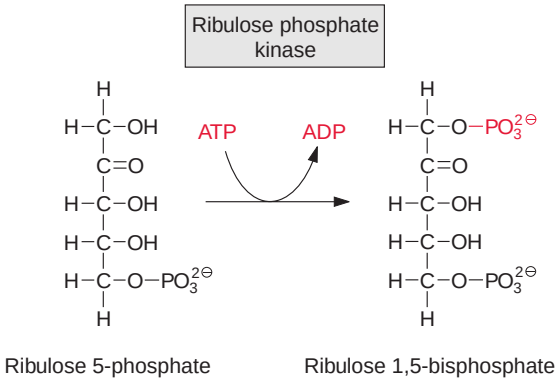

Figure 6.19 Ribulose phosphate kinase catalyzes the irreversible synthesis of ribulose 1,5-bisphosphate.

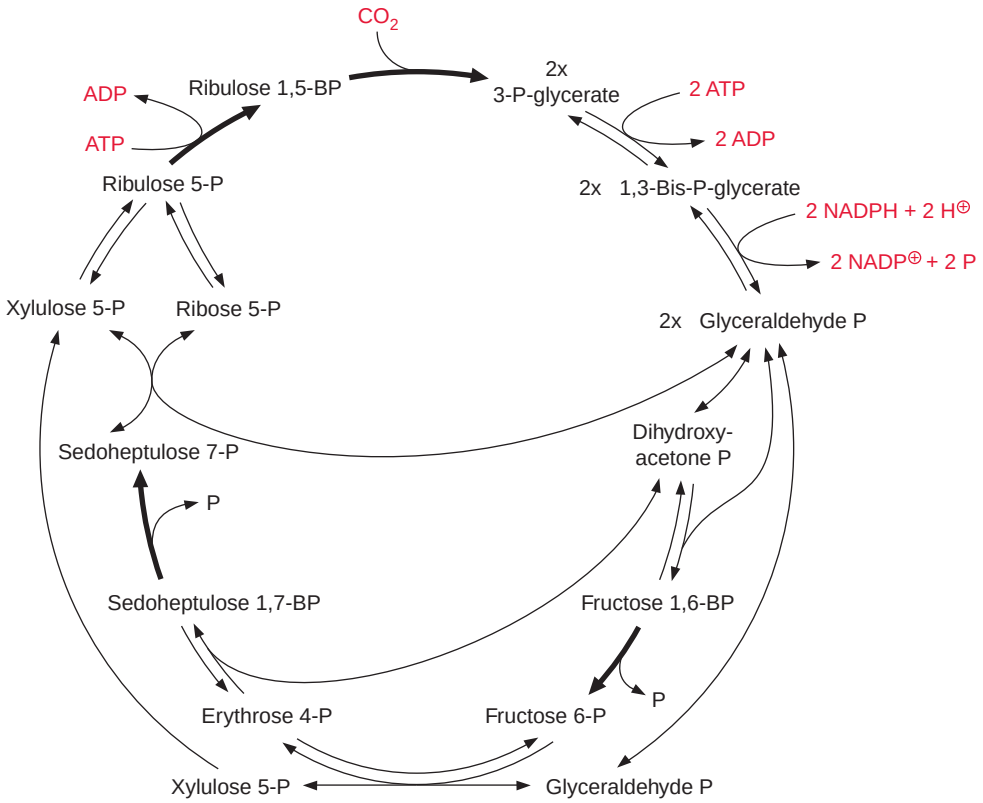

Figure 6.20 The Calvin cycle (reductive pentose phosphate pathway). P, phosphate; BP, bisphosphate. Bold arrows indicate irreversible reactions.

and phosphorylation of ribulose 5-phosphate. The fixation of one molecule of CO_2 requires in total two molecules of NADPH and three molecules of ATP.

6.5 Besides the reductive pentose phosphate pathway there is also an oxidative pentose phosphate pathway

Besides the reductive pentose phosphate pathway discussed in the preceding section, the chloroplasts also contain the enzymes of an oxidative pentose phosphate pathway. This pathway, which occurs both in the plant and animal kingdoms, oxidizes an **hexose phosphate** to a **pentose phosphate**

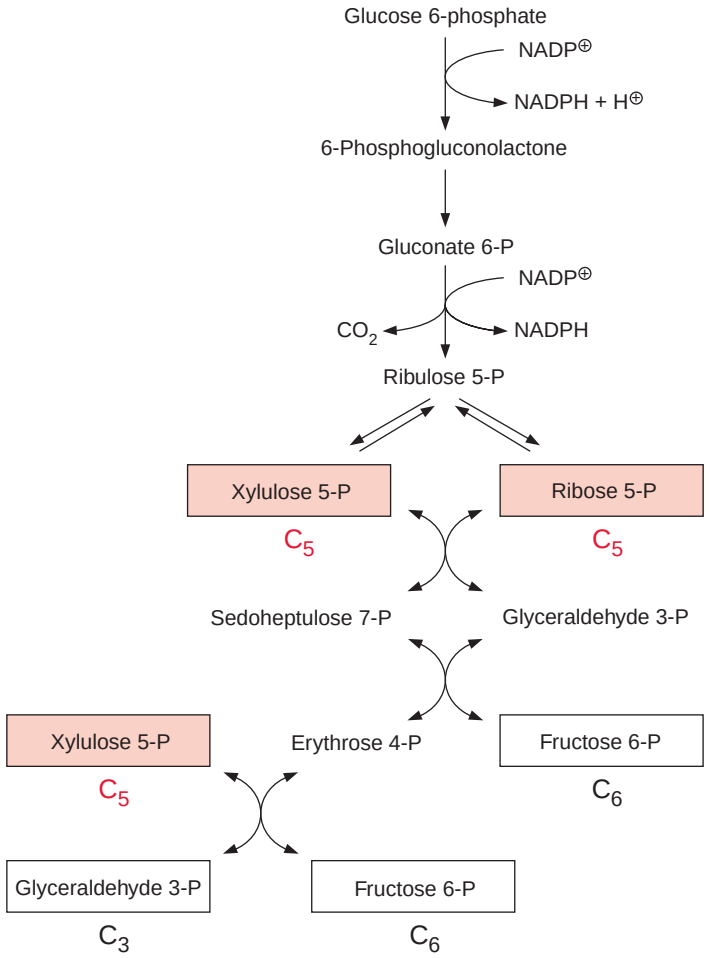

Figure 6.21 Oxidative pentose phosphate pathway.

with the release of one molecule of CO_2. This pathway provides **NADPH** as "high pressure hydrogen" for biosynthetic processes (Fig. 6.21). Glucose 6-phosphate is first oxidized by **glucose 6-phosphate dehydrogenase** to 6-phosphogluconolactone (Fig. 6.22). This reaction is highly exergonic and therefore not reversible. 6-Phosphogluconolactone, an intramolecular ester, is hydrolyzed by **lactonase**. The gluconate 6-phosphate thus synthesized is oxidized to ribulose 5-phosphate by the enzyme **gluconate 6-phosphate dehydrogenase**. In this reaction, CO_2 is released and NADPH is produced.

In the oxidative pathway, xylulose 5-phosphate and ribose 5-phosphate are isomerized from ribulose 5-phosphate by **ribulose phosphate epimerase** and **ribose phosphate isomerase**, respectively. These two products are then converted by **transketolase** to sedoheptulose 7-phosphate and glyceraldehyde

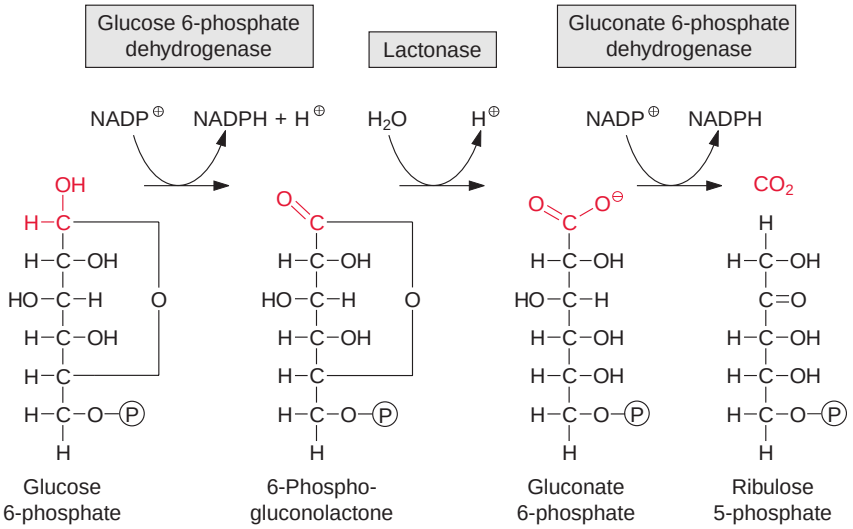

Figure 6.22 The two oxidation reactions of the pentose phosphate pathway. Ⓟ symbolizes $-PO_3^{2-}$.

3-phosphate. This transketolase is TPP-dependent and transfers a C_2 moiety (see Figs. 6.17, 5.4 and 5.5A). This reaction sequence is a reversal of the reductive pentose phosphate pathway. The next reaction is a special feature of the oxidative pathway: **transaldolase** transfers a nonphosphorylated C_3 moiety from sedoheptulose 7-phosphate to glyceraldehyde 3-phosphate, synthesizing fructose 6-phosphate and erythrose 4-phosphate (Fig. 6.23). The reaction mechanism is basically the same as in the aldolase reaction (Fig. 6.13), the only difference is that after the cleavage of the C-C bond, the remaining C_3 moiety continues to be bound to the enzyme via a Schiff base, until it is transferred. Erythrose 4-phosphate reacts with another xylulose 5-phosphate via a **transketolase reaction** to synthesize glyceraldehyde 3-phosphate and fructose 6-phosphate. In this way two hexose phosphates and one triose phosphate are formed from three pentose phosphates:

$$3\,C_5\text{-P} \rightleftarrows 2\,C_6\text{-P} + 1\,C_3\text{-P}$$

This chain of reactions is reversible. It allows the cell to provide ribose 5-phosphate for nucleotide biosynthesis even when no NADPH is required.

In the oxidative pathway, two molecules of NADPH are gained from the oxidation of glucose 6-phosphate and the release of one molecule of CO_2, whereas in the reductive pathway the fixation of one molecule of CO_2 requires not only two molecules of NADPH but also three molecules of ATP (Fig. 6.24). With the expenditure of energy it is possible for the reductive

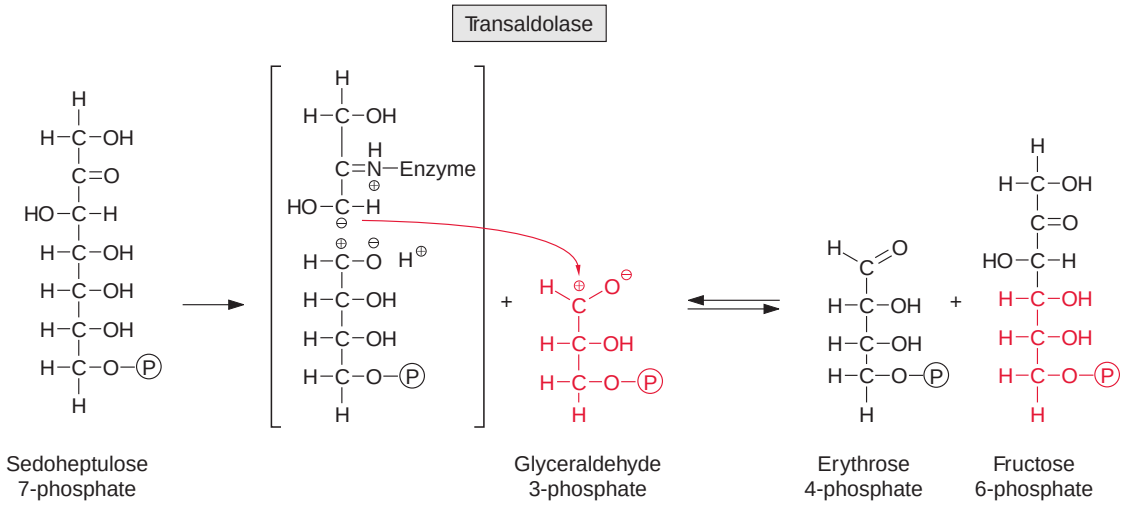

Figure 6.23 Transaldolase catalyzes the transfer of the C_3 moiety from a ketone to an aldehyde. The reaction is reversible. The reaction mechanism is the same as with aldolase, except that after the cleavage of the C-C bond the C_3 moiety remains bound to the enzyme and is released after the transfer to glyceraldehyde phosphate as fructose 6-phosphate.

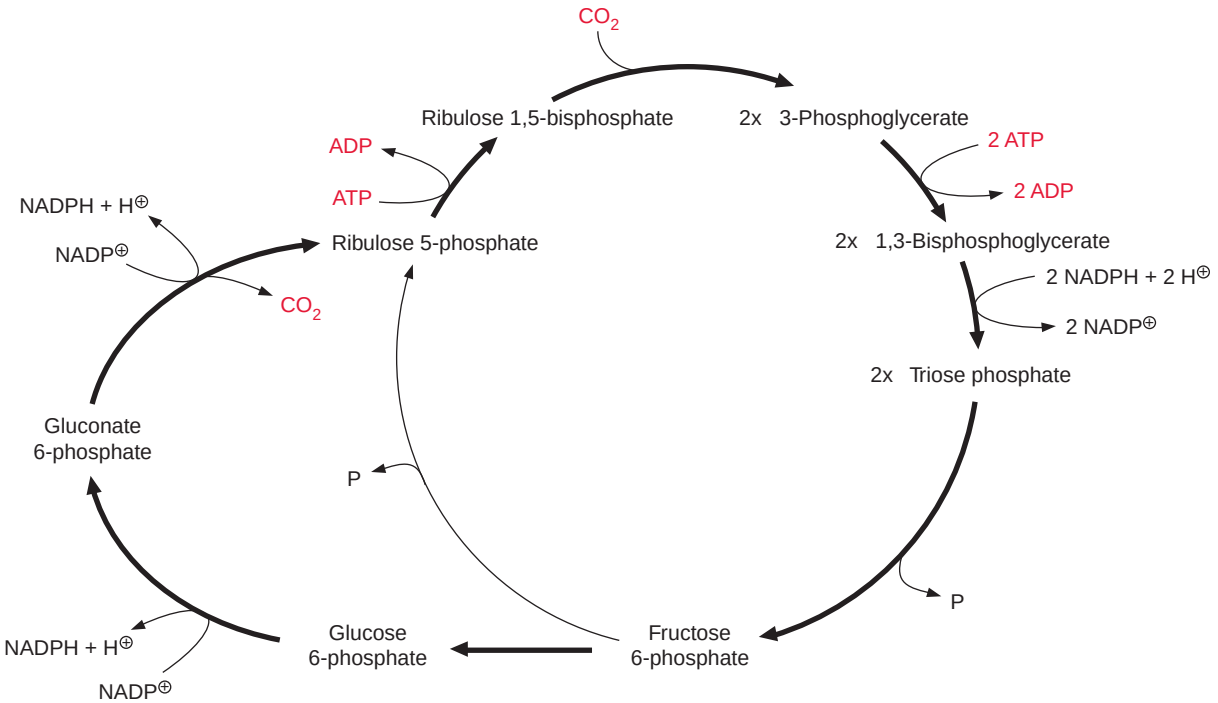

Figure 6.24 A simultaneous operation of the reductive and the oxidative pentose phosphate pathway would result in a futile cycle with the waste of ATP.

pentose phosphate pathway to proceed with a very high flux rate in the opposite direction to the oxidative pathway.

6.6 Reductive and oxidative pentose phosphate pathways are regulated

The enzymes of the reductive as well as the oxidative pentose phosphate pathways are located in the chloroplast stroma (Fig. 6.24). A simultaneous operation of both metabolic pathways, in which one molecule of CO_2 is reduced to a carbohydrate at the expense of three ATP and two NADPH (reductive pentose phosphate pathway), and then reoxidized by the oxidative pathway to CO_2, yielding two molecules of NADPH, would represent a futile cycle. This futile cycle would waste three molecules of ATP in each turn. This is prevented by metabolic regulation, which ensures that key enzymes of the reductive pentose phosphate pathway are active only during illumination and are switched off in darkness, whereas the key enzymes of the oxidative pentose phosphate pathway are only active in the dark.

Reduced thioredoxins transmit the signal "illumination" to the enzymes

An important signal for the state "illumination" is provided by photosynthetic electron transport as reducing equivalents such as reduced thioredoxin (Fig. 6.25). Electrons of reducing equivalents are transferred from ferredoxin to thioredoxin by the enzyme **ferredoxin-thioredoxin reductase**, an iron-sulfur protein of the 4Fe-4S type.

Thioredoxins form a family of small proteins, consisting of about 100 amino acids, which contain as a reactive group the amino acids **Cys-Gly-Pro-Cys**, located at the periphery of the protein. Due to the neighboring cysteine side chains, the thioredoxin can occur in two redox states: the reduced thioredoxin with **two SH-groups** and the oxidized thioredoxin in which the two cysteines are linked by a **disulfide (S-S) bond**.

Thioredoxins are found in all living organisms from archaebacteria to plants and animals. They function as **protein disulfide oxido-reductases**, in reducing disulfide bonds in target proteins to the -SH form and reoxidizing them again to the S-S form. Despite their small size, they possess a relatively high substrate specificity. Thioredoxins participate as redox carriers in the reduction of high as well as low molecular compounds (e.g., the reduction of

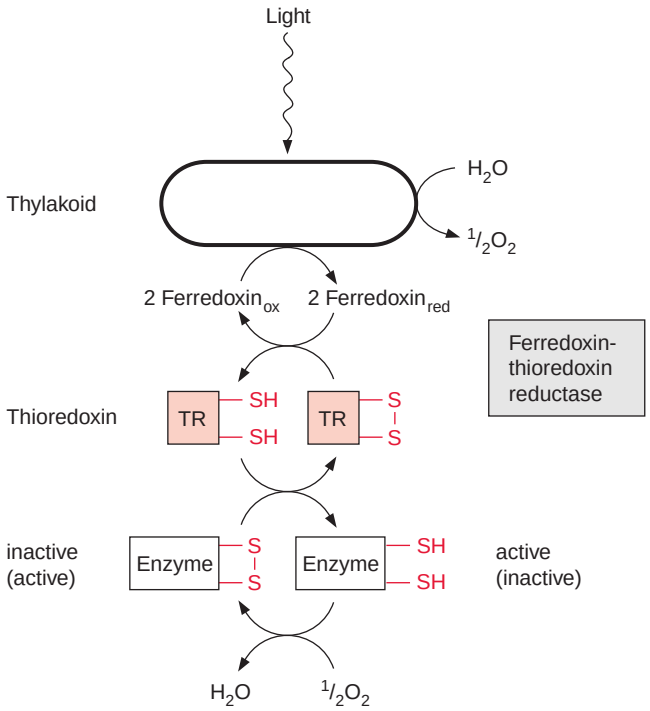

Figure 6.25 The light regulation of chloroplast enzymes is mediated by reduced thioredoxin.

ribonucleotides to deoxyribonucleotides; the reduction of sulfate, a process occurring in plants and microorganisms (section 12.1); and the reductive activation of seed proteins during germination). Furthermore, other processes are known in which thioredoxins play an essential role, for instance the assembly of bacteriophages, and hormone action or the blood-clotting process in animals.

The involvement of thioredoxins in the light regulation of chloroplast enzymes is a very special function which might have occurred during evolution in addition to their general metabolic functions. The chloroplast enzymes **ribulose phosphate kinase**, **sedoheptulose 1,7-bisphosphatase**, **NADP-glyceraldehyde phosphate dehydrogenase** and the chloroplast isoform of **fructose 1,6-bisphosphatase** are converted from an inactive state to an active state via reduction with thioredoxin and are thus switched on by light. This also applies to other chloroplast enzymes such as **NADP-malate dehydrogenase** (section 7.3) and **F-ATP synthase** (section 4.4). Reduced thioredoxin also converts **RubisCO activase** (section 6.2) from a less active state to a more active state. Reduced thioredoxin can also inactivate enzymes, e.g., **glucose**

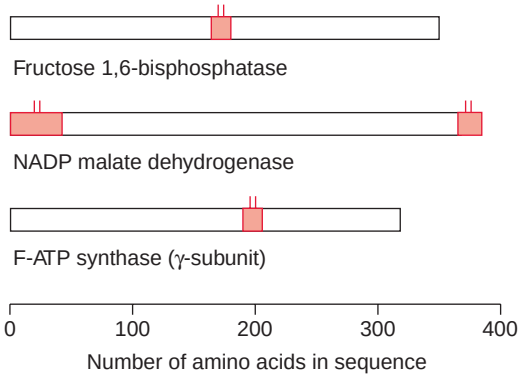

Figure 6.26 In contrast to the nonplastid isoenzymes, several thioredoxin-modulated chloroplast enzymes comprise additional amino acid sequences (shown in red) in which two cysteine residues are located. (After Scheibe, 1990.)

6-phosphate dehydrogenase, the first enzyme of the oxidative pentose phosphate pathway.

The thioredoxin modulated activation of chloroplast enzymes releases a built-in blockage

Important knowledge of the mechanism of thioredoxin action on the chloroplast enzymes has been obtained from comparison with the corresponding isoenzymes from other cellular compartments. Isoenzymes of chloroplast fructose 1,6-bisphosphatase, glyceraldehyde phosphate dehydrogenase and malate dehydrogenase exist in the cytosol and are not regulated by thioredoxin. This also applies to F-ATP synthase in the mitochondria. Comparison of the amino acid sequences shows that at least in some cases the chloroplast isoenzymes possess **additional sequences** at the N- or C-terminus, or in an internal region of their sequence, which provide **two cysteine residues** (Fig. 6.26). The SH-groups of these cysteine residues can be oxidized and form a disulfide bond, which is the substrate for the disulfide oxidoreductase activity of thioredoxin.

Upon exchange of the cysteine residues involved in the regulation by genetic engineering (Chapter 22) enzymes were obtained that are fully active in the absence of reduced thioredoxin. Under oxidizing conditions, the enzymes regulated by thioredoxin are forced by the formation of a disulfide bridge into a conformation in which the catalytic center is inactivated. The reduction of this disulfide bridge by thioredoxin releases this blockage and the enzyme is converted into a relaxed conformation in which the catalytic center is accessible.

The light activation discussed so far is not an all or nothing effect. It is due to a continuous change between the thioredoxin-mediated reduction of the enzyme protein and its simultaneous oxidation by oxygen. The

degree of activation of the enzyme depends on the rate of reduction. This is not only due to the degree of the reduction through thioredoxin (and thus to the degree of reduction of ferredoxin), but also to the presence of other metabolites, e.g., the reductive activation of fructose and sedoheptulose bisphosphatase is enhanced by the corresponding bisphosphates. These effectors cause a decrease of the redox potential of the SH-groups in the corresponding enzymes, which enhances the reduction of the disulfide group by thioredoxin. In this way the activity of these enzymes is increased when the concentration of their substrates rises. Thus the reductive activation of NADP malate dehydrogenase is decreased by the presence of $NADP^+$. This has the effect that the enzyme is only active at a high NADPH/$NADP^+$ ratio. On the other hand, the reductive inactivation of glucose-6-phosphate dehydrogenase is increased by NADPH. Thus with a sufficient supply of NADPH the activity of the oxidative pentose phosphate pathway is turned down. In contrast, the oxidative activation of glucose 6-phosphate dehydrogenase is enhanced by $NADP^+$ which increases the activity of the oxidative pentose phosphate pathway when there is a demand for NADPH.

Multiple regulatory processes tune the reactions of the reductive pentose phosphate pathway

An additional light regulation of the Calvin cycle is based on the effect of light-dependent changes of chloroplast enzyme activities due to the stromal proton and Mg^{++} concentrations. When isolated chloroplasts are illuminated, the acidification of the thylakoid space (Chapter 3) is accompanied by an alkalization and an increase in the Mg^{++} concentration in the stroma. During the dark/light transition, the pH in the stroma may change from about pH 7.2 to 8.0. This correlates with the pH optimum of the CO_2 fixation of isolated chloroplasts of about pH 8.0 with a sharp decline towards the acidic range. An almost identical pH dependence is found with the light-activated enzymes **fructose 1,6-bisphosphatase** and **sedoheptulose 1,7-bisphosphatase**. Moreover, the catalytic activity of both these enzymes is increased by the light-dependent increase of the stromal Mg^{++} concentration. The light activation of these enzymes due to the thioredoxin system and light-induced changes of the stromal pH and Mg^{++} concentration is a very efficient system for switching these enzymes on and off, according to demand. During darkness this system results in an extensive inactivation of the corresponding enzymes.

The activities of several stromal enzymes are also regulated by metabolite levels. The chloroplast **fructose 1,6-bisphosphatase** and **sedoheptulose**

1,7-bisphosphatase are inhibited by their corresponding products, fructose 6-phosphate and sedoheptulose 7-phosphate, respectively. Thus the accumulation of the products has negative effects on the activity of these enzymes. **Ribulose phosphate kinase** is inhibited by 3-phosphoglycerate and also by ADP. Inhibition by ADP is important for coordinating the two kinase reactions of the reductive pentose phosphate pathway. Whereas ribulose phosphate kinase catalyzes an irreversible reaction, the phosphoglycerate kinase reaction is reversible. If both reactions were to compete for ATP in an unrestricted manner, in the case of a shortage of ATP the irreversible phosphorylation of ribulose 5-phosphate would be at an advantage, resulting in an imbalance of the Calvin cycle. A decrease in the activity of ribulose phosphate kinase at an elevated level of ADP can prevent this.

Finally, fructose 1,6-bisphosphatase and sedoheptulose 1,7-bisphosphatase are strongly inhibited by glycerate. As shown in section 7.1, glycerate is an intermediate in the recycling of phosphoglycolate formed by the oxygenase activity of RubisCO. The accumulation of glycerate slows down the regeneration of RuBP and its carboxylation. In this way also the accompanying oxygenation is lowered, decreasing the synthesis of glycolate which is the precursor of glycerate.

Also, **RubisCO** is subject to regulation. Experiments with whole leaves demonstrated that the degree of the activation of RubisCO correlates with the intensity of illumination and the rate of photosynthesis. The activation state of RubisCO is adjusted via a regulation of the **RubisCO activase** (section 6.2). RubisCO-activase is activated by **reduced thioredoxin** and is also dependent on the **ATP/ADP** ratio. When there is a rise in the ATP/ADP ratio in the stroma, the activity of the activase also rises. This scenario explains how the activity of RubisCO can be adjusted to the supply of ATP delivered by the light reaction of photosynthesis. However, many observations suggest that this cannot be the only mechanism for a light regulation of RubisCO, for example the RubisCO activase is regulated by the light-dependent proton gradient across the thylakoid membrane, and the activity of RubisCO is inhibited by its product **3-phosphoglycerate**. In this way the activity of RubisCO could be adjusted according to the product accumulation

Figure 6.27 presents a scheme summarizing the various factors that influence the regulation of the enzymes of the reductive and oxidative pentose pathways. A multitude of regulatory processes ensures that the various steps of both reaction chains are adjusted to each other and to the demand of the cell.

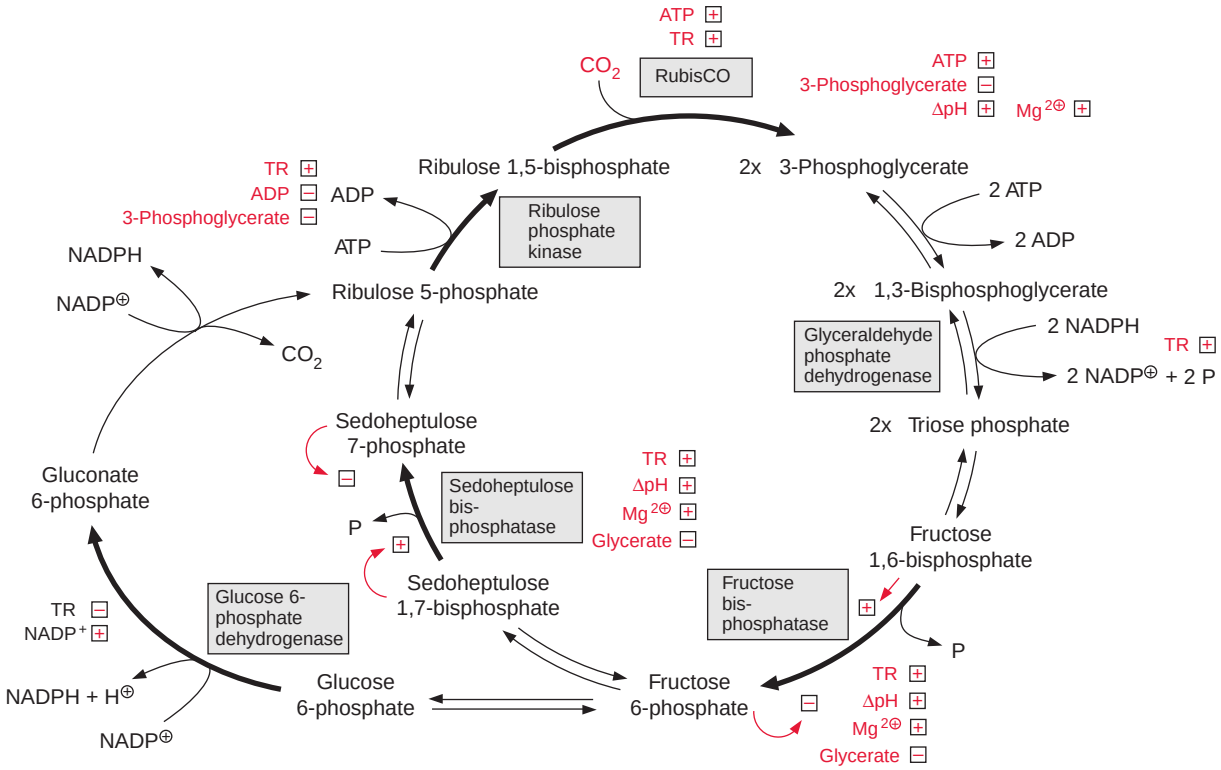

Figure 6.27 Regulation of the reductive and oxidative pentose phosphate pathways. Both pathways are represented in a simplified scheme. Only those enzymes for which regulation has been discussed in the text are highlighted. [+] increase and [−] decrease of activity caused by the factors written in red, such as reduced thioredoxin (TR), light-dependent alkalization (ΔpH), the increase in Mg^{++} concentration in the stroma and the presence of metabolites. The regulation of RubisCO proceeds via a regulation of the RubisCO activase.

Further reading

Allen, D. J., Ort, D. Impact of chilling temperature on photosynthesis in warm-climate plants. Trends in Plant Science 6, 36–42 (2002).

Andersson, I., Backlund, A. Structure and function of RubisCO. Plant Physiology Biochemistry 46, 275–291 (2008).

Andralojc, P. J., Keys, A. J., Kossmann, J., Parry, M. A. J. Elucidating the biosynthesis of 2-carboxyarabinitol-1-phosphate through reduced expression of chloroplastic fructose-1.6-bisphosphate phosphatase and radiotracer studies with $^{14}CO_2$. Proceedings National Academy of Science USA 99, 4742–4747 (2002).

Buchanan, B. B., Balmer, Y. Redox regulation: A broadening horizon. Annual Reviews Plant Biology 56, 187–220 (2005).

Gulliaume, G., Tcherkez, B., Farquhar, G. D., Andrews, T. J. Despite low catalysis and confused substrate specificity, all ribulose bisphosphate carboxylases may be nearly

perfectly optimized. Proceedings National Academy of Science USA 103, 7252–7257 (2006).
Hisabori, T., Motohashi, K., Hosoya-Matsuda, N., Ueoka-Nakanishi, H., Romano, P. G. Towards a functional dissection of thioredoxin networks in plant cells. Photochemistry Photobiology 83, 145–151 (2007).
Kruger, N. J., von Schaewen, A. The oxidative pentose phosphate pathway: Structure and organisation. Current Opinion Plant Biology 6, 236–246 (2003).
Lemaire, S. D., Michelet, L., Zaffagnini, M., Massot, V., Issakidis-Bourguet, E. Thioredoxins in chloroplasts. Current Genetics 51, 343–365 (2007).
Raines, C. A. Transgenic approaches to manipulate the environmental responses of the C3 carbon fixation cycle. Plant Cell Environment 29, 331–339 (2006).
Spreitzer, R. J., Salvucci, M. E. RubisCO: Structure, regulatory interactions and possibilities for a better enzyme. Annual Reviews Plant Biology 53, 449–475 (2002).
Trost, P., Fermani, S., Marri, L., Zaffagnini, M., Falini, G., Scagliarini, S., Pupillo, P., Sparla, F. Thioredoxin-dependent regulation of photosynthetic glyceraldehyde-3-phosphate dehydrogenase: Autonomous vs. CP12-dependent mechanisms. Photosynthesis Research 89, 263–275 (2006).
Von Caemmerer, S., Quick, W. P. RubisCO: Physiology in vivo. In Photosynthesis: Physiology and Metabolism, R. C. Leegood, T. D. Sharkey, S. von Caemmerer (eds.), pp. 85–113. Dordrecht, The Netherlands: Kluwer Academic Publishers. (2000)
Zhang, N., Kallis, R. P., Ewy, R. G., Portis, A. R. Light modulation of Rubisco in Arabidopsis requires a capacity for redox regulation of the larger Rubisco activase isoform. Proceedings National Academy of Science USA 99, 3330–3334 (2002).

7

Phosphoglycolate formed by the oxygenase activity of RubisCO is recycled in the photorespiratory pathway

Section 6.2 described how large amounts of 2-phosphoglycolate are formed as a by-product during CO_2 fixation by RubisCO, due to the oxygenase activity of this enzyme. In the photorespiratory pathway, discovered in 1972 by the American scientist Edward Tolbert, the by-product 2-phosphoglycolate is recycled to ribulose 1,5-bisphosphate. The term *photorespiration* indicates that it involves oxygen consumption in the light, which is accompanied by the release of CO_2. Whereas in mitochondrial respiration (cell respiration; Chapter 5) the oxidation of substrates to CO_2 serves the purpose of producing ATP, and in the course of photorespiration ATP is consumed.

7.1 Ribulose 1,5-bisphosphate is recovered by recycling 2-phosphoglycolate

Figure 7.1 gives an overview of the reactions of the photorespiratory pathway and their localization. The oxygenation of two molecules of ribulose 1,5-bisphosphate yields two molecules of 3-phosphoglycerate and two molecules of 2-phosphoglycolate. The latter are recycled to yield another molecule of 3-phosphoglycerate. This recycling begins with the hydrolytic release of phosphate by **glycolate phosphate phosphatase** present in the chloroplast

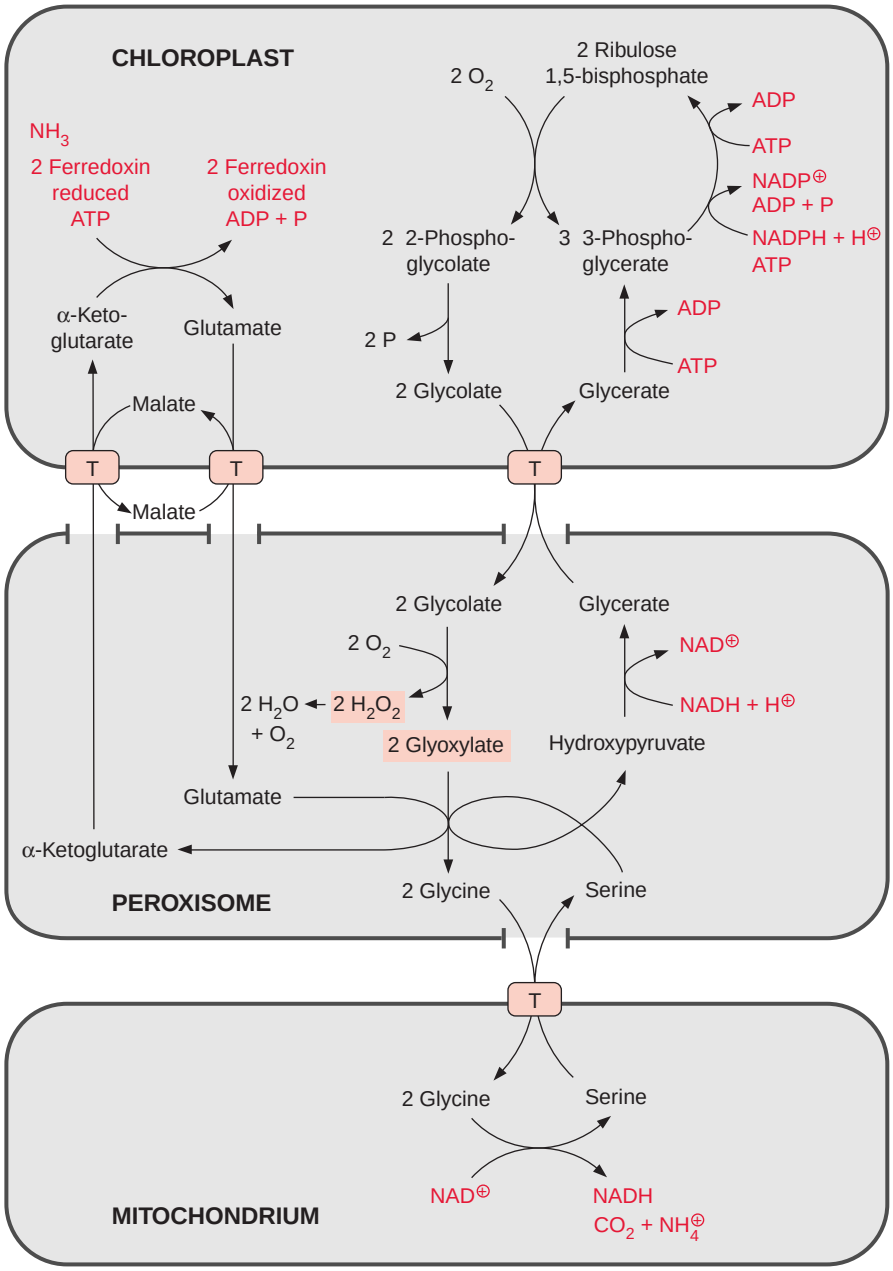

Figure 7.1 Schematic presentation of the compartmentalization of the photorespiratory pathway. Intermediates are shown in black and co-substrates in red. Not shown are the outer membranes of the chloroplasts and mitochondria, which are permeable for metabolites, due to the presence of porins. T = translocator. Translocators for glycine and serine have not been identified yet.

stroma (Fig. 7.2). The resultant glycolate leaves the chloroplasts via a specific translocator located in the inner envelope membrane and enters the peroxisomes via pores in the peroxisomal boundary membrane, probably facilitated by a **porin** (section 1.11).

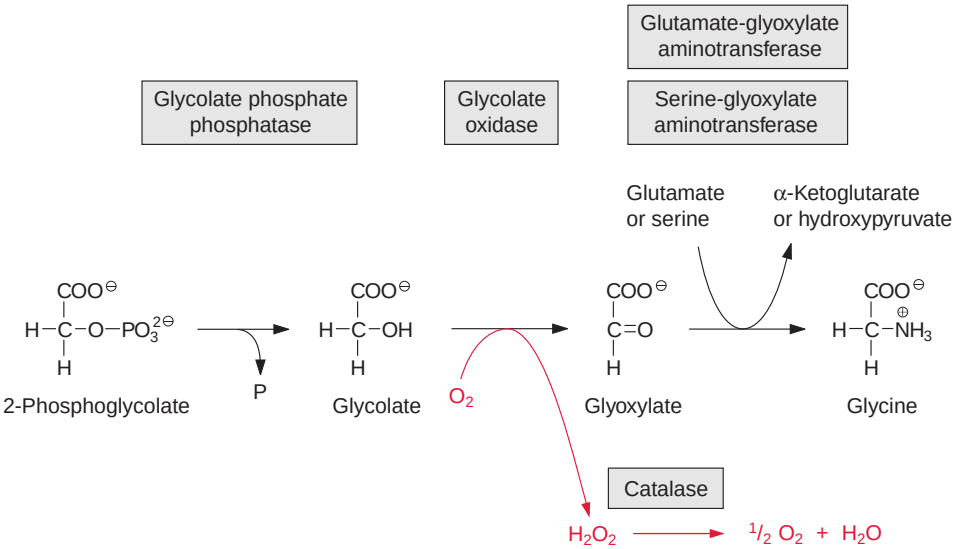

Figure 7.2 Sequence of reactions for the conversion of 2-phosphoglycolate into glycine.

In the peroxisomes the alcoholic group of glycolate is oxidized to a carbonyl group in an irreversible reaction catalyzed by **glycolate oxidase**, resulting in the synthesis of glyoxylate. The reducing equivalents are transferred to molecular oxygen to produce H_2O_2 (Fig. 7.2). Like other H_2O_2 forming oxidases, the glycolate oxidase contains a flavin mononucleotide cofactor (FMN, Fig. 5.16) as redox mediator between glycolate and oxygen. H_2O_2 is then converted to water and oxygen by the enzyme **catalase**, which is present in the peroxisomes. Thus, in total, 0.5 mol of O_2 is consumed for the oxidation of one mole of glycolate to glyoxylate.

The glyoxylate is converted to the amino acid glycine by two different reactions proceeding in the peroxisome simultaneously at a 1:1 ratio. The enzyme **glutamate-glyoxylate aminotransferase** catalyzes the transfer of an amino group from the donor glutamate to glyoxylate. This enzyme also reacts with alanine as amino donor. In the other reaction, the enzyme **serine-glyoxylate aminotransferase** catalyzes the transamination of glyoxylate by serine. These two enzymes, like other aminotransferases (e.g., glutamate-oxaloacetate aminotransferase, see section 10.4) contain bound pyridoxal phosphate with an aldehyde function as reactive group (Fig. 7.3). Figure 7.4 presents the reaction sequence of transamination reactions.

The glycine thus formed leaves the peroxisomes via pores and is transported into the mitochondria. Although this transport has not yet been characterized in detail, it is to be expected that it is facilitated by a specific translocator. In the mitochondria two molecules of glycine are oxidized yielding one molecule of serine with release of CO_2 and NH_4^+ and a transfer of reducing equivalents to NAD^+ (Fig. 7.5). The oxidation of glycine

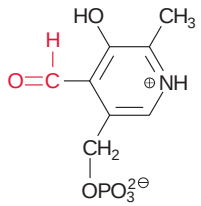

Pyridoxal phosphate

Figure 7.3 Structure of pyridoxal phosphate.

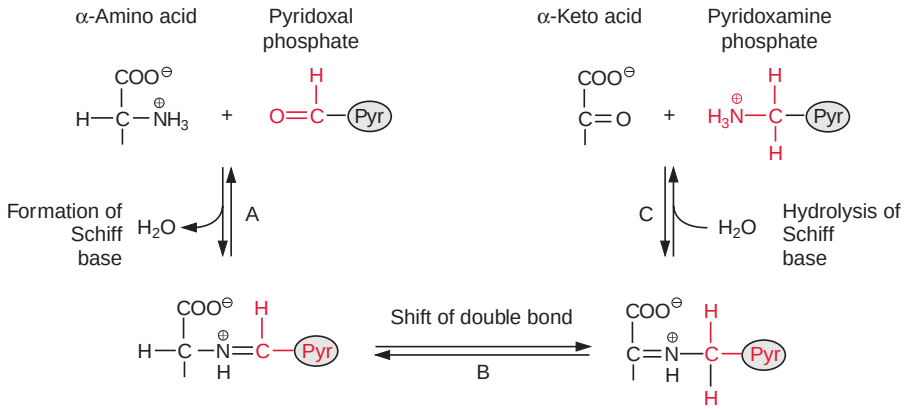

Figure 7.4 Sequence of the aminotransferase reaction. The aldehyde group of pyridoxal phosphate forms a Schiff base with the α-amino group of the amino acid (A), which is subsequently converted to an isomeric form (B) by a base-catalyzed movement of a proton. Hydrolysis of the isomeric Schiff base results in the formation of an α-ketoacid and pyridoxamine phosphate (C). The amino group of this pyridoxamine phosphate then forms a Schiff base with another α-ketoacid and glycine is formed by reversion of the steps C, B, and A. Pyridoxal phosphate is thus regenerated and is available for the next reaction cycle. Pyr = pyridoxal phosphate.

is catalyzed by the **glycine decarboxylase-serine-hydroxymethyl transferase complex**. This is a multi-enzyme complex, consisting of four different subunits (Fig. 7.7), which is similar to the pyruvate dehydrogenase complex (section 5.3). The so-called **H-protein** with the prosthetic group lipoic acid amide (Fig. 5.5) represents the center of the glycine decarboxylase complex. Around this center are positioned the pyridoxal phosphate-containing **P-protein,** the **T-protein** with a tetrahydrofolate (Fig. 7.6) as a prosthetic group, and the **L-protein**, also named **dihydrolipoate dehydrogenase**. The latter is identical to the dihydrolipoate dehydrogenase of the pyruvate and α-ketoglutarate dehydrogenase complex (Figs. 5.4 and 5.8). Since the disulfide group of the lipoic acid amide in the H-protein is located at the end of a flexible polypeptide chain (see also Fig. 5.4), it is able to react with the three other subunits. Figure 7.7 presents the sequence of reactions. The enzyme **serine-hydroxymethyl transferase**, which is in close proximity to the glycine decarboxylase complex, catalyzes the transfer of the methylene residue to another molecule of glycine to synthesize serine.

The NADH produced in the mitochondrial matrix from glycine oxidation can be oxidized by the mitochondrial respiratory chain in order to generate ATP. Alternatively, these reducing equivalents can be exported from the mitochondria to other cell compartments, as will be discussed in section 7.3. The capacity for glycine oxidation in the mitochondria of green plant

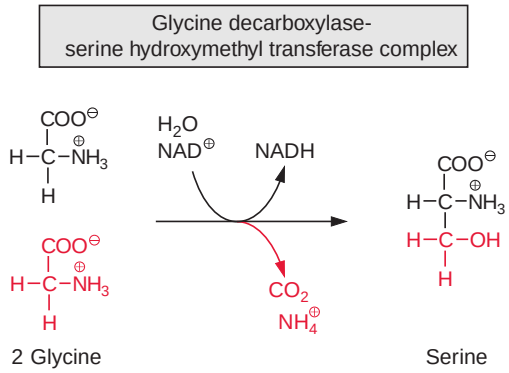

Figure 7.5 Overall reaction of the conversion of two molecules of glycine to synthesize one molecule of serine as catalyzed by the glycine decarboxylase-serine hydroxymethyl transferase complex.

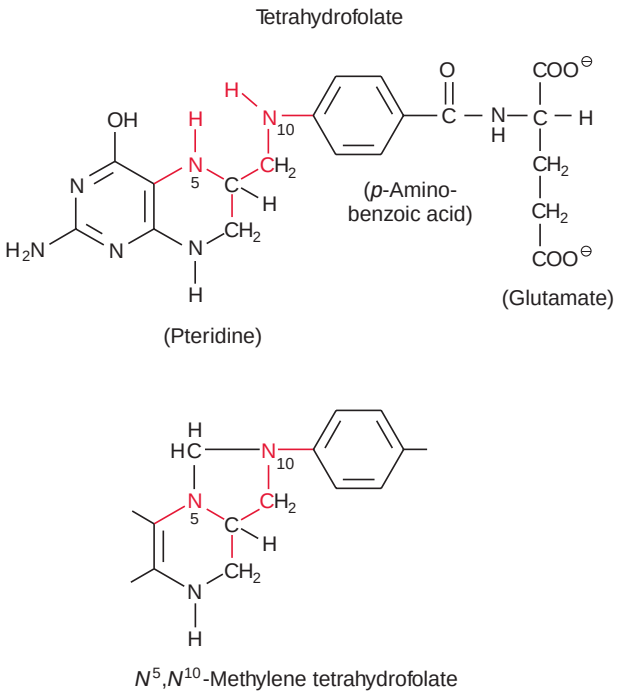

Figure 7.6 Structure of tetrahydrofolate (THF). Atoms in red are involved in binding of the methylene group. THF can also transfer a methyl or formyl moiety.

cells is very high. The glycine decarboxylase complex of the mitochondria can amount to 30% to 50% of the total content of soluble mitochondrial proteins. In mitochondria of nongreen plant cells, however, the proteins of glycine oxidation are present only in very low amounts or are absent.

Serine probably leaves the mitochondria via a specific translocator, possibly the same translocator which is responsible for glycine uptake. After entering the peroxisomes through pores, serine is converted to hydroxypyruvate by

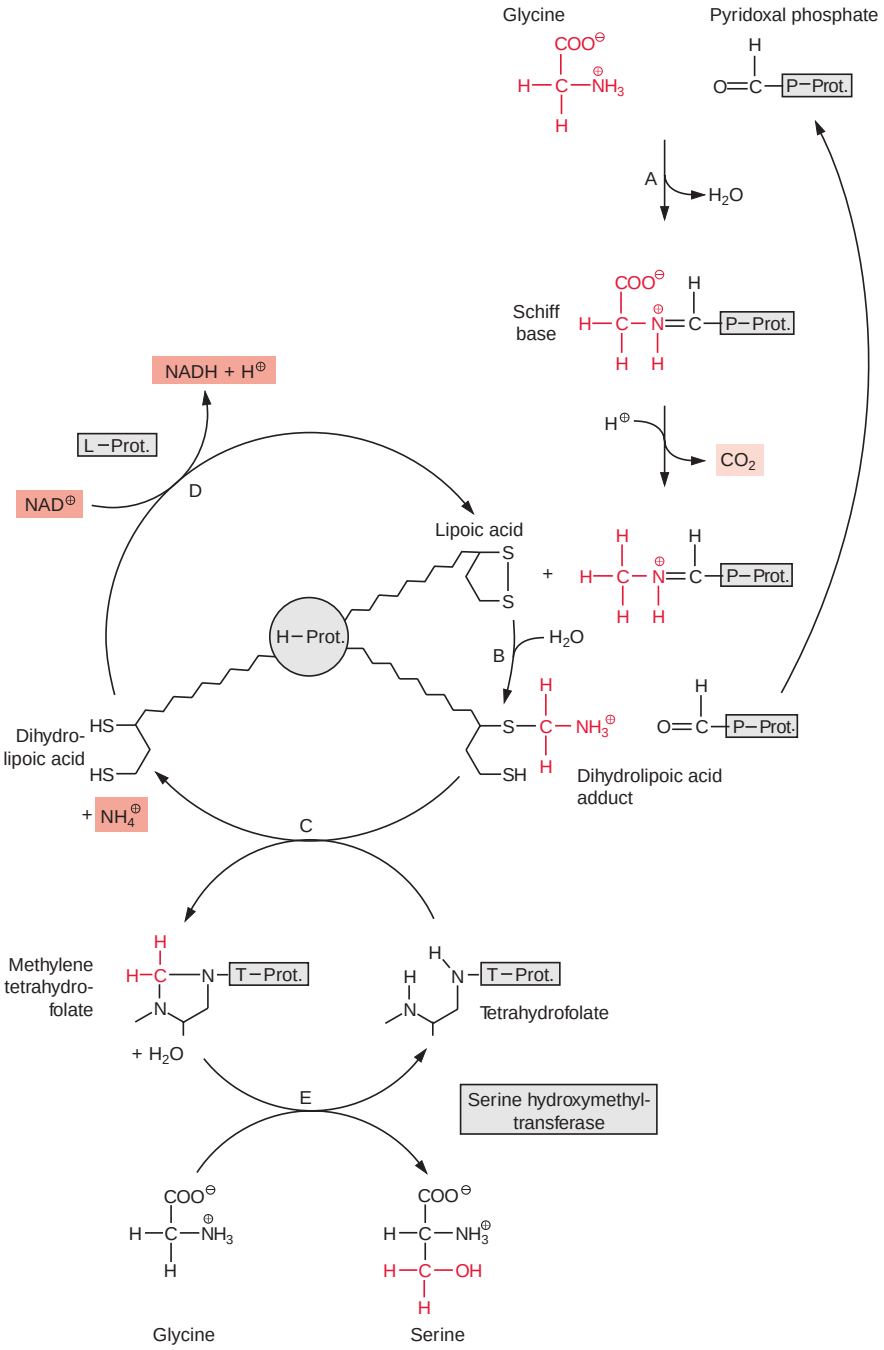

Figure 7.7 Sequence of the reactions converting two molecules of glycine into one molecule of serine. The amino group of glycine reacts first with the aldehyde group of pyridoxal phosphate in the P-protein to form a Schiff base (A). The glycine moiety is then decarboxylated and transferred from the P-protein to the lipoic acid residue of the H-protein (B). This is the actual oxidation step: the C_1 residue is oxidized to a methylene group and the lipoic acid residue is reduced to dihydrolipoic acid. The dihydrolipoic acid adduct reacts then with the T-protein, the methylene C_1 residue is transferred to tetrahydrofolate, and the dihydrolipoic acid residue remains (C). The dihydrolipoic acid is reoxidized via the L-protein (dihydrolipoate dehydrogenase) to lipoic acid and the reducing equivalents are transferred to NAD^+ (D). A new reaction cycle can start. The methylene residue bound to tetrahydrofolate is transferred to a second molecule of glycine by serine hydroxymethyl transferase and serine is synthesized (E).

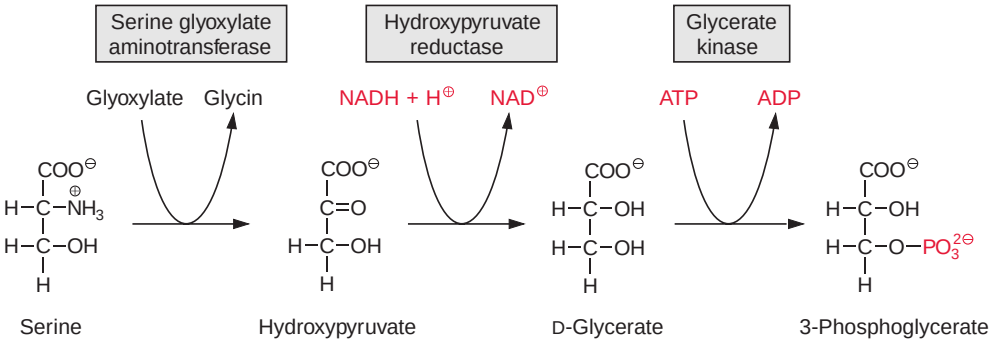

Figure 7.8 Sequence of reactions of the conversion of serine to 3-phosphoglycerate.

the enzyme **serine-glyoxylate aminotransferase** mentioned above (Fig. 7.8). At the expense of NADH, hydroxypyruvate is reduced by **hydroxypyruvate reductase** to synthesize glycerate, which is released from the peroxisomes and imported into the chloroplasts.

The uptake into the chloroplasts proceeds by the same translocator which catalyzed the release of glycolate from the chloroplasts (**glycolate-glycerate translocator**). This translocator facilitates a glycolate-glycerate counter-exchange as well as a co-transport of just glycolate with a proton. In this way, the translocator enables the export of two molecules of glycolate from the chloroplasts in exchange for the import of one molecule of glycerate. Glycerate is converted by **glycerate kinase** to 3-phosphoglycerate, consuming ATP from the chloroplast stroma. Finally, 3-phosphoglycerate is reconverted to ribulose 1,5-bisphosphate via the reductive pentose phosphate pathway (sections 6.3, 6.4). These reactions complete the recycling of 2-phosphoglycolate.

7.2 The NH_4^+ released in the photorespiratory pathway is refixed in the chloroplasts

Nitrogen is an important plant nutrient. Nitrogen supply is often a limiting factor in plant growth. It is therefore necessary for plant metabolism that ammonium, which is released at very high rates in the photorespiratory pathway during glycine oxidation, is completely refixed. This refixation occurs in the chloroplasts. The synthesis is catalyzed by the same enzymes that participate in nitrate assimilation (Chapter 10). However, the rate of NH_4^+ refixation

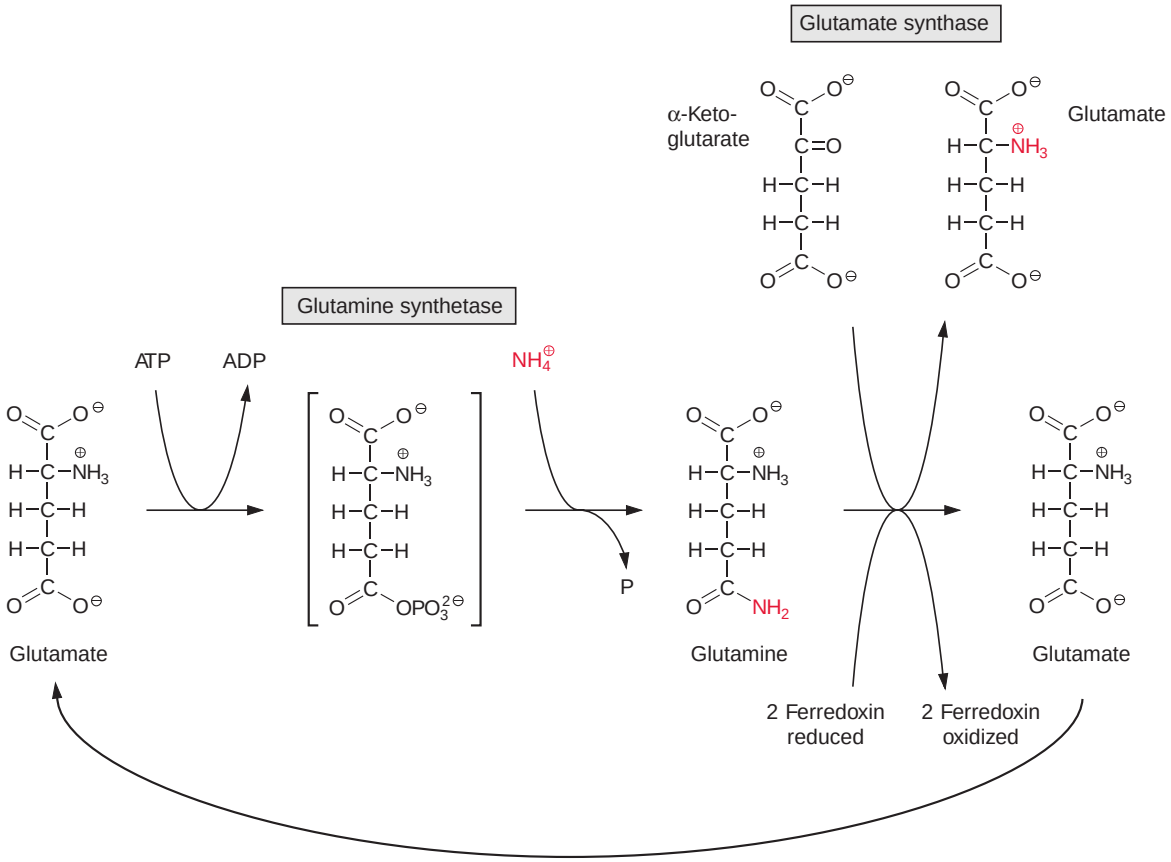

Figure 7.9 Sequence of reactions of the fixation of ammonia with subsequent synthesis of glutamate from α-ketoglutarate.

in the photorespiratory pathway is 5 to 10 times higher than the rate of NH_4^+ fixation in nitrate assimilation.

In a plant cell, chloroplasts and mitochondria are often in close proximity to each other. The NH_4^+ produced during oxidation of glycine passes through the inner membrane of the mitochondria and the chloroplasts. Whether this passage occurs by simple diffusion or is facilitated by specific translocators or ion channels is still a matter of debate. The enzyme **glutamine synthetase**, present in the chloroplast stroma, catalyzes the transfer of an ammonium ion to the δ-carboxyl group of glutamate (Fig. 7.9) to synthesize glutamine. This reaction is driven by the conversion of one molecule of ATP to ADP and phosphate. In an intermediary step, the δ-carboxyl group is activated by reaction with ATP to form a carboxy-phosphate anhydride.

Glutamine synthetase has a high affinity for NH_4^+ and catalyzes an irreversible reaction. This enzyme has a key role in the fixation of NH_4^+ not only in plants, but also in bacteria and animals.

The nitrogen fixed as amide in glutamine is transferred by reductive amination to α-ketoglutarate (Fig. 7.9). In this reaction, catalyzed by **glutamate synthase**, also known as glutamine-2-oxoglutarate aminotransferase (**GOGAT**), two molecules of glutamate are formed. The reducing equivalents are provided by reduced ferredoxin, which is a product of photosynthetic electron transport (see section 3.8). In green plant cells, glutamate synthase is located exclusively in the chloroplasts.

It has been shown in *Arabidopsis* that mitochondria also contain a glutamine synthetase, indicating that mitochondria are also able to fix NH_4^+. Since glutamate synthase is located exclusively in the chloroplasts, the ammonia fixed in the mitochondria has to be transferred to the chloroplasts, perhaps by a glutamine-glutamate shuttle.

Of the two glutamate molecules thus formed in the chloroplasts, one is exported by the **glutamate-malate translocator** in exchange for malate. After entering the peroxisomes, it is available as a reaction partner for the transamination of glyoxylate (Fig. 7.1). The α-ketoglutarate thus formed is re-imported from the peroxisomes into the chloroplasts by a **malate-α-ketoglutarate translocator**, again in counter-exchange for malate.

7.3 Peroxisomes have to be provided with external reducing equivalents for the reduction of hydroxypyruvate

NADH is required as reductant for the conversion of hydroxypyruvate to glycerate in the peroxisomes. Since leaf peroxisomes have no metabolic pathway capable of delivering NADH at the very high rates required, peroxisomes depend on the supply of reducing equivalents from outside.

The cytosolic NADH system of a leaf cell is oxidized to such an extent ($NADH/NAD^+ = 10^{-3}$) that the concentration of NADH in the cytosol is only about 10^{-6}mol/L. This very low concentration does not allow a diffusion gradient to be established, which would be large enough to drive the necessary high diffusion fluxes of reducing equivalents in the form of NADH into the peroxisomes. Instead, the reducing equivalents are imported indirectly into the peroxisomes via the uptake of malate and the subsequent release of oxaloacetate (termed **malate-oxaloacetate shuttle**) (Fig. 7.10).

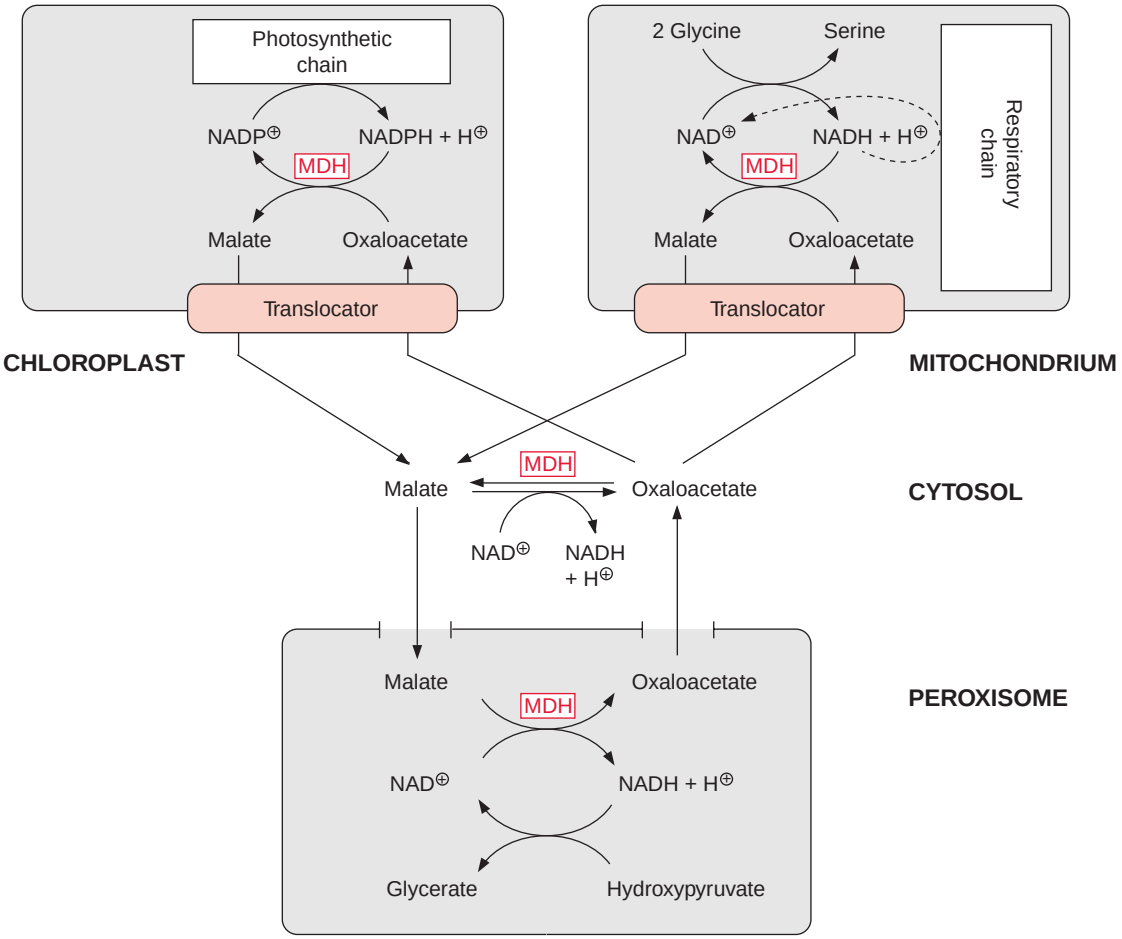

Figure 7.10 Schematic presentation of the transfer of reducing equivalents from the chloroplasts and the mitochondria to the peroxisomes. MDH: malate-dehydrogenase.

Malate dehydrogenase (Fig. 5.9), which catalyzes the oxidation of malate to oxaloacetate in a reversible reaction, has a key function in this shuttle. High malate dehydrogenase activity is found in the cytosol as well as in chloroplasts, mitochondria, and peroxisomes. The malate dehydrogenases in the various cell compartments are considered to be isoenzymes. They show some differences in their structure and are encoded by homologous genes. Apparently, these are all related proteins, which have derived in the course of evolution from a common precursor. Whereas NADH is the redox partner for malate dehydrogenases in the cytosol, mitochondria and peroxisomes, the chloroplast isoenzyme reacts with NADPH.

Mitochondria export reducing equivalents via a malate-oxaloacetate shuttle

In contrast to mitochondria from animal tissues, where the inner membrane is impermeable for oxaloacetate, the inner membrane of plant mitochondria accommodates a **malate-oxaloacetate translocator**, which transports malate and oxaloacetate in a counter-exchange mode. Since the activity of malate dehydrogenase in the mitochondrial matrix is very high, the NADH produced in mitochondria during glycine oxidation can be captured to reduce oxaloacetate to synthesize malate, which can be exported by the **malate-oxaloacetate shuttle**. This shuttle has a high capacity. The amount of NADH generated in the mitochondria from glycine oxidation is equal to the NADH required for the reduction of hydroxypyruvate in the peroxisomes (Fig. 7.1). If all the oxaloacetate synthesized in the peroxisomes were to reach the mitochondria, the NADH generated from glycine oxidation would be totally consumed for the formation of malate and no longer be available to support ATP synthesis by the respiratory chain. However, mitochondrial ATP synthesis is required during photosynthesis to supply energy to the cytosol of mesophyll cells. In fact, mitochondria deliver only about half the reducing equivalents required for peroxisomal hydroxypyruvate reduction, and the remaining portion is provided by the chloroplasts (Fig. 7.10). Thus, only about half of the NADH formed during glycine oxidation is captured by the malate-oxaloacetate shuttle for export and the remaining NADH is oxidized by the respiratory chain for synthesis of ATP.

A "malate valve" controls the export of reducing equivalents from the chloroplasts

Chloroplasts are also able to export reducing equivalents by a malate-oxaloacetate shuttle via a specific malate-oxaloacetate translocator operating in a counter-exchange mode and located in the chloroplast inner envelope membrane. Despite the high activity of the chloroplast malate-oxaloacetate shuttle, a high gradient exists between the chloroplast and cytosolic redox systems: the ratio $NADPH/NADP^+$ in chloroplasts is more than 100 times higher than the corresponding $NADH/NAD^+$ ratio in the cytosol. Whereas malate dehydrogenases usually catalyze a reversible equilibrium reaction, the reduction of oxaloacetate by the chloroplast malate dehydrogenase is virtually irreversible and does not reach equilibrium. This is due to a regulation of chloroplast malate dehydrogenase.

Section 6.6 described how chloroplast malate dehydrogenase is activated by **thioredoxin** and is therefore active only in the light. In addition

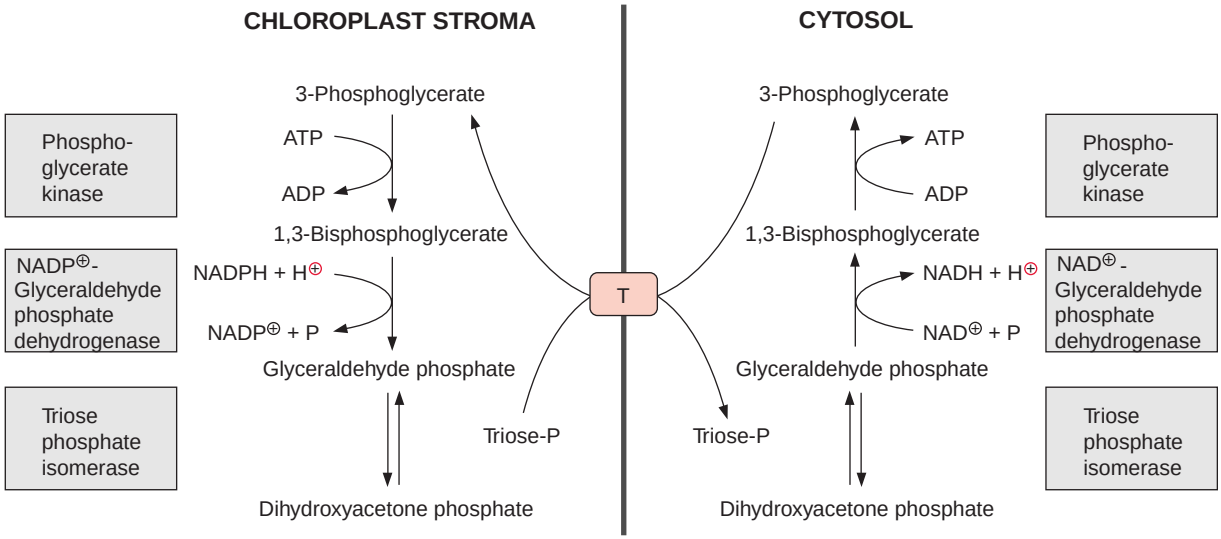

Figure 7.11 Triose phosphate-3-phosphoglycerate shuttle operating between the chloroplast stroma and the cytosol. In the chloroplast stroma triose phosphate is synthesized from 3-phosphoglycerate at the expense of NADPH and ATP. Triose phosphate is transported by the triose phosphate-phosphate translocator across the inner envelope membrane in exchange for 3-phosphoglycerate. In the cytosol, triose phosphate is reconverted to 3-phosphoglycerate with simultaneous generation of NADPH and ATP.

to this, increasing concentrations of $NADP^+$ inhibit the reductive activation of the enzyme by thioredoxin. $NADP^+$ increases the redox potential of the regulatory SH-groups of malate dehydrogenase, with the result that the reductive activation of the enzyme by thioredoxin is lowered. Thus, a decrease in the $NADP^+$ concentration, which corresponds to an increase in the reduction of the NADPH/$NADP^+$ system, switches chloroplast malate dehydrogenase on. This allows the enzyme to function like a **valve**, through which **excessive reducing** equivalents can be released by the chloroplasts to prevent harmful overreduction of the redox carriers of the photosynthetic electron transport chain. At the same time, this valve allows the chloroplasts to provide reducing equivalents for the reduction of hydroxypyruvate in the peroxisomes and also for other processes (e.g., nitrate reduction in the cytosol (section 10.1)).

An alternative way for exporting reducing equivalents from chloroplasts to the cytosol is the **triose phosphate-3-phosphoglycerate shuttle** (Fig. 7.11). This shuttle delivers NADH and ATP simultaneously to the cytosolic compartment.

7.4 The peroxisomal matrix is a special compartment for the disposal of toxic products

Why are two other organelles besides the chloroplasts involved in the recycling process of 2-phosphoglycolate? The conversion of glycine to serine in the mitochondria has the advantage that the respiratory chain can utilize the resultant NADH for the synthesis of ATP. During the conversion of glycolate to glycine, two toxic intermediates are formed: **glyoxylate** and **H_2O_2**. In isolated chloroplasts photosynthesis is completely inhibited by the addition of low concentrations of H_2O_2 or glyoxylate. The inhibitory effect of H_2O_2 is due to the oxidation of SH-groups in thioredoxin-activated enzymes of the reductive pentose phosphate pathway (section 6.6), resulting in their inactivation. Glyoxylate, a very reactive carbonyl compound, also has a strong inhibitory effect on thioredoxin activated enzymes by reacting with their SH-groups. Glyoxylate also inhibits RubisCO. Compartmentalization of the conversion of glycolate to glycine in the peroxisomes serves the purpose of eliminating the toxic intermediates glyoxylate and H_2O_2 at the site of their synthesis, so that they do not invade other cell compartments.

How is such a compartmentalization implemented? Compartmentalization of metabolic processes in cell compartments, such as the chloroplast stroma or the mitochondrial matrix, is achieved by separating membranes. These membranes are impermeable to metabolic intermediates present in these different compartments, and specific translocators facilitate the passage of only certain metabolites. This principle, however, does not apply to the compartmentalization of glycolate oxidation products, since membranes are normally quite permeable to H_2O_2 as well as to glyoxylate. Therefore in this case the membranes would be unable to prevent these compounds from escaping from the peroxisomes.

The very efficient compartmentalization of the conversion of glycolate to glycine and of serine to glycerate in the peroxisomes is due to specific properties of the **peroxisomal matrix**. When the boundary membrane of chloroplasts or mitochondria is disrupted (e.g., by suspending the organelles for a short time in pure water to cause an osmotic shock), the proteins of the stroma or the matrix, which are soluble, are released from the disrupted organelles. After disruption of peroxisomes, however, the peroxisomal matrix proteins remain aggregated in the form of particles of a size similar to peroxisomes. In these aggregates the compartmentalization of peroxisomal reactions is maintained. Glyoxylate, H_2O_2, and hydroxypyruvate, intermediates of peroxisomal metabolism, are not released from these particles in

the course of glycolate oxidation. Apparently, the enzymes of the photorespiratory pathway are arranged in a **multienzyme complex** in the peroxisomal matrix by which the product of one enzymatic reaction efficiently binds to the enzyme of the following reaction and is therefore not released.

This process, termed **metabolite channeling**, probably occurs not only in the peroxisomal matrix but may also apply for other metabolic pathways (e.g., the Calvin cycle in the chloroplast stroma (Chapter 6)) due to a dense packing of the involved enzymes in the stroma. It seems to be a special feature of the peroxisomes, however, that such complexes remain intact after disruption of the boundary membrane. This may have a protective function to avoid the escape of glycolate oxidase after an eventual damage of the peroxisomal membrane. If glycolate oxidase were to escape from the peroxisomes to the cytosol, the oxidation of glycolate would result in the accumulation of the products glyoxylate and H_2O_2 in the cytosol, poisoning the cell.

For any glyoxylate and hydroxypyruvate occasionally leaking out of the peroxisomes despite metabolite channeling, rescue enzymes that are present in the cytosol use NADPH to convert glyoxylate to glycolate (**NADPH-glyoxylate reductase**) and hydroxypyruvate to glycerate (**NADPH-hydroxypyruvate reductase**). Moreover, glyoxylate can also be eliminated by an NADPH-glyoxylate reductase present in the chloroplasts.

7.5 How high are the costs of the ribulose bisphosphate oxygenase reaction for the plant?

On the basis of the metabolic schemes in Figures 6.20 and 7.1, the expenditure in ATP and NADPH (respectively the equivalent of two reduced ferredoxins) for oxygenation and carboxylation of RuBP by RubisCO is listed in Table 7.1. The data illustrate that the consumption of ATP and NADPH required to compensate the consequences of oxygenation is much higher than the ATP and NADPH expenditure for carboxylation. Whereas in CO_2 fixation the conversion of CO_2 to triose phosphate requires three molecules of ATP and two molecules of NADPH, the oxygenation of RuBP costs a total of five molecules of ATP and three molecules of NADPH per molecule O_2. Table 7.2 shows the additional expenditure of ATP and NADPH at two carboxylation/oxygenation ratios. In the leaf, where the carboxylation/oxygenation ratio is usually between two and four, the additional expenditure of NADPH and ATP to compensate for the oxygenation during CO_2 fixation is between 40% and 80%. Thus **the oxygenase side reaction of RubisCO costs the plant more than one-third of the captured photons**.

Table 7.1: Expenditure of ATP and NADPH during carboxylation of ribulose 1,5-bisphosphate (CO_2 assimilation) in comparison to the corresponding expenditure during oxygenation

	Expenditure (mol)	
	ATP	NADPH or 2 reduced Ferredoxin
Carboxylation:		
Fixation of 1 mol CO_2		
1 CO_2 → 0.33 triose phosphate	**3**	**2**
Oxygenation:		
2 ribulose 1,5-bisphosphate + 2 O_2 → 2 3-phosphoglycerate + 2 2-phosphoglycolate		
2 2-phosphoglycolate → 3-phosphoglycerate + 1 CO_2	2	1
1 CO_2 → 0.33 triose phosphate	3	2
3 3-phosphoglycerate → 3 triose phosphate	3	3
3.33 triose phosphate → 2 ribulose 1,5-bisphosphate	2	
	Σ 10	Σ 6
Oxygenation by 1 mol O_2:	**5**	**3**

Table 7.2: Additional consumption of ATP and NADPH for RuBP oxygenation as related to the consumption for CO_2 fixation

Ratio	Additional consumption	
Carboxylation/oxygenation	ATP	NADPH
2	83%	75%
4	42%	38%

7.6 There is no net CO_2 fixation at the compensation point

At a carboxylation/oxygenation ratio of 1/2 there is no net CO_2 fixation, since the amount of CO_2 fixed by carboxylation is equal to the amount of CO_2 released by the photorespiratory pathway due to the oxygenase activity. One

can simulate this situation experimentally by illuminating a plant in a closed chamber. Due to photosynthesis, the CO_2 concentration decreases until it reaches a concentration at which the fixation of CO_2 and the release of CO_2 are counterbalanced. This state is termed the **compensation point**. Although the release of CO_2 is caused not only by the photorespiratory pathway but also by other reactions (e.g., the citrate cycle in mitochondria), the latter sources of CO_2 release are negligible compared with the photorespiratory pathway. For the plants designated as **C_3 plants** (this term is derived from the fact that the first carboxylation product is the C_3 compound 3-phosphoglycerate), the CO_2 concentration in air at the compensation point, depending on the species and temperature, is in the range of 35 to 70 ppm, equivalent to 10% to 20% of the CO_2 concentration in the atmosphere. This corresponds to a CO_2 concentration of $1–2 \times 10^{-6}$ mol/L at 25°C in the aqueous phase. This number matters since the RubisCO reacts with CO_2 in the aqueous phase. For **C_4 plants**, discussed in section 8.4, the CO_2 concentration at the compensation point is only about 5 ppm. How these plants manage to have such a low compensation point in comparison with C_3 plants will be discussed in detail in section 8.4.

With a plant kept in a closed chamber, the CO_2 concentration can be kept below the compensation point by trapping CO_2 with KOH. Upon illumination, the oxygenation by RubisCO and the accompanying photorespiratory pathway result in a net release of CO_2 at the expense of the plant biomass, which is degraded to produce carbohydrates to allow the regeneration of ribulose 1,5-bisphosphate. In such a situation, illumination of a plant causes its own consumption.

7.7 The photorespiratory pathway, although energy-consuming, may also have a useful function for the plant

Due to the high costs of ATP and NADPH during photorespiration, photosynthetic metabolism proceeds at full speed at the compensation point, but without net CO_2 fixation. Such a situation arises when leaves are exposed to full light, and the stomata are closed because of water shortage (section 8.1) and therefore CO_2 cannot be taken up. Since overreduction and overenergization of the photosynthetic electron transport carriers can cause severe damage to the cell (section 3.10), the plant utilizes the energy-consuming photorespiratory pathway to eliminate ATP and NADPH, which have been produced by light reactions, but which cannot be used for CO_2 assimilation.

Photorespiration, the unavoidable side-reaction of photosynthesis, is thus utilized by the plant for its protection. It can therefore be imagined that lowering the oxygenase reaction of RubisCO by molecular engineering (Chapter 22)—as attempted by many researchers, although still without success—may lead to a plant that uses energy more efficiently, but at the same time may increase its vulnerability to excessive illumination or shortage of water and thereby losing a feature of protection (see Chapter 8).

Further reading

Christensen, K. E., MacKenzie, R. E. Mitochondrial one-carbon metabolism is adapted to the specific needs of yeast, plants and mammals. Bioessays 28, 595–605 (2006).

Douce, R., Heldt, H. W. Photorespiration. In R. C. Leegood, T. D. Sharkey, S. von Caemmerer (eds.). Photosynthesis: Physiology and metabolism, pp. 115–136. Dordrecht, Niederlande: Kluwer Academic Publishers (2000).

Douce, R., Bourguignon, J., Neuburger, M., Rébeillé, F. The glycine decarboxylase system: A fascinating complex. Trends in Plant Science 6, 167–176 (2001).

Hayashi, M., Nishimura, M. *Arabidopsis thaliana*—A model organism to study plant peroxisomes. Biochimica Biophysica Acta 1763, 1382–1391 (2006).

Husic, D. W., Husic, H. D. The oxidative photosynthetic carbon (C_2) cycle: An update of unanswered questions. Reviews Plant Biochemistry and Biotechnology 1, 33–56 (2002).

Khan, M. S. Engineering photorespiration in chloroplasts: A novel strategy for increasing biomass production. Trends in Biotechnology 25, 437–440 (2007).

Kunze, M., Pracharoenwattana, I., Smith, S. M., Hartig, A. A central role for the peroxisomal membrane in glyoxylate cycle function. Biochimica Biophysica Acta 1763, 1441–1452 (2006).

Linka, M., Weber, A. P. Shuffling ammonia between mitochondria and plastids during photorespiration. Trends in Plant Science 10, 461–465 (2005).

Reumann, S. The photorespiratory pathway of leaf peroxisomes. In A. Baker & I. A. Graham (eds.), Plant peroxisomes, pp. 141–189. Dordrecht, Niederlande: Kluwer Academic Publishers (2002).

Reumann, S., Weber, A. P. Plant peroxisomes respire in the light: Some gaps of the photorespiratory C2 cycle have become filled, others remain. Biochimica Biophysica Acta 1783, 1496–1510 (2006).

Visser, W. F., van Roermund, C. W., Ijlst, L., Waterham, H. R., Wanders, R. J. Metabolite transport across the peroxisomal membrane. Biochemistry Journal 401, 365–375 (2007).

8

Photosynthesis implies the consumption of water

This chapter describes how photosynthesis is unavoidably linked with a substantial loss of water and therefore is often limited by the lack of water. Biochemical mechanisms that enable certain plants living in hot and dry habitats to reduce their water requirement will be described.

8.1 The uptake of CO_2 into the leaf is accompanied by an escape of water vapor

Since CO_2 assimilation is linked with a high water demand, plants require an ample water supply for their growth. A C_3 plant growing in temperate climates **requires 700 to 1,300 mol of H_2O for the fixation of 1 mol of CO_2**. This calculation does not consider the water consumption necessary for photosynthetic water oxidation since it is negligible in quantitative terms. Water demand is dictated by the fact that water evaporation from the leaves has to be replenished by water taken up through the roots. Thus during photosynthesis there is a steady flow of water, termed the **transpiration stream**, from the roots via the xylem vessels into the leaves.

The loss of water during photosynthesis is unavoidable, as the uptake of CO_2 into the leaves requires openings in the leaf surface, termed **stomata**. The stomata open to allow the diffusion of CO_2 from the atmosphere into the intercellular gas space of the leaf, but at the same time water vapor escapes through the open stomata (Fig. 8.1). The water vapor concentration in the intercellular gas space of a leaf amounts to 31,000 ppm (at 25°C)

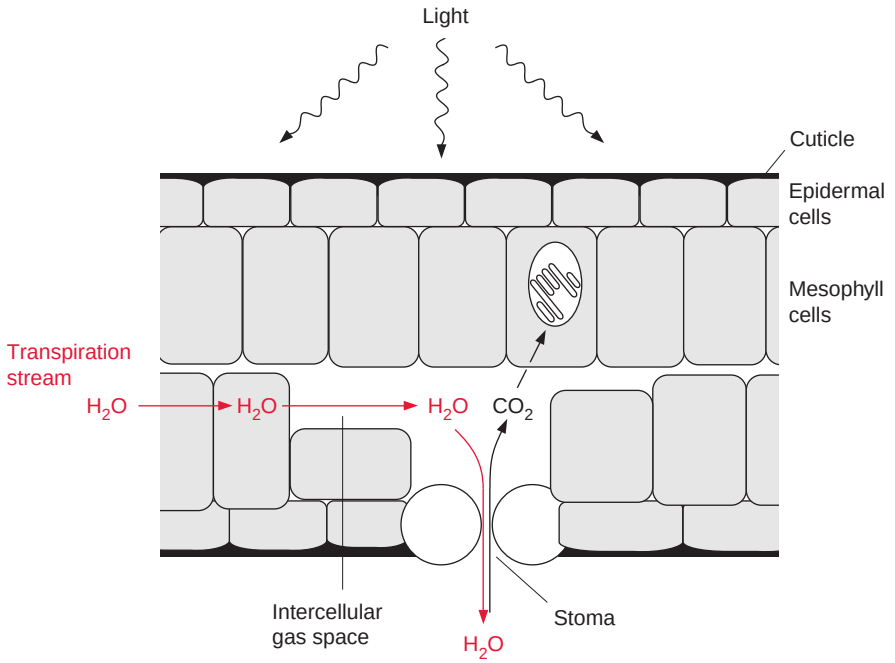

Figure 8.1 Schematic presentation of a cross-section of a leaf. The stomata are often located on the lower surface of the leaf. CO_2 diffuses through the stomata into the intercellular gas space and thus reaches the mesophyll cells carrying out photosynthesis. Water escapes from the cells into the atmosphere by diffusion of water vapor. This scheme is simplified. In reality, a leaf has several cell layers, and the intercellular gas space is much smaller than shown in the drawing.

in equilibrium with the cell water. Since this concentration is two orders of magnitude higher than the CO_2 concentration in the atmosphere (350 ppm), the escape of a very high amount of vaporized water during the influx of CO_2 is inevitable. To minimize the water loss from the leaves, the opening of the stomata is regulated. Thus, when there is a rise in the atmospheric CO_2 concentration, plants lose less water and therefore require less water. Opening and closing of the stomata is caused by biochemical reactions and will be described in the next section.

When the water supply is adequate, plants open their stomata just enough to provide CO_2 for photosynthesis. During water shortage, plants prevent dehydration by closing their stomata partially or completely, which results in the restriction or even cessation of CO_2 assimilation. Therefore water shortage is often a decisive factor limiting plant growth, especially in the warmer and drier regions of our planet. In those habitats a large number of plants have evolved a strategy for decreasing water loss during photosynthesis. In the plants dealt with in the preceding chapter the first product of CO_2 fixation is 3-phosphoglycerate, a compound with three carbon atoms; hence such plants are named **C_3-plants** (see section 6.2). Other plants save water by first producing the C_4 compound oxaloacetate via CO_2 fixation and are therefore named **C_4-plants**.

8.2 Stomata regulate the gas exchange of a leaf

Stomata are formed by two **guard cells**, which are often surrounded by subsidiary cells. Figures 8.2 and 8.3 show a closed and an open stomatal pore. The pore is opened by the increase in osmotic pressure in the guard cells, due to water uptake. The increase of the cell volume **inflates the guard** cells and the **pore opens**.

The best way to study the mechanism of stomata opening is with isolated guard cells. Biochemical and physiological studies are difficult, as the guard cells are very small and can be isolated with only low yields. Nevertheless guard cells are one of the most thoroughly investigated plant cells, but knowledge of the mechanism of stomatal closure is still incomplete.

Malate plays an important role in guard cell metabolism

The increase in osmotic pressure in guard cells during stomatal opening is due mainly to an accumulation of **potassium salts**. The corresponding anions are usually **malate**, but depending on the plant species, sometimes also **chloride**. Figure 8.4 shows a scheme of the metabolic reactions occurring during the opening process with malate as the main anion. An **H^+-P-ATPase** pumps protons across the plasma membrane into the extracellular compartment. The H^+-P-ATPase, which is entirely different from the F-ATPase and V-ATPase (sections 4.3, 4.4), is of the same type as the Na^+/K^+-ATPase in animal cells. An aspartyl residue of the P-ATPase protein is phosphorylated during the transport process (hence the name **P**-ATPase). The potential difference generated by the H^+-P-ATPase drives the influx of K^+ ions into the guard cells via a **K^+ channel**. This channel is open only at a negative voltage (section 1.10) and allows only an inwardly directed flux. For this reason, it is called a **K^+ inward channel**. Most of the K^+ ions taken up into the cell are transported into the vacuole. Probably a vacuolar H^+-ATPase (**V-ATPase**; see section 4.4) is involved, pumping protons into the vacuoles, which could then be exchanged for K^+ ions via a vacuolar potassium channel.

Accumulation of cations in the vacuole leads to the formation of a potential difference across the vacuolar membrane, driving the influx of malate via a channel specific for organic anions. Malate is provided by glycolytic degradation of the starch stored in the chloroplasts. As described in section 9.1, this degradation yields triose phosphate, which is released from the chloroplasts to the cytosol in exchange for inorganic phosphate via the **triose phosphate-phosphate translocator** (section 1.9) and is subsequently converted to phosphoenolpyruvate (see Fig. 10.11). Phosphoenolpyruvate

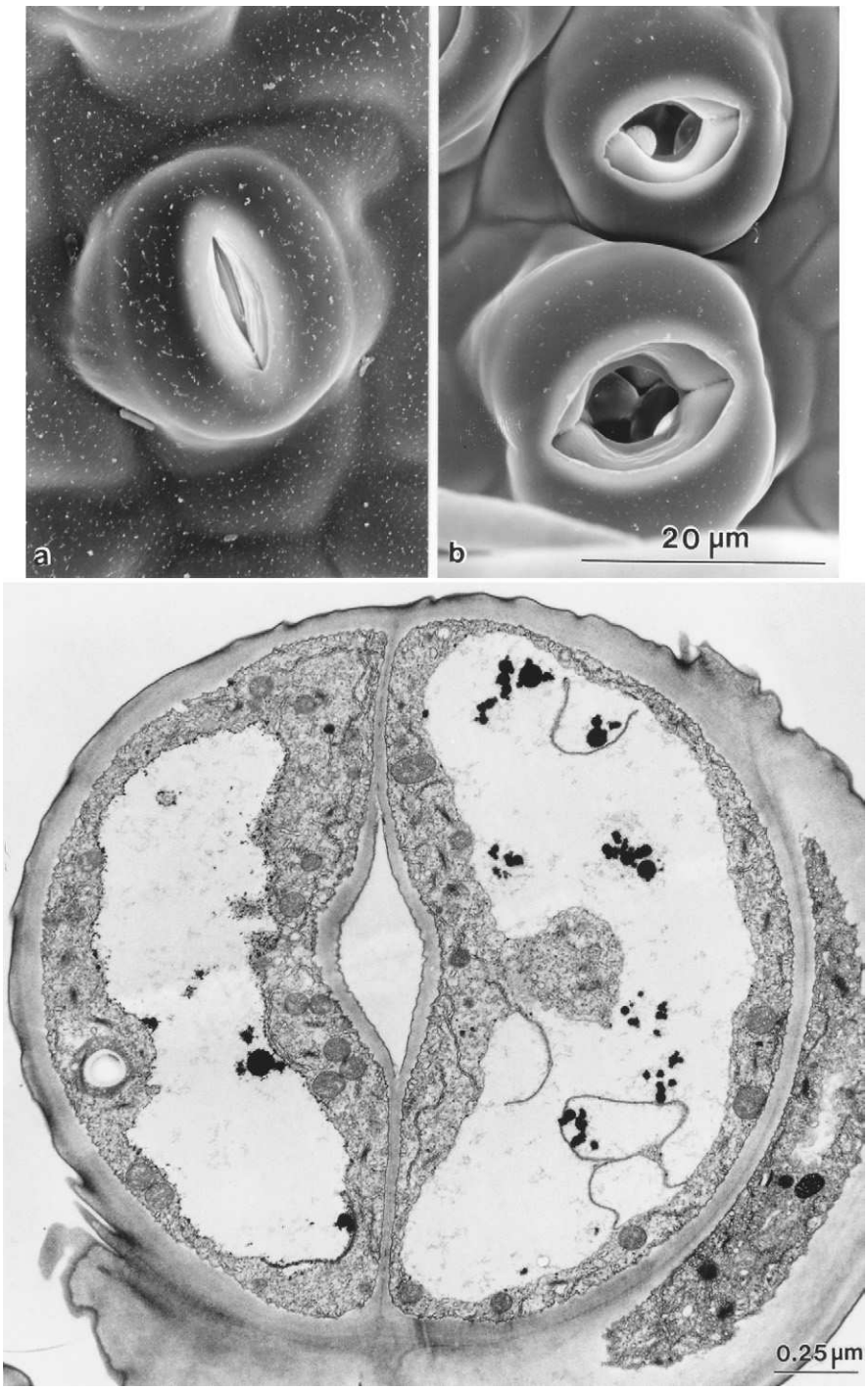

Figure 8.2 Scanning electron micrograph of stomata from the lower epidermis of hazel nut leaves in (a) closed state, and (b) open. (By R.S. Harrison-Murray and C. M. Clay, Wellesbourne.) Traverse section of a pair of guard cells from a tobacco leaf. The large central vacuole and the gap between the two guard cells can be seen. (By D.G. Robinson, Heidelberg.)

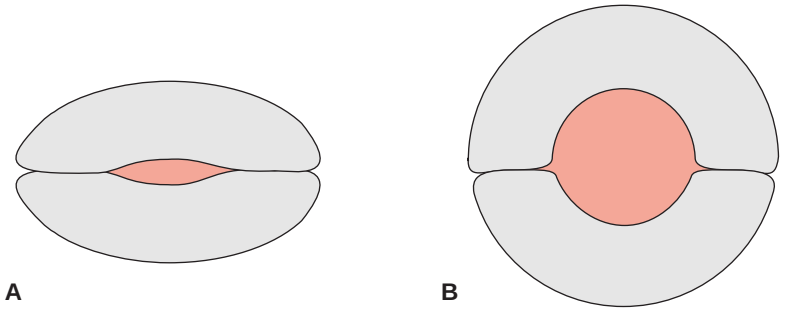

Figure 8.3 Schematic drawing of a stoma formed by two guard cells, (A) closed and (B) open state.

reacts with HCO_3^- to form oxaloacetate in a reaction catalyzed by the enzyme **phosphoenolpyruvate carboxylase** (Fig. 8.5), in which the high energy enol ester bond is cleaved, making the reaction irreversible. The oxaloacetate is transported via a specific translocator into the chloroplasts and is reduced to malate via **NADP-malate dehydrogenase** (Fig. 8.4). Malate is then released into the cytosol, probably by the same translocator which transports oxaloacetate.

During stomatal closure most of the malate is released from the guard cells. The guard cells contain only very low activities of RubisCO, and are therefore unable to fix CO_2 in significant amounts. Starch is regenerated from glucose, which is taken up into the guard cells. In contrast to chloroplasts from mesophyll cells, the guard cell chloroplasts have a **glucose 6-phosphate-phosphate translocator**, which transports not only glucose 6-phosphate and phosphate, but also triose phosphate and 3-phosphoglycerate. This translocator is also found in plastids from nongreen tissues, such as roots (section 13.3).

Complex regulation governs stomatal opening

A number of parameters are known to influence the stomatal opening, resulting in a very complex regulation circuit. The opening is regulated by light via the blue light receptor **phototropin** (section 19.9). An important factor is the CO_2 concentration in the intercellular gas space, although the nature of the CO_2 sensor is not known. At micromolar concentrations, **abscisic acid** (**ABA**) (section 19.6) causes the closure of the stomata. If due to lack of water the water potential sinks below a critical mark, ABA synthesis increases. The effect of ABA on the stomatal opening depends on the intercellular CO_2 concentration and on the presence of the signal compound nitric oxide (NO) (see also section 19.9). The binding of ABA to a membrane receptor triggers one or several signal cascades, which finally control

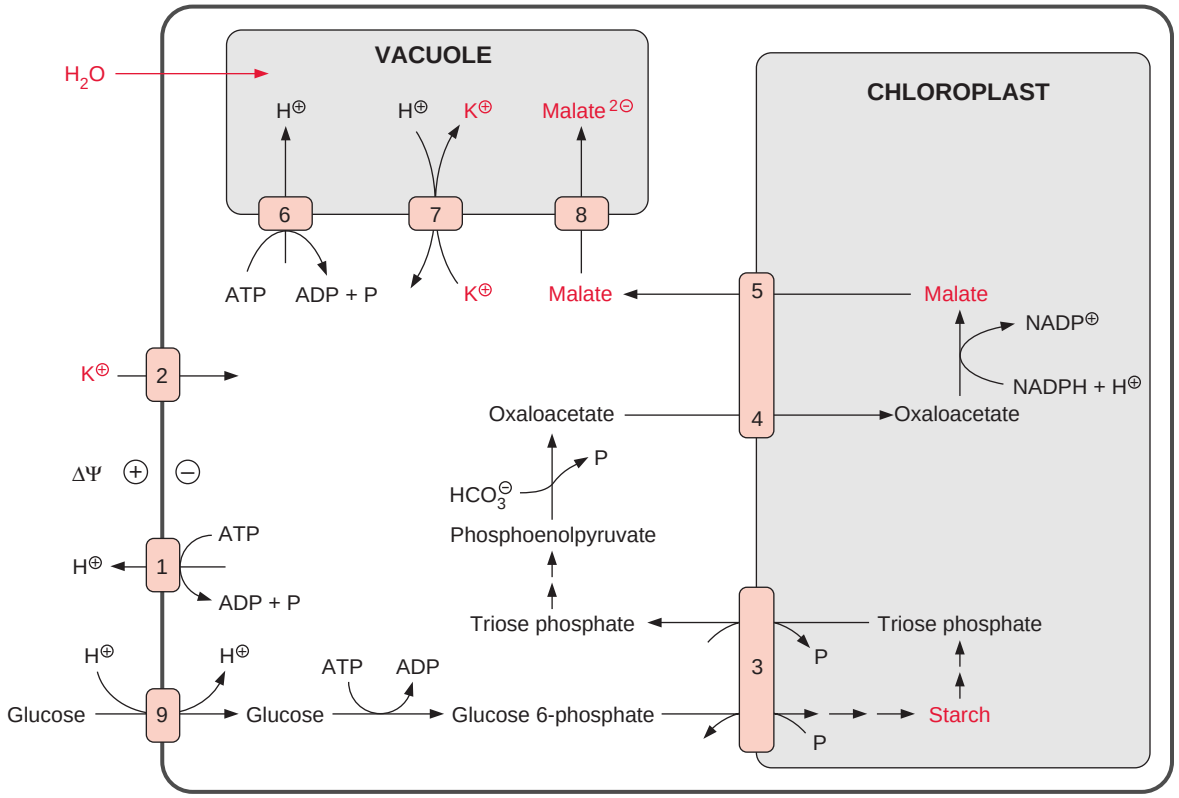

Figure 8.4 Schematic presentation of the processes operating during the opening of stomata with malate as the main anion. The proton transport by H^+-P-ATPase (1) of the plasma membrane of the guard cell results in an increase in the proton potential and in a hyperpolarization. This opens the voltage-dependent K^+ inward channel (2) and the proton potential drives the influx of potassium ions through this channel. Starch degradation occurs simultaneously in the chloroplasts yielding triose phosphate, which is then released from the chloroplasts via the triose phosphate-phosphate translocator (3) and converted in the cytosol to oxaloacetate. Oxaloacetate is transported into the chloroplasts (4) and is converted to malate by reduction. This malate is transported from the chloroplast to the cytosol, possibly via the same translocator responsible for the influx of oxaloacetate (5). Protons are transported into the vacuole (6), probably by an H^+V-ATPase, and these protons are exchanged for potassium ions (7). The electric potential difference formed by the H^+V-ATPase drives the influx of malate ions via a malate channel (8). The accumulation of potassium malate (three ions) increases the osmotic potential in the vacuole and results in an influx of water. For resynthesis of starch, glucose is taken up into the guard cells via an H^+-symport (9), where it is converted in the cytosol to glucose 6-phosphate, which is then transported into the chloroplast via a glucose-phosphate-phosphate translocator (3).

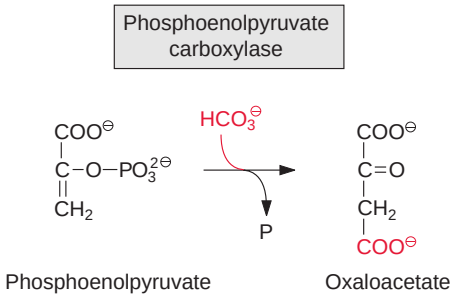

Figure 8.5
Reaction catalyzed by phosphoenolpyruvate carboxylase.

the opening of ion channels. There is strong evidence that protein kinases, cyclic ADP ribose (Fig. 19.13), and inositol trisphosphate (Fig. 19.4) participate in the signal cascades, which open Ca^{++} channels of the plasma membrane and of internal Ca^{++} storage compartments, such as the endoplasmic reticulum. The resulting Ca^{++} ions in the cytosol function as secondary messengers (section 19.6). These cascades also activate ABA-dependent anion channels in the guard cells, resulting in an efflux of anions. This causes depolarization of the plasma membrane and thus leads to the opening of **K^+ outward channels** (section 1.10). NO regulates the Ca^{++}-sensitive ion channels by promoting a Ca^{++} release from intracellular stores so that the cytosolic-free Ca^{++} concentration increases. The resulting release of K^+, $malate^{2-}$, and Cl^- ions from the guard cells by the joint effect of ABA and NO lowers the osmotic pressure, which ultimately leads to a decrease in the guard cell volume and hence to a closure of the stomata. The introduction of the patch clamp technique (section 1.10) has brought important insights into the role of specific ion channels in the stomatal opening process. NO is synthesized by nitric monoxide synthase (section 19.9) or via reduction of nitrite (NO_2^-), and as a by-product is catalyzed by nitrate reductase (sections 10.1, 19.9). In the guard cells, nitrate reductase is induced by ABA. The interaction of ABA and NO in controlling stomatal opening is very complex.

8.3 The diffusive flux of CO_2 into a plant cell

The movement of CO_2 from the atmosphere to the catalytic center of RubisCO—through the stomata, the intercellular gas space, across the plasma membrane, the chloroplast envelope, and the chloroplast stroma—proceeds via diffusion.

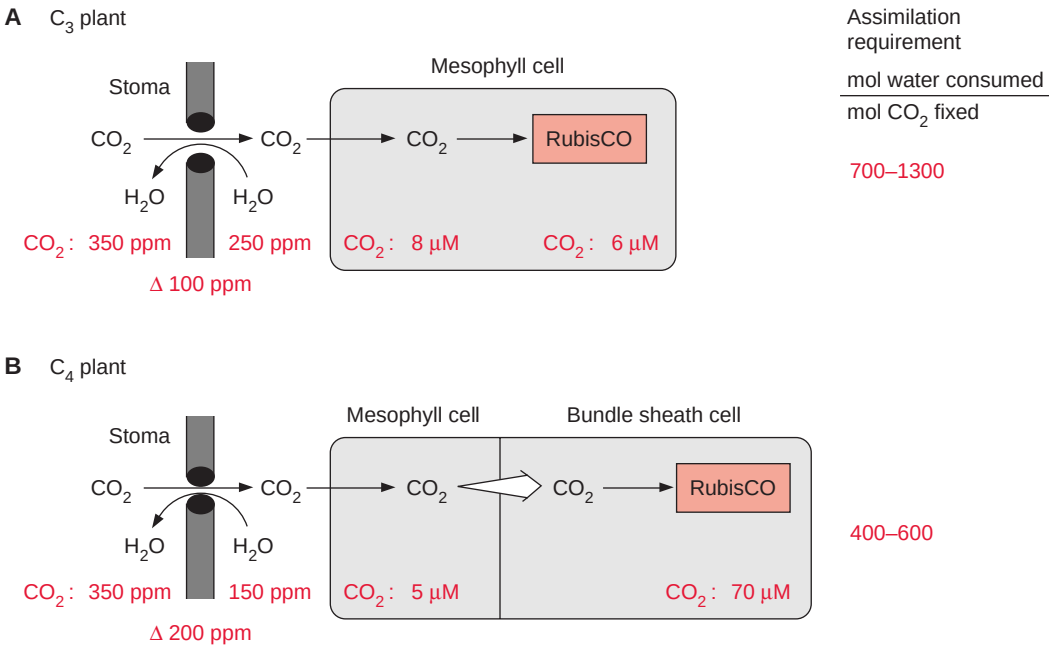

Figure 8.6 Schematic presentation of the uptake of CO_2 in C_3 and C_4 plants. This scheme shows typical stomatal resistances for C_3 and C_4 plants. The values for the CO_2 concentration in the vicinity of RubisCO are taken from von Caemmerer and Evans (C_3 plants) and Hatch (C_4 plants).

According to a simple derivation of the Fick law, the diffusive flux, I, over a certain distance is:

$$I = \frac{\Delta C}{R}$$

where I is defined as the amount of a compound diffusing per unit of time and surface area; ΔC, the diffusion gradient, is the difference of concentrations between start and endpoint; and R is the diffusion resistance. R of CO_2 is 10^4 times larger in water than in air.

In Figure 8.6A a model illustrates the diffusive flux of CO_2 into a leaf of a C_3 plant with a limited water supply. The control of the aperture of the stomata leads to a stomatal diffusion resistance, by which a diffusion gradient of 100 ppm is maintained. The resulting CO_2 concentration of 250 ppm in the intercellular gas space is in equilibrium with the CO_2 concentration in an aqueous solution of 8×10^{-6} mol/L (8 µM). In water saturated with air containing 350 ppm CO_2, the equilibrium concentration of the dissolved CO_2 is 11.5 µM at 25°C.

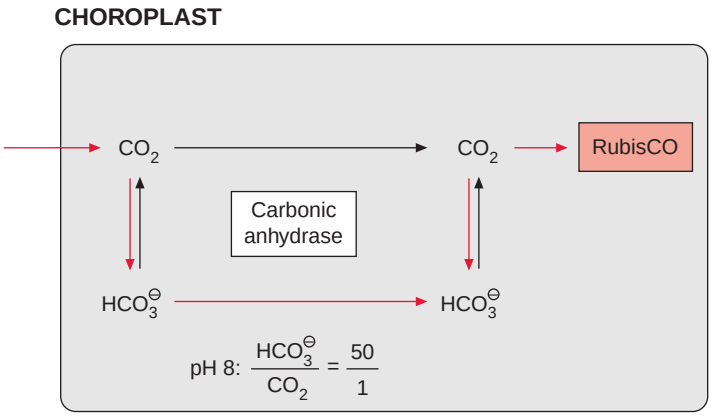

Figure 8.7 Carbonic anhydrase catalyzes the rapid equilibration of CO_2 with HCO_3^- and thus increases the diffusion gradient and hence the diffusive flux of the inorganic carbon across the chloroplast stroma. The example is based on the assumption that the pH is 8.0. Dissociation constant $[HCO_3^-] \cdot [H^+]/[CO_2] = 5 \times 10^{-7}$.

Since the chloroplasts are positioned at the inner surface of the mesophyll cells (see Fig. 1.1), within the mesophyll cell the major distance for the diffusion of CO_2 to the reaction site of RubisCO is the passage through the chloroplast stroma. To facilitate this diffusive flux, the stroma contains high activities of **carbonic anhydrase**. This enzyme allows the CO_2 entering the chloroplast stroma, after crossing the envelope, to equilibrate with **HCO_3^-** (Fig. 8.7). At pH 8.0, 8 μM CO_2 is in equilibrium with 400 μM HCO_3^- (25°C). Thus, in the presence of carbonic anhydrase the gradient for the diffusive movement of HCO_3^- is 50 times higher than that of CO_2. As the diffusion resistance for HCO_3^- is only about 20% higher than that of CO_2, the diffusive flux of HCO_3^- in the presence of carbonic anhydrase is about 40 times higher than that of CO_2. Due to the presence of carbonic anhydrase in the stroma, the diffusive flux of CO_2 from the intercellular gas space to the site of RubisCO in the stroma results in a decrease in CO_2 concentration of only about 2 μM. At the site of RubisCO, a CO_2 concentration of about 6 μM has been measured. In equilibrium with air, the O_2 concentration at the carboxylation site is 250 μM. This results in a carboxylation/oxygenation ratio of about 2.5.

Let us turn our attention again to Figure 8.6. CO_2 and O_2 are competitors for the active site of RubisCO, and the CO_2 concentration in the atmosphere is very low compared to the O_2 concentration. The concentration decrease of CO_2 during the diffusive flux from the atmosphere to the active site of carboxylation is still a limiting factor for efficient CO_2 fixation by RubisCO. This may also account for the high cellular concentration of this enzyme (see section 6.2). Naturally, the stomatal resistance could be decreased by increasing the aperture of the stomata (e.g., by a factor of two). In this case, with still the same diffusive flux, the CO_2 concentration in the

intercellular gas space would increase from 250 to 300 ppm, and the ratio of carboxylation to oxygenation of the RubisCO would increase accordingly. The price, however, for such a reduction of the stomatal diffusion resistance would be a doubling of the water loss. Since the diffusive efflux of vaporized water from the leaves is proportional to the diffusion gradient, the humidity is also a decisive factor governing water loss. These considerations illustrate the important function of stomata for the gas exchange of the leaves. The regulation of the stomatal aperture determines how high the rate of CO_2 assimilation may be, without the plant losing too much essential water.

8.4 C_4 plants perform CO_2 assimilation with less water consumption than C_3 plants

In equilibrium with fluid water, the density of water vapor increases exponentially with the temperature. A temperature increase from 20°C to 30°C leads to almost a doubling of water vapor density. Therefore, at high temperatures the loss of water during CO_2 assimilation becomes a very serious problem for plants. **C_4 plants** developed a way to decrease considerably this water loss. At around 25°C these plants use only 400 to 600 mol of H_2O for the fixation of 1 mol of CO_2, which is almost half the water consumption of C_3 plants, and this difference is even greater at higher temperatures. C_4 plants grow mostly in warm areas, often in dry habitats. They include important crop plants such as maize, sugarcane and millet. The principle by which these C_4 plants save water can be demonstrated by comparing the models of C_3 and C_4 plants in Figure 8.6. By doubling the stomatal resistance prevailing in C_3 plants, the C_4 plant can decrease the diffusive efflux of water vapor by 50%. To maintain the same diffusive flux of CO_2 in the C_4 plants as in C_3 plants, C_4 plants have to increase their diffusion gradient by a factor of two (according to the Fick's law). This means that at 350 ppm CO_2 in the atmosphere, the CO_2 concentration in the intercellular gas space would be only 150 ppm, which is in equilibrium with 5 μM CO_2 in water. At such low CO_2 concentrations C_3 plants would be approaching the compensation point (section 7.6), and therefore the rate of net CO_2 fixation of RubisCO would be very low.

To maintain CO_2 assimilation under these conditions in C_4 plants a crucial factor is a **pumping mechanism** that elevates the concentration of CO_2 at the carboxylation site from 5 μM to about 70 μM. This pumping requires two compartments and the input of energy. However, the energy costs may be recovered, since this high CO_2 concentration at the carboxylation site eliminates the oxygenase reaction to a great extent, and the loss of energy

connected with the photorespiratory pathway is largely decreased (section 7.5). For this reason, C_4 metabolism does not necessarily imply a higher energy demand; in fact, at higher temperatures C_4 photosynthesis is more efficient than C_3 photosynthesis. This is due to the fact that with increasing temperatures the oxygenase activity of RubisCO increases more rapidly than the carboxylase activity. *Therefore, in warm climates C4 plants with their reduced water demand and their suppression of photorespiration have an advantage over C_3 plants.*

The discovery of C_4 metabolism was stimulated by an unexplained experimental result: after Melvin Calvin and Andrew Benson had established that 3-phosphoglycerate is the primary product of CO_2 assimilation by plants, Hugo Kortschak and colleagues studied the incorporation of radioactively labeled CO_2 during photosynthesis of sugarcane leaves at a sugarcane research institute in Hawaii. The result was surprising. The primary fixation product was not as expected, 3-phosphoglycerate, but the **C4** compounds **malate** and **aspartate**. This result questioned whether the then fully accepted Calvin cycle was universally valid for CO_2 assimilation. Perhaps Kortschak was reluctant to raise these doubts and his results remained unpublished for almost 10 years. It is interesting to note that during this time and without knowing these results, Yuri Karpilov in the former Soviet Union observed similar radioactively labeled C_4 compounds during CO_2 fixation in maize.

Following the publication of these puzzling results, in Australia Hal Hatch and Roger Slack set out to solve the riddle by systematic studies. They found that the incorporation of CO_2 in malate was a reaction preceding the CO_2 fixation by the Calvin cycle and that this first carboxylation reaction was part of a CO_2 concentration mechanism; the function of which was elucidated by the two researchers by 1970. This process is known as the Hatch-Slack pathway, but both researchers used the term *C_4 dicarboxylic acid pathway of photosynthesis* which is now abbreviated to **C_4 pathway** or **C_4 photosynthesis**.

The CO_2 pump in C_4 plants

The requirement of two different compartments for pumping CO_2 from a low to a high concentration is reflected in the leaf anatomy of C_4 plants. The leaves of C_4 plants show a so-called **Kranz-anatomy** (Fig. 8.8). The vascular bundles containing the sieve tubes and the xylem vessels are surrounded by a sheath of cells (**bundle sheath cells**), which are encircled by **mesophyll cells**. The latter are in contact with the intercellular gas space of the leaves. In 1884 the German botanist Gustav Haberland described in his textbook *Physiologische Pflanzenanatomie* (*Physiological Plant Anatomy*) that the assimilatory cells in several plants, including sugarcane and millet, are

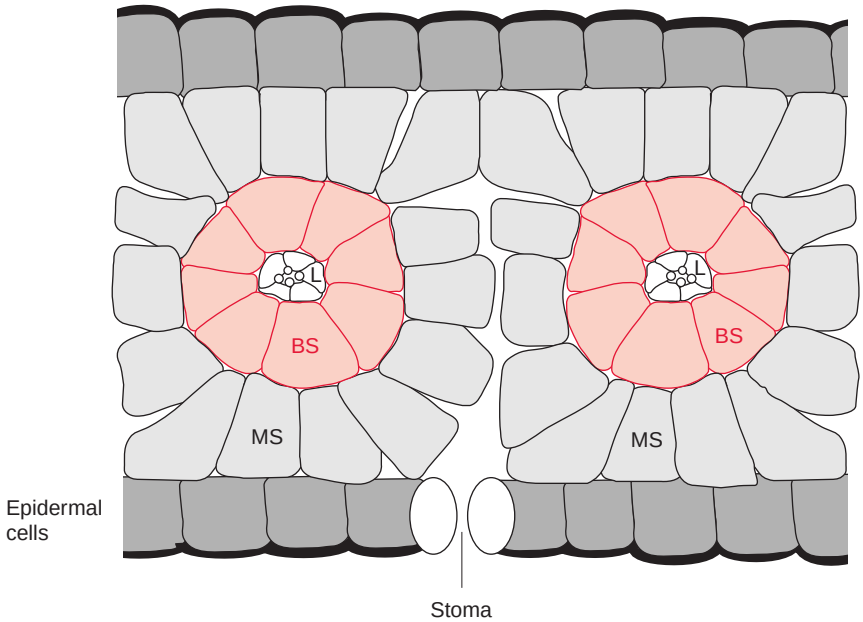

Figure 8.8 Schematic presentation of characteristic leaf anatomy of a C_4 plant. V = Vascular bundle; BS = bundle sheath cells; MS = mesophyll cells.

arranged in what he termed a Kranz (wreath)-type mode. With remarkable foresight, he suggested that this special anatomy may indicate a division of labor between the chloroplasts of the mesophyll and bundle sheath cells.

Mesophyll and bundle sheath cells are separated by a cell wall, in some instances containing a **suberin layer**, which is probably gas-impermeable. Suberin is a polymer of phenolic compounds that are impregnated with wax (section 18.3). The border between the mesophyll and bundle sheath cells is penetrated by a large number of **plasmodesmata** (section 1.1). These plasmodesmata enable the passage of metabolites between the mesophyll and bundle sheath cells.

The CO_2 pumping of C_4 metabolism does not rely on the specific function of a membrane transporter but is due to a prefixation of CO_2. After the conversion of CO_2 to HCO_3^-, phosphoenolpyruvate is carboxylated in the mesophyll cells to form oxaloacetate. After the conversion of this oxaloacetate to malate, malate diffuses through the plasmodesmata into the bundle sheath cells, where CO_2 is released as a substrate for RubisCO. Figure 8.9 shows a simplified scheme of this process. The formation of the CO_2 gradient between the two compartments by this pumping process is due to the fact that the prefixation of CO_2 and its subsequent release are catalyzed by two different reactions, each of which is virtually irreversible. As a crucial feature of C_4 metabolism, RubisCO is located exclusively in the bundle sheath chloroplasts.

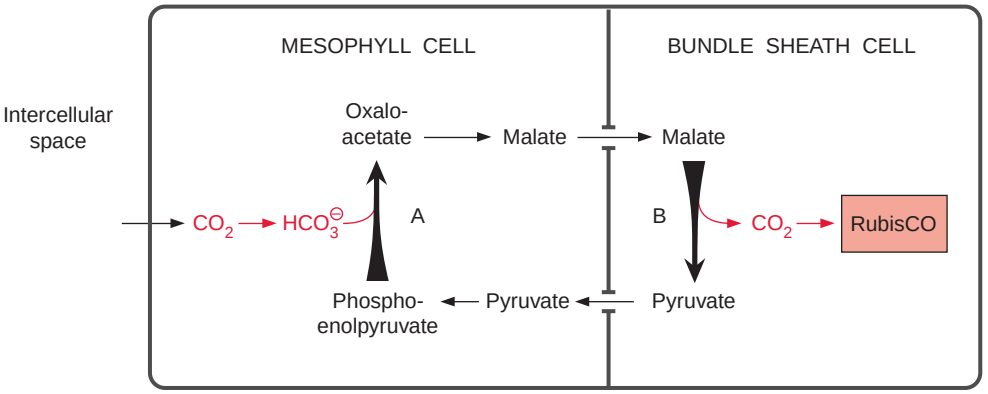

Figure 8.9 Principle mechanism of C_4 metabolism.

The reaction of HCO_3^- with phosphoenolpyruvate is catalyzed by the enzyme **phosphoenolpyruvate carboxylase**. This enzyme has already been mentioned when the metabolism of guard cells was discussed (Figs. 8.4 and 8.5). This reaction is highly exergonic and therefore irreversible. As the enzyme has a very high affinity for HCO_3^-, micromolar concentrations of HCO_3^- are fixed very efficiently. The formation of HCO_3^- from CO_2 is facilitated by carbonic anhydrase present in the cytosol of the mesophyll cells.

The release of CO_2 in the bundle sheath cells occurs in three different ways (Fig. 8.10). In most C_4 species decarboxylation of malate with an accompanying oxidation to pyruvate is catalyzed by **malic enzyme**. In one group of these species termed **NADP-malic enzyme type** plants, the release of CO_2 occurs in the bundle sheath chloroplasts and the oxidation of malate to pyruvate is coupled with the reduction of $NADP^+$. In other plants, termed **NAD-malic enzyme type**, decarboxylation takes place in the mitochondria of the bundle sheath cells and is accompanied by the reduction of NAD^+. In the **phosphoenolpyruvate carboxykinase type** plants, oxaloacetate is decarboxylated in the cytosol of the bundle sheath cells. ATP is required for this reaction which produces phosphoenolpyruvate as well as CO_2. The metabolism and its compartmentation of the three different types of C_4 plants will now be discussed in more detail.

C_4 metabolism of the NADP-malic enzyme type plants

Plants of the NADP-malic enzyme type are important crop plants such as maize and sugarcane. Figure 8.11 shows the reaction chain and its compartmentation. The oxaloacetate arising from the carboxylation of phosphoenolpyruvate is transported via a specific translocator into the chloroplasts where it is reduced by NADP-malate dehydrogenase to malate, which is

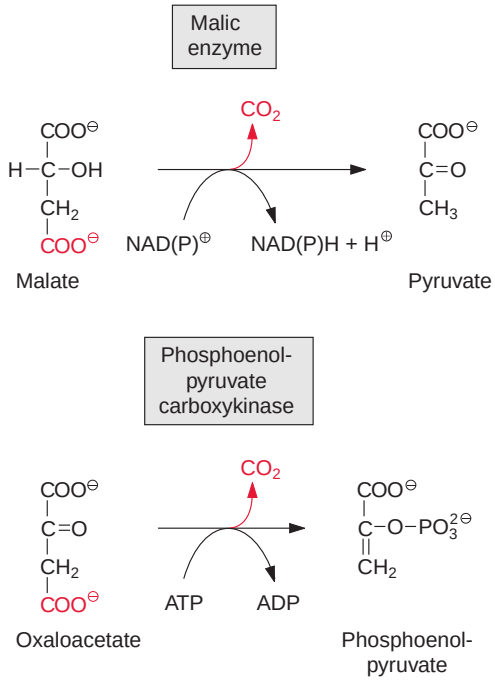

Figure 8.10 Reactions by which CO_2, prefixed in C_4 metabolism in mesophyll cells, can be released in bundle sheath cells.

subsequently transported into the cytosol. (The reduction of oxaloacetate in the chloroplasts has been discussed in section 7.3 in connection with photorespiratory metabolism.) Malate diffuses via plasmodesmata from the mesophyll to the bundle sheath cells. The diffusive flux of malate between the two cells requires a diffusion gradient of about 2×10^{-3} mol/L. The malic enzyme present in the bundle sheath cells catalyzes the conversion of malate to pyruvate and CO_2, and the CO_2 is fixed by RubisCO.

The remaining pyruvate is exported by a specific translocator from the bundle sheath chloroplasts, diffuses through the plasmodesmata into the mesophyll cells, where it is transported by another specific translocator into the chloroplasts. The enzyme **pyruvate-phosphate dikinase** in the mesophyll chloroplasts converts pyruvate to phosphoenolpyruvate by a rather unusual reaction (Fig. 8.12). The name *dikinase* describes an enzyme that catalyzes a twofold phosphorylation. In a reversible reaction one phosphate residue is transferred from ATP to pyruvate and a second one to phosphate, converting it to pyrophosphate. A **pyrophosphatase** present in the chloroplast stroma immediately hydrolyzes the newly formed pyrophosphate and thus makes this reaction irreversible. In this way pyruvate is transformed upon the consumption of two energy-rich phosphates of ATP (which is converted to AMP) irreversibly into phosphoenolpyruvate. The latter is

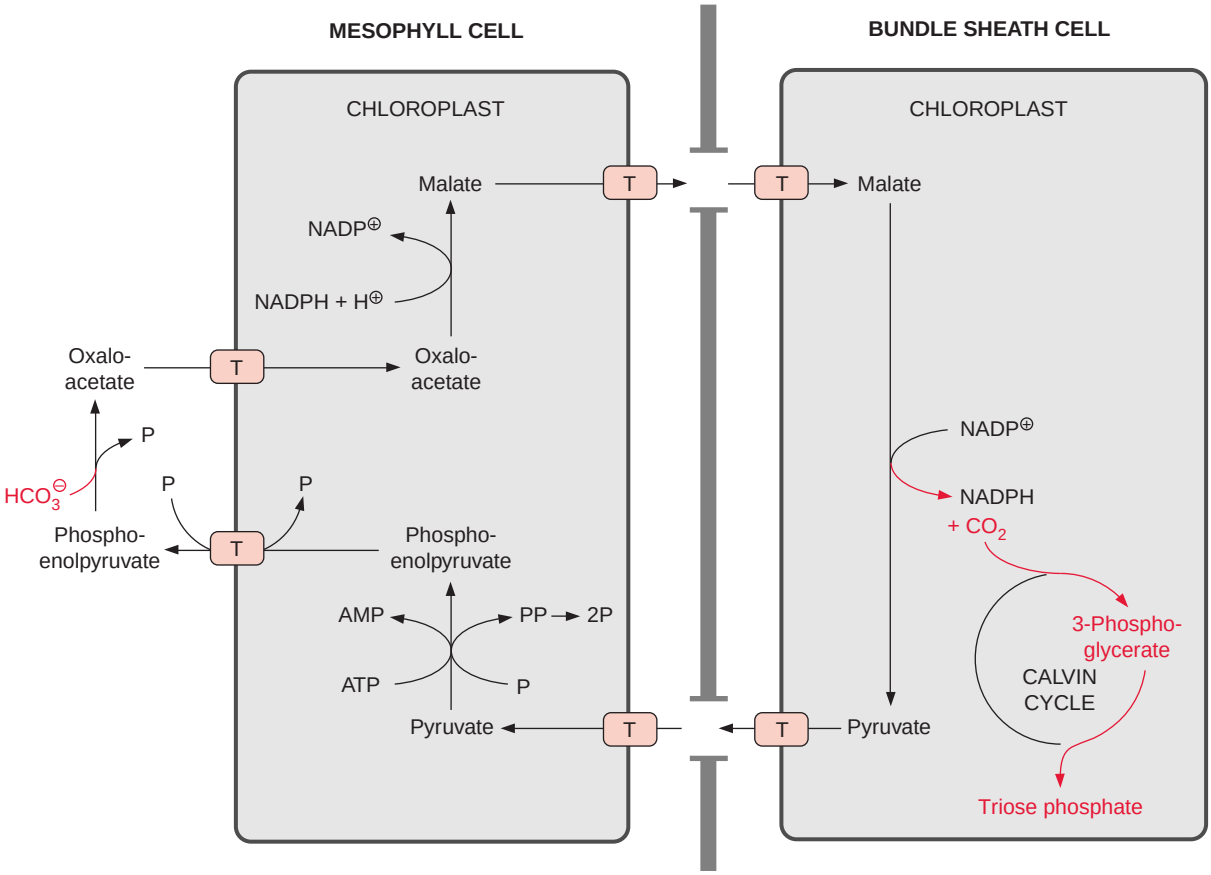

Figure 8.11 Mechanism for concentrating CO_2 in plants of the C_4-NADP-malic enzyme type (e.g., maize). In the cytosol of the mesophyll cells, HCO_3^- is fixed by reaction with phosphoenolpyruvate. The oxaloacetate formed is reduced in the chloroplast to produce malate. After leaving the chloroplasts, malate diffuses into the bundle sheath cells, where it is oxidatively decarboxylated, to produce pyruvate, CO_2, and NADPH. The pyruvate formed is phosphorylated to phosphoenolpyruvate in the chloroplasts of mesophyll cells. The transport across the chloroplast membranes proceeds by specific translocators. The diffusive flux between the mesophyll and the bundle sheath cells proceeds through plasmodesmata. The transport of oxaloacetate into the mesophyll chloroplasts and the subsequent release of malate from the chloroplasts are probably facilitated by the same translocator. T = translocator.

exported in exchange for inorganic phosphate from the chloroplasts via a **phosphoenolpyruvate-phosphate translocator**.

The concentration process produces a high CO_2 gradient between bundle sheath and mesophyll cells. The question arises, why does most of the CO_2 not leak out of the bundle sheath cells before it is fixed by RubisCO?

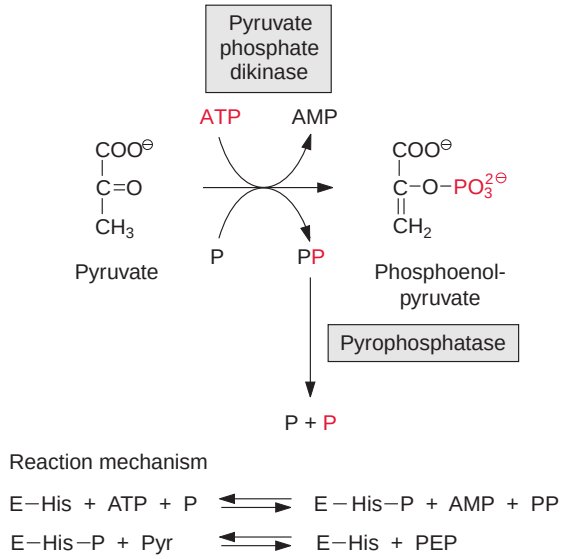

Figure 8.12 Pyruvate-phosphate dikinase. One phosphate moiety is transferred from ATP to inorganic phosphate, resulting in the formation of pyrophosphate, and a second phosphate moiety is transferred to a histidine residue at the catalytic site of the enzyme. In this way a phosphor amide (R-H-N-PO_3^{2-}) is formed as an intermediate, and this phosphate residue is then transferred to pyruvate, resulting in the formation of phosphoenolpyruvate.

As the bundle sheath chloroplasts, in contrast to those from mesophyll cells (see Fig. 8.7), do not contain carbonic anhydrase, the diffusion of CO_2 through the stroma of bundle sheath cells proceeds more slowly than in the mesophyll cells. Furthermore, the suberin layer of some plants between the cells probably prevents the leakage of CO_2 through the cell wall so that there would be only a diffusive loss through plasmodesmata. The portion of CO_2 that is lost by diffusion from the bundle sheath cells back to the mesophyll cells is estimated at 10% to 30% in different species.

In maize leaves the chloroplasts from mesophyll cells differ in their structure from those of bundle sheath cells. Mesophyll chloroplasts have many grana, whereas bundle sheath chloroplasts contain mainly stroma lamellae, with only very few grana stacks and little photosystem II activity (section 3.10). The major function of the bundle sheath chloroplasts is to provide ATP by **cyclic photophosphorylation** via photosystem I (Fig. 3.34). NADPH required for the reductive pentose phosphate pathway (Calvin cycle) is provided mainly by the linear electron transport in the mesophyll cells. This NADPH is delivered in part via the oxidative decarboxylation of malate (by NADP-malic enzyme), but this reducing power is actually provided by the mesophyll cells for the reduction of oxaloacetate. The other part of NADPH required is indirectly transferred along with ATP from the mesophyll chloroplasts to the bundle sheath chloroplasts by a **triose phosphate-3-phosphoglycerate shuttle** via the triose phosphate-phosphate translocators of the inner envelope membranes of the corresponding chloroplasts (Fig. 8.13).

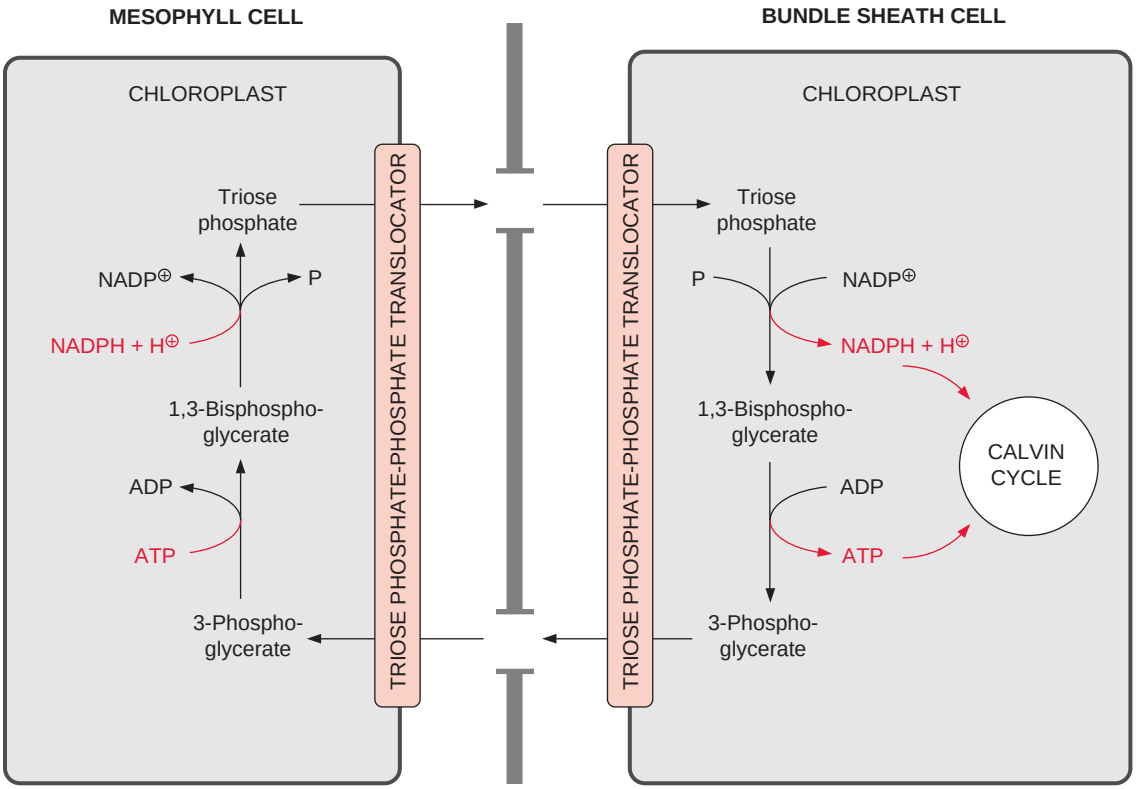

Figure 8.13 C_4 metabolism in maize. Indirect transfer of NADPH and ATP from the mesophyll chloroplast to the bundle sheath chloroplast via a triose phosphate-3-phosphoglycerate shuttle. In the chloroplasts of mesophyll cells, 3-phosphoglycerate is reduced to triose phosphate at the expense of ATP and NADPH. In the bundle sheath chloroplasts, triose phosphate is reconverted to 3-phosphoglycerate, leading to the formation of NADPH and ATP. Transport across the chloroplast membranes proceeds by counter-exchange via triose phosphate-phosphate translocators.

C_4 metabolism of the NAD-malic enzyme type

The NAD-malic enzyme type metabolism (Fig. 8.14) is present in a large number of species including millet. Here the oxaloacetate formed by phosphoenolpyruvate carboxylase is converted to aspartate by transamination via **glutamate-aspartate aminotransferase**. Since the oxaloacetate concentration in the cell is below 0.1×10^{-3} mol/L, oxaloacetate cannot form a high enough diffusion gradient for the necessary diffusive flux into the bundle sheath cells. Because of the high concentration of glutamate in a cell, the transamination of oxaloacetate yields aspartate concentrations in a range between 5 and 10×10^{-3} mol/L, which makes aspartate very suitable for supporting a diffusive flux between the mesophyll and bundle sheath cells.

After diffusing into the bundle sheath cells, aspartate is transported by a translocator into the mitochondria. An isoenzyme of glutamate-aspartate aminotransferase present in the mitochondria catalyzes the conversion of aspartate to oxaloacetate, which is then transformed by **NAD-malate dehydrogenase** to malate. This malate is decarboxylated by **NAD-malic enzyme** to pyruvate and the NAD^+ arising from the malate dehydrogenase reaction is reduced to NADH. CO_2 thus released in the mitochondria diffuses into the chloroplasts, where it is available for assimilation via RubisCO. The pyruvate translocator carries pyruvate into the cytosol where it is converted to alanine by an alanine-glutamate aminotransferase. Since in the equilibrium of this reaction the alanine concentration is much higher than that of pyruvate, a high diffusive flux of alanine into the mesophyll cells is possible. In the mesophyll cells, alanine is transformed to pyruvate by an isoenzyme of the alanine-glutamate aminotransferase. Pyruvate is transported into the chloroplasts, where it is converted to phosphoenolpyruvate by pyruvate-phosphate dikinase in the same way as in the chloroplasts of the NADP-malic enzyme type.

The NADH released by malic enzyme in the mitochondria is sequestered for the reduction of oxaloacetate, and thus there are no reducing equivalents left to be oxidized by the respiratory chain (Fig. 8.14). To enable mitochondrial oxidative phosphorylation to produce ATP, some of the oxaloacetate formed in the mesophyll cells by phosphoenolpyruvate carboxylase is reduced in the mesophyll chloroplasts to malate, as in the NADP-malic enzyme type metabolism. This malate diffuses into the bundle sheath cells, is taken up by the mitochondria, and is oxidized there by malic enzyme to yield NADH. ATP is generated from oxidation of this NADH by the respiratory chain. This pathway also operates in the phosphoenolpyruvate carboxykinase type metabolism, described next.

C_4 metabolism of the phosphoenolpyruvate carboxykinase type

This type of metabolism is found in several of the fast-growing tropical grasses used as forage crops. Figure 8.15 shows a scheme of the metabolism. As in the NAD-malic enzyme type, oxaloacetate is converted in the mesophyll cells to aspartate and the latter diffuses into the bundle sheath cells, where the oxaloacetate is regenerated via an aminotransferase in the cytosol. In the cytosol the oxaloacetate is converted to phosphoenolpyruvate at the expense of ATP via phosphoenolpyruvate carboxykinase. The CO_2 released in this reaction diffuses into the chloroplasts and the remaining phosphoenolpyruvate diffuses back into the mesophyll cells. In this C_4 type metabolism, the pumping of CO_2 into the bundle sheath compartment

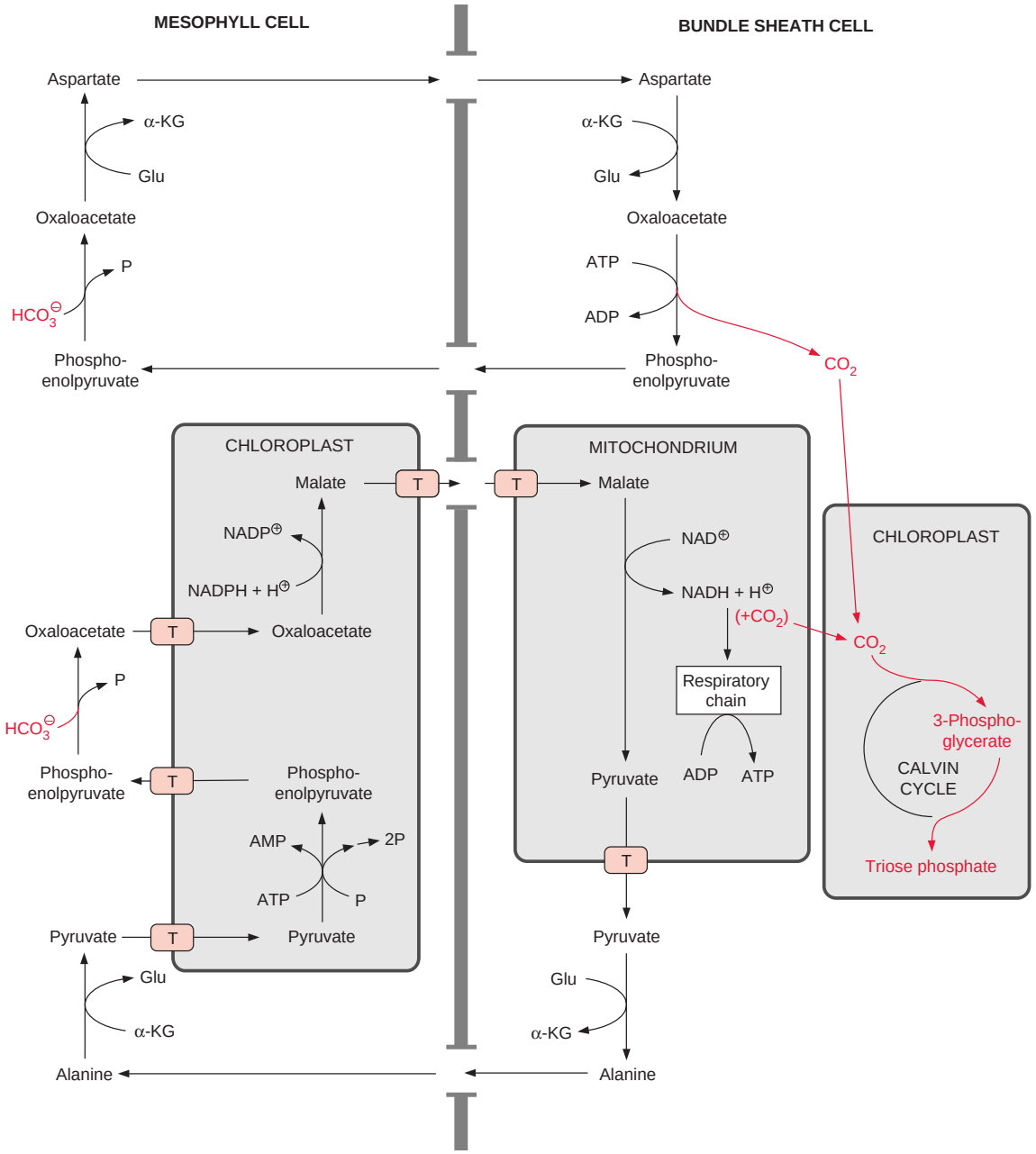

Figure 8.15 Schematic presentation of the CO_2 concentrating mechanism in plants of the C_4-phosphoenolpyruvate carboxykinase type. In contrast to C_4 metabolism described in Figure 8.14, oxaloacetate is formed from aspartate in the cytosol of the bundle sheath cells, and is then decarboxylated to phosphoenolpyruvate and CO_2 via the enzyme phosphoenolpyruvate carboxykinase. Phosphoenolpyruvate diffuses back into the mesophyll cells. Simultaneously, as in Figure 8.11, some malate formed in the mesophyll cells diffuses into the bundle sheath cells and is oxidized there by NAD-malic enzyme in the mitochondria. The NADH thus formed serves as a substrate for the formation of ATP by mitochondrial oxidative phosphorylation in the respiratory chain. This ATP is transported to the cytosol to be used for phosphoenolpyruvate carboxykinase reaction. The CO_2 released in the mitochondria, together with the CO_2 released by phosphoenolpyruvate carboxykinase in the cytosol, serves as substrate for the RubisCO in the bundle sheath chloroplasts. T = translocator.

is due especially to ATP consumption by the **phosphoenolpyruvate carboxykinase** reaction (Fig. 8.10). The mitochondria provide the ATP required for phosphoenolpyruvate carboxykinase reaction by oxidizing malate via NAD-malic enzyme. This malate originates from mesophyll cells in the same way as in the NADP-malic enzyme type (Fig. 8.15). Thus, in the C_4-phosphoenolpyruvate carboxykinase type plants, a minor portion of the CO_2 is released in the mitochondria and the bulk is released in the cytosol.

Kranz-anatomy with its mesophyll and bundle sheath cells is not an obligatory requirement for C_4 metabolism

In individual cases, the spatial separation of the prefixation of CO_2 by PEP carboxylase and the final fixation by RubisCO can also be achieved in other ways. It was demonstrated in a species of *Chenopodiacae* that its C_4 metabolism takes place in uniform extended cells. In these cells PEP carboxylase is in the cytoplasm at one peripheral end and RubisCO is located in the chloroplasts at the proximal end. Although this is a special case, it illustrates the variability of the C_4 system.

Enzymes of C_4 metabolism are regulated by light

Phosphoenolpyruvate carboxylase (PEP carboxylase), the key enzyme of C_4 metabolism, is highly regulated. In a darkened leaf, this enzyme has low activity. In this state, the affinity of the enzyme to its substrate phosphoenolpyruvate is very low and it is inhibited by low concentrations of malate. Therefore, during the dark phase the enzyme in the leaf is practically inactive. Upon illumination of the leaf, a serine protein kinase (see also Figs. 9.18 and 10.9) is activated, which phosphorylates the hydroxyl group of a serine residue in PEP carboxylase resulting in the activation of the enzyme. The enzyme can be inactivated again by hydrolysis of the phosphate group by a protein serine phosphatase. The activated phosphorylated enzyme is also inhibited by malate. In this case much higher concentrations of malate are required for the inhibition of the phosphorylated than for the nonphosphorylated less active enzyme. The rate of irreversible carboxylation of phosphoenolpyruvate can be adjusted through a feedback inhibition by malate in such a way that a certain malate level is maintained in the mesophyll cell. Another important enzyme of the C_4 metabolism, **NADP-malate dehydrogenase**, is activated by light via reduction by thioredoxin as described in section 6.6.

Pyruvate-phosphate dikinase (Fig. 8.12) is also subject to dark/light regulation. It is inactivated in the dark by phosphorylation of a threonine residue. This phosphorylation is rather unusual as it requires ADP rather than

ATP as phosphate donor. The enzyme is activated in the light by the phosphorolytic cleavage of the threonine phosphate group. Thus, the regulation of pyruvate phosphate dikinase proceeds in a completely different way from the regulation of PEP carboxylase.

Products of C_4 metabolism can be identified by mass spectrometry

Measuring the distribution of the ^{12}C and the ^{13}C isotopes in a photosynthetic product (e.g., sucrose) can reveal whether it has been formed by C_3 or C_4 metabolism. ^{12}C and ^{13}C occur as natural carbon isotopes in atmospheric CO_2 in the ratio of 98.89% and 1.11%, respectively. Due to a kinetic isotope effect RubisCO reacts with $^{12}CO_2$ more rapidly than with $^{13}CO_2$. For this reason, the ratio $^{13}C/^{12}C$ is lower in the products of C_3 photosynthesis than in the atmosphere. The ratio $^{13}C/^{12}C$ can be determined by mass spectrometry and is expressed as a $\delta^{13}C$ value.

$$\delta^{13}C\ [‰] = \left(\frac{^{13}C/^{12}C \text{ sample}}{^{13}C/^{12}C \text{ in standard}} - 1 \right) \times 1{,}000$$

As a standard, one uses the distribution of the two isotopes in a defined limestone. Products of C_3 photosynthesis show $\delta^{13}C$ values of 28‰. In the PEP carboxylase reaction of C_4 metabolism the preference for ^{12}C over ^{13}C is less pronounced. As in C_4 plants practically the total amount of CO_2 which is prefixed by PEP carboxylase reacts further in the bundle sheath cells with RubisCO, the photosynthesis of C_4 plants yields a $\delta^{13}C$ value in the range of only 14‰. Based on the different $^{13}C/^{12}C$ ratios in photosynthetic compounds it is possible to determine by mass spectrometry, whether, for instance, sucrose has been formed by sugar beet (C_3 metabolism) or by sugarcane (C_4 metabolism).

C_4 plants include important crop plants but also many persistent weeds

In C_4 metabolism ATP is consumed to concentrate the CO_2 in the bundle sheath cells. This avoids a loss of energy incurred by photorespiration in C_3 plants. The ratio of oxygenation versus carboxylation by RubisCO increases with the temperature (section 6.2). At low temperatures, with resultant low photorespiratory activity, C_3 plants are at an advantage. Under these circumstances C_4 plants offer no benefit and very few C_4 plants occur as wild plants in a temperate climate. At temperatures of 25°C or above, however,

the C_4 plants are at an advantage, as under these conditions, the energy consumption for C_4 photosynthesis (measured as a quantum requirement of CO_2 fixation) is lower than in C_3 plants. As indicated previously, this is due largely to increased photorespiration resulting from an increase in the oxygenase reaction of RubisCO in C_3 plants, whereas in C_4 plants the oxygenase reaction is lowered due to the high CO_2 concentrations in the bundle sheath chloroplasts. A further advantage of C_4 plants is that because of the high CO_2 concentration in the bundle sheath chloroplasts they need less RubisCO. Since RubisCO accounts for the major protein content of leaves (6.2), C_4 plants require less nitrogen than C_3 plants for growth. Last, but not least, C_4 plants require less water. In warmer climates these advantages make C_4 plants very suitable as crop plants. Of the 12 most rapidly growing crop or pasture plants, 11 are C_4 plants. It has been estimated that about 20% of the global photosynthesis of terrestrial plants is by C_4 plants. One disadvantage, however, is that many C_4 crop plants, such as maize, millet, and sugarcane, are very sensitive to chilling, and are therefore restricted to warm areas. Especially persistent weeds are members of the C_4 plants, including 8 of the 10 worldwide worst specimens (e.g., Bermuda grass (*Cynodon dactylon*), and barnyard grass (*Echinochloa crusgalli*)).

8.5 Crassulacean acid metabolism allows plants to survive even during a very severe water shortage

Many plants growing in very dry and often hot habitats have developed a strategy not only for surviving periods of severe water shortage, but also for carrying out photosynthesis under such conditions. Cacti and the succulent ornamental plant *Kalanchoe* are examples of such plants, as are plants that grow as epiphytes in tropical rain forests, including half the orchids. As this metabolism has first been elucidated in *Crassulaceae* and involves the storage of an acid, it has been named **crassulacean acid metabolism** (abbreviated **CAM**). Important CAM crop plants are pineapples and the agave sisal, which provides natural fibers.

First observations on CAM metabolism were made at the beginning of the 19th century. In 1804 the French scientist de Saussure observed that upon illumination and in the absence of CO_2, branches of the cactus *Opuntia* produced oxygen. He concluded that these plants consumed their own matter to produce CO_2, which was then used for CO_2 assimilation. An English gentleman, Benjamin Heyne, noticed in his garden in India that the

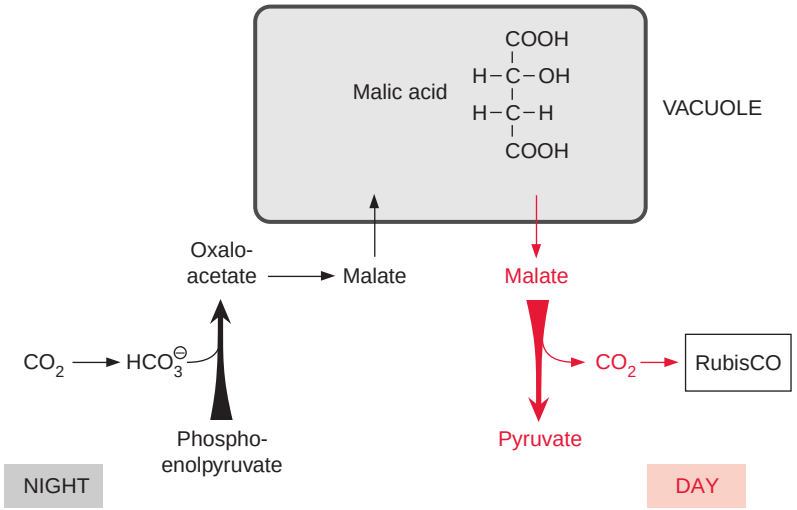

Figure 8.16 Principle mechanism of CAM.

leaves of the very popular ornamental plant *Bryophyllum calycinum* had a herby taste in the afternoon, whereas in the morning the taste was as acid as sorrel. He found this observation so remarkable that, after his return to England in 1813, he communicated it in a letter to the Linnean Society.

CAM plants solve the problem of water loss during photosynthesis by opening their stomata only during the night, when it is cool and humidity is comparatively high. During the night CO_2 is taken up through the open stomata, and fixed in an acid, which is stored until the following day. Then the acid is degraded to release the CO_2, which feeds into the Calvin cycle, proceeding while the stomata are closed. Figure 8.16 shows the basic scheme of this process. Note the strong similarity of this scheme with the scheme of C_4 metabolism in Figure 8.9. The difference is that in C_4 metabolism carboxylation and decarboxylation are spatially separated in two cells whereas in CAM metabolism this separation is temporarily between night and day.

CO_2 fixed during the night is stored as malic acid

Nocturnal fixation of CO_2 is catalyzed by **phosphoenolpyruvate carboxylase**, in the same way as in the metabolism of C_4 plants and guard cells (Fig. 8.4). In many CAM plants the phosphoenolpyruvate required is generated from the degradation of starch, but in other plants soluble carbohydrates, such as sucrose (section 9.2) and fructanes (section 9.5), may also serve as carbon stores. Figure 8.17 shows a scheme of the CAM metabolism using starch as a carbon reservoir. The starch located in the chloroplasts is degraded to triose phosphate (section 9.1), which is then exported via the triose

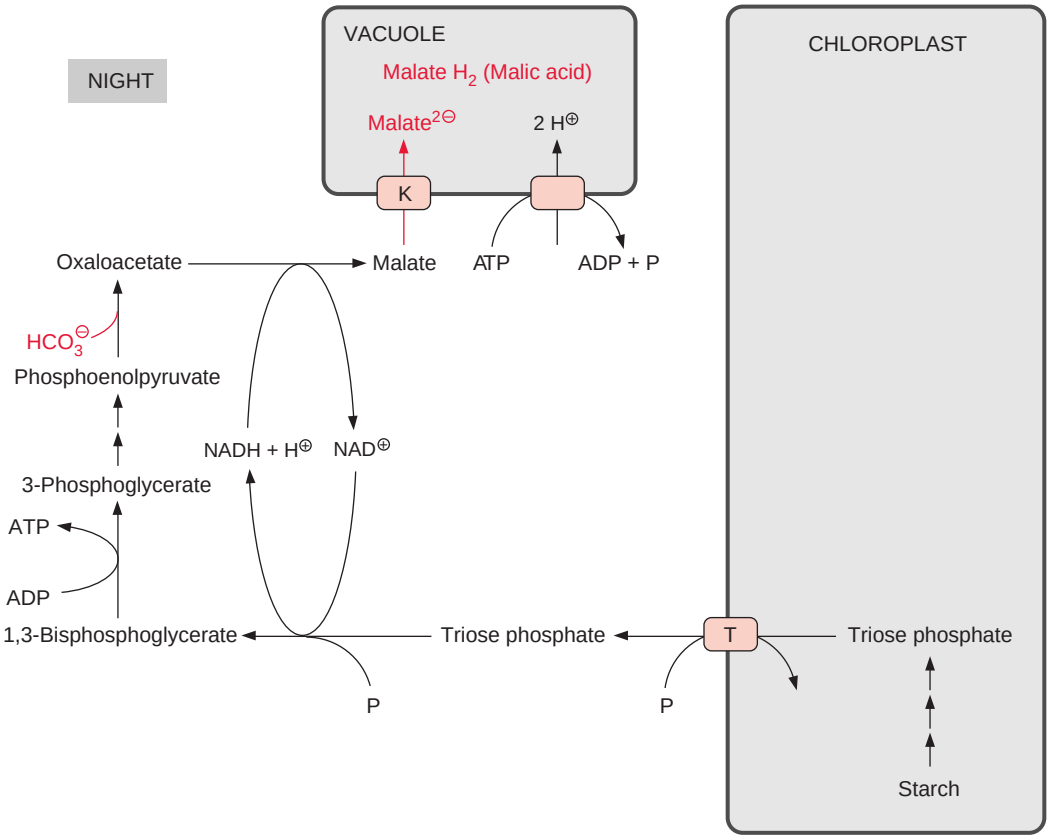

Figure 8.17 CAM during the night. Degradation of starch in the chloroplasts provides triose phosphate, which is converted along with the generation of NADH and ATP to phosphoenolpyruvate, the acceptor for HCO_3^-. The oxaloacetate is reduced in the cytosol to malate. An H^+-V-ATPase in the vacuolar membrane drives the accumulation of malate anions in the vacuole, where they are stored as malic acid. T = translocator; K = channel.

phosphate-phosphate translocator and is converted to phosphoenolpyruvate in the cytosol. The oxaloacetate synthesized as a product of CO_2 prefixation is reduced in the cytosol to malate via NAD-malate dehydrogenase. The NADH required for this reaction is provided by the oxidation of triose phosphate in the cytosol. Malate is pumped into the vacuoles at the expense of energy. As described for the guard cells (section 8.2), the energy-dependent step in this pumping process is the transport of protons by the H^+-V-ATPase (section 4.4) located in the vacuolar membrane. In contrast to the guard cells, in CAM metabolism the transported protons are not exchanged for potassium ions. The malate taken up through a malate channel driven by the proton potential accumulates in the vacuole as malic acid. Thus during the night

the vacuolar content is very acidic and reaches about pH 3. The two carboxyl groups of malic acid have pK values of 3.4 and of 5.1, respectively. Thus at pH 3 malic acid is largely undissociated and the osmotic pressure deriving from the accumulation of malic acid is only about one-third of the osmotic pressure produced by the accumulation of potassium malate ($2K^+ + Mal^{2-}$) in the guard cells. In other words, at a certain osmotic pressure, three times as much malate can be stored as malic acid than as potassium malate. In order to gain a high storage capacity, most CAM plants have unusually large vacuoles and are succulent. The ATP required for CAM metabolism is generated by mitochondrial oxidative phosphorylation of malate.

Photosynthesis proceeds with closed stomata

The malate stored in the vacuoles during the night is released during the day by a regulated efflux through the malate channel. In CAM, as in C_4 metabolism, different plants release CO_2 in various ways: via **NADP-malic enzyme**, **NAD-malic enzyme** or also via **phosphoenolpyruvate carboxykinase**.

CAM of the **NADP-malic enzyme type** is described in Figure 8.18. A specific translocator facilitates the uptake of malate into the chloroplasts, where it is decarboxylated to produce pyruvate, NADPH, and CO_2. The latter reacts as substrate with RubisCO and the pyruvate is converted via pyruvate-phosphate dikinase to phosphoenolpyruvate (see also Figs. 8.11, 8.12, 8.14, and 8.15). Since plastids normally are unable to convert phosphoenolpyruvate to 3-phosphoglycerate (still to be investigated for CAM chloroplasts), the phosphoenolpyruvate is exported in exchange for 3-phosphoglycerate (Fig. 8.18). As in C_4 plants, CAM chloroplasts contain, in addition to a triose phosphate-phosphate translocator (transporting in a counter-exchange triose phosphate, phosphate, and 3-phosphoglycerate), a phosphoenolpyruvate-phosphate translocator (catalyzing a counter-exchange for phosphate). The 3-phosphoglycerate taken up into the chloroplasts is fed into the Calvin cycle. The triose phosphate thus formed is primarily used for resynthesis of the starch which was consumed during the previous night. Only a small surplus of triose phosphate remains and this is the actual gain of CAM photosynthesis.

Since CAM photosynthesis proceeds with closed stomata, the water requirement for CO_2 assimilation (compare Fig. 8.6) amounts to only 5% to 10% of the water needed for the photosynthesis of C_3 plants. Since the storage capacity for malate is limited, the daily increase in biomass in CAM plants is usually very low. Thus the growth rate of plants that rely solely on CAM is limited.

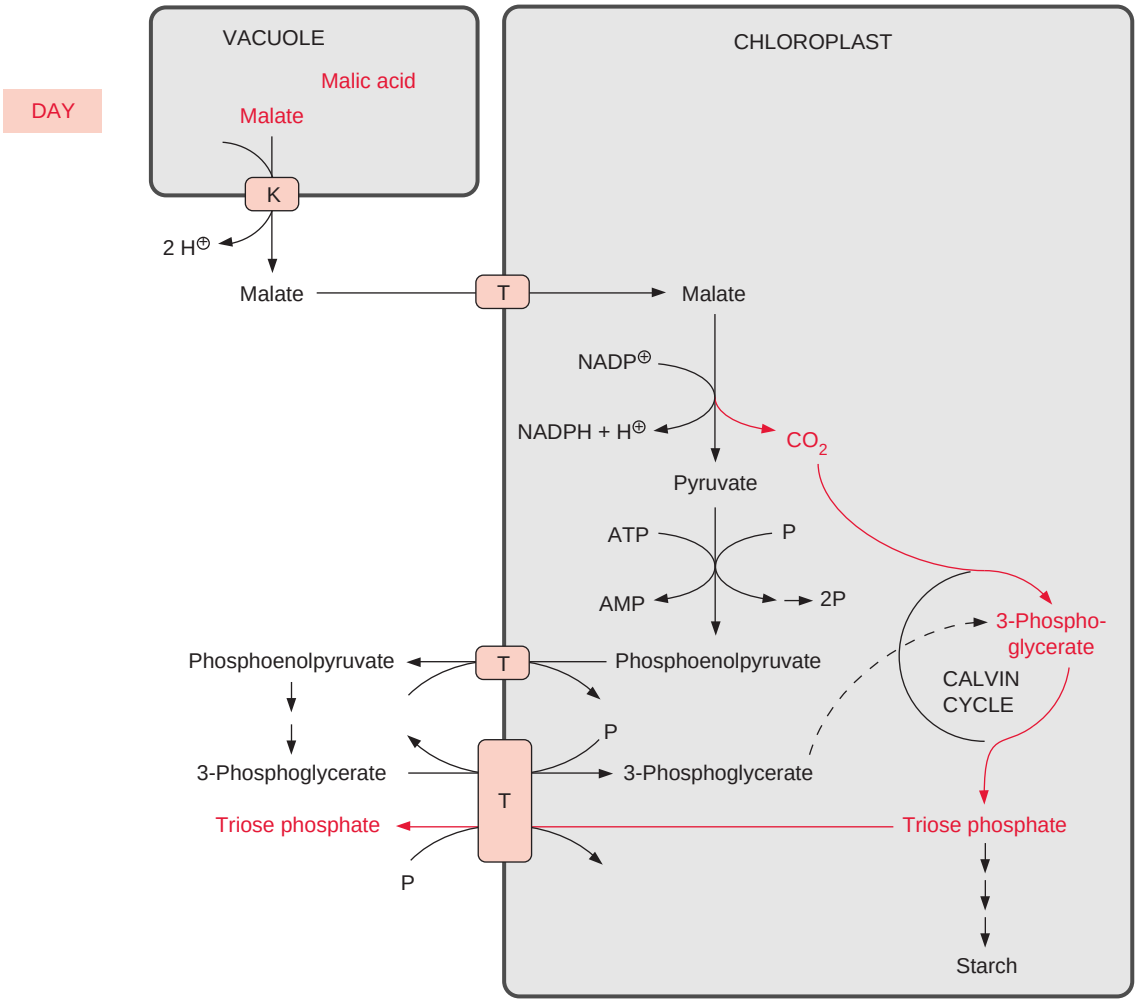

Figure 8.18 CAM during the day. Malate and the accompanying protons are released from the vacuole by a mechanism that is not yet known in detail. In the example given, malate is oxidized in the chloroplasts to pyruvate, yielding CO_2 for the CO_2 fixation by RubisCO. Pyruvate is converted via pyruvate-phosphate dikinase to phosphoenolpyruvate, which is probably converted in the cytosol to 3-phosphoglycerate. After transport into the chloroplasts, 3-phosphoglycerate is converted to triose phosphate, which is used mainly for the regeneration of starch. The transport of phosphoenolpyruvate, 3-phosphoglycerate, triose phosphate and phosphate proceeds via the triose phosphate-phosphate translocator. T = translocator; K = channel.

Quite frequently plants use CAM as a strategy for surviving extended dry periods. Some plants (e.g., *Mesembryanthemum*) perform normal C_3 photosynthesis when water is available, but switch to CAM during drought or salt stress by inducing the corresponding enzymes. It is possible to determine by mass spectrometry the $^{13}C/^{12}C$ ratio (section 8.4) in order to distinguish whether the C_3 metabolism or CAM is performed by a facultative CAM plant. During extreme drought, cacti can survive for a long time without even opening their stomata during the night. Under these conditions, they can conserve carbon by refixing respiratory CO_2 by CAM photosynthesis.

C_4 as well as CAM metabolism developed several times during evolution

C_4 and CAM plants are present in many unrelated families of monocot and dicot plants. This shows that C_4 metabolism and CAM have both evolved independently many times from C_3 metabolism. As the structural elements and the enzymes of C_4 and CAM plants are also present in C_3 plants (e.g., in the guard cells of stomata), the conversion of C_3 plants to C_4 and CAM plants seems to involve relatively simple evolutionary processes.

Further reading

Ainsworth, E. A., Rogers, A. The response of photosynthesis and stomatal conductance to rising [CO2]: Mechanisms and environmental interactions. Plant Cell Environment 30, 258–270 (2007).

Bergmann, D. C., Sack, F. D. Stomatal development. Annual Review Plant Biology 58, 163–181 (2007).

von Caemmerer, S., Furbank, R. T. The C_4 pathway: An efficient CO_2 pump. Photosynthesis Research 77, 191–207 (2003).

Caird, M. A., Richards, J. H., Donovan, L. A. Nighttime stomatal conductance and transpiration in C_3 and C_4 plants. Plant Physiology 143, 4–10 (2007).

Cherel, I. Regulation of K^+ channel activities in plants: From physiological to molecular aspects. Journal Experimental Botany 55, 337–351 (2004).

Edwards, G. E., Franceschi, V. R., Voznesenskaya, E. V. Single-cell C_4 photosynthesis versus the dual-cell (Kranz) paradigm. Annual Review Plant Biology 55, 173–196 (2004).

Farquhar, G. D., Cernusak, L. A., Barnes, B. Heavy water fractionation during transpiration. Plant Physiology 143, 11–18 (2007).

Garcia-Mata, C., Gay, R., Sokolovski, S., Hills, A., Lamattina, L., Blatt, M. R. Nitric oxide regulates K^+ and Cl^- channels in guard cells through a subset of abscisic acid-evoked signaling pathways. Proceedings National Academy Science USA 100, 1116–11121 (2003).

Hatch, M. D. C_4 Photosynthesis: An unlikely process full of surprises. Plant Cell Physiology 33, 333–342 (1992).

Leegood, R. C., Walker, R. P. Regulation and roles of phosphoenolpyruvate carboxykinase in plants. Archives Biochemistry Biophysics 414, 204–210 (2003).
Lüttge, U. Ecophysiology of Crassulacean Acid Metabolism (CAM). Annals Botany (London) 93, 629–652 (2004).
Martinoia, E., Maeshima, M., Neuhaus, H. E. Vacuolar transporters and their essential role in plant metabolism. Journal Experimental Botany 58, 83–102 (2007).
Nimmo, H. G. The regulation of phosphoenolpyruvate carboxylase in CAM plants. Trends in Plant Science 5, 75–80 (2000).
Nimmo, H. G. How to tell the time: The regulation of phosphoenolpyruvate carboxylase in Crassulacean acid metabolism (CAM) plants. Biochemical Society Transactions 31, 728–730 (2003).
Osborne, C. P., Beerling, D. J. Nature's green revolution: The remarkable evolutionary rise of C4 plants. Philosophical Transactions Royal Society London B Biological Science 361(1465), 173–194 (2006).
Pandey, S., Zhang, W., Assmann, S. M. Roles of ion channels and transporters in guard cell signal transduction. FEBS Letters 581, 2325–2336 (2007).
Roelfsema, M. R., Hedrich, R. In the light of stomatal opening: New insights into "the Watergate". New Phytologist 167, 665–691 (2005).
Sage, R. F., Kubien, D. S. The temperature response of C_3 and C_4 photosynthesis. Journal Experimental Botany 30, 1086–1106 (2007).
Shimazaki, K., Doi, M., Assmann, S. M., Kinoshita, T. Light regulation of stomatal movement. Annual Review Plant Biology 58, 219–247 (2007).
Svensson, P., Bläsing, O. E., Westhoff, P. Evolution of C4 phosphoenolpyruvate carboxylase. Archives Biochemistry Biophysics 414, 180–188 (2003).
Zhang, X., Takemiya, A., Kinoshita, T., Shimazaki, K. Nitric oxide inhibits blue light-specific stomatal opening via abscisic acid signaling pathways in *Vicia* guard cells. Plant Cell Physiology 48, 715–723 (2007).

9

Polysaccharides are storage and transport forms of carbohydrates produced by photosynthesis

In higher plants, photosynthesis in the leaves provides substrates, such as carbohydrates, for the various heterotrophic plant tissues (e.g., the roots). Substrates delivered from the leaves are oxidized in the root cells by the large number of mitochondria present. The ATP thus generated is required for driving the ion pumps of the roots by which mineral nutrients are taken up from the surrounding soil. Therefore respiratory metabolism of the roots, supported by photosynthesis of the leaves, is essential for plants. The plant dies when the roots are not sufficiently aerated since not enough oxygen is available for their respiration.

The various plant parts are supplied with carbohydrates via the sieve tubes (Chapter 13). A major transport form is the disaccharide sucrose, but in some plants also tri- and tetrasaccharides or sugar alcohols. Since the synthesis of carbohydrates by photosynthesis occurs only during the day, these carbohydrates have to be stored in the leaves to ensure their continued supply to the rest of the plant during the night or during unfavorable weather conditions. Moreover, plants need to build up carbohydrate stores to tide them over the winter or dry periods, and as a reserve in seeds for the initial phase of germination. For this purpose, carbohydrates are stored primarily in high molecular weight polysaccharides, in particular as starch or fructans, but also as low molecular weight oligosaccharides.

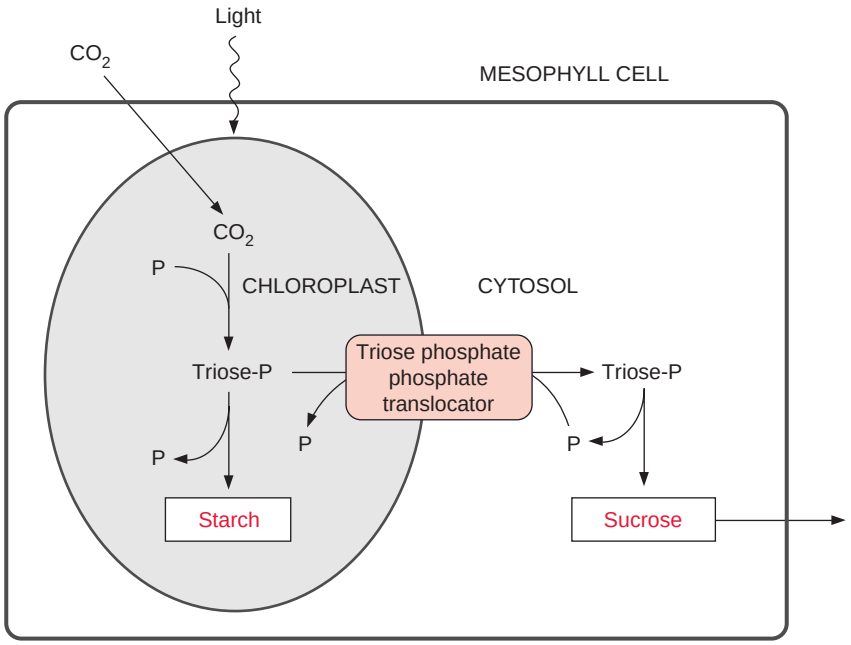

Figure 9.1 Triose phosphate, the product of photosynthetic CO_2 fixation, is either converted in the chloroplasts to starch or, after transport out of the chloroplasts, transformed to sucrose and subsequently exported from the mesophyll cells. P = PO_3^{2-}.

Starch and sucrose are the main products of CO_2 assimilation in many plants

In most crop plants (e.g., cereals, potato, sugar beet, and rapeseed), carbohydrates are stored in the leaves as **starch** and exported as **sucrose** to other parts of the plants such as the roots or growing seeds. CO_2 assimilation in the chloroplasts yields triose phosphate, which is transported by the **triose phosphate-phosphate translocator** (section 1.9) in counter-exchange for phosphate into the cytosol, where it is converted to sucrose, accompanied by the release of inorganic phosphate (Fig. 9.1). It is essential that this phosphate is returned, since phosphate deficiency in the chloroplasts would cause photosynthesis to die down. Part of the triose phosphate generated by photosynthesis is converted in the chloroplasts to starch, serving primarily as a reserve for the following night period.

9.1 Large quantities of carbohydrate can be stored as starch in the cell

Glucose is a relatively unstable compound since its aldehyde group can be spontaneously oxidized to a carboxyl group. Therefore glucose is not a

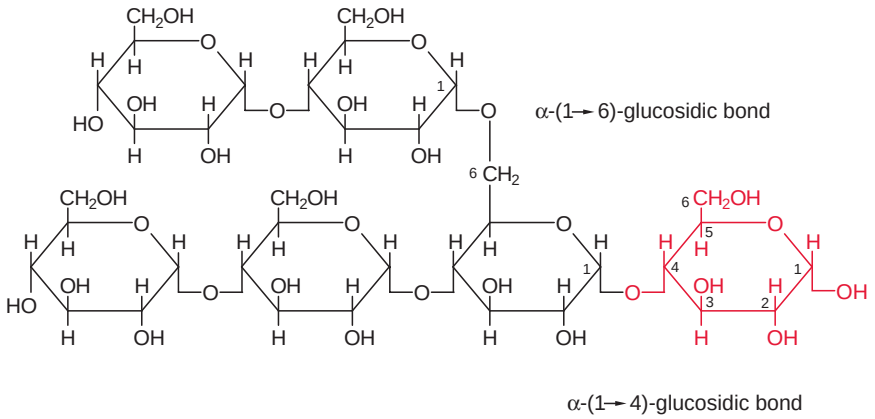

Figure 9.2 The glucose molecules in starch are connected by (α1→4)- and (α1→6)-glycosidic linkages to form a polyglucan. Only the glucose residue (colored red) contains a reducing C1-OH group.

suitable carbohydrate storage compound. Moreover, for osmotic reasons, the cell has a limited storage capacity for monosaccharides. By polymerization of glucose to the osmotically inert starch, large quantities of glucose molecules can be deposited in a cell without affecting an increase in the osmotic pressure of the cell sap. This may be illustrated by an example: at the end of the day the starch content in potato leaves may amount to 10^{-4} mol glucose moiety per mg of chlorophyll. If this amount was dissolved as free glucose in the aqueous phase of the mesophyll cell, it would yield a glucose concentration of 0.25 mol/L. Such an accumulation of glucose would result in an increase of the osmotic pressure in the cell sap by more than 50%.

The glucose molecules in starch are primarily connected by (α1→4)-glycosidic linkages (Fig. 9.2). These linkages protect the aldehyde groups of the glucose molecules against oxidation; only the first glucose molecule, colored red in Figure 9.2, is unprotected. In this way long glucose chains are synthesized, which eventually can be branched by (α1→6)-glycosidic linkages. Branched starch molecules contain many terminal glucose residues at which the starch molecule can be elongated.

In plants the formation of starch is restricted to plastids (section 1.3), namely, **chloroplasts** in leaves and green fruits and **leucoplasts** in heterotrophic tissues. Starch is deposited in the plastids as **starch granules** (Fig. 9.3). The starch granules in a leaf are very large at the end of the day and are usually degraded extensively during the following night. This starch is called **transitory starch**. In contrast, the starch in storage organs (e.g., seeds or tubers) is deposited for longer time periods, and therefore is called **reserve starch**. The granules of the reserve starch are usually larger than those of the transitory starch. In cereals the reserve starch often represents 65% to 75% and in potato tubers even 80% of the dry weight. Additionally small α-glucans are present in the cytosol which play a role in starch degradation via maltose metabolism as will be discussed in a following section.

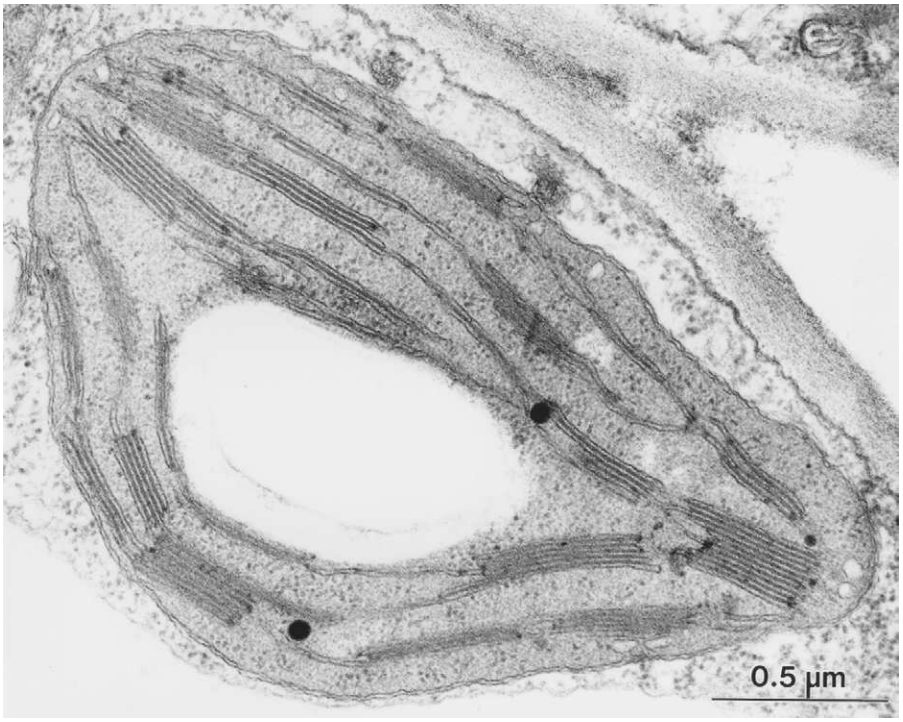

Figure 9.3 Transitory starch in a chloroplast of a mesophyll cell of a tobacco leaf at the end of the day. The starch granule in chloroplasts appears as a large white area. (By D.G. Robinson, Heidelberg.)

Table 9.1: Constituents of plant starch

	Number of glucose residues	Number of glucose residues per branching	Absorption maximum of the glucan iodine complex
Amylose	10^3		660 nm
Amylopectin	10^4–10^5	20–25	530–550 nm

Starch granules consist primarily of **amylopectin**, and **amylose** (Table 9.1). Starch granules contain the enzymes for starch synthesis and degradation. These enzymes are present in several isoforms, some of which are bound to the starch granules whereas others are soluble. Amylose consists mainly of unbranched chains of about 1,000 glucose molecules. Amylopectin, with 10^4 to 10^5 glucose molecules, is much larger than amylose and has a branching point at every 20 to 25 glucose residues (Fig. 9.4). Results of X-ray structure analysis (section 3.3) show that a starch granule is constructed of concentric layers. The amylopectin molecules are arranged in a radial fashion (Fig. 9.5). The reducing glucose (colored red in Figs. 9.2 and 9.4) is

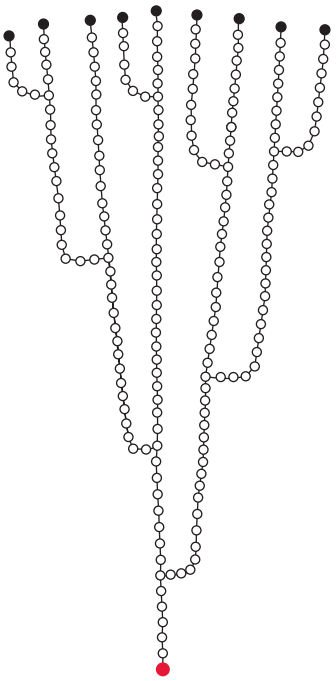

Figure 9.4 The polyglucan chains of amylopectin have a branch point at every 20 to 25 glucose residues. Neighboring chains are arranged in an ordered structure. The glucose residue, colored red at the beginning of the chain, contains a reducing group. The groups colored black at the end of the branches are the acceptors for the addition of further glucose residues catalyzed by starch synthase.

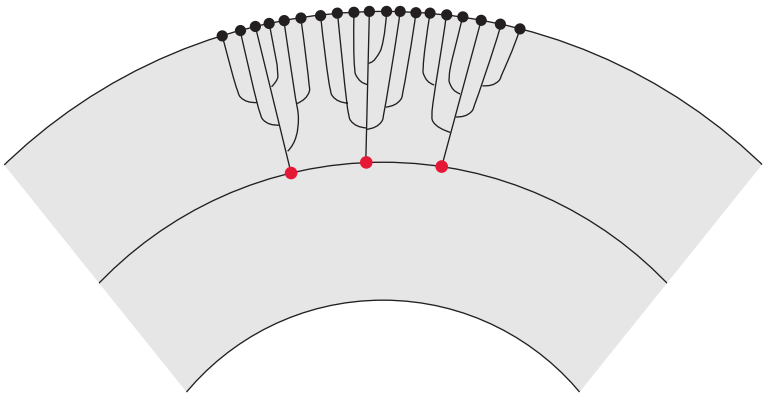

Figure 9.5 In a starch granule the amylopectin molecules are arranged in layers. Compare with Figure 9.4.

directed towards the inside, and glucose residues at the ends of the branches (colored black) are directed towards the outside. The arrangement of amylose within these layers is still a matter of debate.

A starch granule usually contains 20% to 30% amylose and 70% to 80% amylopectin. Wrinkled peas, which Gregor Mendel used in his classic breeding experiments, have an amylose content of up to 80%. In the so-called waxy maize mutants, the starch granules consist almost entirely

of amylopectin. On the other hand, the starch of the maize variety amylomaize consists of 50% amylose. Transgenic potato plants have been generated that contain only amylopectin in their tubers. Uniform starch content in potato tubers is of importance for the use of starch as a multipurpose raw material in the chemical industry.

Amylose and amylopectin form blue- to violet-colored complexes with iodine molecules (Table 9.1). This makes it very easy to detect starch in a leaf by a simple iodine test.

Starch is synthesized via ADP-glucose

Fructose 6-phosphate, an intermediate of the Calvin cycle, is the precursor for starch synthesis in chloroplasts (Fig. 9.6). Fructose 6-phosphate is converted by hexose phosphate isomerase to glucose 6-phosphate, and a *cis*-enediol is formed as an intermediate of this reaction. Phosphoglucomutase transfers the phosphate residue from the 6-position of glucose to the 1-position. A crucial step for starch synthesis is the activation of glucose 1-phosphate by reaction with ATP to **ADP-glucose**, accompanied by the release of pyrophosphate. This reaction, catalyzed by the enzyme **ADP-glucose pyrophosphorylase** (Fig. 9.7), is reversible. The high activity of pyrophosphatase in the chloroplast stroma, however, ensures that the pyrophosphate formed is immediately hydrolyzed to phosphate and thus withdrawn from the equilibrium. Therefore the formation of ADP-glucose

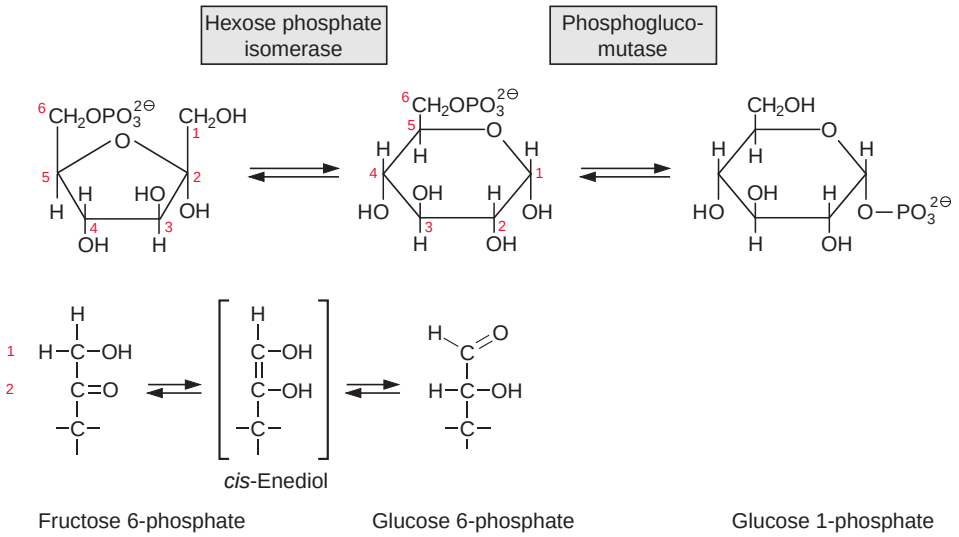

Figure 9.6
Conversion of fructose 6-phosphate to glucose 1-phosphate. The hexose phosphate isomerase reaction forms a *cis*-enediol intermediate.

is an **irreversible process** and is very suitable for regulating starch synthesis. The American biochemist Jack Preiss, who has studied the properties of ADP-glucose pyrophosphorylase in detail, found that this enzyme is allosterically activated by 3-phosphoglycerate and inhibited by phosphate. The significance of this regulation will be discussed at the end of this section. The glucose residue is transferred by **starch synthases** from ADP-glucose to the OH-group in the 4-position of the terminal glucose molecule in the polysaccharide chain of starch (Fig. 9.7). The deposition of glucose residues in a starch grain proceeds by an interplay of several isoenzymes of starch synthase.

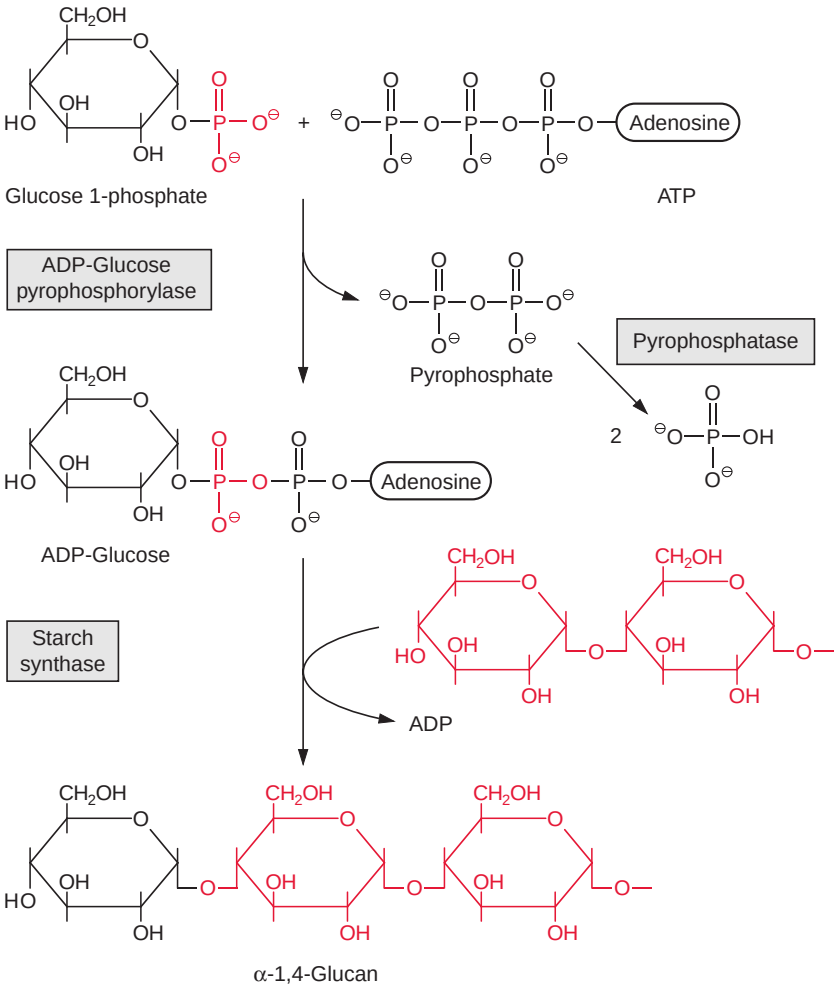

Figure 9.7 Biosynthesis of starch. Glucose 1-phosphate reacts with ATP to synthesize ADP-glucose. The pyrophosphate is hydrolyzed by pyrophosphatase and in this way the formation of ADP-glucose becomes irreversible. The activated ADP-glucose is transferred by starch synthase to a terminal glucose residue of a glucan chain.

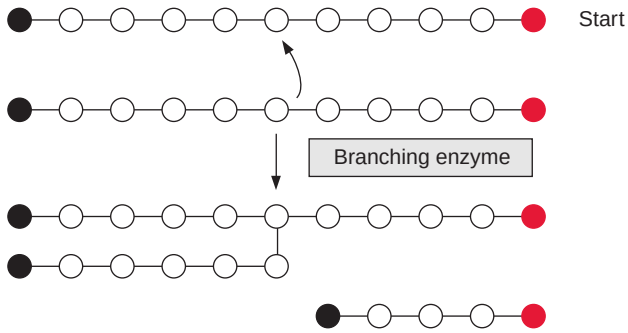

Figure 9.8 In a polyglucan chain an (α1→4)-linkage is cleaved by the branching enzyme and the disconnected fragment is linked to a neighboring chain by a (α1→6)-glycosidic linkage.

Branches are formed by a **branching enzyme**. At certain chain lengths, the polysaccharide chain is cleaved at the (α1→4) glycosidic bond (Fig. 9.8) and the polysaccharide fragment thus separated is connected via a newly formed (α1→6) bond to a neighboring chain. These chains are elongated further by starch synthase until a new branch develops. In the course of starch synthesis, branches are also cleaved again by a **debranching enzyme**, which will be discussed later. It is assumed that the activities of the branching and the debranching enzymes determine the degree of branching in starch. The wrinkled peas with the high amylose content are the result of a decrease in the activity of the branching enzyme in these plants, leading in total to lowered starch content.

Degradation of starch proceeds in two different ways

Degradation of starch proceeds in two basically different reactions (Fig. 9.9). **Amylases** catalyze a hydrolytic cleavage of (α1→4) glycosidic bonds. Different amylases attack the starch molecule at different sites (Fig. 9.10). **Exoamylases** start to hydrolyze starch from the end of the molecules. **β-Amylase** is an important exoamylase that splits off the disaccharide maltose which consists of two glucose residues (Fig. 9.11). The enzyme is named after its product β-maltose, in which the OH-group in the 1-position is present in the β-configuration. Amylases that hydrolyze starch in the interior of the glucan chain (**endoamylases**) produce cleavage products in which the OH-group in the 1-position is in α-configuration and are therefore named **α-amylases**. (α1→6) Glycosidic bonds at the branch points are hydrolyzed by **debranching enzymes**.

Phosphorylases (Fig. 9.9) cleave (α1→4) bonds phosphorolytically to form glucose 1-phosphate. The energy of the glycosidic bond is preserved

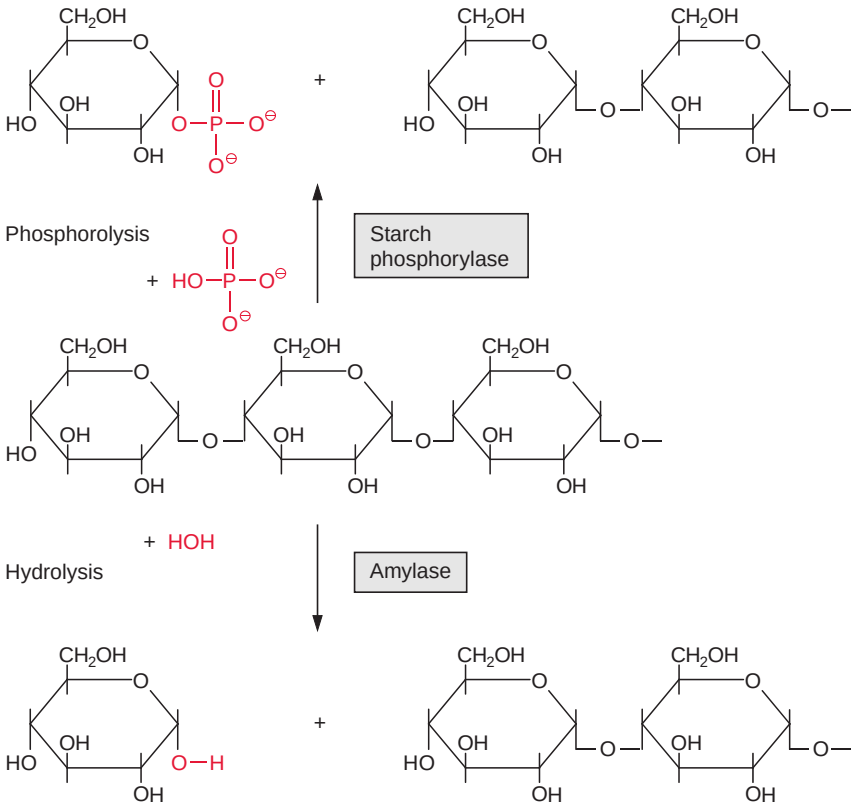

Figure 9.9 The (α1→4)-linkage in a starch molecule can be cleaved by hydrolysis or by phosphorolysis.

in a phosphate ester bond. In this case ultimately only one molecule of ATP is consumed for the storage of a glucose residue as starch; whereas two molecules of ATP are needed when the starch is mobilized by amylases (see also Fig. 9.7). It has been shown, however, that the degradation of starch is primarily facilitated by amylases.

In plant tissue an **α-glucan-water dikinase** was discovered, through which glucose residues in starch molecules are phosphorylated at the 6-C position by ATP. The phosphorylation is a typical dikinase reaction (see also Fig. 8.12) in which three substrates, an α-polyglucan, ATP, and H_2O, are converted into the three products, α-polyglucan-P, AMP, and phosphate.

$$\alpha\text{-polyglucan} + \text{ATP} + \text{H}_2\text{O} \xrightarrow{\textit{α-Glucan-water dikinase}} \alpha\text{-polyglucan-P} + \text{AMP} + \text{P}$$

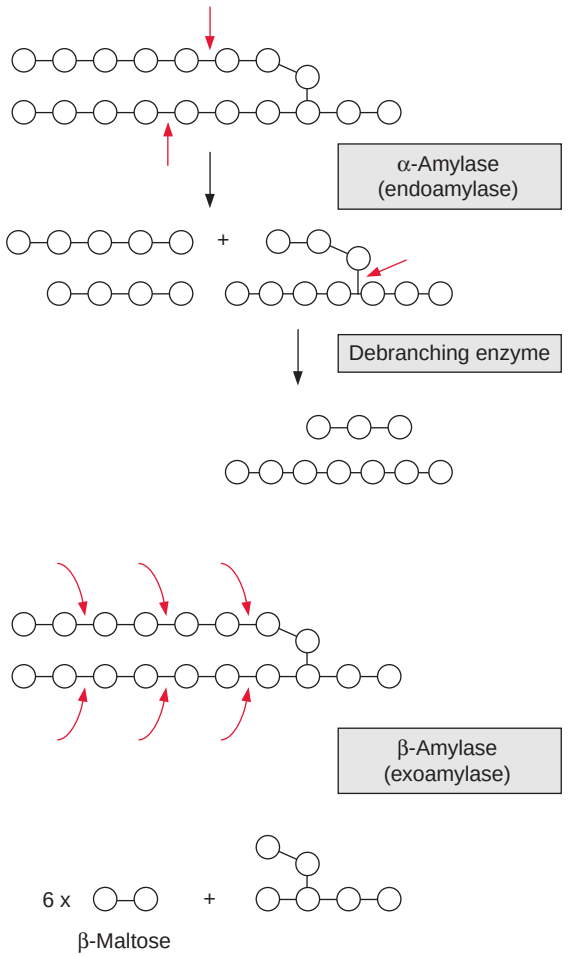

Figure 9.10 (α1→4)-Glycosidic linkages in the interior of the starch molecule are hydrolyzed by α-amylases. The debranching enzyme hydrolyzes (α1→6)-linkages. β-Amylases release the disaccharide β-maltose by hydrolysis of (α1→4)-linkages successively from the end of the starch molecules.

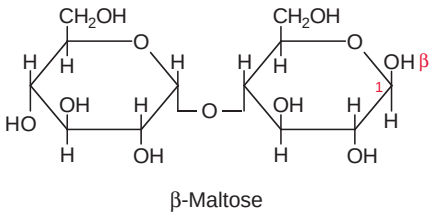

Figure 9.11 In the disaccharide β-maltose, the OH-group in position 1 is in the β-configuration.

Starch phosphorylated at 6-C is further phosphorylated by an α-glucan-water kinase at 3-C, which already occurs during starch synthesis and is essential for starch degradation. *Arabidopsis* mutants devoid of this enzyme showed impaired starch degradation.

Surplus of photosynthesis products can be stored temporarily in chloroplasts as starch

Figure 9.12 outlines the synthesis and degradation of transitory starch in chloroplasts. The regulation of ADP-glucose pyrophosphorylase by **3-phosphoglycerate** (3-PGA) and **phosphate** (P) enables the control of the flux of carbohydrates into starch. The activity of the enzyme is governed by the 3-PGA/P concentration ratio. 3-PGA is a major metabolite in the chloroplast stroma. Due to the equilibrium of the reactions catalyzed by phosphoglycerate kinase and glyceraldehyde phosphate dehydrogenase (section 6.3), the stromal 3-PGA concentration is much higher than that of triose phosphate. In the chloroplast stroma the total amount of phosphate and phosphorylated intermediates of the Calvin cycle is virtually kept constant by the counter-exchange of the triose phosphate-phosphate translocator (section 1.9). Therefore, an increase of the 3-PGA concentration results in a decrease of the phosphate concentration. The 3-PGA/P ratio is therefore a very sensitive indicator of the metabolite status in the chloroplast stroma. When sucrose synthesis is decreased, leading to a decrease of phosphate release in the cytosol, the chloroplasts would suffer from phosphate deficiency, which would limit photosynthesis in the chloroplasts (Fig. 9.1). Under such conditions, however, the PGA/P quotient increases, which enhances starch synthesis and the resulting release of phosphate allows photosynthesis to continue. In this case starch acts as a buffer. Assimilates that are not utilized for synthesis of sucrose or other metabolites are deposited temporarily in the chloroplasts as transitory starch. Moreover, starch synthesis is programmed in such a way (by a mechanism largely unknown) that sufficient starch is deposited each day for use during the following night.

So far very little is known about the regulation of transitory starch degradation. It probably is stimulated by an increase in the stromal phosphate concentration, but the mechanism for this is still unclear. An increase in the stromal phosphate concentration indicates a shortage of substrates. Hydrolytic starch degradation leads to the release of maltose and glucose, which are transported into the cytosol via specific translocators. Maltose, frequently the main product of starch degradation, is split in the cytosol by a **transglucosidase**. This enzyme transfers one glucose molecule of maltose to an **α-glucan** present in the cytosol with the release of the remaining glucose molecule, which is phosphorylated by ATP via a **hexokinase** to glucose 6-phosphate. The cytosolic α-glucan is degraded by a cytosolic **phosphorylase**.

Glucose 1-phosphate, derived from **phosphorolytic starch degradation**, is converted in a reversal of the starch synthesis pathway to fructose 6-phosphate

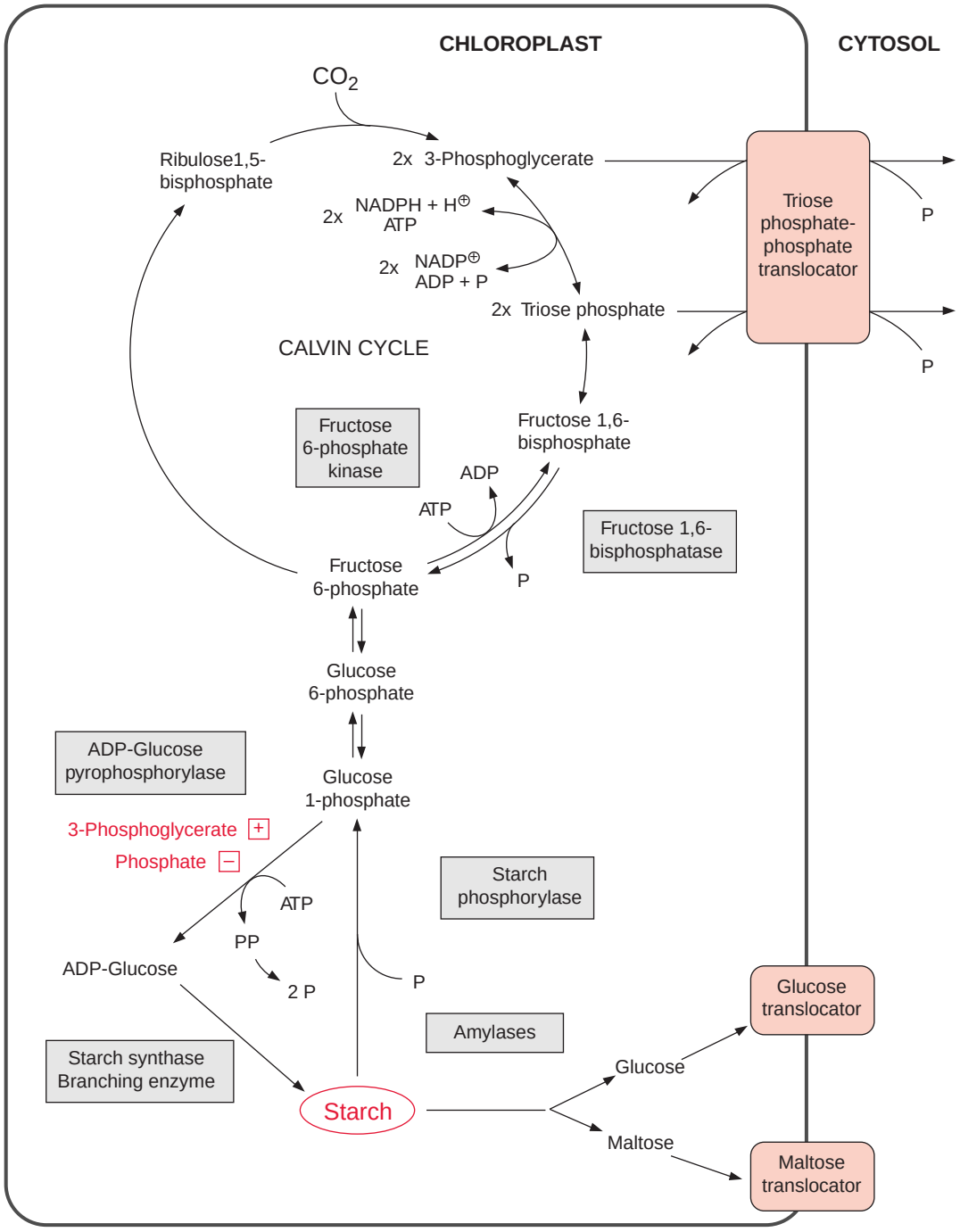

Figure 9.12 Synthesis and degradation of starch in a chloroplast.

and the latter to fructose 1,6-bisphosphate by fructose 6-phosphate kinase. Triose phosphate formed from fructose 1,6-bisphosphate by aldolase is released from the chloroplasts via the **triose phosphate-phosphate translocator**. Part of the triose phosphate is oxidized within the chloroplasts to 3-phosphoglycerate and is subsequently exported also via the triose phosphate-phosphate translocator. This translocator as well as the glucose translocator is thus involved in the mobilization of the chloroplast transitory starch.

9.2 Sucrose synthesis takes place in the cytosol

The synthesis of sucrose, a disaccharide of glucose and fructose (Fig. 9.13), takes place in the cytosol of the mesophyll cells. As in starch synthesis, the glucose residue is activated as nucleoside diphosphate-glucose, although in this case via UDP-glucose pyrophosphorylase:

$$\text{glucose 1-phosphate} + \text{UTP} \xrightleftharpoons{\textit{UDP-glucose pyrophosphorylase}} \text{UDP-glucose} + \text{PP}$$

In contrast to the chloroplast stroma, a pyrophosphatase is not present in the cytosol of mesophyll cells. Since pyrophosphate cannot be withdrawn from the equilibrium, the UDP-glucose pyrophosphorylase reaction is reversible. **Sucrose phosphate synthase** (abbreviated SPS, Fig. 9.13) catalyzes the transfer of the glucose residue from UDP-glucose to fructose 6-phosphate forming sucrose 6-phosphate. **Sucrose phosphate phosphatase,** forming an enzyme complex together with SPS, hydrolyzes sucrose 6-phosphate, thus withdrawing it from the sucrose phosphate synthase reaction equilibrium. Therefore, the overall reaction of sucrose synthesis is an irreversible process.

In addition to sucrose phosphate synthase, plants also contain a **sucrose synthase**:

$$\text{sucrose} + \text{UDP} \xrightleftharpoons{\textit{Sucrose synthase}} \text{UDP-glucose} + \text{fructose}$$

This reaction is reversible. It is not primarily involved in sucrose synthesis but in the utilization of sucrose by catalyzing the formation of

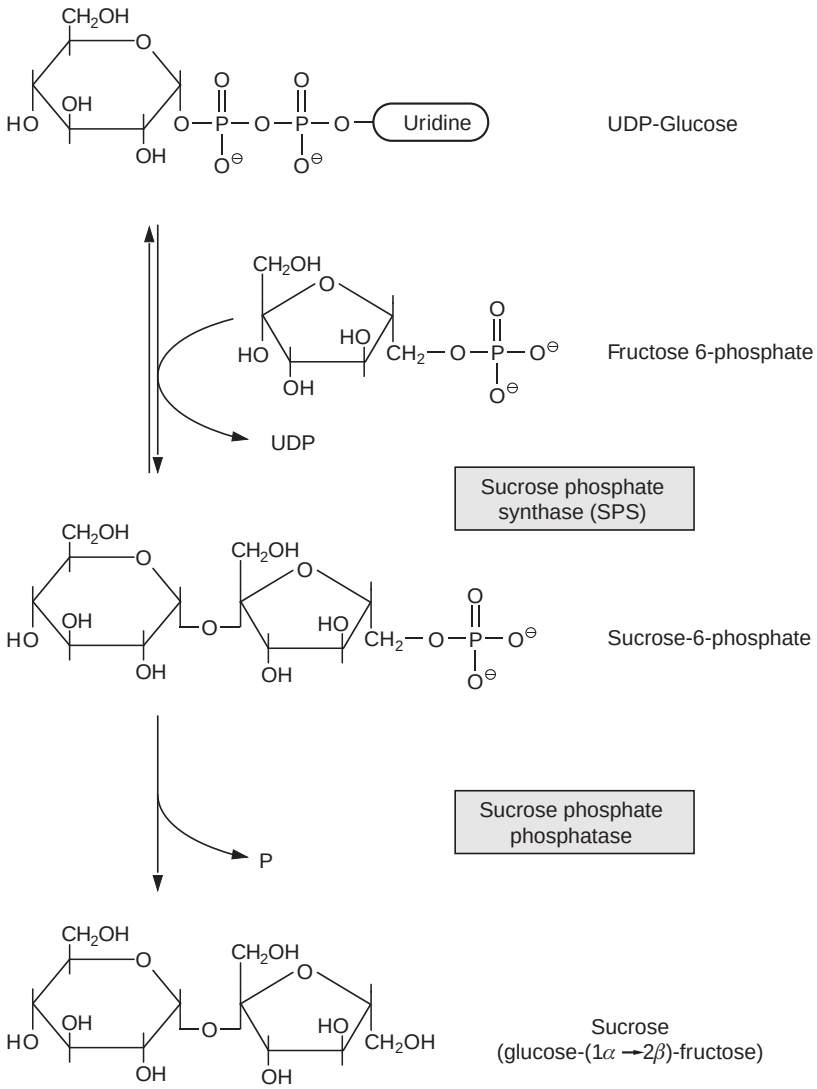

Figure 9.13 Synthesis of sucrose. The glucose activated by UDP is transferred to fructose 6-phosphate. The total reaction becomes irreversible by hydrolysis of the formed sucrose 6-phosphate.

UDP-glucose and fructose from UDP and sucrose. This enzyme occurs mostly in nonphotosynthetic tissues. It is for instance involved in sucrose breakdown in amyloplasts of storage tissue such as potato tubers to support starch synthesis (section 13.3). It also plays a role in the synthesis of cellulose and callose, where the sucrose synthase, otherwise soluble, is membrane-bound (see section 9.6).

9.3 The utilization of the photosynthesis product triose phosphate is strictly regulated

As shown in Figure 6.11, five of the six triose phosphate molecules generated in the Calvin cycle are required for the regeneration of the CO_2 acceptor ribulose bisphosphate. Therefore, a maximum of one-sixth of the triose phosphate produced is available for export from the chloroplasts. In fact, due to photorespiration (Chapter 7), the portion of available triose phosphate is only about one-eighth of the triose phosphate synthesized in the chloroplasts. If more triose phosphate would be withdrawn from the Calvin cycle, the CO_2 acceptor ribulose bisphosphate could no longer be regenerated and the Calvin cycle would collapse. To keep the Calvin cycle running it is crucial that the withdrawal of triose phosphate does not exceed this limit. On the other hand, photosynthesis of chloroplasts can only proceed if its product triose phosphate is utilized (e.g., for synthesis of sucrose), and consequently phosphate is released. A phosphate deficiency would result in a decrease or even a total cessation of photosynthesis. Thus, it is important for a plant to match the increase of the photosynthesis rate (e.g., during strong sunlight) with the increase in the synthesis and utilization of assimilation products. Therefore the utilization of the triose phosphate generated by photosynthesis should be regulated in such a way that as much as possible is utilized without exceeding the limit, to ensure the regeneration of the CO_2 acceptor ribulose bisphosphate.

Fructose 1,6-bisphosphatase is an entrance valve of the sucrose synthesis pathway

In mesophyll cells, sucrose synthesis is normally the main consumer of triose phosphate generated by CO_2 fixation. The withdrawal of triose phosphate from chloroplasts for the synthesis of sucrose is not regulated via translocation between chloroplast and cytosol. Due to the hydrolysis of fructose 1,6-bisphosphate and sucrose 6-phosphate, the complete reaction of sucrose synthesis (Fig. 9.14) is an irreversible process, which has a high synthetic capacity due to high enzymatic activities. Sucrose synthesis must be strictly regulated to ensure that not more than the permitted amount of triose phosphate (see preceding paragraph) is withdrawn from the Calvin cycle.

The first irreversible step of sucrose synthesis is catalyzed by the **cytosolic fructose 1,6-bisphosphatase**. This reaction is an important control

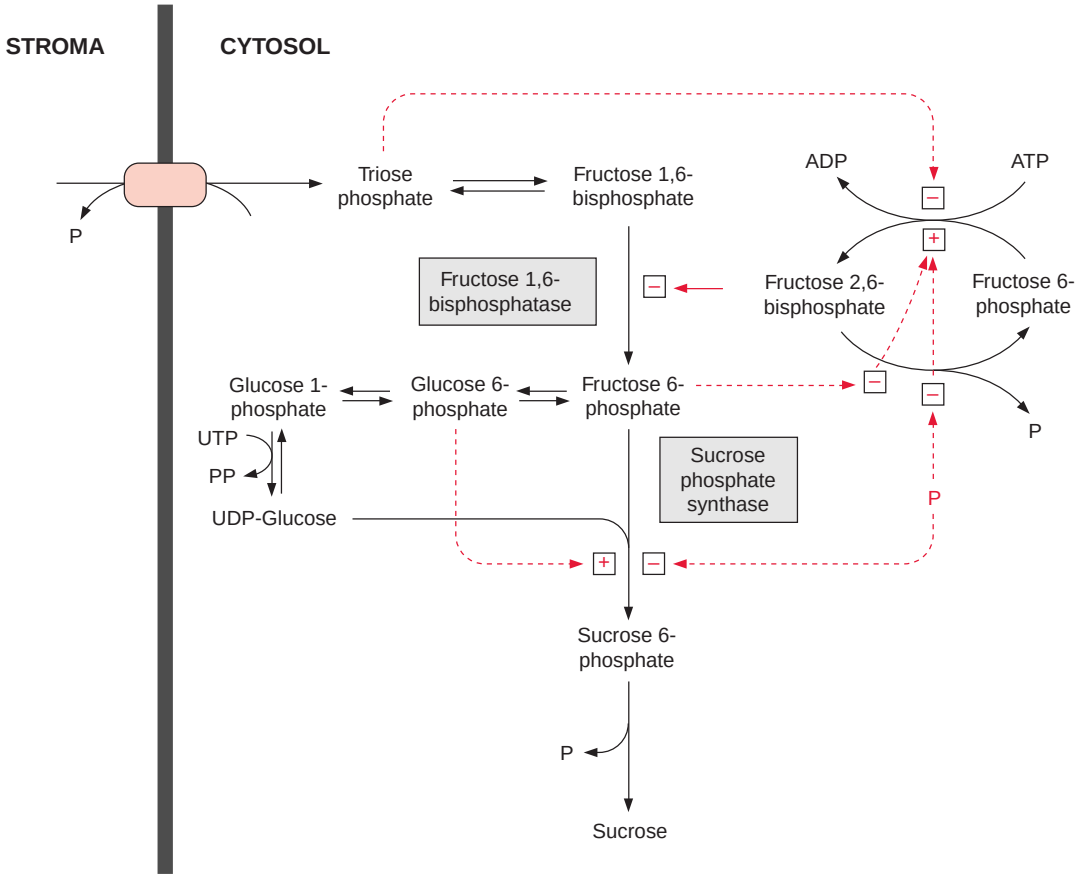

Figure 9.14 Conversion of triose phosphate into sucrose. The dashed red lines represent the regulation by metabolites, (−) inhibition, (+) activation. The effect of the regulatory compound fructose 2,6-bisphosphate is explained in detail in Figure 9.15. P = PO_3^{2-}, PP = pyrophosphate.

point and is the entrance valve where triose phosphate is recruited for the synthesis of sucrose. Figure 9.15 shows how this valve is regulated. An important role is played by **fructose 2,6-bisphosphate** (Fru2,6BP), a regulatory compound that differs from the metabolic fructose 1,6-bisphosphate only in the positioning of one phosphate group (Fig. 9.16).

Fru2,6BP was discovered to be a potent activator of ATP-dependent fructose 6-phosphate kinase and an inhibitor of fructose 1,6-bisphosphatase in liver. Later it became apparent that Fru2,6BP has a general function in controlling glycolysis and gluconeogenesis in animals, plants, and fungi. It is a powerful regulator of cytosolic fructose 1,6-bisphosphatase in mesophyll cells. At micromolar concentrations Fru2,6BP decreases the affinity

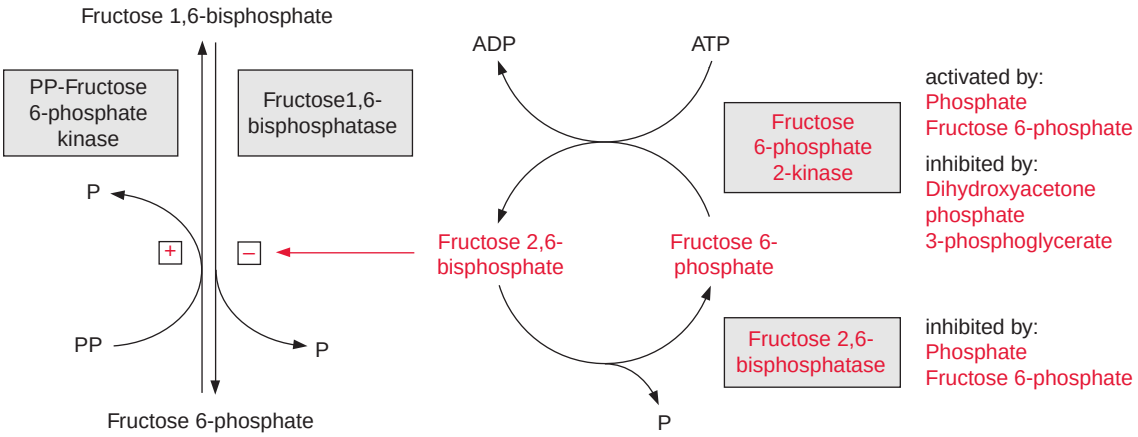

Figure 9.15 Fructose 1,6-bisphosphatase represents the entrance valve for the conversion of the CO_2 assimilates into sucrose. The enzyme is inhibited by the regulatory metabolite fructose 2,6-bisphosphate (Fru2,6BP). The pyrophosphate-dependent fructose 6-phosphate kinase, which synthesizes fructose 1,6-bisphosphate from fructose 6-phosphate, with the consumption of pyrophosphate, is active only in the presence of Fru2,6BP. The concentration of Fru2,6BP is adjusted by continuous synthesis and degradation. The enzymes catalyzing Fru2,6BP synthesis and degradation are regulated by metabolites. In this way the presence of triose phosphate and 3-phosphoglycerate decreases the concentration of Fru2,6BP and thus increases the activity of fructose 1,6-bisphosphatase. P = PO_3^{2-}, PP = pyrophosphate.

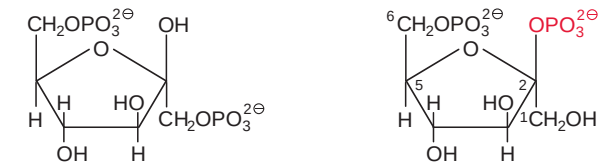

Figure 9.16 The regulatory compound fructose 2,6-bisphosphate differs from the metabolite fructose 1,6-bisphosphate only in the position of one phosphate group.

of the enzyme towards its substrate fructose 1,6-bisphosphate. On the other hand, Fru2,6BP activates a **pyrophosphate-dependent fructose 6-phosphate kinase** present in the cytosol of plant cells. This enzyme is inactive when Fru2,6BP is lacking. The pyrophosphate-dependent fructose 6-phosphate kinase can utilize pyrophosphate, which is produced in the UDP-glucose pyrophosphorylase reaction.

Fru2,6BP is synthesized from fructose 6-phosphate by a specific kinase (**fructose 6-phosphate 2-kinase**) and is degraded hydrolytically to fructose 6-phosphate by a specific phosphatase (**fructose 2,6-bisphosphatase**). The cellular concentration of the regulatory metabolite Fru2,6BP is adjusted by

regulation of the relative rates of synthesis and degradation. Triose phosphate and 3-phosphoglycerate inhibit the synthesis of Fru2,6BP, whereas fructose 6-phosphate and phosphate stimulate synthesis and decrease hydrolysis. Consequently the increase of triose phosphate concentration results in a decrease in the level of Fru2,6BP and thus in an increased affinity of the cytosolic fructose 1,6-bisphosphatase towards its substrate fructose 1,6-bisphosphate. Moreover, due to the equilibrium catalyzed by cytosolic aldolase, an increase in the triose phosphate concentration results in an increase in the concentration of fructose 1,6-bisphosphate. The simultaneous increase in substrate concentration and substrate affinity has the effect that only after a threshold level of triose phosphate is reached, does the rate of sucrose synthesis increase following rising concentrations of triose phosphate (Fig. 9.17). In this way the rate of sucrose synthesis can be adjusted effectively to the supply of triose phosphate.

The principal mechanism of this regulation can be compared with an overflow valve. Only when a certain threshold concentration of triose phosphate is overstepped can an appreciable metabolite flux via fructose 1,6-bisphosphatase occur. This mechanism ensures that the triose phosphate level in chloroplasts does not decrease below the minimum level which is required for the Calvin cycle reactions to proceed. When this threshold is reached, a further increase in triose phosphate results in a large increase in enzyme activity, whereby the surplus triose phosphate can be channeled very efficiently into sucrose synthesis.

Cytosolic fructose 1,6-bisphosphatase adjusts its activity, as shown above, not only to the substrate supply, but also to the demand for its product. With an increase in fructose 6-phosphate, the level of the regulatory metabolite Fru2,6BP is increased by stimulation of fructose 6-phosphate 2-kinase and simultaneous inhibition of fructose 2,6-bisphosphatase, resulting in a reduction of cytosolic fructose 1,6-bisphosphatase activity (Fig. 9.15).

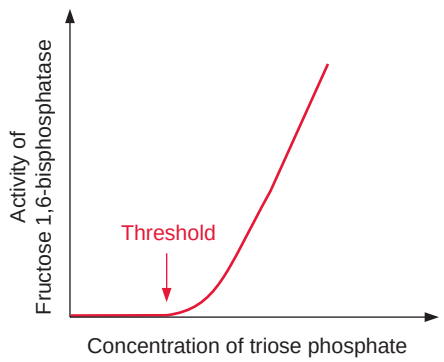

Figure 9.17 Cytosolic fructose 1,6-bisphosphatase acts as an entrance valve to adjust the synthesis of sucrose to the supply of triose phosphate. Increasing triose phosphate leads, via aldolase, to an increase in the substrate fructose 1,6-bisphosphate (Fig. 9.14), and in parallel (Fig. 9.15) to a decrease in the concentration of the regulatory metabolite fructose 2,6-bisphosphate. As a consequence of these two synergistic effects, fructose 1,6-bisphosphatase is activated only after triose phosphate reaches a threshold concentration and then increases its activity according to the triose phosphate concentrations.

Sucrose phosphate synthase is regulated by metabolites and by covalent modification

Sucrose phosphate synthase (Fig. 9.14) is also subject to strict metabolic control. This enzyme is activated by glucose 6-phosphate and is inhibited by phosphate. Due to hexose phosphate isomerase, the activator glucose 6-phosphate is in equilibrium with fructose 6-phosphate. In this equilibrium the concentration of glucose 6-phosphate greatly exceeds the concentration of fructose 6-phosphate. Therefore, the change in the concentration of the substrate fructose 6-phosphate results in a much larger change in the concentration of the activator glucose 6-phosphate. In this way the activity of the enzyme is adjusted effectively to the supply of the substrate.

Moreover, the activity of sucrose phosphate synthase is altered by a covalent modification of the enzyme. At **position 158** the enzyme has a **serine residue**, of which the OH-group is phosphorylated by a special protein kinase, termed **sucrose phosphate synthase kinase** (SPS kinase) and is dephosphorylated by the corresponding **SPS phosphatase** (Fig. 9.18a). The SPS phosphatase is inhibited by **okadaic acid**, an inhibitor of protein phosphatases of the so-called 2A type (not discussed in more detail here). The activity of SPS kinase is probably regulated by metabolites such as glucose 6-phosphate.

The phosphorylated form of sucrose phosphate synthase is less active than the dephosphorylated form. The activity of the enzyme is adjusted

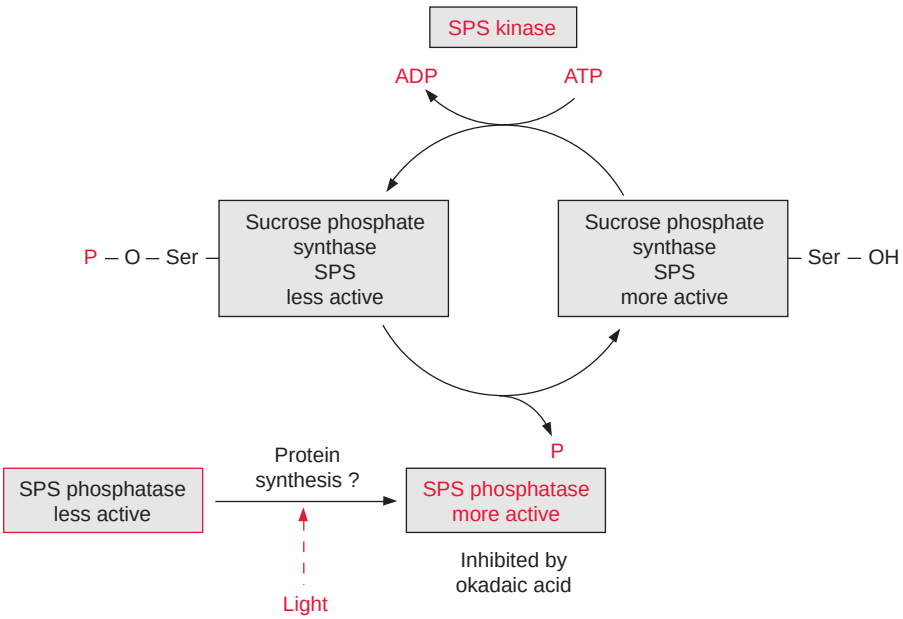

Figure 9.18a Sucrose-phosphate synthase (SPS) is converted to a less active form by phosphorylation of a serine residue via SPS kinase. The hydrolysis of the phosphate residue by SPS phosphatase results in an increase of the activity. The activity of SPS phosphatase is increased by illumination, probably via *de novo* synthesis of the enzyme protein. (After Huber, 1996.)

by the relative rates of its phosphorylation and dephosphorylation. When leaves are illuminated the activity of SPS phosphatase increases and thus the sucrose phosphate synthase is converted into the more active form. The mechanism for this is still not fully known. It is discussed that the decrease of SPS phosphatase activity during darkness is due to a lowered rate of the synthesis of the SPS phosphatase. In **position 424** sucrose phosphate synthase has a **second serine residue**, which is phosphorylated by another protein kinase (activated by osmotic stress), resulting in an activation of SPS. Thus the regulation of SPS is very complex. The phosphorylation of one serine residue by the corresponding protein kinase causes an inhibition, while the phosphorylation of another serine residue by a different protein kinase leads to activation. Moreover, SPS has a **third phosphorylation site**, to which a **14.3.3 protein** is bound (similarly as in the case of nitrate reductase, section 10.3). The physiological role of this binding remains to be resolved.

Partitioning of assimilates between sucrose and starch is due to the interplay of several regulatory mechanisms

The preceding section discussed various regulatory processes involved in the regulation of sucrose synthesis. Metabolites acting as enzyme inhibitors or activators can adjust the rate of sucrose synthesis immediately to the prevailing metabolic conditions in the cell. Such an immediate response is called **fine control**. The covalent modification of enzymes, influenced by diurnal factors and probably also by phytohormones (Chapter 19), results in a **general regulation of metabolism** according to the metabolic demand of the plant, including partitioning of assimilates between sucrose, starch, and amino acids (Chapter 10). Thus, slowing down sucrose synthesis, which results in an increase in triose phosphate and also of 3-phosphoglycerate, can lead to an increase in the rate of **starch synthesis** (Fig. 9.12). During the day a large part of the photo assimilates is deposited temporarily in the chloroplasts of leaves as transitory starch, to be converted during the following night to sucrose and delivered to other parts of the plant. However, in some plants, such as barley, during the day large quantities of the photo assimilates are stored as sucrose in the leaves. Therefore during darkness the rate of sucrose synthesis varies in leaves of different plants.

Trehalose is an important signal mediator

For a long time trehalose (Fig. 9.18b), occurring in plant cells only in small concentrations, was regarded as being of minor importance. Only recently it was shown that trehalose and trehalose phosphate are very important signal

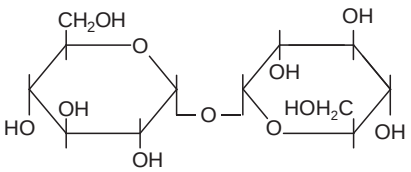

Figure 9.18b
α,α-Trehalose is a disaccharide consisting of two glucose molecules connected by a (α1→1α) glucosidic linkage.

metabolites involved in the regulation of plant metabolism. Precursors for trehalose synthesis are glucose 6-phosphate and UDP-glucose:

$$\text{glucose 6-P} + \text{UDP-glucose} \xrightarrow{\textit{Trehalose phosphate synthase}} \text{trehalose 6-P} + \text{UDP}$$

$$\text{trehalose 6-P} \xrightarrow{\textit{Trehalose phosphate phosphatase}} \text{trehalose} + \text{phosphate}$$

The importance of trehalose is illustrated by the fact that the *Arabidopsis* genome provides more genes for its synthesis than for the synthesis of sucrose. Trehalose and trehalose phosphate stimulate in plants the synthesis of starch, increase the resistance to dryness, and are involved in triggering flowering and maturation of embryos. The mechanisms of these actions remain to be elucidated.

9.4 In some plants assimilates from the leaves are exported as sugar alcohols or oligosaccharides of the raffinose family

Not all plants use sucrose for the translocation of assimilates from the leaves to other parts of the plant. In some plants photo assimilates are translocated as **sugar alcohols**, also called **polyols**, including sorbitol and mannitol (Fig. 9.19). *Rosaceae* (including orchard trees in temperate regions) translocate assimilates in the form of **sorbitol** (Fig. 9.19). Other plants, such as squash, several deciduous trees (e.g., lime, hazelnut, elm), and olive trees, translocate in their sieve tubes oligosaccharides of the **raffinose family**. In these oligosaccharides sucrose is linked by a glycosidic bond to one or more galactose molecules (Fig. 9.20). Oligosaccharides of the raffinose family include **raffinose** with one, **stachyose** with two, and **verbascose** with three galactose residues. These oligosaccharides also serve

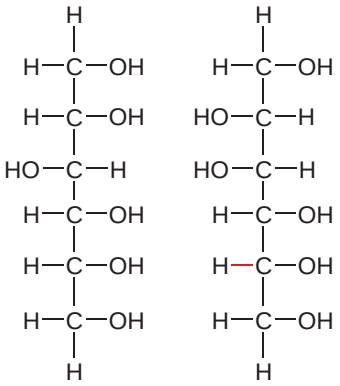

Figure 9.19 In some plants assimilated CO_2 is exported from the leaves via sugar alcohols (polyols) such as sorbitol and mannitol.

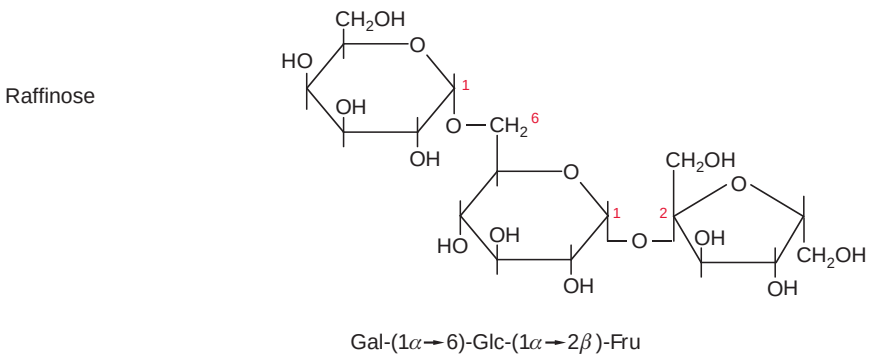

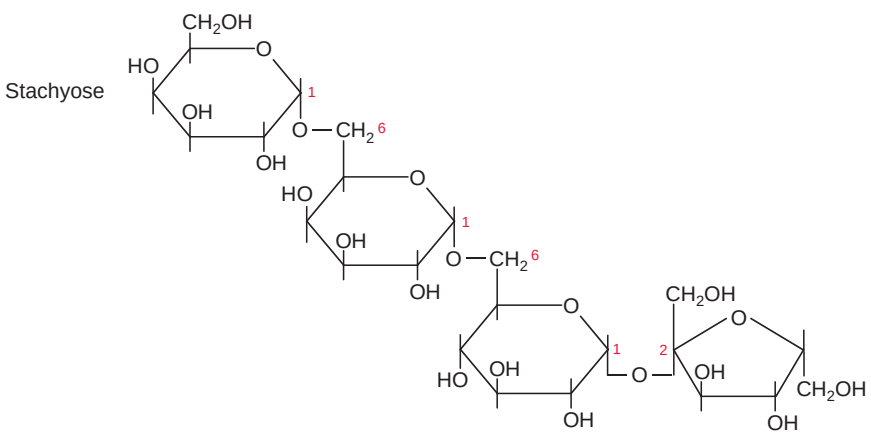

Verbascose

Gal-(1α→6)-Gal-(1α→6)-Gal-(1α→6)-Glc-(1α→2β)-Fru

Figure 9.20 In the oligosaccharides of the raffinose family, one to three galactose residues are linked to the glucose residue of sucrose in position 6. Abbreviations: Gal = galactose; Glc = glucose; Fru = fructose.

as storage compounds and, for example, in pea and bean seeds make up 5% to 15% of the dry matter. Humans do not have the enzymes that catalyze the hydrolysis of α-galactosides and are therefore unable to digest oligosaccharides of the raffinose family. When these sugars are ingested, they are decomposed in the last section of the intestines by anaerobic bacteria, which metabolize the sugars and release digestive gases.

The galactose required for raffinose synthesis is formed by epimerization of UDP-glucose (Fig. 9.21). **UDP-glucose epimerase** catalyzes the oxidation of the OH-group in position 4 of the glucose molecule by NAD^+, which is

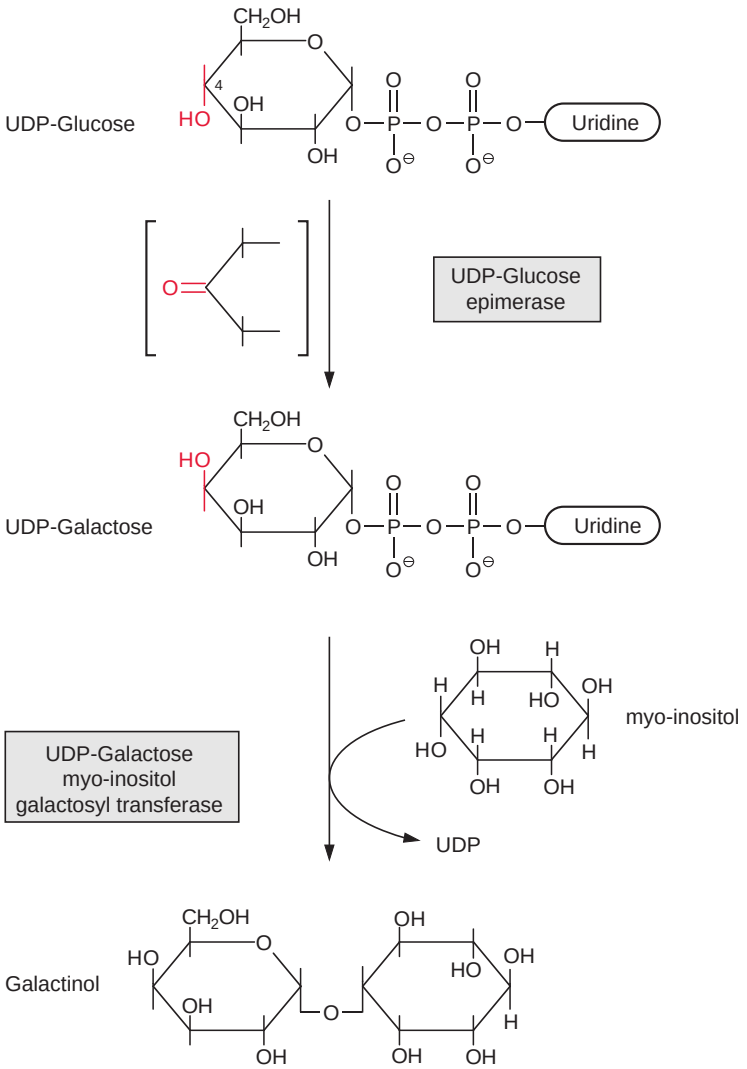

Figure 9.21 Synthesis of galactinol as an intermediate in raffinose synthesis from UDP-glucose and myo-inositol. The epimerization of UDP-glucose to UDP-galactose proceeds via the formation of a keto group as intermediate in position 4.

tightly bound to the enzyme. Remaining bound to the enzyme the intermediate is subsequently reduced to galactose. As the reaction is reversible, UDP-glucose epimerase catalyzes an equilibrium between glucose and galactose. The galactose residue is transferred by a transferase to the cyclic alcohol myo-inositol producing galactinol. **Myo-inositol-galactosyl-transferases** catalyze the transfer of the galactose residue from galactinol to sucrose, to synthesize raffinose, and correspondingly also stachyose and verbascose.

sucrose + galactinol → raffinose + myo-inositol

raffinose + galactinol → stachyose + myo-inositol

stachyose + galactinol → verbascose + myo-inositol

9.5 Fructans are deposited as storage compounds in the vacuole

In addition to starch, many plants use **fructans** as carbohydrate storage compounds. Whereas starch is an insoluble polyglucose formed in the plastids, fructans are soluble polyfructoses that are synthesized and stored in the vacuole. They were first detected in the tubers of ornamental flowers such as dahlias. Fructans are stored, often in the leaves and stems, of many grasses from temperate climates, such as wheat and barley. Fructans are also the major carbohydrate present in onions and, like the raffinose sugars, cannot be digested by humans. Because of their sweet taste, fructans are used as natural calorie-free sweeteners. Fructans are also used in the food industry as a replacement for fat.

The precursor for the polysaccharide chain of fructans is a sucrose molecule to which additional fructose molecules are attached by glycosidic linkages. The basic structure of a fructan in which sucrose is linked with one additional fructose molecule to a trisaccharide is called **kestose**. Figure 9.22 shows three major types of fructans.

In fructans of the **6-kestose type**, the fructose residue of sucrose is glycosidically linked at position 6 with the 2β-position of another fructose. Chains of different lengths (10–200 fructose residues) are elongated by (6→2β)-linkages of additional fructose residues. These fructans are also called **levan type fructans** and are often found in grasses.

The fructose residues in fructans of the **1-kestose type** are linked to the sucrose molecule by (1→2β) glycosidic linkages. These fructans, also called

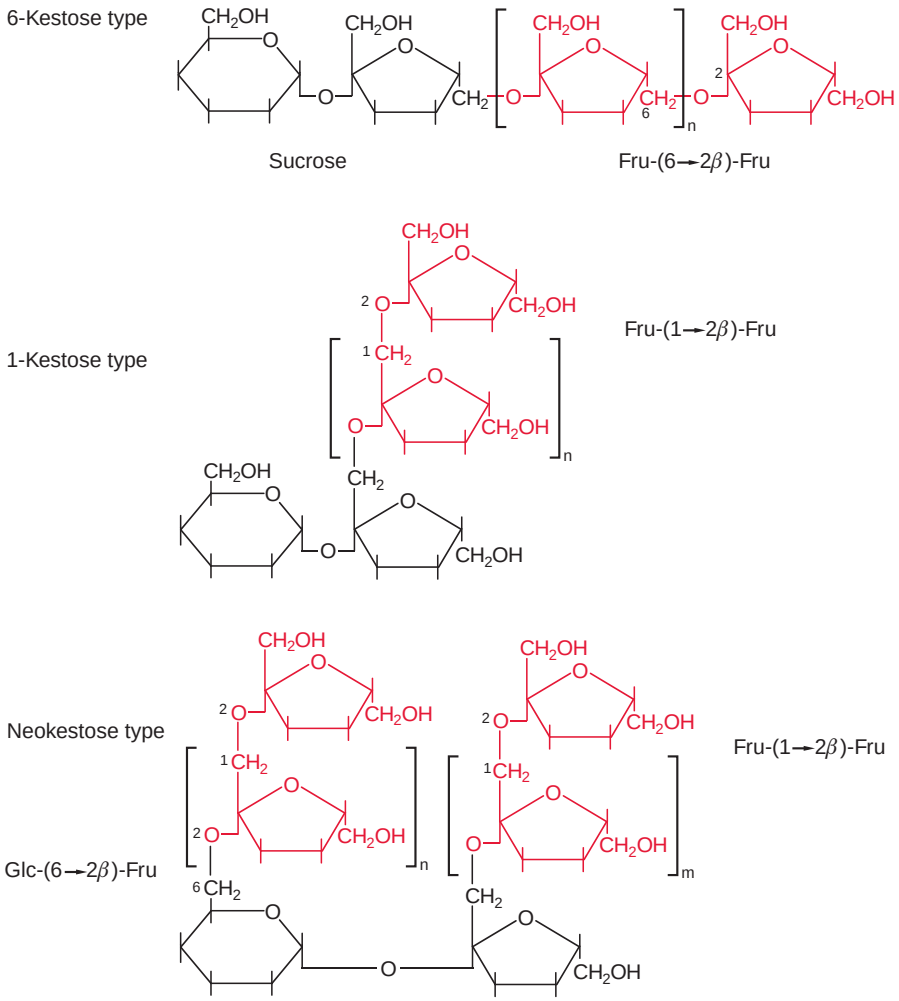

Figure 9.22 Fructans are derived from kestoses. They are formed by the linkage of fructose residues to a sucrose molecule. In fructans of the 6-kestose type, the chain consists of $n = 10$ to 200 and in the 1-kestose type $n < 50$ fructose residues, and in the neokestose type, n and m are <10.

inulin type fructans, consist of up to 50 fructose molecules. Inulin is found in dahlia tubers.

In fructans of the **neokestose type**, two polyfructose chains are connected to the fructose moiety of sucrose, one via (1→2β) glycosidic linkage, and the other in a (6→2β) glycosidic linkage with the glucose residue of the sucrose molecule. The fructans of the neokestose type are comprised of only 5 to 10 fructose residues. Branched fructans in which the fructose molecules are connected by both (1→2β)- and (6→2β)-glycosidic linkages are found in wheat and barley and are called **graminanes**.

Although fructans appear to have an important function in the metabolism of many plants, our knowledge of their function and metabolism is

still fragmentary. Fructan synthesis occurs in the vacuoles, and sucrose is the precursor for its synthesis. The fructose moiety of a sucrose molecule is transferred by a **sucrose-sucrose fructosyl transferase** to a second sucrose molecule, resulting in the formation of a 1-kestose with a glucose molecule remaining (Fig. 9.23A). Additional fructose residues are transferred not from another sucrose molecule but from another kestose molecule for the elongation of the kestose chain (Fig. 9.23B). The enzyme **fructan-fructan 1-fructosyl transferase** transfers preferentially the fructose residue from a trisaccharide to a longer chain kestose. Correspondingly, the formation of 6-kestoses is catalyzed by a **fructan-fructan 6-fructosyl transferase**. For the formation of neokestoses, a fructose residue is transferred via a **6-glucose-fructosyl transferase** from a 1-kestose to the glucose residue of sucrose (Fig. 9.23C). The trisaccharide thus formed is a precursor for further chain elongation as shown in Figure 9.23B.

The degradation of fructans proceeds by successive hydrolysis of fructose residues from the end of the fructan chain which is catalyzed by exohydrolytic enzymes. In many grasses, fructans accumulate for a certain time in the leaves and in the stems, and then constitute up to 30% of the dry matter. Often these carbohydrates accumulate before the onset of flowering and are available for rapid seed growth after pollination of the flowers. In plants growing in meager habitats, where periods of high photosynthesis

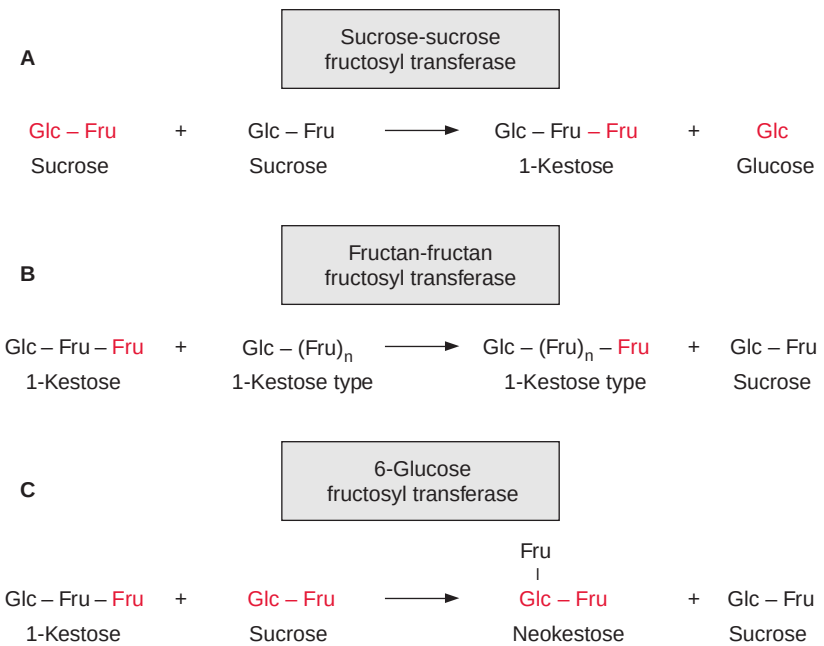

Figure 9.23 Sucrose is the precursor for the synthesis of kestoses. Three important reactions of the kestose biosynthesis pathway proceed in the vacuole.

are succeeded by periods with limited and inadequate photosynthesis, fructans are a reserve for surviving unfavorable conditions. Thus in many plants fructans are formed when these are subjected to water or cold stress.

Plants that accumulate fructans usually also store sucrose and starch in their leaves. Figure 9.24 shows a simplified scheme of fructan synthesis as an alternative storage compound in leaves. For the synthesis of fructans, sucrose is first synthesized in the cytosol (see Figure 9.14 for details). The UDP-glucose required is synthesized from glucose that is released from the vacuole in the course of fructan synthesis and subsequently phosphorylated by hexokinase. Fructose 6-phosphate, generated by photosynthesis and UDP-glucose, is converted into fructan, which requires altogether two ATP equivalents per molecule of fructan.

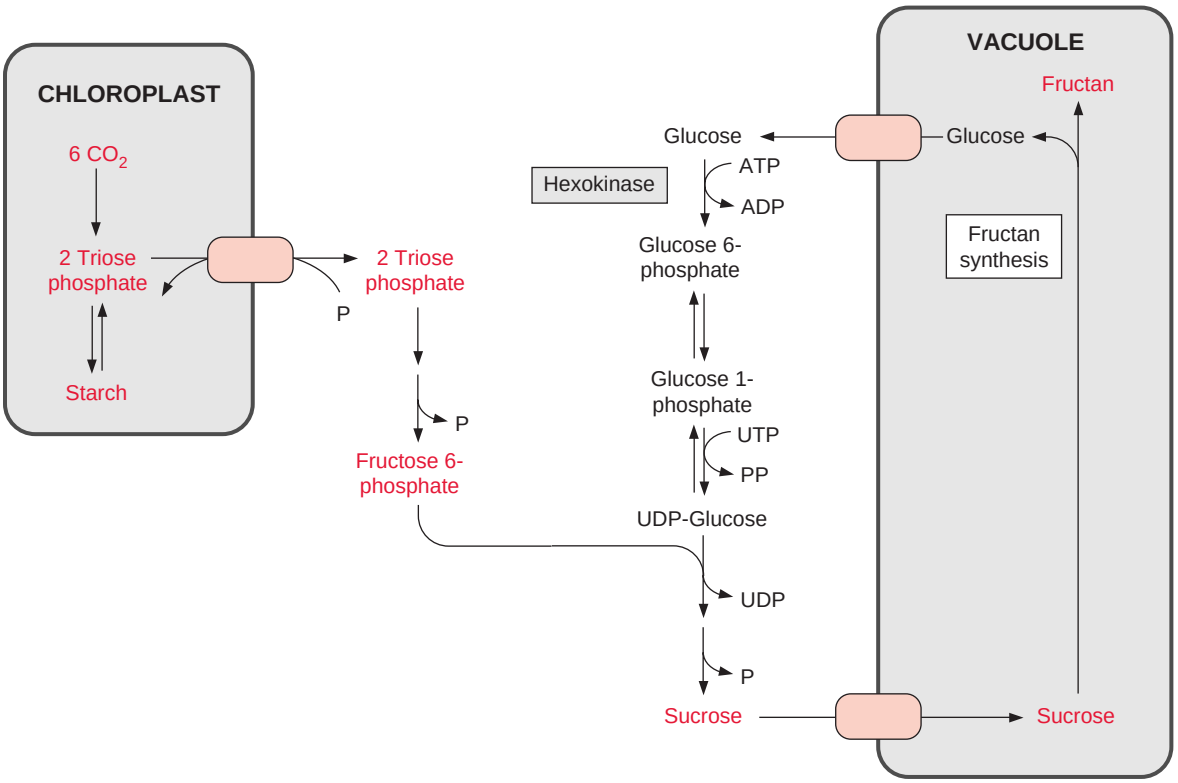

Figure 9.24 The conversion of CO_2 assimilates to fructan. Fructose 6-phosphate, which is provided as a product of photosynthesis to the cytosol, is first converted to sucrose. The glucose required for this reaction is synthesized as a by-product in the synthesis of fructan in the vacuole (see Fig. 9.23). Phosphorylation is catalyzed by a cytosolic hexokinase. The entry of sucrose into the vacuole and the release of glucose from the vacuole are facilitated by different translocators.

The large size of the leaf vacuoles, often comprising about 80% of the total cellular volume, provides the plant with a very advantageous storage capacity for carbohydrates in the form of fructans. Thus, in leaves, on top of the diurnal carbohydrate stores such as transitory starch and sucrose, an additional carbohydrate reserve is maintained to serve purposes such as rapid seed production or endurance of unfavorable growth conditions.

9.6 Cellulose is synthesized by enzymes located in the plasma membrane

Cellulose, an important cell constituent (section 1.1), is a glucan in which the glucose residues are linked by (β1→4)-glycosidic bonds forming a very long chain (Fig. 9.25). The synthesis of cellulose is catalyzed by **cellulose synthase** located in the plasma membrane. The required glucose molecules are delivered as **UDP-glucose** from the cytosol, and the newly synthesized cellulose chain is excreted into the extracellular compartment (Fig. 9.26). It has been shown in cotton-producing cells—a useful system for studying cellulose synthesis—that UDP-glucose is supplied from cytosolic sucrose by the action of a membrane-bound **sucrose synthase** (see section 9.2). The UDP-glucose released is transferred directly to the cellulose synthase.

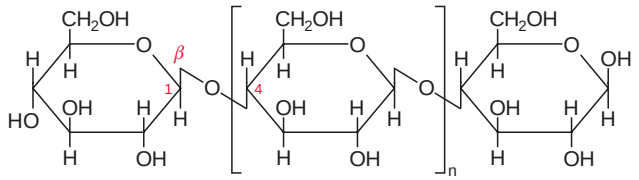

β-1,4-Glucan: cellulose

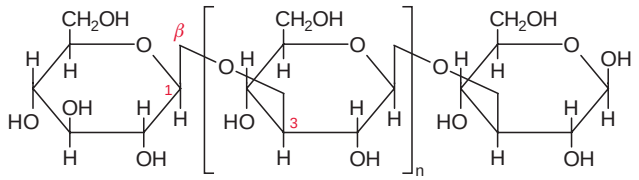

β-1,3-Glucan: callose

Figure 9.25 Cellulose and callose.

Alternatively UDP-glucose is synthesized from glucose 1-phosphate and UTP, catalyzed by UDP-glucose pyrophosphorylase (section 9.2). The synthesis of cellulose starts with the transfer of a glucose residue from UDP-glucose to **sitosterol** (Fig. 15.3), a plasma membrane lipid. The glucose residue is bound to the hydroxyl group of the membrane lipid via a glycosidic linkage and acts as a primer for the cellulose synthesis, thus anchoring the growing cellulose chain to the membrane. Cellulose never occurs in single chains but always in a crystalline array of many chains called a **microfibril** (section 1.1). It is assumed that, due to the many neighboring cellulose synthases in the membrane, all β-1,4-glucan chains of a microfibril are synthesized simultaneously and spontaneously assemble to a microfibril.

Synthesis of callose is often induced by wounding

Callose is a **β-1,3-glucan** (Fig. 9.25) with a long unbranched helical chain. Callose forms very compact structures and functions as a **universal insulation material** in the plant. In response to wounding of a cell, large amounts of callose can be synthesized very rapidly at the plasma membrane. According to present knowledge, its synthesis proceeds like the synthesis of cellulose (shown in Fig. 9.26). Membrane-bound sucrose synthase provides UDP-glucose for callose synthesis. Callose synthesis is stimulated by an increase in the cytosolic Ca^{++} concentration. Wounding is accompanied by a Ca^{++} influx and an increase of the cytosolic Ca^{++} concentration, thus inducing the synthesis of callose for insulation. Plasmodesmata of injured cells are closed by callose formation in order to prevent damage to other cells of the symplast (section 1.1). Moreover, callose serves as a filling material to close defective sieve tubes (section 13.2).

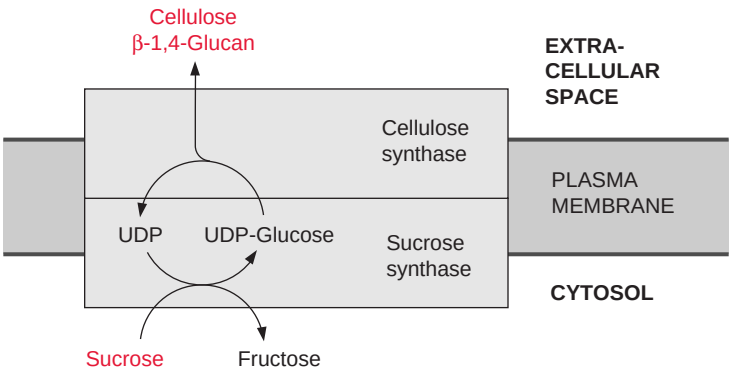

Figure 9.26 Synthesis of β-1,4-glucan chains is catalyzed by a membrane-bound cellulose synthase. The UDP-glucose required is delivered from sucrose by a membrane-bound sucrose synthase.

Cell wall polysaccharides are also synthesized in the Golgi apparatus

In contrast to the synthesis of cellulose and callose localized outside of the plasma membrane, the synthesis of the cell wall polysaccharides hemicellulose and pectin takes place in the Golgi apparatus. In the synthesis GDP activated hexoses (e.g., **GDP-mannose** and **GDP-fucose)** are involved. The transfer of the polysaccharides synthesized in the Golgi apparatus to the cell wall proceeds via exocytotic vesicle transport.

Further reading

Ball, S. G., Mrell, M. From bacterial glycogen to starch: Understanding of the biogenesis of the plant starch granule. Annual Review Plant Biology, 54, 207–233 (2003).

Blennow, A., Engelsen, S. B., Nielson, T. H., Baunsgaard, L., Mikkelsen, R. Starch phosphorylation: A new front line in starch research. Trends in Plant Science 7, 445–449 (2002).

Cairns, A. J., Pollock, C. J., Gallagher, J. A., Harrison, J. Fructans: Synthesis and regulation. In Photosynthesis: Physiology and Metabolism. R. C. Leagood, T. D. Sharkey, S. von Caemmerer (eds.) pp. 301–351. Kluwer Academic Publishers, Dordrecht, Nederland (2000).

Cairns, A. J. Fructan biosynthesis in transgenic plants. Journal Experimental Botany 54, 549–567 (2003).

Fischer, K., Weber, A. Transport of carbon in non-green plastids. Trends in Plant Science 7, 345–351 (2002).

Joshi, C. P., Mansfield, S. D. The cellulose paradox—Simple molecule, complex biosynthesis. Current Opinion in Plant Biology 10, 220–226 (2007).

Lloyd, J. R., Kossmann, J., Ritte, G. Leaf starch degradation comes out of the shadow. Trends in Plant Science 10, 130–137 (2005).

Lu, Y., Sharkey, T. D. The importance of maltose in transitory starch breakdown. Plant Cell Environment 29, 353–366 (2006).

Lytovchenko, A., Sonnewald, U., Fernie, A. The complex network of non-cellulosic carbohydrate metabolism. Current Opinion in Plant Biology 10, 227–235 (2007).

Matthew, P. Trehalose-6-phosphate. Current Opinion in Plant Biology 10, 303–309 (2007).

Mendel, G. Versuche über Pflanzen-Hybriden. Verhandlung Naturforscher-Verein Brünn 4, 3–47 (1865).

Neuhaus, H. E. Transport of primary metabolites across the plant vacuolar membrane. FEBS Letters 581, 2223–2226 (2007).

Nielsen, T. H., Rung, J. H., Villadsen, D. Fructose-2,6-bisphosphate: A traffic signal in plant metabolism. Trends in Plant Science 9, 556–563 (2004).

Niittylä, T., Messerli, G., Trevisan., M., Chen, J., Smith, A. M., Zeeman, S. C. A previously unknown maltose transporter essential for starch degradation in leaves. Science 303, 87–89 (2004).

Paul, M. Trehalose 6-phosphate. Current Opinion Plant Biology 10, 303–309 (2007).

Peng, L., Kawagoe, Y., Hogan, P., Delmer, D. Sitosterol-β-glucoside as primer for cellulose synthesis in plants. Science 295, 147–150 (2002).

Ramon, M., Rolland, F. Plant development; introducing trehalose metabolism. Trends in Plant Science 12, 185–188 (2007).
Ritsema, T., Smeekens, S. Fructans: Beneficial for plants and humans. Current Opinion Plant Biology 6, 223–230 (2003).
Smith, A. M., Stitt, M. Coordination of carbon supply and plant growth. Plant Cell Environment 30, 1126–1149 (2007).
Somerville, C. Cellulose synthesis in higher plants. Annual Review Cell Development Biology 22, 53–78 (2006).
Winter, H., Huber, S. C. Regulation of sucrose metabolism in higher plants: Localization and regulation of activity of key enzymes. Critical Reviews Plant Science 19, 31–67 (2000).
Zeeman, S. C., Smith, S. M., Smith, A. M. The diurnal metabolism of leaf starch. Biochemical Journal 401, 13–28 (2007).
Zimmermann, M. H., Ziegler, H. (1975). List of sugars and sugar alcohols in sieve-tube exudates. In (Zimmermann, M. H.; Milburn, J. A. (eds.)) Encyclopedia of plant physiology, Springer Verlag, Heidelberg, Vol. 1, 480–503 (1975).

10

Nitrate assimilation is essential for the synthesis of organic matter

Living matter contains a large amount of nitrogen incorporated in proteins, nucleic acids, and many other biomolecules. This organic nitrogen is present in oxidation state −III (as in NH_3). During autotrophic growth the nitrogen demand for the formation of cellular matter is met by inorganic nitrogen in two alternative ways:

1. Fixation of molecular nitrogen from air; or
2. Assimilation of the nitrate or ammonia present in water or soil.

Only some bacteria, including cyanobacteria, are able to fix nitrogen (N_2) from air. Some plants enter a symbiosis with N_2-fixing bacteria, which supply them with organic bound nitrogen (Chapter 11). However, about 99% of the organic nitrogen in the biosphere is derived from the assimilation of nitrate. NH_4^+ is formed as an end product of the degradation of organic matter, primarily by the metabolism of animals and bacteria, and is oxidized to nitrate again by nitrifying bacteria in the soil. Thus a continuous cycle exists between the nitrate in the soil and the organic nitrogen in the plants. NH_4^+ accumulates only in poorly aerated soils with insufficient drainage, where, due to lack of oxygen, nitrifying bacteria cannot grow. Mass animal production can lead to a high ammonia input into the soil, not only from manure but also from the air. If NH_4^+ instead of nitrate is available, many plants can utilize it as a nitrogen source.

10.1 The reduction of nitrate to NH_3 proceeds in two reactions

Nitrate is assimilated in the leaves and also in the roots. In most fully grown herbaceous plants, nitrate assimilation occurs primarily in the leaves, although nitrate assimilation in the roots often plays a major role at an early growth state of these plants. In contrast, many woody plants (e.g., trees, shrubs), as well as legumes such as soybean, assimilate nitrate mainly in the roots.

The transport of nitrate into the root cells proceeds via symport with two protons (Fig. 10.1). A proton gradient across the plasma membrane, generated by an H^+-P-ATPase (section 8.2), drives the uptake of nitrate against a concentration gradient. The ATP required for the formation of the proton gradient is provided mostly by **mitochondrial respiration**. When inhibitors or uncouplers of respiration abolish mitochondrial ATP synthesis in the roots, nitrate uptake normally comes to a stop. Root cells contain several **nitrate transporters** in their plasma membrane; among these are a transporter with a relatively low affinity (half saturation $>500 \times 10^{-6}$ mol/L nitrate) and a transporter with a very high affinity (half saturation $20–100 \times 10^{-6}$ mol/L nitrate), where the latter is induced only when required by metabolism. In this way the capacity of nitrate uptake into the roots is adjusted to the environmental conditions. The efficiency of the nitrate uptake systems enables plants to grow when the external nitrate concentration is as low as 10×10^{-6} mol/L.

The nitrate taken up into the root cells can be stored temporarily in the vacuole. As discussed in section 10.2, nitrate is reduced to NH_4^+ in the epidermal and cortical cells of the root. This NH_4^+ is used mainly for the synthesis of **glutamine** and **asparagine** (collectively named amide in Fig. 10.1). These two amino acids can be transported to the leaves via the **xylem vessels**. However, when the capacity for nitrate assimilation in the roots reaches its maximum, nitrate is released from the roots into the xylem vessels and is carried by the transpiration stream to the leaves. The uptake into the mesophyll cells occurs probably also by a proton symport. Large quantities of nitrate can be stored in the vacuole. This vacuolar store may be emptied by nitrate assimilation during the day and replenished during the night. Thus for instance in spinach leaves the highest nitrate content is found in the early morning.

The nitrate in the mesophyll cells is first reduced to nitrite by **nitrate reductase** present in the **cytosol** and then to NH_4^+ by **nitrite reductase** in the **chloroplasts** (Fig. 10.1).

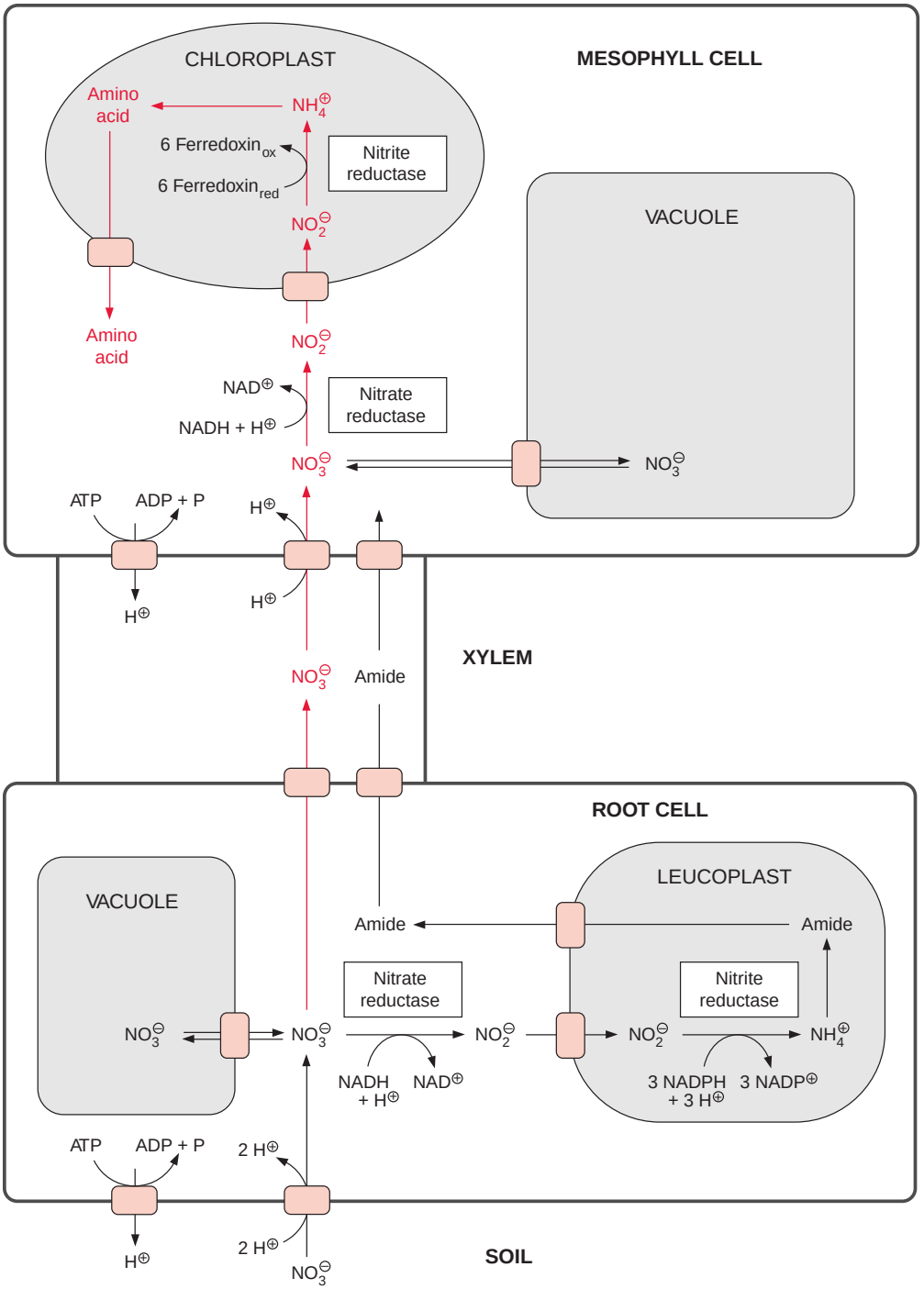

Figure 10.1 Nitrate assimilation in the roots and leaves of a plant. Nitrate is taken up from the soil by the root. It can be stored in the vacuoles of the root cells or assimilated in the cells of the root epidermis and the cortex. Surplus nitrate is carried via the xylem vessels to the mesophyll cells, where nitrate can be stored temporarily in the vacuole. Nitrate is reduced to nitrite in the cytosol and then nitrite is reduced further in the chloroplasts to NH_4^+, from which amino acids are formed. H^+ transport out of the cells of the root and the mesophyll proceeds via an H^+-P-ATPase.

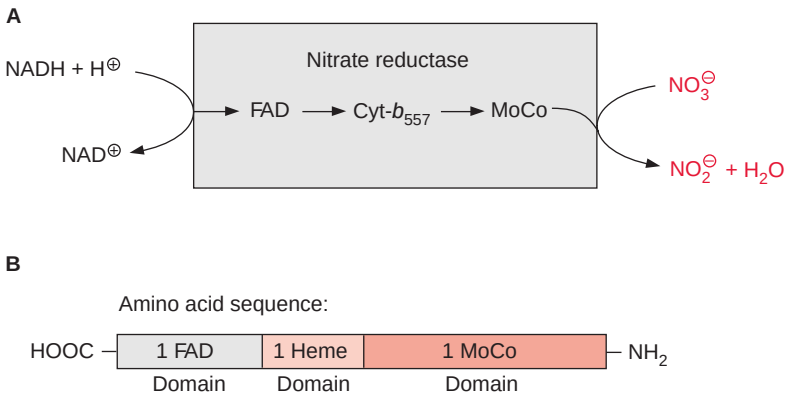

Figure 10.2 A. Nitrate reductase transfers electrons from NADH to nitrate. B. The enzyme contains three domains where FAD, heme, and the molybdenum cofactor (MoCo) are bound.

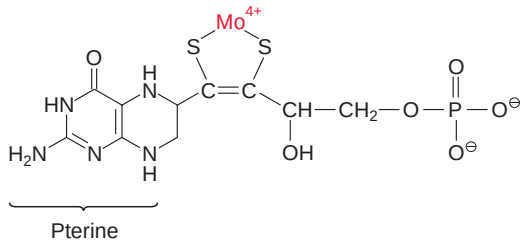

Figure 10.3 The molybdenum cofactor (MoCo).

Nitrate is reduced to nitrite in the cytosol

Nitrate reduction uses mostly NADH as reductant, although some plants contain a nitrate reductase reacting with NADPH as well as with NADH. The **nitrate reductase** of higher plants consists of two identical subunits. The molecular mass of each subunit varies from 99 to 104 kDa, depending on the species. Each subunit comprises an electron transport chain (Fig. 10.2) consisting of one **flavin adenine dinucleotide** molecule (FAD), one heme of the **cytochrome-*b*** type (cyt-b_{557}), and one cofactor containing molybdenum (Fig. 10.3). The latter is a **pterin** with a side chain to which the molybdenum is attached by two sulfur bonds and is called the **molybdenum cofactor**, abbreviated **MoCo**. The bound Mo atom probably changes between oxidation states +IV and +VI. The three redox carriers of nitrate reductase are each covalently bound to the subunit of the enzyme. The protein chain of the subunit can be cleaved by limited proteolysis into three domains, each of which contains only one of the redox carriers. These separated domains, as well as the holoenzyme, are able to catalyze via their redox carriers electron transport to artificial electron acceptors (e.g., from NADPH to Fe^{+++} ions via the FAD domain or from reduced methylviologen (Fig. 3.39) to

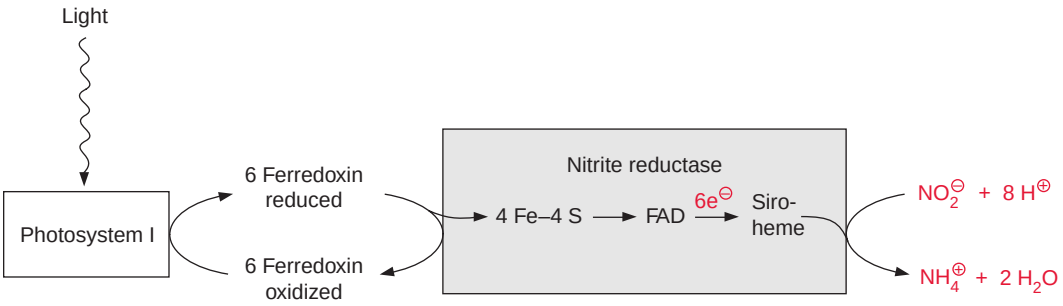

Figure 10.4 Nitrite reductase in chloroplasts transfers electrons from ferredoxin to nitrite. Reduction of ferredoxin by photosystem I is shown in Figure 3.16.

nitrate via the Mo domain). Moreover, nitrate reductase reduces chlorate (ClO_3^-) to chlorite (ClO_2^-). The latter is a very strong oxidant and therefore highly toxic to plant cells. In the past chlorate was used as an inexpensive nonselective herbicide for keeping railway tracks free of vegetation.

The reduction of nitrite to ammonia proceeds in the plastids

The reduction of nitrite to ammonia requires the uptake of six electrons. This reaction is catalyzed by only one enzyme, the **nitrite reductase** (Fig. 10.4), which is located exclusively in plastids. This enzyme utilizes reduced ferredoxin as electron donor, which is supplied as a product of photosynthetic electron transport by photosystem I (Fig. 3.31). To a much lesser extent, the reduced ferredoxin can also be provided during darkness via reduction by NADPH. The latter is generated by the oxidative pentose phosphate pathway present in chloroplasts and leucoplasts (Figs. 6.21, 10.8).

Nitrite reductase contains a covalently bound **4Fe-4S cluster** (see Fig. 3.26), one molecule of **FAD**, and one siroheme. **Siroheme** (Fig. 10.5) is a cyclic tetrapyrrole with one Fe atom in the center. Its structure is different from that of heme as it contains additional acetyl and propionyl residues deriving from pyrrole synthesis (see section 10.5).

The 4Fe-4S cluster, FAD, and siroheme form an electron transport chain by which electrons are transferred from ferredoxin to nitrite. Nitrite reductase has a very high affinity for nitrite. The capacity for nitrite reduction in the chloroplasts is much greater than that for nitrate reduction in the cytosol. Therefore all nitrite formed by nitrate reductase can be completely converted to ammonia. This is important since nitrite is toxic to

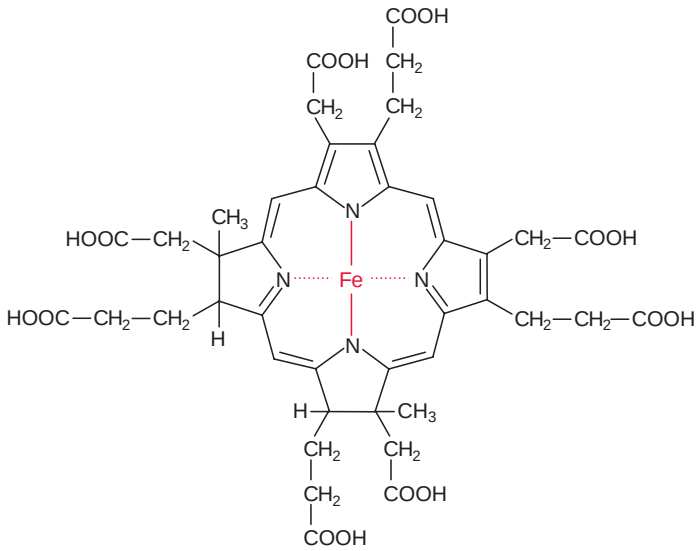

Siroheme

Figure 10.5 Structure of siroheme.

the cell. It forms diazo compounds with amino groups of nucleobases ($R–NH_2$), which are converted into alcohols with the release of nitrogen.

$$R - NH_2 + NO_2^- \rightarrow [R - N = N - OH + OH^-] \rightarrow R - OH + N_2 + OH^-$$

Thus, for instance, cytosine can be converted to uracil. This reaction can lead to mutations in nucleic acids. The very efficient reduction of nitrite by plastid nitrite reductase prevents nitrite from accumulating in the cell.

The fixation of NH_4^+ proceeds in the same way as in the photorespiratory cycle

Glutamine synthetase in the chloroplasts transfers the newly formed NH_4^+ at the expense of ATP to glutamate, forming glutamine (Fig. 10.6). The activity of glutamine synthetase and its affinity for NH_4^+ ($Km \approx 5 \cdot 10^{-6}$ mol/L) are so high that the NH_4^+ produced by nitrite reductase is completely assimilated into glutamine. Glutamine synthetase also fixes the NH_4^+ released during photorespiration (see Fig. 7.9). Due to the high rate of photorespiration, the amount of NH_4^+ produced by the oxidation of glycine is about 5 to 10 times higher than generated by nitrate assimilation. Thus only a minor proportion of glutamine synthesis in the leaves results from nitrate assimilation. Leaves also contain an isoenzyme of glutamine synthetase in their cytosol.

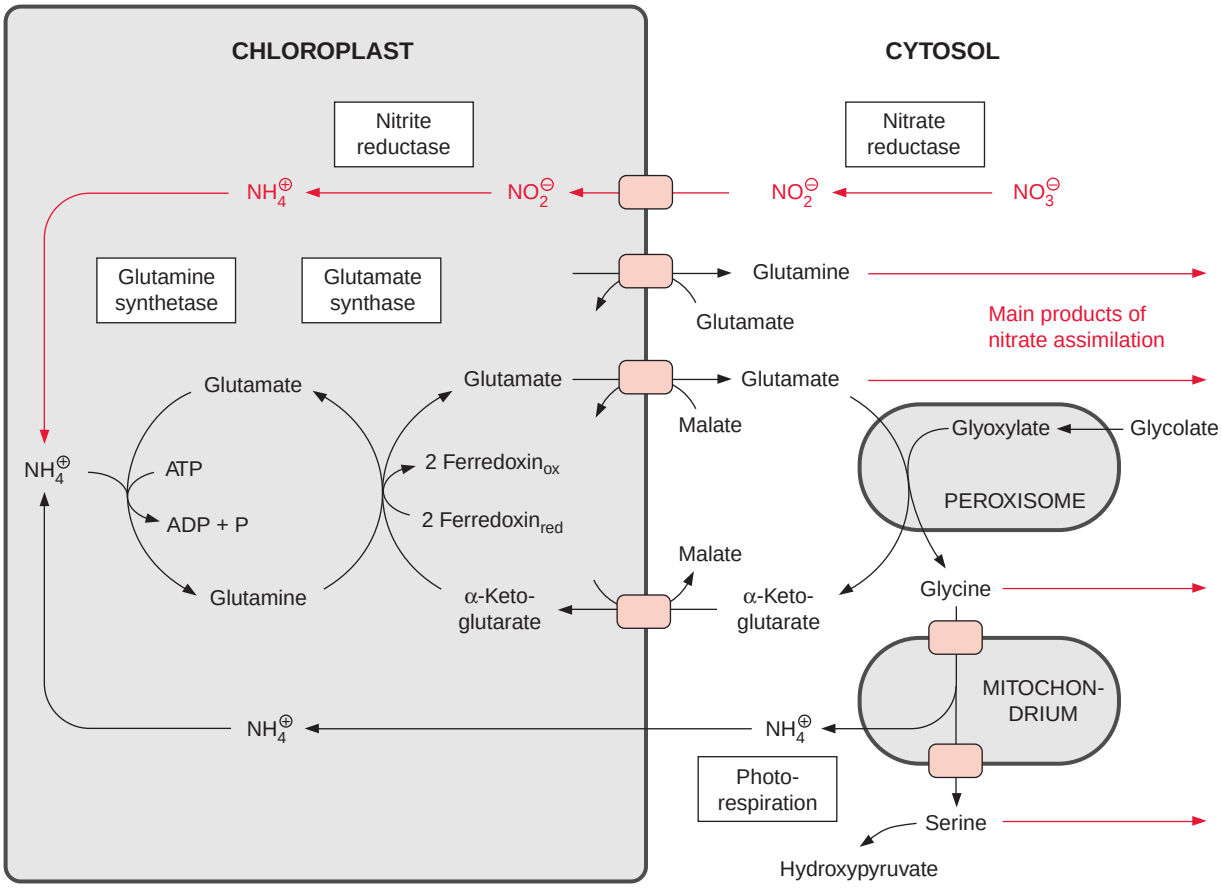

Figure 10.6 Compartmentation of nitrate assimilation reactions and the photorespiratory pathway in mesophyll cells. NH_4^+ formed in the photorespiratory pathway is colored black and NH_4^+ formed by nitrate assimilation is colored red. The main products of nitrate assimilation are marked with a red arrow.

Glufosinate (Fig. 10.7), a substrate analogue of glutamate, is a strong inhibitor of the glutamine synthetase. When glufosinate is applied to plants the synthesis of glutamine is inhibited and subsequently toxic levels of ammonia accumulate. Glufosinate is a herbicide (section 3.6) and commercially available under the trade name Basta (Bayer Crop Science). This herbicide degrades rapidly in the soil, without the accumulation of toxic degradation products. Recently glufosinate-resistant crop plants have been generated by genetic engineering, enabling the use of glufosinate as a selective herbicide for weed control in growing cultures (section 22.6).

Glutamine together with α-ketoglutarate is converted by **glutamate synthase** (also called glutamine-oxoglutarate aminotransferase, abbreviated

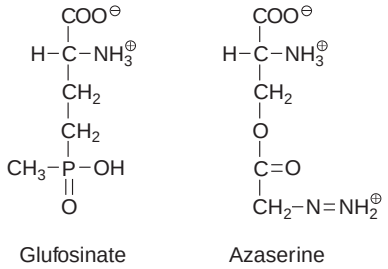

Figure 10.7
Glufosinate (also called phosphinotricin) is a substrate analogue of glutamate and a strong inhibitor of glutamine synthetase. Ammonium glufosinate is a herbicide (Basta, Bayer Crop Science). Azaserine is also a substrate analogue of glutamate and an inhibitor of glutamate synthase.

GOGAT), to two molecules of glutamate (see also Fig. 7.9). Ferredoxin is used as reductant in this reaction. Some chloroplasts and leucoplasts also contain an NADPH-dependent glutamate synthase. Glutamate synthases are inhibited by the substrate analogue **azaserine** (Fig. 10.7), which is toxic to plants.

α-Ketoglutarate, which is required for the glutamate synthase reaction, is transported into the chloroplasts by a specific translocator in counter-exchange for malate, and the glutamate formed is transported out of the chloroplasts into the cytosol by another translocator, also in exchange for malate (Fig. 10.6). Yet another translocator in the chloroplast envelope transports glutamine in counter-exchange for glutamate, enabling the export of glutamine from the chloroplasts.

10.2 Nitrate assimilation also takes place in the roots

As mentioned, nitrate assimilation occurs in part, and in some species even mainly, in the roots. NH_4^+ taken up from the soil is normally fixed in the roots. The reduction of nitrate and nitrite as well as the fixation of NH_4^+ proceeds in the root cells analogously to that of the mesophyll cells. However, in the root cells the necessary reducing equivalents are supplied exclusively by oxidation of carbohydrates. In roots the reduction of nitrite and the subsequent fixation of NH_4^+ (Fig. 10.8) occur in the leucoplasts, a differentiated form of plastids (section 1.3).

The oxidative pentose phosphate pathway in leucoplasts provides reducing equivalents for nitrite reduction

In leucoplasts the reducing equivalents required for the reduction of nitrite and the formation of glutamate are provided by oxidation of glucose

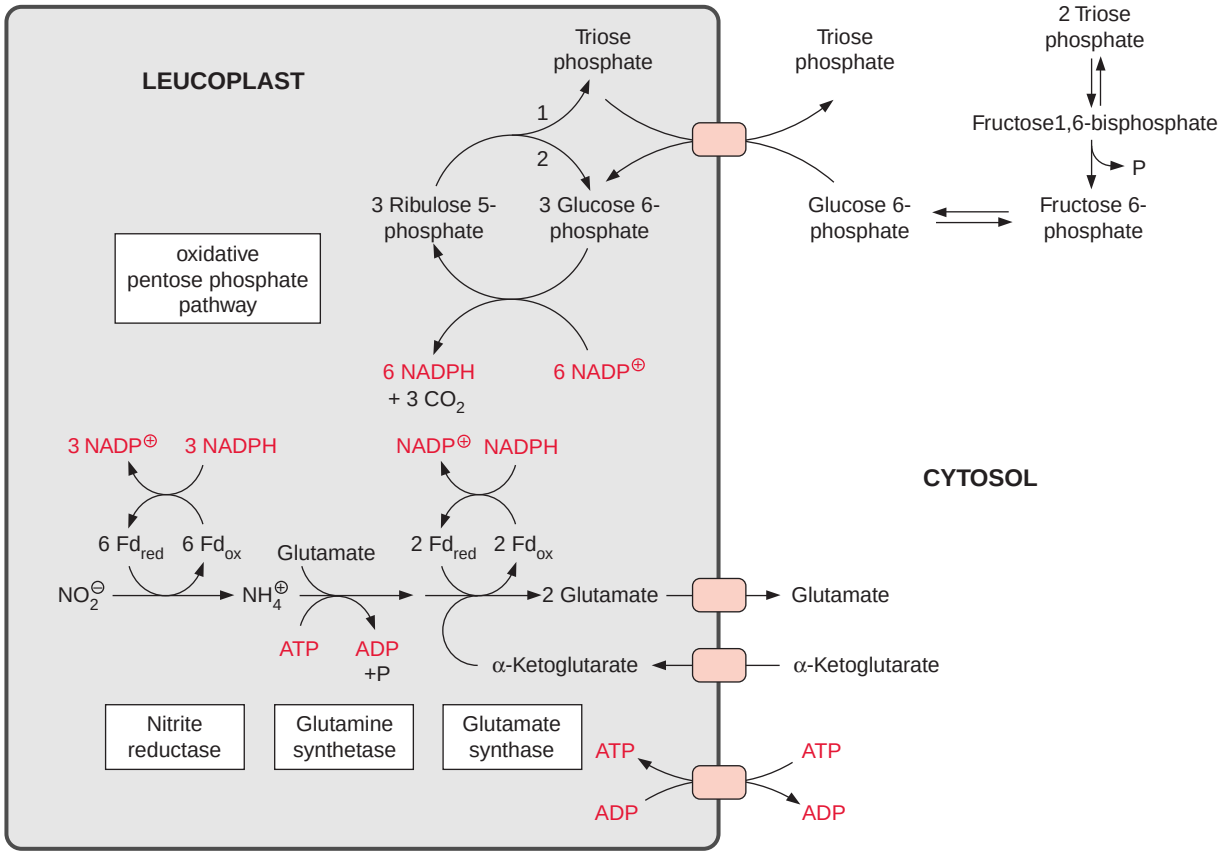

Figure 10.8 The oxidative pentose phosphate pathway provides the reducing equivalents for nitrite reduction in plastids (leucoplasts) from non-green tissues. In some plastids, glucose 1-phosphate is transported in counter-exchange for triose phosphate or phosphate. Fd = ferredoxin.

6-phosphate via the oxidative pentose phosphate pathway (section 6.5, Fig. 10.8). The uptake of glucose 6-phosphate proceeds in counter-exchange for triose phosphate. The **glucose 6-phosphate-phosphate translocator** of leucoplasts differs from the triose phosphate-phosphate translocator of chloroplasts in transporting glucose 6-phosphate in addition to phosphate, triose phosphate, and 3-phosphoglycerate. In the oxidative pentose phosphate pathway, three molecules of glucose 6-phosphate are converted to three molecules of ribulose 5-phosphate with the release of three molecules of CO_2, yielding six molecules of NADPH. The subsequent reactions yield one molecule of triose phosphate and two molecules of fructose 6-phosphate; the latter are reconverted to glucose 6-phosphate via hexose phosphate isomerase. In the cytosol, glucose 6-phosphate is regenerated from two

molecules of triose phosphate via aldolase, cytosolic fructose 1,6-bisphosphatase, and hexose phosphate isomerase. In this way glucose 6-phosphate can be completely oxidized to CO_2 in order to produce NADPH.

As in chloroplasts, nitrite reduction in leucoplasts also requires reduced ferredoxin as reductant. In the leucoplasts, ferredoxin is reduced by NADPH, which is generated by the oxidative pentose phosphate pathway. The ATP required for glutamine synthesis in the leucoplasts can be generated by the mitochondria and transported into the leucoplasts by a plastid ATP translocator in counter-exchange for ADP. Also, the glutamate synthase of the leucoplasts uses reduced ferredoxin as redox partner, although some leucoplasts also contain a glutamate synthase that utilizes NADPH or NADH directly as reductant. Nitrate reduction in the roots provides the shoot with organic nitrogen compounds mostly as **glutamine** and **asparagine** via the transpiration stream in the xylem vessels. This is also the case when NH_4^+ is the nitrogen source in the soil.

10.3 Nitrate assimilation is strictly controlled

During photosynthesis, CO_2 assimilation and nitrate assimilation have to be matched to each other. Nitrate assimilation can progress only when CO_2 assimilation provides the carbon skeletons for the amino acids. Moreover, nitrate assimilation must be regulated in such a way that the production of amino acids does not exceed the demand. Finally, it is important that nitrate reduction does not proceed faster than nitrite reduction, to prevent the accumulation of toxic levels of nitrite (section 10.1). For example, dangerous levels of nitrite may accumulate under anaerobic soil conditions in the case of excessive moisture. Flooded roots are able to release nitrite into the soil water, avoiding the buildup of toxic levels of nitrite. This escape route, however, does not function in leaves, and there the strict control of nitrate reduction is especially important.

The NADH required for nitrate reduction in the cytosol can also be provided during darkness (e.g., by glycolytic degradation of glucose). The reduction of nitrite and fixation of NH_4^+ in the chloroplasts depends largely on photosynthesis providing reducing equivalents and ATP, whereas the oxidative pentose phosphate pathway can offer only limited amounts of reducing equivalents in the dark. Therefore, during darkness nitrate reduction in the leaves has to be slowed down or even switched off to prevent an accumulation of nitrite. This illustrates how essential it is for a plant to regulate the activity of nitrate reductase, which is the entrance step of nitrate assimilation.

The synthesis of the nitrate reductase protein is regulated at the level of gene expression

Nitrate reductase is an exceptionally short-lived protein. Its half-life time is only a few hours. The rate of *de novo* synthesis of this enzyme is very high. Thus, by regulating its synthesis, the activity of nitrate reductase in the tissue can be altered within hours.

Various factors control the synthesis of the enzyme at the level of gene expression. Nitrate and light stimulate the enzyme synthesis. Part of the light effect is caused by carbohydrates generated by photosynthesis. The synthesis of the nitrate reductase protein is stimulated by glucose and other carbohydrates generated by photosynthesis, and is inhibited by NH_4^+, glutamine and other amino acids (Fig. 10.9). Sensors seem to be present in the cell that adjust via regulation of gene expression the capacity of nitrate reductase both to the demand for amino acids and to the supply of carbon skeletons from CO_2 assimilation for its synthesis.

Nitrate reductase is also regulated by reversible covalent modification

The regulation of *de novo* synthesis of nitrate reductase (NR) allows regulation of the enzyme activity within a time span of hours. This would not be sufficient to prevent an acute accumulation of nitrite in the plants during darkening or sudden shading of the plant. Rapid inactivation within minutes of nitrate reductase occurs via **phosphorylation of the nitrate reductase protein** (Fig. 10.9). Upon darkening, a **serine** residue, which is located in the nitrate reductase protein between the heme and the MoCo domain, is phosphorylated by a protein kinase termed **nitrate reductase kinase**. This protein kinase is inhibited by the photosynthesis product triose phosphate and other phosphate esters and is stimulated by Ca^{++} ions, a messenger compound of many signal transduction chains (section 19.1). The phosphorylated nitrate reductase binds an **inhibitor protein**, which interrupts the electron transport between cytochrome-b_{557} and the MoCo domain (Fig. 10.2). The **nitrate reductase phosphatase** hydrolyzes the enzyme's serine phosphate and this causes the inhibitor protein to be released from the enzyme and thus nitrate reductase is restored to an activated state. **Okadaic acid** inhibits nitrate reductase phosphatase and in this way also inhibits the reactivation of nitrate reductase. Since the phosphorylation of the serine residue and the binding of the inhibitor protein are reversible, there is a dynamic equilibrium between the active and inactive form of the nitrate reductase. The inhibition of nitrate reductase kinase by triose phosphate and other phosphate esters ensures that nitrate reductase is active

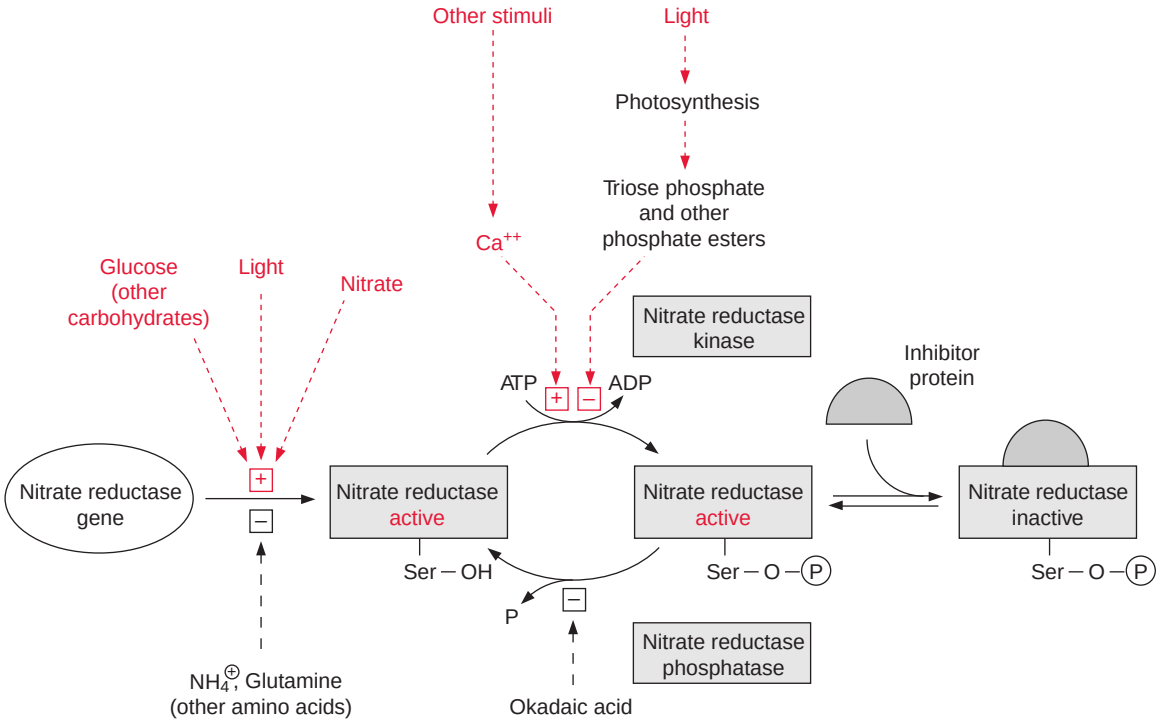

Figure 10.9 Regulation of nitrate reductase (NR). Synthesis of the NR protein is stimulated by carbohydrates (perhaps glucose or its metabolic products) and light [+], and inhibited by glutamine or other amino acids [–]. The newly formed NR protein is degraded within a few hours. Nitrate reductase is inhibited by phosphorylation of a serine residue and the subsequent interaction with an inhibitor protein. After hydrolytic liberation of the phosphate residue by a protein phosphatase, the inhibitor is dissociated and nitrate reductase regains its full activity. There is a dynamic equilibrium between the active and inactive form of the enzyme. The activity of the nitrate reductase kinase is inhibited by products of photosynthesis in the light, such as triose phosphate and other phosphate esters. In this way nitrate reductase is active in the light. Through the effect of Ca^{++} on nitrate reductase kinase other still not identified factors may modulate the activity of nitrate reductase. Okadaic acid, an inhibitor of protein phosphatases, counteracts the activation of nitrate reductase. (After Huber et al., 1996.)

only when CO_2 fixation is operating for delivery of the carbon skeletons for amino acid synthesis, which is discussed in the next section.

14-3-3 proteins are important metabolic regulators

It was discovered that the nitrate reductase inhibitor protein belongs to a family of highly conserved regulatory proteins called **14-3-3 proteins**, which are widely spread throughout the animal and plant worlds. 14-3-3 proteins

bind to a specific binding site of the **target protein with six amino acids** (Arg-X-X-SerP/ThrP-X-Pro), which contain a serine or threonine phosphate in position 4. The importance of these latter amino acids for nitrate reductase was verified in an experiment, in which the serine in the 14-3-3 protein binding site of nitrate reductase was exchanged for alanine via **site directed mutagenesis**; the altered nitrate reductase was no longer inactivated by phosphorylation. 14-3-3 proteins bind to a variety of proteins and change their activity. They form a large family of **multifunctional regulatory proteins**, many isoforms of which occur in a single plant. Thus 14-3-3 proteins regulate in plants the activity of the **H^+-P-ATPase** (section 8.2) of the plasma membrane. 14-3-3 proteins regulate the function of transcription factors (section 20.2) and protein transport into chloroplasts (section 21.3). There are indications that 14-3-3 proteins are involved in the regulation of signal transduction (section 19.1) as they bind to various protein kinases and play a role in defense processes against biotic and abiotic stress. The elucidation of these various functions of 14.3.3 proteins is at present a very hot topic in research.

This important function of the 14-3-3 proteins in metabolic regulation is exploited by the pathogenic fungus *Fusicoccum amygdalis* to attack plants. This fungus forms the compound **fusicoccin**, which binds specifically to the 14-3-3 protein binding sites of various proteins and thus cancels the regulatory function of 14-3-3 proteins. In this way fusicoccin disrupts the metabolism to such an extent that the plant finally dies. This attack proceeds in a subtle way. When *F. amygdalis* infects peach or almond trees, at first only a few leaves are affected. In these leaves the fungus excretes fusicoccin into the apoplasts, from which it is spread via the transpiration stream through the other parts of the plant. Finally, fusicoccin arrives in the guard cells; where it causes an irreversible transformation of the H^+-P-ATPase into the active form resulting in continuously opened stomata (Fig. 8.4). This leads to a very high loss of water; consequently, the leaves wilt, the tree dies, which ultimately is the nutrient source of the fungus.

There are great similarities between the regulation of nitrate reductase and sucrose phosphate synthase

The regulation principle of nitrate reduction by phosphorylation of serine residues by special protein kinases and protein phosphatases is remarkably similar to the regulation of sucrose phosphate synthase discussed in Chapter 9 (Fig. 9.18). Upon darkening, both enzymes are inactivated by phosphorylation, which in the case of nitrate reductase also requires a binding of an inhibitor protein. Both enzymes are reactivated by protein phosphatases, which are inhibited by okadaic acid. Also, sucrose phosphate synthase has

a binding site for 14-3-3 proteins, but its significance for regulation is not yet clear. Although many details are still not known, it is obvious that the basic mechanisms for the rapid light regulation of sucrose phosphate synthase and nitrate reductase are similar.

10.4 The end product of nitrate assimilation is a whole spectrum of amino acids

As described in Chapter 13, the carbohydrates formed as the product of CO_2 assimilation are transported from the leaves via the sieve tubes to various parts of the plants. The transport forms of the carbohydrates are sucrose, sugar alcohols (e.g., sorbitol), or raffinoses, depending on the species. There are no such special transport forms for the products of nitrate assimilation. All amino acids present in the mesophyll cells are exported via the sieve tubes. Therefore the sum of amino acids can be regarded as the final product of nitrate assimilation. Synthesis of these amino acids takes place mainly in the chloroplasts. The pattern of the amino acids synthesized varies largely, depending on the species and the metabolic conditions. In most cases **glutamate** and **glutamine** represent the major portion of the synthesized amino acids. Glutamate is exported from the chloroplasts in exchange for malate and glutamine in exchange with glutamate (Fig. 10.6). Also, **serine** and **glycine**, which are synthesized as intermediate products in the photorespiratory cycle, represent a considerable portion of the total amino acids present in the mesophyll cells. Large amounts of **alanine** are often formed in C_4 plants.

CO_2 assimilation provides the carbon skeletons to synthesize the end products of nitrate assimilation

CO_2 assimilation provides the carbon skeletons required for the synthesis of the various amino acids. Figure 10.10 gives an overview of the origin of the carbon skeletons of individual amino acids.

3-Phosphoglycerate is the most important carbon precursor for the synthesis of amino acids. It is generated in the Calvin cycle and exported from the chloroplasts to the cytosol by the triose phosphate-phosphate translocator in exchange for phosphate (Fig. 10.11). 3-Phosphoglycerate is converted in the cytosol by **phosphoglycerate mutase** and **enolase** to phosphoenolpyruvate (PEP). From PEP two pathways branch off, the reaction via pyruvate kinase leading to **pyruvate**, and via PEP carboxylase to **oxaloacetate**.

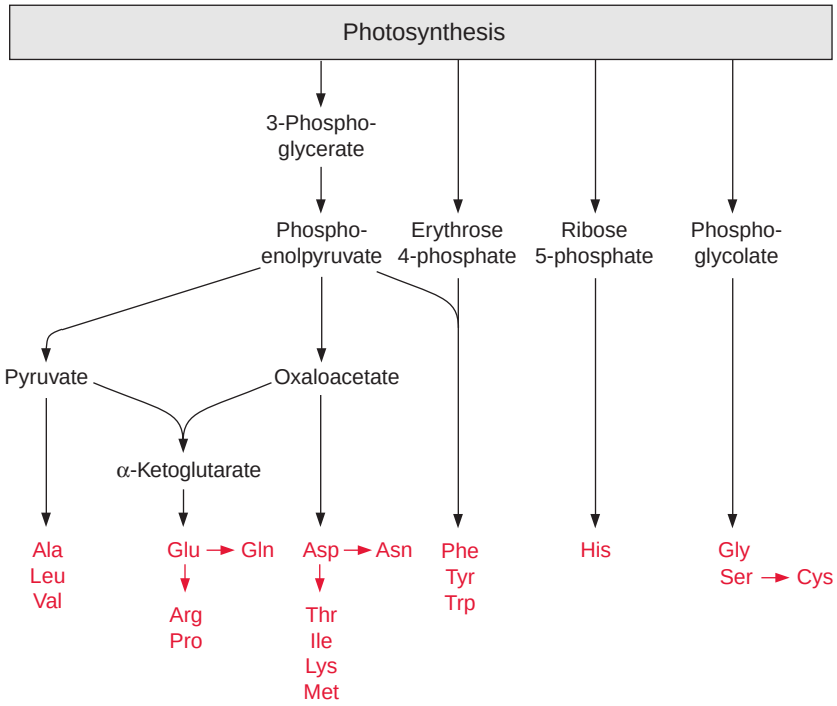

Figure 10.10 Origin of carbon skeletons for various amino acids.

Moreover, PEP together with erythrose 4-phosphate is the precursor for the synthesis of aromatic amino acids via the **shikimate pathway**, discussed later in this chapter. Since the shikimate pathway is located in the chloroplasts, the PEP required is transported via a specific **PEP-phosphate translocator** into the chloroplasts.

The PEP carboxylase reaction has already been discussed in conjunction with the metabolism of stomatal cells (section 8.2) and C_4 and CAM metabolism (sections 8.4 and 8.5). Oxaloacetate formed by PEP carboxylase has two functions in nitrate assimilation:

1. It is converted by transamination to aspartate, which is the precursor for the synthesis of five other amino acids (asparagine, threonine, isoleucine, lysine, and methionine).
2. Together with pyruvate it is the precursor for the formation of α-ketoglutarate, which is converted by transamination to glutamate, being the precursor of three other amino acids (glutamine, arginine, and proline).

Glycolate synthesized by photorespiration is the precursor for the formation of glycine and serine (see Fig. 7.1), and from the latter cysteine is

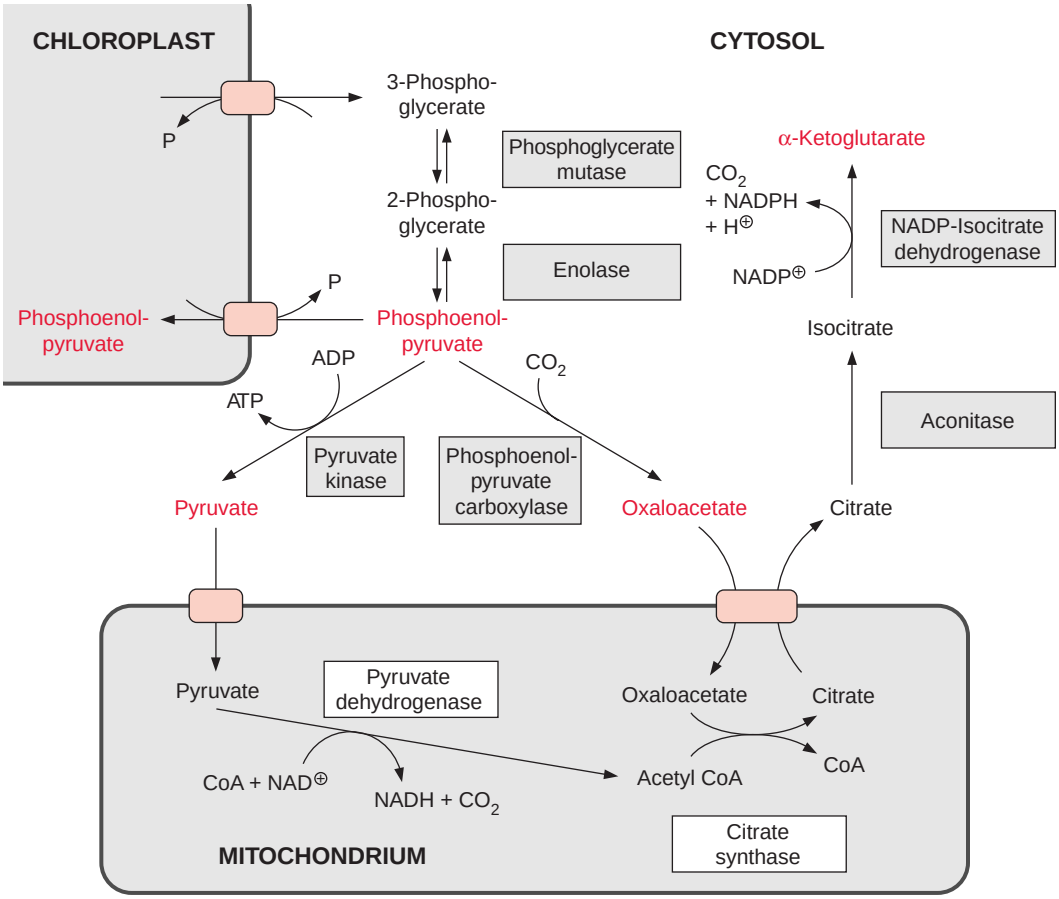

Figure 10.11 Carbon skeletons for the synthesis of amino acids are provided by CO_2 assimilation. Important precursors for amino acid synthesis are colored red.

formed (Chapter 12). In non-green cells, serine and glycine can also be synthesized from 3-phosphoglycerate. Details of this are not discussed here. Ribose 5-phosphate is the precursor for the synthesis of histidine. This pathway has not yet been fully resolved in plants.

The synthesis of glutamate requires the participation of mitochondrial metabolism

Figure 10.6 shows that glutamate is synthesized in the chloroplasts from α-ketoglutarate, which originates from the mitochondrial citrate cycle (Fig. 10.11). Pyruvate and oxaloacetate are transported from the cytosol to the mitochondria by specific translocators. Pyruvate is oxidized by the **pyruvate**

dehydrogenase complex (see Fig. 5.4), and the acetyl-CoA thus generated condenses with oxaloacetate to citrate (see Fig. 5.6). This citrate can be converted in the mitochondria via the citric acid cycle enzyme **aconitase** (Fig. 5.7), oxidized further by **NAD-isocitrate dehydrogenase** (Fig. 5.8), and the resultant α-ketoglutarate can be transported into the cytosol by a specific translocator. Often a major part of the citrate produced in the mitochondria is exported to the cytosol and converted there to α-ketoglutarate by cytosolic isoenzymes of aconitase and NADP-isocitrate dehydrogenase. Citrate is released from the mitochondria by a specific translocator in exchange for oxaloacetate.

Biosynthesis of proline and arginine

Glutamate is the precursor for the synthesis of **proline** (Fig. 10.12). Its δ-carboxylic group is first converted by a **glutamate kinase** to an energy-rich phosphoric acid anhydride and is then reduced by NADPH to an aldehyde. The accompanying hydrolysis of the energy-rich phosphate, resembling the reduction of 3-phosphoglycerate to glyceraldehyde 3-phosphate in the Calvin cycle, drives the reaction. A ring is formed by the intramolecular condensation of the carbonyl group with the α-amino group. Reduction by NADPH results in the formation of proline.

Besides its role as a protein constituent, proline has a special function as a **protective substance against dehydration damage** in leaves. When exposed to aridity or to a high salt content in the soil (both leading to water stress), many plants accumulate very high amounts of proline in their leaves, in some cases several times the sum of all the other amino acids. It is assumed that the accumulation of proline during water stress is caused by the induction of the synthesis of the enzyme protein of **pyrrolin-5-carboxylate reductase**.

Proline protects a plant against dehydration, because, in contrast to inorganic salts, it has no inhibitory effect on enzymes even at very high concentrations. Therefore proline is classified as a **compatible solute**. Other compatible solutes, formed in certain plants in response to water stress, are sugar alcohols such as **mannitol** (Fig. 10.13), and **betains**, consisting of amino acids, such as proline, glycine, and alanine, of which the amino groups are methylated. The latter are termed proline, glycine, and alanine betains. The accumulation of such compatible solutes, especially in the cytosol, chloroplasts, and mitochondria, minimizes the damaging effects of water shortage or high salt content of the soil. These compounds also participate as antioxidants in the elimination of reactive oxygen species (**ROS**) (section 3.9). Water shortage and high salt content of the soil causes an inhibition of CO_2 assimilation, resulting in an overreduction of photosynthetic electron transport carriers, which in turn leads to an increased formation of ROS.

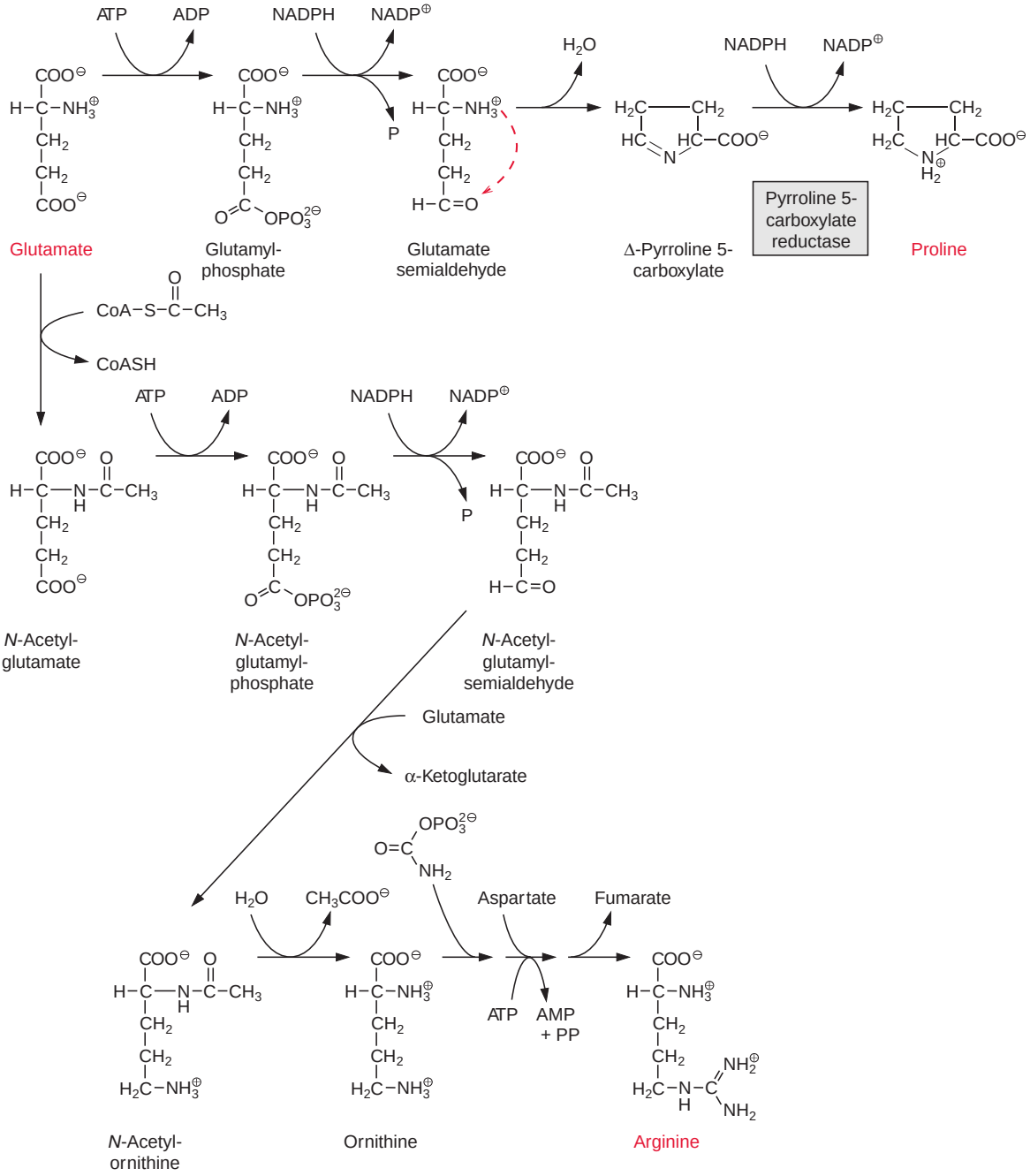

Figure 10.12 Biosynthetic pathways for proline and arginine starting with glutamate as precursor.

In the first step of the synthesis of **arginine**, the α-amino group of glutamate is acetylated by reaction with acetyl-CoA and is thus protected. Subsequently, the δ-carboxylic group is phosphorylated and reduced to a semi-aldehyde in basically the same reaction as in proline synthesis. Here the α-amino group is protected and the formation of a ring is not possible. By transamination with glutamate, the aldehyde group is converted to an amino group, and after cleavage of the acetyl residue, ornithine is formed. The conversion of ornithine to arginine (not shown in detail in Fig. 10.12) proceeds in the same way as in the urea cycle of animals by condensation with carbamoyl phosphate to citrulline. An amino group is transferred from aspartate to citrulline, resulting in the formation of arginine and fumarate.

Aspartate is the precursor of five amino acids

Aspartate is formed from oxaloacetate by transamination with glutamate by **glutamate-oxaloacetate amino transferase** (Fig. 10.14). The synthesis of **asparagine** from aspartate requires a transitory phosphorylation of the terminal carboxylic group by ATP, as in the synthesis of glutamine. In contrast to glutamine synthesis, however, it is not NH_4^+ but the amide group of glutamine that usually serves as the amino donor in asparagine synthesis. Therefore, the energy expenditure for the amidation of aspartate is twice as high as for the amidation of glutamate. Asparagine is formed to a large extent in the roots (section 10.2), especially when NH_4^+ is the nitrogen source in the soil. Synthesis of asparagine in the leaves often plays only a minor role.

For the synthesis of **lysine**, **isoleucine**, **threonine** and **methionine**, the first two steps are basically the same as for proline synthesis: after phosphorylation by a kinase, the γ-carboxylic group is reduced to a semi-aldehyde. For the synthesis of lysine (not shown in detail in Fig. 10.14), the semi-aldehyde condenses with pyruvate and, in a sequence of six reactions involving reduction by NADPH and transamination by glutamate, *meso*-2,6-diaminopimelate is synthesized and from this lysine arises by decarboxylation.

For the synthesis of **threonine**, the semi-aldehyde is further reduced to homoserine. After phosphorylation of the hydroxyl group by homoserine kinase, threonine is formed by isomerization of the hydroxyl group, accompanied by the removal of phosphate. The synthesis of isoleucine from threonine will be discussed in the following paragraph, and the synthesis of methionine in conjunction with sulfur metabolism is discussed in Chapter 12.

Synthesis of amino acids from aspartate is subject to strong feedback control by its end products (Fig. 10.15). Aspartate kinase, the entrance valve for these pathways, is present in two isoforms. One is inhibited by

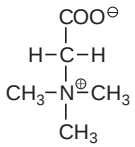

Glycine betaine

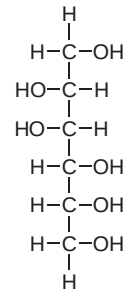

D-Mannitol

Figure 10.13 Two compatible solutes which like proline are accumulated in plants as protective agents against desiccation and high salt levels in the soil.

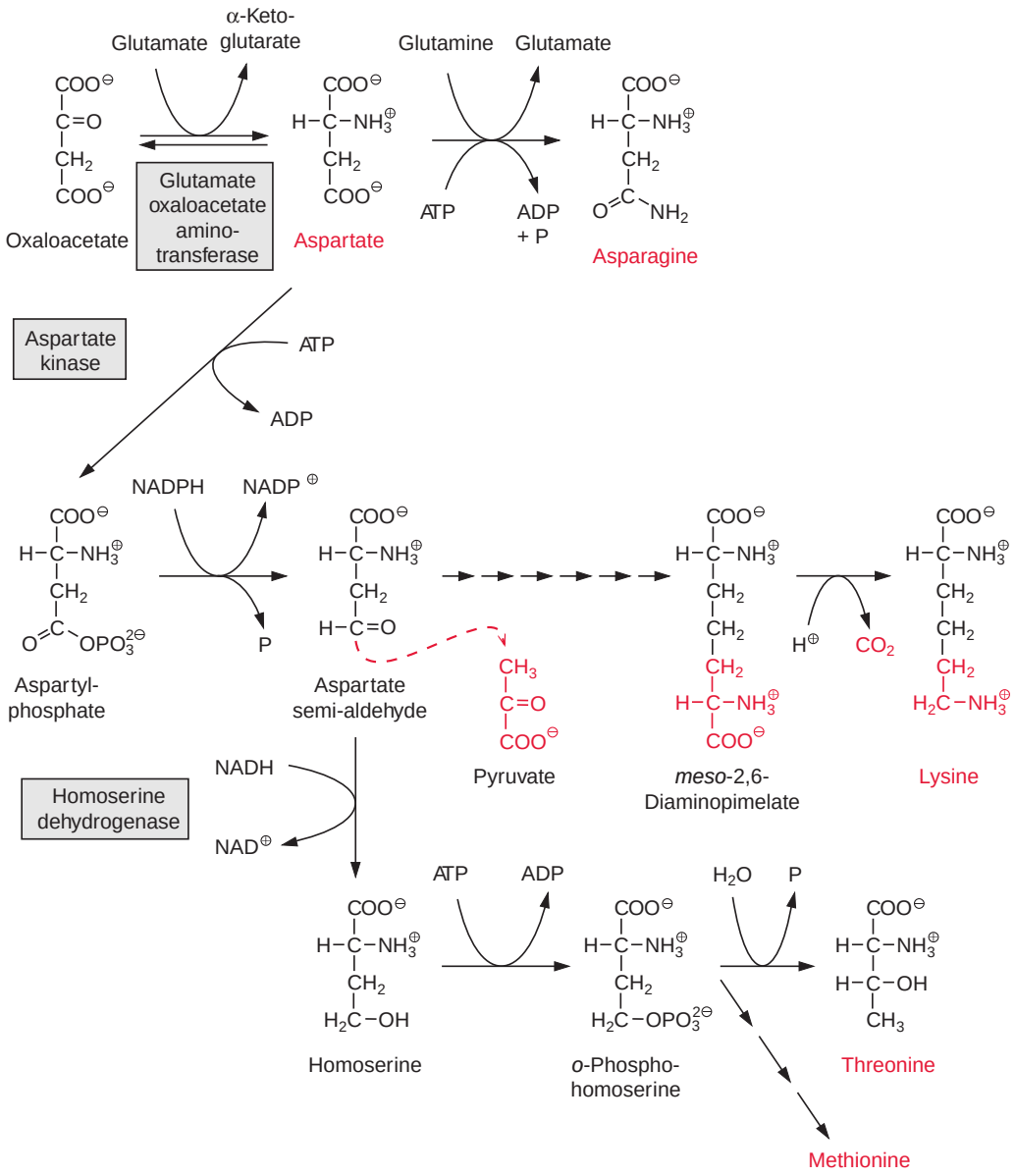

Figure 10.14 The biosynthetic pathway of asparagines, lysine, threonine and methionine starting with aspartate as precursor.

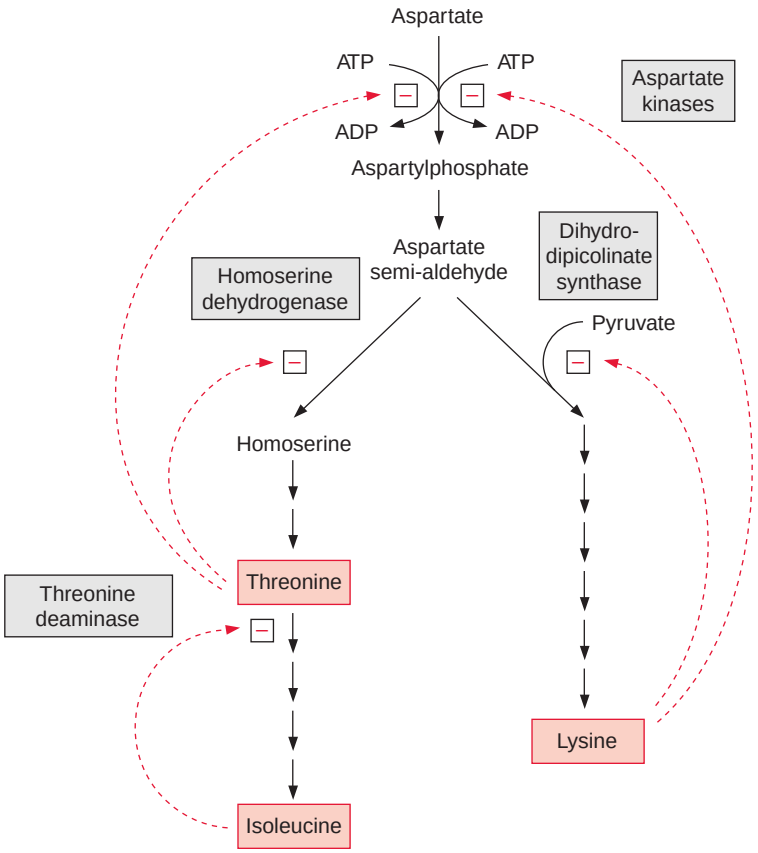

Figure 10.15 End product feedback inhibition regulates the entrance enzyme for the synthesis of amino acids deriving from aspartate according to the cellular demand. [–] indicates inhibition. Aspartate kinase exists in two isoforms.

threonine and the other by lysine. In addition, the reactions that follow aspartate semi-aldehyde at the branch point of both biosynthetic pathways are inhibited by the corresponding end products.

Acetolactate synthase participates in the synthesis of hydrophobic amino acids

Pyruvate can be converted by transamination to **alanine** (Fig. 10.16A). This reaction plays a special role in C_4 metabolism (see Figs. 8.14 and 8.15).

Synthesis of **valine** and **leucine** begins with the formation of acetolactate from two molecules of pyruvate. **Acetolactate synthase**, catalyzing this reaction, contains **thiamine pyrophosphate** (TPP) as prosthetic group. The reaction of TPP with pyruvate yields hydroxyethyl-TPP and CO_2, in the same way as in the pyruvate dehydrogenase reaction (see Fig. 5.4). The hydroxyethyl residue is transferred to a second molecule of pyruvate and thus **ace-**

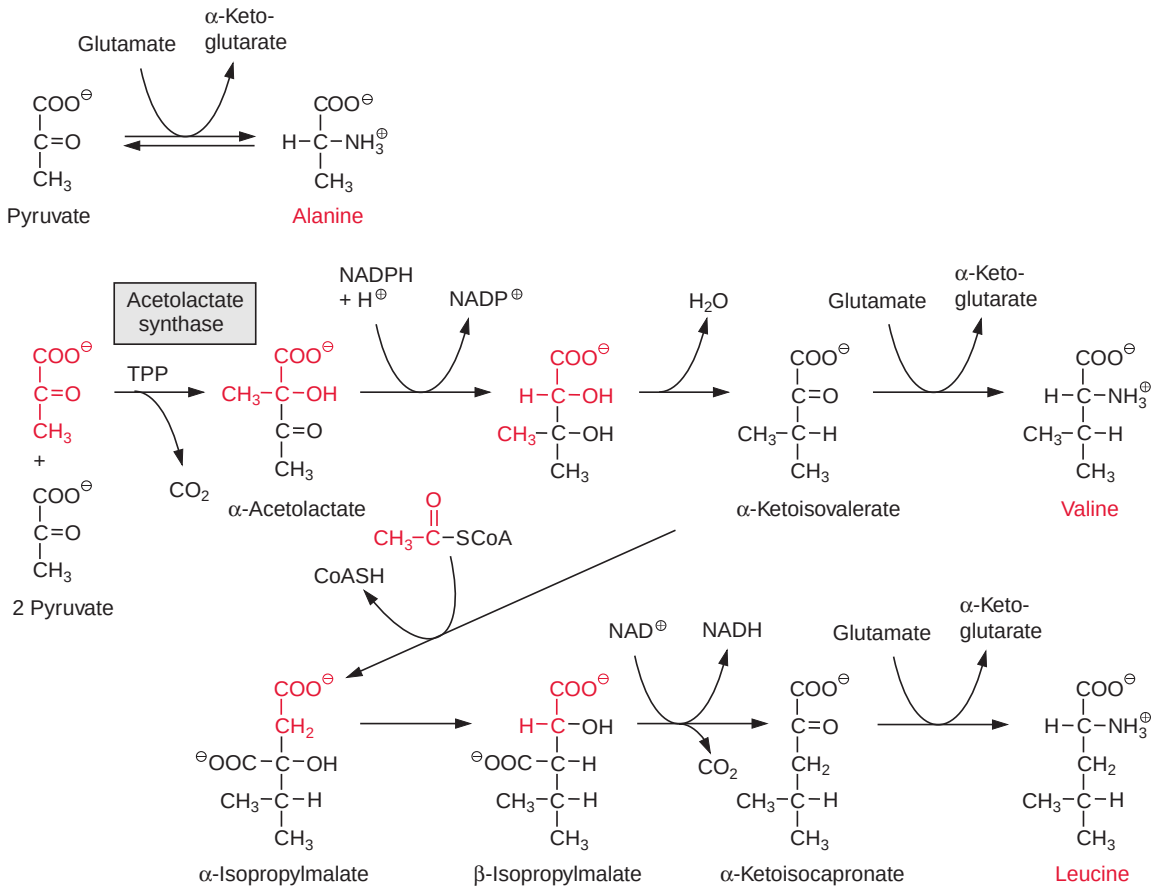

Figure 10.16A Biosynthetic pathway for the synthesis of alanine, valine, and leucine with pyruvate as precursor.

tolactate is synthesized. Its reduction and rearrangement and the release of water yields α-ketoisovalerate and a subsequent transamination by glutamate produces valine.

The formation of **leucine** from α-ketoisovalerate proceeds with basically the same reaction sequences as for the synthesis of glutamate from oxaloacetate shown in Figure 5.3. First, acetyl-CoA condenses with α-ketoisovalerate (analogous to the formation of citrate), the product α-isopropylmalate isomerizes (analogous to isocitrate formation), and the β-isopropylmalate thus formed is oxidized by NAD^+ with the release of CO_2 to α-ketoisocapronate (analogous to the synthesis of α-ketoglutarate by isocitrate dehydrogenase). Finally, in analogy to the synthesis of glutamate, α-ketoisocapronate is transaminated to leucine.

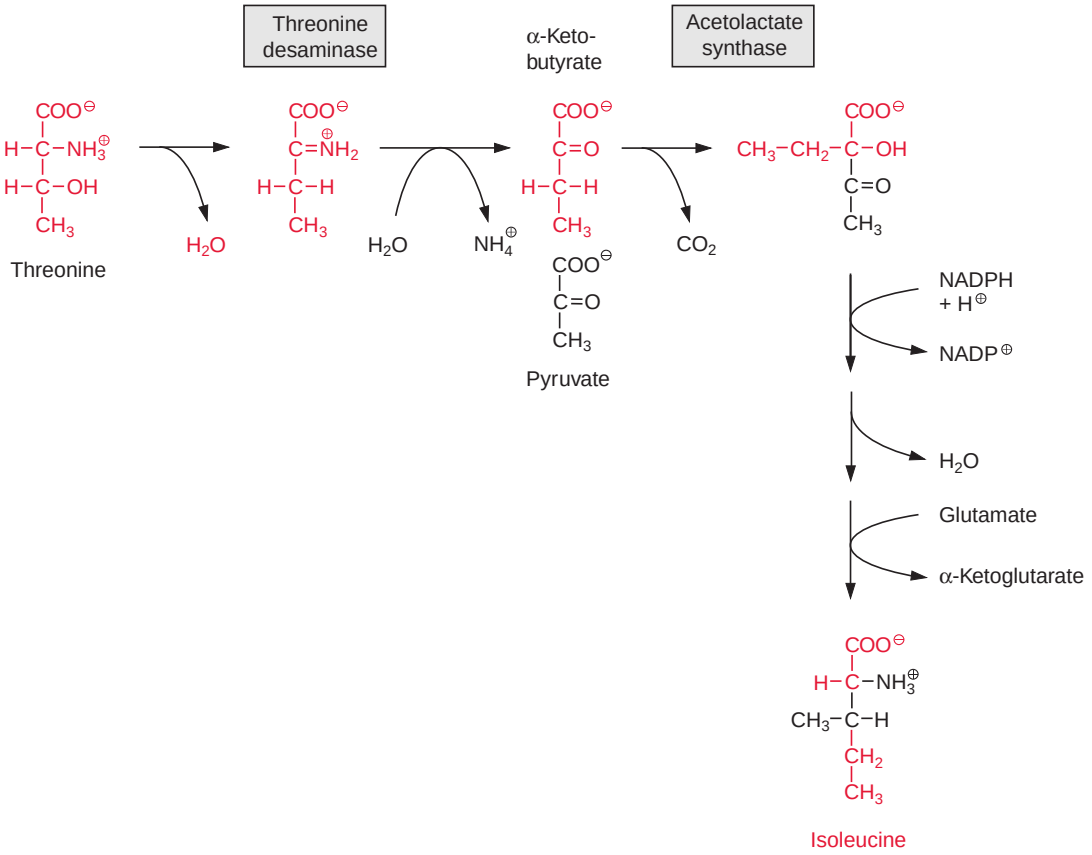

Figure 10.16B Biosynthetic pathway for the synthesis of isoleucine from threonine and pyruvate.

For the synthesis of **isoleucine** from threonine, the latter is first converted by a deaminase to α-ketobutyrate (Fig. 10.16B). Acetolactate synthase condenses α-ketobutyrate with pyruvate in a reaction analogous to the synthesis of acetolactate from two molecules of pyruvate (Fig. 10.16A). Further reactions of the synthesis of isoleucine correspond to the reaction sequence of the synthesis of valine.

The synthesis of leucine, valine, and isoleucine is also subject to feedback control by the end products. Isopropylmalate synthase is inhibited by leucine (Fig. 10.17) and threonine deaminase is inhibited by isoleucine (Fig. 10.15). The first enzyme, **acetolactate synthase** (ALS), is inhibited by valine and leucine. Sulfonyl ureas (e.g., chlorsulfurone) and imidazolinones (e.g., imazethapyr) (Fig. 10.18), are very strong inhibitors of ALS, since these compounds bind to the pyruvate binding site. A concentration as low as

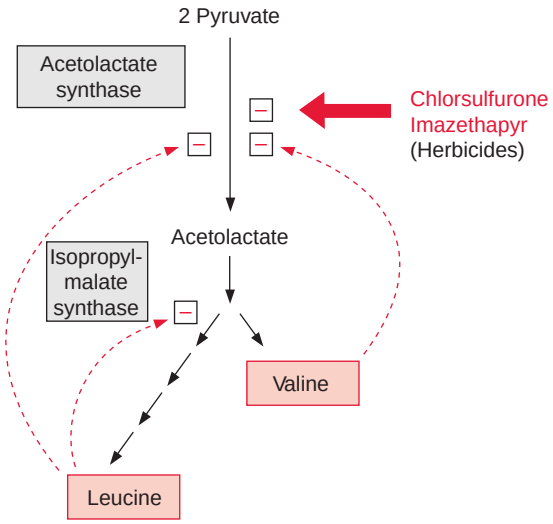

Figure 10.17 Synthesis of valine and leucine is adjusted to the cellular demand by feedback regulation of both amino acids inhibiting acetolactate synthase and leucine inhibiting isopropyl malate synthase. The herbicides chlorsulfurone and imazethapyr also inhibit acetolactate synthase. [–] indicates inhibition.

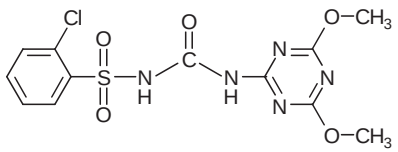

Chlorsulfurone

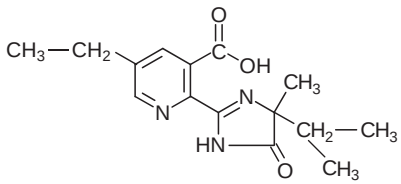

Imazethapyr

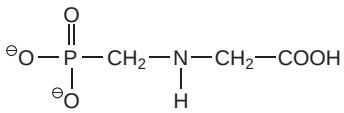

Glyphosate

Figure 10.18 Herbicides: chlorsulfurone, a sulfonyl urea (trade name Glean, DuPont), and imazethapyr, an imidazolinone (trade name Pursuit, ACC), inhibit acetolactate synthase (Fig. 10.16A). Glyphosate (trade name Roundup, Monsanto) inhibits EPSP synthase (Fig. 10.19).

10^{-9}mol/L of chlorsulfurone is sufficient to inhibit ALS by 50%. Since the pathway for the formation of valine, leucine, and isoleucine is present only in plants and microorganisms, the aforementioned inhibitors are suitable to kill specifically plants and are therefore used as **efficient herbicides** (section 3.6).

Chlorsulfurone (trade name Glean, DuPont) is applied as a selective herbicide in the cultivation of cereals, and Imazethapyr (Pursuit, American Cyanamide Co.) is used for protecting soybeans. The application of these herbicides resulted in naturally evolved mutants of maize, soybean, rapeseed, and wheat, which are resistant to sulfonyl ureas or imidazolinones, or even to both herbicides. In each case, a mutation was found in the gene for acetolactate synthase, making the enzyme insensitive to the herbicides without affecting its enzyme activity. By crossing these mutants with other lines, herbicide-resistant varieties have been bred and are, in part, already commercially cultivated.

Aromatic amino acids are synthesized via the shikimate pathway

Precursors for the formation of aromatic amino acids are erythrose 4-phosphate and phosphoenolpyruvate. These two compounds condense to form cyclic dehydrochinate accompanied by the liberation of both phosphate groups (Fig. 10.19). Following the removal of water and the reduction of the carbonyl group, **shikimate** is formed. After protection of the 3′-hydroxyl group by phosphorylation, the 5′-hydroxyl group of shikimate reacts with phosphoenolpyruvate to synthesize the enolether 5′-enolpyruvyl shikimate-3-phosphate (**EPSP**). From this chorismate is formed by the removal of phosphate and represents a branch point for two biosynthetic pathways:

1. Tryptophan is synthesized via four reactions, which are not discussed in detail here.
2. Prephenate is produced by a rearrangement, in which the side chain is transferred to the 1′-position of the ring, and arogenate is formed after transamination of the keto group. Removal of water results in the formation of the third double bond and **phenylalanine** is synthesized by decarboxylation. Oxidation of arogenate by NAD^+, accompanied by a decarboxylation, results in the formation of **tyrosine**. According to recent results, the enzymes of the shikimate pathway are located exclusively in the **plastids**. The synthesis of aromatic amino acids is also controlled at several steps in the pathway by the end products (Fig. 10.20).

Glyphosate acts as a herbicide

Glyphosate (Fig. 10.18), a structural analogue of phosphoenolpyruvate, is a very strong inhibitor of **EPSP synthase**. Glyphosate inhibits specifically the synthesis of aromatic amino acids but has only a low effect on other

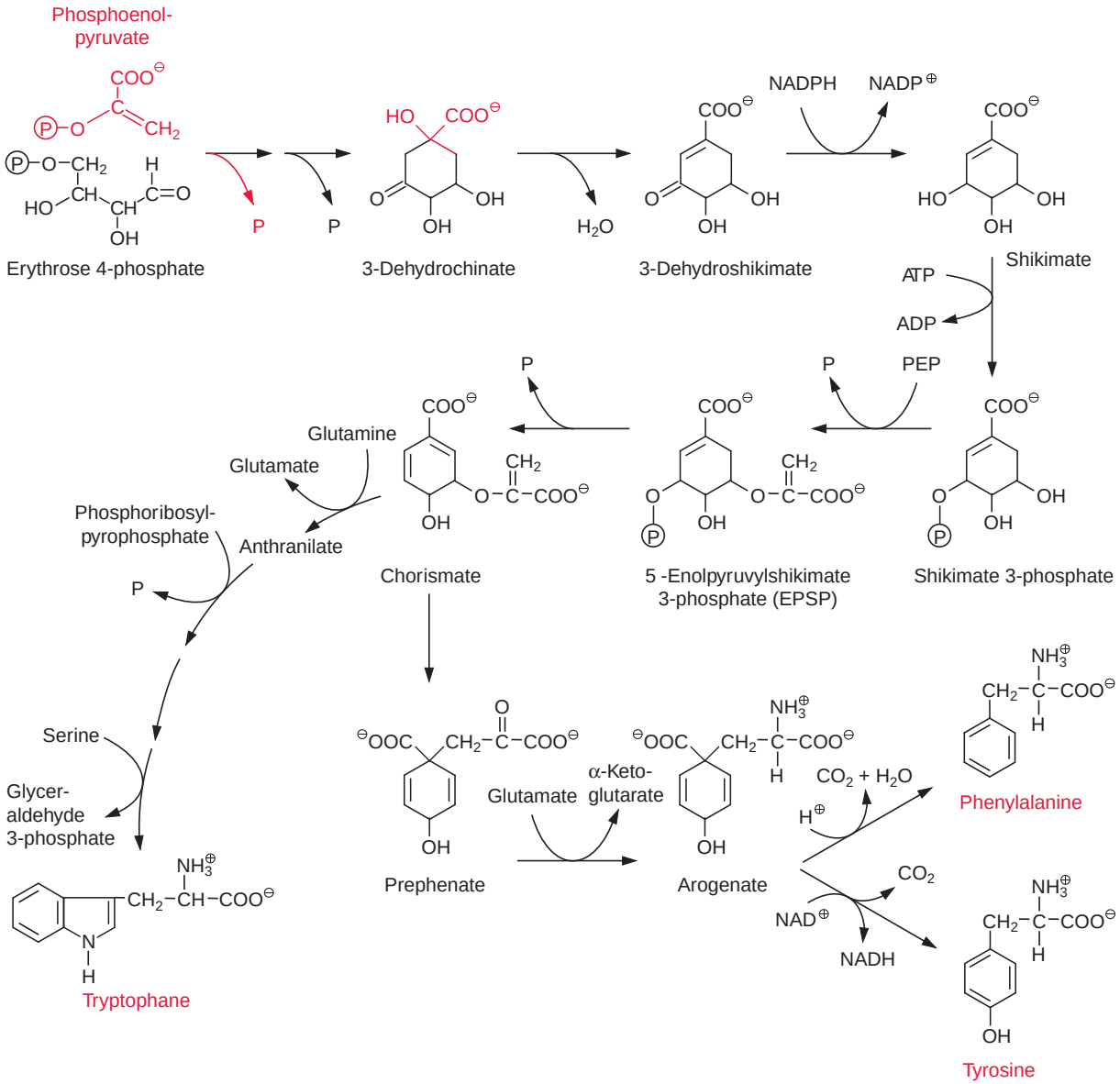

Figure 10.19 Aromatic amino acids (tryptophan, tyrosine, and phenylalanine) are synthesized by the shikimate pathway. PEP = phosphoenolpyruvate.

phosphoenolpyruvate metabolizing enzymes (e.g., pyruvate kinase or PEP carboxykinase). Interruption of the shikimate pathway by glyphosate has a lethal effect on plants. Since the shikimate pathway is not present in animals, glyphosate (under the trade name Roundup, Monsanto) is used as

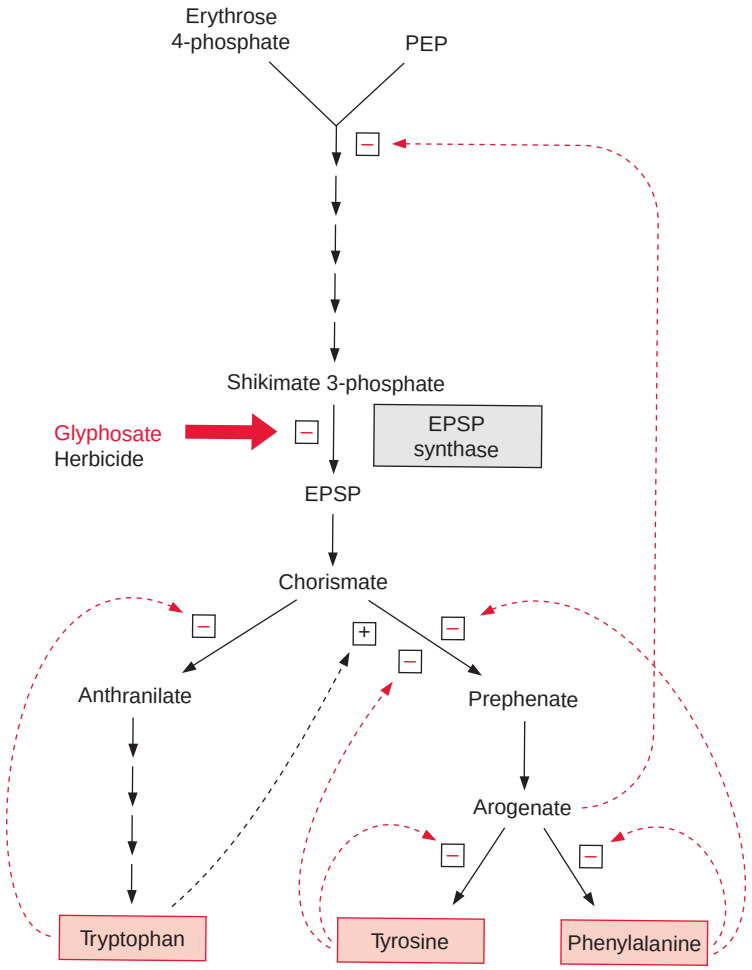

Figure 10.20 Several steps in the synthesis of aromatic amino acids are regulated by product feedback inhibition, thus adjusting the rate of synthesis to the cellular demand. Tryptophan stimulates the synthesis of tyrosine and phenylalanine [+]. The herbicide glyphosate (Fig. 10.18) inhibits EPSP synthase [–].

a selective herbicide (section 3.6). Due to its simple structure glyphosate is relatively quickly degraded by soil bacteria. Glyphosate is the herbicide with the highest sales worldwide. Genetic engineering successfully created glyophosate-resistant crop plants (section 22.6), which allows an efficient weed control in the presence of such transgenic crop plants.

A large proportion of the total plant matter can be formed by the shikimate pathway

The shikimate pathway is not restricted to the generation of amino acids for protein biosynthesis. It also provides precursors for a large variety of other compounds (Fig. 10.21) formed by plants in large quantities, particularly

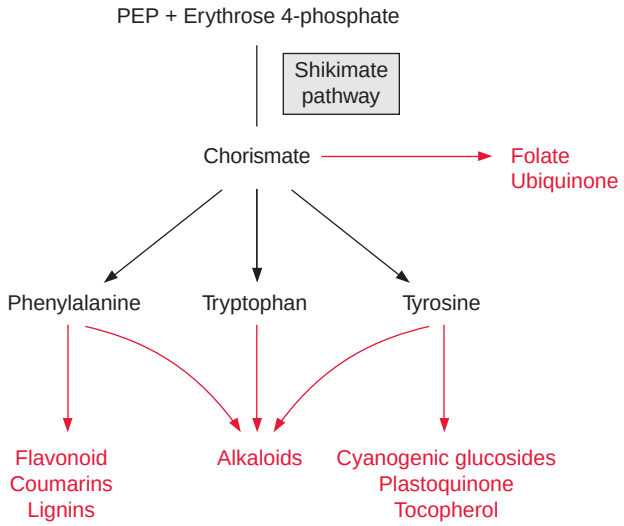

Figure 10.21 Several secondary metabolites are synthesized via the shikimate pathway.

phenylpropanoids such as **flavonoids** and **lignin** (Chapter 18). These products can amount to a high proportion of the total cellular matter, in some plants up to 50% of the dry matter. Therefore the shikimate pathway can be regarded as one of the pronounced biosynthetic pathways of plants.

10.5 Glutamate is the precursor for chlorophylls and cytochromes

Chlorophyll amounts to 1% to 2% of the dry matter of leaves. Its synthesis proceeds in the plastids. As shown in Figure 2.4, chlorophyll consists of a **tetrapyrrole** ring with **magnesium** as the central atom and with a **phytol side chain** as a hydrophobic membrane anchor. **Heme**, likewise a tetrapyrrole, but with **iron** as the central atom, is a constituent of cytochromes and catalase.

Porphobilinogen, a precursor for the synthesis of tetrapyrroles, is formed by the condensation of two molecules of **δ-amino levulinate**. δ-Amino levulinate is synthesized in animals, yeast, and some bacteria from succinyl-CoA and glycine, accompanied by the liberation of CoASH and CO_2. In contrast, the synthesis of δ-amino levulinate in plastids, cyanobacteria, and many eubacteria proceeds by reduction of **glutamate**. As discussed in section 6.3, the difference in redox potentials between a carboxylate and an aldehyde is so high that a reduction of a carboxyl group by NADPH is only

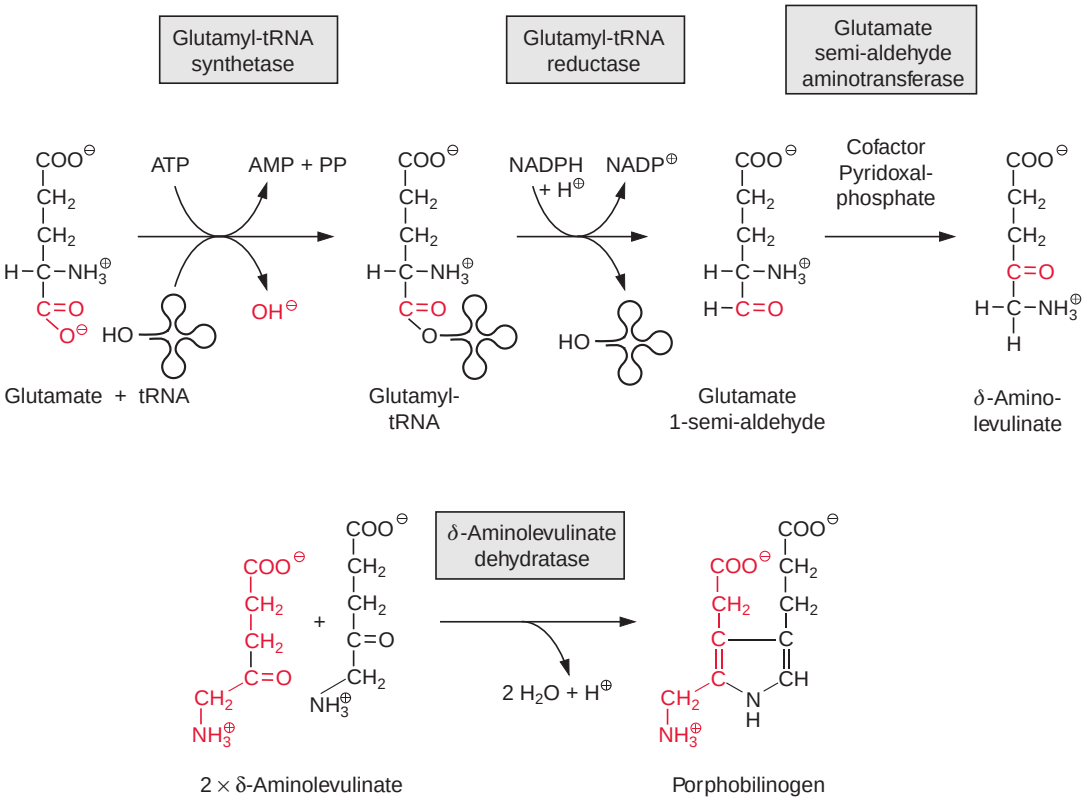

Figure 10.22 In chloroplasts, glutamate is the precursor for the synthesis of δ-amino levulinate. Two molecules are condensed to porphobilinogen.

possible when this carboxyl group has been previously activated (e.g., as a thioester (Fig. 6.10) or as a mixed phosphoric acid anhydride (Fig. 10.12)). In the plastid δ-amino levulinate synthesis, glutamate is activated in a very unusual way by a covalent linkage to a **transfer RNA** (tRNA) (Fig. 10.22). This tRNA for glutamate is encoded in the plastid genome and is involved in the plastids in the synthesis of δ-amino levulinate as well as in protein biosynthesis. As in protein biosynthesis (see Fig. 21.1), the linkage of the carboxyl group of glutamate to tRNA is accompanied by consumption of ATP. During reduction of glutamate tRNA by **glutamate tRNA reductase**, tRNA is liberated and in this way the reaction becomes irreversible. The **glutamate 1-semi-aldehyde** thus formed is converted to δ-amino levulinate by an aminotransferase with **pyridoxal phosphate** as a prosthetic group. This reaction proceeds according to the same mechanism as the aminotransferase reaction shown in Figure 7.4, the only difference being that

the amino group (as amino donor) and the keto group (as amino acceptor) is present in the same molecule.

Two molecules of δ-amino levulinate condense to form porphobilinogen (Fig. 10.22). The open-chain tetrapyrrole hydroxymethylbilan is synthesized from four molecules of porphobilinogen via **hydroxymethylbilan synthase** (Fig. 10.23). The enzyme contains a dipyrrole as cofactor. After the exchange of the two side chains on ring d the closure of the tetrapyrrole ring produces uroporphyrinogen III. Subsequently, protoporphyrin IX is formed by reaction with a decarboxylase and two oxidases (not shown in detail). Mg^{++} is incorporated into the tetrapyrrole ring by **magnesium chelatase** and the resultant Mg-protoporphyrin IX is converted by three more enzymes to protochlorophyllide. The tetrapyrrole ring of protochlorophyllide contains the same number of double bonds as protoporphyrin IX. The reduction of one double bond in ring d by NADPH yields chlorophyllide. **Protochlorophyllide oxido-reductase**, which catalyzes this reaction, is only active when protochlorophyllide is activated by absorption of light. The transfer of a pyrophosphate activated phytyl chain to protochlorophyllide via a prenyl transferase (**chlorophyll synthetase**, see section 17.7) completes the synthesis of chlorophyll.

The light dependence of the protochlorophyllide reductase allows a developing shoot to green only when it reaches the light. Also, the synthesis of the chlorophyll binding proteins of the light harvesting complexes is light-dependent. The exceptions are some gymnosperms (e.g., pine), in which protochlorophyllide reduction as well as the synthesis of chlorophyll binding proteins also progresses during darkness. Unprotected and unbound porphyrins may lead to photochemical cell damage. It is therefore important that intermediates of chlorophyll biosynthesis do not accumulate. To prevent this, the synthesis of δ-amino levulinate is light-dependent, but the mechanism of this regulation is not yet fully understood. Moreover, δ-amino levulinate synthesis is subject to feedback inhibition by chlorophyllide. The end products protochlorophyllide and chlorophyllide inhibit magnesium chelatase (Fig. 10.24). Moreover, intermediates of chlorophyll synthesis control the synthesis of light harvesting proteins (section 2.4) via the regulation of gene expression.

Protophorphyrin is also precursor for heme synthesis

Incorporation of an iron ion into protoporphyrin IX by a **ferro-chelatase** results in the formation of heme. By assembling the heme with apoproteins, chloroplasts are able to synthesize their own cytochromes and phytochromes. Also, mitochondria possess the enzymes for the biosynthesis of cytochromes from protoporphyrin IX, but the corresponding enzyme

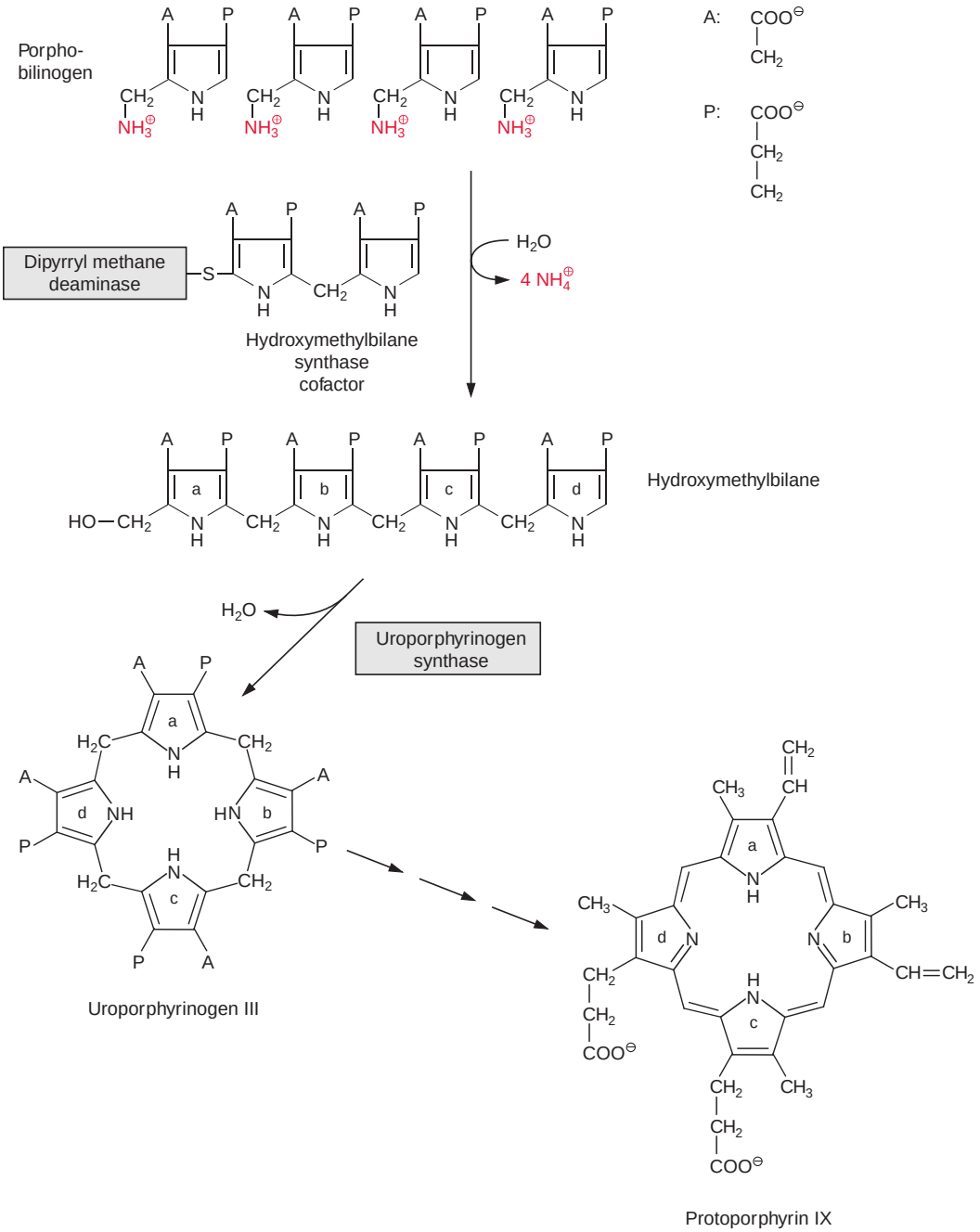

Figure 10.23 Four molecules of porphobilinogen condense and form protoporphyrin.

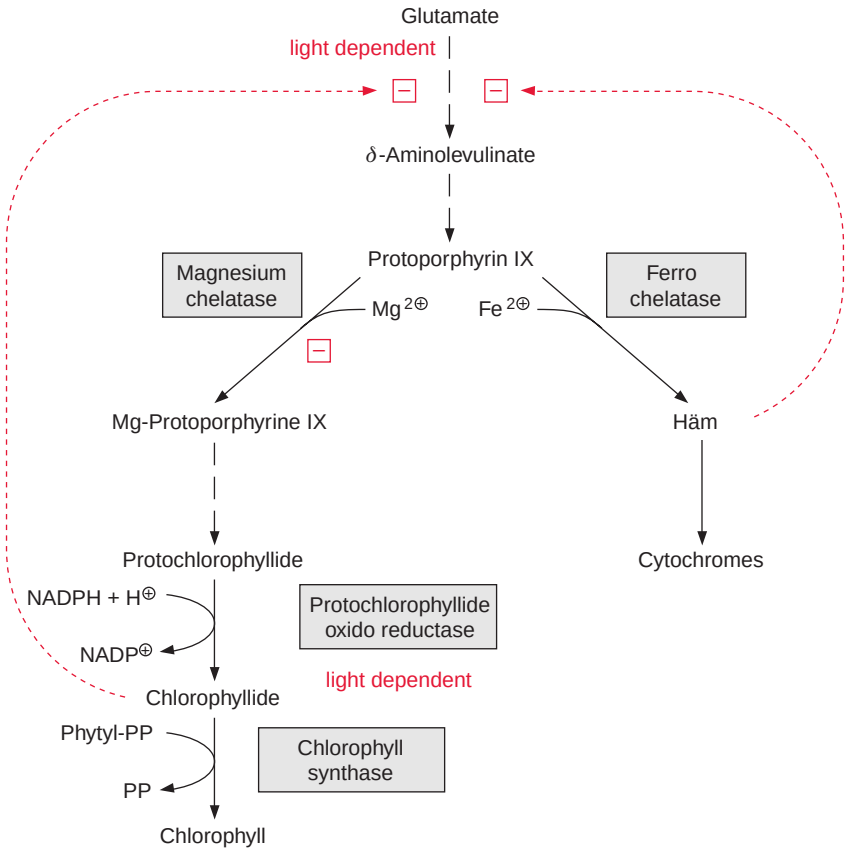

Figure 10.24 Overview of the synthesis of chlorophyll and heme in chloroplasts. The dashed red lines symbolize feedback inhibition of enzymes. Isoenzymes of the biosynthetic pathway from protoporphyrin IX to cytochromes are present in the mitochondria.

proteins are different from those in the chloroplasts. Present knowledge suggests that the heme for mitochondrial cytochromes is synthesized in the mitochondria whereas the heme synthesis of chloroplasts not only serves their own demand but also provides hemes for cytosolic heme proteins.

Further reading

Cornah, J. E., Terry, M. J., Smith, A. G. Green or red: What stops the traffic in the tetrapyrrole pathway? Trends in Plant Science 8, 224–230 (2003).

Curien, G., Biou, V., Mas-Droux, C., Robert-Genthon, M., Ferrer, J. L., Dumas, R. Amino acid biosynthesis: New architectures in allosteric enzymes. Plant Physiology Biochemistry 46, 325–339 (2008).

De Angeli, A., Monachello, D., Ephritikhine, G., Franchisse, J. M., Thomine, S., Gambale, F., Barbier-Brygoo, H. The nitrate/proton antiporter AtCLCa mediates nitrate accumulation in plant vacuoles. Nature 442, 939–942 (2006).

Forde, B. G. Local and long-range signaling pathways regulating plant responses to nitrate. Annual Review Plant Biology 53, 203–224 (2002).

Forde, B. G., Lea, P. Glutamate in plants: Metabolism, regulation, and signaling. Journal Experimental Botany 58, 2339–2358 (2007).

Hasegawa, P. M., Bressan, R. A., Zhu, J.-K., Bohnert, H. J. Plant cellular and molecular responses to high salinity. Annual Review Plant Physiology Plant Molecular Biology 51, 463–499 (2000).

Hermann, K. M., Weaver, L. M. The shikimate pathway. Annual Review Plant Physiology Plant Molecular Biology 50, 473–503 (1999).

Huber, S. C., Mackintosh, C., Kaiser, W. M. Metabolic enzymes as targets for 14-3-3 proteins. Plant Molecular Biology 50, 1053–1063 (2002).

Kaiser, W. M., Stoimenova, M., Man, H.-M. What limits nitrogen reduction in leaves? In C. H. Foyer and G. Noctor (eds.), Advances in Photosynthesis: Photosynthetic Assimilation and Associated Carbon Metabolism (pp. 63–70). Dordrecht, Niederlande: Kluwer Academic Publishers (2002).

Kopriva, S., Rennenberg, H. Control of sulphate assimilation and glutathione synthesis: Interaction with N and C metabolism. Journal Experimental Botany 55, 1831–1842 (2004).

Lillo, C., Meyer, C., Lea, U. S., Provan, F., Oltedal, S. Mechanism and importance of posttranslational regulation of nitrate reductase. Journal Experimental Botany 55, 1275–1282 (2004).

Masuda, T. Recent overview of the Mg branch of the tetrapyrrole biosynthesis leading to chlorophylls. Photosynthesis Research 96, 121–143 (2008).

Miller, A. J., Fan, X., Orsel, M., Smith, S. J., Wells, D. M. Nitrate transport and signalling. Journal Experimental Botany 58, 2297–2306 (2007).

McNiel, S. D., Nuccio, M. L., Hanson, A. D. Betaines and related osmoprotectants. Targets for metabolic engineering of stress resistance. Plant Physiology 120, 945–949 (1999).

Roberts, M. R. 14-3-3 proteins find new partners in plant cell signalling. Trends in Plant Science 8, 218–223 (2003).

Seki, M., Umezawa, T., Urano, K., Shinozaki, K. Regulatory metabolic networks in drought stress responses. Current Opinion Plant Biology 10, 296–302 (2007).

Streatfield, S. J., Weber, A., Kinsman, E. A., Häusler, R. E., Li, J., Post-Breitmiller, D., Kaiser, W. M., Pyke, K. A., Flügge, U.-I., Chory, J. The phosphoenolpyruvate/phosphate translocator is required for phenolic metabolism. Plant Cell 11, 1609–1622 (1999).

Tabuchi, M., Abiko, T., Yamaya, T. Assimilation of ammonium ions and reutilization of nitrogen in rice (*Oryza sativa* L.). Journal Experimental Botany 58, 2319–2327 (2007).

Tanaka, R., Tanaka, A. Tetrapyrrole biosynthesis in higher plants. Annual Review Plant Biology 58, 321–346 (2007).

Zhang, H., Rong, H., Pilbeam, D. Signalling mechanisms underlying the morphological responses of the root system to nitrogen in *Arabidopsis thaliana*. Journal Experimental Botany 58, 2329–2338 (2007).

11

Nitrogen fixation enables plants to use the nitrogen of the air for growth

In a closed ecological system, the nitrate required for plant growth is derived from the degradation of the biomass. In contrast to other plant nutrients (e.g., phosphate or sulfate), nitrate cannot be delivered by the weathering of rocks. Smaller amounts of nitrate are generated by lightning and carried into the soil by rain water (in temperate areas about 5 kg N/ha per year). Due to the effects of civilization (e.g., car traffic, mass animal production, etc.), the amount of nitrate, other nitrous oxides and ammonia carried into the soil by rain can be in the range of 15 to 70 kg N/ha per year. Fertilizers are essential for agricultural production to compensate for the nitrogen that is lost by the withdrawal of harvest products. For the cultivation of maize, for instance, about 200 kg N/ha per year have to be added as fertilizers in the form of nitrate or ammonia. Ammonia, the primary product for the synthesis of nitrate fertilizer, is produced from nitrogen and hydrogen by the **Haber-Bosch process**:

$$3\,H_2 + N_2 \rightarrow 2\,NH_3\ (\Delta H - 92.6\,kJ/mol)$$

Because of the high bond energy of the N≡N triple bond, this synthesis requires a high activation energy and therefore has to be carried out at a pressure of several hundred atmospheres and temperatures of 400–500°C. This involves very high energy costs. The synthesis of nitrogen fertilizer amounts to about one-third of the total energy expenditure for the cultivation of maize. If it were not for the production of nitrogen fertilizer by the Haber-Bosch synthesis, large parts of the world's population could no

longer be fed. Using "organic cycle" agriculture, one hectare of land can feed about 10 people, whereas with the use of nitrogen fertilizer the amount is increased fourfold.

The majority of cyanobacteria and some bacteria are able to synthesize ammonia from atmospheric nitrogen. A number of plants live in symbiosis with N_2-fixing bacteria, which supply the plant with organic nitrogen. In return, the plants provide these bacteria with metabolites for their nutrition. The symbiosis of legumes with **nodule-inducing bacteria** (**rhizobia**) is widespread and important for agriculture. **Legumes**, which include soybean, lentil, pea, clover, and lupines, form a large family (***Leguminosae***) with about 20,000 species. A very large part of the legumes have been shown to form a symbiosis with rhizobia. In temperate climates, the cultivation of legumes can lead to an N_2 fixation of 100 to 400 kg N_2/ha per year. Therefore legumes are important as green manure; in crop rotation they are an inexpensive alternative to artificial fertilizers. The symbiosis of the water fern *Azolla* with the cyanobacterium ***Nostoc*** supplies rice fields with nitrogen. N_2-fixing actinomycetes of the genus ***Frankia*** form a symbiosis with woody plants such as the alder or the Australian *Casuarina*. The latter is a pioneer plant on nitrogen-deficient soils.

11.1 Legumes form a symbiosis with nodule-inducing bacteria

Initially it was thought that the nodules of legumes (Fig. 11.1) were caused by a plant disease, until their function in N_2 fixation was recognized by Hermann Hellriegel (Germany) in 1888. He found that beans containing these nodules were able to grow without nitrogen fertilizer.

The nodule-inducing bacteria include, among other genera, ***Rhizobium***, ***Bradyrhizobium***, and ***Azorhizobium*** and are collectively called **rhizobia**. Species of *Rhizobium* form nodules with peas, species of *Bradyrhizobium* with soybean and species of *Azorhizobium* with the tropical legume *Sesbania*. The rhizobia are strictly aerobic gram-negative rods, which live in the soil and grow heterotrophically in the presence of organic compounds. Some species (*Bradyrhizobium*) are also able to grow **autotrophically** in the presence of H_2, although at a low growth rate.

The uptake of rhizobia into the host plant is a **controlled infection**. The molecular basis of specificity and recognition is still only partially known. The rhizobia form species-specific nodulation factors (**Nod factors**). These are lipochito-oligosaccharides that acquire a high structural specificity (e.g., by acylation, acetylation, and sulfatation). They are like a security key with many notches and open the house of the specific host with which the rhizobia

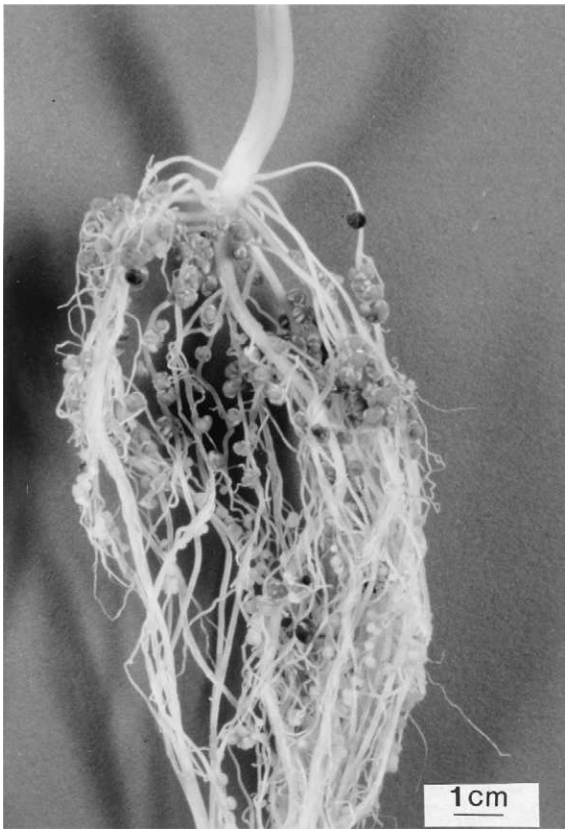

Figure 11.1 Root system of *Phaseolus vulgaris* (bean) with a dense formation of nodules after infection with *Rhizobium etli.* (By P. Vinuesa-Fleischmann and D. Werner, Marburg.)

associate. The Nod factors bind to specific **receptor kinases** of the host**,** which are part of signal transduction chains (section 19.1). In this way the "key" induces the root hair of the host to curl and the root cortex cells to divide, forming the **nodule primordium**. After the root hair has been invaded by the rhizobia, an **infection thread** forms (Fig. 11.2), which extends into the cortex of the roots, branches there and infects the cells of the nodule primordium. A **nodule** thus develops from the infection thread. The morphogenesis of the nodule is of similarly high complexity as any other plant organ such as the root or shoot. The nodules are connected with the root via vascular tissues, which supply them with substrates produced by photosynthesis. The bacteria incorporated into the plant cell are enclosed by a **peribacteroid membrane** (also called a symbiosome membrane), which derives from the plasma membrane of the infected plant cell. The incorporated bacteria are thus separated from the cytoplasm of the host cell in a so-called **symbiosome** (Fig. 11.3). In the symbiosome, the rhizobia differentiate to **bacteroids**. The volume of these bacteroids can be 10 times the

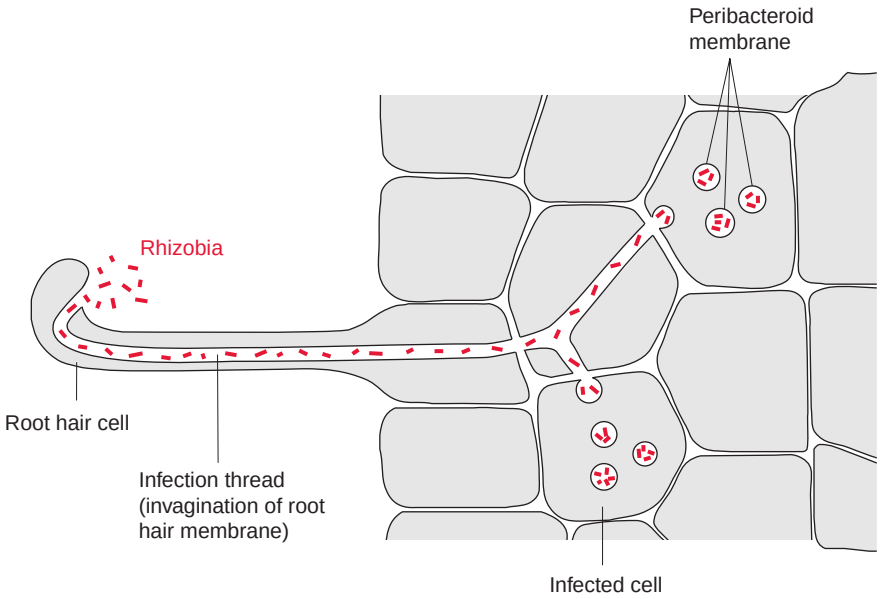

Figure 11.2 Controlled infection of a host cell by rhizobia is induced by an interaction with the root hairs. The rhizobia induce the formation of an infection thread, which is formed by invagination of the root hair cell wall and protrudes into the cells of the root cortex. In this way the rhizobia invaginate the host cell where they are separated by a peribacteroid membrane from the cytosol of the host cells. The rhizobia grow and differentiate into large bacteroids.

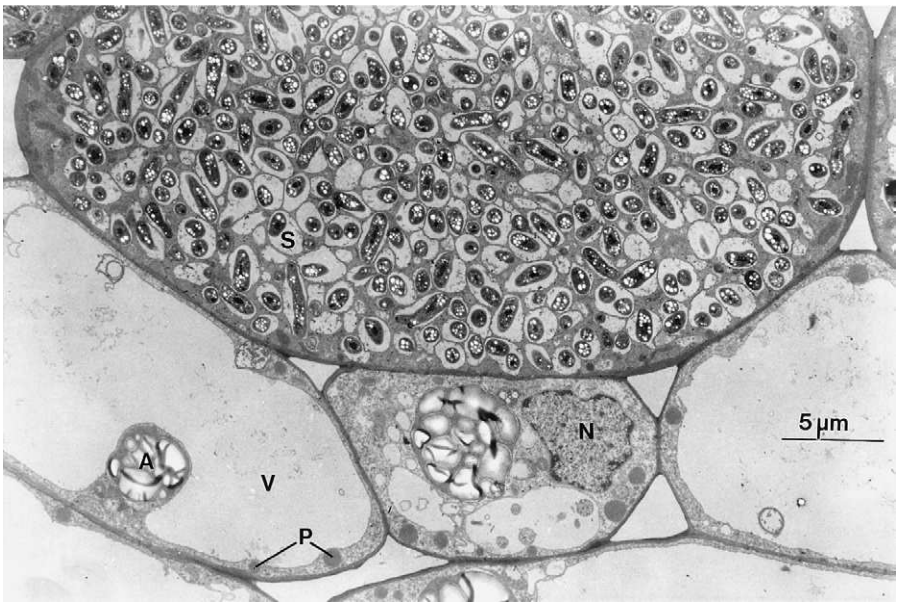

Figure 11.3 Electron microscopic cross-section through a nodule of *Glycine max cv. Caloria* (soybean) infected with *Bradyrhizobium japonicum*. The upper large infected cell shows intact symbiosomes (S) with one or two bacteroids per symbiosome. In the lower section, three noninfected cells with nucleus (N), central vacuole (V), amyloplasts (A), and peroxisomes (P) are to be seen. (By E. Mörschel and D. Werner, Marburg.)

volume of an individual bacterium. Several of these bacteroids are surrounded by a peribacteroid membrane.

Rhizobia possess a respiratory chain which corresponds to the mitochondrial respiratory chain (see Fig. 5.15). In a *Bradyrhizobium* species, an

additional electron transport path develops during differentiation of the rhizobia to bacteroids. This path branches at the cyt-bc_1 complex of the respiratory chain and conducts electrons to another terminal oxidase, enabling an increased respiratory rate. It is encoded by symbiosis-specific genes.

The nodule formation relies on a balanced interplay of bacterial and plant gene expression

Symbiotic rhizobia provide a large number of genes, which are switched off in the free-living bacteria and are activated only after an interaction with the host, to contribute to the formation of an N_2-fixing nodule. The bacterial genes encoding proteins required for N_2 fixation are named ***nif*** and ***fix*** **genes**, and those that induce the formation of the nodules are called ***nod***, ***nol*** and ***noe*** **genes**.

The host plant signals its readiness to form nodules by excreting several **flavonoids** (section 18.5) as signal compounds for the chemo-attraction of rhizobia. These flavonoids bind to a bacterial ***nod*** **gene** protein, which is constitutively expressed (expressed at all times). The protein, to which the flavonoid is bound, activates the transcription of the other *nod*, *nol* and *noe* genes. The proteins encoded by these *nod* genes are involved in the synthesis of the Nod factors. Four, so-called "general" *nod* genes are present in nearly all rhizobia. In addition, more than 20 other *nod* genes are known, which are responsible for the host's specificity.

Those proteins, which are required especially for the formation of nodules, and which are synthesized by the **host plant** in the course of nodule formation, are called **nodulins**. These nodulins include leghemoglobin (section 11.2), the enzymes of carbohydrate degradation (including sucrose synthase (section 9.2)), enzymes of the citrate cycle and the synthesis of glutamine and asparagines, and, if applicable, also of ureide synthesis. They also include an aquaporin of the peribacteroid membrane. Together, these proteins belong to the normal outfit of root cells, but are synthesized at elevated levels during nodule formation. The plant genes encoding these proteins are called **nodulin genes**. One differentiates between "**early**" and "**late**" **nodulins**. "Early" nodulins are involved in the process of infection and formation of nodules, and the expression of the corresponding genes is induced in part by signal compounds released from the rhizobia. "Late" nodulins are only synthesized after the formation of the nodules.

Metabolic products are exchanged between bacteroids and host cells

The main substrate provided by the host cells to the bacteroids is **malate** (Fig. 11.4), synthesized from sucrose, which is delivered by the sieve tubes.

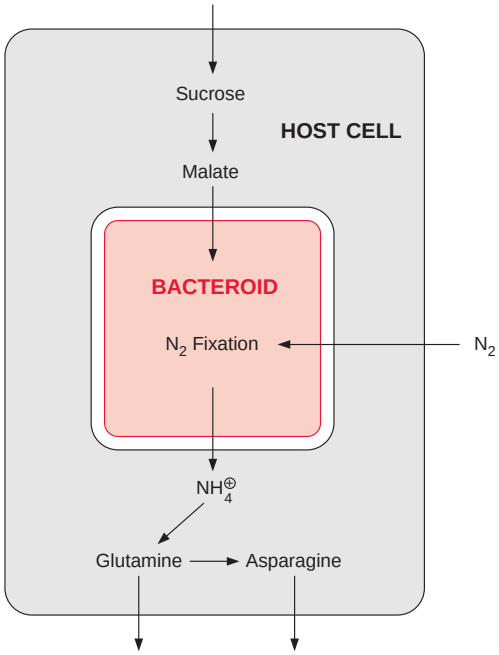

Figure 11.4 Metabolism of infected cells in a root nodule. Glutamine and asparagine are synthesized as the main products of N_2 fixation (see also Fig. 11.5).

The sucrose is metabolized by sucrose synthase in the plant cell (Fig. 13.5), and further converted by glycolysis to phosphoenolpyruvate, which is subsequently carboxylated to oxaloacetate (see Fig. 10.11), and the latter is reduced to malate. Nodule cells contain high activities of phosphoenolpyruvate carboxylase. NH_4^+ is delivered as a product of N_2 fixation via a specific transporter to the host cell, where it is subsequently converted mainly into **glutamine** (Fig. 7.9) and **asparagine** (Fig. 10.14) and then transported via the xylem vessels to the other parts of the plant. It was recently shown that alanine can also be exported from bacteroids.

The nodules of some plants (e.g., soybean) export the fixed nitrogen as ureides (urea degradation products), especially **allantoin** and **allantoic acid** (Fig. 11.5). These compounds have a particularly high nitrogen to carbon (N/C) ratio. The formation of ureides in the host cells requires a complicated synthetic pathway. First, inosine monophosphate is synthesized via the pathway of purine synthesis, which is present in all cells for the synthesis of AMP and GMP, and then it is degraded via xanthine and ureic acid to the ureides.

Malate taken up into the bacteroids (Fig. 11.4) is oxidized by the citrate cycle (Fig. 5.3). The reducing equivalents thus generated are the fuel for the fixation of N_2 (Fig. 11.6).

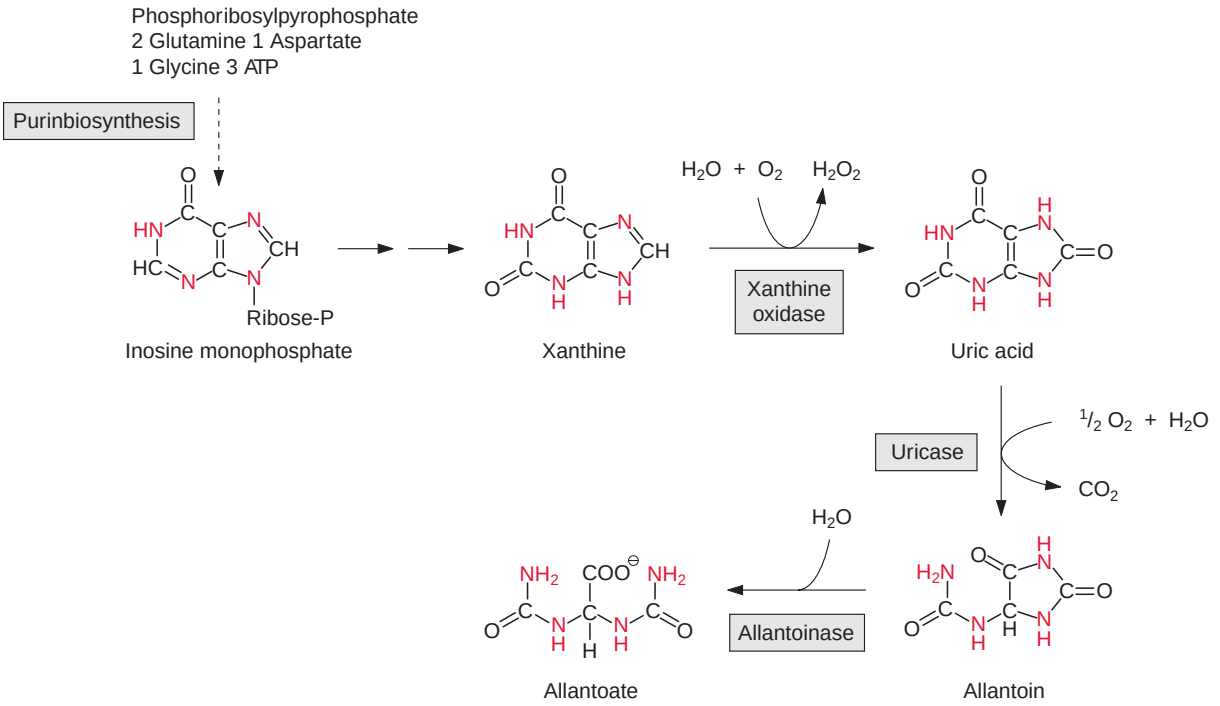

Figure 11.5 In some legumes (e.g., soy bean and cow pea), allantoin and allantoic acid are synthesized as products of N_2 fixation and are delivered via the roots to the xylem. Their formation proceeds via inosine monophosphate by the purine synthesis pathway. Inosine monophosphate is oxidized to xanthine and then further to ureic acid. Allantoin and allantoic acid are formed by hydrolysis and opening of the ring.

Dinitrogenase reductase delivers electrons for the dinitrogenase reaction

Nitrogen fixation is catalyzed by the **nitrogenase complex**, a very intricate system with nitrogenase reductase and dinitrogenase as the main components (Fig. 11.6). This complex is highly conserved and is present in the cytoplasm of the bacteroids. NADH formed in the citrate cycle delivers electrons via soluble ferredoxin to **dinitrogenase reductase**. The latter is a one-electron carrier, consisting of two identical subunits, which together form a **4Fe-4S cluster** (see Fig. 3.26) and comprise two binding sites for ATP. After the reduction of dinitrogenase reductase, two molecules of ATP are bound, resulting in a conformational change of the protein, by which the redox potential of the 4Fe-4S cluster is raised from −0.25 to −0.40 V. After transfer of an electron to the dinitrogenase, the two ATP molecules are hydrolyzed to ADP and phosphate, and then released from the protein.

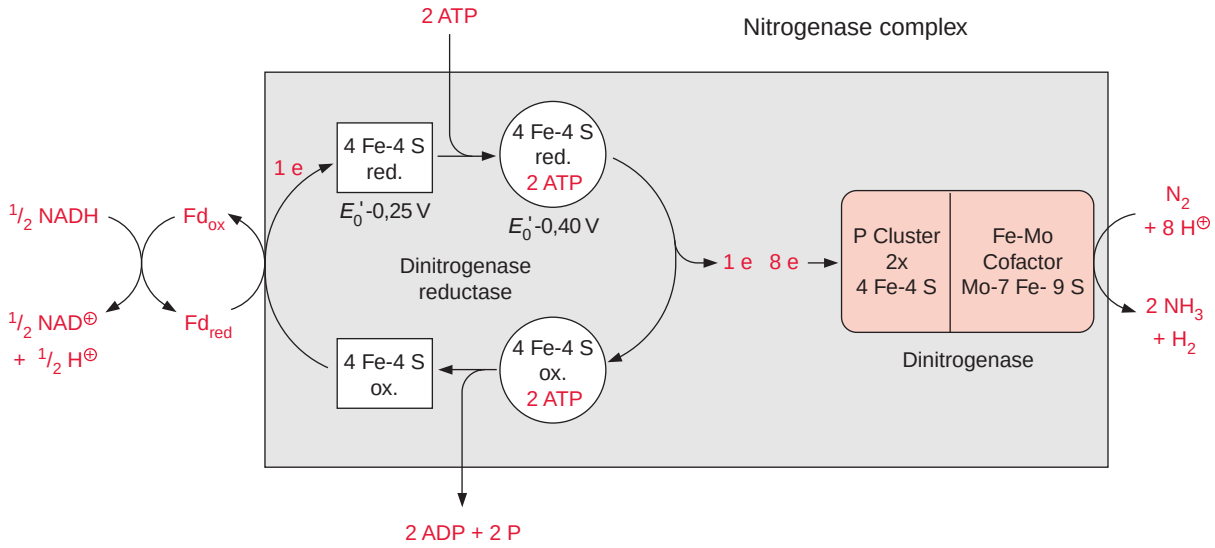

Figure 11.6 The nitrogenase complex comprises the dinitrogenase reductase and the dinitrogenase. Their structures and functions are described in the text. The reduction of one molecule of N_2 is accompanied by the reduction of at least two protons to form molecular hydrogen.

As a result, the conformation with the lower redox potential is restored and the enzyme is once more ready to take up one electron from ferredoxin. Thus, with the hydrolysis of two molecules of ATP, one electron is transferred from NADH to dinitrogenase via dinitrogenase reductase.

N_2 as well as H^+ are reduced by dinitrogenase

Dinitrogenase is an $\alpha_2\beta_2$ tetramer. The α and β subunits are similar in size and structure. The tetramer contains two catalytic centers, probably reacting independently of each other, and each contains a so-called P cluster, consisting of two **4Fe-4S clusters** and an iron molybdenum cofactor (**FeMoCo**). FeMoCo is a large redox center built of Fe_4S_3 and Fe_3MoS_3, which are linked to each other via three inorganic sulfide bridges (Fig. 11.7). Another constituent of the cofactor is **homocitrate**, which is linked via oxygen atoms of the hydroxyl and carboxyl group to molybdenum. Another ligand of molybdenum is the imidazole ring of a histidine residue of the protein. The function of the Mo atom is still unclear. Alternative nitrogenases are known in which molybdenum is replaced by vanadium or iron, but these nitrogenases are much more unstable than the nitrogenase containing FeMoCo. The Mo atom possibly causes a more favorable geometry and electron structure of the center. It is not yet known how

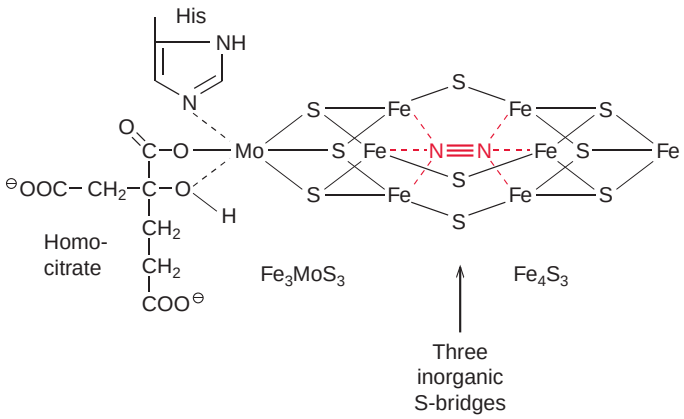

Figure 11.7 The iron-molybdenum cofactor consists of Fe_4S_3 and $MoFe_3S_3$ clusters, which are linked to each other by three inorganic sulfide bridges. In addition, the molybdenum is ligated with homocitrate and the histidine side group of the protein. The cofactor binds one N_2 molecule and reduces it to two molecules of NH_3 by successive uptake of electrons. The position where N_2 is bound in the cofactor has not yet been experimentally verified. (After Karlin, 1993.)

nitrogen reacts with the iron-molybdenum cofactor. One possibility would be that the N_2 molecule is bound in the cavity of the FeMoCo center (Fig. 11.7) and that the electrons required for N_2 fixation are transferred by the P cluster to the FeMoCo center.

The nitrogenase complex is able to reduce other substrates beside N_2 (e.g., protons, which are reduced to molecular hydrogen):

$$2\,H^+ + 2\,e^- \xrightarrow{\textit{Dinitrogenase}} H_2$$

During N_2 fixation at least one molecule of hydrogen is formed per N_2 reduced:

$$8\,H^+ + 8\,e^- + N_2 \xrightarrow{\textit{Dinitrogenase}} 2\,NH_3 + H_2$$

Thus the balance of N_2 fixation is at least:

$$N_2 + 4\,NADH + 4\,H^+ + 16\,ATP \rightarrow 2\,NH_3 + H_2 + 4\,NAD^+ + 16\,ADP + 16\,P$$

In the presence of sufficient concentrations of acetylene, only this is reduced and ethylene is formed:

$$HC\tilde{}\ CH + 2\,e^- + 2\,H^+ \xrightarrow{\textit{Dinitrogenase}} H_2C\cdot\cdot\ CH_2$$

This reaction is used to measure the activity of dinitrogenase.

It is not known why H_2 evolves during N_2 fixation. It may be part of the catalytic mechanism or a side reaction or a reaction to protect the active center against the inhibitory effect of oxygen. The formation of molecular hydrogen during N_2 fixation can be observed in a clover field. Many bacteroids, however, possess hydrogenases by which H_2 is reoxidized by electron transport:

$$2\,H_2 + O_2 \xrightarrow{Hydrogenase} 2\,H_2O$$

It is questionable, however, whether in the bacteroids this reaction is coupled to the generation of ATP.

11.2 N_2 fixation can proceed only at very low oxygen concentrations

The dinitrogenase is extremely sensitive to oxygen. Therefore N_2 fixation can proceed only at very low oxygen concentrations. The nodules form an anaerobic compartment. Since N_2 fixation depends on the uptake of nitrogen from the air, the question arises how the enzyme is protected against the oxygen present in the air. The answer is that oxygen, which has diffused together with nitrogen into the nodules, is consumed by the **respiratory chain** present in the bacteroid membrane. Due to a very high affinity of the bacteroid cytochrome-*a*/a_3 complex, respiration is still possible with an oxygen concentration of only 10^{-9} mol/L. As described previously, at least a total of 16 molecules of ATP are required for the fixation of one molecule of N_2. Upon oxidation of one molecule of NADH, about 2.5 molecules of ATP are generated by the mitochondrial respiratory chain (section 5.6). In the bacterial respiratory chain, which normally has a lower degree of coupling than that of mitochondria, only about two molecules of ATP may be formed per molecule of NADH oxidized. Thus about four molecules of O_2 have to be consumed to facilitate the formation of 16 molecules of ATP (Fig. 11.8). If the bacteroids additionally possess a hydrogenase, required for the oxidation of H_2 that is released during N_2 fixation, oxygen consumption is further increased by half an O_2 molecule. Thus for each N_2 molecule at least four O_2 molecules are consumed by bacterial respiration ($O_2/N_2 \geq 4$). In contrast, the O_2/N_2 ratio in air is about 0.25. This comparison shows that air required for N_2 fixation contains far too little oxygen in relation to nitrogen.

The outer layer of the nodules is a considerable **diffusion barrier** for the entry of air. The diffusive resistance is so high that bacteroid respiration

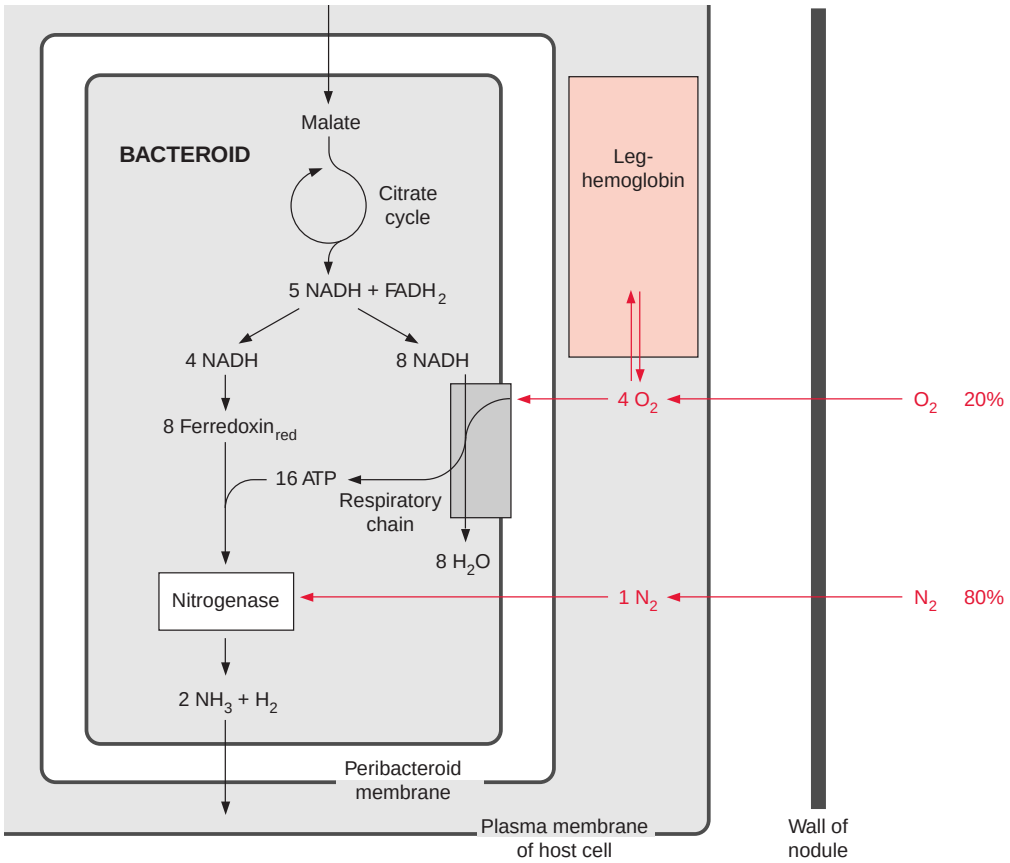

Figure 11.8 N_2 fixation by bacteroids. The total oxidation of malate by the citrate cycle yields five NADH and one $FADH_2$ (see Fig. 5.3). The formation of two NH_3 from N_2 and the accompanying reduction of $2H^+$ to H_2 require at least 16 molecules of ATP. Generation of this ATP by the respiratory chain localized in the bacteroid membrane requires the oxidation of at least eight molecules of NADH. Thus, for each molecule of N_2 fixed, at least four molecules of O_2 are consumed.

is limited by the uptake of oxygen. This leads to the astonishing situation that N_2 fixation is limited by influx of O_2 which is needed for the formation of the ATP required. Experiments by Fraser Bergersen (Australia) verified this. He observed in soybean nodules that a doubling of the O_2 content in air (with a corresponding decrease of the N_2 content) resulted in a doubling of the rate of N_2 fixation. Because of the O_2 sensitivity of the nitrogenase, however, a further increase in O_2 resulted in a steep decline in N_2 fixation.

Since the bacterial respiratory chain is located in the plasma membrane and nitrogenase in the interior of the bacteroids, O_2 is kept at a safe distance

from the nitrogenase complex. The high diffusive resistance for O_2, which can limit N_2 fixation, ensures that even at low temperatures, at which N_2 fixation and the bacterial respiration are slowed down, the nitrogenase complex is protected from O_2.

The cells infected by rhizobia accumulate **leghemoglobin**, which is very similar to the myoglobin of animals, but has a 10-fold higher affinity for oxygen. The oxygen concentration required for half saturation of leghemoglobin amounts to only 10–20 $\times$ 10^{-9} mol/L. Leghemoglobin is located in the cytosol of the host cell—outside the peribacteroid membrane—and present there in unusually high concentrations (3×10^{-3} mol/L in soybeans). Leghemoglobin can amount to 25% of the total soluble protein of the nodules and gives them a pink color. It has been proposed that leghemoglobin plays a role in the transport of oxygen within the nodules. However, it is more likely that it serves as an **oxygen buffer** to ensure continuous electron transport in the bacteroids at the very low prevailing O_2 concentration in the nodules.

11.3 The energy costs for utilizing N_2 as a nitrogen source are much higher than for the utilization of NO_3^-

As shown in Figure 11.8, at least six molecules of NADH are consumed in the production of one molecule of NH_4^+ during molecular nitrogen fixation. Assimilation of nitrate, in contrast, requires only four NAD(P)H equivalents for the formation of NH_4^+ (Fig. 10.1). In addition, nodule formation costs the plant much metabolic energy. Therefore it is cheaper for plants to satisfy their nitrogen demand by nitrate assimilation instead of N_2 fixation with the help of the symbionts. As a consequence the formation of nodules has to be balanced according to the cellular demands and environmental conditions. Nodules are formed only when the soil is nitrate-deficient. The advantage of this symbiosis is that legumes and actinorhizal plants can grow in soils with very low nitrogen content, where other plants do not survive.

11.4 Plants improve their nutrition by symbiosis with fungi

Frequently plant growth is limited by the supply of nutrients other than nitrate, e.g., phosphate. Because of its low solubility, the extraction of phosphate by the roots from the soil requires very efficient uptake systems. For

this reason, plant roots possess very high affinity transporters, with a half saturation of 1 to 5μM phosphate, where the phosphate transport is driven by proton symport, similar to the transport of nitrate (section 10.1). In order to increase the uptake of phosphate, but also of other mineral nutrients (e.g., nitrate and potassium), most plants enter a symbiosis with fungi. Fungi are able to form a mycelium with hyphae that have a much lower diameter than root hairs and are therefore well suited to penetrate soil particles, thereby mobilizing the nutrients. The symbiotic fungi (microsymbionts) deliver these nutrients to the plant root (macrosymbiont) and are in turn supplied by the plant with carbon metabolites for maintaining their own metabolism.

The arbuscular mycorrhiza is widespread

The **arbuscular mycorrhiza** has been detected in more than 80% of all terrestrial plant species. In this symbiosis the fungus penetrates the cortex of plant roots by a plant controlled process and forms a network of hyphae, which protrude into cortical cells and form treelike invaginations, termed **arbuscules** (Fig. 11.9), or form **hyphal coils**. The boundary membranes of fungus and host remain intact. The arbuscules form a large surface, enabling an efficient exchange of compounds between the fungus and the host. The fungus delivers phosphate, nitrate, K^+ ions, and water, and the host delivers carbohydrates. The arbuscules have a lifetime of less than two weeks, but the subsequent degeneration

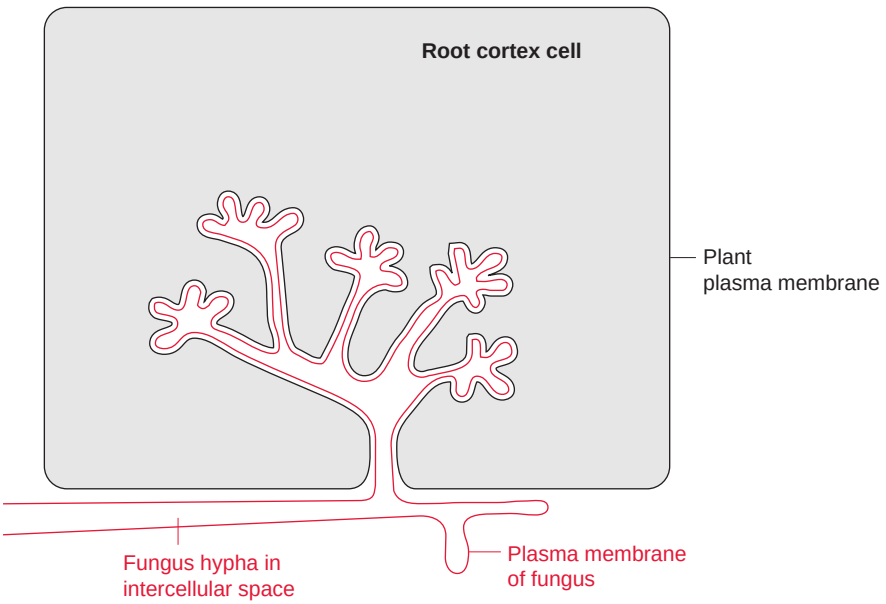

Figure 11.9 Schematic representation of an arbuscel. The hypha of a symbiotic fungus traverses the rhizodermis cells and spreads into the intercellular space of the root cortex. From there tree-like invaginations into the inner layer of the cortex are formed. The cell walls of the plant and of the fungus (not shown in the figure) and the plasma membranes remain intact. The large contact area between the host and the microsymbiont enables an efficient exchange of compounds.

does not damage the corresponding host cell. Therefore, the maintenance of symbiosis requires a constant formation of new arbuscules. The arbuscular mycorrhiza evolved at a very early stage of plant evolution about 450 million years ago. Whereas the number of plant species capable of forming an arbuscular mycorrhiza is very large (about 80% of terrestrial plants), there are only six genera of fungi capable of forming microsymbionts, resulting in rather unspecific plant-fungus combinations. Since the supply of the symbiotic fungi by the roots demands a high amount of assimilates, in many plants the establishment of mycorrhiza depends on the phosphate availability in the soil.

Ectomycorrhiza supply trees with nutrients

Many trees in temperate and cool climates form a symbiosis with fungi termed **ectomycorrhiza**. In this the hyphae of the fungi do not penetrate the cortex cells, but colonize only the surface and the intercellular space of the cortex with a network of hyphae, termed **Hartig net**, which is connected to a very extensive mycel in the soil. Microsymbionts are *Asco-* and *Basiodiomycetae* from more than 60 genera, including several mushrooms. The plant roots colonized by the fungi become thicker and do not form root hairs. The uptake of nutrients and water is delegated to the microsymbiont, which in turn is served by the plant with carbon metabolites to maintain its metabolism. The exchange of compounds occurs, as in arbuscular mycorrhiza, via closely neighbored fungal and plant plasma membranes. The ectomycorrhiza also enables a transfer of assimilates between adjacent plants. Ectomycorrhiza are of great importance for the growth of trees, such as beech, oak, and pine, as it increases the uptake of phosphate by a factor of three to five. It has been observed that the formation of ectomycorrhiza is negatively affected when the nitrate content of the soil is high. This may explain the damaging effect of nitrogen input to forests by air pollution.

Other forms of mycorrhiza (e.g., the endomycorrhiza with orchids and *Ericaceae*) will not be discussed here.

11.5 Root nodule symbioses may have evolved from a pre-existing pathway for the formation of arbuscular mycorrhiza

There are parallels between the establishing of arbuscular mycorrhiza and of root nodule symbiosis. In both cases, **receptor-like kinases** (**RLK**, section 19.1) appear to be involved, linked to **signal cascades**, which induce

the synthesis of the proteins required for the controlled infection. These signal cascades probably involve G-proteins, MAP-kinases, and Ca^{++} ions as messengers (section 19.1). For several legume species, mutants are known that have lost the ability to establish both root nodule symbiosis and arbuscular mycorrhiza. One of the genes that causes such a defect in different legume species has been identified as encoding an RLK, indicating that this RLK has an essential function in the formation of both arbuscular mycorrhiza and root nodule symbiosis. Fungi and bacteria, despite their different natures, apparently induce similar genetic programs upon infection.

Molecular phylogenetic studies have shown that all plants with the ability to enter root nodule symbiosis, rhizobial or actinorhizal, belong to a single clade (=branch of phylogenetic tree, named **Eurosid I**). This implies that these species go back to a common ancestor, although not all descendants of this ancestor are symbiotic. Obviously, this ancestor has acquired a property on the basis of which a bacterial symbiosis could develop. Based on this property, root nodule symbiosis evolved about 50 million years ago, not as a single evolutionary event, but reoccurred about eight times. In order to transfer the ability to enter a root nodule symbiosis to agriculturally important monocots, such as rice, maize, and wheat by genetic engineering, it will be necessary to find out which properties of the Eurosid I clade plants allowed the evolution of such symbiosis.

Further reading

Atkins, C. A., Smith, P. M. C. Translocation in legumes: Assimilates, nutritients, and signaling molecules. Plant Physiology 144, 550–561 (2007).

Chalot, M., Blaudez, D., Brun, A. Ammonia: A candidate for nitrogen transfer at the mycorrhizal interface. Trends in Plant Science 11, 263–266 (2006).

Christiansen, J., Dean, D. R. Mechanistic feature of the Mo-containing nitrogenase. Annual Review Plant Physiology Molecular Biology 52, 269–295 (2002).

Giraud, E., Fleischmann, D. Nitrogen-fixing symbiosis between photosynthetic bacteria and legumes. Photosynthesis Research 82, 115–130 (2004).

Govindarajulu, M., et al. Nitrogen transfer in the arbuscular mycorrhizial symbiosis. Nature 435, 819–823 (2005).

Igarashi, R. Y., Seefeld, L. C. Nitrogen fixation: The mechanism of the Mo-dependent nitrogenase. Critical Reviews Biochemistry Molecular Biology 38, 351–384 (2003).

Karandashov, V., Bucher, M. Symbiotic phosphate transport in arbuscular mycorrhizas. Trends in Plant Science 10, 22–29 (2005).

Karlin, K. D. Metalloenzymes, structural motifs and inorganic models. Science 701–708 (1993).

Limpens, E., Franken, C., Smit, P., Willemse, J., Bisseling, T., Geurts, R. LysM domain receptor kinases regulating rhizobial Nod factor-induced infection. Science 302, 630–633 (2003).

MacLean, A. M., Finan, T. M., Sadowsky, M. J. Genomes of the symbiotic nitrogen-fixing bacteria of legumes. Plant Physiology 144, 615–622 (2007).

Martin, F., Kohler, A., Duplessis, S. Living in harmony in the wood underground: Ectomycorrhizal genomics. Current Opinion Plant Biology 10, 204–210 (2007).
Mylona, P., Pawlowski, K., Bisseling, T. Symbiotic nitrogen fixation. Plant Cell 7, 869–885 (1995).
Ott, T., et al. Symbiotic leghemoglobins are crucial for nitrogen fixation in legume root nodules but not for general plant growth and development. Current Biology 15, 531–535 (2005).
Pauly, N., Pucciariello, C., Mandon, K., Innocenti, G., Jamet, A., Baudouin, E., Hérouart, D., Frendo, P., Puppo, A. Reactive oxygen and nitrogen species and glutathione: Key players in the legume-Rhizobium symbiosis. Journal Experimental Botany 57, 1769–1776 (2006).
Prell, J., Poole, P. Metabolic changes of rhizobia in legume nodules. Trends in Microbiology 14, 161–168 (2006).
Samac, D. A., Graham, M. A. Recent advances in legume-microbe interactions: Recognition, defense response, and symbiosis from a genomic perspective. Plant Physiology 144, 582–587 (2007).
Sawers, R. J., Gutjahr, C., Paszkowski, U. Cereal mycorrhiza: An ancient symbiosis in modern agriculture. Trends in Plant Science 13, 93–97 (2008).
Smith, P. M. C., Atkins, C. A. Purine biosynthesis. Big in cell division, even bigger in nitrogen assimilation. Plant Physiology 128, 793–802 (2002).
Smith, F. A., Smith, S. E. Structural differences in arbuscular mycorrhizal symbioses: More than 100 years after Gallaud, where next? Mycorrhiza 17, 375–938 (2007).
Sprent, J. I., James, E. K. Legume evolution: Where do nodules and mycorrhizas fit in? Plant Physiology 144, 575–581 (2007).
Stacey, G., Libault, M., Brechenmacher, L., Wan, J., May, G. D. Genetics and functional genomics of legume nodulation. Current Opinion Plant Biology 9, 110–121 (2006).
van der Heijden, M. G., Bardgett, R. D., van Straalen, N. M. The unseen majority: Soil microbes as drivers of plant diversity and productivity in terrestrial ecosystems. Ecology Letters 11, 296–310 (2008).
White, J., Prell, J., James, E. K., Poole, P. Nutrient sharing between symbionts. Plant Physiology 144, 604–614 (2007).
Zhu, H., Choi, H.-K., Cook, D. R., Shoemaker, R. C. Bridging model and crop legumes through comparative genomics. Plant Physiology 137, 1189–1196 (2005).

12

Sulfate assimilation enables the synthesis of sulfur containing compounds

Sulfate is an essential constituent of living matter. In the oxidation state -II, it is present in the two amino acids cysteine and methionine, in the detoxifying agent glutathione, in various iron sulfur redox clusters, in peroxiredoxins, and in thioredoxins. Plants, bacteria, and fungi are able to synthesize these compounds by assimilating sulfate taken up from the environment. The animal metabolism is dependent on sulfur containing nutrients such as methionine and cysteine. Therefore sulfate assimilation of plants is a prerequisite for animal life, just like the carbon and nitrate assimilation discussed previously.

Whereas the plant uses nitrate only in its reduced form for syntheses, sulfur, also in the form of sulfate, is an essential plant constituent. Sulfate is present in sulfolipids, which comprise about 5% of the lipids of the thylakoid membrane (Chapter 15). In sulfolipids sulfur is attached as sulfonic acid via a C-S bond to a carbohydrate residue of the lipid.

12.1 Sulfate assimilation proceeds primarily by photosynthesis

Sulfate assimilation in plants occurs primarily in the **chloroplasts** and is then a part of photosynthesis, but it also takes place in the **plastids** of the roots. The rate of sulfate assimilation is relatively low, amounting to only about 5% of the rate of nitrate assimilation and only 0.1% to 0.2% of the rate of CO_2

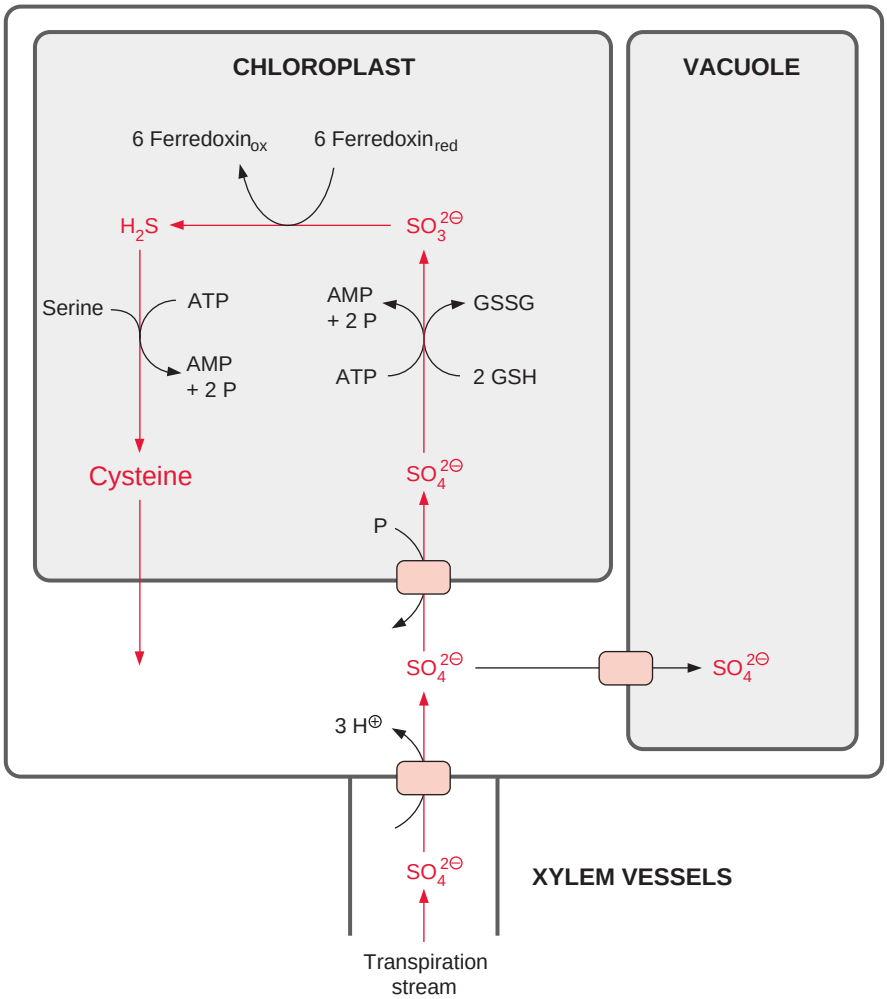

Figure 12.1 Schematic presentation of the sulfate metabolism in a leaf. Sulfate is carried by the transpiration stream into the leaves and is transported into the mesophyll cells, where it is transported to the chloroplast via the phosphate translocator. Sulfate is reduced there to H_2S and subsequently converted to cysteine. Sulfate can also be deposited in the vacuole. Serine is activated as acetylserine prior to the reaction with H_2S (Fig. 12.4).

assimilation. The activities of the enzymes involved in sulfate assimilation are minute, a reason why it is very difficult to elucidate the reactions involved. Therefore our knowledge about sulfate assimilation is still fragmentary.

Sulfate assimilation has some parallels to nitrogen assimilation

Plants take up **sulfate** via a specific translocator of the roots, in a manner similar to that described for nitrate (Chapter 10). The transpiration stream in the xylem vessels carries the sulfate to the leaves, where it is taken up by a specific translocator, probably a symport with three protons, into the mesophyll cells (Fig. 12.1). Surplus sulfate is transported to the vacuole and is deposited there.

The basic scheme for sulfate assimilation in the mesophyll cells corresponds to that of nitrate assimilation. Sulfate is reduced to **sulfite** by the uptake of two electrons and then by the uptake of another six electrons, to **hydrogen sulfide**:

$$SO_4^{2-} + 2\,e^- + 2\,H^+ \rightarrow SO_3^{2-} + H_2O$$

$$SO_3^{2-} + 6\,e^- + 8\,H^+ \rightarrow H_2S + 3\,H_2O$$

Whereas the NH_3 synthesized during nitrite reduction is fixed in the amino acid glutamine (Fig. 10.6), the hydrogen sulfide formed during sulfite reduction is integrated into the amino acid cysteine. A distinguishing difference between nitrate assimilation and sulfate assimilation is that the latter requires a much higher input of energy. This is shown in an overview in Figure 12.1. The reduction of sulfate to sulfite, which in contrast to nitrate reduction occurs in the chloroplasts, requires in total the cleavage of two energy-rich phosphate anhydride bonds, and the fixation of the hydrogen sulfide into cysteine requires another two. Thus the ATP consumption of sulfate assimilation is four times higher than that of nitrate assimilation.

Sulfate is activated prior to reduction

Sulfate is probably taken up into the chloroplasts via the **triose phosphate-phosphate translocator** (section 1.9) in counter-exchange for phosphate. Sulfate cannot be directly reduced in the chloroplasts because the redox potential of the substrate pair SO_3^{2-}/SO_4^{2-} ($\Delta E^{0\prime} = 517\,mV$) is too high. No reductant is available in the chloroplasts that could reduce SO_4^{2-} to SO_3^{2-} in one reaction step. To make the reduction of sulfate possible, the redox potential difference to sulfite is lowered by activation of the sulfate prior to reduction.

As shown in Figure 12.2a, activation of sulfate proceeds via the formation of an anhydride bond with the phosphate residue of AMP. Sulfate is exchanged by the enzyme **ATP-sulfurylase** for a pyrophosphate residue of ATP to form AMP-sulfate (**APS**). Since the free energy of the hydrolysis of the sulfate-phosphate anhydride bond ($\Delta G^{o\prime} = -71\,kJ/mol$) is very much higher than that of the phosphate-phosphate anhydride bond in ATP ($\Delta G^{o\prime} = -31\,kJ/mol$), the equilibrium of the reaction lies far towards ATP. This reaction can proceed only because pyrophosphate is withdrawn from the equilibrium by a high **pyrophosphatase activity** in the chloroplasts.

Sulfate present in the form of APS is reduced by **glutathione** (Figs. 12.5, 3.38) to sulfite. The **APS reductase** involved in this reaction catalyzes not only the reduction, but also the subsequent liberation of sulfite from AMP.

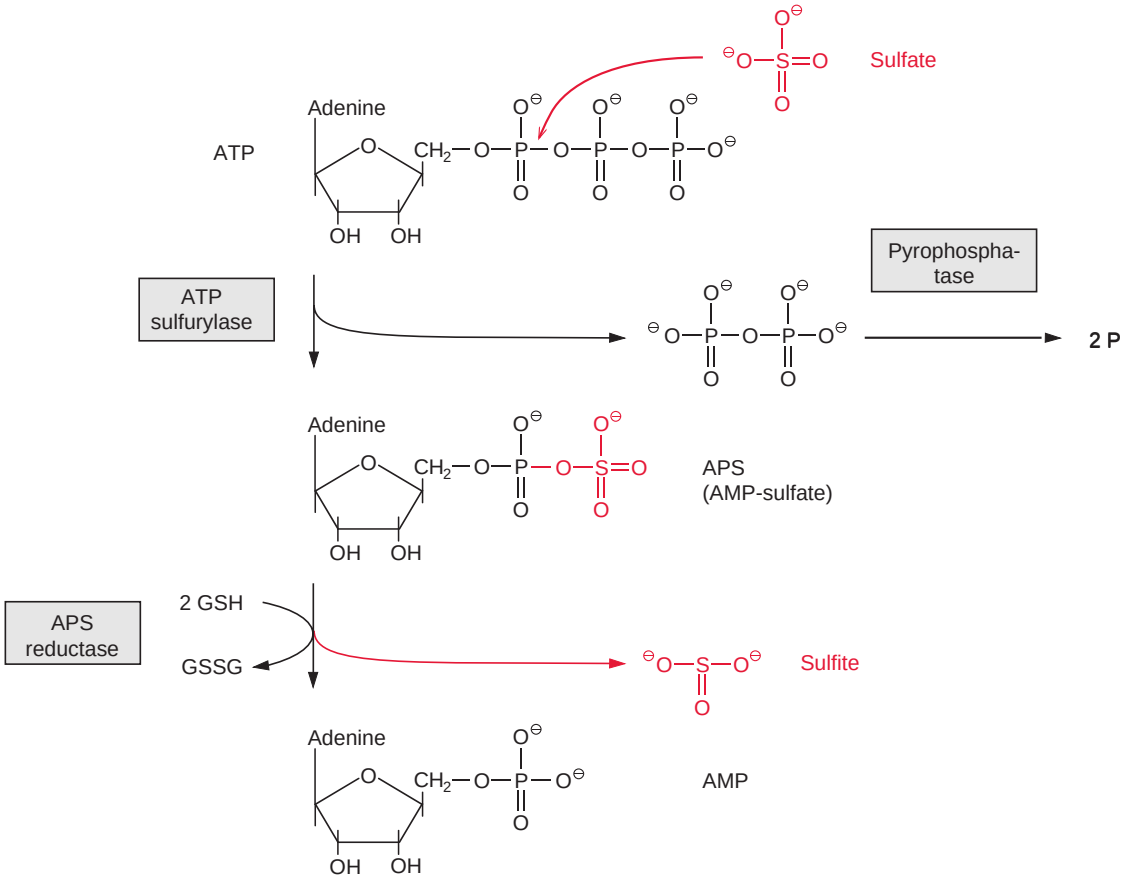

Figure 12.2a Reduction of sulfate to sulfite.

The redox potential difference from sulfate to sulfite is lowered, since the reduction of sulfate is driven by hydrolysis of the very energy-rich sulfite anhydride bond. The mechanism of the APS reductase reaction remains to be elucidated.

Alternatively APS is phosphorylated via **APS kinase** to 3-phospho AMP sulfate (**PAPS**) (Fig. 12.2b), resulting in an activation of the sulfate residue. Because of its high sulfate transfer potential PAPS is an important precursor for the introduction of sulfate residues into biological molecules such as glucosinolates (section 16.4).

Sulfite reductase is similar to nitrite reductase

As in nitrite reduction, six molecules of reduced ferredoxin are required as reductant for the reduction of sulfite in the chloroplasts (Fig. 12.3). The **sulfite reductase** is homologous to the nitrite reductase; it also contains a

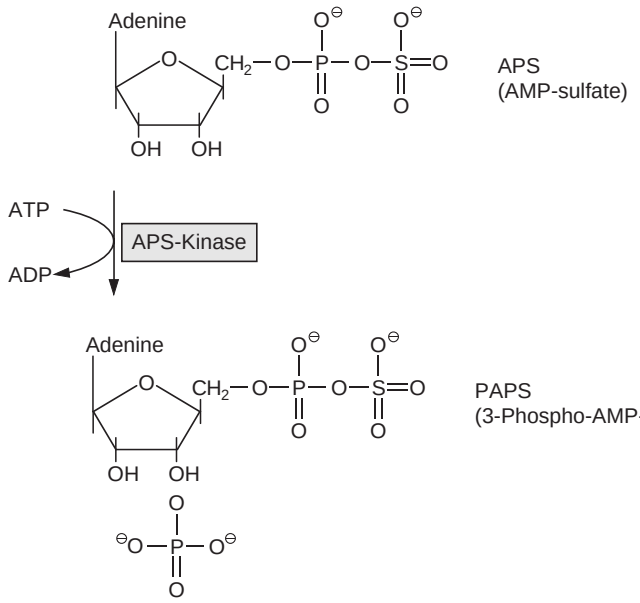

Figure 12.2b Synthesis of PAPS (3-phospho-AMP-sulfate), the "active sulfate".

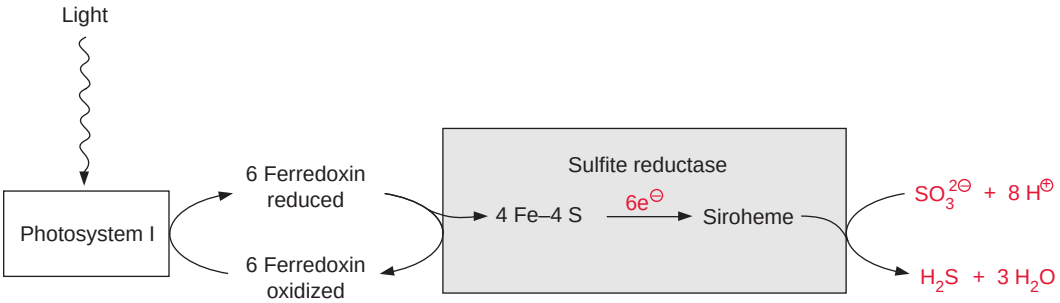

Figure 12.3 Reduction of sulfite to hydrogen sulfide by sulfite reductase in the chloroplasts. Reduced ferredoxin from photosystem delivers electrons for the reaction.

siroheme (Fig. 10.5) and a **4Fe-4S cluster**. The enzyme is half saturated at a sulfite concentration in the range of 10^{-6}mol/L and thus is suitable to reduce efficiently the newly formed sulfite to hydrogen sulfide. The ferredoxin required by sulfite reductase, as in the case of nitrite reductase (Fig. 10.1), can be reduced by NADPH. This feature allows the sulfite reduction to occur also in heterotrophic tissues.

H_2S is fixed in the amino acid cysteine

The fixation of the newly formed H_2S requires the activation of **serine** and for this the hydroxyl group of serine is acetylated by **acetyl-CoA** via a **serine transacetylase** (Fig. 12.4). The latter is formed from acetate and CoA

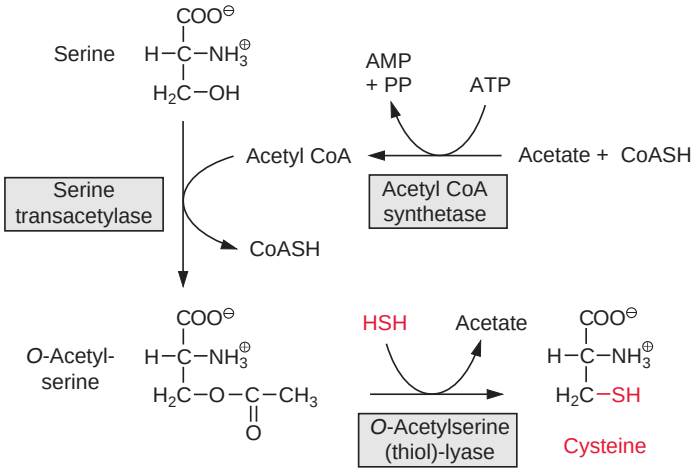

Figure 12.4 Activation of serine precedes the reaction of cysteine synthesis. The hydrogen sulfide formed by sulfite reduction is incorporated into cysteine.

with the consumption of ATP (which is converted to AMP and pyrophosphate) by the enzyme **acetyl-CoA synthetase**. As the pyrophosphate released in this reaction is hydrolyzed by the pyrophosphatase present in the chloroplasts, the activation of the serine costs the chloroplasts in total two energy-rich phosphates.

Fixation of H_2S is catalyzed by the **enzyme *O*-acetyl serine (thiol) lyase**. The enzyme contains pyridoxal phosphate as a prosthetic group and has a high affinity for H_2S and acetyl serine. The incorporation of the SH group can be described as a cleavage of the ester linkage by H-S-H. In this way **cysteine** is formed as the end product of sulfate assimilation.

Cysteine has an essential function in the structure and activity of the catalytic site of many enzymes and a replacement by any other amino acids would alter the catalytic properties. Moreover, cysteine residues form iron-sulfur clusters (Fig. 3.26) and are constituents of thioredoxin (Fig. 6.25).

12.2 Glutathione serves the cell as an antioxidant and is an agent for the detoxification of pollutants

A relatively large proportion of the cysteine produced by the plant is used for synthesis of the tripeptide **glutathione** (Fig. 12.5). The synthesis of glutathione proceeds via two enzymatic steps: first, an amide linkage between the γ-carboxyl group of glutamate with the amino group of the cysteine is formed by **γ-glutamyl-cysteine-synthetase** accompanied by the hydrolysis of ATP; and second, a peptide bond between the carboxyl group of

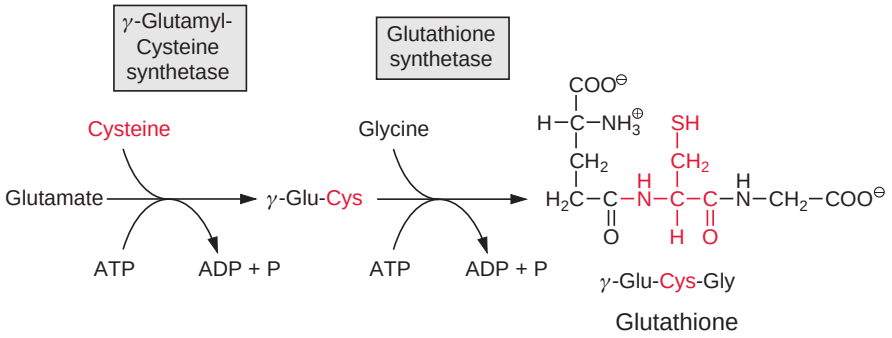

Figure 12.5 Biosynthesis of glutathione.

the cysteine and the amino group of the glycine is produced by **glutathione synthetase**, again with the consumption of ATP. Glutathione, abbreviated **GSH**, is present at relatively high concentrations in all plant cells, where it has various functions. The function of GSH as a reducing agent was discussed in a previous section. As an antioxidant, it protects cell constituents against oxidation. Together with ascorbate, it eliminates the oxygen radicals formed as by-products of photosynthesis (section 3.9). In addition, glutathione has a protective function for the plant in forming conjugates with xenobiotics and also as a precursor for the synthesis of **phytochelatins**, which are involved in the detoxification of heavy metals. Moreover, glutathione acts as a reserve for organic sulfur. If required, cysteine is released from glutathione by enzymatic degradation.

Xenobiotics are detoxified by conjugation

Toxic compounds produced by the plant or which are taken up (xenobiotics, including herbicides) are detoxified by reaction with glutathione. Catalyzed by **glutathione-*S* transferases**, the reactive SH group of glutathione can form a thioether by reacting with electrophilic carbon double bonds, carbonyl groups, and other reactive groups. **Glutathione conjugates** (Fig. 12.6) synthesized in this way in the cytosol are transported into the vacuole by a specific **glutathione translocator** against a concentration gradient. In contrast to the transport processes, where metabolite transport against a gradient proceeds by secondary active transport, the uptake of glutathione conjugates into the vacuole proceeds by an ATP-driven primary active transport (Fig. 1.20). This translocator belongs to the superfamily of the **ABC-transporter** (ATP binding cassette), which is ubiquitous in plants and animals and is also present in bacteria. Various ABC transporters with different specificities are localized in the vacuolar membrane. The imported conjugates are often modified (e.g., by degradation to a cysteine conjugate)

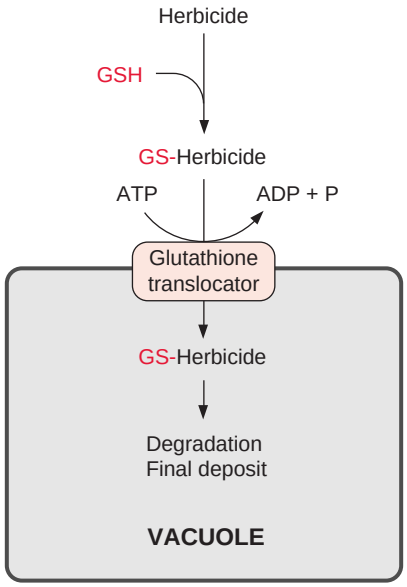

Figure 12.6 Detoxification of a herbicide. Glutathione (GSH) is conjugated to the herbicide, which is subsequently pumped into the vacuole by a specific glutathione translocator. After degradation the herbicide is deposited there. Alternatively GS conjugates can also be degraded in the cytosol.

and are finally deposited in the vacuole. In this way plants can also detoxify herbicides. Herbicide resistance (e.g., resistance of maize to atrazine) can be due to the activity of a specific glutathione-*S* transferase. In an attempt to develop herbicides that selectively attack weeds and not crop plants, the plant protection industry has produced a variety of different compounds that increase the tolerance of crop plants to certain herbicides. These protective substances are called **safeners**. Such safeners, like other xenobiotics, stimulate the increased expression of glutathione-*S* transferase and of the vacuolar glutathione translocator, resulting in a rapid detoxification of the herbicides in the plants. Formation of glutathione conjugates and their transport into the vacuole is also involved in the deposition of flower pigments (section 18.6).

Phytochelatins protect the plant against heavy metals

Glutathione is also a precursor for the formation of **phytochelatins** (Fig. 12.7). **Phytochelatin synthase**, a transpeptidase, transfers the amino group of glutamate to the carboxyl group of the cysteine of a second glutathione molecule, accompanied by liberation of one glycine molecule. The repetition of this process results in the formation of chains of up to 11 Glu-Cys residues with a glycine residue at the carboxyl terminus. Phytochelatins have been found in all plants investigated so far, although sometimes in a

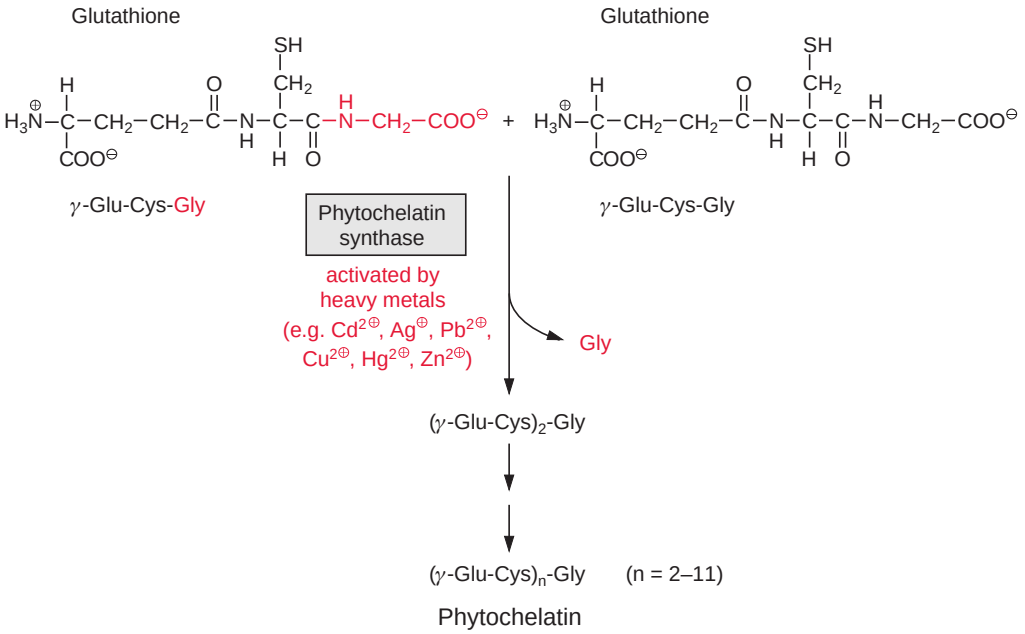

Figure 12.7 Phytochelatin synthesis. The phytochelatin synthase (a transpeptidase) cleaves the peptide bond between the cysteine and the glycine of a glutathione molecule and transfers the α-amino group of the glutamate residue of a second glutathione molecule to the liberated carboxyl group of the cysteine. Long chain phytochelatins are formed by repetition of this reaction.

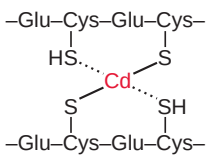

Figure 12.8 Detoxification of heavy metals by phytochelatins: heavy metals form complexes with the thiol groups of the cysteine and are thus rendered harmless.

modified form as *iso*-phytochelatins, in which glycine is replaced by serine, glutamate, or β-alanine.

Phytochelatins protect plants against heavy metal poisoning. Mutants of *Arabidopsis* with a defect in the phytochelatin synthase are extremely sensitive to Cd^{++}. Phytochelations are storage compounds for Cu^{++} and Zn^{++}. Through the thiol groups of the cysteine residues, they form tight complexes with metal ions such as Cd^{++}, Ag^{+}, Pb^{++}, Cu^{++}, Hg^{++}, and Zn^{++} as well as with the semimetal As^{3+} (Fig. 12.8). The phytochelatin synthase present in the cytosol is activated by the ions of at least one of the heavy metals listed. Upon the exposure of plants to heavy metals, phytochelatins required for detoxification are immediately *de novo* synthesized from glutathione.

Exposure to heavy metals can therefore lead to a dramatic depletion of the glutathione reserves in the cell. The phytochelatins loaded with heavy metals are pumped, like the glutathione conjugates, into the vacuoles. This transport is ATP dependent. Because of the acidic environment in the vacuole, the heavy metals are liberated from the phytochelatins and finally deposited there as sulfides, often as microcrystalline sulfide complexes.

The capacity of plants to sequester heavy metal ions by binding them to phytochelatins has been utilized in recent times to detoxify soils which are polluted with heavy metals. This procedure, termed **phytoremediation**, may be important in the future, since it is much less costly than other methods of remediating soils polluted with heavy metals. Plants with a particularly high capacity for heavy metal uptake by roots and for phytochelatin biosynthesis were developed by breeding or genetical engineering specifically to facilitate this purpose.

12.3 Methionine is synthesized from cysteine

Cysteine is a precursor for **methionine**, which is another sulfur-containing amino acid. *O*-Phosphohomoserine, which has already been mentioned as an intermediate of threonine synthesis (Fig. 10.14), reacts with cysteine, while a phosphate group is liberated to form cystathionine (Fig. 12.9). The thioether is cleaved by **cystathionine-β-lyase** to release homocysteine and an unstable enamine, which spontaneously degrades into pyruvate and NH_4^+. The sulfhydryl group of homocysteine is methylated by methyl tetrahydrofolate (**methyl-THF**) (see Fig. 7.6), and thus the end product methionine is synthesized.

S-Adenosylmethionine is a universal methylation reagent

The methyl group delivered as methyl-THF derives from a formiate molecule, which has been bound upon the consumption of ATP to THF and subsequently reduced by two molecules of NADPH to methyl-THF. Methyl-THF has only a relatively low methyl transfer potential. ***S*-Adenosylmethionine**, however, has a more general role as a methyl donor. It is involved in the methylation of nucleic acids, proteins, carbohydrates, membrane lipids, and many other compounds such as chlorophyll, plastoquinone, biotin and polyamines and can therefore be regarded as a universal methylating agent of the cell.

S-Adenosylmethionine is formed by the transfer of an adenosyl residue from ATP to the sulfur atom of methionine, with the release of phosphate

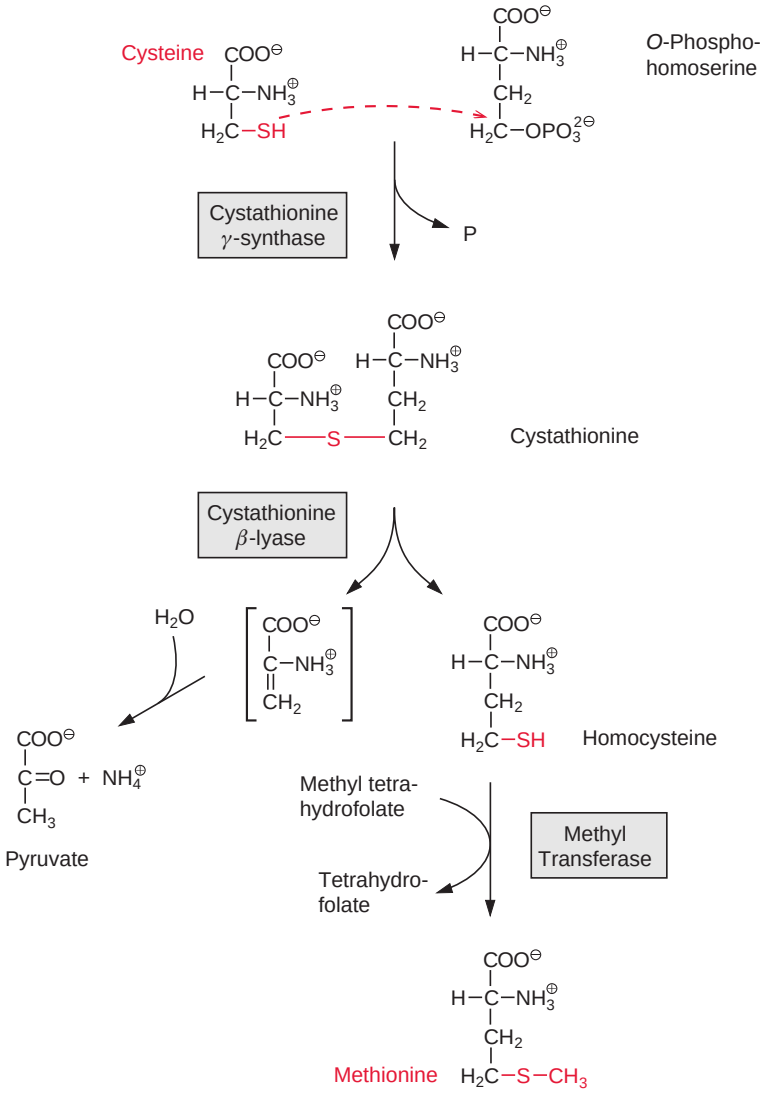

Figure 12.9 Biosynthesis of methionine from cysteine.

and pyrophosphate (Fig. 12.10). The methyl group to which the positively charged *S* atom is linked is activated and can thus be transferred by corresponding methyl transferases to other acceptors. The remaining *S*-adenosyl homocysteine is hydrolyzed to adenosine and homocysteine and from the latter methionine is recovered by reduction with **methyl tetrahydrofolate** (Fig. 12.9).

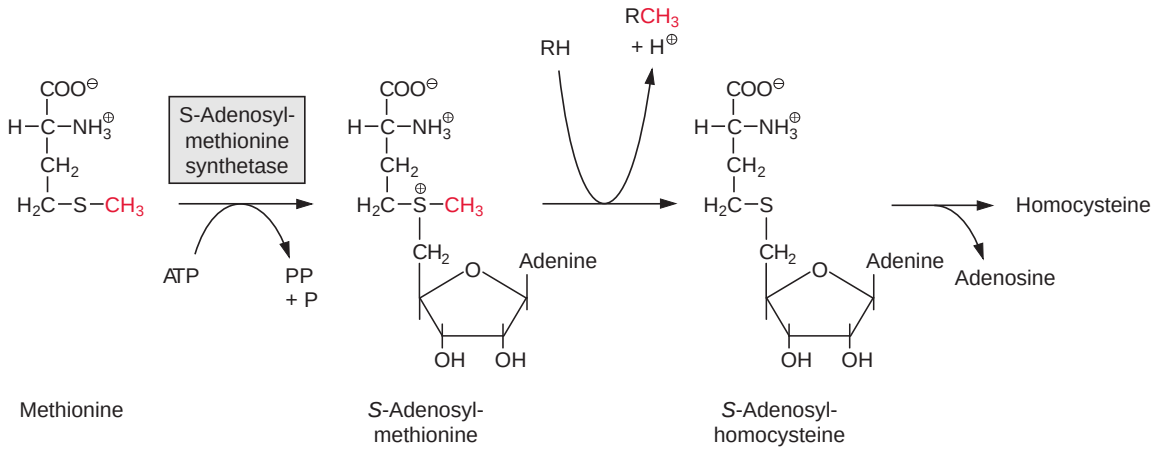

Figure 12.10 *S*-Adenosylmethionine is synthesized from methionine and ATP and is a general methylating agent.

12.4 Excessive concentrations of sulfur dioxide in the air are toxic for plants

Sulfur dioxide in the air, which is formed in particularly high amounts during the smelting of sulfur containing ores, and also during the combustion of fossil fuel, can cover the total nutritional sulfur requirement of a plant. In higher concentrations, however, it leads to dramatic damage in plants. Gaseous SO_2 is taken up via the stomata into the leaves, where it is converted to sulfite:

$$SO_2 + OH^- \rightarrow SO_3^{2-} + H^+$$

Plants possess protective mechanisms for removing the sulfite which has been formed in the leaves, e.g., sulfite is converted by the sulfite reductase (section 12.1) to hydrogen sulfide and then further into cysteine. When cysteine is formed in increasing amounts it can be converted to glutathione. Therefore, in SO_2-polluted plants an accumulation of glutathione is observed in the leaves. Excessive hydrogen sulfide can leak out of the leaves through the stomata, although only in small amounts. Alternatively, sulfite can be oxidized, possibly by peroxidases in the leaf, to sulfate. Since this sulfate cannot be removed by transport from the leaves, it is finally deposited in the vacuoles of the leaf cells as K^+ or Mg^{++}-sulfate. When the deposit site is full, the leaves are abscised. This explains in part the toxic

effect of SO_2 on pine trees: the early loss of the pine needles of SO_2-polluted trees is due to a large extent to the fact that the capacity of the vacuoles for the final deposition of sulfate is exhausted. In cation-deficient soils, the high cation demand for the final deposition of sulfate can lead to a serious K^+ or Mg^{++} deficiency in leaves or pine needles. The bleaching of pine needles, often observed during SO_2 pollution, is partly attributed to a decreased availability of Mg^{++} ions resulting in a reduced chlorophyll content.

Further reading

Blum, R., Beck, A., Korte, A., Stengel, A., Letzel, T., Lendzian, K., Grill, E. Function of phytochelatin synthase in catabolism of glutathion-conjugates. The Plant Journal 49, 740–749 (2007).

Clemens, S. Evolution and function of phytochelatin synthases. Journal Plant Physiology 163, 319–332 (2006).

Cobbett, C., Goldsbrough, P. Phytochelatins and metallothionins: roles in heavy metal detoxification and homeostasis. Annual Review Plant Biology 53, 159–182 (2002).

Hawkesford, M. J., de Kok, L. J. Managing sulphur metabolism in plants. Plant Cell Environment 29, 382–395 (2006).

Heber, U., Kaiser, W., Luwe, M., Kindermann, G., Veljovic-Iovanovic, S., Yin, Z.-H., Pfanz, H., Slovik, S. Air pollution, photosynthesis and forest decline. Ecological Studies 100, 279–296 (1994).

Kopriva, S., Wiedemann, G., Reski, R. Sulfate assimilation in basal land plants—what does genomic sequencing tell us? Plant Biology 9, 556–564 (2007).

Martin, M. N., Tarczynski, M. C., Shen, B., Leustek, T. The role of 5′-adenylylsulfate reductase in controlling sulfate reduction in plants. Photosynthesis Research 83, 309–323 (2005).

Pilon-Smits, E. Phytoremediation. Annual Review of Plant Biology, 56, 15–39 (2005).

Rausch, T., Wachter, A. Sulfur metabolism: A versatile platform for launching defence operations. Trends in Plant Science 10, 503–509 (2005).

Ravanel, S., Block, M. A., Rippert, P., Jabrin, S., Curien, G., Rebeille, F., Douce, R. Methionine metabolism in plants. Journal of Biological Chemistry 279, 22548–22557 (2004).

Rea, P. A., Vatamaniuk, O. K., Ridgen, D. J. Update on phytochelatin synthase; weeds, worms, and more. Papains long-lost cousin, phytochelatin synthase. Plant Physiology 136, 2463–2474 (2004).

Rea, P. A. Plant ATP-binding cassette transporters. Annual Reviews of Plant Biology 58, 347–375 (2007).

Saito, K. Sulfur assimilatory metabolism. The long and smelly road. Plant Physiology 136, 2443–2450 (2004).

Suresh, B., Ravishankar, G. A. Phytoremediation—a novel and promising approach for environmental clean-up. Critical Review Biotechnology 24, 97–124 (2004).

Tong, Y.-P., Kneer, R., Zhu, Y.-G. Vacuolar compartmentation: a second-generation approach to engineering plants for phytoremediation. Trends in Plant Science 9, 7–9 (2004).

Wirtz, M., Hell, R. Functional analysis of the cysteine synthase protein complex from plants: structural, biochemical and regulatory properties. Journal of Plant Physiology, 163, 273–286 (2006).

13

Phloem transport distributes photoassimilates to the various sites of consumption and storage

This chapter deals with the export of photoassimilates from the leaves to the other parts of the plant. Besides having the xylem as a long-distance translocation system for transport from the root to the leaves, plants have a second long-distance transport system, the phloem, which exports the photoassimilates formed in the leaves to wherever they are required. The **xylem** and **phloem** together with the parenchyma cells form **vascular bundles** (Fig. 13.1). The xylem (*xylon*, Greek for wood) consists of lignified tubes, which translocate water and dissolved mineral nutrients from the root to the leaves. Several translocation vessels arranged mostly on the outside of the vascular bundles comprise the phloem (*phloios*, Greek for bark), which transports photoassimilates from the site of synthesis (**source**) (e.g., the mesophyll cell of a leaf) to the sites of consumption or storage (**sink**) (e.g., roots, tubers, fruits, or areas of growth). The phloem system thus connects the sink and source tissues.

The phloem is built from elongated cells, joined by **sieve plates**, the latter consisting of diagonal cell walls perforated by pores. The single cells are called **sieve elements** and their longitudinal arrangement is called the **sieve tube** (Fig. 13.2). The pores of the sieve plate are widened plasmodesmata lined with **callose** (section 9.6). The sieve elements can be regarded as living cells that have lost their nucleus, Golgi apparatus, and vacuoles, and contain only a few mitochondria, plastids, and some endoplasmic reticulum. The absence of many cellular structures specializes the sieve tubes for the long-distance transport of carbon- and nitrogen-containing metabolites and of various inorganic and organic compounds. In most plants sucrose is the main transport form for carbon, but some plants also transport oligosaccharides

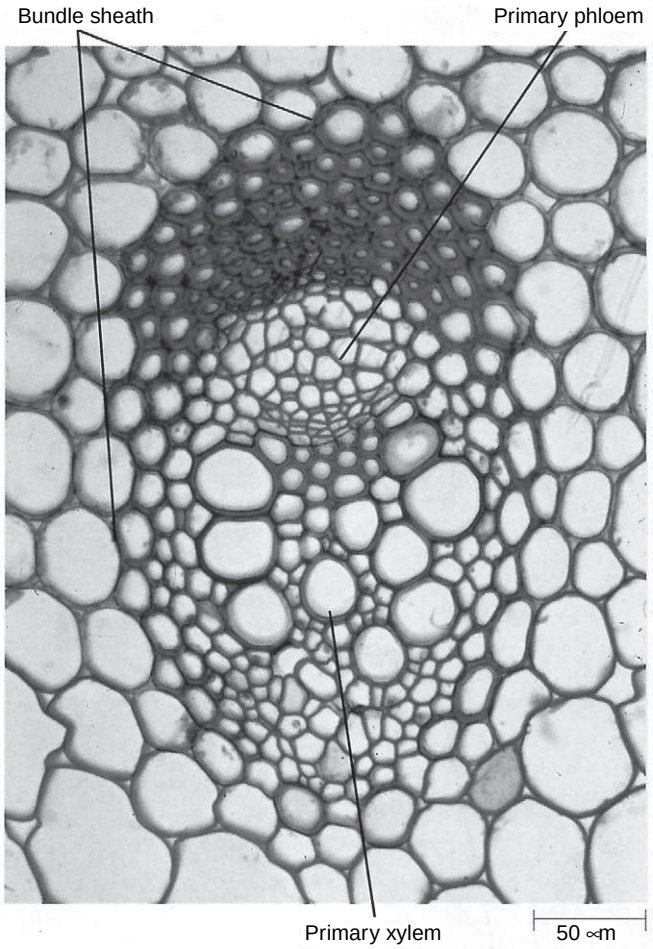

Figure 13.1 Transverse section through a vascular bundle of *Ranunculus* (buttercup), a herbaceous dicot plant. The phloem and xylem are surrounded by bundle sheath cells. (From Raven, Evert, and Curtis: Biologie der Pflanzen, De Gruiter Verlag, Berlin, by permission.)

from the raffinose family, or sugar alcohols (**polyols**), such as **sorbitol** and **mannitol** (Fig. 9.19). Nitrogen is transported in the sieve tubes almost exclusively in the organic form as amino acids. Organic acids, nucleotides, proteins, signal molecules and phytohormones are also present in the phloem sap, but in much lower concentrations. In addition to these organic compounds the sieve tubes transport inorganic ions, mainly K^+ ions.

Companion cells are localized adjacent to the sieve elements of angiosperms. These cells contain all the constituents of a normal living plant cell, including the nucleus, many mitochondria and ribosomes. Companion cells supply the adjacent sieve elements with energy and synthesized proteins. Sieve elements and companion cells have developed from a common precursor cell. They are connected to each other by numerous **plasmodesmata** (section 1.1) and are important for phloem loading.

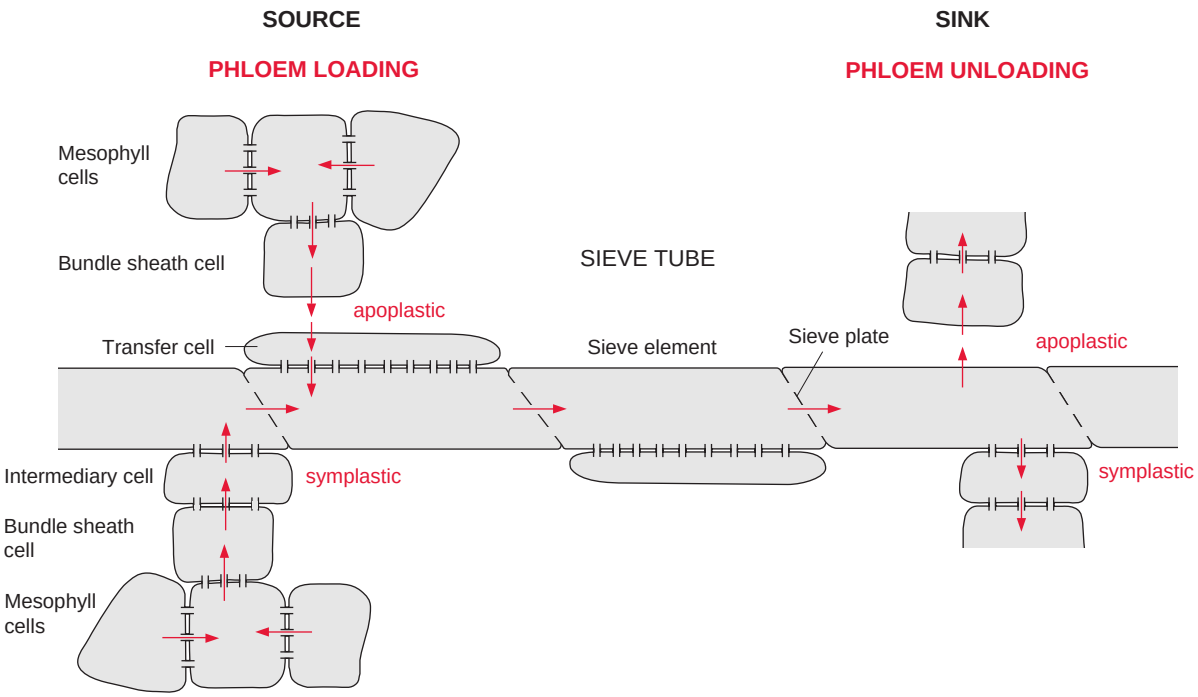

Figure 13.2 Schematic presentation of the sieve tubes and their loading and unloading via the apoplastic and symplastic pathways. The plasmodesmata indicated by the double line allow unhindered diffusion of sugar and amino acids. The structures are not shown to scale. The companion cells participating in apoplastic loading are also called transfer cells. Intermediary cells are specialized companion cells involved in symplastic phloem loading.

Depending on the kind of phloem loading, the companion cells are named **transfer cells** or **intermediary cells**.

13.1 There are two modes of phloem loading

Photoassimilates generated in the mesophyll cells, such as sucrose, various oligosaccharides, polyols as well as amino acids, diffuse via plasmodesmata to the **bundle sheath cells**. The subsequent transport of photoassimilates from the bundle sheath cells to the sieve tubes can occur in two different ways:

1. Plants in which oligosaccharides from the **raffinose** family (section 9.4) are translocated into the sieve tubes (e.g., squash plants), the bundle

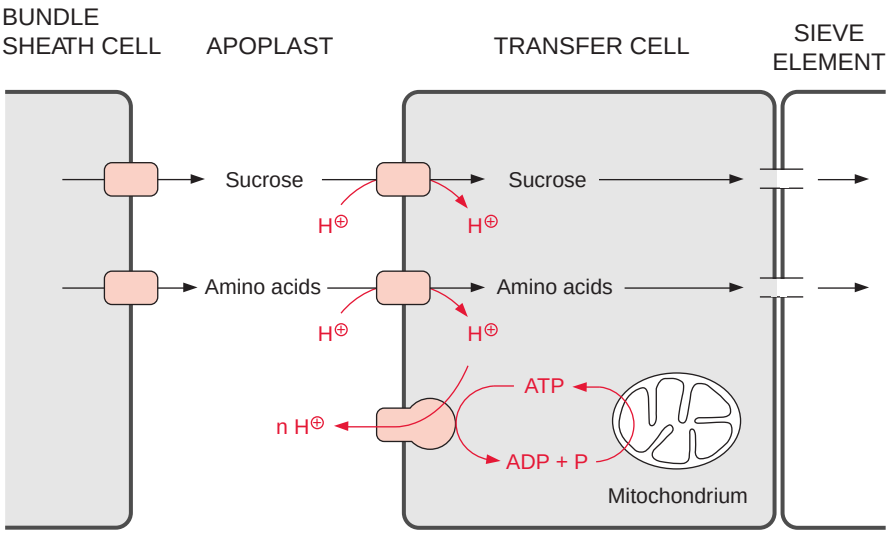

Figure 13.3 Apoplastic phloem loading. Transfer of the photoassimilates from the bundle sheath cells to the sieve tubes. Many observations indicate that active loading takes place in the plasma membrane of the transfer cells and that the subsequent transfer to the sieve elements occurs by diffusion via plasmodesmata.

sheath cells are connected to specialized companion cells (**intermediary cells**) and further to the sieve tubes via a large number of plasmodesmata. These plants transfer the photoassimilates to the sieve tubes via plasmodesmata in a process termed **symplastic phloem loading**.

2. In contrast, in **apoplastic** phloem loading, found for instance in the leaves of cereals, sugar beet, rapeseed, and potato, photoassimilates are first transported from the source cells via the bundle sheath cells to the extracellular compartment, the **apoplast**, and then by **active transport** into the sieve tube compartment (Fig. 13.3). Since the concentration of sucrose, polyols and amino acids in the source cells is very much higher than in the apoplast, this export does not seem to require any energy input. The translocators mediating the export from the bundle sheath to the apoplast have not yet been characterized.

The companion cells participating in the apoplastic phloem loading are termed **transfer cells**. The transport of sucrose and amino acids from the apoplasts to the phloem proceeds via a **proton symport** (Fig. 13.3). This is driven by a proton gradient between the apoplast and the interior of the companion cells and the sieve tubes. The proton gradient is generated by an **H^+-P ATPase** (section 8.2) present in the plasma membrane. The required ATP is produced by mitochondrial oxidation. By now a number of H^+-driven symporters involved in the phloem loading of sucrose, polyols and amino acids have been identified and characterized in several plants. In the vascular bundles of *Plantago major* using specific antibodies, an H^+-sucrose translocator and two

H^+-polyol translocators have been localized in the plasma membrane of transfer cells (Fig. 13.3). The substrates for mitochondrial respiration are provided by degradation of sucrose via sucrose synthase (see also Fig. 13.5) to hexose phosphates, which are further degraded by glycolytic metabolism. Another substrate for respiration is glutamate (section 5.3). In many plants this amino acid is present in relatively high concentrations in the phloem sap.

In the plants with apoplastic phloem loading, **sucrose**, also in combinations with the polyols sorbitol and mannitol, is the transport form for carbohydrates (hexoses are not transported), while no special transport form exists for amino nitrogen. In principle, all protein-building amino acids are transported. The ratio of a single amino acid versus the sum of amino acids is very similar in the phloem sap and in the source cells. The amino acids most frequently found in the phloem sap are glutamate, glutamine, and aspartate, but also much alanine is found in some plants. Several amino acid translocators with a broad specificity for various amino acids were identified, which are presumed to participate in the phloem loading.

13.2 Phloem transport proceeds by mass flow

The proton-substrate-co-transport results in very high concentrations of sucrose and amino acids in the sieve tubes. Depending on the plant and on growth conditions, the concentration of sucrose in the phloem sap amounts to 0.6 to 1.5 mol/L, that of polyols 0.5 mol/L and the sum of the amino acids ranges from 0.05 to 0.5 mol/L. **Aphids** turned out to be useful helpers for obtaining phloem sap samples for such analyses. An aphid, after some attempts, can insert its stylet exactly into a sieve tube. As the phloem sap is under pressure, it flows through the tube of the stylet and is consumed by the aphid (Fig. 13.4). The aphid takes up more sucrose than it can metabolize and excretes the surplus as honeydew, which is a sticky sugary layer e.g., covering aphid-infested house plants. When the stylet of a feeding aphid is severed by a laser beam, the phloem sap exudes from the sieve tube through the stump of the stylet. Although only very small amounts of phloem sap can be obtained ($0.05–0.1 \times 10^{-6}$ L/h), it is sufficient for quantitative assays using modern technology.

In plants performing photosynthesis in the presence of radioactively labeled CO_2, phloem transport velocities of 30 to 150 cm/h have been measured. This rapid transport proceeds by **mass flow**, driven by very efficient pumping of sucrose, polyols and amino acids into the sieve tubes and by their withdrawal at the sites of consumption. This mass flow is driven by many transversal osmotic gradients. The surge of this mass flow carries along compounds present at low concentrations, such as **phytohormones**. The direction

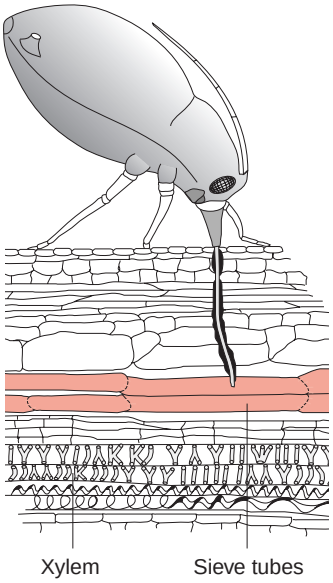

Figure 13.4 Aphids know where to insert their stylet into the sieve tubes to feed from the exuding phloem sap. (Figure by A.F.G. Dixon, Encyclopaedia of Plant Physiology, Vol. 1, Springer-Verlag, by permission.)

of mass flow is governed entirely by the consumption of the phloem contents. Depending on what is required, phloem transport can proceed in an upward direction (e.g., from the mature leaf to the growing shoot or flower) or downwards into the roots or storage tubers. Since the phloem sap is under high pressure and the phloem is highly branched, wounding the vascular tissue might result in the phloem sap "bleeding". Protective mechanisms prevent this. Due to the presence of substrates in the phloem sap and the enzymes of sucrose synthase and **callose synthase**, which are probably membrane-bound, the sieve pores of damaged sieve tubes are sealed by the formation of **callose** (section 9.6), and damaged sieve tubes are disconnected. Sieve tubes are also rapidly sealed by the so-called P proteins.

13.3 Sink tissues are supplied by phloem unloading

The delivered photosynthate is utilized in the sink tissues to sustain the metabolism, but may also be deposited there as reserves, mainly in the form of starch. There are again two possibilities for phloem unloading (Fig. 13.2). In **symplastic unloading**, the sucrose and amino acids reach the cells of the sink organs directly from the sieve elements via plasmodesmata. In **apoplastic unloading**, the compounds are first transported from the sieve tubes to the extracellular compartment and are then taken up into the cells of the sink organs. Electron microscopic investigations of the frequency of

plasmodesmatal appearance indicate that in vegetative tissues, such as roots or growing shoots, phloem unloading proceeds primarily symplastically, whereas in storage tissues unloading is often, but not always, apoplastic.

Starch is deposited in plastids

In storage tissues, the delivered carbohydrates are mostly converted to starch and stored as such. In apoplastic phloem unloading, this may proceed by two alternative pathways. In the pathway colored red in Figure 13.5, the sucrose is taken up from the apoplast into the storage cells and converted there via **sucrose synthase** and **UDP-glucose-pyrophosphorylase** to fructose and glucose 1-phosphate. In this reaction, pyrophosphate is consumed and UTP is generated. **Phosphoglucomutase** converts glucose 1-phosphate to glucose 6-phosphate. Alternatively, the enzyme **invertase** first hydrolyzes sucrose in the apoplast to glucose and fructose, and these two hexoses are then transported into the cell. This pathway is colored black in Figure 13.5. A **fructokinase** and a **hexokinase** (the latter phosphorylating mannose as well as glucose) catalyze the formation of the corresponding hexose phosphates. Glucose 6-phosphate is transported via the **glucose 6-phosphate-phosphate translocator** (see section 8.2) in counter-exchange for phosphate to the amyloplast, where starch is formed via the synthesis of ADP-glucose (section 9.1). Some leucoplasts transport glucose 1-phosphate in counter-exchange for phosphate. In potato tubers, the storage of starch probably proceeds mainly via sucrose synthase. In the taproots of sugar beet, the carbohydrates are stored as sucrose in the vacuoles. In some fruits (e.g., grapes), carbohydrates are stored in the vacuole as glucose.

The glycolysis pathway plays a central role in the utilization of carbohydrates

The carbohydrates delivered by phloem transport to the sink cells are fuel for the energy metabolism and also a carbon source for the synthesis of the cell matter. The **glycolysis pathway**, which is present at least in part in almost all living organisms, has a fundamental role in the utilization of carbohydrates. The enzymes of this pathway not only occur in sink tissues but are also present in all plant cells. Each cell has two sets of glycolytic enzymes, one in the **cytosol** and one in the **plastids**. Some of the plastidic enzymes participate in the Calvin cycle, as discussed in Chapter 6. In the plastids of some plants, the glycolysis pathway is incomplete because one or two enzymes are lacking. The corresponding glycolytic enzymes in the cytosol and in the plastids are isoenzymes encoded by different genes.

Figure 13.6 depicts the glycolysis pathway present in the cytosol. Glucose 6-phosphate, deriving from either the degradation of sucrose (Fig. 13.5)

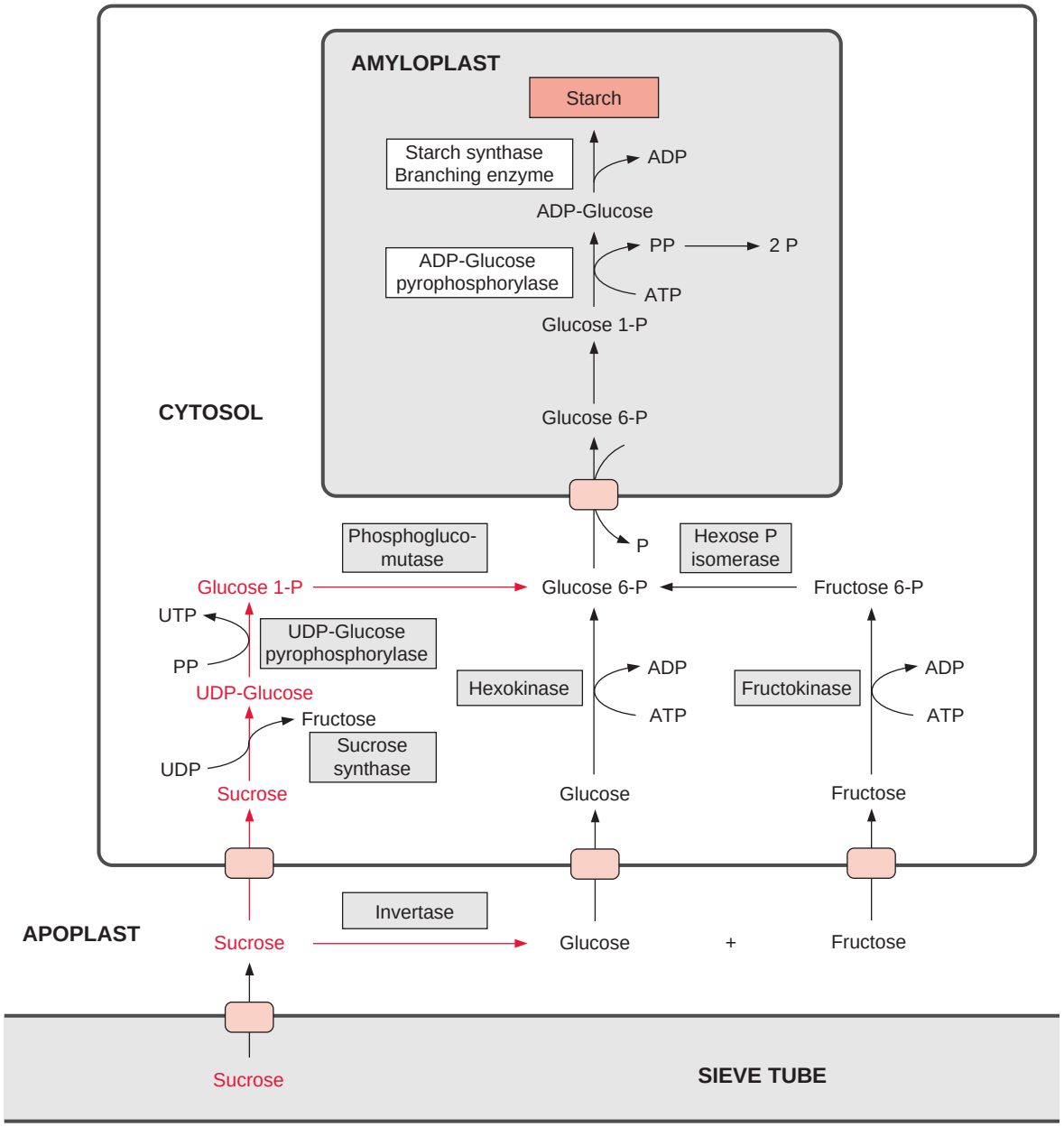

Figure 13.5 Apoplastic phloem unloading and synthesis of starch. Some storage cells take up sucrose, whereas others take up glucose and fructose, synthesized by the hydrolysis of sucrose catalyzed by invertase. It is not yet known whether glucose and fructose are transported by the same or by different translocators. For details see section 9.1. Some amyloplasts transport glucose-1-phosphate in exchange for phosphate.

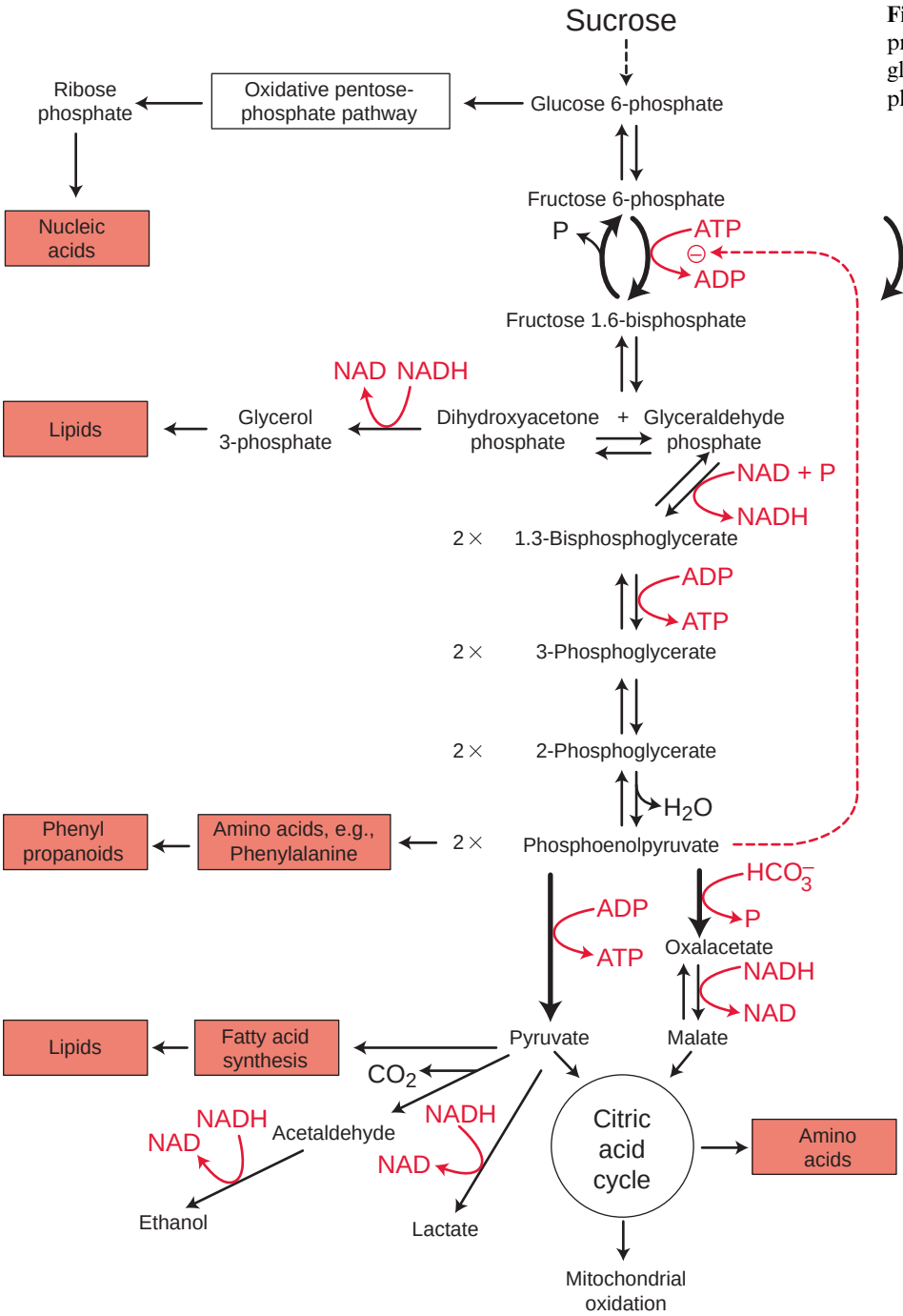

Figure 13.6 Schematic presentation of the cytosolic glycolysis pathway in plants.

or the degradation of starch (Fig. 9.12), is converted in a reversible reaction by **hexose phosphate isomerase** to fructose 6-phosphate. This reaction proceeds in analogy to the isomerization of ribose 5-phosphate (Fig. 6.18). Fructose 6-phosphate is phosphorylated by ATP to fructose 1.6-bisphosphate, as catalyzed by **ATP-phosphofructokinase** (Fig. 9.15). Alternatively, it is also phosphorylated by inorganic pyrophosphate via **pyrophosphate-phosphofructokinase**. The latter enzyme does not occur in plastids. Since in both reactions the free energy for the hydrolysis of the anhydride phosphate donor is much higher than that of the phosphate ester, the formation of fructose 1.6-bisphosphate is an irreversible process. For this reason, the conversion of fructose 1.6-bisphosphate to fructose 6-phosphate proceeds via another reaction, namely, the hydrolysis of phosphate, as catalyzed by **fructose 1.6-bisphosphatase** (Fig. 6.15). Fructose 1.6-bisphosphate is split in a reversible reaction into glyceraldehyde phosphate and dihydroxyacetone phosphate as catalyzed by **aldolase** (Fig. 6.14). Dihydroxyacetone phosphate is converted to glyceraldehyde phosphate by **triose phosphate isomerase**, again in analogy to the isomerization of ribose 5-phosphate (Fig. 6.18). In the reaction sequence of the glycolysis pathway discussed so far, the hexose phosphate was prepared for the generation of reducing equivalents and of ATP. Glyceraldehyde phosphate is oxidized in a reversible reaction by **glyceraldehyde phosphate dehydrogenase** to 1.3-bisphosphoglycerate yielding the reduction of NAD^+. This reaction has already been discussed, although in the opposite direction, as part of the Calvin cycle in Figures 6.9 and 6.10. The change in free energy during the oxidation of the aldehyde to a carboxylate is conserved to form a phosphate anhydride, and by the reversible conversion of 1.3-bisphosphoglycerate to 3-phosphoglycerate, as catalyzed by **phosphoglycerate kinase**, this is utilized for the synthesis of ATP (Fig. 6.9). In order to prepare the remaining phosphate group for the synthesis of ATP, 3-phosphoglycerate is first converted by **phosphoglycerate mutase** to 2-phosphoglycerate (in analogy to the phosphogluco mutase reaction, Fig. 9.6) and then H_2O is split off in a reversible reaction catalyzed by **enolase**, yielding phosphoenol pyruvate**.** In this way a phosphate ester is converted to an enol ester, of which the free energy of hydrolysis is considerably higher than that of the anhydride bond of ATP. Therefore the subsequent conversion of phosphoenolpyruvate to pyruvate coupled to the phosphorylation ADP by **pyruvate kinase** is an irreversible reaction. Alternatively, phosphoenolpyruvate can be converted in the cytosol via **PEP carboxylase** (Fig. 8.5) to oxaloacetate, and the latter can be reduced by **malate dehydrogenase** (Fig. 5.9) to malate. Malate can be converted to pyruvate by malic enzyme, as described in Figure 8.10. Both pyruvate and malate can be fed into the citrate cycle of the mitochondria for the generation of ATP via the respiratory chain.

Under usual aerobic conditions, the glycolysis pathway makes only a minor contribution to the energy demand of a cell. The conversion of glucose 6-phosphate to pyruvate produces just **three molecules** of **ATP**. In contrast, mitochondrial oxidation of pyruvate and of the NADH formed by glyceraldehyde phosphate dehydrogenase yields about **25 molecules** of **ATP** per glucose 6-phosphate. But in the absence of oxygen, which may occur when roots are flooded or during imbibition of water by germinating seeds, the ATP production by the glycolysis pathway is crucial for maintaining a minimal metabolism. In such a situation, the NADH generated in the glycolysis pathway can be reoxidized by the reduction of pyruvate to lactate, as catalyzed by **lactate dehydrogenase**. In roots and developing seeds, this enzyme is induced by a shortage of oxygen. The lactate formed is excreted as **lactic acid**. Alternatively, the NADH produced by glycolysis can be consumed in converting pyruvate to **ethanol**, in the same way as in ethanol fermentation by yeast. In this reaction, pyruvate is first decarboxylated by **pyruvate decarboxylase** to acetaldehyde, involving thiamine pyrophosphate as cofactor, similar as in Figure 5.4. Subsequently, **alcohol dehydrogenase** catalyzes the reduction of acetaldehyde to ethanol, which is excreted. In plant cells, the activity of alcohol dehydrogenase is largely increased as a response to oxygen deficit. In most plants, ethanol is the main product of anaerobic metabolism, with smaller amounts of lactic acid synthesized.

Apart from the generation of ATP, the glycolysis pathway provides **precursors for a multitude of cell components**. Here are a few examples: the oxidation of glucose 6-phosphate by the oxidative pentose phosphate pathway (Fig. 6.21) yields ribose 5-phosphate as a precursor for the synthesis of nucleotides and nucleic acids. The reduction of dihydroxyacetone phosphate by **glycerol phosphate dehydrogenase** yields glycerol 3-phosphate, a precursor for the synthesis of lipids. Phosphoenolpyruvate is the precursor of a number of amino acids (e.g., phenylalanine), which is the precursor for the synthesis of phenylpropanoids, such as lignin (Fig. 18.9) and tannin (Fig. 18.16). Pyruvate is the precursor for the synthesis of fatty acids (Fig. 15.7) and hence the synthesis of lipids.

The glycolysis pathway is governed by a very complex regulation, particularly as most of the enzymes are located in the cytosol as well as in the plastids. In both compartments, the phosphorylation of fructose 6-phosphate by **ATP-phosphofructokinase** is inhibited by **phosphoenolpyruvate**, allowing a feedback control of the glycolysis pathway. The phosphorylation by the **pyrophosphate-dependent phosphofructokinase** is activated by **fructose 2.6-bisphosphate**, whereas the hydrolysis of fructose 1.6-bisphosphate by **fructosebisphosphatase** is inhibited by this compound (see Fig. 9.15).

Further reading

Britto, D. T., Kronzucker, H. J. Cellular mechanisms of potassium transport in plants. Physiologia Plantarum 133, 637–650 (2008).

Fukao, T., Bailey-Serres, J. Plant responses to hypoxia—is survival a balancing act? Trends in Plant Science 9, 449–456 (2004).

Godt, D., Roitsch, T. The developmental and organ specific expression of sucrose cleaving enzymes in sugar beet suggests a transition between apoplastic and symplastic phloem unloading in the tap roots. Plant Physiology Biochemistry 44, 656–665 (2006).

Hammond, J. P., White, P. J. Sucrose transport in the phloem: Integrating root responses to phosphorus starvation. Journal Experimental Botany 59, 109–193 (2008).

Kehr, J. Phloem sap proteins: Their identities and potential roles in the interaction between plants and phloem-feeding insects. Journal Experimental Botany 57, 767–774 (2006).

Kehr, J., Buhtz, A. Long distance transport and movement of RNA through the phloem. Journal Experimental Botany 59, 85–92 (2008).

Kutchan, T. M. A role for intra- and intercellular translocation in natural product biosynthesis. Current Opinion Plant Biology 8, 292–300 (2005).

Lalonde, S., Wipf, D., Frommer, W. B. Transport mechanisms for organic forms of carbon and nitrogen between source and sink. Annual Review Plant Biology 55, 341–372 (2004).

Lohaus, G., Fischer, K. Intracellular and intercellular transport of nitrogen and carbon. In C. H. Foyer and G. Noctor (eds.), Advances in Photosynthesis: Photosynthetic Assimilation and Associated Carbon Metabolism, pp. 239–263. Kluwer Academic Publishers, Dordrecht, Niederlande (2002).

Lough, T. J., Lucas, W. J. Integrative plant biology: Role of phloem long-distance macromolecular trafficking. Annual Review Plant Biology 57, 203–232 (2006).

Minchin, P. E., Lacointe, A. New understanding of phloem physiology and possible consequences for modelling long-distance carbon transport. New Phytologist 166, 771–779 (2005).

Sauer, N. Molecular physiology of higher plant sucrose transporters. FEBS Letters 581, 2309–2317 (2007).

Thompson, M. V. Phloem: The long and the short of it. Trends in Plant Science 11, 26–32 (2006).

Voitsekhovskaja, O. V., Koroleva, O. A., Bantashev, D. R., Tomos, A. D., Gamalei, Y. V., Heldt, H. W., Lohaus, G. Phloem loading models for two Scrophulariaceae species: What drives symplastic flow via plasmodesmata? Plant Physiology 140, 383–395 (2006).

14

Products of nitrate assimilation are deposited in plants as storage proteins

Whereas the products of CO_2 assimilation are deposited in plants in the form of oligo- and polysaccharides, as discussed in Chapter 9, the amino acids formed as products of nitrate assimilation are stored as proteins. These are mostly special **storage proteins**, which have no enzymatic activity and are often deposited in the cell within **protein bodies**. Protein bodies are enclosed by a single membrane that derived from the endomembrane system of the endoplasmic reticulum and the Golgi apparatus or the vacuoles. In potato tubers, storage proteins are also stored in the vacuole.

Storage proteins can be deposited in various plant organs, such as leaves, stems, and roots. They are stored in seeds and tubers and also in the cambium of tree trunks during winter to enable the rapid formation of leaves during seed germination and sprouting. Storage proteins are located in the endosperm in cereal seeds and in the cotyledons of most legume seeds. Whereas in cereals the protein content amounts to 10% to 15% of the dry weight, in some legumes (e.g., soybean) it is as high as 40% to 50%. About 85% of these proteins are storage proteins.

Globally, about 70% of the human demand for protein is met by the consumption of seeds, either directly or indirectly by feeding them to animals for meat production. Therefore plant storage proteins are the important basis for human nutrition. However, in many plant storage proteins the content of nutritionally essential amino acids is too low. In cereals, for example, the storage proteins are limited in **threonine**, **tryptophan**, and particularly in **lysine**, whereas in legumes there is a shortage of **methionine**. Since these amino acids cannot be synthesized by the human metabolism, humans have to take up essential amino acids through their food. In

Table 14.1: Some examples of plant storage proteins

Plant	Globulin	Prolamin (incl. glutelin)	2S-Protein
Rape seed			Napin*
Pea, bean	Legumin, vicilin		
Wheat, rye		Gliadin, glutenin	
Maize		Zein	
Potato	Patatin		

*Structurally related to prolamins, which, according to the solubility properties, are classified as globulins

humans with an entirely vegetarian diet, the deficiency of essential amino acids can lead to irreparable physical and mental damage, especially in children. It can also be a serious problem in pig and poultry fodder. A research goal in plant genetic engineering is to improve the amino acid composition of the storage proteins of harvest products.

Scientists have long been interested in plant proteins. In 1745 the Italian Jacopo Beccari isolated proteins from wheat. In 1924, Thomas Osborne, at the Connecticut Agricultural Experimental Station, classified plant proteins according to their solubility properties. He fractionated plant proteins into **albumins** (soluble in pure water), **globulins** (soluble in diluted salt solutions), **glutelins** (soluble in diluted solutions of alkali and acids), and **prolamins** (soluble in aqueous ethanol). Later, when the structures of these proteins were determined, it turned out that glutelins and prolamins were structurally closely related. Therefore, in more recent literature, glutelins are regarded as members of the group of prolamins. Table 14.1 shows some examples of various plant storage proteins.

14.1 Globulins are the most abundant storage proteins

Storage globulins occur in varying amounts in practically all plants. The most important globulins are **legumin** and **vicilin**, both of which are encoded by a multigene family. These multigene families descend from a common ancestor. Legumin is the main storage protein of leguminous seeds. In broad bean, for instance, 75% of the total storage protein consists of legumin.

Legumin is a hexamer with a molecular mass of 300 to 400 kDa. The monomers contain two different peptide chains (α, β), which are linked by a disulfide bridge. The large α-chain usually has a molecular mass of about 35 to 40 kDa, and the small β-chain has a molecular mass of about 20 kDa. Hexamers can be composed of different (α, β) monomers some of which contain methionine. In the hexamer, the protein molecules are arranged in a very regular package and can be deposited in this form in the protein bodies. Protein molecules, in which some of the protein chains are not properly folded, do not fit into this package and are degraded by peptidases. Although it is easy nowadays to exchange amino acids in a protein by genetic engineering, it turned out to be difficult for storage proteins, most likely because the three-dimensional structure of the molecule was altered by such exchanges. Recent progress was made in obtaining protein crystals which enabled the analysis of the three-dimensional protein structure of the precursor trimers as well as of the mature storage proteins. These studies revealed that the stability of the storage proteins towards the proteases in the storage vacuoles is due to possible cleavage sites being hidden within the protein structure and in this way protected against proteolysis.

Vicilin shows similarities in its amino acid sequence to legumin, and primarily forms trimers, of which the monomers consist of only one peptide chain. Due to the lack of cysteine, the vicilin monomers are unable to form S-S bridges. In contrast to legumins, vicilins are often glycosylated; they contain carbohydrate residues, such as mannose, glucose, and *N*-acetylglucosamine.

14.2 Prolamins are formed as storage proteins in grasses

Prolamins are only present in grasses, such as cereals. They form polymorphic mixtures of many different subunits of 30 to 90 kDa. Some of these subunits contain cysteine residues and are linked by S-S bridges. Also in **glutenins** which occur in the grains of wheat and rye, monomers are linked by S-S bridges. The glutenin molecules differ in size. Flour for baking bread depends on the content of high molecular glutenins. Flour from barley, oats or maize that lacks glutenin is not suitable for baking bread. Since the glutenin content is a critical factor in determining the quality of bread grain, investigations are in progress to improve the glutenin content of grains by genetic engineering.

14.3 2S-Proteins are present in seeds of dicot plants

2S-Proteins are also widely distributed storage proteins. They represent a heterogeneous group of proteins, of which the sole definition is their sedimentation coefficient of about 2 Svedberg (S). Structural investigations have revealed that most 2S-proteins have a related structure and therefore possibly derive, along with the prolamins, from a common ancestor protein. **Napin**, the predominant storage protein in rape seed, is an example of a 2S-protein. This protein is of substantial economic importance since, after the oil has been extracted, the remainder of the rape seed is used as fodder. Napin and other related 2S-proteins consist of two relatively small polypeptide chains of 9 kDa and 12 kDa, which are linked by S-S bridges. So far, little is known about the packing of the prolamins and 2S-proteins in the protein bodies.

14.4 Special proteins protect seeds from being eaten by animals

The protein bodies of some seeds contain additional proteins, which, although also acting as storage proteins, protect the seeds from being eaten. Some examples are: the storage protein **vicilin** has a defense function as it binds to the chitin matrix of fungi and insects. In some insects, vicilin interferes with the development of the larvae. The seeds of some legumes contain **lectins**, which bind to sugar residues, irrespective of whether these are free sugars or constituents of glycolipids or glycoproteins. When these seeds are consumed by animals, the lectins bind to glycoproteins in the intestine and thus interfere with the absorption of food. The seeds of some legumes and other plants also contain **proteinase inhibitors**, which block the digestion of proteins by inhibiting proteinases in the animal digestive tract. Because of their content of lectins and proteinase inhibitors, many beans and other plant products are suitable for human consumption only after being denatured by cooking. This is one reason why humans have learned to cook. Castor beans contain the extremely toxic protein **ricin** of which a few milligrams are sufficient to kill a human being. Beans also contain **amylase inhibitors**, which specifically inhibit the hydrolysis of starch by amylases in the digestive tract of certain insects. Using genetic engineering, α-amylase inhibitors from beans have been successfully expressed in the

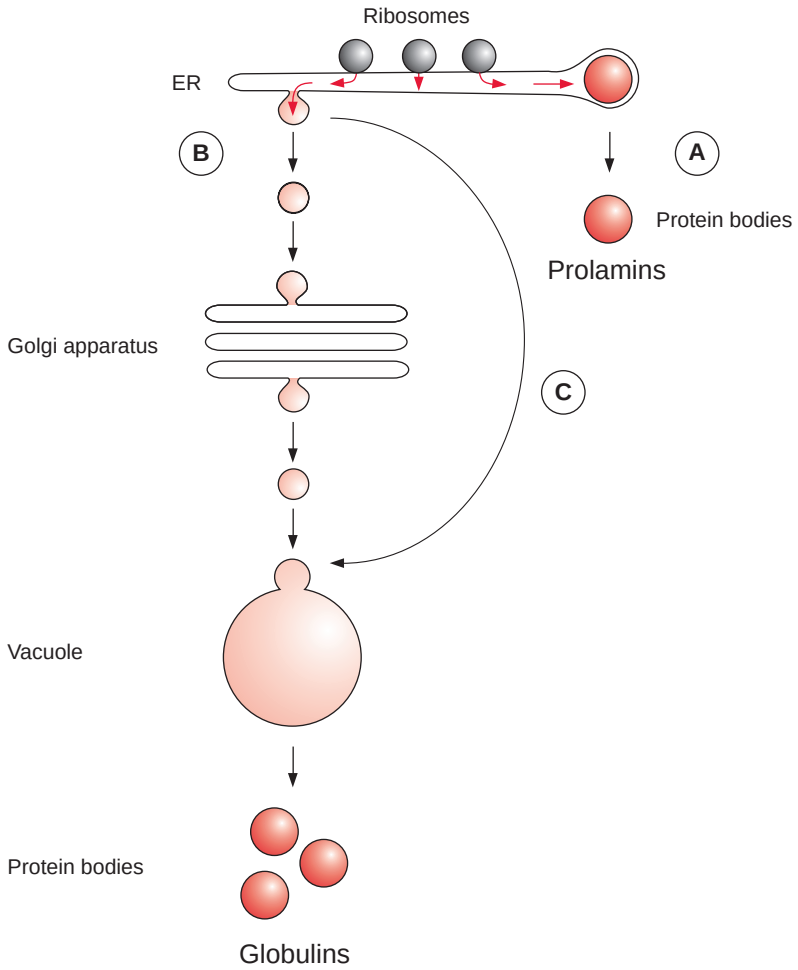

Figure 14.1 Three ways of depositing storage proteins in protein bodies; their presence depending on plant species.
A. During formation of prolamin in cereal grains, the prolamin aggregates in the lumen of the ER and the protein bodies are formed by budding off from the ER.
B. The proteins that appear in the lumen of the ER are transferred via the Golgi apparatus to the vacuole. The protein bodies are formed by fragmentation of the vacuole. This is probably the most common pathway.
C. In a third alternative, the proteins that appear in the lumen of the ER are directly transferred to the vacuole circumventing the Golgi apparatus.

seeds of pea. Whereas the larvae of the pea beetle normally cause large losses during storage of peas, the peas from the genetically modified plants were protected against these losses.

14.5 Synthesis of the storage proteins occurs at the rough endoplasmic reticulum

Seed storage proteins are formed by ribosomes at the rough endoplasmic reticulum (ER) (Fig. 14.1). The newly synthesized proteins occur in the

lumen of the ER, and the storage proteins are finally deposited in the **protein bodies**. In the case of 2S-proteins and prolamins, the protein bodies are formed by budding from the ER. The globulins are mostly transferred from the ER by vesicle transfer via the Golgi apparatus (section 1.6), first to the vacuole, from which protein bodies are formed by fragmentation. There is also a pathway by which certain proteins (e.g., globulins in wheat endosperm) are transported directly by vesicle transfer from the ER to the vacuole without passing the Golgi apparatus.

Figure 14.2 shows the formation of legumin in detail. The protein formed by the ribosome contains, at the N-terminus of the polypeptide chain, a hydrophobic section called a **signal sequence**. After the synthesis of this signal sequence, translation is attenuated, and the signal sequence forms a complex with three other components:

1. **A signal recognition particle,**
2. A **binding protein** attached at the ER membrane, and
3. A **pore protein** present in the ER membrane.

The formation of this complex anchors the ribosome on the ER membrane for the duration of protein synthesis and supports the continuation of translation. The newly formed protein chain (e.g., pre-pro-legumin) reaches the lumen of the ER. Immediately after the peptide chain enters the lumen, the signal sequence is removed by a **signal peptidase** located on the inside of the ER membrane. The remaining polypeptide, termed a **pro-legumin**, comprises the future α- and β-chains of the legumin. An S-S linkage within the pro-legumin is formed in the ER lumen. Three pro-legumin molecules form a **trimer**, facilitated by chaperones (section 21.2). A quality control occurs during this association: Trimers without the correct conformation are degraded. The trimers are transferred via the Golgi apparatus to the vacuoles, where the α- and β-chains are separated by a peptidase. The subunits of the legumins are now assembled to **hexamers** and are deposited in this form. The protein bodies, the final storage site of the legumins, are derived from fragmentation of the vacuole. The carbohydrate chains of glycosylated vicilins (e.g., of the phaesolins from the bean *Phaseolus vulgaris*) are processed in the Golgi apparatus.

The pre-pro-forms of newly synthesized **2S-proteins** and **prolamins**, which occur in the lumen of the ER, also contain a signal sequence. Completion and aggregation of these proteins takes place in the lumen of the ER, from which the protein bodies are formed by budding.

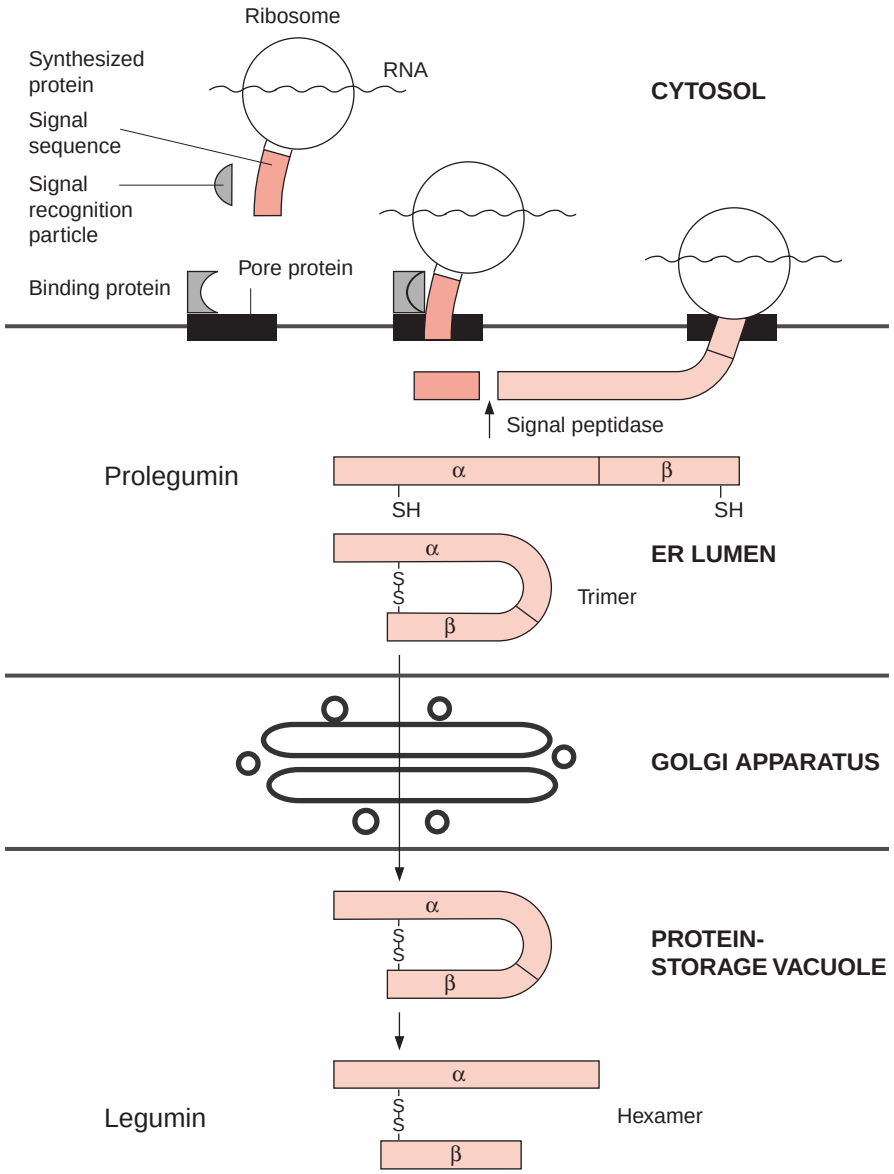

Figure 14.2 Legumin synthesis. The pre-pro-form of the legumin formed by the ribosome is first processed in the lumen of the ER and then further in the vacuole to yield the end product.

14.6 Proteinases mobilize the amino acids deposited in storage proteins

Our knowledge about the mobilization of the amino acids from storage proteins derives primarily from investigations of processes during seed germination. In most cases, germination is induced by the uptake of water, and as a result of this protein bodies fuse to form a vacuole. The hydrolysis of the storage proteins is catalyzed by proteinases, which are in part deposited as inactive pro-forms together with the storage proteins in the protein bodies. Other proteinases are newly synthesized and transferred via the lumen of the ER and the Golgi apparatus to the vacuoles (Fig. 14.2). These enzymes are initially synthesized as inactive pro-forms. Activation of these pro-proteinases proceeds by limited proteolysis, in which a section of the sequence is removed by a specific peptidase. The remainder of the polypeptide represents the active proteinase.

The degradation of the storage proteins is also initiated by limited proteolysis. A specific proteinase first removes small sections of the protein sequence, resulting in a conformational change of the storage protein. In cereal grains, S-S bridges of storage proteins are cleaved by reduced thioredoxin (section 6.6). The unfolded protein is then susceptible to hydrolysis by various proteinases, for example exopeptidases, which split off amino acids one after the other from the end of the protein molecule, and endopeptidases, which cleave within the molecule. In this way storage proteins are completely degraded in the vacuole and the liberated amino acids are provided as building material to the germinating plant.

Further reading

Adachi, M., Takenaka, Y., Gidamis, A. B., Mikami, B., Utsumi, S. Crystal structure of soybean proglycinin A1aB1b homotrimer. Journal Molecular Biology 305, 291–305 (2001).

Anjum, F. M., Khan, M. R., Din, A., Saeed, M., Pasha, I., Arshad, M. U. Wheat gluten: High molecular weight glutenin subunits—Structure, genetics, and relation to dough elasticity. Journal Food Science 72, 56–63 (2007).

Bethke, P. C., Jones, R. L. Vacuoles and prevacuolar compartments. Current Opinion in Plant Biology 3, 469–475 (2000).

Hadlington, J. L., Denecke, J. Sorting of soluble proteins in the secretory pathway of plants. Current Opinion in Plant Biology 3, 461–468 (2000).

Haq, S. K., Atif, S. M., Khan, R. H. Protein proteinase inhibitor genes in combat against insects, pests, and pathogens: Natural and engineered phytoprotection. Archives Biochemistry Biophysics 431, 145–159 (2004).

Jolliffe, N. A., Craddock, C. P., Frigerio, L. Pathways for protein transport to seed storage vacuoles. Biochemical Society Transactions 33, 1016–1018 (2005).

Matsuoka, K., Neuhaus, J.-M. *Cis*-elements of protein transport to the plant vacuoles. Journal Experimental Botany 50, 165–174 (1999).

Morton, R. L., Schroeder, H. E., Bateman, K. S., Chrispeels, M. J., Armstrong, E. Bean α-amylase inhibitor 1 in transgenic peas (*Pisum sativum*) provides complete protection from pea weevil (*Bruchus pisorum*) under field conditions. Proceedings National Academy USA 97, 3820–3825 (2000).

Muentz, K., Shutov, A. D. Legumains and their functions in plants. Trends in Plant Science 7, 340–344 (2002).

Müntz, K. Protein dynamics and proteolysis in plant vacuoles. Journal Experimental Botany 58, 2391–2407 (2007).

Payan, F. Structural basis for the inhibition of mammalian and insect alpha-amylases by plant protein inhibitors. Biochimica Biophysica Acta 1696, 171–180 (2004).

Peumans, W. J., van Damme, E. J. M. Lectins as plant defense proteins. Plant Physiology 109, 247–352 (1995).

Robinson, D. G., Oliviusson, P., Hinz, G. Protein sorting to the storage vacuoles of plants: A critical appraisal. Traffic 6, 615–625 (2005).

Shewry, P. R., Napier, J. A., Tatham, A. S. Seed storage proteins: Structures and biosynthesis. Plant Cell 7, 945–956 (1995).

Shutov, A. D., Bäumlein, H., Blattner, F. R., Müntz, K. Storage and mobilization as antagonistic functional constraints on seed storage globulin evolution. Journal Experimental Botany 54, 1645–1654 (2003).

Somerville, C. R., Bonetta, D. Plants as factories for technical materials. Plant Physiology 125, 168–171 (2001).

Van Damme, E. J. M., Barre, A., Rouge, P., Peumans, W. J. Cytoplasmic/nuclear plant lectins: A new story. Trends in Plant Science 9, 484–489 (2004).

Vitale, A., Hinz, G. Sorting of proteins to storage vacuoles: How many mechanisms? Trends in Plant Science 10, 316–323 (2005).

15

Lipids are membrane constituents and function as carbon stores

Lipids subdivide into **glycerolipids**, **shingolipids**, and **steroids**. **Glycerolipids** are fatty acid esters of glycerol (Fig. 15.1). **Triacylglycerols** (also called triglycerides) consist of a glycerol molecule that is esterified with three fatty acids. Whereas in animals triacylglycerols serve primarily as an energy store, they function in plants mainly as a carbon store in seeds, which are used by humans as vegetable oils. In **polar glycerolipids**, the glycerol is esterified with only two fatty acids, and a hydrophilic group is linked to the third -OH group. These polar lipids are the main constituents of membranes.

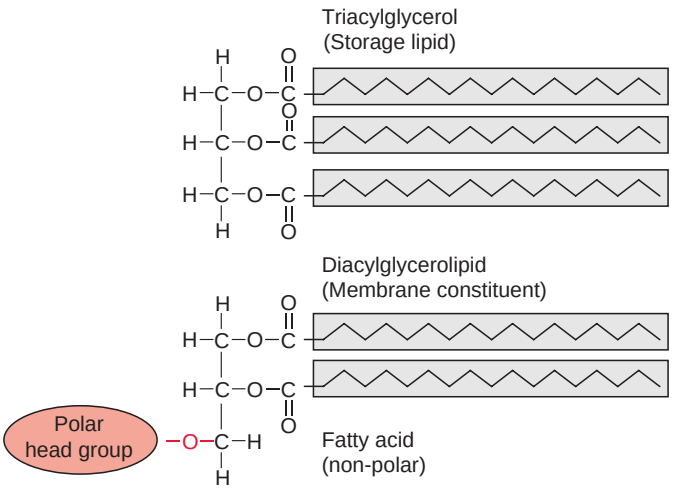

Figure 15.1
Triacylglycerols are comprised of three fatty acids of nonpolar nature. In contrast, polar lipids are amphiphilic compounds, since, besides the hydrophobic tail consisting of two fatty acids, a polar hydrophilic head group is present in the molecule.

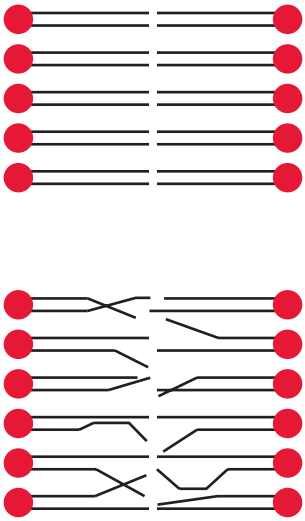

Figure 15.2
Membrane lipids with saturated fatty acids form a very regular lipid bilayer. The kinks caused in the hydrocarbon chain by *cis*-carbon-carbon double bonds in unsaturated fatty acids result in disturbances in the lipid bilayer and lead to an increase in its fluidity.

15.1 Polar lipids are important membrane constituents

The polar **glycerolipids** are **amphiphilic molecules**, consisting of a hydrophilic head and a hydrophobic tail. This property enables them to form **lipid bilayers**, in which the hydrocarbon tails are held together by hydrophobic interactions and the hydrophilic heads protrude into the aqueous phase, thus forming the basic structure of a membrane (bilayer) (Fig. 15.2). Since the middle C atom of the glycerol in a polar glycerolipid is asymmetric, a distinction can be made between the two esterified groups of glycerol at the C-1- and C-3-positions.

Other membrane lipids in plants are **sphingolipids** (Fig. 15.5C) which are important constituents of plasma membranes. The **sterols** shown in Figure 15.3 are also amphiphilic, the hydroxyl groups form the hydrophilic head and the sterane skeleton with the side chain serves as the hydrophobic tail. In addition to the sterols shown here, plants contain a large variety of other sterols as membrane constituents, many of them are present in the outer membrane of mitochondria, in the membranes of the endoplasmatic reticulum, and in the plasma membrane. Sterols determine to a large extent the properties of these membranes (see below).

The polar glycerolipids are comprised mainly of fatty acids with 16 or 18 carbon atoms (Fig. 15.4). The majority of these fatty acids are unsaturated and contain one to three carbon-carbon double bonds. These double bonds are almost exclusively in the ***cis***-configuration and rarely in the

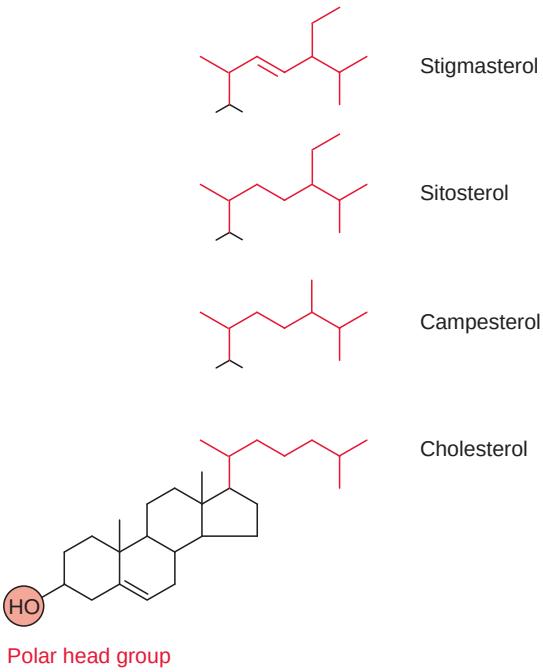

Figure 15.3 Cholesterol and the related sterols (only side chains are shown) are membrane constituents.

trans-configuration. The double bonds are usually not conjugated. Figure 15.4 shows the number code for the structure of fatty acids: number of C atoms, number of double bonds, Δ-position of the first C atom of the double bond, c = *cis*-configuration (t = *trans*).

The storage lipids of plants often contain unusual fatty acids (e.g., with conjugated double bonds, carbon-carbon triple bonds, or hydroxyl-, keto- or epoxy groups). By now more than 500 of these unusual fatty acids are known. There are also glycerolipids, in which the carbon chain is connected with the glycerol via an ether linkage.

The fluidity of the membrane is governed by the proportion of unsaturated fatty acids and the content of sterols

The hydrocarbon chains in saturated fatty acids are packed in a regular bilayer (Fig. 15.2), whereas in unsaturated fatty acids the packing is disturbed due to kinks in the hydrocarbon chain, caused by the *cis*-carbon-carbon double bonds, resulting in a more fluid layer and having an effect on the melting points of various fatty acids (Table 15.1). The melting point increases with increasing chain length as the packing becomes tighter, whereas the melting point decreases with an increasing number of double

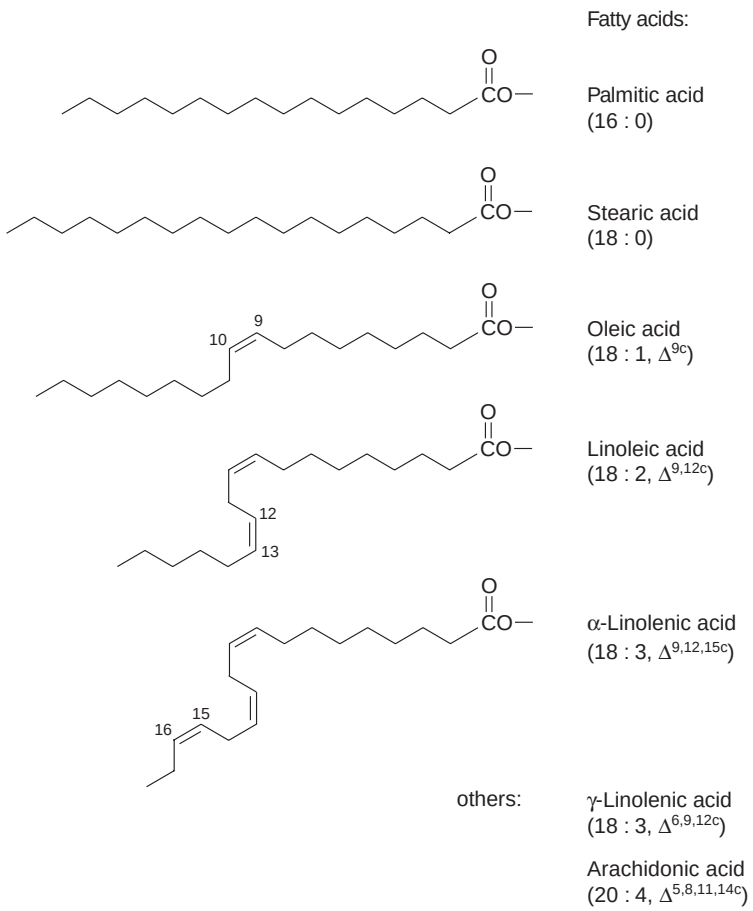

Figure 15.4 Fatty acids as hydrophobic constituents of membrane lipids.

Table 15.1: Influence of chain length and the number of double bonds on the melting point of fatty acids

Fatty acid	Chain length: double bonds	Melting point
Lauric acid	12:0	40°C
Stearic acid	18:0	70°C
Oleic acid	18:1	13°C
Linoleic acid	18:2	−5°C
Linolenic acid	18:3	−11°C

bonds. This feature also applies to the corresponding fats. Cocoa fat, for instance, consisting only of saturated fatty acids, is solid at room temperature, whereas plant oils, with a very high natural content of unsaturated fatty acids, are liquid.

Likewise, the **fluidity of membranes** is governed by the proportion of **unsaturated fatty acids** in the membrane lipids. This is why in some plants, during growth at a low temperature, more highly unsaturated fatty acids are incorporated into the membrane to compensate for the decrease in membrane fluidity. It has been demonstrated that it is possible to enhance the cold tolerance of tobacco by increasing the proportion of unsaturated fatty acids in the membrane lipids by genetic engineering. Sterols (Fig. 15.3) decrease the fluidity of membranes and probably also play a role in the adaptation of membranes to temperature. On the other hand, a decrease of unsaturated fatty acids in the lipids of thylakoid membranes, as achieved by genetic engineering, made tobacco plants more tolerant to heat.

Membrane lipids contain a variety of hydrophilic head groups

The head groups of the polar glycerolipids, which provide the lipid molecule with a polar group, are formed in plants by a variety of compounds (Fig. 15.5). In the **phospholipids**, the head group consists of a phosphate residue that is esterified with a second alcoholic compound such as ethanolamine, choline, serine, glycerol, or inositol. Phosphatidic acid is only a minor membrane constituent, but it plays a role as a signaling compound (section 19.1).

The phospholipids are found as membrane constituents in bacteria as well as in animals and plants. As a specialty of plants and cyanobacteria the **galactolipids** monogalactosyldiacylglycerol (MGDG) and digalactosyldiacylglycerol (DGDG), and the sulfolipid sulfoquinovosyldiacylglycerol (SL) are additionally present in the membranes. In SL a glucose moiety to which a sulfonic acid residue is linked at the C-6-position forms the polar head group (Fig. 15.5B).

There are great differences in the lipid composition of the various membranes in a plant (Table 15.2). The main constituents of the chloroplast thylakoid and envelope membranes are **galactolipids**. The membranes of the mitochondria and the plasma membrane do not contain galactolipids but have phospholipids as the main membrane constituents. **Cardiolipin** is a specific component of the inner mitochondrial membrane in animals and plants (Fig. 15.5A).

In a green plant cell, about 70% to 80% of the total membrane lipids are constituents of the thylakoid membranes. Plants represent the largest part of the biosphere, and this is why the galactolipids MGDG and DGDG are the most abundant membrane lipids on earth. In many habitats plant growth is limited by the phosphate content in the soil, therefore it was probably advantageous during evolution for plants to synthesize—independent

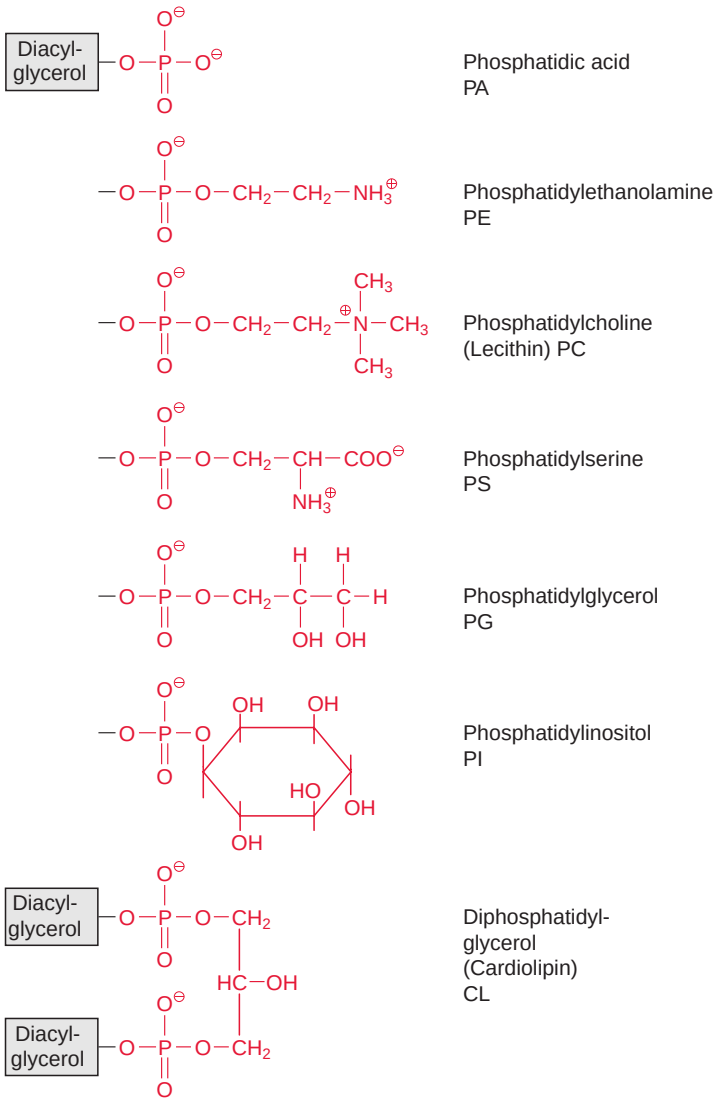

Figure 15.5A Hydrophilic constituents of membrane lipids: phosphate and phosphate esters.

of the phosphate supply of the soil—galactolipids rather than phospholipids as dominant membrane lipids.

Sphingolipids are important constituents of the plasma membrane

Sphingolipids (Fig. 15.5C) are present in the plasma and ER membranes. The sphingolipids consist of a so-called **sphingo base**. This is a hydrocarbon

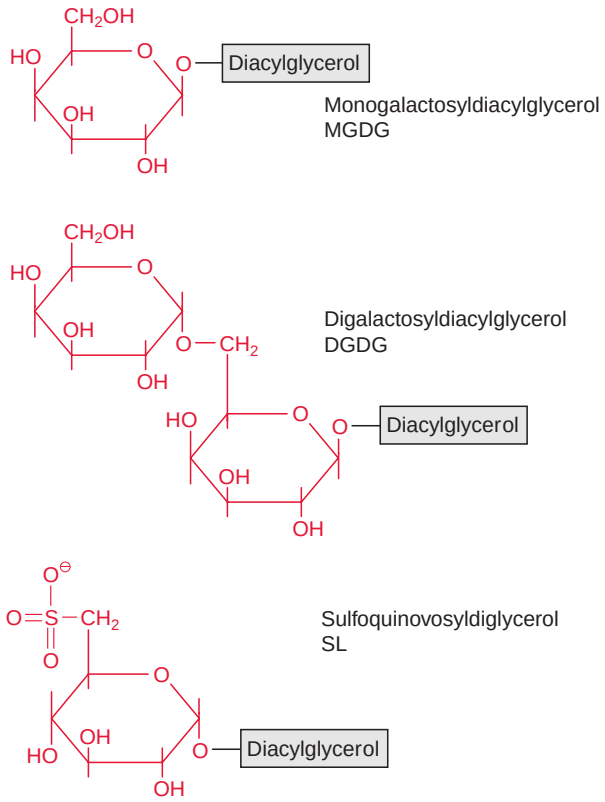

Figure 15.5B Hydrophilic constituents of membrane lipids: hexoses.

chain containing double bonds, an amino group in position 2, and two to three hydroxyl groups in positions 1, 3, and 4. The sphingo base is connected by an amide link to a fatty acid (C16–24, with up to two double bonds). As an example of one of the many sphingolipids, **ceramide**, with sphinganine as base, is shown in Figure 15.5C. In **glucosylsphingolipids**, the terminal hydroxyl group is linked to a glucose residue, whereas **phosphorylsphingolipids** (not shown in Fig. 15C) are esterified with phosphate or phosphocholine.

Sphingolipids are known to have an important signaling function in animals and yeast. Research on the function of sphingolipids in plants is still in its infancy. Recent results indicate that sphinganine 1-phosphate acts in guard cells as a **Ca^{++}-mobilizing messenger**, which is released upon the action of abscisic acid (**ABA**) (see also sections 8.2 and 19.6). Plant sphingolipid metabolites may be also involved as signals in **programmed cell death**.

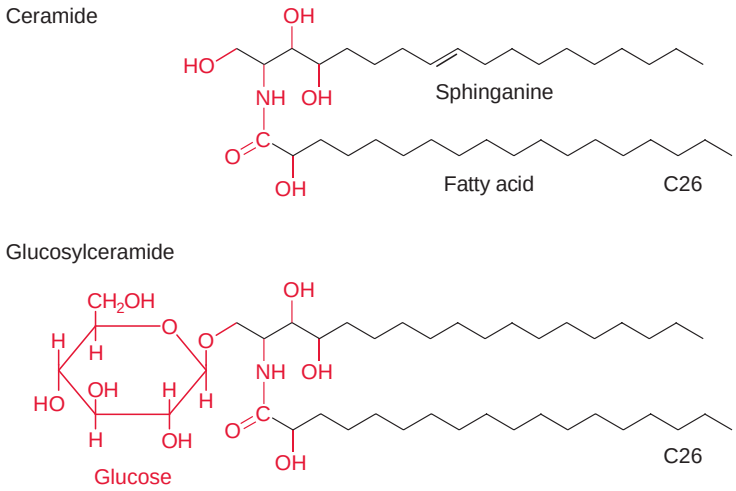

Figure 15.5C Hydrophilic constituents of membrane lipids: sphingolipids.

Table 15.2: The composition of membrane lipids in various organelle membranes

Membrane lipids*	Chloroplast thylakoid membrane	ER membrane	Plasma membrane
		Mol %	
Monogalactosyldiglyceride	42	1	2
Digalactosyldiglyceride	33	2	3
Sulfolipide	5	0	0
Phosphatidylcholine	5	45	19
Phosphatidylethanolamine	1	15	17
Phosphatidylserine	0	1	3
Phosphatidylglycerol	11	6	12
Phosphatidylinositol	0	8	2
Sphingolipids	0	10	7
Sterols	0	5	31

Leaves from Rye, after Lochnit et al. (2001)

15.2 Triacylglycerols are storage compounds

Triacylglycerols are primarily present in seeds but also in some fruits such as olives or avocados. The purpose of triacylglycerols in fruits is to attract animals to consume these fruits in order to obtain a wide distribution of the seeds. The triacylglycerols in seeds are a carbon store to supply the carbon required for biosynthetic processes during seed germination. Triacylglycerols

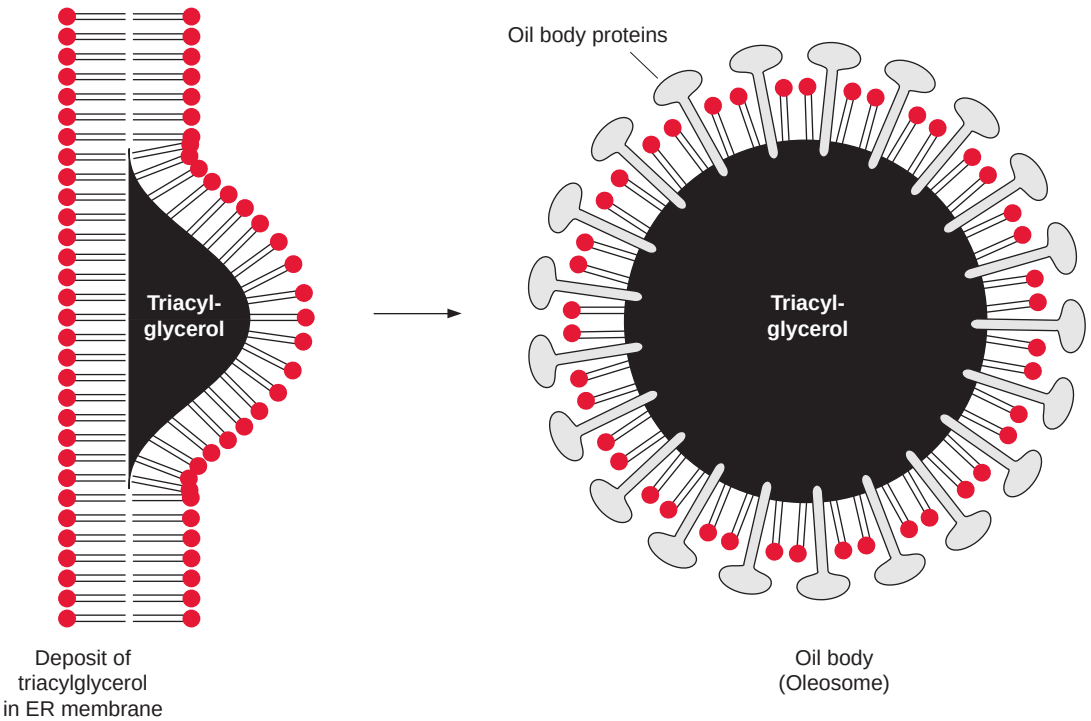

Figure 15.6 The incorporation of triacylglycerols in the ER membrane results in the formation of oil bodies that are enclosed by a lipid monolayer. Oil body proteins such as oleosins, caloleosins and steroleosins are anchored to the lipid monolayer.

have an advantage over carbohydrates as storage compounds, because their weight/carbon content ratio is much lower. A calculation illustrates this: in starch the glucose residue, containing six C atoms, has a molecular mass of 162 Da. The mass of one stored carbon atom thus amounts to 27 Da. In reality, this value is higher, since starch is hydrated. A triacylglycerol with three palmitate residues contains 51 C atoms and has a molecular mass of 807 Da. The mass of one stored carbon atom thus amounts to only 16 Da. Since triacylglycerols, in contrast to starch, are not hydrated, carbon stored as fat in the seed requires less than half the weight as when it is stored as starch. Low seed weight is advantageous for dispersal.

Triacylglycerols are deposited in **oil bodies**, also termed **oleosomes** or **lipid bodies** (Fig. 15.6). They are oil droplets, which are surrounded by a lipid monolayer. A variety of **oil body proteins** (oleosines, caloleosines, steroleosines) are anchored to the lipid monolayer and catalyze the mobilization of fatty acids from the triacylglycerol store during seed germination (section 15.6). These oil body proteins are present only in oil bodies of the endosperm and embryonic tissue of seeds. The oil bodies in the pericarp of

olives or avocados, where the triacylglycerols are not used for storage but to lure animals, do not possess oil body proteins. With 10 to 20 μm in diameter these are much larger than the oil bodies of storage tissues (diameter 0.5–2 μm). It is assumed that newly synthesized triacylglycerol accumulates between the lipid bilayer of the ER membrane, until the full size of the oil body is reached (Fig. 15.6; section 15.5). When the oil body buds off from the ER membrane, it is surrounded by a phospholipid monolayer.

15.3 The *de novo* synthesis of fatty acids takes place in the plastids

The carbon fixed by CO_2 assimilation in the chloroplasts is the precursor not only for the synthesis of carbohydrates and amino acids, but also for the synthesis of fatty acids and various secondary metabolites discussed in Chapters 16 to 18. Whereas the production of carbohydrates and amino acids by the mesophyll cells is primarily destined for export to other parts of the plants, the synthesis of fatty acids occurs only for the cell's own requirements, except in seeds and fruits. Plants are not capable of long-distance fatty acid transport. Since fatty acids are present as constituents of membrane lipids in every cell, each cell must contain the enzymes for the synthesis of membrane lipids and thus also for the synthesis of fatty acids.

In plants the *de novo* synthesis of fatty acids always occurs in the plastids: in the chloroplasts of green cells and the leucoplasts and chromoplasts of non-green cells. Although in plant cells enzymes of fatty acid synthesis are also found in the membrane of the ER, these enzymes appear to be involved only in the **modification** of fatty acids, which have been synthesized earlier in the plastids. These modifications include a chain elongation of fatty acids, as catalyzed by **elongases** and the introduction of further double bonds by **desaturases** (Fig. 15.15B).

Acetyl CoA is a precursor for the synthesis of fatty acids

Acetyl CoA is provided in different ways**.** Like mitochondria (see Fig. 5.4), plastids contain a **pyruvate dehydrogenase complex**, by which pyruvate is oxidized to acetyl CoA, accompanied by the reduction of NAD^+ (Fig. 15.7). In chloroplasts, however, depending on the developmental state of the cells, the activity of pyruvate dehydrogenase is often low. On the other hand, chloroplasts contain a high activity of **acetyl CoA synthetase**, which can convert acetate upon consumption of ATP to acetyl CoA. In many

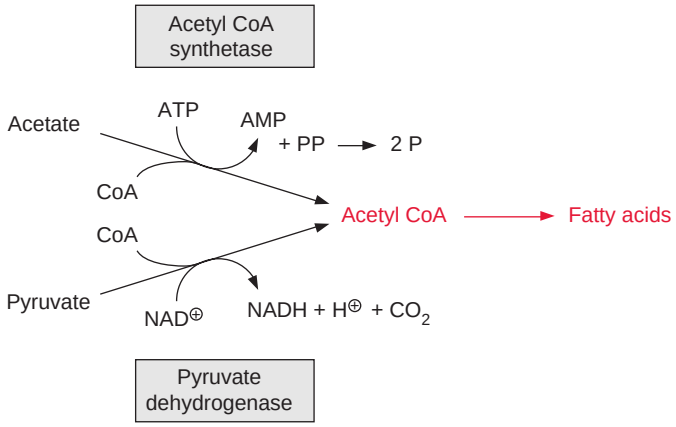

Figure 15.7 Acetyl CoA can be synthesized in two ways.

plants, **acetate** is often a major precursor for the formation of acetyl CoA in the chloroplasts and leucoplasts. Thus, when chloroplasts are supplied with radioactively labeled acetate, the radioactivity is very rapidly incorporated into fatty acids. Our knowledge about the origin of the acetate is still fragmentary. One possibility is that it is formed in the mitochondria by hydrolysis of acetyl CoA, which derived from the oxidation of pyruvate by the mitochondrial pyruvate dehydrogenase complex.

In chloroplasts, photosynthesis provides the **NADPH** required for the synthesis of fatty acids. In leucoplasts, the NADPH required for fatty acid synthesis is provided by the oxidation of glucose 6-phosphate via the **oxidative pentose phosphate pathway** (Fig. 6.21). Glucose 6-phosphate is transported by a **glucose phosphate-phosphate translocator** to the plastids (see Fig. 13.5).

Fatty acid synthesis starts with the carboxylation of acetyl CoA to malonyl CoA by **acetyl CoA carboxylase**, with the consumption of ATP (Fig. 15.8). In a subsequent reaction, CoA is exchanged by **acyl carrier protein** (**ACP**) (Fig. 15.9). ACP comprises a serine residue to which a pantetheine is linked via a phosphate group. The pantetheine is also a functional constituent of CoA. Both ACP and CoA are covalently bound to a protein. The enzyme **β-ketoacyl-ACP synthase III** (**KAS III**) catalyzes the condensation of acetyl CoA with malonyl-ACP. The reaction is irreversible due to the liberation of CO_2. The function of the enzymes KAS I and KAS II will be discussed later (Fig. 15.14). The acetoacetate thus formed remains bound as a thioester to ACP and is reduced by NADPH to β-D-hydroxyacyl-ACP. Following the release of water, the carbon-carbon double bond formed is reduced by NADPH to produce acyl ACP. The product is a **fatty acid** that has been elongated by two carbon atoms (Fig. 15.8).

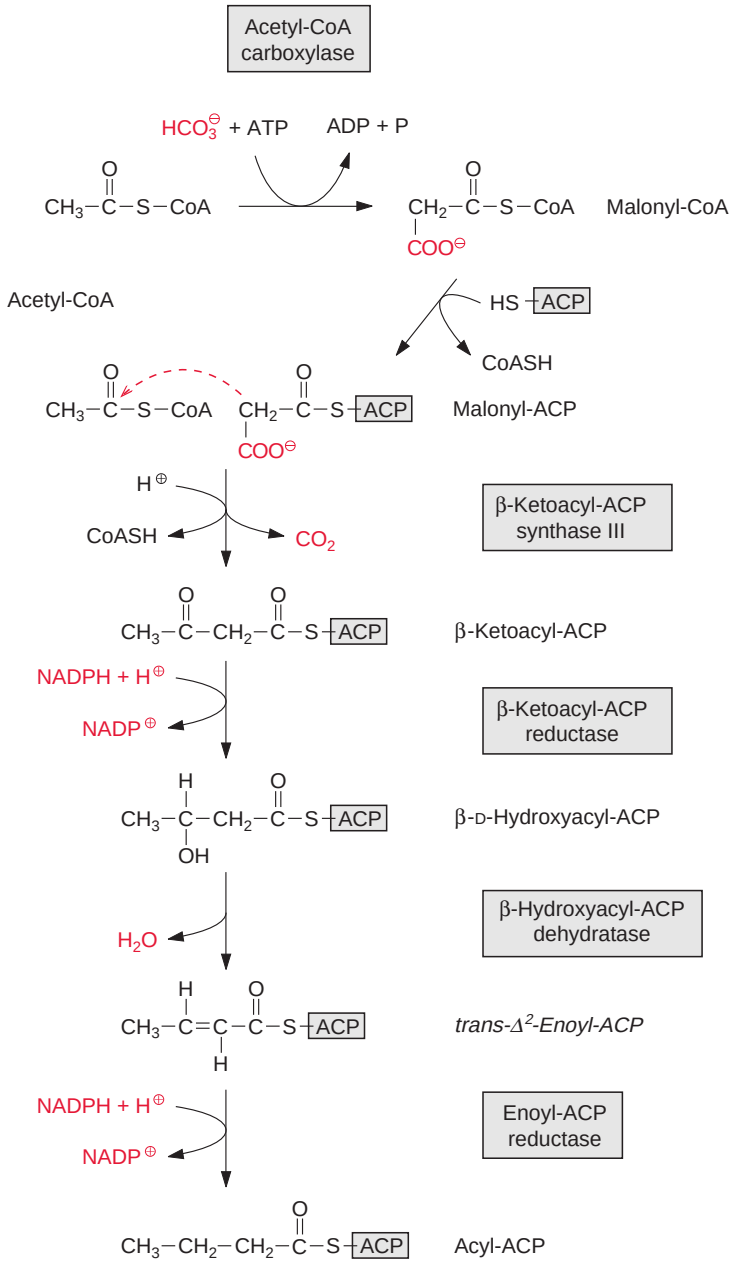

Figure 15.8 Reaction sequence for the synthesis of fatty acids: activation, condensation, reduction, release of water, and another reduction ultimately elongate a fatty acid by two carbon atoms.

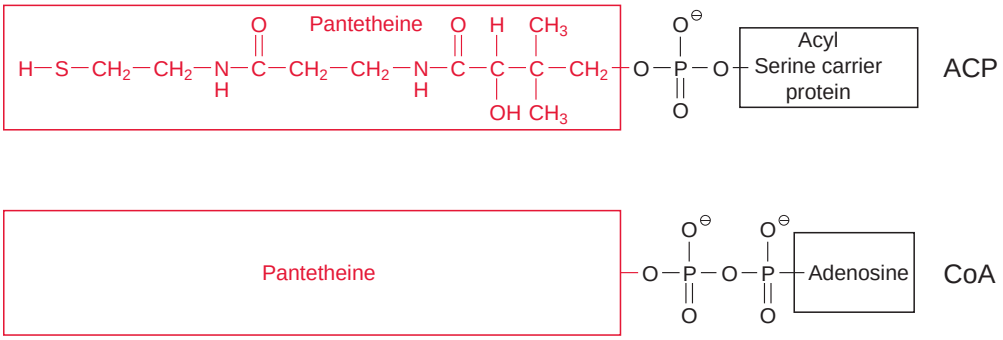

Figure 15.9 The acyl carrier protein (ACP) comprises pantetheine, the same functional group as in coenzyme-A.

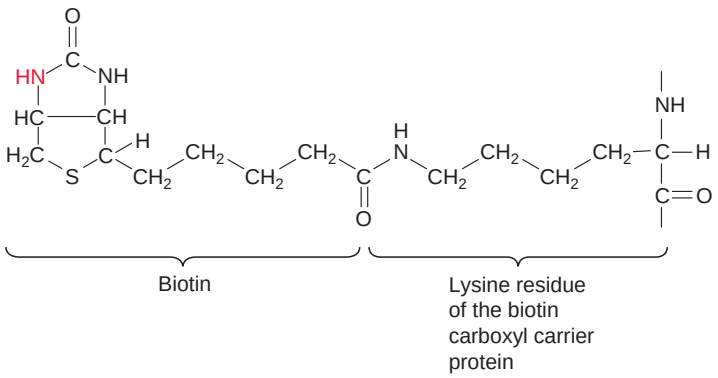

Figure 15.10 Biotin is linked via a lysine residue to the biotin carboxyl carrier protein.

Acetyl CoA carboxylase is the first enzyme of fatty acid synthesis

The carboxylation of acetyl CoA involves **biotin** which acts as a carrier for "**activated CO_2**" (Fig. 15.10). Biotin is covalently linked with its carboxyl group to the ε-amino group of a lysine residue of the **biotin carboxyl carrier protein**, and its -NH-group can form a carbamate with HCO_3^- (Fig. 15.11). This reaction is driven by the hydrolysis of ATP. Therefore the acetyl CoA carboxylation requires two steps:

1. Biotin is carboxylated at the expense of ATP by **biotin carboxylase**.
2. Bicarbonate is transferred to acetyl CoA by **carboxyl transferase**.

All three proteins—the biotin carboxyl carrier protein, biotin carboxylase, and carboxyl transferase—form a single multienzyme complex. Since

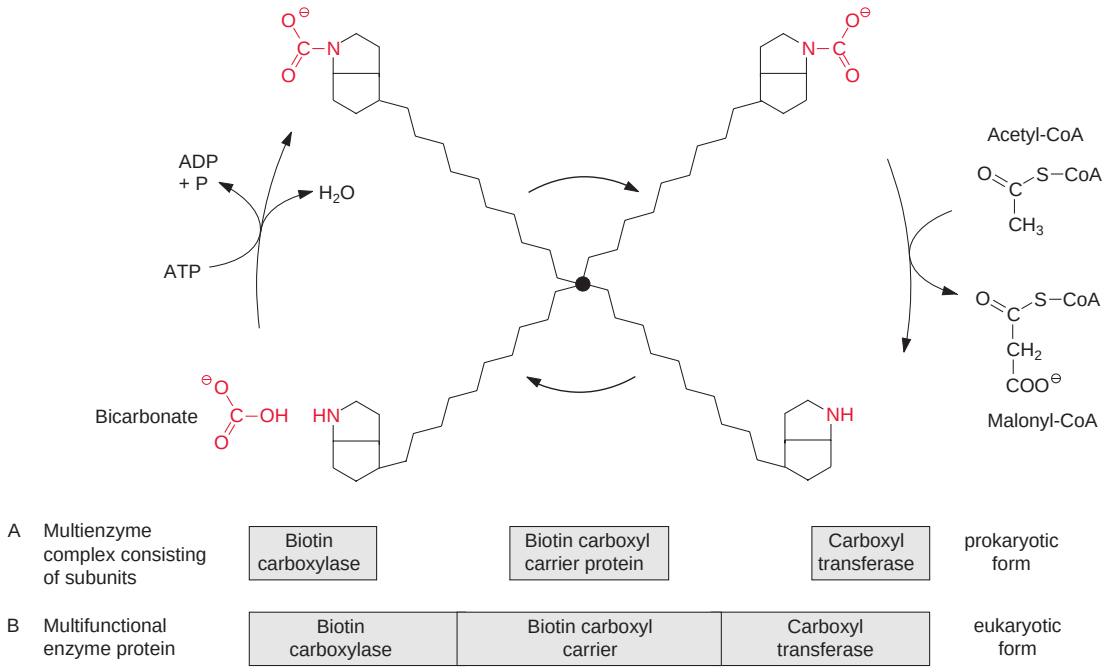

Figure 15.11 Acetyl CoA carboxylase: reaction scheme. The biotin linked to the biotin carboxyl carrier protein reacts in turn with biotin carboxylase and carboxyl transferase. The circular presentation was chosen for the sake of clarity; in reality it is probably a pendulum-like movement. The eukaryotic acetyl CoA carboxylase is present as a multifunctional protein.

the biotin is attached to the carrier protein by a long flexible hydrocarbon chain, it reacts alternately with the carboxylase and carboxyl transferase in this multienzyme complex (Fig. 15.11).

The acetyl CoA carboxylase multienzyme complex in the stroma of plastids consists of several subunits, resembling the acetyl CoA carboxylase in cyanobacteria and other bacteria, and is referred to as the **prokaryotic form** of the acetyl CoA carboxylase. Acetyl CoA carboxylase is also present outside the plastids, probably in the cytosol. The malonyl CoA formed outside the plastids is used for chain elongation of fatty acids and is the precursor for the formation of flavonoids (see section 18.5). The extra-plastidic acetyl CoA carboxylase, in contrast to the prokaryotic type, is a single large **multifunctional protein** in which the biotin carboxyl carrier, the biotin carboxylase, and the carboxyl transferase are located on different sections of the same polypeptide chain (Fig. 15.11). Since this multifunctional protein also occurs in a very similar form in the cytosol of yeast and animals, it is referred to as the **eukaryotic form**. It should be emphasized, however, that

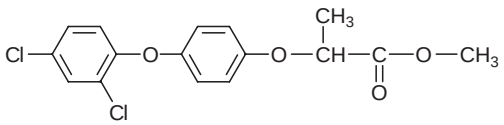

Diclofop methyl

Figure 15.12 Diclofop methyl, a herbicide (Hoe-Grass, Bayer, Crop Science), inhibits the eukaryotic multifunctional acetyl CoA carboxylase.

the eukaryotic form as well as the prokaryotic form of acetyl CoA carboxylase are encoded in the nucleus. Possibly only one protein of the prokaryotic enzyme is encoded in the plastid genome.

In *Gramineae* (grasses), including the various species of cereals, the prokaryotic form is not present. In these plants, the multifunctional eukaryotic acetyl CoA carboxylase is located in the cytosol as well as in the chloroplasts. The eukaryotic acetyl CoA carboxylase is inhibited by various arylphenoxypropionic acid derivatives, such as, for example, **diclofop methyl** (Fig. 15.12). Since eukaryotic acetyl CoA carboxylase in *Gramineae* is involved in the *de novo* fatty acid synthesis of the plastids, this inhibitor severely impairs lipid biosynthesis in this group of plants. Diclofop methyl (trade name Hoe-Grass, Bayer, Crop Science) and similar substances are therefore used as **selective herbicides** (section 3.6) to control grass weeds.

Acetyl CoA carboxylase, the first enzyme of fatty acid synthesis, is an important regulatory enzyme and its reaction is regarded as a rate-limiting step in fatty acid synthesis. In chloroplasts, the enzyme is fully active only during illumination and is inhibited during darkness. This ensures that fatty acid synthesis proceeds mainly during the day, when photosynthesis provides the necessary NADPH. The mechanism of light regulation is similar to the light activation of the enzymes of the Calvin cycle (section 6.6): The acetyl CoA carboxylase is reductively activated by thioredoxin and the activity is further enhanced by the increase of the pH and the Mg^{++} concentration in the stroma.

Further steps of fatty acid synthesis are also catalyzed by a multienzyme complex

β-Ketoacyl ACP formed by the condensation of acetyl CoA and malonyl ACP (Fig. 15.8) is reduced by NADPH to β-D-hydroxyacyl ACP, and after the release of water the carbon-carbon double bond of the resulting enoyl ACP is reduced again by NADPH to acyl ACP. This reaction sequence resembles the reversal of the formation of oxaloacetate from succinate in the citrate cycle (Fig. 5.3). Fatty acid synthesis is catalyzed by a multienzyme complex. Figure 15.13 shows a schematic presentation of the interplay of the various reactions. The ACP, comprising the acyl residue bound

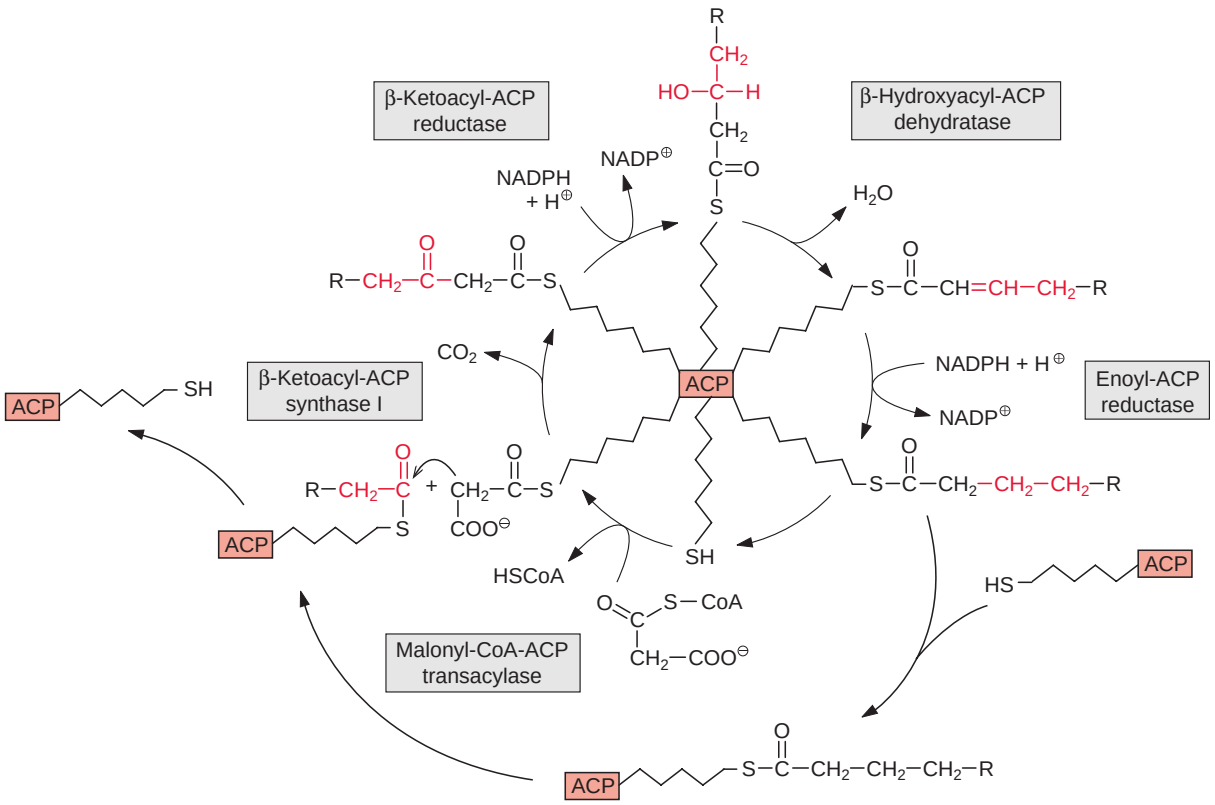

Figure 15.13 The interplay of the various enzymes during fatty acid synthesis. The acyl carrier protein (ACP), located in the center, carries the fatty acid residue, bound as thioester, from enzyme to enzyme. The circular presentation is for the sake of clarity, but does not represent reality.

as a thioester, is located in the center of the complex. Thus the acyl residue is attached to a flexible chain, to be transferred from enzyme to enzyme during this reaction cycle.

A fatty acid is elongated by transferring it to another ACP which is then condensed with malonyl ACP. The enzyme **β-ketoacyl-ACP synthase I**, catalyzing this reaction, enables the formation of fatty acids with a chain length of up to C-16. A further chain elongation to C-18 is catalyzed by **β-ketoacyl-ACP synthase II** (Fig. 15.14).

It should be mentioned that in animals and fungi the enzymes of fatty acid synthesis (Fig. 15.13) are present in one multifunctional protein, or two multifunctional proteins which form a complex (**eukaryotic fatty acid synthase complex**). Since the fatty acid synthase complex of the plastids, consisting of several proteins, is similar to those of many bacteria, it is called the **prokaryotic fatty acid synthase complex**.

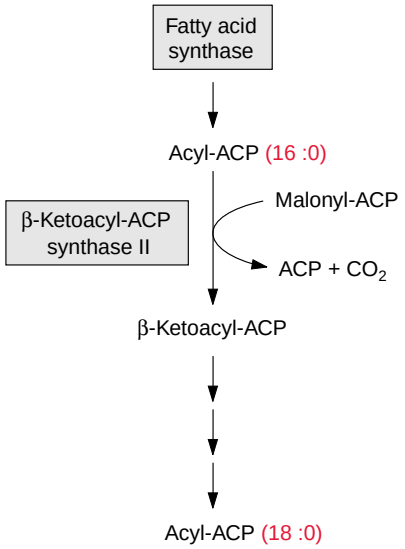

Figure 15.14 Elongation and desaturation of fatty acids in plastids.

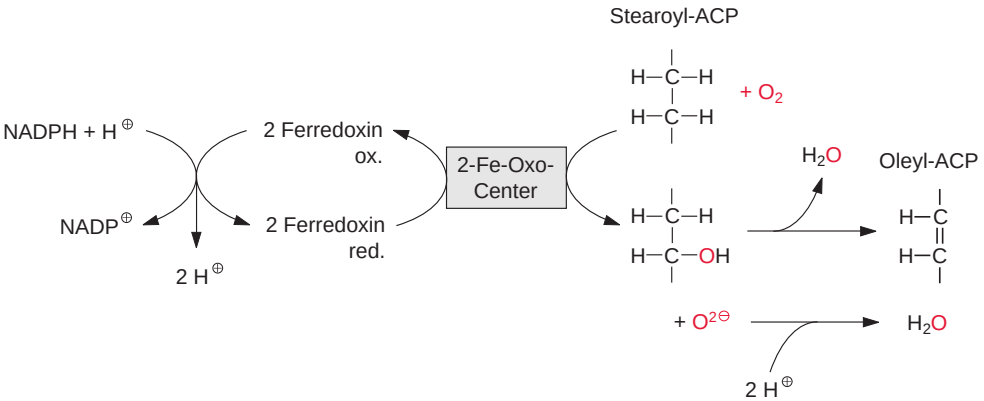

Figure 15.15A Stearoyl ACP desaturase, localized in the plastids, catalyzes the desaturation of stearoyl ACP to oleyl ACP. The reaction can be regarded as a monooxygenation with subsequent release of water.

The first double bond in a newly synthesized fatty acid is formed by a soluble desaturase

The synthesized stearoyl ACP (18:0) is desaturated to oleoyl ACP (18:1) in the plastid stroma (Fig. 15.15A). This reaction can be regarded as a **monooxygenation** (section 18.2), in which one O atom from an O_2 molecule is reduced to water and the other is incorporated into the hydrocarbon chain of the fatty acid as hydroxyl group (Fig. 15.15B). A carbon-carbon

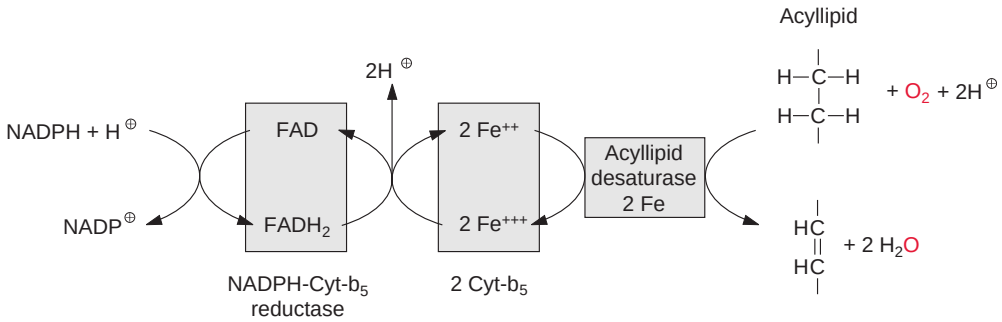

Figure 15.15B Acyl lipid desaturases, integral proteins of the ER membrane, catalyze the desaturation of fatty acids, which are parts of phospholipids. The reaction can be regarded as a monooxygenation followed by water cleavage (not shown in the figure). Electron transport from NADPH to the desaturase requires two additional proteins, one NADPH-cyt-*b* and cytochrom-b_5.

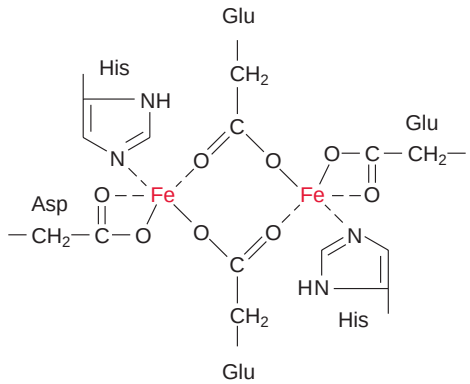

Figure 15.16 In a di-iron-oxo cluster, two Fe atoms are bound to glutamate, aspartate, and histidine side chains of the protein. (After Karlin, 1993.)

double bond is formed by subsequent liberation of H_2O (analogous with the β-hydroxyacyl ACP dehydratase reaction, Fig. 15.8), which, in contrast to fatty acid synthesis, has a *cis*-configuration. The monooxygenation requires two electrons, which are provided by NADPH via reduced ferredoxin. Monooxygenases are widespread in bacteria, plants, and animals. In most cases, O_2 is activated by a special cytochrome, **cytochrome P_{450}**. However, in the **stearoyl ACP desaturase**, the O_2 molecule reacts with a **di-iron-oxo cluster** (Fig. 15.16). In previous sections, we have discussed iron-sulfur clusters as redox carriers, in which the Fe atoms are bound to the protein via cysteine residues (Fig. 3.26). In the di-iron-oxo cluster of the desaturase, two iron atoms are bound to the enzyme via the carboxyl groups of glutamate and

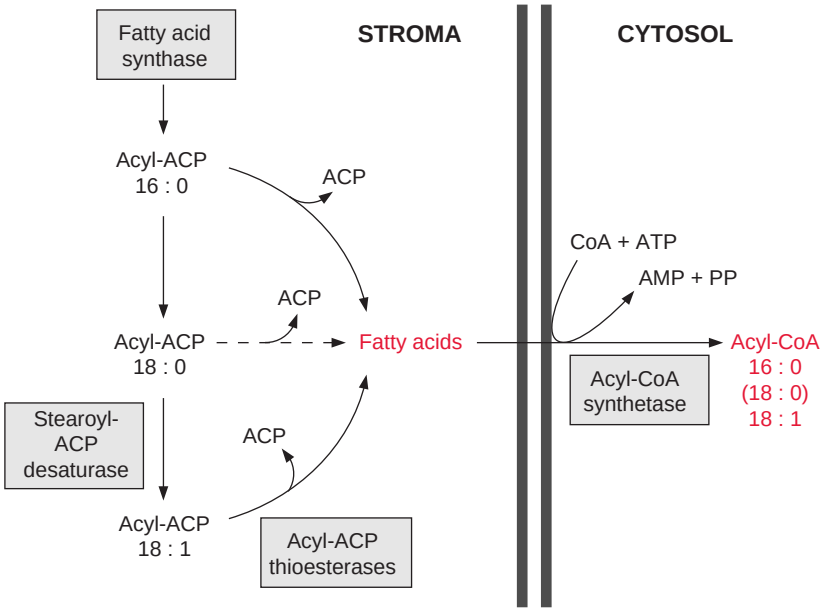

Figure 15.17 Acyl ACP-thioesterases synthesize primarily 16:0- and 18:1-fatty acids and only low amounts of 18:0-fatty acids. After the transfer of fatty acids from the stroma to the cytosol, they are immediately converted to acyl CoA.

aspartate. The two Fe atoms alternate between oxidation state +IV, +III and +II. An O_2 molecule is activated by the binding of the two Fe atoms.

Stearoyl ACP desaturase is a soluble protein that is localized in chloroplasts and other plastids. The enzyme is so active that normally the newly formed stearoyl ACP is almost completely converted to oleyl ACP (18:1) (Fig. 15.17). This soluble desaturase is capable of introducing only one double bond into fatty acids. The introduction of further double bonds is catalyzed by other desaturases, which are integral membrane proteins of the ER and of the plastidal inner envelope membrane. These desaturases react only with fatty acids that are constituents of membrane lipids. For this reason, they are termed **acyl lipid desaturases**. These membrane-bound desaturases also require O_2 and reduced ferredoxin, similar to the aforementioned ACP desaturases, but have a different electron transport chain (Fig. 15.15B). The required reducing equivalents are transferred from NADPH via an FAD containing **NADPH-cytochrome-b_5-reductase** to cytochrome-b_5 and from there further to the actual desaturase, which contains **two Fe atoms** probably bound to histidine residues of the protein. In plastids ferredoxin acts as a reductant. The acyl lipid desaturases belong to a large family of enzymes. Members of this family catalyze the introduction of hydroxyl groups (hydroxylases), epoxy groups (epoxygenases), conjugated double bonds (conjugases), and carbon triple bonds (acetylenases) into fatty acids of acyl lipids.

Acyl ACP synthesized as a product of fatty acid synthesis in the plastids serves two purposes

Acyl ACP produced in the plastids has two important functions:

1. It acts as an acyl-donor for the synthesis of plastid membrane lipids. The enzymes of glycerolipid synthesis are in part located in both the inner and outer envelope membranes. Therefore the lipid biosynthesis is a division of labor between these two membranes. In the following text no distinction will be made between the lipid biosynthesis of the inner and outer envelope membranes.
2. For biosynthesis outside the plastids, acyl ACP is hydrolyzed by **acyl ACP thioesterases** to release **fatty acids**, which then leave the plastids (Fig. 15.17). It is not known whether this export proceeds via non-specific diffusion or by specific transport. These free fatty acids are immediately captured outside the outer envelope membrane by conversion to acyl CoA, a reaction catalyzed by an **acyl CoA synthetase** with consumption of ATP. Since the thioesterases in the plastids hydrolyze primarily 16:0- and 18:1-acyl ACP, and to a small extent 18:0-acyl ACP, the plastids mainly provide CoA esters with the acyl residues of 18:1 and 16:0 (also a low amount of 18:0) for lipid metabolism outside the plastids.

15.4 Glycerol 3-phosphate is a precursor for the synthesis of glycerolipids

Glycerol 3-phosphate is synthesized by reduction of dihydroxyacetone phosphate with NADH as reductant (Fig. 15.18). **Dihydroxyacetone phosphate reductases** are present in the plastid stroma as well as in the cytosol. In plastid lipid biosynthesis, the acyl residues are transferred directly from acyl ACP to glycerol 3-phosphate. For the first acylation step, mostly an 18:1-, less frequently a 16:0-, and more rarely an 18:0-acyl residue is esterified to carbon position 1 of glycerol 3-phosphate. The C-2-position, however, is always esterified with a 16:0-acyl residue. Since this specificity is also observed in cyanobacteria, the glycerolipid biosynthesis pathway of the plastids is called the **prokaryotic pathway**.

For glycerolipid synthesis in the ER membrane, the acyl residues are transferred from acyl CoA. Here again, the hydroxyl group in the C-1-position of glycerol 3-phosphate is esterified with an 18:1-, 16:0-, or 18:0-acyl residue, and position C-2 is always linked with a desaturated 18:*n*-acyl residue. The glycerolipid pathway of the ER membrane is called the **eukaryotic pathway**.

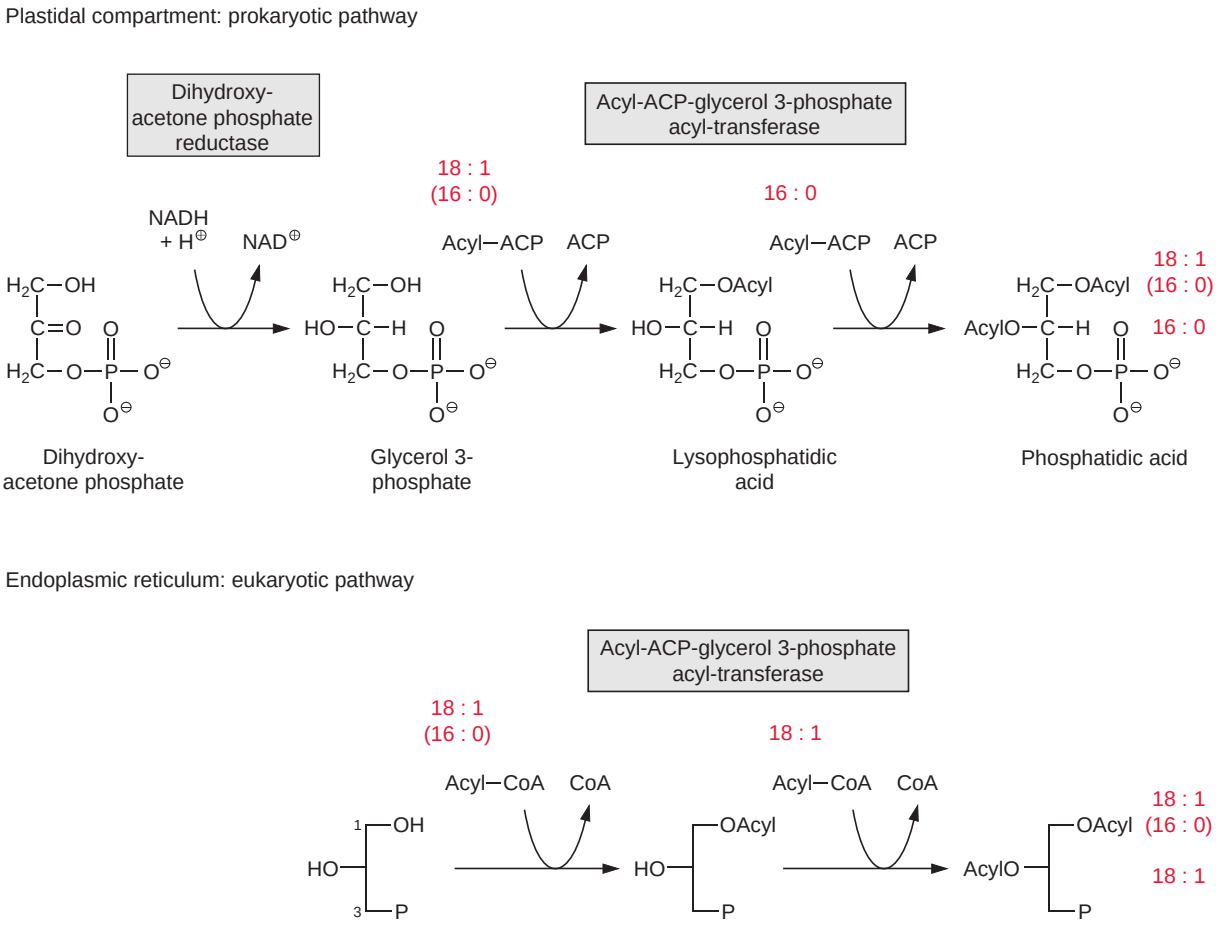

Figure 15.18 The membrane lipids synthesized in the plastids and at the ER have different fatty acid compositions.

The linkage of the polar head group to diacylglycerol proceeds mostly via activation of the head group, but in some cases also by an activation of diacylglycerol. Choline and ethanolamine are activated by phosphorylation via specific kinases and are then converted via cytidyl transferases by reaction with CTP to **CDP choline** and **CDP ethanolamine** (Fig. 15.19). A galactose head group is activated as **UDP galactose** (Fig. 15.20). The latter is synthesized from glucose 1-phosphate and UTP via the UDP glucose pyrophosphorylase (section 9.2) and UDP glucose epimerase (Fig. 9.21). For the synthesis of digalactosyldiacylglycerol (DGDG) from monogalactosyldiacylglycerol (MGDG), a galactose residue is transferred from UDP galactose. Also, sulfoquinovose is activated as a UDP derivative, but details of the synthesis of this moiety will not be discussed here. The acceptor for

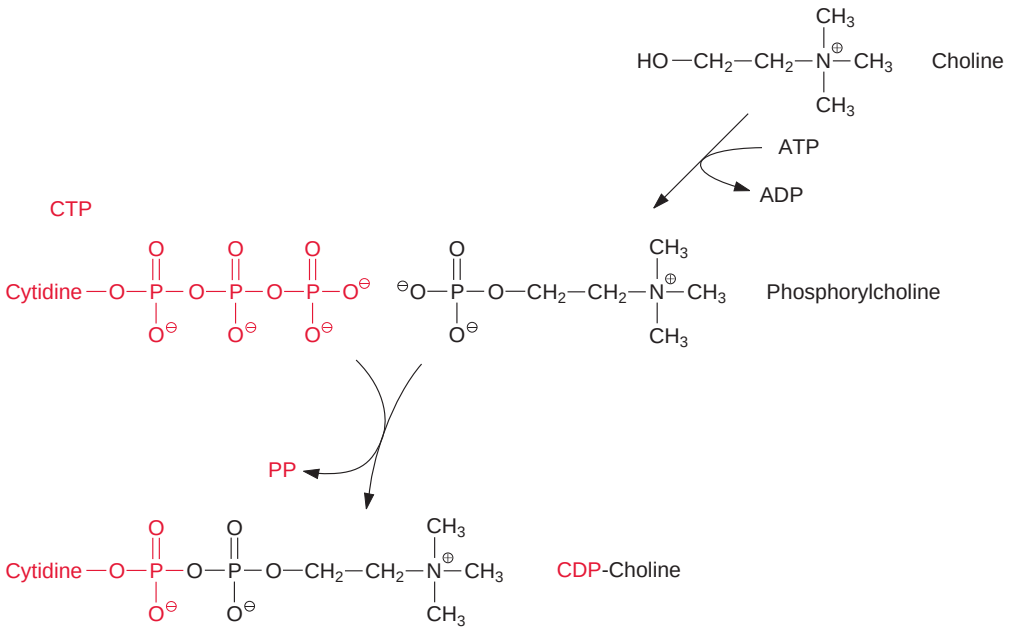

Figure 15.19 Synthesis of CDP choline.

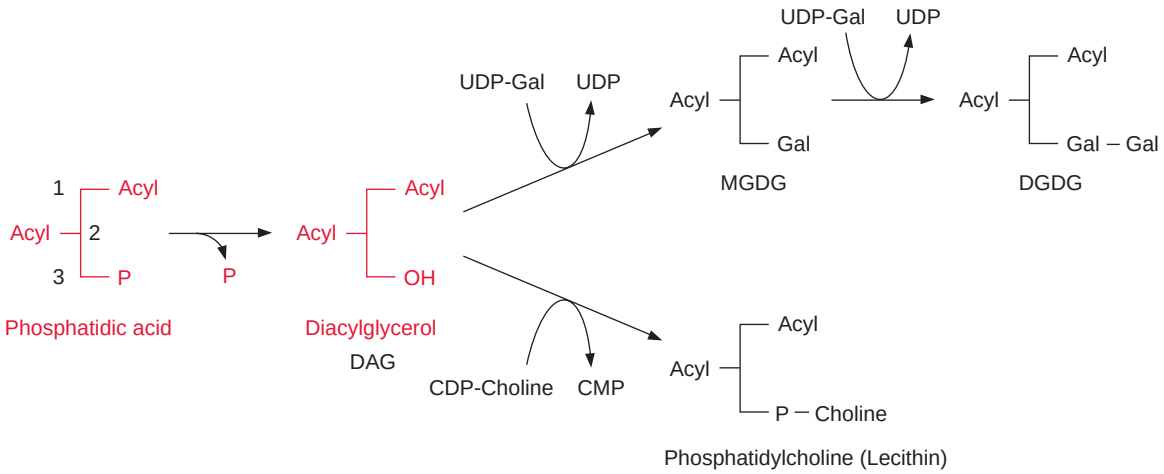

Figure 15.20 Overview of the synthesis of membrane lipids.

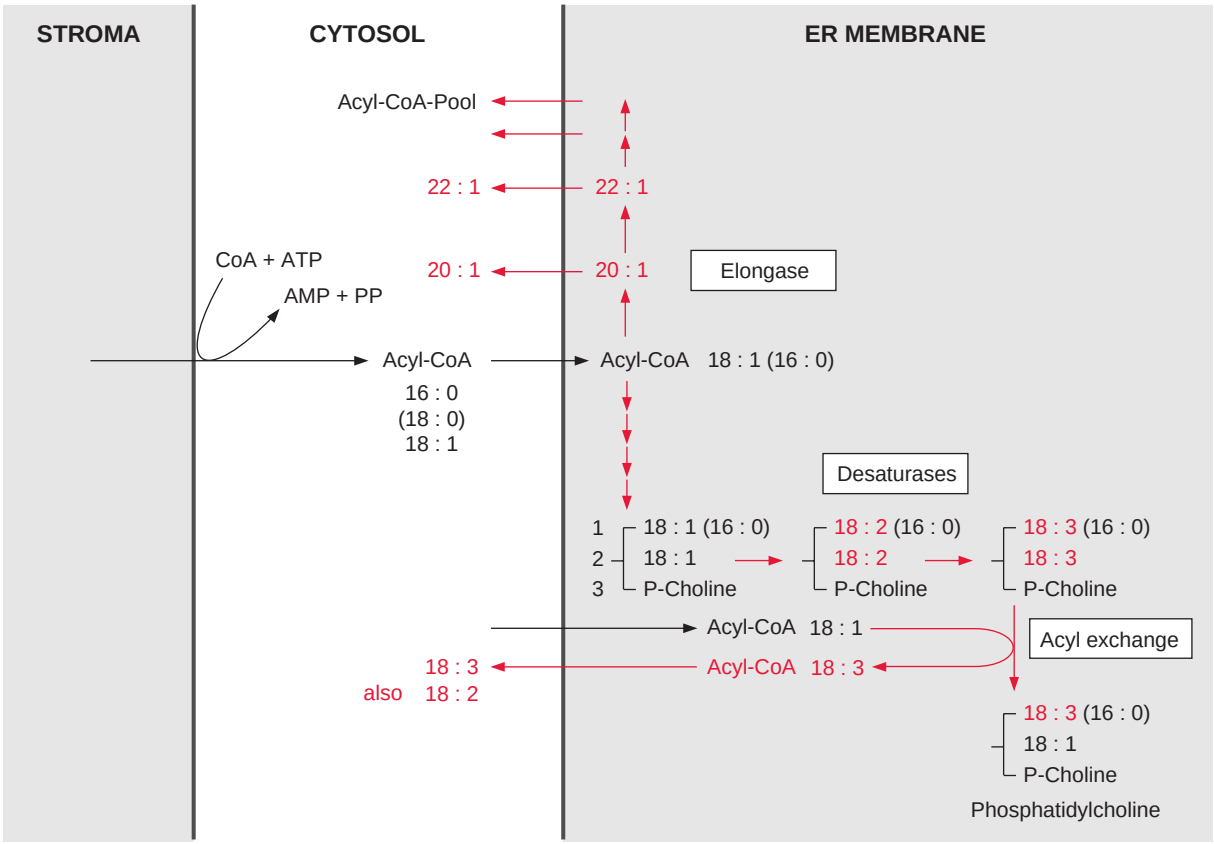

Figure 15.21 A pool of acyl CoA with various chain lengths and desaturation is present in the cytosol. Acyl residues delivered from the plastids as acyl CoA are elongated by elongases located at the ER. After incorporation in phosphatidylcholine, 18:1-acyl residues are desaturated to 18:2 and 18:3 by desaturases present in the ER membrane. The more highly desaturated fatty acids in position 2 can be exchanged for 18:1-acyl CoA. In this way the cytosolic pool is provided with 18:2- and 18:3-acyl CoA.

the activated head group is diacylglycerol, which is formed from phosphatidic acid by the hydrolytic release of the phosphate residue.

The ER membrane is the site of fatty acid elongation and desaturation

As shown in Figure 15.17, the plastids produce 16:0-, 18:1-, and to a lesser extent 18:0-acyl residues. However, some storage lipids contain fatty acids with longer chains. This also applies to waxes, which are esters of long chain fatty acid (C_{20}–C_{24}) and very long chain acyl alcohols (C_{24}–C_{32}). The

elongation of fatty acids longer than C_{18} is catalyzed by **elongases**, which are located in the membranes of the ER (Fig. 15.21). Elongation proceeds in the same way as fatty acid synthesis, with the differences that other enzymes are involved and the acyl and malonyl residues are activated as acyl CoA thioesters.

The ER membrane is also the site for further desaturations of the acyl residue. For desaturation, the acyl groups are first incorporated into phospholipids, such as phosphatidylcholine (Fig. 15.21). **Desaturases** bound to the membrane of the ER convert oleate (18:1) to linoleate (18:2) and then to linolenate (18:3). The 18:2- or 18:3-acyl residues in the C-2-position of glycerol can be exchanged for an 18:1-acyl residue, and the latter can then be further desaturated.

The interplay of the desaturases in the plastids and the ER provides the cell with an **acyl CoA pool** to cover the various needs of the cytosol. The 16:0-, 18:0-, and 18:1-acyl residues for this pool are delivered by the plastids, and the longer chains and more highly unsaturated acyl residues are provided through modifications by the ER membrane.

Some of the plastid membrane lipids are synthesized via the eukaryotic pathway

The synthesis of glycerolipids destined for the plastid membranes occurs in the envelope membranes of the plastids (Fig. 15.22). Besides the prokaryotic pathway of glycerolipid synthesis, in which the acyl residues are directly transferred from acyl ACP, glycerolipids are also synthesized via the eukaryotic pathway. In the latter case, the desaturases of the ER membrane can provide double unsaturated fatty acids for plastid membrane lipids. A precursor is, for instance, phosphatidylcholine with double unsaturated fatty acids, which has been synthesized in the ER membrane (Fig. 15.21). This phosphatidylcholine is transferred to the envelope membrane of the plastids and hydrolyzed to diacylglycerol and then substituted with a head group consisting of one or two galactose residues. The acyl residues can be further desaturated to 18:3 by a desaturase present in the envelope membrane.

Some desaturases in the plastid envelope are able to desaturate lipid-bound 18:1- and 16:0-acyl residues. A comparison of the acyl residues in the C-2-position (in the prokaryotic pathway 16:0 and in the eukaryotic pathway 18:*n*) demonstrated, however, that a large proportion of the highly unsaturated galactolipids in the plastids are synthesized via a detour through the eukaryotic pathway. The membrane lipids of the envelope membranes are probably transferred by a special transfer protein to the thylakoid membrane.

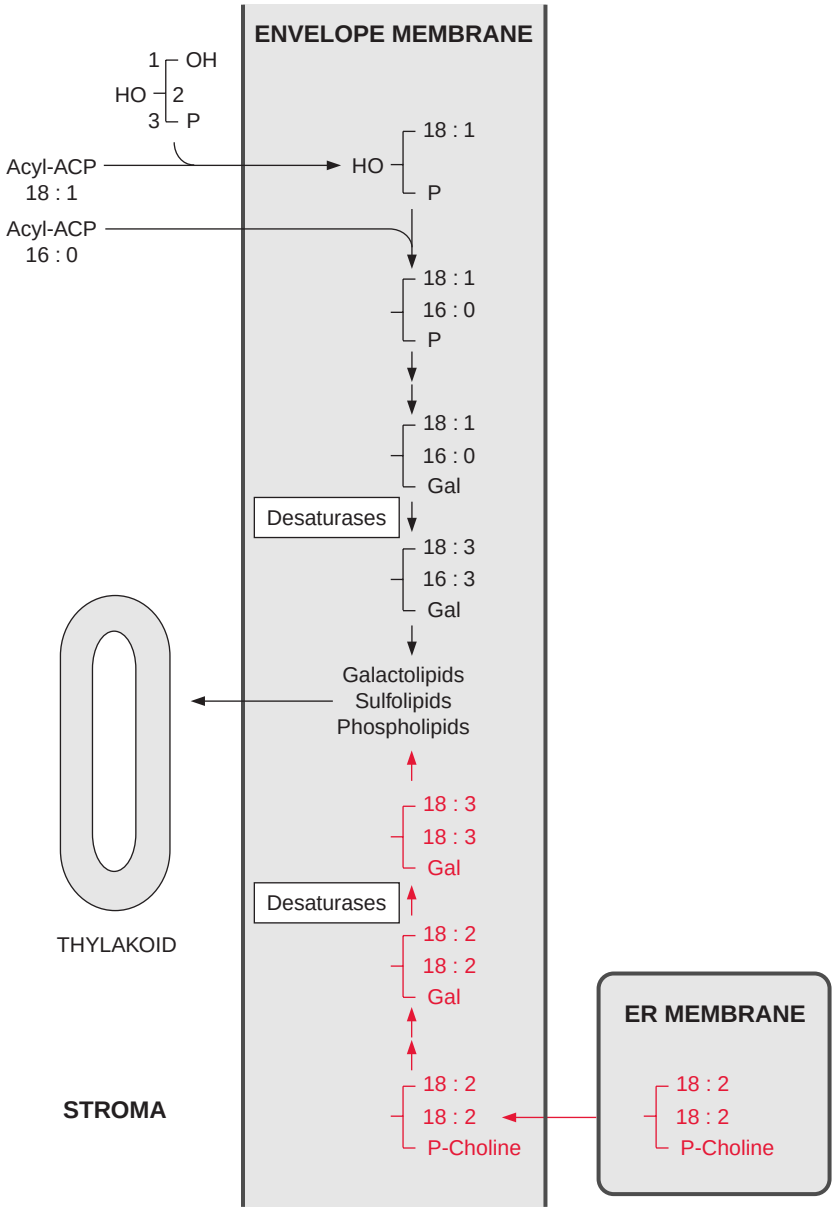

Figure 15.22 Membrane lipids of the thylakoid membranes are synthesized via the eukaryotic pathway (red) and via the prokaryotic pathway (black).

15.5 Triacylglycerols are synthesized in the membranes of the endoplasmatic reticulum

The lipid content of mature seeds can amount to 45% of the dry weight, but in some cases (e.g., Ricinus) up to 85%. The precursor for the synthesis of triacylglycerols is again glycerol 3-phosphate. There are at least four pathways for its synthesis, the two most important will be discussed here (Fig. 15.23):

1. **Phosphatidic acid** is formed by acylation of the hydroxyl groups at position C-1 and C-2 of glycerol and, after hydrolysis of the phosphate residue, the C-3-position is also acylated. The total cytosolic acyl CoA pool is available for these acylations, but due to the eukaryotic pathway, position 2 is mostly esterified by a C_{18} acyl residue (Fig. 15.21).
2. **Phosphatidylcholine** is formed first, and its acyl residues are further desaturated. The choline phosphate residue is transferred to CMP, and the corresponding diacylglycerol is esterified with a third acyl residue.

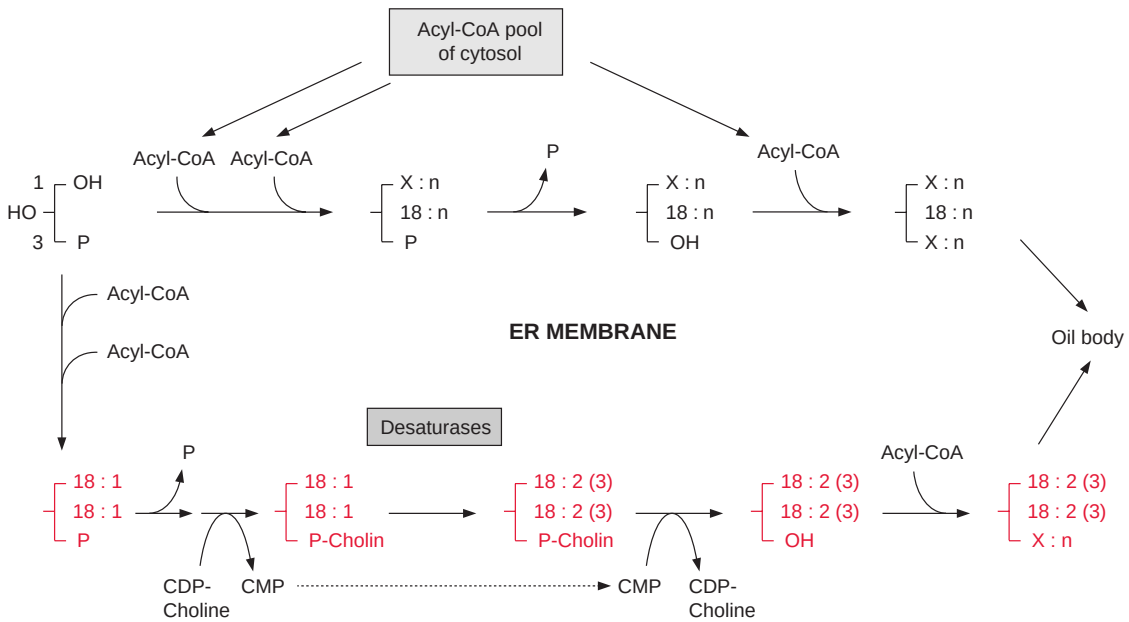

Figure 15.23 Overview of triacylglycerol synthesis in the ER membrane. The synthesis occurs either by acylation of glycerol phosphate (black) or via the intermediary synthesis of a phospholipid, of which the fatty acids are desaturated by desaturases in the ER membrane (red).

This pathway operates frequently during the synthesis of highly unsaturated triacylglycerols.

Cross-connections exist between the two pathways, but for the sake of simplicity these are not discussed in Figure 15.23.

Plant fat is used for human nutrition and also as a raw material in industry

About 20% of the human caloric nutritional uptake in industrialized countries is due to the consumption of plant fats. Plant fats have a nutritional advantage over animal fats since they contain a higher portion of unsaturated fatty acids. Human metabolism requires unsaturated fatty acids with two or more carbon-carbon double bonds, but is not able to introduce double bonds at position 12 and 15. This is why **linoleic acid** and **linolenic acid** (Fig. 15.4) are essential fatty acids, which are absolutely necessary in the human diet.

Plant fats are also important as industrial raw materials. Fatty acids are obtained after the hydrolysis of triacylglycerols. They have been in use as alkali salts in soap since ancient times. Fatty acid alcohols and fatty acid methyl esters are also used as detergents. Moreover, fatty acid methyl esters synthesized from rape seed oil are used as car fuel (bio diesel). The high quantities of glycerol released during the hydrolysis of fats are an important industrial raw material.

Table 15.3 shows that the fatty acid composition of various plant oils is very divergent. Triacylglycerols of some plants comprise large quantities

Table 15.3: World production and fatty acid composition of the most important vegetable oils

World production 10^6 t 2005		% of fatty acid content						
		C 12:0	C 14:0	C 16:0	C18:0	C 18:1	C.18:2	others
Soybean	30	0	0	8	4	28	53	7
Palm	25	0	2	42	5	41	10	0
Rape seed	13	0	0	4	1	60	20	15
Sunflower	9	0	0	6	4	28	61	1
Peanut	5	0	0	10	3	50	30	3
Coconut	3	48	17	9	2	7	1	16
Palm kernel	3	50	15	7	2	15	1	10
Total production plant fats	**98**							

Table 15.4: Industrial utilization of fatty acids from vegetable oils

	Main source	Utilization for
Lauric acid (12:0)	Palm kernel, coconut	Soap, detergents, cosmetics
Linolenic acid (18:3)	Flax seed	Paints, lacquers
Ricinoleic acid (18:1, Δ9, 12-OH)	Castor bean	Surface protectants, lubricant
Erucic acid (22:1, Δ13)	Rape seed	Tensides
		Foam control for detergents, lubricant, synthesis of artificial fibers

of rare fatty acids, which are used for industrial purposes (Table 15.4). Oil from palm kernels has a high content of the short-chain **lauric acid** (12:0), which is used for the production of detergents and cosmetics. Large plantations of oil palms in Southeast Asia ensure its supply to the oleochemical industry. **Linolenic acid** from European flax seed is used for the production of paints. **Ricinoleic acid**, a rare fatty acid that comprises a hydroxyl group at the C-12-position, accounts for about 90% of the fatty acids in castor oil. It is used in industry as a lubricant and as a surface protectant. **Erucic acid** is used for similar purposes. Earlier varieties of rape seed had erucic acid in their triacylglycerols, and for this reason rape seed oil was then of inferior value for human nutrition. About 40 years ago, successful crossings led to a breakthrough in the breeding of rape seed free of erucic acid, with the result that rape seed oil is now highly suitable for human consumption. The values given in Table 15.3 are indicative for this new type of rape seed, which is now cultivated worldwide. However, rape seed varieties containing a high percentage of erucic acid are recently cultivated again for industrial demands.

Plant fats are customized by genetic engineering

The progress in gene technology now makes it possible to alter the quality of plant fats in a defined way by changing the enzymatic profile of the cell. The procedures for the introduction of a new enzyme into a cell, or for eliminating the activity of an enzyme present in the cell, will be described in detail in Chapter 22. Three cases of the alteration of oil crops by genetic engineering will be illustrated here.

1. The lauric acid present in palm kernel and coconut oil (12:0) is an important raw material for the production of soaps, detergents, and cosmetics. Recently, rape seed plants that contained oil with a lauric acid content

of 66% were generated by genetic transformation. The synthesis of fatty acids is terminated by the hydrolysis of acyl ACP (Fig. 15.17). An **acyl ACP thioesterase**, which specifically hydrolyzes lauroyl ACP, was isolated and cloned from the seeds of the California bay tree (*Umbellularia californica*), which contains a very high proportion of lauric acid in its storage lipids. The introduction of the gene for this acyl ACP thioesterase into the developing rape seed terminates its fatty acid synthesis at acyl (12:0), and the released lauric acid is incorporated into the seed oil. Field studies have shown that these plants grow normally and yields are as expected.

2. A relatively high content of stearic acid (18:0) improves the heat stability of fats for deep frying and for the production of margarine. The stearic acid content in rape seed oil has been increased from 1%–2% to 40% by decreasing the activity of stearoyl ACP desaturase using antisense technique (see section 22.5). On the other hand, genetic engineering has been employed to increase highly unsaturated fatty acids (e.g., in rape seed) providing the oil with a higher nutritional quality. In soybeans, the proportion of double unsaturated fatty acids in the oil could be increased to 30%. Nutritional physiologists discovered that highly unsaturated fatty acids (20:4, 20:5, 22:6), which are only present in fish oil, are very beneficial for human health. Investigations by genetic engineering are now in progress to develop rape lines with highly unsaturated fatty acids of C20 and C22 length. This is an example where gene technology is applied for the production of "healthy food."

Erucic acid (Fig. 15.24) could be an important industrial raw material, for instance for the synthesis of synthetic fibers and for foam control in detergents. Presently, however, its utilization is limited, since conventional breeding has not succeeded in increasing the erucic acid content to more than 50% of the fatty acids in the seed oil. The costs of separating erucic acid and disposal of the other fatty acids are so high that for many purposes the industrial use of rape seed oil as a source of erucic acid from presently available cultivars is not economically viable. Attempts are being made to increase further the erucic acid content of rape seed oil by overexpression of elongase genes and by transferring genes encoding enzymes that catalyze the specific incorporation of erucic acid to the C-2-position of triacylglycerols. If this were to be successful, present petrochemical-based industrial processes could be replaced with processes using rape seed oil as a renewable resource.

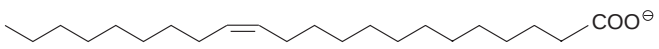

Erucic acid (22 :1,Δ^{13}-*cis*)

Figure 15.24 Erucic acid, an industrial raw material.

15.6 Storage lipids are mobilized for the production of carbohydrates in the glyoxysomes during seed germination

At the onset of germination, storage proteins (Chapter 14) are degraded to amino acids, from which enzymes required, for example, for the mobilization of the storage lipids, are synthesized. These enzymes include **lipases**, which catalyze the hydrolysis of triacylglycerols to glycerol and fatty acids. They bind to the oil body proteins (section 15.2). The **glycerol** released by the hydrolysis of triacylglycerol, after phosphorylation to glycerol 3-phosphate and its subsequent oxidation to dihydroxyacetone phosphate, is fed into the **gluconeogenesis** or glycolytic pathway (Chapter 9). The **free fatty acids** are first activated by reaction with CoA to form thioesters and are then degraded to acetyl CoA by **β-oxidation** (Fig. 15.25). This process proceeds in specialized peroxisomes called **glyoxysomes**. It has been observed that for a transfer of fatty acids, oil bodies and glyoxysomes come into close contact with each other.

Although in principle β-oxidation represents the reversal of fatty acid synthesis (Fig. 15.8), there are distinct differences that enable high metabolic fluxes through these two metabolic pathways operating in opposite directions. The differences between β-oxidation and fatty acid synthesis are:

1. In acyl CoA dehydrogenation, hydrogen is transferred via an **FAD-dependent oxidase** to O_2 to form H_2O_2. A catalase irreversibly eliminates the toxic H_2O_2 at the site of its production by conversion to water and oxygen (section 7.1). Sometimes, for example at a very high rate of β-oxidation during seed maturation, the amount of H_2O_2 can be so high that it leaks out of the glyoxysomes causing cell damage.
2. **β-L Hydroxyacyl CoA** is synthesized during the hydration of enoyl CoA, in contrast to the corresponding D-enantiomer during fatty acid synthesis.
3. Hydrogen is transferred to **NAD^+** during the second dehydrogenation step. Normally, most of the NAD^+ in the cell is highly oxidized (section 7.3), driving the reaction to hydroxyacyl CoA oxidation. It is not known which reactions utilize the NADH synthesized in the peroxisomes.
4. In an irreversible reaction, **CoA-SH-mediated thiolysis** cleaves β-ketoacyl CoA to synthesize one molecule each of acetyl CoA and of acyl CoA shortened by two C atoms.

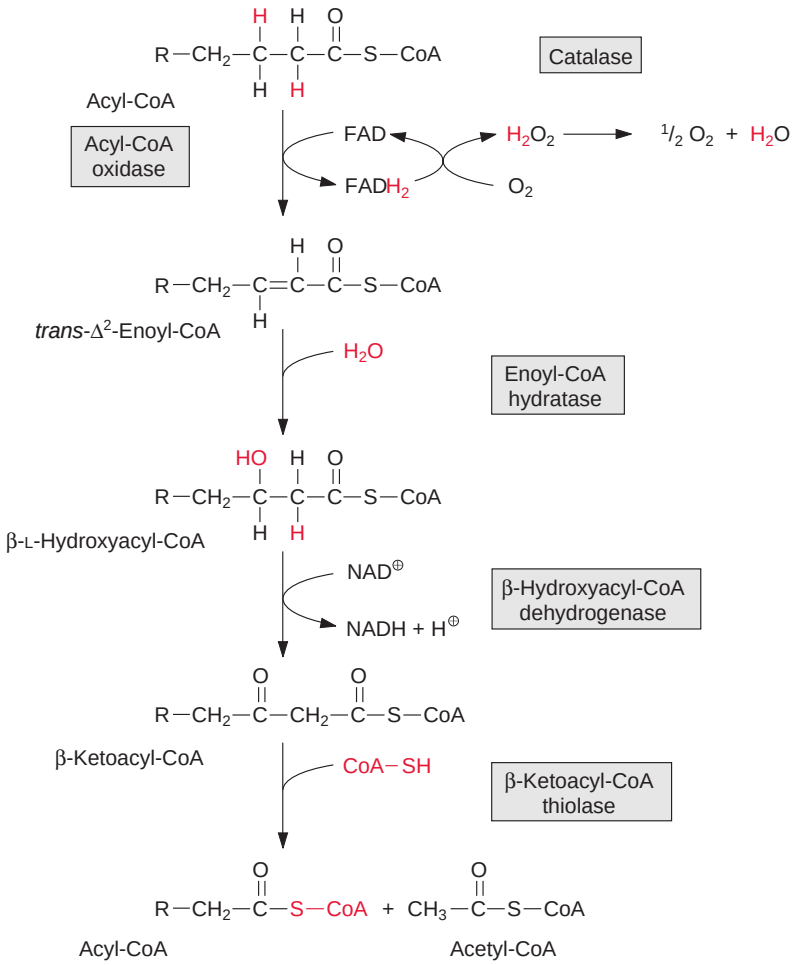

Figure 15.25 β-Oxidation of fatty acids in the glyoxysomes. The fatty acids are first activated (CoA-thioesters) and then converted to acetyl CoA and a fatty acid shortened by two carbon atoms. The sequence of reactions involve dehydrogenation via an FAD-dependent oxidase, addition of water (hydroxylation), a second dehydrogenation (by NAD^+), and finally a thiolysis by CoA-SH.

During the degradation of unsaturated fatty acids, sometimes intermediate products are produced that cannot be metabolized by the reactions of β-oxidation. **Δ_3-*cis*-enoyl CoA** (Fig. 15.26), which is synthesized during the degradation of oleic acid, is converted by an **isomerase** which shifts the double bond to **Δ_2-*trans*-enoyl CoA**, an intermediate of β-oxidation. In the β-oxidation of linoleic or linolenic acid, the second double bond in the corresponding intermediate is at the correct position but in the *cis*-configuration. Consequently its hydration by enoyl CoA hydratase results in the formation of β-D-hydroxyacyl CoA. The latter is converted by a dehydratase to Δ_2-*trans*-enoyl-CoA, which is an intermediate of β-oxidation.

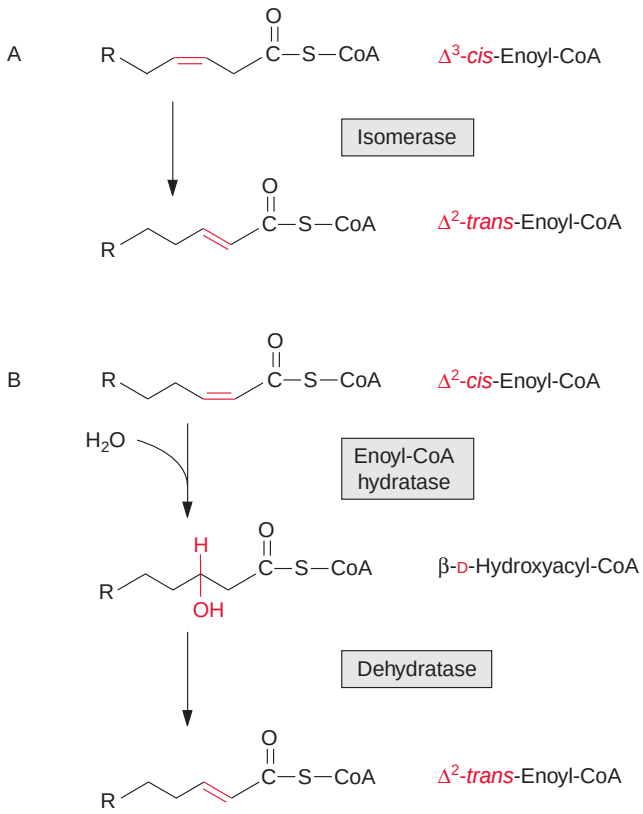

Figure 15.26 The intermediates synthesized during β-oxidation of unsaturated fatty acids are isomerized to enable subsequent metabolization.

The glyoxylate cycle enables plants to synthesize hexoses from acetyl CoA

In contrast to animals, which are unable to synthesize glucose from acetyl CoA, plants are capable of gluconeogenesis from lipids, as they possess the enzymes of the glyoxylate cycle (Fig. 15.27). Like β-oxidation, this cycle is located in the glyoxysomes, which are named after this cycle. The two starting reactions of the cycle are identical to those of the citrate cycle (see Fig. 5.3). Acetyl CoA condenses with oxaloacetate, as catalyzed by **citrate synthase**, to produce citrate, which is then converted by aconitase to isocitrate. The following reaction with isocitrate, however, is a specialty of the glyoxylate cycle: isocitrate is split by **isocitrate lyase** into succinate and glyoxylate (Fig. 15.28). **Malate synthase**, the second special enzyme of the glyoxylate cycle, catalyzes the instantaneous condensation of glyoxylate with acetyl CoA to synthesize malate. Due to the hydrolysis of the CoA-thioester this reaction

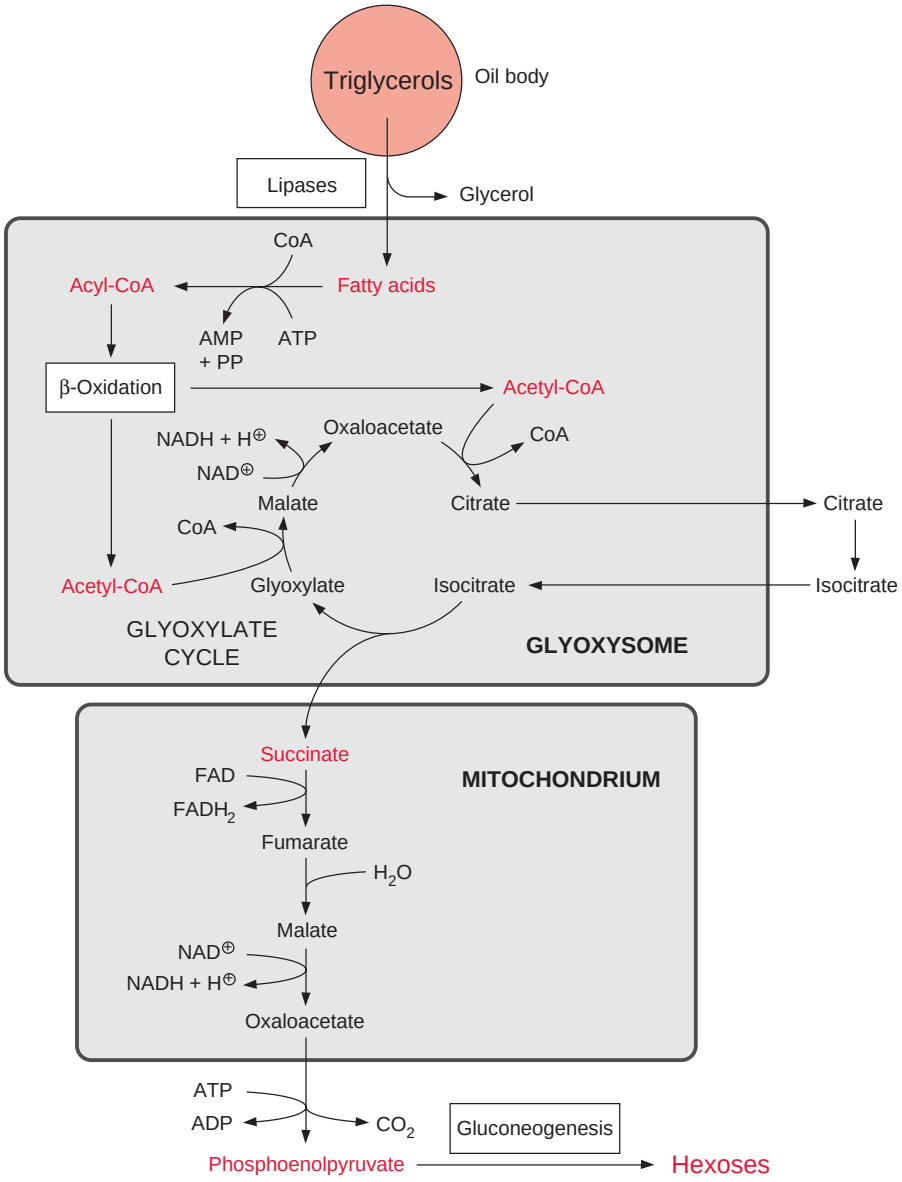

Figure 15.27 Mobilization of storage lipids for the synthesis of hexoses needed during germination. The hydrolysis of the triacylglycerols of the oil bodies is catalyzed by oil body protein-bound lipases. Released fatty acids, which are activated in the glyoxysomes to form CoA-thioesters, are subsequently degraded by β-oxidation to acetyl CoA. From two molecules of acetyl CoA, the glyoxylate cycle forms one molecule of succinate, which is converted by the citrate cycle to oxaloacetate in the mitochondria. Phosphoenolpyruvate synthesized from oxaloacetate in the cytosol is a precursor for the synthesis of hexoses via the gluconeogenesis pathway.

becomes irreversible. As in the citrate cycle, malate is oxidized by **malate dehydrogenase** to oxaloacetate, thus completing the glyoxylate cycle. In this way one molecule of succinate is generated from two molecules of acetyl CoA. The succinate is transferred to the mitochondria and converted to oxaloacetate by a partial reaction of the citrate cycle. The oxaloacetate is

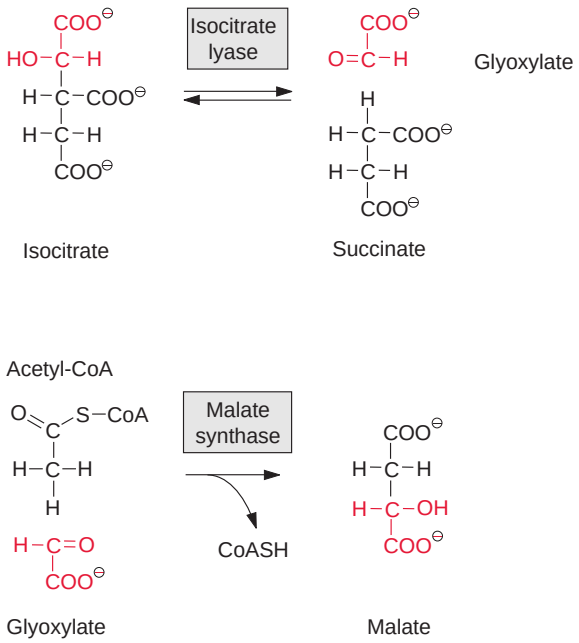

Figure 15.28
Key reactions of the glyoxylate cycle.

released from the mitochondria by the oxaloacetate translocator and transformed in the cytosol by phosphoenolpyruvate carboxykinase to phosphoenolpyruvate (Fig. 8.10). Phosphoenolpyruvate is a precursor for the synthesis of hexoses by the **gluconeogenesis pathway** and for other biosynthetic processes.

Reactions with toxic intermediates take place in peroxisomes

There is a simple explanation for the fact that β-oxidation and the closely related glyoxylate cycle proceed in specialized peroxisomes (**glyoxysomes**). As in photorespiration, in which peroxisomes participate (section 7.1), the toxic compounds **H_2O_2** and **glyoxylate** are also synthesized as intermediates in the conversion of fatty acids to succinate. Compartmentation in the peroxisomes prevents these toxic compounds entering the cytosol (section 7.4). β-Oxidation also takes place, although at a much lower rate, in leaf peroxisomes, where it serves the purpose of recycling the fatty acids that are no longer required or have been damaged. This recycling plays a role in **senescence**,

when carbohydrates are synthesized from the degradation products of membrane lipids in the senescent leaves and are transferred to the stem via the phloem (section 19.7). During senescence, one can indeed observe a differentiation of leaf peroxisomes into **glyoxysomes** (alternatively termed **gerontosomes**). The hydrophobic amino acids leucine and valine are also degraded in peroxisomes.

15.7 Lipoxygenase is involved in the synthesis of oxylipins, which are defense and signal compounds

Oxylipins, which derive from the oxygenation of unsaturated fatty acids, comprise a multiplicity of various signal compounds in animals and plants. In animals, oxylipins include prostaglandins, leucotriens, and thromboxans, of which the specific roles in the regulation of physiological processes are known to a large extent. Likewise, plant oxylipins comprise a very large number of compounds mostly different from those in animals. They are involved in defense reactions (e.g., as signal components to regulate defense cascades), but also as fungicides, bactericides, and insecticides, or as volatile signals to attract predators, such as insects that feed on herbivores. Moreover, they participate in wound healing, regulate vegetative growth, and induce senescence. Our knowledge about these important compounds is still fragmentary.

In plants, oxylipins are synthesized primarily via **lipoxygenases**. These are **dioxygenases**, mediating the incorporation of both atoms of the oxygen molecule into the fatty acid molecule, in contrast to monooxygenases, which catalyze the incorporation of only one O atom of an O_2 molecule (section 15.3). The lipoxygenases are a family of enzymes catalyzing the dioxygenation of multiple-unsaturated fatty acids, such as linoleic acid and linolenic acid, with an intramolecular ***cis*, *cis*-1,4-pentadiene** sequence (colored red in Fig. 15.29). At one end of this sequence, a hydroperoxide group is introduced by oxygenation and the neighboring double bond is shifted by one C-position to the direction of the other double bond, thereby attaining a *trans*-configuration. The **hydroperoxide lyase** catalyzes the cleavage of hydroperoxylinolenic acid into a 12-oxo-acid and a 3-*cis*-hexenal. Other hexenals are synthesized by shifting the double bond, and reduction leads to the formation of hexenols (Fig. 15.29).

Hexanals, **hexenals**, **hexanols**, and **hexenols** are volatile **aromatic compounds** that are important components of the characteristic odor and taste of many fruits and vegetables. The wide range of aromas includes fruity, sweet, spicy, and grass like. Work is in progress to improve the taste of tomatoes by increasing their hexenol content by genetic engineering. The quality of olive oil, for instance, depends on its content of hexenals and hexenols. Hexenals are responsible for the aroma of black tea. Green tea is processed to black tea by heat and fermentation, resulting in the condensation of hexenals to aromatic compounds, which give black tea its typical taste. Large amounts of hexenals and hexenols are produced industrially as aromatic components for the food industry or the production of perfumes.

The characteristic smell of freshly cut grass is caused primarily by the release of hexenals and hexenols, indicating that the activity of lipoxygenase and hydroperoxide lyase is greatly increased by tissue wounding. This is part of a defense reaction, e.g., when leaves are damaged by feeding larvae, enemies of the herbivores are attracted by the emission of the volatiles. To give an example: after the wounding of corn or cotton by caterpillars, parasitic wasps are attracted, which inject their eggs into the feeding caterpillar and the developing larvae of the wasps subsequently destroy the herbivore. Moreover, 2-*trans*-hexenal itself (colored red in Fig. 15.29) is a strong bactericide, fungicide, and insecticide. Hexenals also interact with transcription factors in defense reactions. 12-Oxo-dodec-10-enic acid, which is released as a cleavage product of hydroperoxylinolenic acid by the shifting of a double bond, has the properties of a wound hormone and has therefore been named **traumatin**. Traumatin induces cell division in neighboring cells, resulting in the formation of calli and wound sealing. However, our knowledge of latter defense processes is still fragmentary.

Hydroperoxy-α-linonelic acid is converted by divinyl ether synthase into a **divinyl ether** (Fig. 15.30). Such divinyl ethers are formed as fungicide in very high amounts in potato after infection with the noxious fungus *Phytophtera infestans*. Allene oxide synthase and cyclase catalyze the cyclization of 13-hydroperoxy-α-linolenic acid (Fig. 15.30). Shortening of the hydrocarbon chain of the product by β-oxidation (Fig. 15.25) results in the formation of **jasmonic acid**. Plants contain many derivatives of jasmonic acid, including sulfatated compounds and methyl esters, which are collectively termed **jasmonates**. They represent a family of compounds with distinct hormone-like functions. It has been estimated that the jasmonates in total regulate the expression of several hundred genes. They play, for instance, an important role in plant resistance to insects and disease; the formation of flowers, fruits, and seeds; and the initiation of senescence (section 19.9).

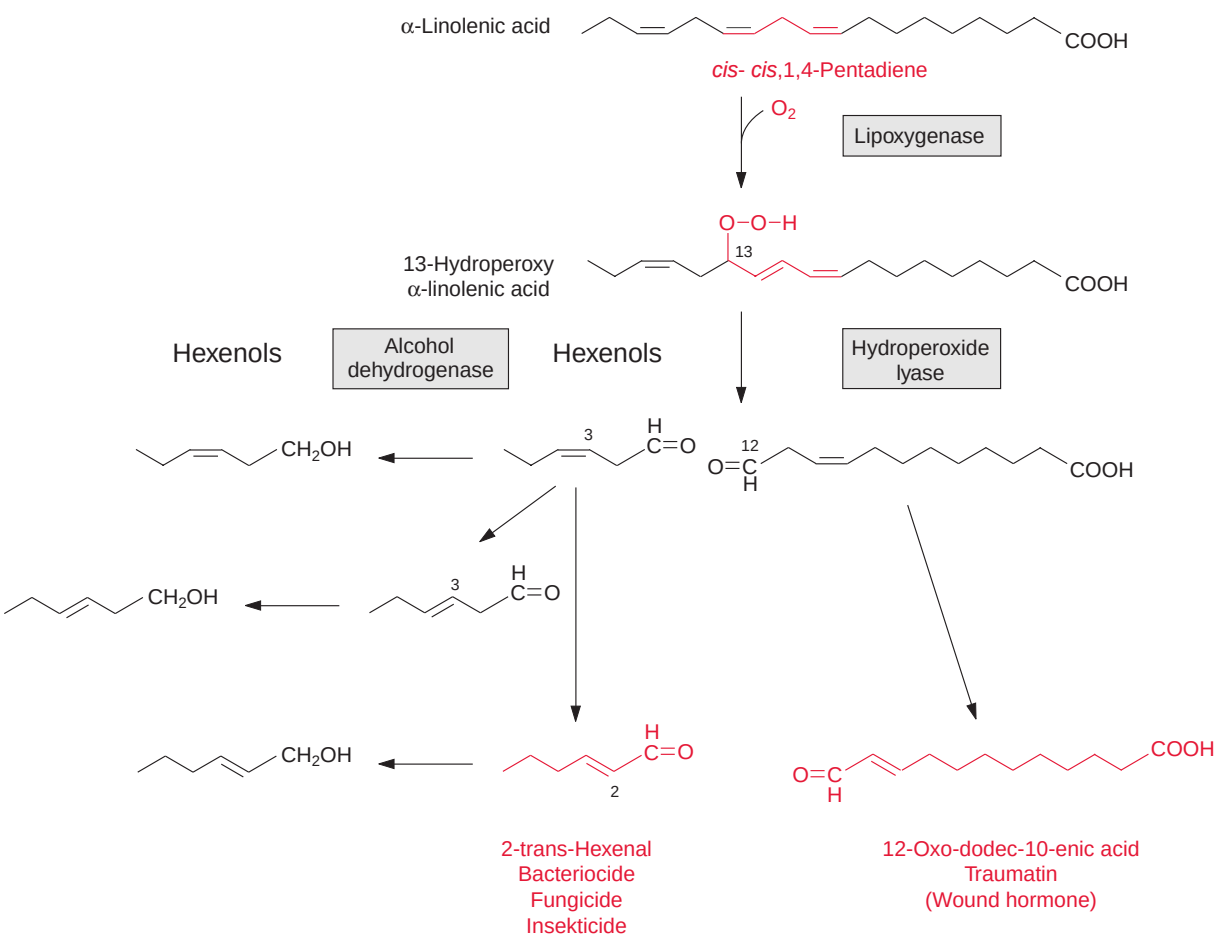

Figure 15.29 By reaction with O_2, lipoxygenase catalyzes the introduction of a peroxide group at one end of a *cis*, *cis*-1,4-pentadiene intramolecular sequence (red). Hydroperoxide lyase cleaves the C-C bond between C atoms 12 and 13. The hexenal thus synthesized can be isomerized by shifting the double bond, probably due to enzymatic catalysis. The hexenals are reduced to the corresponding hexenols by an alcohol dehydrogenase. The 12-oxo-acid synthesized as a second product is isomerized to traumatin. There are also lipoxygenases, which insert the peroxy group at position C9.

It was also shown that lipoxygenases are involved in the mobilization of storage lipids present in oil bodies. The lipid monolayer enclosing the oil bodies contains among other proteins lipoxygenases. The latter catalyze the introduction of peroxide groups into multiple-unsaturated fatty acids, as long as they are constituents of triacylglycerols (Fig. 15.31). Only after

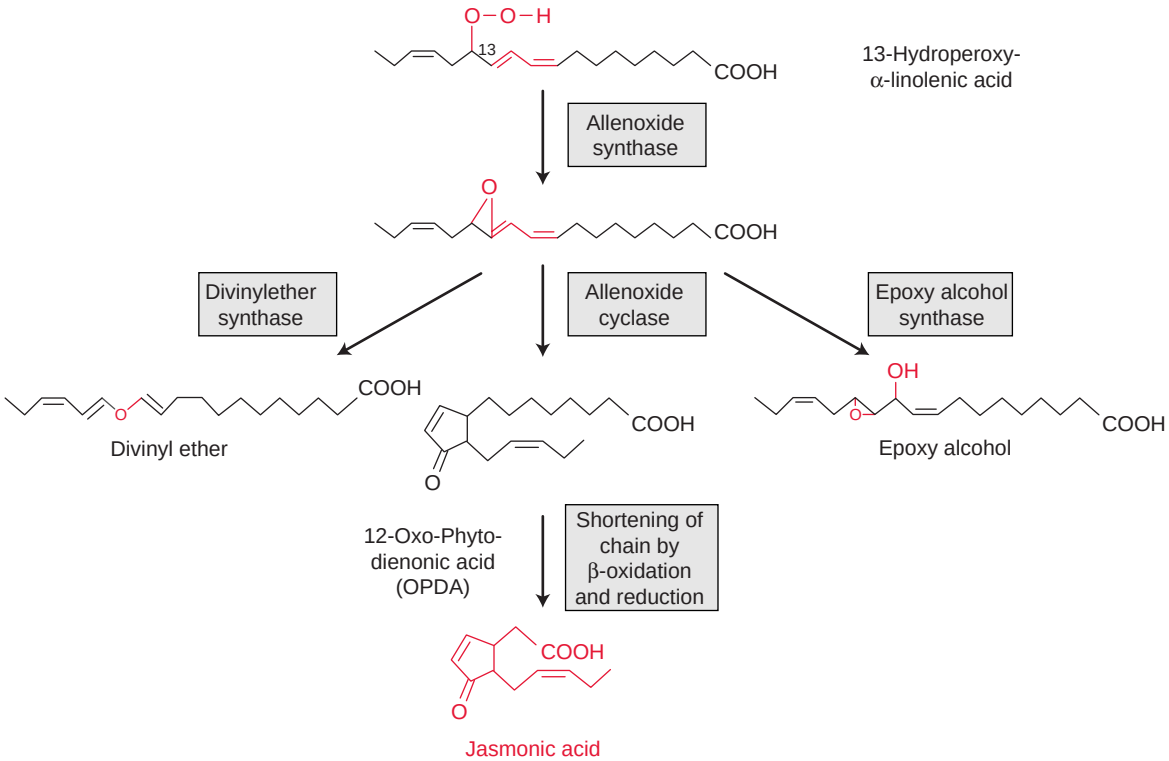

Figure 15.30 An allene oxide synthase and allene oxide cyclase (both belong to the P_{450} family of enzymes, see section 18.2) catalyze the cyclization of the hydroperoxyl linolenic acid by shifting the oxygen. These reactions take place in the chloroplasts. The shortening of the fatty acid chain by six C atoms via β-oxidation leads to the synthesis of jasmonic acid, a phytohormone and signal compound. The peroxisomes are the site of the β-oxidation. Divinyl ether synthase catalyzes the conversion to divinyl ethers and epoxy alcohol synthase to epoxy alcohols. Both compounds are produced as fungicides in response to fungal infection.

this peroxidation are these triacylglycerols hydrolyzed by a lipase, which is also bound to the oil body. The released peroxy fatty acids are reduced to hydroxy fatty acids, which are concomitantly degraded in the glyoxysomes to acetyl CoA by β-oxidation (Fig. 15.25). This pathway for the mobilization of storage lipids exists in parallel to the "classic" pathway of triacylglycerol mobilization initiated by the activity of lipases, as discussed previously. The contribution of each pathway in lipid mobilization varies in the different plant species. The acetyl CoA thus generated is substrate for gluconeogenesis via the glyoxylate cycle (Fig. 15.27).

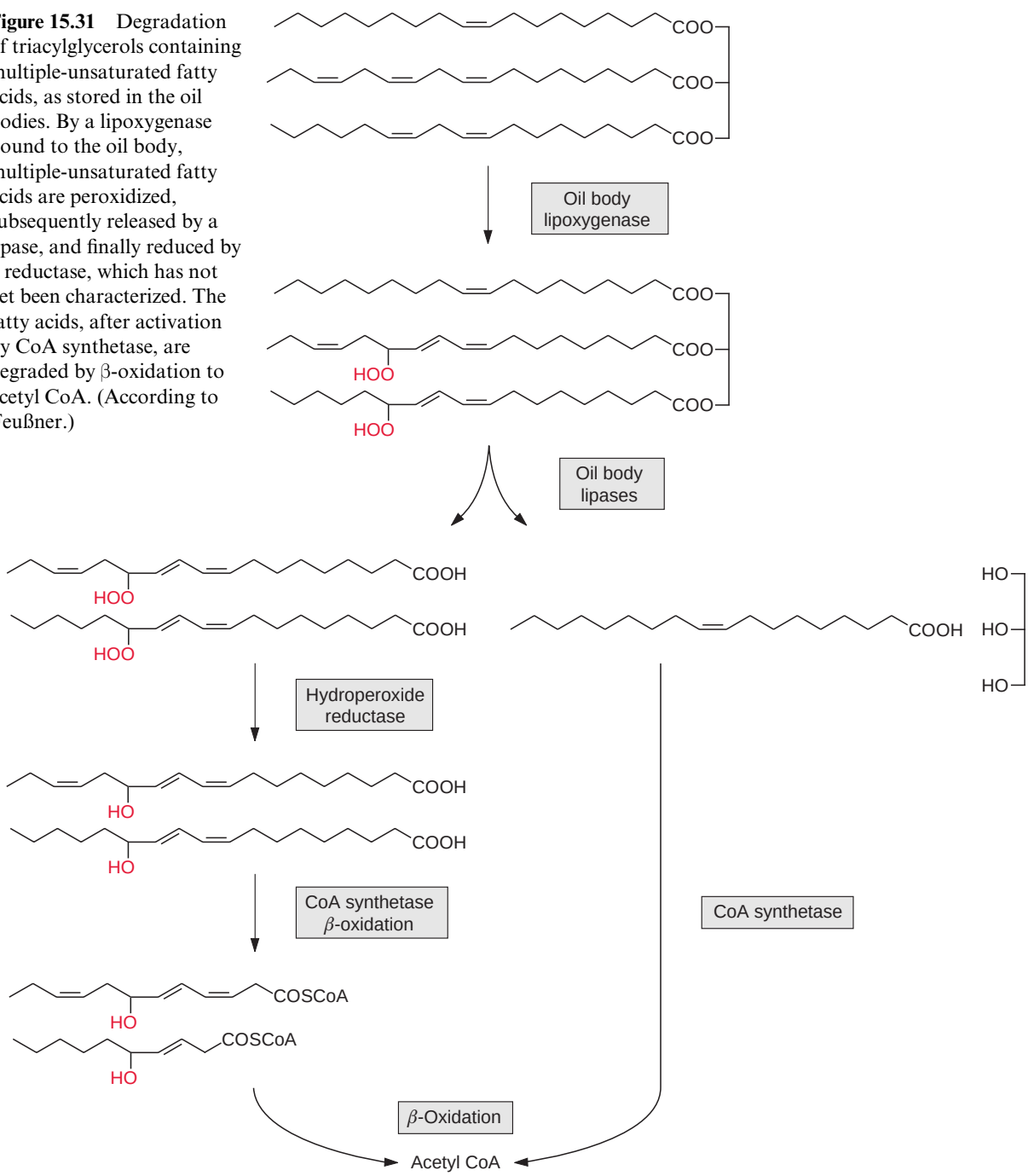

Figure 15.31 Degradation of triacylglycerols containing multiple-unsaturated fatty acids, as stored in the oil bodies. By a lipoxygenase bound to the oil body, multiple-unsaturated fatty acids are peroxidized, subsequently released by a lipase, and finally reduced by a reductase, which has not yet been characterized. The fatty acids, after activation by CoA synthetase, are degraded by β-oxidation to acetyl CoA. (According to Feußner.)

Further reading

Blee, E. Impact of phyto-oxylipins in plant defense. Trends in Plant Science 7, 315–321 (2002).

Caboon, E. B., Ripp, K. G., Hall, S. E., Kinney, A. J. Formation of conjugated Δ8, Δ10 double bonds by delta12-oleic acid desaturase related enzymes. Journal Biological Chemistry 276, 2083–2087 (2001).

Capuano, F., Beaudoin, F., Napier, J. A, Shewry, P. R. Properties and exploitation of oleosins. Biotechnology Advances 25, 203–206 (2007).

Delker, C., Stenzel, I., Hause, B., Miersch, O., Feussner, I., Wasternack, C. Jasmonate biosynthesis in *Arabidopsis thaliana*—enzymes, products, regulation. Plant Biology 8, 297–306 (2006).

Dörmann, P., Benning, C. Galactolipids rule in seed plants. Trends in Plant Science 7, 112–117 (2002).

Feussner, I., Wasternack, C. The lipoxygenase pathway. Annual Reviews Plant Physiology Plant Molecular Biology 53, 275–297 (2002).

Goepfert, S., Poirier, Y. β-Oxidation in fatty acid degradation and beyond. Current Opinion in Plant Biology 10, 245–251 (2007).

Halim, V. A., Vess, A., Scheel, D., Rosahl, S. The role of salicylic acid and jasmonic acid in pathogene defence. Plant Biology 8, 307–313 (2006).

Hsieh, K., Huang, A. H. C. Endoplasmatic reticulum, oleosins, and oils in seeds and tapetum cells. Plant Physiology 136, 3427–3434 (2004).

Kader, J.-C. Lipid-transfer proteins: A puzzling family of plant proteins. Trends in Plant Science 2, 66–70 (1997).

Liavonchanka, A., Feussner, I. Lipoxygenases: Occurrence, functions and catalysis. Journal Plant Physiology 163, 348–357 (2006).

Murakami, Y., Tsuyama, M., Kobayashi, Y., Kodama, H., Ida, K. Trienoic fatty acids and plant tolerance of high temperature. Science 287, 476–479 (2000).

Napier, J. A. The production of unusual fatty acids in transgenic plants. Annual Review Plant Biology 58, 295–319 (2007).

Ryu, S. B. Phospholipid-derived signaling mediated by phospholipase A in plants. Trends in Plant Science 9, 1360–1385 (2004).

Schaller, H. The role of sterols in plant growth. Progress in Lipid Research 42, 163–175 (2003).

Sperling, P., Heinz, E. Plant sphingolipids: Structural diversity, biosynthesis, first genes and functions. Biochimica Biophysica Acta 1632, 1–5 (2003).

Voelker, T., Kinney, A. J. Variations in the biosynthesis of seed-storage lipids. Annual Reviews Plant Physiology Plant Molecular Biology 52, 335–361 (2001).

Warude, D., Joshi, K., Harsulkar, A. Polyunsaturated fatty acids: Biotechnology. Critical Reviews Biotechnology 26, 83–93 (2006).

Wasternack, C. Jasmonates: An update on biosynthesis, signal transduction and action in plant stress response, growth and development. Annals Botany (London) 100, 681–697 (2007).

Worrall, D., Ng, C. K.-J., Hetherington, A. M. Sphingolipids, new players in plant signalling. Trends in Plant Science 8, 317–320 (2003).

Yalovsky, S., Rodriguez-Concepción, M., Gruissem, W. Lipid modifications of proteins—slipping in and out of membranes. Trends in Plant Science 4, 439–445 (1999).

16

Secondary metabolites fulfill specific ecological functions in plants

In addition to **primary** metabolites such as carbohydrates, amino acids, fatty acids, cytochromes, chlorophylls, and metabolic intermediates of the anabolic and catabolic pathways, which occur in all plants and where they all have the same metabolic functions, plants also produce a large variety of compounds, with no apparent function in the primary metabolism, and therefore are called **secondary** metabolites. Certain secondary metabolites are restricted to a few plant species where they fulfill specific ecological functions, such as attracting insects to transfer pollen, or animals for consuming fruits to distribute seeds, or as **natural pesticides** that act as defense compounds to combat herbivores and pathogens.

16.1 Secondary metabolites often protect plants from pathogenic microorganisms and herbivores

Plants, because of their protein and carbohydrate content, are an important food source for many animals, such as insects, snails, and many vertebrates. Since plants cannot run away, they have had to evolve strategies that make them indigestible or poisonous to protect them from being eaten. Many plants protect themselves by producing toxic proteins (e.g., amylase, proteinase inhibitors or lectins), which impair the digestion of herbivores (section 14.4). In response to caterpillar feeding, maize plants mobilize a protease that destroys the caterpillar's intestine. To secondary metabolites belong alkaloids (this chapter), isoprenoids (Chapter 17), and phenylpropanoids (Chapter 18),

all of which include natural pesticides that protect plants against herbivores and pathogenic microorganisms. In some plants these natural pesticides amount to 10% of the dry matter.

Some defense compounds against herbivores are part of the permanent outfit of plants; they are **constitutive**. Other defense components are only synthesized by the plant after browsing damage (**induced defense**). Section 18.7 describes how acacias, after feeding damage, produce more tannins, thus making the leaves inedible. Another example, as described in section 15.7, is when plants damaged by caterpillars use the synthesis of scents (volatile secondary metabolites) to attract parasitic wasps, which lay their eggs in the caterpillars, thus killing them (**indirect defense**).

Microorganisms can be pathogens

Certain fungi and bacteria infect plants in order to utilize their resources for their own nutritional requirements. As this often leads to plant diseases, these infectants are called **pathogens**. In order to infect the plants effectively, the pathogenic microbes produce aggressive substances such as enzymes, which degrade the cell walls, or toxins, which damage the plant. An example is **fuscicoccin** (section 10.3), which is produced by the fungus *Fusicoccum amygdalis*. The production of compounds for infecting plants requires the presence of specific **virulence genes**. Plants protect themselves against pathogens by producing defense compounds that are encoded by specific **resistance genes**. The interaction of the virulence genes and resistance genes decides the success of the attack and defense.

When a plant is susceptible and the pathogen is aggressive, it leads to a disease, and the pathogen is called **virulent**. Such is termed a **compatible interaction**. If, on the other hand, the infecting pathogen is killed or at least its growth is very much retarded, this is an **incompatible interaction**, and the plant is regarded as **resistant**. Often just a single gene decides on compatibility and resistance between pathogen and host.

Plants synthesize phytoalexins in response to microbial infection

Defense compounds against microorganisms, especially fungi, are synthesized mostly in response to an infection (induced defense). These inducible defense substances, which are produced within hours, are called **phytoalexins** (*alekein*, Greek, to defend). Phytoalexins comprise a large number of compounds with very different structures such as isoprenoids, flavonoids, and stilbenes, many of which act as antibiotics against a broad spectrum of pathogenic fungi and bacteria. Plant root exudates contain bacteriostatic

compounds such as cumaric acid, 3-indol propionic acid and methyl *p*-hydroxybenzoate that can render a plant resistant against pathogens. Plants produce for defense aggressive oxygen compounds such as superoxide radicals ($\bullet O_2^-$) and H_2O_2, as well as nitrogen monoxide (NO) (section 19.9), and enzymes, such as β-glucanases, chitinases, and proteinases, which damage the cell walls of bacteria and fungi. Also the emission of volatile metabolites is induced after pathogen attack, which directly or indirectly can alarm defense reactions in the plant or in plants in the neighborhood. The synthesis of these various defense substances is induced by so-called **elicitors**. Elicitors are often proteins excreted by the pathogens to attack plant cells (e.g., cell-degrading enzymes). Moreover, polysaccharide segments of the cell's own wall, produced by degradative enzymes of the pathogen, function as elicitors. But elicitors can also be fragments from the cell wall of the pathogen, released by defense enzymes of the plant. These various elicitors are bound to specific receptors on the outer surface of the plasma membrane of the plant cell. The binding of the elicitor releases signal cascades in which protein kinases (section 19.1) and signal substances such as salicylic acid (section 18.2) and jasmonic acid (section 15.7) participate, and which finally induce the **transcription of genes** for the synthesis of phytoalexins, reactive oxygen compounds, and defense enzymes (section 19.9).

Elicitors may also cause an infected cell to die and the surrounding cells to die with it. In other words, the infected cells and those surrounding it commit suicide. This can be caused, for instance, by the production of phenols of the infected cells to poison not only themselves but also their surrounding cells. This programmed cell death, called a **hypersensitive response**, serves to protect the plant. The cell walls around the necrotic tissue are strengthened by increased biosynthesis of lignin, and in this way the plant barricades itself against further spreading of the infection.

Plant defense compounds can also be a risk for humans

Substances toxic for animals are, in many cases, also toxic for humans. In crop plants, toxic or inedible secondary metabolites have been eliminated or at least decreased by breeding. This is why cultivated plants usually are more sensitive to pests than wild plants, thus necessitating the use of external pest control, which is predominantly achieved by the use of chemicals. Attempts to breed more resistant crop plants by crossing them with wild plants, however, may lead to problems, e.g., a newly introduced variety of insect-resistant potato had to be taken off the market because the highly toxic solanine content (an alkaloid, see following section) made these potatoes unsuitable for human consumption. In a new variety of insect-resistant celery cultivated in the United States, the 10-fold increase in the content

of psoralines (section 18.2) caused severe skin damage to people harvesting the plants. This illustrates that natural pest control is not without risk.

A number of plant constituents that are harmful to humans (e.g., proteins such as lectins, amylase inhibitors, proteinase inhibitors, and cyanogenic glycosides or glucosinolates (dealt with in this chapter)) decompose when cooked. But most secondary metabolites are not destroyed in this way. In higher concentrations, many plant secondary metabolites are cancerogenic. It has been estimated that in industrialized countries more than 99% of all cancerogenic compounds that humans normally consume with their diet are plant secondary metabolites that are natural constituents of the food. However, experience has shown that the human metabolism usually provides sufficient protection against many harmful natural substances particularly at lower concentrations. As will be discussed in the following, plants also contain many compounds which are used as pharmaceuticals to combat illnesses.

16.2 Alkaloids comprise a variety of heterocyclic secondary metabolites

Alkaloids belong to a group of secondary metabolites that are synthesized from **amino acids** and contain one or several N atoms as constituents of **heterocycles**. Many of these alkaloids act as defense compounds against animals and microorganisms. Since alkaloids usually are bases, they are stored in the protonated form, mostly in the vacuole which is acidic. Since ancient times humans have used alkaloids in the form of plant extracts as poisons, stimulants, and narcotics, and, last but not least, as medicine. In 1806 the pharmacy assistant Friedrich Wilhelm Sertürner isolated morphine from poppy seeds. Another 146 years had to pass before the structure of morphine was finally resolved in 1952. More than 10,000 alkaloids of very different structures are now known. Their biosynthesis pathways are very diverse, to a large extent still not known, and will not be discussed here.

Figure 16.1 shows a small selection of important alkaloids. Alkaloids are classified according to their heterocycles. **Coniine**, a piperidine alkaloid, is a very potent poison in hemlock. Socrates died when he was forced to drink this poison. **Nicotine**, which also is very toxic, contains a pyridine and a pyrrolidine ring. It is synthesized in the roots of tobacco plants and is carried along with the xylem sap into the stems and leaves. Nicotine sulfate, a by-product of the tobacco industry, is used as a very potent insecticide (e.g., for fumigating greenhouses). There is no insect known to be resistant to nicotine. Genetically modified tobacco plants where the nicotine content

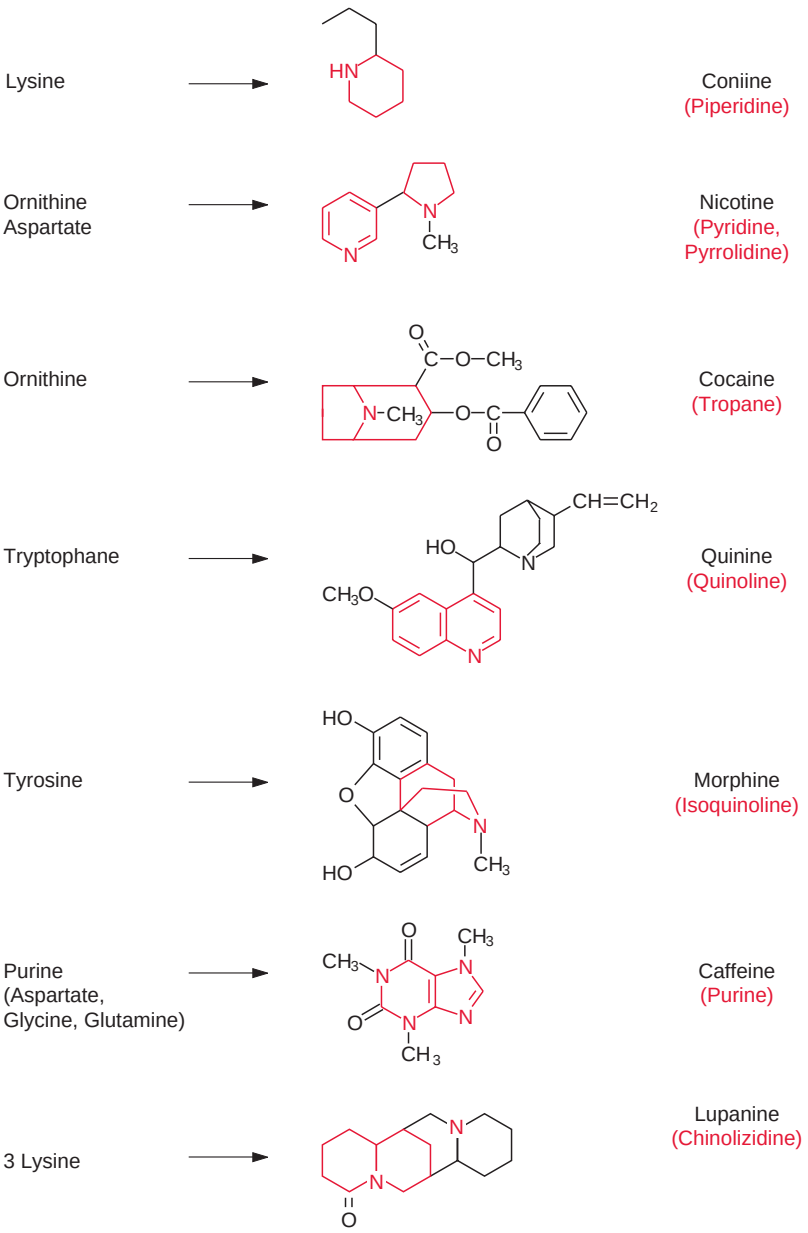

Figure 16.1 Some alkaloids and the amino acids from which they are synthesized. The heterocycles, after which the alkaloids are classified, are colored red; their names are given in brackets. A synthesis of coniine from acetyl CoA has also been described. Purine is synthesized from aspartate, glycine, and glutamine.

was decreased by 96% were shown to be highly infested by the caterpillar *Maduca sexta*. **Cocaine**, the well-known narcotic, contains **tropane** as a heterocycle, in which the N atom is a constituent of two rings. A further well-known tropane alkaloid is **atropine** (formula not shown), a poison accumulated in deadly nightshade (*Atropa belladonna*). In low doses, it dilates

the pupils of the eye and is therefore used in medicine for eye examination. Cleopatra allegedly used extracts containing atropine to dilate her pupils to appear more attractive. **Quinine**, a quinoline alkaloid from the bark of *Chinchuna officinalis* growing in South America, was known by the Spanish conquerors to be an antimalarial drug. The isoquinoline alkaloid **morphine** is an important pain killer and is also a precursor for the synthesis of heroin. **Caffeine**, the stimulant of coffee, has purine as the heterocycle. **Chinolizidin alkaloids**, such as **lupinin** and **lupanin**, which primarily accumulate in varieties of lupines, are synthesized from three lysine molecules. Due to the toxicity of these compounds sheep frequently die in the autumn from eating too much lupine seed. **Pyrrolizidin** alkaloids, such as **senecionin** (formula not shown) are synthesized by plants to combat herbivores. These compounds, however, are not harmful to certain specifically adapted herbivores, which accumulate them and thus render themselves poisonous towards predators, parasitoids and pathogens.

In order to search for new medicines, large numbers of plants are being analyzed for their secondary metabolite contents. One result is the alkaloid **taxol**, isolated from the yew tree *Taxus brevifolia*, now used for cancer treatment. Derivatives of the alkaloid camptothezine from the Chinese "happy tree" *Camptotheca acuminata* are also being clinically tested as cancer therapeutics. The search for new medicines against malaria and viral infections continues. Since large quantities of pharmacologically interesting compounds often cannot be gained from plant material, attempts are being made with the aid of genetic engineering either to increase production in the corresponding plants or to transfer the plant genes into microorganisms in order to use the latter for production.

16.3 Some plants emit prussic acid when wounded by animals

Since **prussic acid** (**HCN**) inhibits cytochrome oxidase which is the final step of the respiratory chain, it is a very potent poison (section 5.5). Ten percent of all plants are estimated to use this poison as a defense strategy against being eaten by animals. The consumption of peach kernels, for instance, or bitter almonds can have fatal consequences for humans. Since plants also possess a mitochondrial respiratory chain, in order not to poison themselves, prussic acid is bound in a non-toxic form as **cyanogenic glycoside**, e.g., amygdalin (Fig. 16.2), which is present in the kernels and roots of peaches. The cyanogenic glycosides are stored as stable compounds in the vacuole. The **glycosidase**, which catalyzes the hydrolysis of the glycoside, is present in

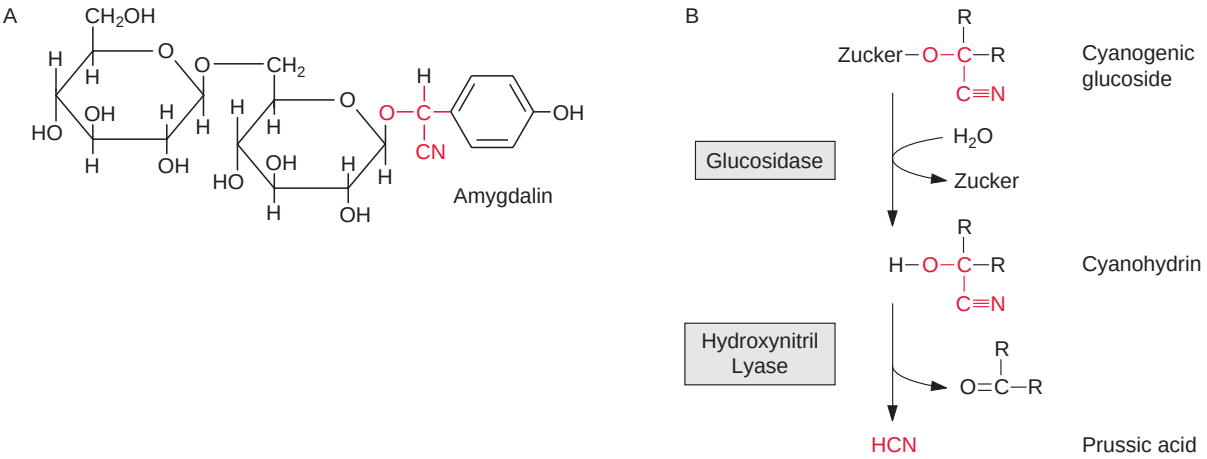

Figure 16.2 A. Amygdalin, a cyanogenic glycoside, accumulates in some stone fruit kernels. B. After the sugar residue has been cleaved off by hydrolysis, cyanohydrin is released from cyanogenic glycosides, which decomposes spontaneously to prussic acid and a carbonyl compound.

another compartment (cytosol). If the cell is wounded by feeding animals, the compartmentation is disrupted and the glycosidase comes into contact with the cyanogenic glycoside. After the hydrolysis of the glucose residue, the remaining cyanhydrin is very unstable and decomposes spontaneously to prussic acid and an aldehyde. A **hydroxynitrile lyase** enzyme accelerates this reaction. The aldehydes synthesized from cyanogenic glycosides are often very toxic. For a feeding animal, the detoxification of these aldehydes can be even more difficult than that of prussic acid. Due to the formation of the two different toxic compounds, cyanogenic glycosides are a very effective defense system.

16.4 Some wounded plants emit volatile mustard oils

Glucosinolates, also called mustard oil glycosides, have a similar protective function against herbivores as cyanogenic glycosides. Glucosinolates can be found, for instance, in radish, several cabbage varieties, and mustard. Cabbage contains the glycoside glucobrassicin (Fig. 16.3), which is synthesized from tryptophan. The hydrolysis of the glycoside by a **thioglucosidase** results in a very unstable product from which, after the liberation and rearrangement of the sulfate residue, an isothiocyanate, also termed **mustard oil**,

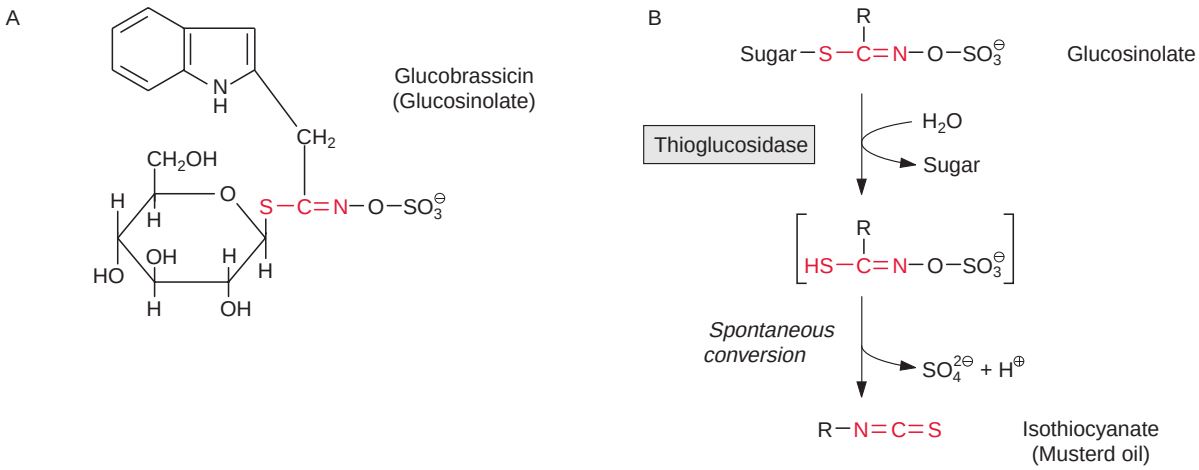

Figure 16.3 A. Glucobrassicin, a glucosinolate from cabbage. B. The hydrolysis of the glycoside by thioglucosidase results in an unstable product, which decomposes spontaneously into sulfate and isothiocyanate.

is spontaneously released. Depending on the cellular pH nitriles, thiocyanate and oxazolidin 3-thion can also be formed as glucosinolate products. Mustard oils are toxic in higher concentrations. As is the case of the cyanogenic glycosides, glucosinolates and the hydrolyzing enzyme thioglucosidase are also located in separate compartments of the plant tissues. The enzyme comes into contact with its substrate only after wounding. When cells of these plants have been damaged, the pungent smell of mustard oil can easily be detected (e.g., in freshly cut radish). The high glucosinolate content in early varieties of rape seed made the pressed seed unsuitable for fodder. Nowadays, as a result of successful breeding, rape seed varieties are cultivated without glucosinolate in the seeds and the pressed seeds are a valuable fodder due to their high protein content.

16.5 Plants protect themselves by tricking herbivores with false amino acids

Many plants contain unusual amino acids with a structure very similar to that of protein building amino acids (e.g., **canavanine** from Jack bean (*Canavalia ensiformis*), a structural analogue of **arginine** (Fig. 16.4)). Herbivores take up canavanine with their food. During protein biosynthesis, the arginine-transfer RNAs of animals cannot distinguish between arginine

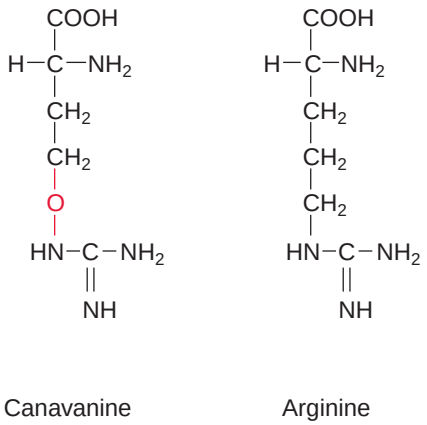

Figure 16.4 Canavanine is a structural analogue of arginine.

and canavanine and incorporate canavanine instead of arginine into proteins. This exchange can alter the three-dimensional structure of proteins, which then lose their biological function partially or even completely. Therefore canavanine is toxic for herbivores. In those plants which synthesize canavanine, the arginine transfer RNA does not react with canavanine, therefore it is not toxic for these plants. This same protective mechanism is used by some insects, which are specialized in eating leaves containing canavanine.

Further reading

Bais, H. P., Weir, T. L., Perry, L. G., Gilroy, S., Vivanco, J. M. The role of root exudates in rhizophere interactions with plants and other organisms. Annual Review Plant Biology 57, 233–266 (2006).

Baldwin, I. T., Halitschke, R., Paschold, A., von Dahl, C. C. Volatile signaling in plant-plant interactions: "talking tress" in the genomics era. Science 311, 812–815 (2006).

Beers, E. P., McDowell, J. M. Regulation and execution of programmed cell death in response to pathogens, stress and developmental cues. Current Opinion in Plant Biology 4, 561–567 (2001).

Facchini, P. J. Regulation of alkaloid biosynthesis in plants. Alkaloids Chemistry Biology 63, 1–44 (2006).

Friedman, M. Potato glycoalkaloids and metabolites: Roles in the plant and in the diet. Journal Agricultural Food Chemistry 54, 8655–8681 (2006).

Grant, J. J., Loake, G. J. Role of reactive oxygen intermediates and cognate redox signaling in disease resistance. Plant Physiology 124, 21–29 (2000).

Grubb, D. C., Abel, S. Glucosinolate metabolism and its control. Trends in Plant Science 11, 89–100 (2006).

Halkier, B. A., Gershenzon, J. Biology and biochemistry of glucosinolates. Annual Reviews Plant Biology 57, 303–333 (2006).

Hartmann, T. Plant-derived secondary metabolites as defensive chemicals in herbivorous insects: A case study in chemical ecology. Planta 219, 1–4 (2004).

Heil, M., Bueno, J. C. S. Within-plant signaling by volatiles leads to induction and priming of an indirect plant defense in nature. Proceedings of National Academic Society USA 104, 5467–5472 (2007).

Kingston, D. G., Newman, D. J. Taxoids: Cancer-fighting compounds from nature. Current Opinion Drug Discovery Development 10, 130–144 (2007).

Paul, N. D., Hatcher, P. E., Taylor, J. E. Coping with multiple enemies: An integration of molecular and ecological perspectives. Trends in Plant Science 5, 220–225 (2000).

Shitan, N., Yazaki, K. Accumulation and membrane transport of plant alkaloids. Current Pharmacology Biotechnology 8, 244–252 (2007).

Stahl, E. A., Bishop, J. G. Plant pathogen arms races at the molecular level. Current Opinion in Plant Biology 3, 299–304 (2000).

Yan, X., Chen, S. Regulation of plant glucosinolate metabolism. Planta 226, 1343–1352 (2007).

Zagrobelny, M., Bak, S., Rasmussen, A. V., Jørgensen, B., Naumann, C. M., Lindberg-Møller, B. Cyanogenic glucosides and plant-insect interactions. Phytochemistry 65, 293–306 (2004).

17

A large diversity of isoprenoids has multiple functions in plant metabolism

Isoprenoids are present in all living organisms, but with a remarkable diversity in plants. More than 40,000 different plant isoprenoids are known and new compounds are being constantly identified. These isoprenoids have many different functions (Table 17.1). In primary metabolism, they function as membrane constituents, photosynthetic pigments, electron transport carriers, growth substances, and plant hormones. They act as glucosyl carriers in glucosylation reactions and are involved in the regulation of cell growth.

Plant isoprenoids (also known as **terpenoids**) are important commercially, for example as aroma substances for food, beverages, and cosmetics, as vitamins (A, D, and E), natural insecticides (e.g., pyrethrin), solvents (e.g., turpentine), and as rubber and gutta-percha. The plant isoprenoids also comprise important natural compounds, which are utilized as pharmaceuticals or their precursors. Investigations are in progress to increase the ability of plants to synthesize isoprenoids by genetic engineering.

Plant ethereal oils have long been of interest to chemists. A number of mainly cyclic compounds containing 10, 15, 20, or correspondingly more C atoms have been isolated from turpentine oil. Such substances have been found in many plants and were given the collective name **terpenes**. Figure 17.1 shows some examples of terpenes. Limonene, an aromatic substance from lemon oil, is a terpene with 10 C atoms and is called a monoterpene. Carotene, with 40 C atoms, is accordingly a tetraterpene**.** Rubber is a polyterpene with about 1,500 C atoms. It is obtained from the latex of the rubber tree *Hevea brasiliensis*.

Table 17.1: Isoprenoids of higher plants

Precursor	Class	Example	Function
C_5: Dimethylallyl-PP	Hemiterpene	Isoprene	Protection of the photosynthetic apparatus against heat
Isopentenyl-PP		Side chain of cytokinin	Growth regulator
C_{10}: Geranyl-PP	Monoterpene	Pinene	Defense substance attractant
		Linalool	
C_{15}: Farnesyl-PP	Sesquiterpene	Capsidiol	Phytoalexin
C_{20}: Geranylgeranyl-PP	Diterpene	Gibberellin	Plant hormone
		Phorbol	Defense substance
		Casbene	Phytoalexin
C_{30}: 2 Farnesyl-PP	Triterpene	Cholesterol	Membrane constituents
		Sitosterol	
C_{40}: 2 Geranylgeranyl-PP	Tetraterpene	Carotenoids	Photosynthesis pigments
n Geranylgeranyl-PP or *n* Farnesyl-PP	Polyprenols	Prenylated proteins	Regulation of cell growth
		Prenylation of plastoquinone, ubiquinone, chlorophyll, cyt *a*	Membrane solubility of photosynthesis pigments and electron transport carriers
		Dolichols	Glucosyl carrier
		Rubber	

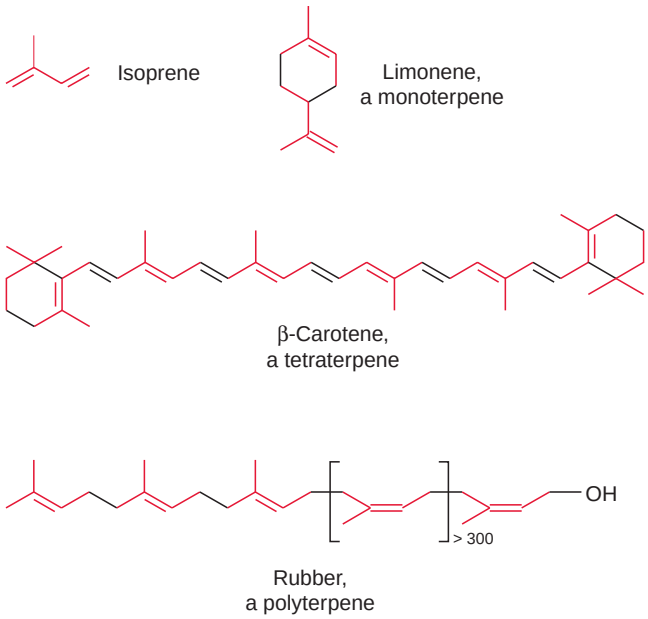

Figure 17.1
Various isoprenoids.

Otto Wallach (Bonn, Göttingen), who in 1910 was awarded the Nobel Prize in Chemistry for his basic studies on terpenes, recognized that isoprene is the basic constituent of terpenes (Fig. 17.1). Continuing these studies, Leopold Ruzicka (Zürich) found that isoprene is the universal basic element for the synthesis of many natural compounds, including steroids, and for this he was awarded the Nobel Prize in Chemistry in 1939. He postulated the biogenic isoprene rule, according to which all terpenoids (derivatives of terpenes) are synthesized via a hypothetical precursor, which he named **active isoprene**. This speculation was verified by Feodor Lynen in Munich (1964 Nobel Prize in Medicine), when he identified **isopentenyl pyrophosphate** to be the "active isoprene."

17.1 Higher plants have two different synthesis pathways for isoprenoids

Precursor for the synthesis of isoprenoids is isopentenyl pyrophosphate. Its synthesis proceeds in higher plants and some groups of algae in two different ways, one located in the cytosol and the other in the plastids.

Acetyl CoA is a precursor for the synthesis of isoprenoids in the cytosol

The basis for the elucidation of this isoprenoid biosynthesis pathway was the discovery by Konrad Bloch (USA, likewise a joint winner of the Nobel Prize in Medicine in 1964) that **acetyl CoA** is a precursor for the biosynthesis of steroids. Figure 17.2 shows the synthesis of the intermediary product isopentenyl pyrophosphate: two molecules of acetyl CoA react to produce **acetoacetyl CoA** and then with another acetyl CoA yielding **β-hydroxy-β-methylglutaryl CoA** (HMG CoA). In yeast and animals, these reactions are catalyzed by two different enzymes, whereas in plants a single enzyme, **HMG CoA synthase**, catalyzes both reactions. The esterified carboxyl group of HMG CoA is reduced by two molecules of NADPH to a hydroxyl group, accompanied by hydrolysis of the energy-rich thioester bond. Thus **mevalonate** is formed in an irreversible reaction. The formation of mevalonate from HMG CoA is an important regulatory step of isoprenoid synthesis in animals. It has not yet been resolved whether this also applies to plants. A pyrophosphate ester is formed in two successive phosphorylation steps, catalyzed by two different kinases. With consumption of a third molecule of ATP, involving the transitory formation of a phosphate

Figure 17.2 Isopentenyl pyrophosphate synthesis in the cytosol proceeds via the acetate-mevalonate pathway.

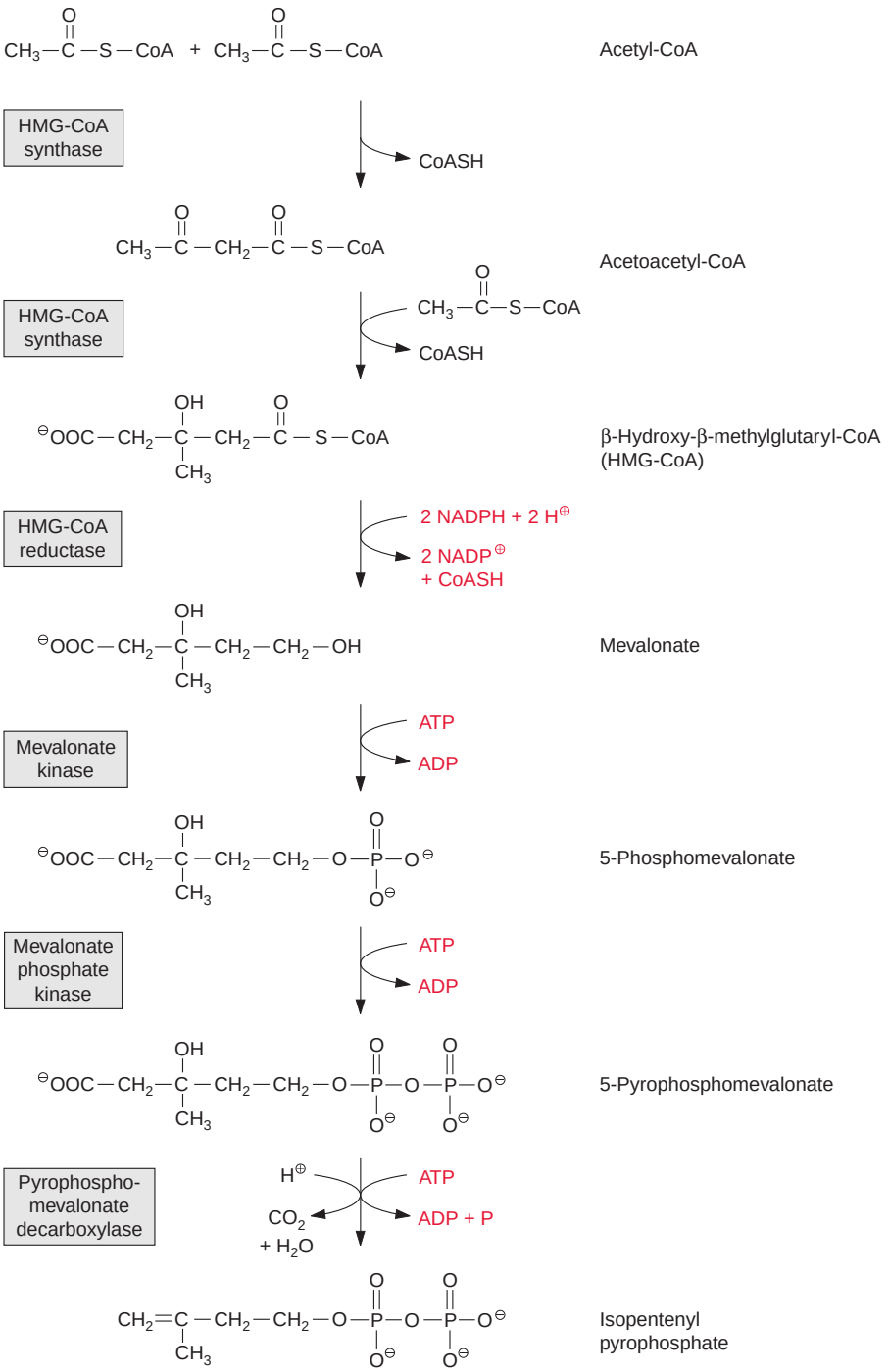

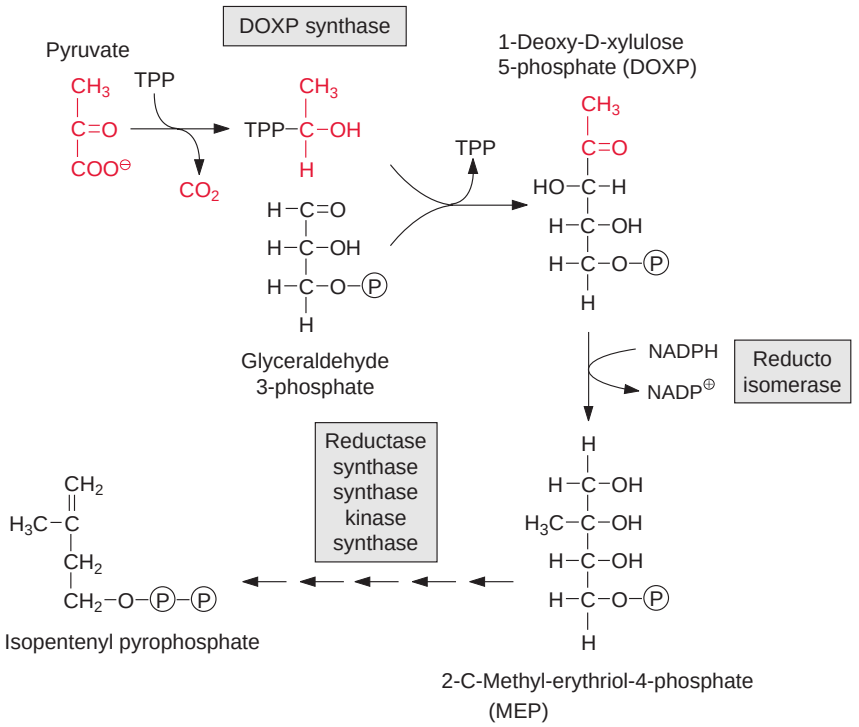

Figure 17.3
The isopentenyl pyrophosphate synthesis in the plastids proceeds via the 2-methyl erythriol 4-phosphate pathway (MEP). For the conversion of MEP to isopentenyl pyrophosphate only the enzymes involved are listed, the intermediates are not shown.

ester, a carbon-carbon double bond is generated and the remaining carboxyl group is removed. Isopentenyl pyrophosphate thus formed is the basic element for the formation of an isoprenoid chain. This synthesis of isopentenyl pyrophosphate, termed the **acetate-mevalonate pathway**, is located in the cytosol. It is responsible for the synthesis of sterols, certain sesquiterpenes, and the side chain of ubiquinone.

Pyruvate and D-glyceraldehyde-3-phosphate are the precursors for the synthesis of isopentyl pyrophosphate in plastids

The acetate-mevalonate pathway can be blocked by **mevilonin**, a very specific inhibitor of HMG CoA reductase. Experiments with plants showed that mevilonin inhibits the isoprenoid synthesis in the cytosol, but not in the plastids. These findings led to the discovery that the synthesis of isopentenyl pyrophosphate in the plastids follows a different pathway from that in the cytosol (Fig. 17.3). For the plastidal synthesis pathway, the precursors are **pyruvate** and **D-glyceraldehyde-3-phosphate**. As in the pyruvate dehydrogenase reaction (Fig. 5.4), pyruvate is decarboxylated via thiamine pyrophosphate (TPP), and then, as in the transketolase reaction (Fig. 6.17), is transferred

to D-glyceraldehyde-3-phosphate to yield **1-deoxy-D-xylulose-5-phosphate** (**DOXP**). After isomerization and reduction by NADPH, 2-C-methyl-D-erythritol-4-phosphate (**MEP**) is synthesized. MEP is then activated by reacting with CTP to yield CDP methyl erythriol. Two further reduction steps, followed by dehydration and phosphorylation, finally yield **isopentenyl pyrophosphate**. The **MEP-synthase pathway** for isoprenoids is present in bacteria, algae, and plants, but not in animals. A large part of plant isoprenoids, including the hemiterpene isoprene, monoterpenes like pinene and limonene, diterpenes (e.g., phytol chains, gibberellin, abietic acid as oleoresin constituent) as well as tetraterpenes (carotenoids) are synthesized via the MEP synthase pathway located in the plastids. Also, the side chains of chlorophyll and plastoquinone are synthesized by this pathway. Sesquiterpenes and triterpenes, on the other hand, according to our present knowledge are synthesized by the mevalonate pathway in the cytosol (Fig. 17.2).

17.2 Prenyl transferases catalyze the association of isoprene units

Dimethylallyl pyrophosphate, which is formed by isomerization of isopentenyl pyrophosphate, is the acceptor for successive transfers of isopentenyl moieties (Fig. 17.4). With the liberation of the pyrophosphate residue, dimethylallyl-PP condenses with isopentenyl-PP to produce geranyl-PP. In an analogous way, chain elongation is attained by further head-to-tail condensations with isopentenyl-PP, and so farnesyl-PP and geranylgeranyl-PP are formed one after the other.

The transfer of the isopentenyl moieties is catalyzed by **prenyl transferases**. Prenyl residues are a collective term for isoprene or polyisoprene residues. A special prenyl transferase is required for the production of each of the prenyl pyrophosphates mentioned. For example, the prenyl transferase termed **geranyl-PP synthase** catalyzes only the synthesis of geranyl-PP. However, **farnesyl-PP synthase** synthesizes farnesyl-PP in two discrete steps: from dimethylallyl-PP and isopentenyl-PP, first geranyl-PP is formed, but this intermediate remains bound to the enzyme and reacts further with another isopentenyl-PP to produce farnesyl-PP. Analogously, **geranylgeranyl-PP synthase** catalyzes all three steps of the formation of geranylgeranyl-PP. Table 17.1 shows that each of these prenyl pyrophosphates is the precursor for the synthesis of structurally and functionally specific isoprenoids, including hemiterpenes, monoterpenes, and sesquiterpenes. As these prenyl pyrophosphates are synthesized by different enzymes, the synthesis of a certain prenyl

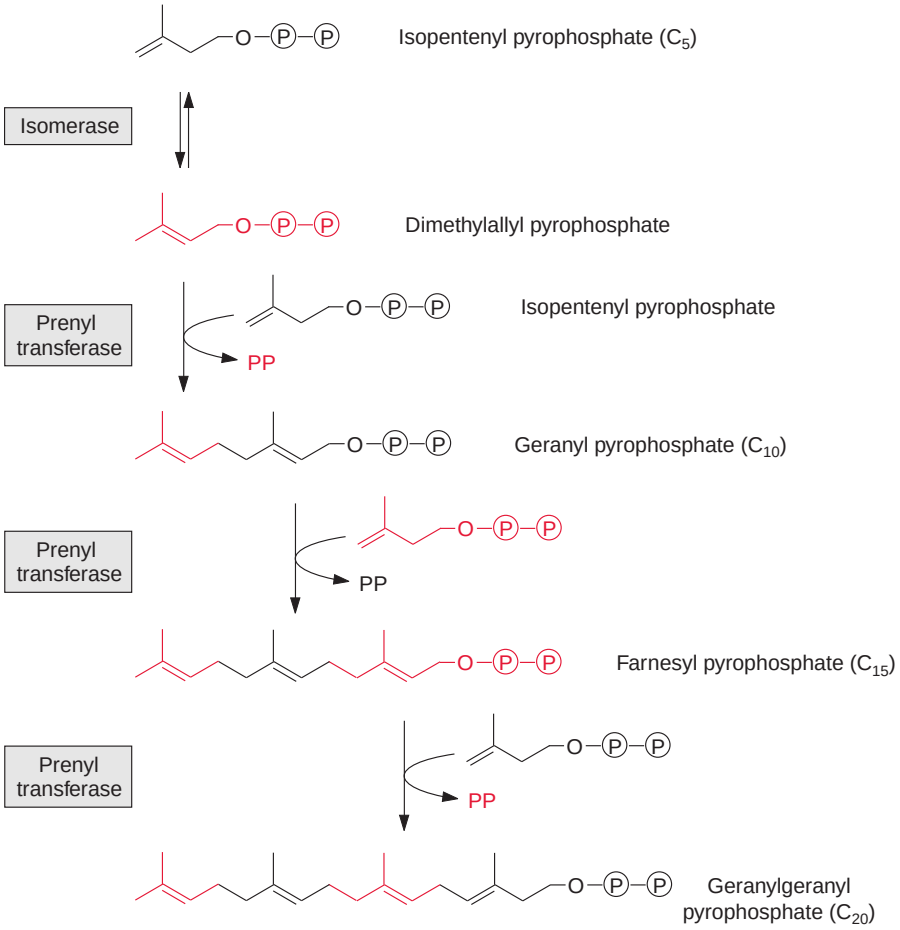

Figure 17.4 Higher molecular prenyl phosphates are formed by head-to-tail addition of active isoprene units.

pyrophosphate can be regulated by induction or repression of the corresponding enzyme. It appears that there is a synthesis pathway from isopentenyl pyrophosphate to geranylgeranyl pyrophosphate, not only in the cytosol but also in the plastids. The differences between these two pathways have not yet been resolved in detail.

The formation of a C-C linkage between two isoprenes proceeds by nucleophilic substitution (Fig. 17.5): an Mg^{++} ion, bound to the prenyl transferase, facilitates the release of the negatively charged pyrophosphate residue from the acceptor molecule, whereby a positive charge remains at the terminal C atom (C-1), which is stabilized by the neighboring double bond. The allyl cation thus formed reacts with the terminal C-C double bond of the donor molecule and a new C-C bond is formed with the release of a proton. According to the same reaction mechanism, not only isoprene chains, but also rings are formed, leading to the exceptional diversity of isoprenoids.

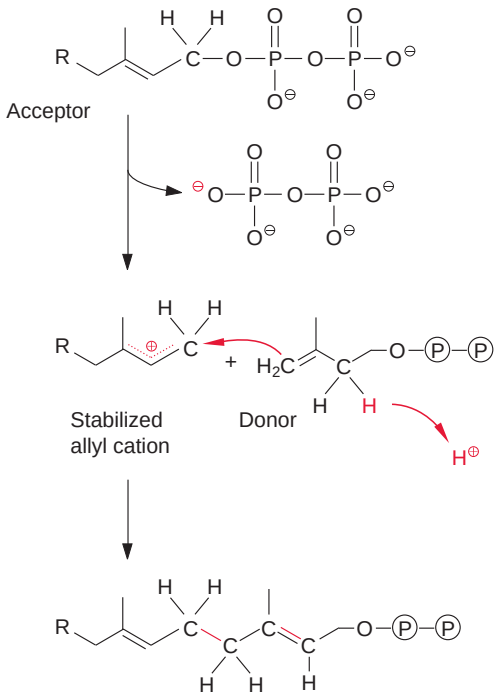

Figure 17.5 The head-to-tail addition of two prenyl phosphates by prenyl transferase is a nucleophilic substitution according to the S_N1 mechanism. First, pyrophosphate is released from the acceptor molecule. An allyl cation is formed, which reacts with the double bond of the donor molecule and forms a new C-C bond. The double bond is restored by release of a proton, but it is shifted by one C atom. The reaction scheme is simplified.

17.3 Some plants emit isoprenes into the air

The **hemiterpene** isoprene is formed from dimethyallyl-PP upon the release of pyrophosphate by an **isoprene synthase**, which is present in many plants (Fig. 17.6). Isoprene is volatile (boiling point 33°C) and leaks from the plant in gaseous form. Trees, such as oak, willow, planes, and poplar, emit isoprene during the day at temperatures of 30°C to 40°C. At such high temperatures, as much as 5% of the photosynthetically fixed carbon in oak leaves can be emitted as isoprene. Isoprene emissions of up to 20% of the total photoassimilate have been observed for the kudzu vine (*Pueraria lobota*), a climbing plant that is grown in Asia for fodder. Together with monoterpenes and other compounds, isoprene emission is responsible for the blue haze that can be observed over forests during hot weather.

Isoprene is produced in the chloroplasts from dimethylallyl pyrophosphate, which is formed via the MEP synthase pathway (Fig. 17.3). Isoprene synthase is induced when leaves are exposed to high temperatures. The physiological function of isoprene formation is still a matter of debate. There are indications that low amounts of isoprene stabilize photosynthetic membranes against high temperature damage. The global isoprene emission

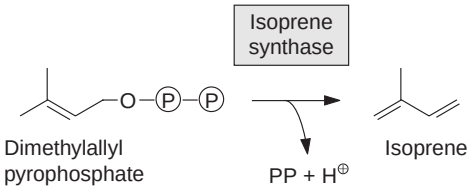

Figure 17.6 Via isoprene synthase some leaves form isoprene, which escapes as a volatile.

by plants is considerable. It is estimated to be about as high as the global methane emission. But, in contrast to methane, isoprene decomposes in the atmosphere rather rapidly.

17.4 Many aromatic compounds derive from geranyl pyrophosphate

The monoterpenes comprise a large number of open chain and cyclic isoprenoids, many of which, due to their high volatility and their lipid character, are classified as essential oils. Many of them have a distinctive, often pleasant odor and are, for example, responsible for the typical scents of pine needles, thyme, lavender, roses, and lily of the valley. Flower scents attract insects for the distribution of pollen, but in addition some volatiles also repel insects and other animals and thus protect the plants from herbivores.

The hydrolysis of geranyl-PP results in the formation of the alcohol geraniol (Fig. 17.7), the main constituent of rose oil. Geraniol has the typical scent of freshly cut geraniums. Geranyl-PP is a precursor for the synthesis of monoterpenes via monoterpene synthases. These enzymes belong to a common enzyme family, which typically possess characteristic sequence motifs and similar active centers, and produce a great variety of products. Figure 17.8 shows the products of two closely related monoterpene synthases. Whereas the linalool synthase from *Nicotiana alata* produces only one product linalool, the cineol synthase from *Nicotiana suaveolens*, as a multiproduct enzyme, yields eight products (60% cineol, 10% each myrcene, limonene and sabinene and 2% each ocimen, terpineol, α-pinene and β-pinene). Thus a variety of compounds can be synthesized by a single enzyme. Monoterpenes occur as scents in flowers to lure insects, but they are also contained in plants as insect repellent. The monoterpenes myrcene, limonene, α-pinene and β-pinene are major constituents of the resin (termed **olioresin**) of conifers. They are toxic for many insects and thus act as a protection against herbivores. Conifers respond to an attack by bark beetles with a strong increase of

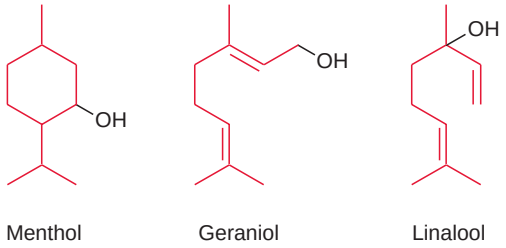

Figure 17.7 Menthol, a constituent of peppermint oil; geraniol, a constituent of rose oil as well as an aromatic compound in geranium scent; and linalool, an aromatic compound of the *Compositae*.

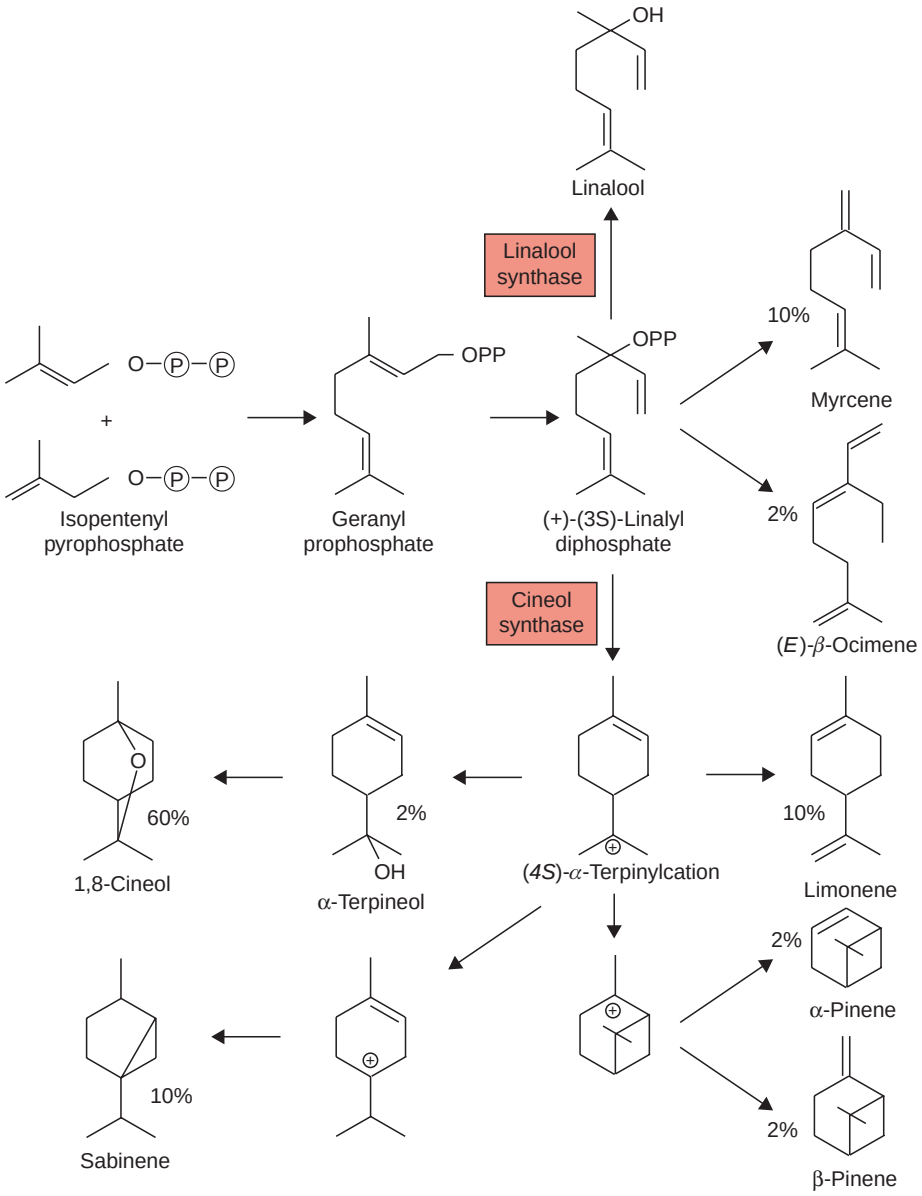

Figure 17.8 Example for the reaction products of two monoterpene synthases. The conversion of linalyl diphosphate, as catalyzed by the linalool synthase from *Nicotiana alata*, yields a single product, whereas the conversion by the cineol synthase of *Nicotiana suaveolens* results in eight products (yields are indicated in %).

cyclase activity, which results in enhanced formation of cyclic monoterpenes, e.g., pinene, limonene. Limonene is also found in the leaves and peel of lemons. Another example of a monoterpene is menthol (Fig. 17.7), the main constituent of peppermint oil. It serves the plant as an insect repellent. Many other monoterpenes containing carbonyl and carboxyl groups can be synthesized by plants, which are not discussed here.

17.5 Farnesyl pyrophosphate is the precursor for the synthesis of sesquiterpenes

The number of possible products is even larger for the cyclization of farnesyl-PP, according to the same mechanism of cyclization of geranyl-PP (Fig. 17.8). This is illustrated in Figure 17.9. The reaction of the intermediary carbonium ion with the two double bonds of the molecule alone can lead

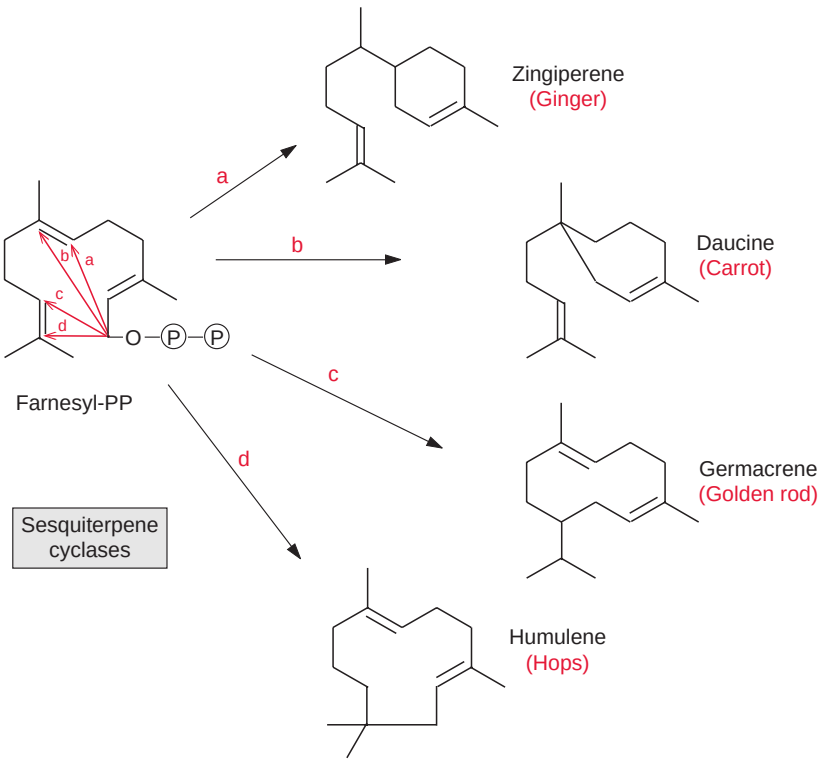

Figure 17.9 Without rearrangement of the double bonds there are four different possibilities for the cyclization of farnesyl pyrophosphate.

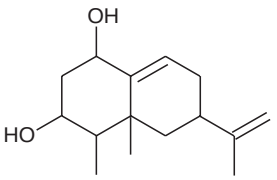

Capsidiol

Figure 17.10 Some sesquiterpenes.

to four different products. The number of possible products is multiplied by simultaneous rearrangements. Sesquiterpenes form the largest group of isoprenoids; they comprise more than 200 different ring structures. The sesquiterpenes include many aromatic compounds such as valencene of oranges, caryophyllene of carnations and several constituents of hops and eucalyptus oil. Capsidiol (Fig. 17.10), a phytoalexin (section 16.1) synthesized in pepper and tobacco, is a sesquiterpene.

Steroids are synthesized from farnesyl pyrophosphate

The triterpene squalene is formed from two molecules of farnesyl-PP by an NADPH-dependent **reductive head-to-head condensation** (Fig. 17.11). Squalene is the precursor for membrane constituents such as cholesterol and sitosterol, the functions of which have been discussed in section 15.1, and also for **brassinosteroids**, which function as phytohormones (section 19.8).

A class of glucosylated steroids, named **saponins** because of their soap-like properties (Fig. 17.12), functions in plants as toxins against herbivores and fungi. The glucosyl moiety of the saponins consists of a branched oligosaccharide built from glucose, galactose, xylose, and other hexoses. The hydrophilic polysaccharide chain and the hydrophobic steroid give the saponins the properties of a **detergent**. Saponins are toxic, as they dissolve the plasma membranes of fungi and cause hemolysis of the red blood cells in animals. Some grasses contain saponins and are therefore a hazard for grazing cattle. **Yamonin**, a saponin from the yam plant (*Dioscorea*), is used in the pharmaceutical industry as a precursor for the synthesis of progesterones, a component of contraceptive pills. A number of very toxic glucosylated steroids called **cardenolides**, which inhibit the **Na^+/K^+ pump** present in animals, also belong to the saponins. A well-known member of this class of compounds is **digitoxigenin** (Fig. 17.12), a poison from foxglove. Larvae of certain butterflies can ingest cardenolides without being harmed. They store these compounds, which then make them poisonous for birds. In low doses, cardenolides are widely used as a medicine against heart disease. Other plant defense substances are the **phytoecdysones**, a

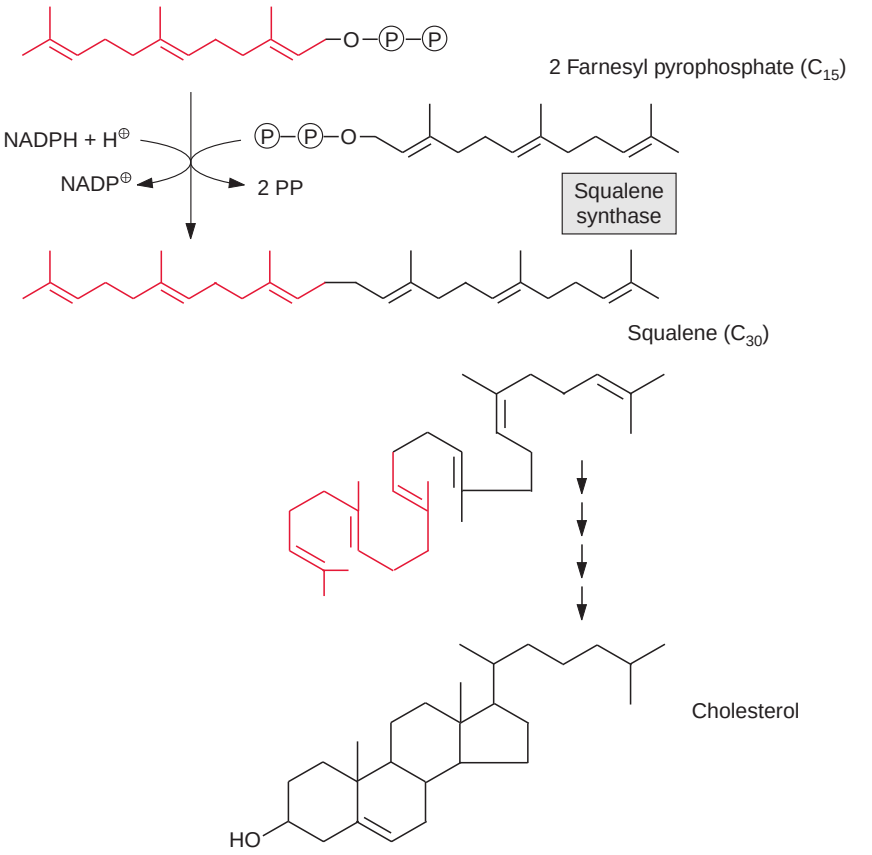

Figure 17.11 Squalene is formed from two farnesyl-PP molecules by head-to-head addition, accompanied by a reduction. After the introduction of an -OH group by a monooxygenase and cyclizations, cholesterol is formed in several reaction steps.

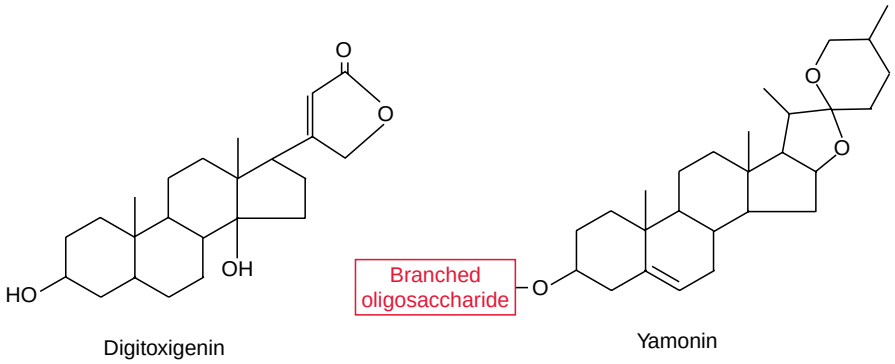

Figure 17.12 Digitoxigenin, a cardenolide, and yamonin, a saponin.

group of steroids with a structure similar to that of the insect hormone ecdysone. Ecdysone controls the pupation of larvae. When insects eat plants which accumulate phytoecdysone, the pupation process is disturbed and the larvae die.

17.6 Geranylgeranyl pyrophosphate is the precursor for defense compounds, phytohormones, and carotenoids

The cyclization of geranylgeranyl-PP leads to the formation of the diterpene casbene (Fig. 17.13). Casbene is a phytoalexin (section 16.1) of castor bean (*Ricinus communis*). The diterpene phorbol is an ester in the latex of plants of the spurge family (*Euphorbiae*). Phorbol acts as a toxin against herbivores; even skin contact causes severe inflammation. Since phorbol esters induce the formation of tumors, they are widely used in medical research. Geranylgeranyl-PP is also the precursor for the synthesis of gibberellins, a group of phytohormones (section 19.4).

Oleoresins protect trees from parasites

In forests of the temperate zone, conifers are widely spread and often reach an old age, some species being far over 1,000 years old. This demonstrates that conifers have been very successful in protecting themselves from browsing enemies. One of the greatest threats is the bark beetle, which not only causes damage itself, but also opens the destroyed bark to fungal infections.

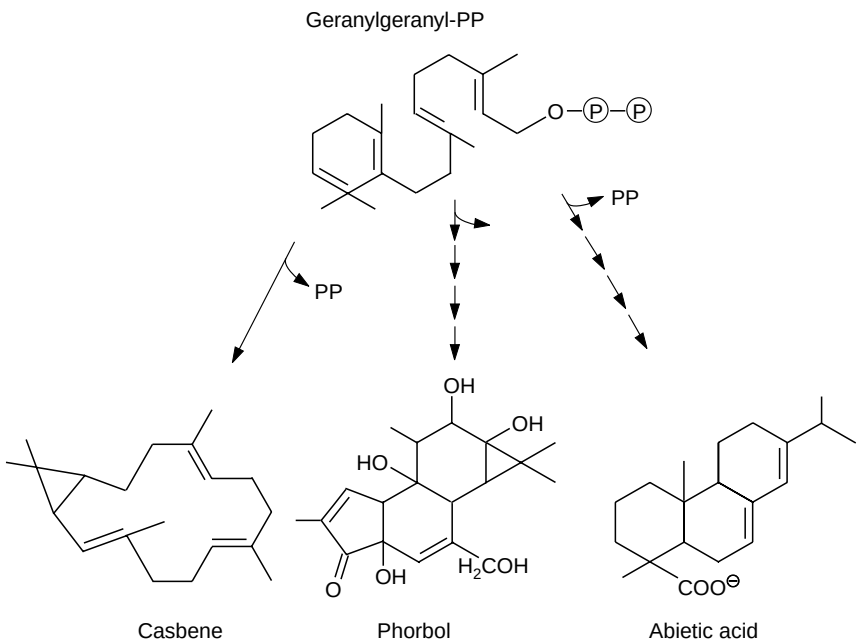

Figure 17.13 The phytoalexin casbene is formed in one step by cyclization from geranylgeranyl pyrophosphate. The synthesis of the defense compound phorbol requires several steps, including hydroxylations, some of which are catalyzed by monooxygenases. Abietic acid, which is also synthesized from geranylgeranyl pyrophosphate, is one of the main components of oleoresins.

To protect themselves, the trees secrete **oleoresins** (tree resins), which seal the wound site and kill insects and fungi. The conifer oleoresins are a complex mixture of terpenoids, about half of which consist of a volatile **turpentine fraction** (many monoterpenes and some sesquiterpenes) and the other half of a non-volatile **rosin fraction** (diterpenes). The turpentine fraction contains a number of compounds that are toxic for insects and fungi (e.g., **limonene** (Fig. 17.5)). The rosin fraction is comprised of resin acids, the main component of which is **abietic acid** (Fig. 17.13). When the tree is wounded, stored oleoresin leaks through channels or is synthesized directly at the infected sites. It is presently being investigated how the toxic properties of the different components of the oleoresins affect different insects and fungi. Scientists are hopeful that such knowledge will make it possible to employ genetic engineering to enhance the parasite resistance of trees growing in large forests.

Carotene synthesis delivers pigments to plants and provides an important vitamin for humans

The function of **carotenoids** in photosynthesis has been discussed in detail in Chapters 2 and 3. Additionally, carotenoids function as pigments, e.g., in flowers and fruits (tomato, bell pepper). The synthesis of carotenoids requires two molecules of geranylgeranyl-PP, which, as in the synthesis of squalene, are linked by head-to-head condensation (Fig. 17.14). Upon release of the first pyrophosphate, the intermediate pre-phytoene pyrophosphate is formed, and the subsequent release of the second pyrophosphate results in the formation of **phytoene**, where the two prenyl residues are linked to each other by a carbon-carbon double bond. Catalyzed by two different desaturases, phytoene is converted to **lycopene**. According to recent results, these desaturations proceed via dehydrogenation reactions, in which hydrogen is transferred via FAD to O_2. Cyclization of lycopene then results in the formation of **β-carotene**. Another cyclase generates α-carotene. The hydroxylation of β-carotene leads to the xanthophyll **zeaxanthin**. The formation of the xanthophyll violaxanthin from zeaxanthin is described in Figure 3.41.

β-Carotene is the precursor for the synthesis of the visual pigment **rhodopsin**. Since β-carotene cannot be synthesized by humans, it is as **provitaminA** an essential part of the human diet. Hundreds of millions of people, especially in Asia, where rice dominates the diet and there is a lack of β-carotene in the food supply, suffer from severe provitaminA deficiency. Because of this, many children become blind. A recent success was the introduction of all the enzymes of the synthesis pathway from geranylgeranyl pyrophosphate to β-carotene into the endosperm of rice grains by genetic engineering. These transgenic rice lines produce β-carotene containing grains, with a yellowish color, and have therefore been called "**golden**

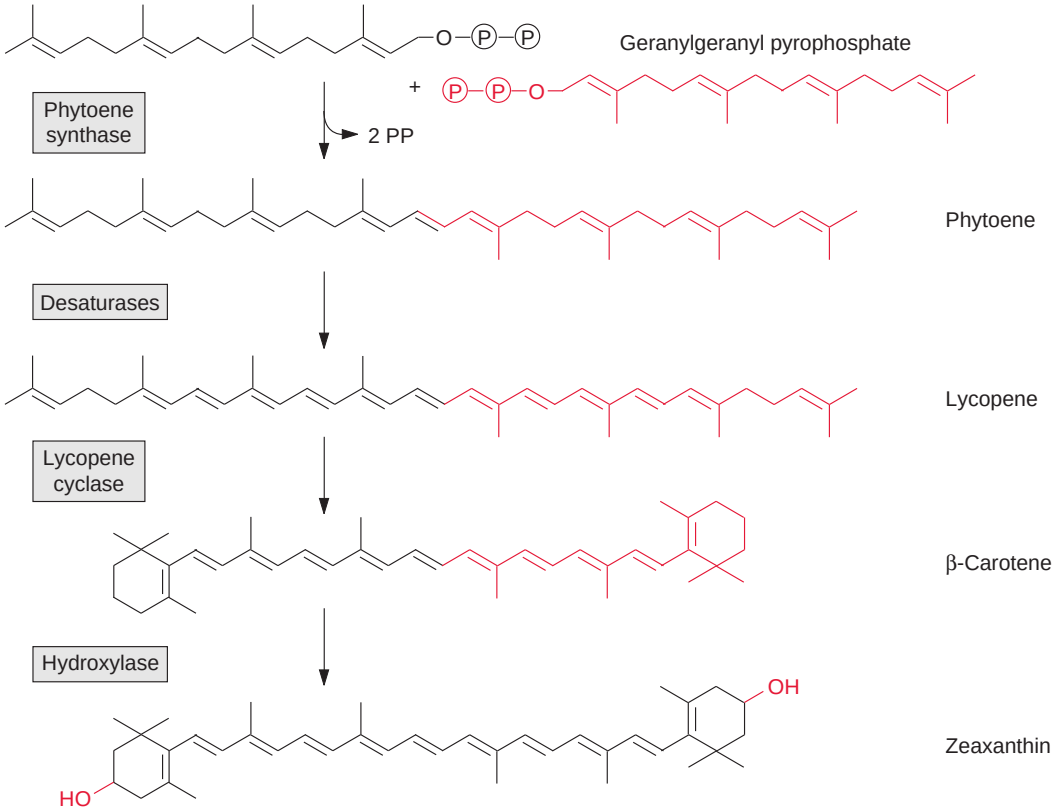

Figure 17.14 Carotenoid biosynthesis. The phytoene synthase catalyzes the head-to-head addition of two molecules of geranylgeranyl-PP to phytoene. The latter is converted by desaturases with neurosporene as the intermediate (not shown) to lycopene. β-Carotene is formed by cyclization and zeaxanthin by additional hydroxylation.

rice." Non-profit organizations have placed these transgenic rice lines at the disposal of many breeding stations in Asian countries, where they are at present crossed with local rice varieties. It is hoped that the serious provitaminA deficiency in wide parts of the world populations can be overcome through the cultivation of "golden rice."

17.7 A Prenyl chain renders compounds lipid-soluble

Ubiquinone (Fig. 3.5), plastoquinone (Fig. 3.19), and cytochrome-*a* (Fig. 3.24) are anchored in membranes by isoprenoid chains of various sizes. At the biosynthesis of these electron carriers, the **prenyl chains** are

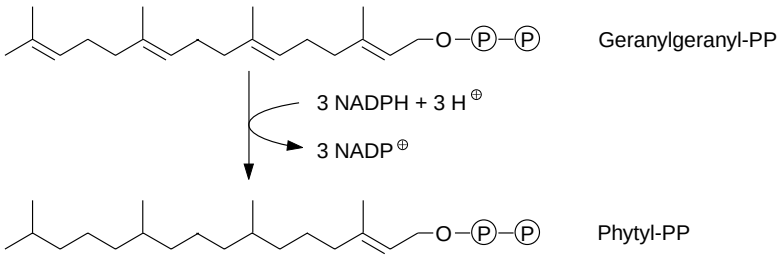

Figure 17.15 Synthesis of phytyl-PP from geranylgeranyl-PP.

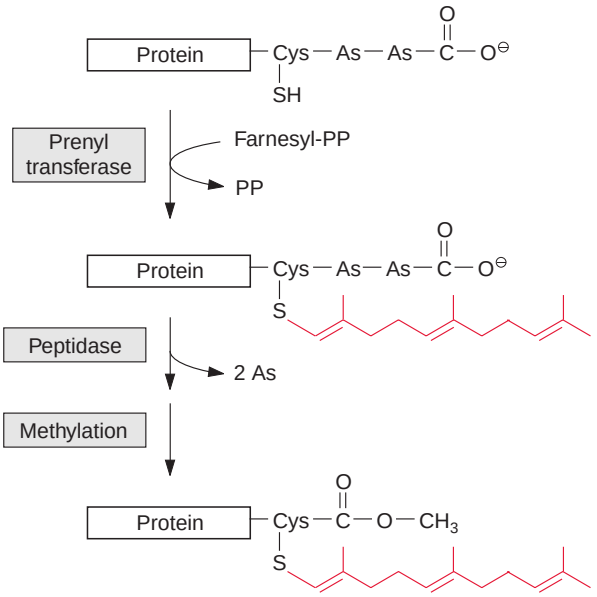

Figure 17.16 Prenylation of a protein. A farnesyl residue is transferred to the -SH group of a cysteine residue at the C terminus of the protein by a prenyl transferase. After hydrolytic release of the terminal amino acids (AS), the carboxyl group of the cysteine is methylated. The prenyl residue provides the protein with a membrane anchor.

introduced from prenyl phosphates by reactions similar to those catalyzed by **prenyl transferases**. Chlorophyll (Fig. 2.4), tocopherols, and phylloquinone (Fig. 3.32), on the other hand, contain phytol side chains. These are synthesized from geranylgeranyl-PP by reduction with NADPH and are incorporated correspondingly (Fig. 17.15).

Proteins can be anchored in a membrane by prenylation

A large number of membrane proteins present in yeast and animals possess a characteristic C terminal sequence with a cysteine, which binds a farnesyl or geranyl residue via a thioether (Fig. 17.16). The connection of these molecules is catalyzed by a specific prenyl transferase. In many cases, the terminal amino acids following the cysteine residue are eliminated after

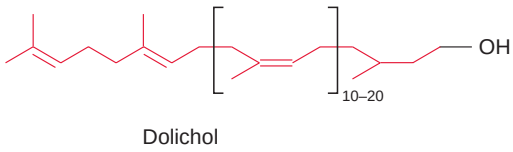

Figure 17.17 Dolichol, a polyprenol.

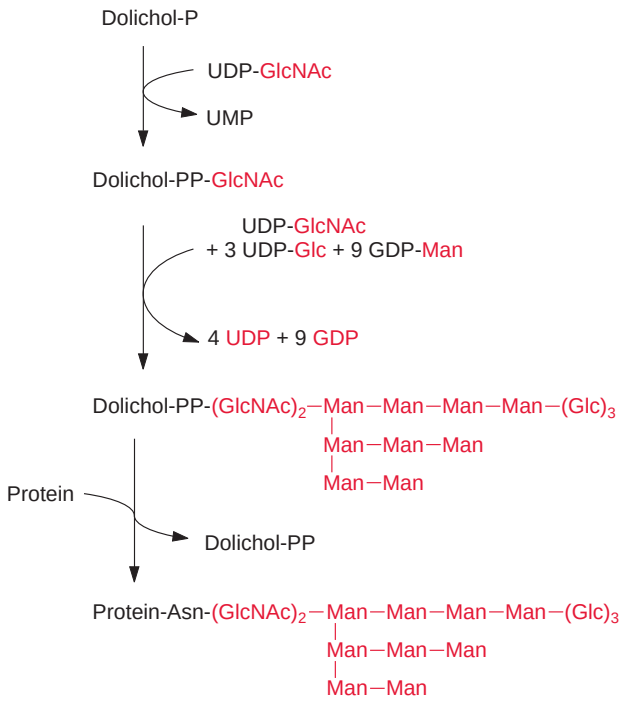

Figure 17.18 Dolichol as glucosyl carrier. For the synthesis of a branched oligosaccharide, successively sugar moieties are added from *N*-acetylglucosamine (GlcNAc), the corresponding UDP- and GDP-hexoses mannose (Man) and glucose (Glc) to dolichol. The first *N*-acetylglucose residue is attached to the -OH group of the dolichol via a pyrophosphate group. The complete oligosaccharide is then transferred to an asparagine residue of a protein. Asn = asparagine.

prenylation by a peptidase, and the carboxylic group of the cysteine is methylated. Prenylation and methylation modify the protein so that it becomes lipid-soluble and can be anchored in a membrane. Recent results indicate that this prenylation of proteins plays important roles in plants.

Dolichols mediate the glucosylation of proteins

Dolichols (Fig. 17.17) are isoprenoids with a very long chain length, occurring in the membranes of the endoplasmatic reticulum and the Golgi network. They have an important function in the **transfer of oligosaccharides**. Many membrane proteins and secretory proteins are *N*-glucosylated by branched oligosaccharide chains. This glucosylation proceeds in the endoplasmatic reticulum utilizing membrane-bound dolichol (Fig. 17.18). The oligosaccharide structure is successively synthesized at the dolichol molecule,

and after completion it is transferred to an asparagine residue of the protein to be glucosylated. By subsequent modification in the Golgi network, in which certain carbohydrate residues are split off and others are added, a large variety of oligosaccharide structures are generated.

17.8 The regulation of isoprenoid synthesis

In plants, isoprenoids are synthesized in different organs and tissues according to the specific demand. Large amounts of hydrophobic isoprenoids are synthesized in specialized tissues such as the glandular and epidermis cells of leaves and the osmophores of flowers. The enzymes for synthesis of isoprenoids are present in the plastids, the cytosol, and the mitochondria. Each of these cellular compartments is essentially self-sufficient with respect to its isoprenoid content. Some isoprenoids, such as the phytohormone gibberellic acid, are synthesized in the plastids and then supplied to the cytosol of the cell. As mentioned in section 17.2, the various prenyl pyrophosphates, from which all the other isoprenoids are derived, are synthesized by different enzymes.

This spatial distribution of the synthetic pathways makes it possible that, despite their very large diversity, the different isoprenoids synthesized by basically similar processes, can be efficiently controlled in their rate of synthesis via regulation of the corresponding enzyme activities (e.g., terpene synthases) in the various compartments. Results so far indicate that the synthesis of the different isoprenoids is regulated primarily at the level of gene expression. This is especially obvious when, after infections or wounding, the isoprenoid metabolism is very rapidly activated by elicitor-controlled gene expression (section 16.1). Competition may occur between isoprenoid synthesis for maintenance and for defense. In tobacco, for instance, the fungal elicitor induced phytoalexin synthesis blocks steroid synthesis. In such a case, the cell focuses its capacity for isoprenoid synthesis on defense.

17.9 Isoprenoids are very stable and persistent substances

Little is known about the catabolism of isoprenoids in plants. Biologically active compounds, such as phytohormones, are converted by the introduction of additional hydroxyl groups and glucosylation into inactive derivatives,

which are often deposited in the vacuole. It is questionable whether, after degradation, isoprenoids can be recycled in a plant. Some isoprenoids are remarkably stable. Large amounts of isoprenoids are found as relics of early life in practically all sedimentary rocks as well as in crude oil. In archaebacteria, the plasma membranes contain glycerol ethers with isoprenoid chains instead of fatty acid glycerol esters. Isoprenoids are probably constituents of very early forms of life.

Further reading

Eisenreich, W., Rohdich, F., Bacher, A. Deoxyxylulose phosphate pathway. Trends in Plant Science 6, 78–84 (2001).

Hirschberg, J. Carotinoid biosynthesis in flowering plants. Current Opinion in Plant Biology 4, 210–218 (2001).

Holopainen, J. K. Multiple functions of inducible plant volatiles. Trends in Plant Science 9, 529–533 (2004).

Hunter, W. N. The non-mevalonate pathway of isoprenoid precursor biosynthesis. Journal Biological Chemistry 282, 21573–21577 (2007).

Knudsen, J. T., Eriksson, R., Gershenzon, J., Stahl, B. Diversity and distribution of floral scent. The Botanical Review 72, 1–120 (2006).

Lichtenthaler, H. K. The 1-deoxy-D-xylulose-5-phosphate pathway of isoprenoid biosynthesis in plants. Annual Review of Plant Physiology and Plant Molecular Biology 50, 47–65 (1999).

Lichtenthaler, H. K. Biosynthesis, accumulation and emission of carotenoids, alpha-tocopherol, plastoquinone, and isoprene in leaves under high photosynthetic irradiance. Photosynthesis Research 92, 163–179 (2007).

McGarvey, D. J., Croteau, R. Terpenoid metabolism. The Plant Cell 7, 1015–1026 (1995).

Osbourn, A. Saponins and plant defence—a soap story. Trends in Plant Science 1, 4–9 (1996).

Peñueales, J., Munné-Bosch, S. Isoprenoids: an evolutionary pool for photoprotection. Trends in Plant Science 10, 166–169 (2005).

Roeder, S., Hartmann, A. M., Effmert, U., Piechulla, B. Regulation of simultaneous synthesis of floral scent terpenoids by the 1.8 cineole synthase of *Nicotiana suaveolens*. Plant Molecular Biology 65, 107–124 (2007).

Römer, S., Fraser, P. D. Recent advances in carotenoid biosynthesis, regulation and manipulation. Planta 221, 305–308 (2005).

Sharkey, T. D., Wiberley, A. E., Donohue, A. R. Isoprene emission from plants: Why and how. Annals Botany (London) 101, 5–18 (2008).

Strack, D., Fester, T. Isoprenoid metabolism and plastid reorganization in arbuscular mycorrhizal roots. New Phytologist 172, 22–34 (2006).

Tholl, D. Terpene synthases and the regulation, diversity and biological roles of terpene metabolism. Current Opinion Plant Biology 9, 297–304 (2006).

Trapp, S., Croteau, R. Defensive resin biosynthesis in conifers. Annual Review of Plant Physiology and Plant Molecular Biology 52, 689–724 (2001).

Ye, X., Al-Babili, S., Kloeti, A., Thang, J., Lucca, P., Beyer, P., Potrykus, I. Engineering the provitamin A (β-carotene) biosynthetic pathway into (carotenoid-free) rice endosperm. Science 287, 303–305 (2000).

18

Phenylpropanoids comprise a multitude of plant secondary metabolites and cell wall components

Plants contain a large variety of phenolic derivatives, which contain a phenyl ring and a C_3 side chain and are collectively termed **phenylpropanoids**. As well as simple phenols, these comprise flavonoids, stilbenes, tannins, lignans and lignin (Fig. 18.1). Together with long chain carboxylic acids, phenylpropanoids are also components of suberin and cutin. These rather structurally divergent compounds have important functions as antibiotics, natural pesticides, signal substances for the establishment of symbiosis with rhizobia, attractants for pollinators, protective agents against ultraviolet (UV) light, insulating materials to make cell walls impermeable to gases and water, and structural material to assist plant stability (Table 18.1). All these substances are derived from phenylalanine, and in some plants also from tyrosine. Phenylalanine and tyrosine are synthesized by the **shikimate pathway**, described in section 10.4. The flavonoids, including flavones,

Table 18.1: Some functions of phenylpropanoids

Coumarins	Antibiotics, toxins against browsing animals
Lignan	Antibiotics, toxins against browsing animals
Lignin	Cell wall constituent
Suberin and cutin	Formation of impermeable layers
Stilbenes	Antibiotics, especially fungicides
Flavonoids	Antibiotics, signal for interaction with symbionts, flower pigments, light protection substances
Tannin	Tannins, fungicides, protection against herbivores

isoflavones, and also anthocyanidins inherit the phenylpropane structure, and additionally a second aromatic ring that is built from three molecules of malonyl CoA (Fig. 18.1). This also applies to the stilbenes, but here, after the introduction of the second aromatic ring, one C atom of the phenylpropane is split off.

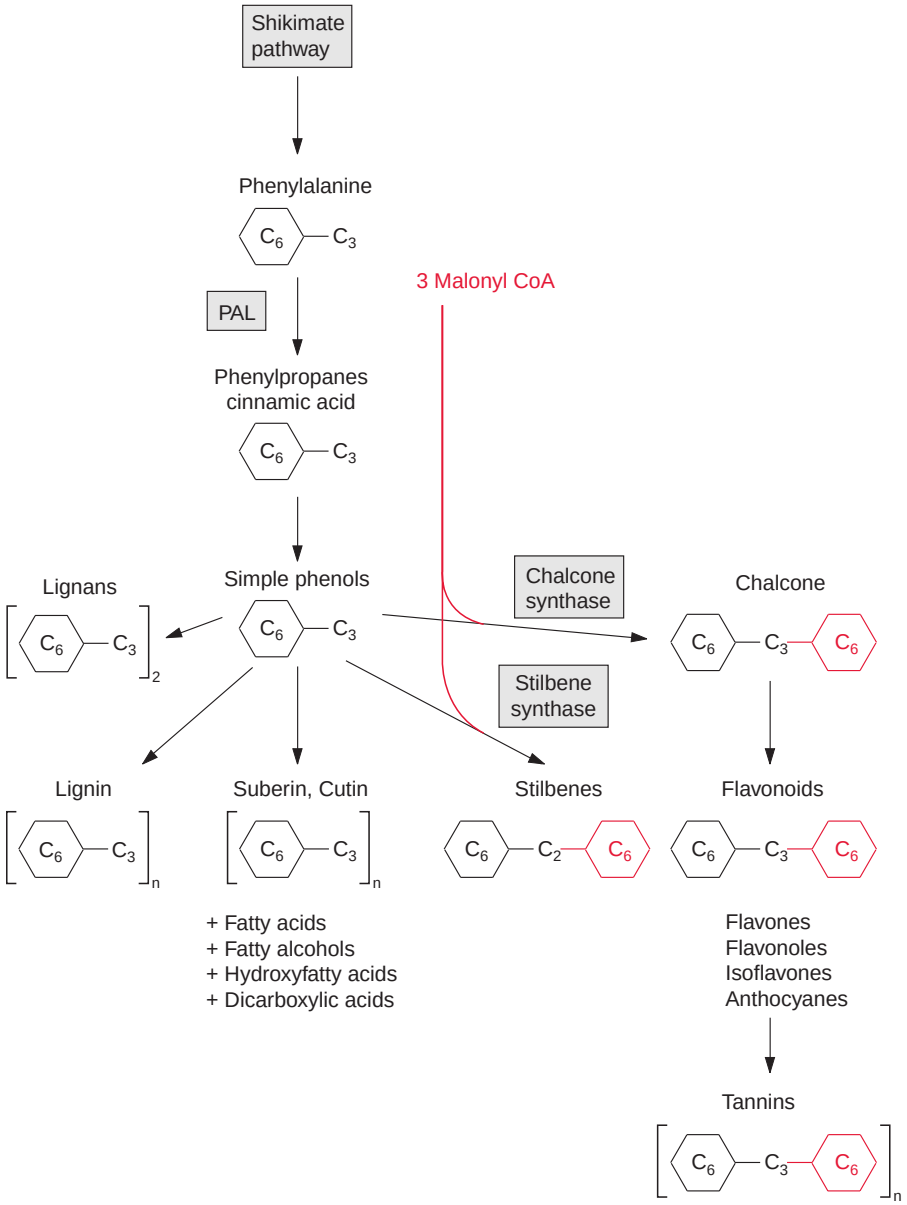

Figure 18.1 Overview of products of the phenylpropanoid metabolism. Cinnamic acid, synthesized from phenylalanine by phenylalanine ammonia lyase (PAL), is the precursor for the various phenylpropanoids. In some plants, 4-hydroxycinnamic acid is synthesized from tyrosine in an analogous way (not shown in the figure). An additional aromatic ring is built either by chalcone or stilbene synthase from three molecules of malonyl CoA.

18.1 Phenylalanine ammonia lyase catalyzes the initial reaction of phenylpropanoid metabolism

Phenylalanine ammonia lyase, abbreviated **PAL**, catalyzes a deamination of phenylalanine (Fig. 18.2): a carbon-carbon double bond is formed during the release of NH_3, yielding *trans*-cinnamic acid. In some grasses, tyrosine is converted to 4-hydroxycinnamic acid in an analogous way by **tyrosine ammonia lyase**. The released NH_3 is probably refixed by the glutamine synthetase reaction (section 10.1).

PAL is one of the most intensively studied enzymes of plant secondary metabolism. The enzyme consists of a tetramer with subunits of 77 to 83 kDa. The formation of phenylpropanoid **phytolalexins** after fungal infection involves a very rapid induction of PAL. PAL is inhibited by its product *trans*-cinnamic acid. The phenylalanine analogue aminoxyphenylpropionic acid (Fig. 18.3) is also a very potent inhibitor of PAL.

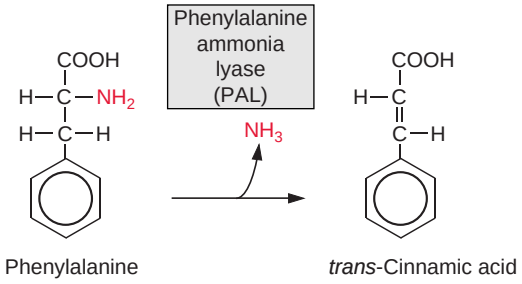

Figure 18.2 Synthesis of *trans*-cinnamic acid.

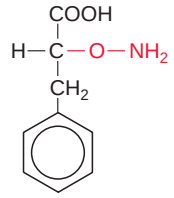

Figure 18.3 Aminooxyphenylpropionic acid, a structural analogue of phenylalanine, inhibits PAL.

18.2 Monooxygenases are involved in the synthesis of phenols

The introduction of the hydroxyl group into the phenyl ring of cinnamic acid (hydroxylation, Fig. 18.4) proceeds via a **monooxygenase catalyzed reaction** utilizing cytochrome P_{450} as the O_2 binding site according to:

$$NADPH + H^+ + R\text{-}CH_3 + \mathbf{O_2} \rightarrow NADP^+ + RCH_2\text{-}\mathbf{OH} + \mathbf{H_2O}$$

In this reaction, electrons are transferred from NADPH via FAD (Fig. 5.16) to cytochrome-P_{450} (pigment with absorption maximum at 450 nm) and subsequently to O_2. From the O_2 molecule, only one O atom is incorporated into the hydroxyl group; the remaining O atom is reduced to yield H_2O. Since both O atoms are incorporated into two different molecules, it is a **monooxygenase reaction**. Like cyt-a_3 (section 5.5), cyt-P_{450} can bind CO instead of O_2. Therefore, P_{450}-monooxygenases are inhibited by CO.

P_{450}-monooxygenases are widely distributed in the animal and plant kingdoms. Genomic analyses of the model plant *Arabidopsis thaliana*

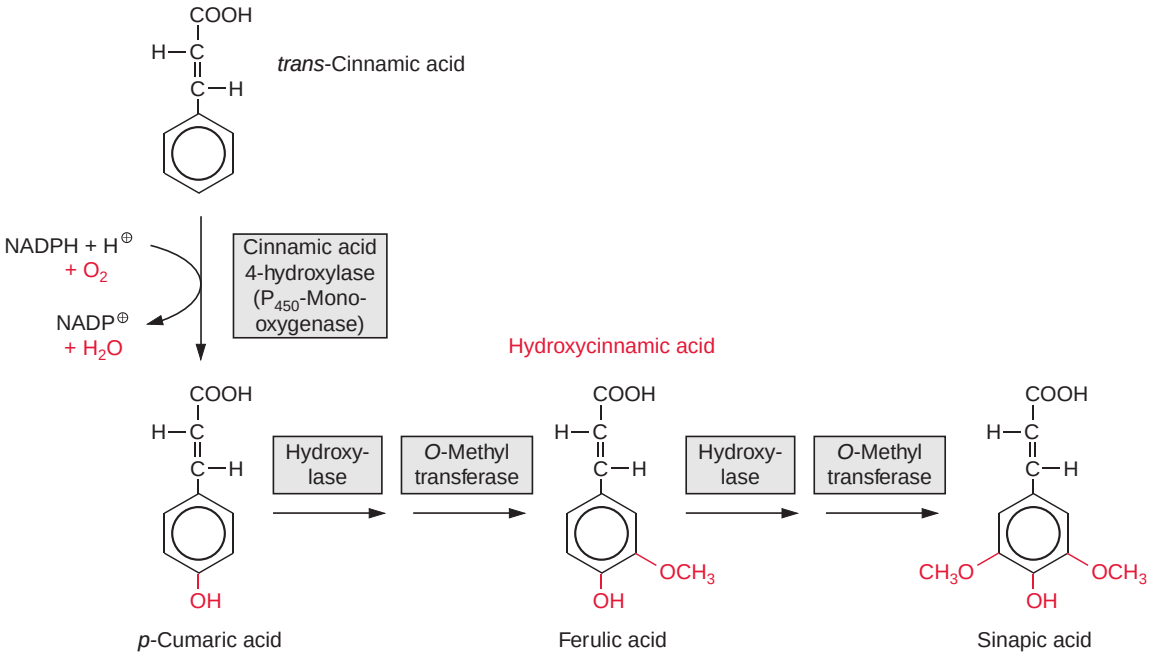

Figure 18.4 Synthesis of various hydroxycinnamic acids from *trans*-cinnamic acid.

revealed about 300 different genes that encode P_{450}-proteins. It seems to be the largest gene family in plants. The majority of these proteins is probably involved in the generation of hydroxyl groups for the synthesis of plant hormones and secondary metabolites, but they also play an important role in detoxification processes (e.g., the detoxification of herbicides) (section 3.6).

Like all P_{450}-monooxygenases, the cinnamic acid hydroxylase is bound at the membranes of the endoplasmatic reticulum. *p*-Coumaric acid can be hydroxylated further at positions 3 and 5 by hydroxylases, again by the P_{450}-monooxygenase reaction type. The -OH groups thus generated are methylated mostly via *O*-methyl transferases with ***S*-adenosylmethionine** as the methyl donor (Fig. 12.10). In this way ferulic acid and sinapic acid are synthesized, which, together with *p*-coumaric acid, are the precursors for the synthesis of lignin (section 18.3).

Benzoic acid derivatives, including **salicylic acid** as well as a derivative of benzaldehyde, **vanillin** (the aroma substance of vanilla), are formed by cleavage of a C_2 fragment from the phenylpropanes (Fig. 18.5). Under the trade name aspirin, the acetyl ester of salicylic acid is widely used as a remedy against pain, fever, and other illnesses and is probably the most frequently used pharmaceutical worldwide. The name salicylic acid is derived from *Salix*, the Latin name for willow, since it was first isolated from the bark of the willow tree, where it accumulates in high amounts. Since ancient times, the salicylic acid content of willow bark was used as medicine in the Old and New Worlds. In the fourth century BC Hippocrates gave women willow bark to chew to relieve pain during childbirth. Native Americans also used extracts from willow bark as pain killers.

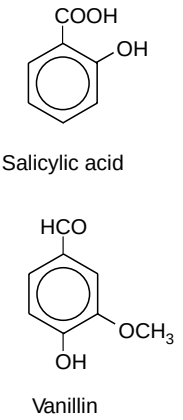

Figure 18.5 Salicylic acid and vanillin are phenylpropanoids.

Salicylic acid also affects plants. It has been observed that tobacco plants treated with aspirin or salicylic acid have enhanced resistance to pathogens, such as the *Tobacco mosaic* virus. Many plants show an increase in their salicylic acid content after being infected by viruses or fungi, but also after being exposed to UV radiation or ozone stress. Salicylic acid is an important signal component of signal transduction chains that lead to the expression of enzymes involved in **defense reactions** against viruses, bacteria, and fungi (sections 16.1 and 19.9). *Arabidopsis* mutants, which have lost the ability to produce salicylic acid, are more prone to infection, while a dose of salicylic acid can give better protection against pathogens. This principle is now used commercially. A salicylic acid analogue with the trade name **Bion** (Syngenta) is being sprayed on wheat to prevent mildew infection.

However, salicylic acid not only triggers defense reactions, but can also induce blooming in some plants. By stimulating the mitochondrial alternative oxidase (section 5.7), it activates the production of heat in the spadix of the voodoo lily, emitting a carrion-like stench.

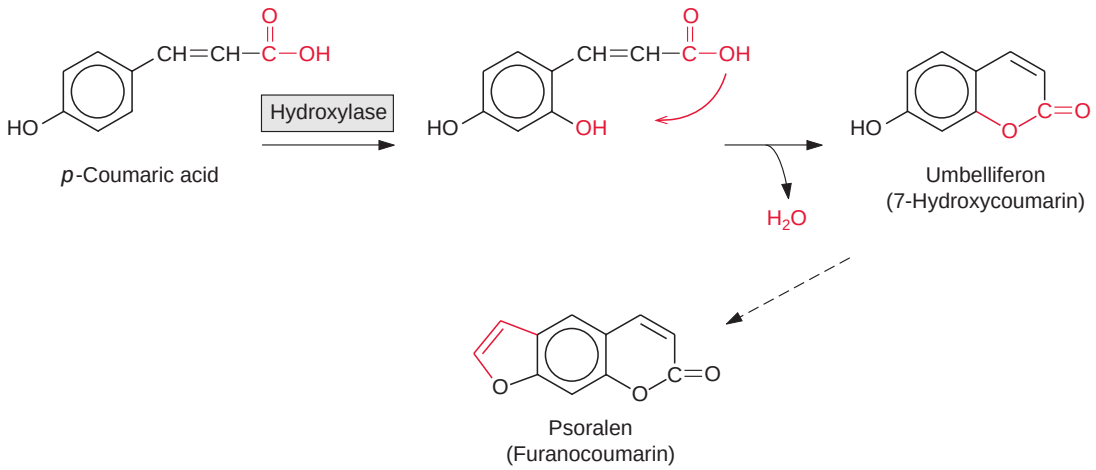

Figure 18.6
Umbelliferone, which is the precursor for the synthesis of the defense compound psoralen, is formed by hydroxylation of *p*-coumaric acid and the formation of a ring.

7-Hydroxycoumarin, also called **umbelliferone**, is synthesized from *p*-coumaric acid by hydroxylation and the formation of an intermolecular ester, a lactone (Fig. 18.6). The introduction of a C_2 group into umbelliferone yields psoralen, a **furanocoumarin**. Illumination with UV light turns psoralen into a toxic compound. The illuminated psoralen reacts with the pyrimidin bases of the DNA, causing blockage of transcription and DNA repair mechanisms, which finally results in the death of the cell. As mentioned in section 16.1, some celery varieties contain very high concentrations of psoralen and caused severe skin inflammation of workers involved in the harvest. Many furanocoumarins have antibiotic properties. In some cases, they are constitutive components of the plants, whereas in other cases, they are formed only after infection or wounding as phytoalexins.

18.3 Phenylpropanoid compounds polymerize to macromolecules

As mentioned in section 1.1, after cellulose, **lignin** is the second most abundant natural substance on earth. The basic components for lignin synthesis are ***p*-coumaryl**, **sinapyl**, and **coniferyl alcohols**, which are collectively termed **monolignols** (Fig. 18.7). Synthesis of the monolignols requires reduction of the carboxylic group of the corresponding acids to an alcohol. In the discussion on the glyceraldehyde phosphate dehydrogenase reaction in section 6.3, it was shown that a carboxyl group can be reduced by NADPH

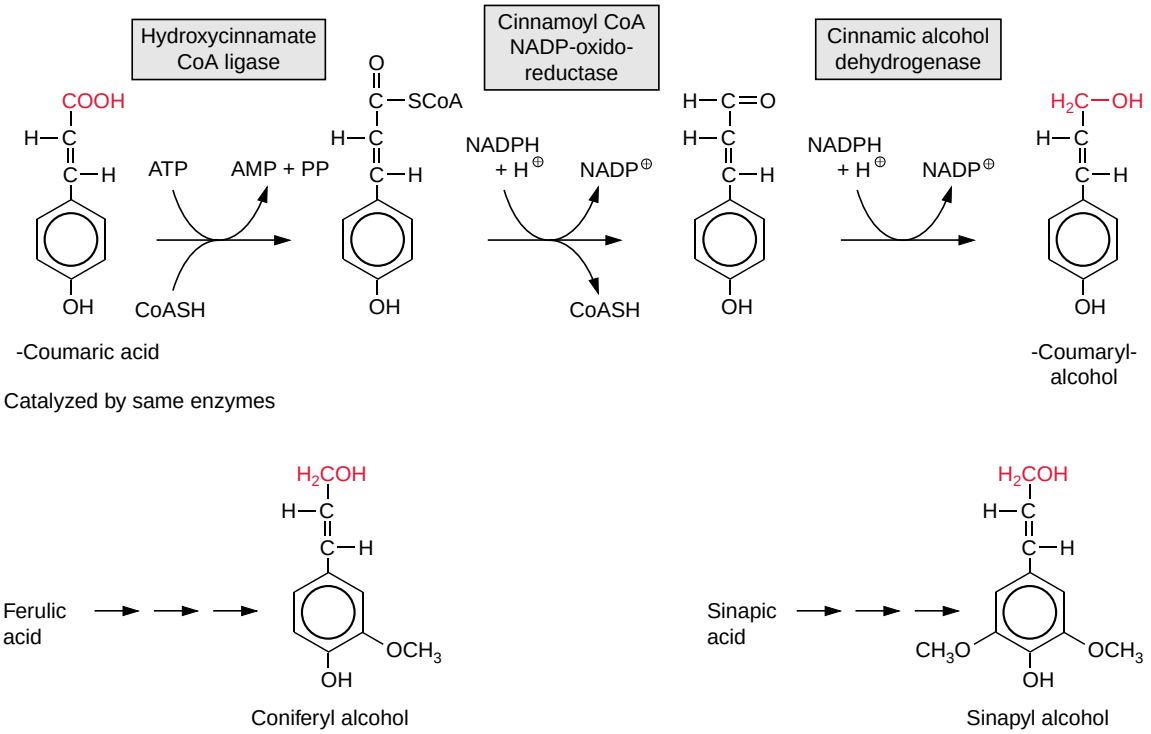

Figure 18.7 Reduction of the hydroxycinammic acids to the corresponding alcohols (monolignols).

to an aldehyde only if it is activated via the formation of a thioester. For the reduction of *p*-coumaric acid by NADPH (Fig. 18.7) a similar activation occurs. The required thioester is formed with CoA at the expense of ATP in a reaction analogous to fatty acid activation described in section 15.6. The cleavage of the energy-rich thioester bond drives the reduction of the carboxylate to the aldehyde. In the subsequent reduction to an alcohol, NADPH is again the reductant. The synthesis of sinapyl- and coniferyl alcohols from sinapic and ferulic acids follows the same principle, but there are specific enzymes involved. Alternatively, coniferyl and sinapyl alcohols can also be formed from *p*-coumaryl alcohol by hydroxylation followed by methylation (Fig. 18.4).

Lignans act as defense substances

The dimerization of monolignols leads to the formation of **lignans** (Fig. 18.8). This takes place mostly by a reductive 8,8-linkage of the side chains, but

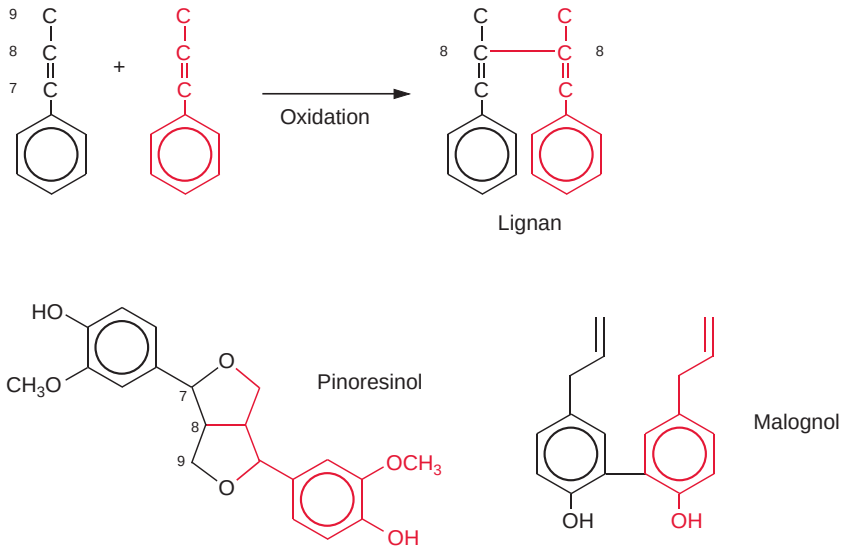

Figure 18.8 Lignans are formed by dimerization of monolignols. Pinoresinol and malognol are examples of two lignans.

sometimes also by a condensation of the two phenol rings. The mechanism of lignan synthesis is still not clear. Probably free radicals are involved (see next section). Plant lignans also occur as higher oligomers. In the plant world, lignans are widely distributed as defense substances. The lignan **pinoresinol** is a constituent of the resin of forsythia and is formed when the plant is wounded. Its toxicity to microorganisms is caused by an inhibition of cAMP phosphodiesterase. Pinoresinol thus averts the regulatory action of cAMP, which acts as a messenger component in many organisms (whether also in plants is still undecided (section 19.1)). Malognol inhibits the growth of bacteria and fungi.

Some lignans have interesting pharmacological effects. Two examples may be used to illustrate this: podophyllotoxin, from *Podophyllum*, a member of the Berberidaceae family growing in America, is a mitosis toxin. Derivatives of podophyllotoxin are used to combat cancer. Arctigenin and tracheologin (from tropical climbing plants) have antiviral properties. Investigations are under way to try to utilize this property to cure AIDS.

Lignin is formed by radical polymerization of phenylpropanoid derivatives

Lignin is formed by polymerization of monolignols, in angiosperms primarily of sinapyl and coniferyl alcohol, and in gymnospermes mainly of coniferyl alcohol. The synthesis of lignin takes place outside the cell, but the mechanism by which the monolignols are exported from the cell for lignin synthesis is still not known. There are indications that the monolignols are

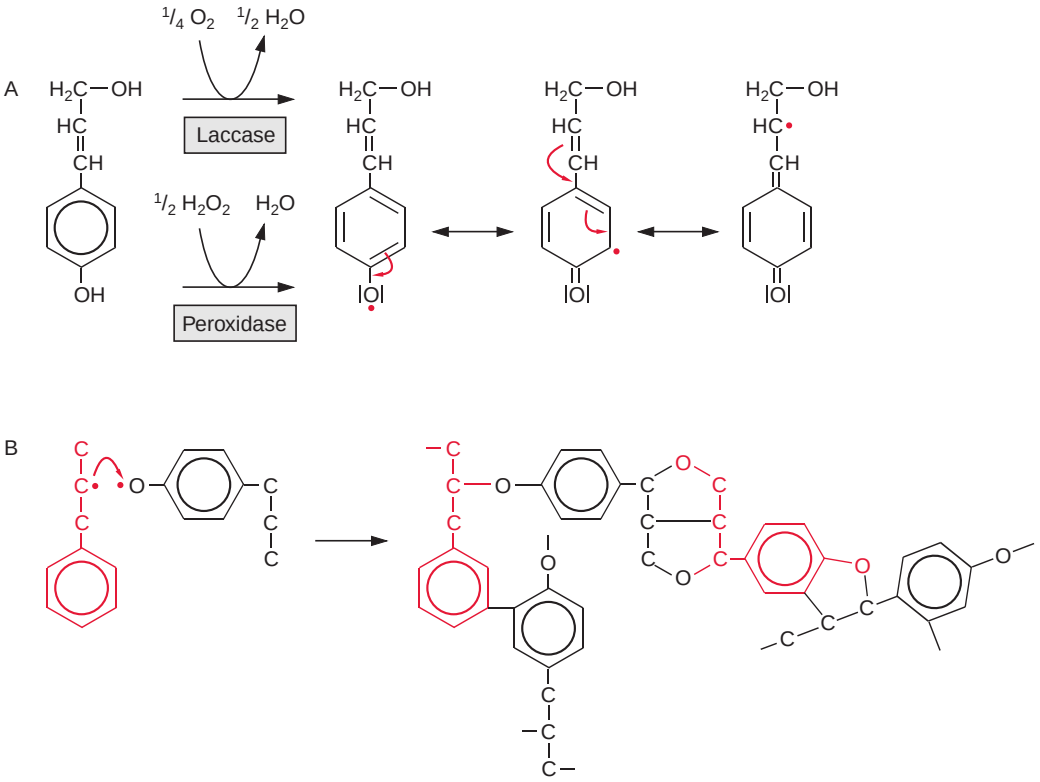

Figure 18.9 A. Oxidation of a monolignol by laccase or a peroxidase results in the formation of a phenol radical. The unpaired electron is delocalized and can react with various resonance structures of the monolignol. B. Two monolignols can form a dimer and polymerize further. Finally, highly branched lignin is formed.

exported as glucosides that are hydrolyzed outside the cell by glucosidases, but this is still a matter of controversy. The mechanism of lignin formation also remains unclear. Both **laccase** and **peroxidases** probably play a role in the linkage of the monolignols. Laccase is a **monophenol oxidase** that oxidizes a phenol group to a radical and transfers hydrogen via an enzyme-bound Cu^{++} ion to molecular oxygen. The enzyme was given this name as it was first isolated from the lac tree (*Rhus vermicifera*), which grows in Japan. In the case of peroxidases, H_2O_2 functions as an oxidant, but the origin of the required H_2O_2 is not certain. As shown in Figure 18.9A, the oxidation of a phenol by H_2O_2 presumably results in the formation of a resonance-stabilized phenol radical. These phenol radicals can dimerize nonenzymatically and finally polymerize nonenzymatically (Fig. 18.9B). Due to the various resonance structures, many combinations are possible in the polymer. Monolignols react to form several C-C or C-O-C linkages,

building a highly branched phenylpropanoid polymer. Free hydroxyl groups are present in only a few side chains of lignin and sometimes are oxidized to aldehyde and carboxyl groups.

Although until now the primary structure of lignins has not been fully established in all its details, it is recognized that even in a single cell lignins of **different structure** are deposited in **discrete sections of the cell wall**. It has been postulated that certain extracellular glycoproteins, termed **dirigent proteins**, control the polymerization of monolignol radicals in such a way that defined lignin structures are formed. It is still a matter of debate to what extent lignin is formed by chance and formed specifically through the action of dirigent proteins.

The composition of lignin varies greatly in different plants. Lignin of conifers, for instance, has a high coniferyl content, whereas the coumaryl moiety prevails in the straw of cereals. Lignin is covalently bound to cellulose in the cell walls. **Lignified cell walls** have been compared with **reinforced concrete**, in which the cellulose fibers are the steel and lignin is the concrete. In addition to giving mechanical strength to plant parts such as stems or twigs, or providing stability for the vascular tissues of the xylem, lignin has a function in defense. Its mechanical strength and chemical composition make plant tissues difficult for herbivores to digest. In addition, lignin inhibits the growth of pathogenic microorganisms. Lignin is synthesized in many plants in response to wounding. Only a few bacteria and fungi are able to cleave lignin. A special role in the **degradation of lignin** is played by **woodrot fungi**, which are involved in the rotting of tree trunks.

Often one-third of dry wood consists of lignin. For the production of cellulose and paper, this lignin has to be removed, which is very costly and the methods used ultimately contribute significantly to the pollution of rivers. Attempts are being made to reduce the content of lignin in wood by means of genetic engineering. Experiments have shown that it is possible to lower the lignin content of wood by antisense constructs (section 22.5) that inhibit the expression of genes encoding lignin biosynthesis enzymes.

Suberins form gas- and water-impermeable layers between cells

Suberin is a polymeric compound formed from phenylpropanoids, long chain fatty acids and fatty alcohols (C_{18}–C_{30}), as well as hydroxyfatty acids and dicarboxylic acids (C_{14}–C_{20}) (Fig. 18.10). In suberin, the phenylpropanoids are to some extent linked with each other as in lignin. However, most of the 9′-OH groups are not involved in these linkages and instead form esters with fatty acids. Often two phenylpropanoids are connected by

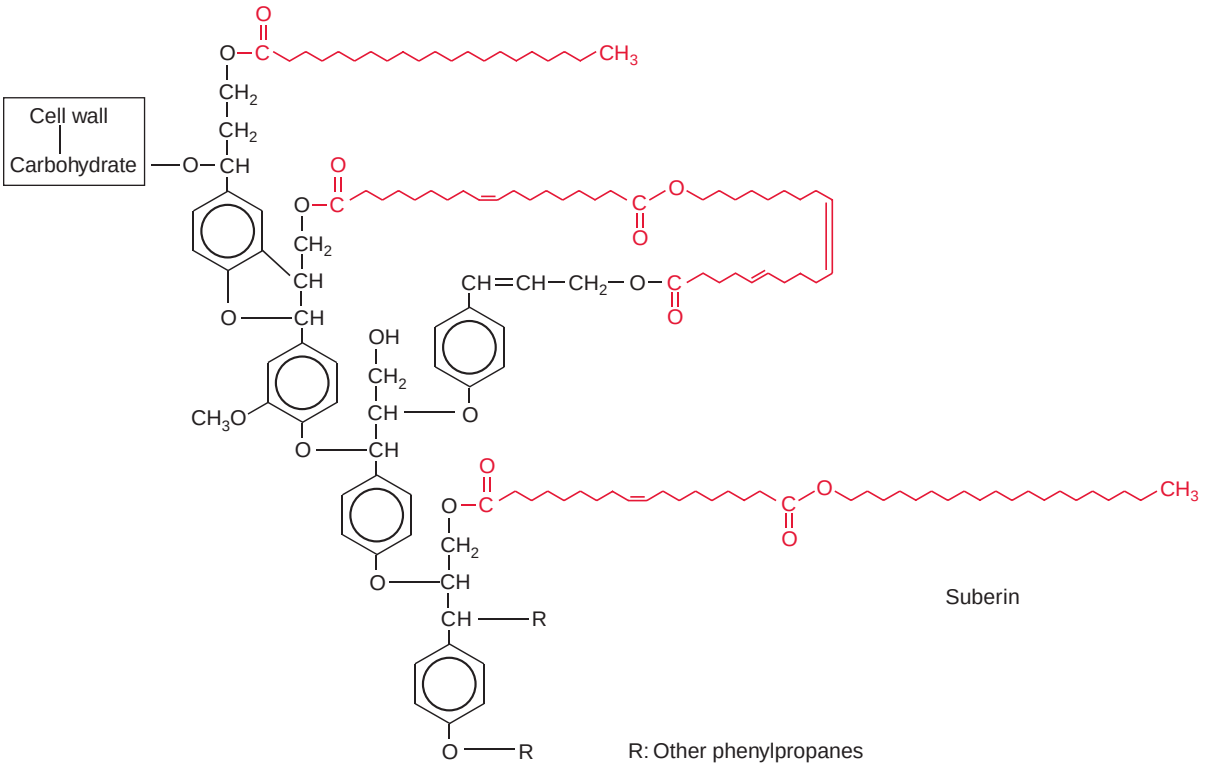

Figure 18.10 In suberin, the monolignols are connected similarly as in lignin, but the 9′-OH groups usually remain free. Instead they form esters with long-chain fatty acids and hydroxyfatty acids. Carboxylic acid esters provide a link between two monolignols.

dicarboxylic acids via ester linkages, and fatty acids and hydroxyfatty acids also can form esters with each other. Although the mechanism of suberin synthesis is to a large extent still not known, it appears that peroxidases are also involved in this process.

Suberin is a cell wall constituent that forms gas- and watertight layers. It is part of the **Casparian strip** of the root endodermis, where it acts as a diffusion barrier between the apoplast of the root cortex and the central cylinder. Suberin is present in many C_4 plants as an impermeable layer between the bundle sheath and mesophyll cells. Cork tissue, consisting of dead cells surrounded by alternating layers of suberin and wax, has a particularly high suberin content. **Cork cells** are found in a secondary protective layer called the periderm and in the bark of trees. Cork layers containing suberin protect plants against loss of water, infection by

microorganisms, and heat exposure. Due to this, some plants even survive short fires and are able to continue growing afterwards.

Cutin is a gas- and water-impermeable constituent of the cuticle

The epidermis of leaves and shoots is surrounded by a gas- and water-impermeable cuticle (Chapter 8). It consists of a cell wall that is impregnated with cutin and in addition is covered by a wax layer. **Cutin** is a polymer similar to suberin, but with a relatively small proportion of phenylpropanoids and dicarboxylic acids, mainly composed of esterified hydroxyfatty acids (C_{16}–C_{18}).

18.4 The synthesis of flavonoids and stilbenes requires a second aromatic ring derived from acetate residues

Probably the largest group of phenylpropanoids is that of the flavonoids, in which a second aromatic ring is linked to the 9′-C atom of the phenylpropanoid moiety. A precursor for the synthesis of flavonoids is chalcone (Fig. 18.11), synthesized by **chalcone synthase** (**CHS**) from *p*-coumaryl-CoA and three molecules of malonyl-CoA**.** This reaction is also called the **malonate pathway**. The release of three CO_2 molecules and four CoA molecules makes chalcone synthesis an irreversible process. In the overall reaction, the new aromatic ring is formed from three acetate residues. Since CHS represents the first step of flavonoid biosynthesis, this enzyme has been thoroughly investigated. In some plants, one or two different isoforms of the enzyme have been found, while in others there are up to nine. CHS is the most abundant enzyme protein of phenylpropanoid metabolism in plant cells, probably because this enzyme has only a low catalytic activity. As in the case of phenylalanine ammonia lyase (section 18.1), the *de novo* synthesis of CHS is subject to multiple controls of gene expression by internal and external factors, including elicitors.

Some stilbenes are very potent natural fungicides

Some plants, including pine, grapevine and peanuts, possess a **stilbene synthase** activity, by which *p*-coumaroyl-CoA reacts with three molecules of

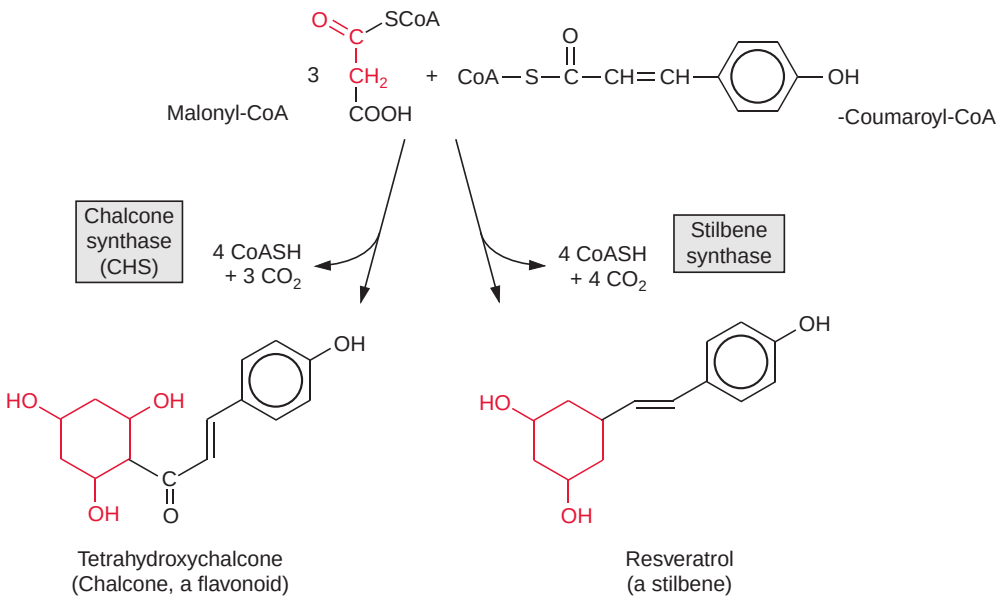

Figure 18.11 An additional aromatic ring is formed by chalcone synthase and stilbene synthase.

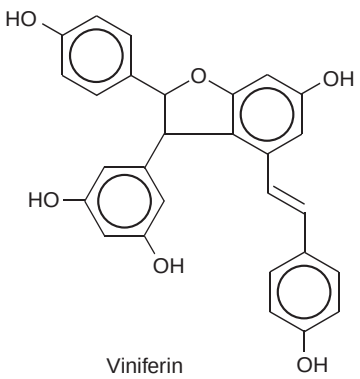

Figure 18.12 A natural fungicide from grapevine.

malonyl CoA. In contrast to CHS, the 9′-C atom of the phenylpropane is released as CO_2 (Fig. 18.11). **Resveratrol**, synthesized by this process, is a phytoalexin belonging to the stilbene group. A number of very potent plant fungicides are stilbenes, including **viniferin** (Fig. 18.12), which is contained in grapevine. The elucidation of stilbene synthesis has opened new possibilities to combat fungal infections. A gene from grapevine for the formation of resveratrol has been expressed by genetic engineering in tobacco, and the

resultant transgenic tobacco plants were resistant to the pathogenic fungus *Botrytis cinerea*.

18.5 Flavonoids have multiple functions in plants

Chalcone is converted to flavanone by **chalcone isomerase** (Fig. 18.13). As a key enzyme of flavonoid synthesis, the synthesis of the enzyme protein of chalcone isomerase is subject to strict control. It is induced like PAL and

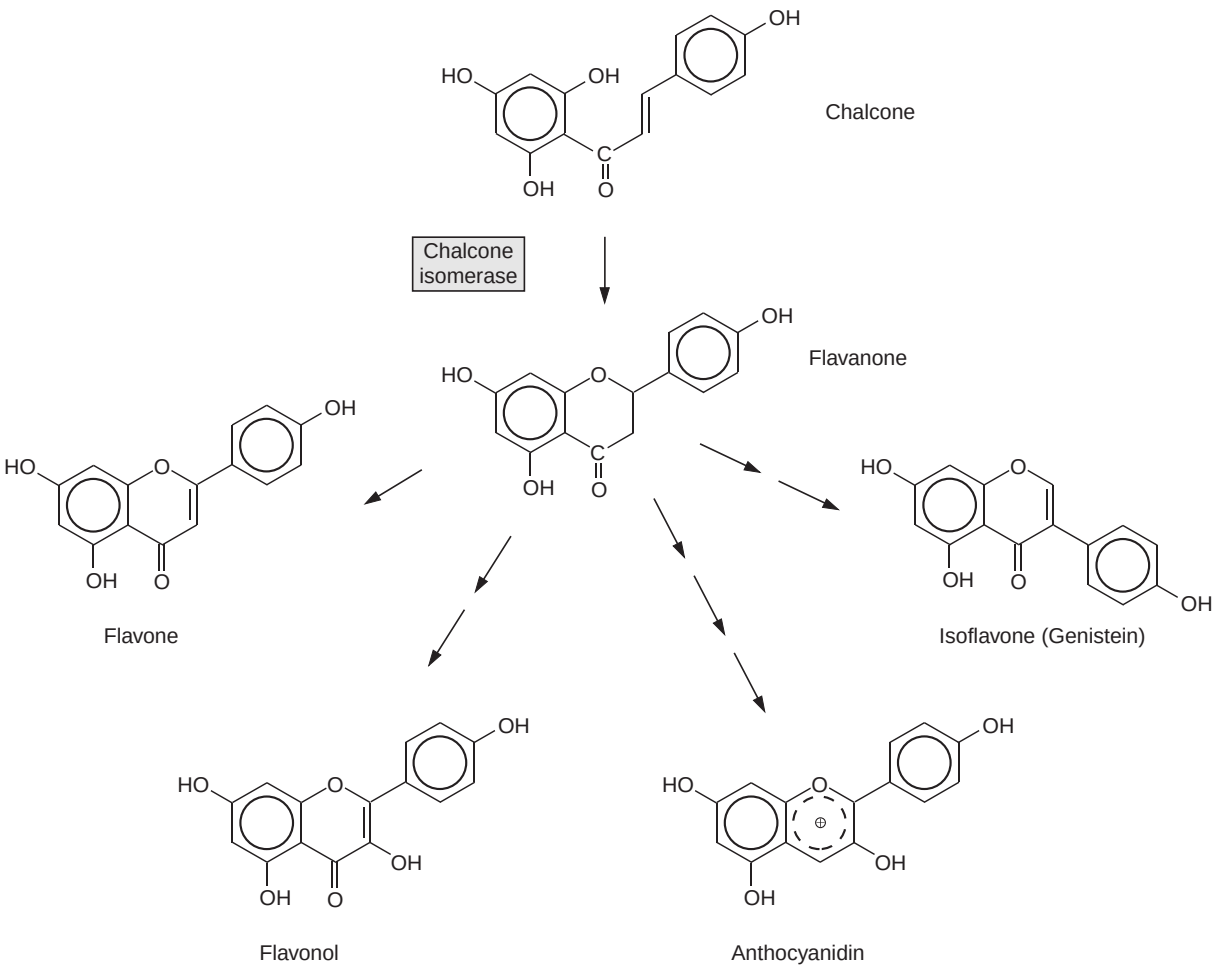

Figure 18.13 Chalcone is the precursor for the synthesis of various flavonoids.

CHS by elicitors. The middle ring is formed by the addition of a phenolic hydroxyl group to the double bond of the carbon chain connecting the two phenolic rings. Flavanone is the precursor for a variety of flavonoids; the details of the synthesis pathways of flavonoids will not be described here.

The flavonoids include protectants against herbivores and many are phytoalexins. An example of this is the poisonous isoflavone dimer **rotenone**, an inhibitor of the respiratory chain (section 5.5), which accumulates in the leaves of a tropical legume. Aboriginals in South America used to kill fish by flinging the leaves of these plants into the water. The isoflavone **medicarpin** from alfalfa (*Medicago sativa*) is a phytoalexin (Fig. 18.14). Flavonoids also serve as signals for interactions of the plant with symbionts. Flavones and flavonols are emitted from leguminous roots in order to attract rhizobia by chemotaxis and to induce in these the genes required for the nodulation (section 11.1).

Flavones and flavonols have an absorption maximum in the UV region. As **protective pigments**, they shield plants from the damaging effect of UV light. The irradiation of leaves with UV light induces a strong increase in flavonoid biosynthesis. Mutants of *Arabidopsis thaliana*, which, because of a defect in either chalcone synthase or chalcone isomerase, are not able to synthesize flavones, are extremely sensitive to the damaging effects of UV light. In some plants, fatty acid esters of sinapic acid (section 18.2) can also act as protective pigments against UV light.

Many flavonoids are **antioxidants** in acting as radical scavengers for reactive oxygen species (ROS), thus preventing the peroxidation of lipids. As constituents of nutrients, they are assumed to be protectants against cardiovascular diseases and cancer. For this reason, nutrients containing flavonoids (e.g., green tea, soy sauce, and red wine) have been regarded as beneficial for health.

Recently, particular attention has been focused on certain isoflavones that are found primarily in legumes. It had been observed earlier that sheep became infertile after grazing on certain legumes. It turned out that these forage plants contained isoflavones, which in animals (and in humans) have an effect similar to that of estrogens. For this reason, they have been named **phytoestrogens**. **Genistein,** shown in Figure 18.13, has a strong estrogen effect. Some of these phytoestrogens are used for medical purposes.

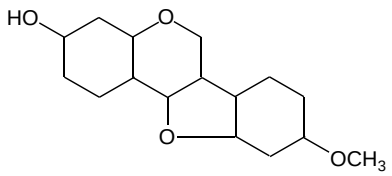

Medicarpin

Figure 18.14 A phytoalexin from *Medicago sativa*.

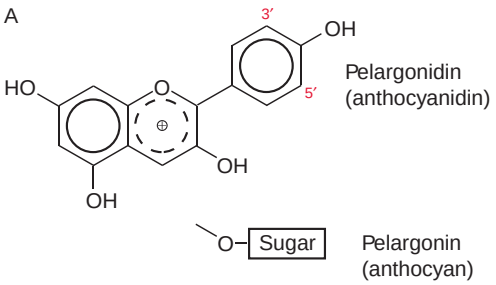

Figure 18.15
A. Pelargonidin, an anthocyanidin, is a flower pigment. It is present in the petals as a glucoside, named pelargonin. B. More plant pigments are synthesized by additional -OH groups at 3′ and 5′ positions and subsequent methylation.

B

Anthocyanidin	Substituent	Color
Pelargonidin	—	Orange-red
Cyanidin	3′-OH	Red
Peonidin	3′-OCH_3	Pink
Delphinidin	3′-OH, 5′-OH	Bluish-purple
Petunidin	3′-OCH_3, 5′-OH	Purple
Malvidin	3′-OCH_3, 5′-OCH_3	Reddish-purple

18.6 Anthocyanins are flower pigments and protect plants against excessive light

As discussed earlier, carotenoids provide yellow and orange flower pigments (section 17.6). Other widely distributed flower pigments are the yellow **chalcones**, light yellow **flavones**, and red and blue **anthocyanins**. Anthocyanins are glucosides of anthocyanidins (Fig. 18.15) in which the sugar component, consisting of one or more hexoses, is usually linked to the -OH group of the pyrylium ring. Anthocyanins are contained in the vacuole. They are transported as glutathione conjugates via the glutathione translocator to the vacuole (section 12.2) and are deposited there. The anthocyanin pelargonin, shown in Figure 18.15, contains **pelargonidin** as chromophore. The introduction of two -OH groups at 3′ and 5′ positions of the phenyl residue by P_{450} dependent monooxygenases (section 18.2) and their successive methylation yields five additional flower pigments, each with a different color. Hydroxylations at other positions result in even more pigments. A change in the pH in the vacuole leads additionally to alterations of the color. This in part explains the change of color when plants fade. Moreover, the color of the pigment is altered by the formation of complexes with metal ions. Thus, upon complexation with Al^{+++} or Fe^{+++}, the color of pelargonin changes from orange red to blue. These

various pigments and their mixtures lead to the multitude of color nuances of flowers. With the exception of pelargonidin, all the pigments listed in Figure 18.15 are found in the flowers of petunia. To date, 35 genes that are involved in the coloring of flowers have been isolated from petunia.

Anthocyanins not only contain flower pigments to attract pollen-transferring insects, but also function as protective pigments for shading leaf mesophyll cells. Plants in which growth is limited by environmental stress factors, for instance phosphate deficiency, chilling, or high salt content of the soil, often have red leaves, due mainly to the accumulation of anthocyanins. Stress conditions, in general, reduce the utilization of NADPH and ATP, which are provided by the light reactions of photosynthesis. Shading the mesophyll cells by anthocyanins decreases the light reactions and thus prevents overenergization and overreduction of the photosynthetic electron transport chain (see section 3.10).

18.7 Tannins bind tightly to proteins and therefore have defense functions

Tannins are a collective term for a variety of plant polyphenols used in the tanning of rawhides to produce leather. Tannins are widely distributed in plants and occur in especially high amounts in the bark of certain trees (e.g., oak) and in galls. Tannins are classified as condensed and hydrolyzable tannins (Fig. 18.16A). The **condensed tannins** are flavonoid polymers and thus are products of phenylpropanoid metabolism. Radical reactions are probably involved in their synthesis, but few details of the biosynthesis pathways are known. The **hydrolyzable tannins** consist of **gallic acids** (Fig. 18.16B). Many of these gallic acids are linked to hexose molecules. Gallic acid in plants is synthesized from shikimate (Fig. 10.19).

The phenolic groups of the tannins bind very tightly to proteins by forming hydrogen bonds with the -NH groups of peptides and these bonds cannot be cleaved by digestive enzymes. In the tanning process, tannin binds to the collagen of the animal hides and thus produces leather that is able to withstand the attack of microorganisms. Tannins have a sharp unpleasant taste; binding of tannins to the proteins of the mucous membranes and saliva draws the mouth together. In this way animals are discouraged from eating plant leaves that accumulate tannin. When an animal eats these leaves, the destruction of leaf cells results in the binding of tannins to plant proteins, which renders the leaves less digestible and thus unsuitable as fodder. Tannins also react with enzymes of the herbivore digestive tract. For

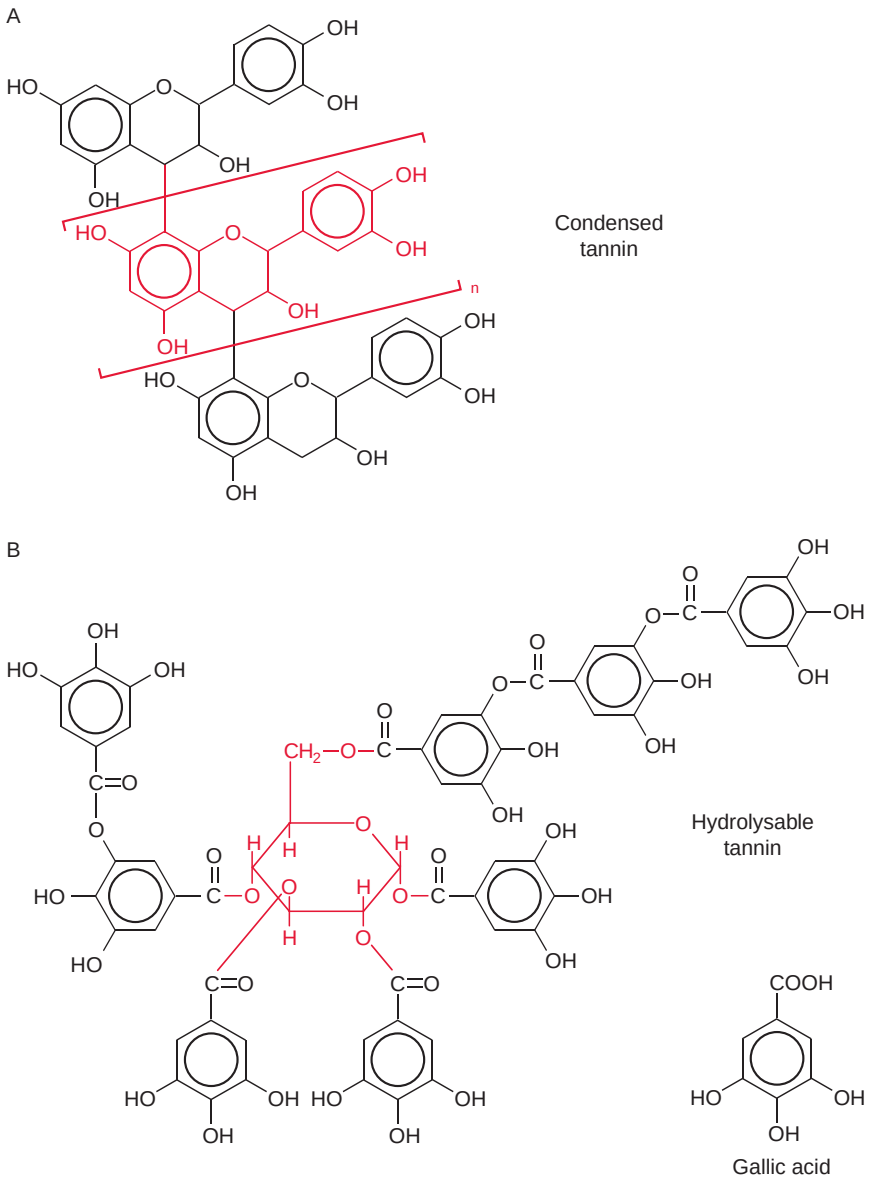

Figure 18.16 A. Composition of a condensed tannin (n = 1–10). The terminal phenyl residue can also contain three hydroxyl groups. B. Example of hydrolyzable tannin. The hydroxyl groups of a hexose are esterified with gallic acids (from *Anarcadia* plants).

these reasons, tannins are very effective in protecting leaves from being eaten by animals. To illustrate this: in the South African savannah, the leaves of the acacia are the main source of food for the kudu antelope. These leaves contain tannin, but in such low amounts that it does not affect the nutritional quality. Trees injured by feeding animals emit volatile ethylene

(section 19.5), and within 30 minutes the synthesis of tannin is induced in the leaves of neighboring acacias. If too many acacia leaves are eaten, the tannin content can increase to such a high level that the kudu could die when feeding from these leaves. Thus the acacias protect themselves from complete defoliation by a collective warning system. Investigations are in progress to decrease the tannin content of forage plants by genetic engineering.

Tannins also protect plants against attack by microorganisms. Infection of plant cells by microorganisms is often initiated by the secretion of enzymes for lytic digestion of plant cell walls. These aggressive enzymes are inactivated when tannins are bound to them.

Further reading

Boerjan, W., Ralph, J., Baucher, M. Lignin biosynthesis. Annual Review Plant Biology 54, 519–546 (2003).

Boudet, A. M., Kajita, S., Grima-Pettenati, J., Goffner, D. Lignins and lignocellulosics: A better control of synthesis for new and improved uses. Trends in Plant Science 8, 576–581 (2003).

Chen, F., Dixon, R. A. Lignin modification improves fermentable sugar yields for biofuel production. Nature Biotechnology 25, 759–761 (2007).

Davin, L. B., Lewis, N. G. Dirigent phenoxy radical coupling: Advances and challenges. Current Opinion Biotechnology 16, 398–406 (2005).

Dembitsky, V. M. Astonishing diversity of natural surfactants: 5. Biologically active glycosides of aromatic metabolites. Lipids 40, 869–900 (2005).

Dixon, R. A. Phytoestrogens. Annual Review Plant Biology 55, 225–261 (2004).

Grotewold, E. The genetics and biochemistry of floral pigments. Annual Review Plant Biology 57, 761–780 (2006).

Hatfield, R., Vermeris, W. Lignin formation in plants. The dilemma of linkage specificity. Plant Physiology 126, 1351–1357 (2001).

Iason, G. The role of plant secondary metabolites in mammalian herbivory: Ecological perspectives. Proceedings Nutritional Society 64, 123–131 (2005).

Koes, R., Verweig, W., Quattrocio, T. Flavonoids: A colorful model for the regulation and evolution of biochemical pathways. Trends in Plant Science, 10, 236–242 (2005).

Pérez, J., Muñoz-Dorado, J., de la Rubia, T., Martínez, J. Biodegradation and biological treatments of cellulose, hemicellulose and lignin: An overview. Interactions Microbiology 5, 53–63 (2002).

Schijlen, E. G., Ric de Vos, C. H., van Tunen, A. J., Bovy, A. G. Modification of flavonoid biosynthesis in crop plants. Phytochemistry 65, 2631–2648 (2004).

Springob, K., Nakajima, J., Yamazaki, M., Saito, K. Recent advances in the biosynthesis and accumulation of anthocyanins. Natural Products Report 20, 288–303 (2003).

Treutter, D. Significance of flavonoids in plant resistance and enhancement of their biosynthesis. Plant Biology 7, 581–591 (2005).

Winkel-Shirley, B. Biosynthesis of flavonoids and effects of stress. Current Opinion Plant Biology 5, 218–223 (2002).

19

Multiple signals regulate the growth and development of plant organs and enable their adaptation to environmental conditions

In complex multicellular organisms such as higher plants and animals, metabolism, growth, and development of the various organs are coordinated by the emission of signal compounds. In animals these signals can be hormones, which are secreted by glandular cells. Hormones are classified in paracrine hormones, which function as signals to neighboring cells, and endocrine hormones, which are emitted to distant cells (e.g., via the blood circulation). Also in plants, signal compounds are released from certain organs, often signaling to neighboring cells, but also to distant cells via the xylem or the phloem. All these plant signal compounds are termed **phytohormones**. Some of the phytohormones (e.g., brassinosteroids) resemble animal hormones in their structure, whereas others are structurally completely different. Like animal hormones, phytohormones also have many different signal functions. They control the adjustment of plant metabolism to environmental conditions, such as water supply, temperature, and day length, and regulate plant development**.** Light sensors including **phytochromes**, which recognize red and far-red light, and **cryptochromes** and **phototropin** monitoring blue light, control the growth and the differentiation of plants depending on the intensity and quality of light.

The signal transduction chain between the binding of a certain hormone to the corresponding receptor and its effect on specific cellular targets, such as the transcription of genes or the activity of enzymes, is now known for many animal hormones. In contrast, signal transduction chains have not been fully resolved for any of the phytohormones or light sensors. However,

partial results indicate that certain components of the signal transduction chain in plants may be similar to those in animals. The phytohormone receptors and light sensors apparently act as a **multicomponent system**, in which the signal transduction chains are interwoven to a **network**.

19.1 Signal transduction chains known from animal metabolism also function in plants

G-proteins act as molecular switches

A family of proteins, which by binding of GTP or GDP can alternate between two conformational states, is widely distributed in the animal and plant kingdoms. These proteins are **GTP-binding proteins**, or simply **G-proteins**. The heterotrimeric G-proteins, discussed in the following, are bound at the inner side of the plasma membrane interacting with integral membrane receptor proteins consisting of seven transmembrane helices (Fig. 19.1). The receptors have a binding site for the signal molecule at the outside and a binding site for G-proteins at the cytoplasmic site of the plasma membrane, and are therefore well suited to pass external signals into the cell. **Heterotrimeric-G-proteins** are composed of three different subunits: $\mathbf{G_\alpha}$ (molecular mass 45–55 kDa), $\mathbf{G_\beta}$ (molecular mass 35 kDa), and $\mathbf{G_\gamma}$ (molecular mass 8 kDa). In *Arabidopsis thaliana* the α- and β-subunits are each encoded by one gene, whereas the γ-subunit is encoded by two genes. Subunit G_α has a binding site that can be occupied by either GDP or GTP. In animals, binding of the heterotrimer to a receptor (e.g., an adrenaline receptor occupied by adrenaline) enables the exchange of the GDP for GTP at the G_α subunit.

The binding of GTP results in a **conformational change** of the G_α subunit, which subsequently dissociates from the trimer. The liberated G_α-GTP unit functions as an activator of various enzymes that synthesize components of the signal transduction chain. For instance, G_α-GTP stimulates a **GMP-cyclase** that forms the signal compound guanosine-3′-5′-monophosphate (**cGMP**) from GTP (Fig. 19.2), as has been found in plants and animals. G_α-GTP also stimulates **phospholipase C** (see Fig. 19.4). The function of this reaction in the liberation of Ca^{2+} as a signal component will be discussed in the following section. In fungi and animals, G_α-GTP also stimulates the synthesis of the signal compound adenosine-3′-5′-monophosphate (**cAMP**) from ATP via an activation of AMP-cyclase. It has so far not been definitely proved whether cAMP plays a role also in plant metabolism.

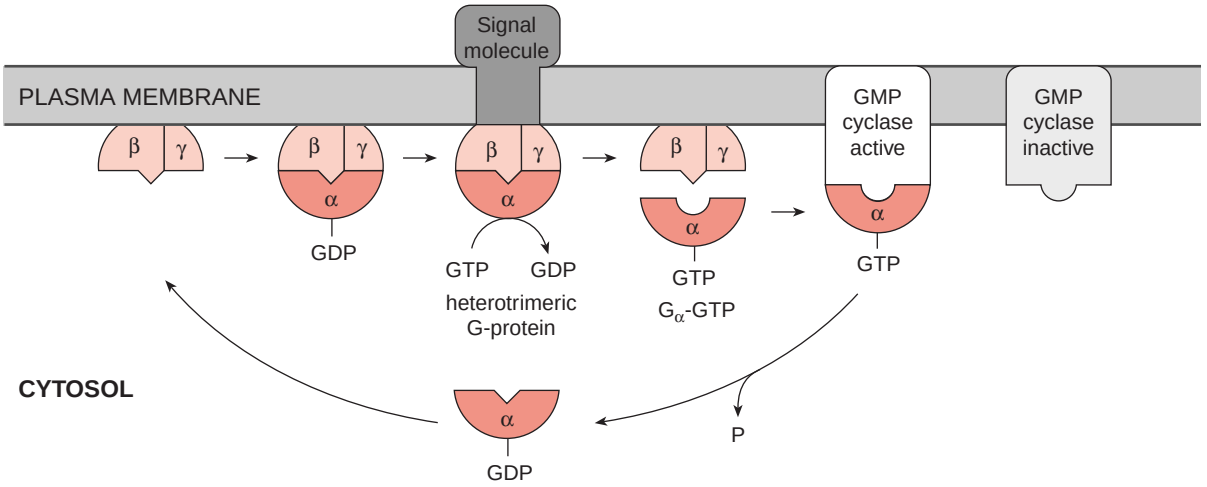

Figure 19.1 Schematic presentation of G-protein action.

G_α-GTP has a half-life of only a few minutes. Bound GTP is hydrolyzed to GDP by an intrinsic GTPase activity, and the resulting conformational change causes the G_α subunit to lose its activator function. It binds again to the dimer to form a trimer and a new cycle can begin. The short life of G_α-GTP makes the signal transduction very efficient.

Small G-proteins have diverse regulatory functions

All eukaryotes also contain **small G-proteins**, which have only one subunit and are related to the α-subunit of heterotrimeric G-proteins discussed in the preceding. All small G-proteins belong to a superfamily termed the **Ras superfamily**. These small G-proteins, located in the cytosol, have binding domains for GDP/GTP and an effector domain. Binding of a GDP renders the protein inactive and that of GTP active. When stimulated by a signal, the small G-protein interacts with an **exchange factor**, which converts the GDP-bound inactive protein to a GTP-active conformation by GTP/GDP replacement. Through its effector domain the active GTP-conformation interacts with other proteins in analogy to the G_α-GTP of the heterotrimeric G-protein. It has been predicted from genomic analyses that the *Arabidopsis* genome encodes more than 90 small G-proteins. Small G-proteins have various regulatory functions, such as the regulation of defense reactions, ABA responses, vesicle transport, cell polarity, and the growth of pollen tubes and root hairs. Present knowledge about the role of small G-proteins in plants is still at an early stage.

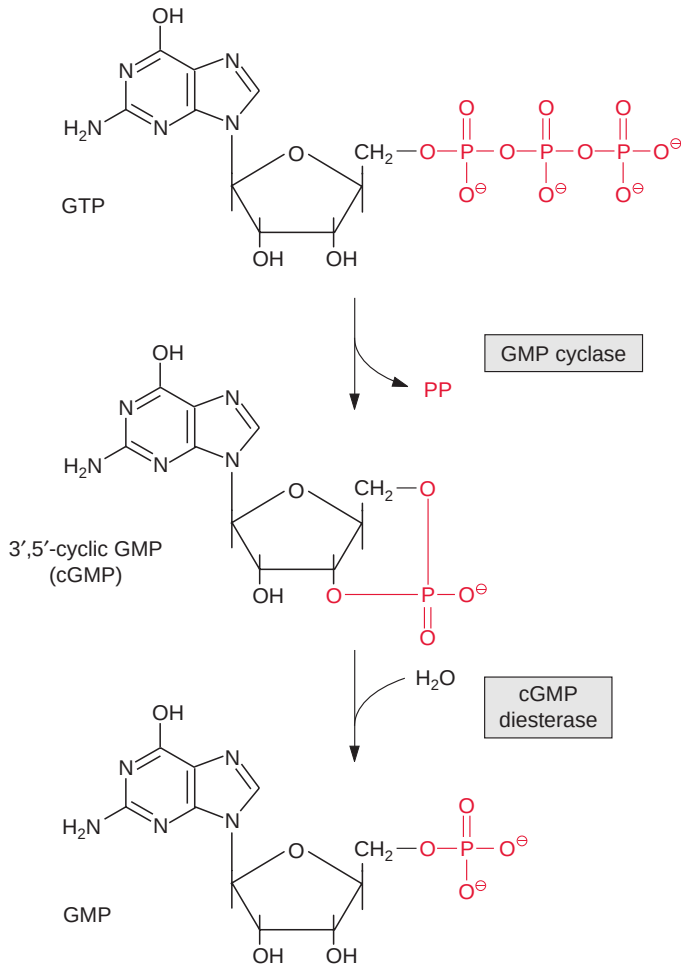

Figure 19.2 cGMP is synthesized by GMP-cyclase from GTP and is degraded to GMP by a diesterase.

Ca^{2+} is a component of signal transduction chains

In animal cells as well as in plant cells, the cytosolic concentration of free Ca^{2+} is normally lower than 10^{-7}mol/L. These very low Ca^{2+} concentrations are maintained by ATP-dependent pumps (Ca^{2+}-P-ATPases, section 8.2), which accumulate Ca^{++} in the lumen of the endoplasmatic reticulum and the vacuole (in plants) or transport Ca^{2+} via the plasma membrane to the extracellular compartment (Fig. 19.3). Alternatively, Ca^{2+} can be taken up into mitochondria by H^+/Ca^{2+} antiporters. Signals (e.g., salt, ABA, dryness or coldness) induce Ca^{2+} channels in the endomembranes of intracellular stores to open for a short time, resulting in a rapid increase in the cytosolic concentration of free Ca^{2+}. In almost all cells free Ca^{2+} stimulates

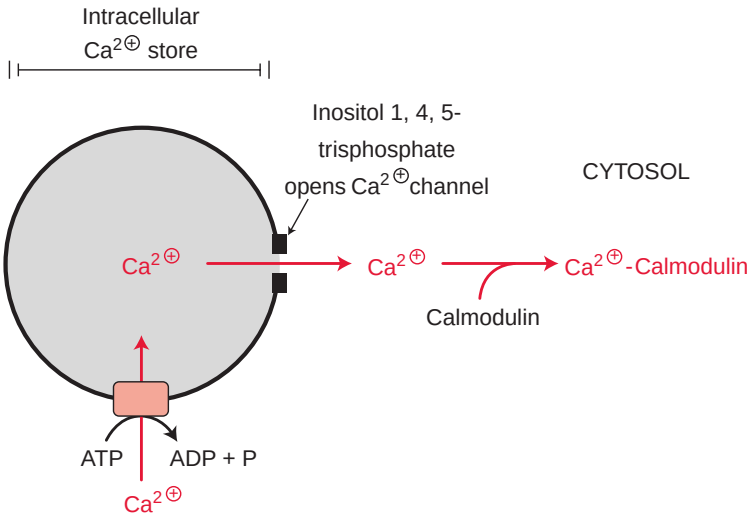

Figure 19.3 The endoplasmatic reticulum of animals and plants and the plant vacuole (designated here as intracellular Ca^{2+} store) contain in their membrane a Ca^{2+}-P-ATPase (section 8.2), which pumps Ca^{2+} into the lumen or into the vacuole. Ca^{2+} can be released into the cytosol by an IP_3-dependent Ca^{2+} channel.

regulatory enzymes such as protein kinases that are often components of signal cascades regulating a multitude of cellular processes (see following section).

The phosphoinositol pathway controls the opening of Ca^{2+} channels

Ca^{2+} channels can be controlled by the phosphoinositol signal transduction cascade (Fig. 19.4), which has initially been resolved in animal metabolism, but has also been shown to exist in plants. **Phosphatidyl inositol** is present, although in relatively low amounts, as a constituent of cell membranes. In animal cells, the two fatty acids of phosphatidyl inositol are usually stearic acid and arachidonic acid. The inositol residue is phosphorylated at the hydroxyl groups in 4′ and 5′ position by a kinase. **Phospholipase C**, stimulated by a G-protein, cleaves the lipid to **inositol-1,4,5-trisphosphate** (**IP_3**) and **diacylglycerol** (DAG). IP_3 causes a rise in the cytosolic Ca^{2+} concentration, whereas in animals diacylglycerol stimulates a Ca^{2+}-dependent protein kinase. In plants, diacylglycerol as such does not seem to play a role in the metabolism. However, it has an indirect effect, since **phosphatidic acid** (Fig. 15.5) deriving from the phosphorylation of diacylglycerol affects protein kinases and ion channels.

Patch-clamp studies (see section 1.10) demonstrated that in plant vacuoles and other Ca^{2+} stores, such as the endoplasmatic reticulum, IP_3 causes Ca^{2+} channels to open. The rapid influx of Ca^{2+} into the cytosol is limited

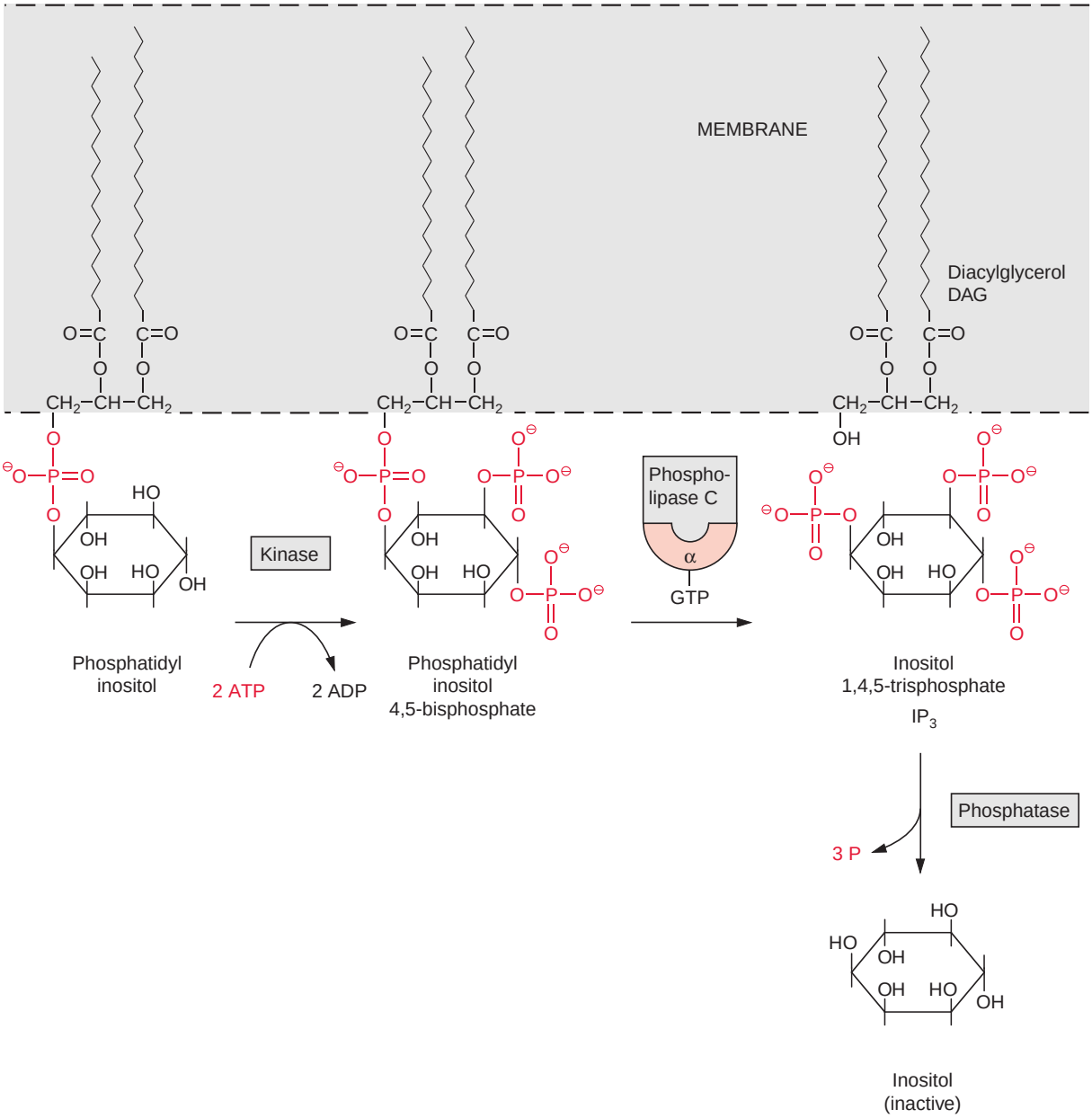

Figure 19.4 Inositol-1,4,5-trisphosphate (IP_3) is part of a signal transduction chain. Two hydroxyl groups of the inositol bound to a membrane anchored phospholipid are phosphorylated by a kinase and IP_3 is liberated by a G-protein ($G_\alpha GTP$)-dependent phospholipase C. The signal component IP_3 formed in this way can be degraded by phosphatases.

by the very short life of IP_3 (often less than 1 s). The rapid elimination of IP_3 proceeds either via additional phosphorylation of IP_3 or the hydrolytic liberation of the phosphate groups by a phosphatase. The short lifetime of IP_3 enables a very efficient signal transduction.

In plants the phosphoinositol cascade has an important role in transmitting signals from the environment to cellular functions (e.g., in adjusting the stomata opening to the water supply). A specific kinase has been identified in plants, which catalyzes the phosphorylation of phosphatidyl inositol to **phosphatidyl inositol-3-phosphate**. This modified membrane lipid functions as a signal for vesicle transfer (Fig. 1.16) (e.g., in the transfer of hydrolytic enzymes from the ER to the vacuole).

Calmodulin mediates the signal function of Ca^{2+} ions

Ca^{2+} often does not act directly as a signal component but by binding to calmodulin. **Calmodulin** is a soluble protein (molecular mass 17 kDa) that occurs in animals as well as in plants. It is a highly conserved protein; the identity of the amino acid sequences between the calmodulin from wheat and cattle is as high as 91%. Calmodulin is present mainly in the cytosol. It consists of a flexible helix connecting the two loops of both ends. Each loop possesses a binding site for a Ca^{2+} ion and contains glutamate (E) and phenylalanine (F). For this reason these loops are designated **EF hands** (Fig. 19.5). The binding of Ca^{2+} to all four EF hands results in a conformational change of calmodulin by which its hydrophobic domain is exposed. This domain interacts with certain protein kinases **(calmodulin-binding kinases** (**CBK**)), which are subsequently activated. The activated protein kinase-CBK II first catalyzes its own phosphorylation (autophosphorylation), and then reaches its full activity, and even retains it after the dissociation of calmodulin, until the phosphate residue is released by hydrolysis.

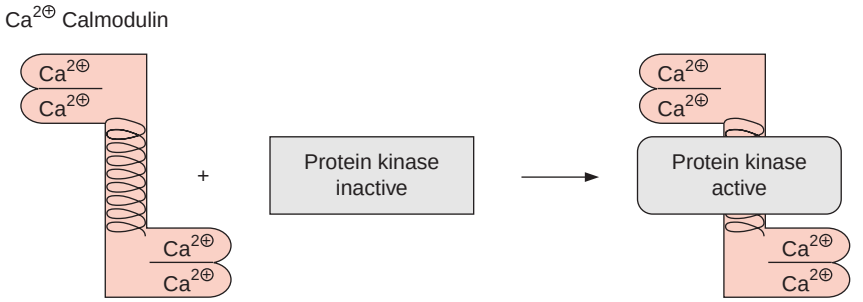

Figure 19.5 The protein calmodulin contains two Ca^{2+} binding domains, which are connected by a flexible α-helix. Ca^{2+}-calmodulin activates certain protein kinases, e.g., CBK.

Ca^{2+}-calmodulin also binds to other proteins, thus changing their activity, and is therefore an important component of signal transduction chains.

Moreover, plants encode a family of protein kinases, which possess Ca^{2+}-binding EF hands as essential domains of the protein. They are termed Ca^{2+}-dependent protein kinases (**CDPK**). By now more than 30 genes of the CDPK-family have been detected in *Arabidopsis*, although the function of part of them is still not known. CDPK kinases are involved in the phosphorylation of sucrose phosphate synthase (Fig. 9.18) and nitrate reductase (Fig. 10.9), pathogen defense reaction, and the response to various abiotic stresses.

There are also other proteins with calmodulin domains, the so-called **calmodulin-related proteins** (**CRK**), but their functions are to a large extent not known.

Phosphorylated proteins are components of signal transduction chains

Protein kinases, several of which have been discussed previously, and **protein phosphatases** are important elements in the regulation of intracellular processes. Phosphorylation and dephosphorylation change proteins between two activity states. Similarly many protein kinases are switched on or off by phosphorylation; therefore protein kinases represent a **network of on-off switches in the cell**, comparable to those of computer chips. These switches control differentiation, metabolism, defense against pests, and many other cell processes. It is estimated that in a eukaryotic cell 1% to 3% of the functional genes encode protein kinases. Initially protein kinases were investigated primarily in yeast and animals, but in the meantime several hundred genes encoding protein kinases have been identified in plants, although the physiological functions of only some of them are known. The elucidation of the interacting cellular components of protein kinases is at present a dynamic field in plant biochemistry.

Most protein kinases in eukaryotes, such as fungi, animals, or plants, encompass 12 structurally conserved regions. Since all these protein kinases are homologous and thus descend from a common ancestor, they are grouped in a **superfamily of eukaryotic protein kinases** (Table 19.1). They phosphorylate mainly the -OH group of **serine** and/or **threonin**e and in some cases also of **tyrosine**. Protein kinases phosphorylating histidine (e.g., receptors for ethylene and cytokinin) and aspartate residues are not members of this family (see section 19.7). The protein kinases, which are regulated by cGMP, are named **protein kinases G**. The existence in plants of **protein kinases A**, regulated by cAMP, is still a matter of dispute. The

Table 19.1: Some members of the eukaryotic protein kinase super family

	Modulator
Protein kinase-A	cAMP
Protein kinase-G	cGMP
Ca^{2+}-dependent protein kinase (CDPK)	Ca^{2+}
Calmodulin-binding kinase (CBK)	Ca^{2+}-Calmodulin
Receptor-like protein kinase (RLK)	e.g., Phytohormones
Cyclin-dependent protein kinase (CDK)	Cyclin
Mitogen-activated protein kinase (MAPK)	Mitogen
MAPK-activated protein kinase (MAPKK)	MAPK
MAPKK-activated protein kinase (MAPKKK)	MAPKK

protein kinases regulated by Ca^{2+}-calmodulin (**CBK**) were already mentioned, as well as the Ca^{2+}-dependent protein kinases (**CDPK**). Further members of the superfamily are the **receptor-like protein kinases (RLK**). These protein kinases are generally located in plasma membranes. They contain an extra cytoplasmatic domain with a receptor function (e.g., for a phytohormone). The occupation of this receptor by a signal molecule results in the activation of a protein kinase at the cytoplasmatic side of the membrane, and subsequent reaction with cellular proteins. Genome sequencing revealed that the *Arabidopsis* genome contains more than 400 genes encoding RLKs.

The superfamily of eukaryotic protein kinases also encompasses the **cyclin-dependent-protein kinases** (**CDK**) (Table 19.1). **Cyclin** is a protein that is present in all eukaryotic cells, as it has an essential function in the cell cycle. CD kinases activate a number of proteins that are involved in mitosis. Additional members of the superfamily are the **mitogen-activated-protein kinases** (**MAPK**). **Mitogen** is a collective term for a variety of compounds, many of them of unknown structure, which stimulate mitosis, and thus the cell cycle, but also other reactions. G-proteins and phytohormones may act as mitogens. MAPKs play an important role in **protein kinase cascades**, where protein kinases are regulated through phosphorylation by other protein kinases. In such a cascade, a G-protein, for example, activates an MAP-kinase-kinase-kinase (**MAPKKK**), which activates by phosphorylation an MAP-kinase-kinase (**MAPKK**), which activates an MAP-kinase (**MAPK**). The MAP-kinase in turn phosphorylates various cellular components. In a

plant several of these signal cascades with different target proteins operate in parallel. Some of the cascade components overlap. The signal cascades regulate the expression of different genes by phosphorylation of a series of transcription factors (section 20.2). The **MAP-kinase-cascade** thus has an important regulatory function in the process of cell development and differentiation. Moreover, the MAP-kinase system is also involved in the signal cascades of **pathogen defense systems**, which are triggered by elicitors (section 16.1), and in the response to abiotic stress (e.g., heavy metals, salt, dryness, coldness, wounding). Genome sequencing revealed that 20 MAPKs, 10 MAPKKs, and 60 MAPKKKs exist in *Arabidopsis*.

Recently, protein kinases have been identified that phosphorylate **histidine** and **aspartate** residues of proteins and which do not belong to the superfamily mentioned previously. As will be discussed in section 19.7, histidine protein kinases are involved in the function of the receptors for ethylene and cytokinin.

Also, **protein phosphatases** exist in eukaryotes as a superfamily, with **serine-threonine-phosphatases** and **tyrosine-phosphatases** as different groups. Many of these phosphatases are regulated similarly to protein kinases (e.g., by binding of Ca^{2+} plus calmodulin or by phosphorylation). In this way the protein phosphatases also play an active role in signal transduction cascades. Research in this field is still at the beginning.

19.2 Phytohormones contain a variety of very different compounds

Phytohormones (Fig. 19.6) have very diverse structures and functions. Only a few examples of these functions will be summarized here. Indole acetic acid, an **auxin** derived from indole, stimulates cell elongation**. Gibberellins**, derivatives of gibberellane, induce elongation growth of internodes. Zeatin, a **cytokinin**, is a prenylated adenine and stimulates cell division. **Abscisic acid**, which is formed from carotenoids, regulates the water balance. **Ethylene** and **jasmonic acid** (the latter being a derivative of fatty acids, section 15.7) enhance senescence; **methyl jasmonate** plays a role in pathogene defense. **Brassinosteroids** have a key function in the regulation of cell development. **Peptide hormones** regulate plant development, and, in addition to **salicylic acid** and jasmonic acid, play a role in pathogen defense. In many cases, phytohormone function is caused by a pair of antagonistic phytohormones. Thus abscisic acid induces seed dormancy, and gibberellic acid terminates it.

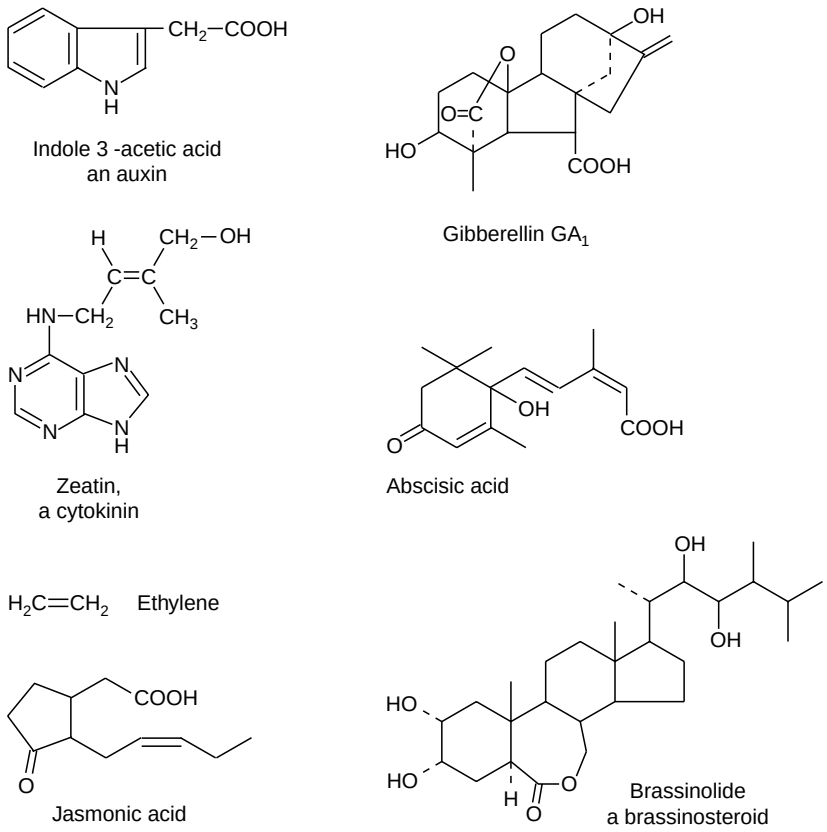

Figure 19.6 Chemical structures of some important phytohormones.

19.3 Auxin stimulates shoot elongation growth

Charles Darwin and his son Francis had already observed in 1880 that growing plant seedlings bend towards sunlight. They found that illumination of the tip initiated the bending of seedlings of canary grass (*Phalaris canariensis*). Since the growth zone is only a few millimeters from the tip, they assumed that a signal is transmitted from the tip to the growth zone. In 1926 the Dutch researcher Frits Went isolated from the tip of oat seedlings a growth-stimulating compound, which he named **auxin** and which was later identified as **indoleacetic acid** (**IAA**). Besides IAA, some other compounds are known with auxin properties (e.g., phenylacetic acid) (Fig. 19.8). The synthesis of IAA occurs not only in the shoot but also in the root. Different biosynthesis pathways are operating in different plants. Figure 19.7 shows two of these pathways.

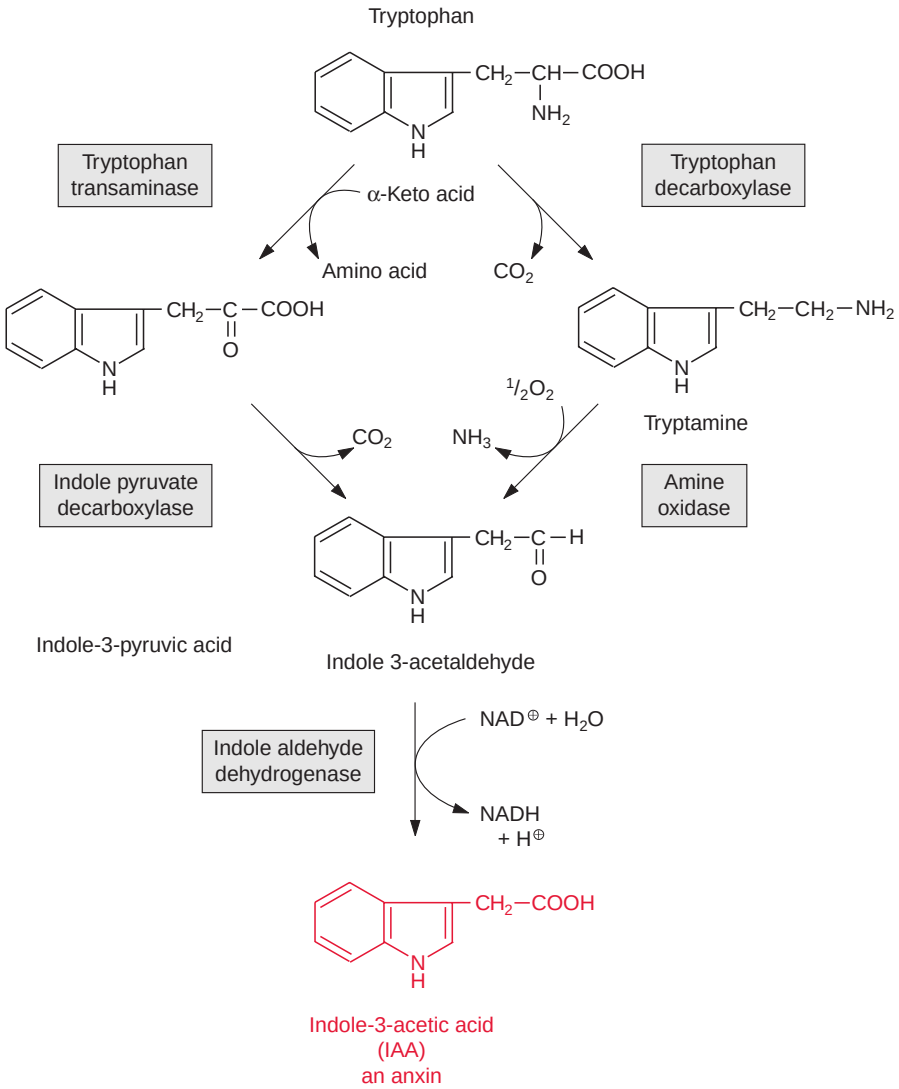

Figure 19.7 Presentation of two biosynthetic pathways for the synthesis of indole-3-acetic acid from tryptophan.

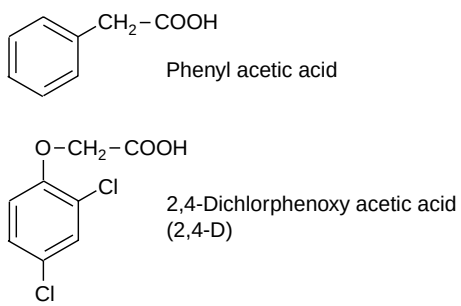

Figure 19.8 Phenylacetic acid, a compound with auxin properties, and 2,4D, a structural analogue of auxin, applied as a herbicide.

The synthetic auxin **2,4-dichlorophenoxyacetic acid** (**2,4-D**, Rohm & Haas) is used as a **herbicide**. It kills plants by acting as an especially powerful auxin, resulting in disordered morphogenesis and an increased synthesis of ethylene, which leads to a premature senescence of leaves. In the Vietnam War it was used as **Agent Orange** to defoliate forests. 2,4-D is a selective herbicide that destroys dicot plants. Monocots are insensitive to it, because they eliminate the herbicide by degradation. For this reason, 2,4-D is used for combating weeds in cereal crops.

Auxin functions in many ways. It influences embryogenesis, all types of organogenesis, maintenance of the root meristem, differentiation of vascular tissue, elongation growth of hypocotyls and roots, curvature of the coleoptiles, apical dominance, fruit ripening and the effects of the environment on plant growth. For a long time it was not clear how auxin was able to affect all these different processes. The key to this is the **polar transport** of auxin between different cells, resulting in its **asymmetric accumulation** in tissues and cells. Auxin is primarily synthesized at the tip of the shoot. From there it is transported from cell to cell by specific **influx** and **efflux carriers** of the plasma membrane. The protonated form of IAA (IAAH) is transported by a proton driven influx carrier (AUX1) into the cell where it is deprotonated and trapped. The efflux of IAA proceeds via another specific carrier (PIN). The polar transport is caused by an asymmetric distribution of these carriers. The membrane-bound efflux carrier proteins are transferred in a reversible fashion between membrane regions by vesicle transport via the Golgi apparatus. In this way the efflux carriers can be moved rapidly from one area of the plasma membrane to another to facilitate a polar transport. During the curvature of the coleoptiles, IAA is transported laterally to one side. The resulting differential stimulation of cell elongation at only one side of the shoot leads to the bending. IAA is also transported via the phloem from the leaves to distant parts of the plant.

The effect of IAA on cell growth in the shoot can be shown experimentally to occur within a few minutes after adding IAA. The hyperpolarization of the cell and an increase of phospholipase activity result in the opening of Ca^{2+} channels (section 19.1). The subsequent activation of **H^+-P-ATPases** (section 8.2) leads to the acidification of the cell wall region and subsequently to a loosening of the normally rigid cell wall. Shortly thereafter (15–30 min), the synthesis of proteins and xyloglucans begins, both as part of the epidermal cell wall synthesis and the elongation growth.

The **auxin receptor** (TIR) has been identified recently. The binding of auxin to this receptor recruits **AUX/IAA transcription factors** (section 20.2), which at low auxin concentrations together with other transcription factors (ARF) repress the expression of certain genes. Increased auxin concentrations result in a derepression of these genes and the formation

of auxin-inducible proteins. AUX/IAA transcription factors have a very short lifetime and are degraded in the proteasome after conjugation with **ubiquitin** (section 21.4). For this reason the AUX/IAA proteins are very well suited to function as on/off switches. A plant contains many genes of these TIR and AUX/IAA proteins, which explains the large repertoire of diverse auxin effects in different tissues.

In different tissues and organs IAA has different cellular impacts. IAA stimulates cell division in the cambium, enhances **apical dominance** by suppression of lateral bud growth, and controls embryo development. Moreover, IAA prevents the formation of an abscission layer for leaves and fruits and is thus an antagonist to ethylene (section 19.7). On the other hand, increased IAA concentrations can induce the synthesis of ethylene.

Moreover, auxin induces the **formation of fruits**. Normally, seeds produce IAA only after fertilization. Transformants of eggplants that express a bacterial enzyme of IAA synthesis in the unfertilized seed were generated by genetic engineering. This IAA prevents the formation of seeds, resulting in seedless eggplants of normal consistency which are four times larger than usual. This is an impressive example of the importance of auxin for fruit growth and shows the possibilities of generating genetically altered vegetables.

19.4 Gibberellins regulate stem elongation

The discovery of gibberellins is related to a plant disease. The infection of rice by the fungus *Gibberella fujikuroi* results in the formation of extremely tall plants that fall over and bear no seeds. In Japan this disease was called "foolish seedling disease." In 1926 Eiichi Kurozawa and collaborators (Japan) isolated a compound from this fungus that induces unnatural growth. It was named **gibberellin**. These results were known in the West only after World War II. Structural analysis revealed that gibberellin is a mixture of various compounds with similar structures, which also occur in plants and act there as phytohormones.

Gibberellins are derived from the hydrocarbon ***ent*-gibberellane** (Fig. 19.9). More than 100 gibberellin derivatives are now known in plants, which are numbered in the order of their identification. Therefore the numbering gives no information about structural relationships or functions. Many of these gibberellins are intermediates or by-products of the biosynthetic pathway. Only a few of them have been shown to act as phytohormones. Whether other gibberellins have a physiological function is not

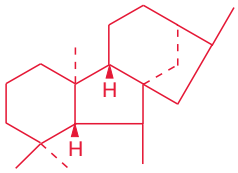

ent-Gibberellane

Figure 19.9 Hydrocarbon from which gibberellins are derived.

A

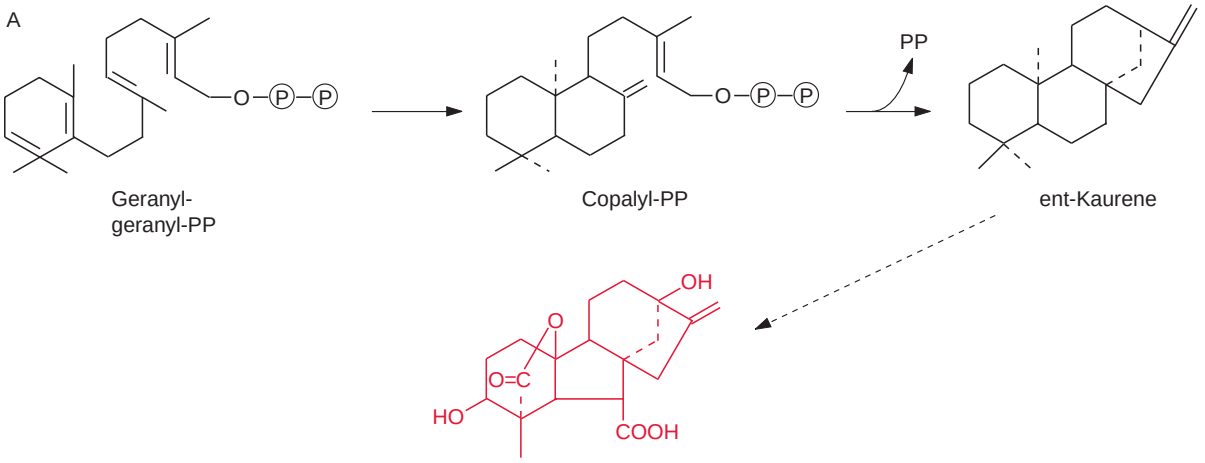

Geranyl-geranyl-PP

Copalyl-PP

ent-Kaurene

Gibberellin GA_1

B

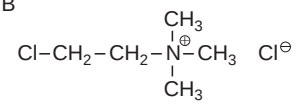

2-Chlorethyltrimethylammonium-chloride (Cycocel, BASF)

Figure 19.10 A. Synthesis of gibberellin GA_1. B. Cycocel (BASF), a retardant that decreases the growth of stalks in wheat and other cereals, inhibits kaurene synthesis and thus also the synthesis of gibberellins.

known. The most important gibberellins are GA_1 (Fig. 19.10A) and GA_4 (not shown). Gibberellins derive from **isoprenoids** (Chapter 17). The synthesis proceeding in 13 steps takes place in three compartments. At first geranylgeranyl pyrophosphate is converted in the **plastids** to *ent*-kaurene. Subsequently *ent*-kaurene is transformed to GA_{12}-aldehyde by a cyt-P450 monooxygenase located in the membrane of the endoplasmatic reticulum

(**ER**) (section 18.2). Finally gibberellin (GA_{12}) is synthesized in the **cytosol**. This reaction involves the catalysis by oxoglutarate-dependent dioxygenases (GA oxidases).

Similar to IAA, gibberellins **stimulate shoot elongation**, especially in the internodes of the stems. A pronounced gibberellin effect is that it induces rosette plants (e.g., spinach or lettuce) to initiate and regulate the formation of flowers and flowering. Additionally, gibberellins have a number of other functions such as the preformation of fruits and the stimulation of their growth. Gibberellins terminate **seed dormancy**, probably by softening the seed coat, and facilitate seed germination by the expression of genes for the necessary enzymes (e.g., amylases).

The use of gibberellins is of economic importance for the production of **long**, **seedless grapes**. In these grapes, GA_1 causes not only extension of the cells, but also parthenocarpy (the generation of the fruit as a result of parthogenesis). Moreover, in the malting of barley for beer brewing, gibberellin is added to induce the formation of α-amylase in the barley grains. The gibberellin GA_3, produced by the fungus *Gibberella fujikuroi*, is generally used for these purposes. Inhibitors of gibberellin biosynthesis are commercially used as **retardants** (growth inhibitors). A number of substances that inhibit the synthesis of the gibberellin precursor *ent*-kaurene, such as **chloroethyltrimethyl ammonia chloride** (trade name Cycocel, BASF) (Fig. 19.10B) are sprayed on cereal fields to decrease the **growth of the stalks**. This enhances the strength of the cereal stalks and at the same time increases the proportion of total biomass in seeds. Slowly degradable gibberellin synthesis inhibitors are used in horticulture to keep indoor plants small.

Gibberellins influence gene expression. A soluble protein (GID1), which resembles a hormone-sensitive lipase, has been identified as a GA receptor. *Arabidopsis* contains three genes for GID1 proteins. When GA binds to this receptor, the complex then transmits the information to so-called cytosolic **DELLA proteins**. The latter usually repress plant growth. In this way the binding of GA to the receptor ultimately leads to an increase of gene expression, resulting in an increase of elongation growth. Thus, GA causes **the relief of a restraint**.

Mutants, in which the synthesis of GA or the function of GA on growth was impaired, turned out to be important for agriculture. The dramatic increase in the yield of cereal crops achieved after 1950, often named the "**green revolution**," is in part due to the introduction of **dwarf wheat lines**. At that time, attempts to increase the crop yield of traditional wheat varieties by an increased application of nitrogen fertilizer failed, since it produced more straw biomass instead of enhancing the grain yield. This was averted by breeding wheat varieties with **reduced stalk growth**, where the portion of grains in the total biomass (harvest index) was increased

considerably. It turned out that the decreased stalk growth in these varieties was due to the mutation of genes encoding transcription factors of the gibberellin signal transduction chain. In wheat, the mutated genes have been termed **Rht** (reduced height).

19.5 Cytokinins stimulate cell division

Cytokinins are prenylated derivatives of adenine. In **zeatin**, which is the most common cytokinin, the amino group of adenine is linked with the hydroxylated isoprene residue in the *trans*-position (Fig. 19.11). In other cytokinins benzyl derivatives, sugars or sugar phosphates are attached to the adenine. Cytokinins enhance plant growth by stimulating **cell division** and increase the sprouting of lateral buds. As cytokinins override apical dominance, they are antagonists of the auxin IAA. Cytokinins **retard senescence** and thus counteract the phytohormone ethylene (section 19.7). The larvae of some butterflies (e.g., *Stigmella,* which invade beech trees) use this principle for their nutrition. They excrete cytokinin with their saliva and thus prevent senescence of the leaves on which they are feeding. As a result, **green islands** of intact leaf material remain in yellowing autumn leaves, which provide, beyond the actual vegetation period, the caterpillars with the forage they need to form pupae.

Mature (i.e., differentiated) plant cells normally stop dividing. By adding cytokinin and auxin, differentiated cells can be induced to initiate cell division again. When a leaf piece is placed on a solid culture medium containing auxin and cytokinin, leaf cells start unlimited growth, resulting in the formation of a callus that can be propagated in tissue culture. Upon the application of a certain cytokinin/auxin ratio, a new shoot can be regenerated from single cells of this callus. The use of tissue culture for the generation of transgenic plants will be described in section 22.3.

In nature some plant associated bacteria and fungi produce auxin and cytokinin to induce unlimited cell division, which results in tumor growth of the plant. The formation of the **crown gall** induced by ***Agrobacterium tumefaciens*** (see section 22.2) is caused by a stimulation of the production of cytokinin and auxin. The bacterium does not produce these phytohormones itself, but transfers the genes for the biosynthesis of cytokinin and auxin from its T_i plasmid to the plant genome.

Zeatin is formed from AMP and dimethyallylpyrophosphate (Fig. 19.11). The isoprene residue is transferred by **cytokinin synthase** (a prenyl transferase, see section 17.2) to the amino group of the AMP and is then hydroxylated. Cytokinin synthesis takes place primarily in the meristematic

tissues. Transgenic tobacco plants in which the activity of cytokinin synthase in the leaves is increased have a much longer lifespan than normal plants, since their senescence is suppressed by the enhanced production of cytokinin.

Cytokinin receptors, like ethylene receptors, are **dimeric histidine kinases**. They are located in the plasma membrane, where the receptor site is directed to the extracellular compartment and the kinase is directed to the cytoplasm. The kinase moiety of the dimer comprises two histidine residues and two aspartyl residues. Upon binding of cytokinin, the two histidine kinases phosphorylate their histidine residues reciprocally (**autophosphorylation**). Subsequently, the phosphate groups are transferred to histidine residues or aspartyl residues of **transmitter proteins** (signal components). The transmitter proteins are channeled into the nucleus, where they function as transcription factors and thus regulate the expression of many genes.

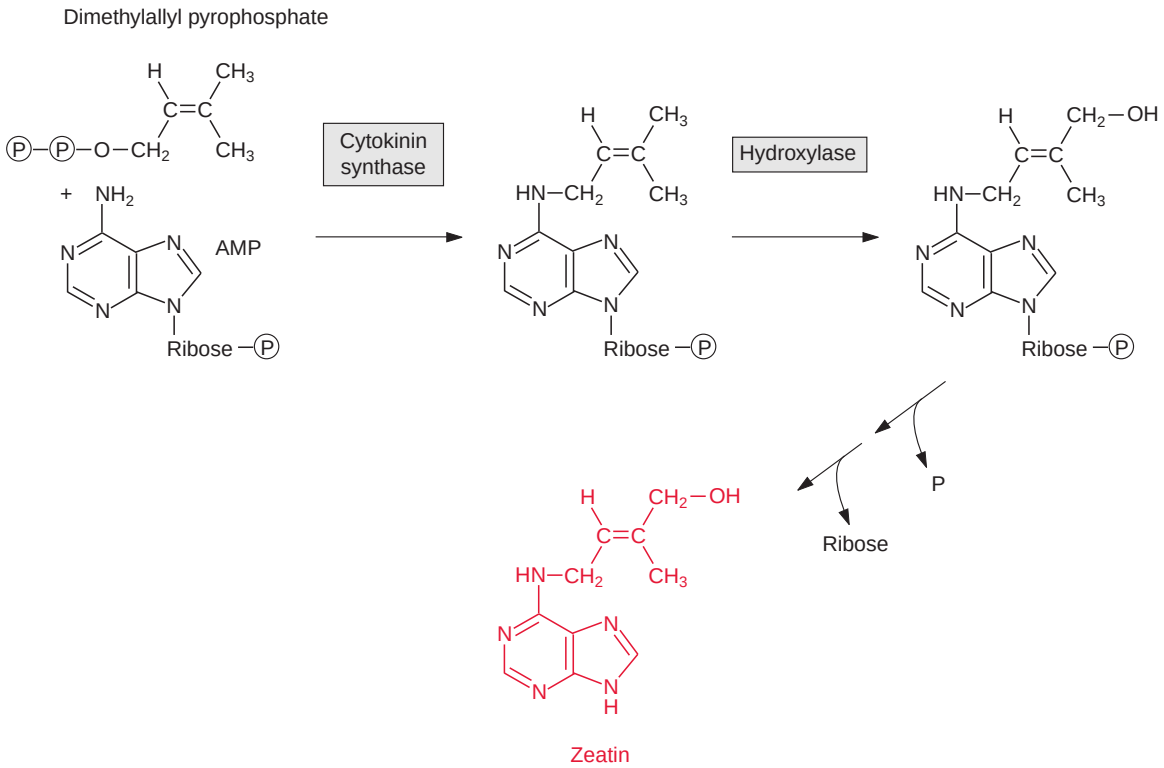

Figure 19.11 Synthesis of zeatin, a cytokinin.

19.6 Abscisic acid controls the water balance of the plant

When searching for what causes the abscission of leaves and fruits, **abscisic acid** (**ABA**) (Fig. 19.12) was found to be an inducing factor and was named accordingly. Later it turned out that the formation of the abscission layer for leaves and fruits is induced primarily by ethylene (section 19.7). An important function of the phytohormone ABA, however, is the induction of **dormancy** (endogenic rest) of seeds and buds. Moreover, ABA has a major function in maintaining the **water balance of plants**, since it induces with nitric oxide (**NO**) the closure of the stomata during water shortage (section 8.2). In addition, ABA prevents germination before the seeds are mature (vivipary). ABA deficient tomato mutants have wilting leaves and fruits, due to the disturbance of the water balance. In these wilting mutants, the immature seeds germinate within the tomato fruits while they are still attached to the mother plant.

ABA is a product of isoprenoid metabolism. The synthesis of ABA proceeds in two different ways via oxidation of **violaxanthin** (Fig. 19.12, see also Fig. 3.41). ABA synthesis occurs in leaves and also in roots, where water shortage would have a direct impact. ABA can be transported by the transpiration stream via the xylem vessels from the roots to the leaves, where it induces closure of the stomata (section 8.2).

In leaves, beside stoma closure ABA also causes rapid alterations in metabolism by influencing gene expression. Two ABA receptors have been identified, a soluble receptor named **FCA** (flowering time control) and a

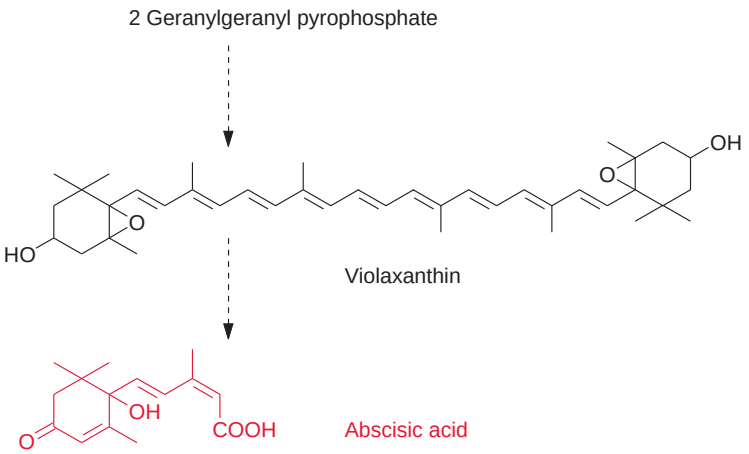

Figure 19.12 Abscisic acid is synthesized in several steps by the oxidative degradation of violaxanthin.

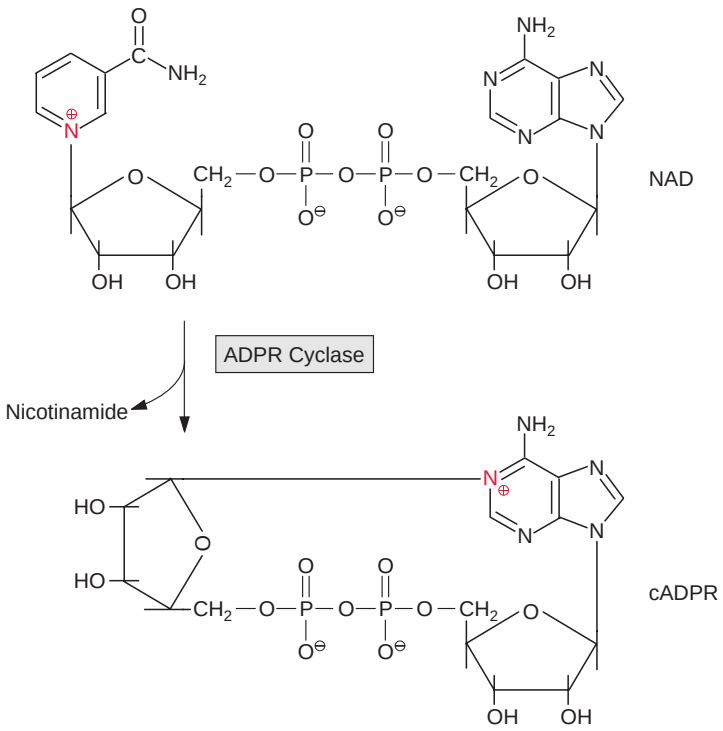

Figure 19.13 Cyclic ADP-ribose, a signaling component, causes Ca^{2+} ions to be released into the cytosol. This compound is ubiquitous in the plant and animal kingdoms. The synthesis of cyclic ADP-ribose from NAD^+ by an ADPR-cyclase: the ribose moiety (left side of the figure) is transferred from the positively charged N atom of the pyridine ring (nicotinamide) to the likewise positively charged N atom in the adenine ring.

membrane bound receptor **GRC2** (G-protein coupled receptor). The formation of the soluble FCA-ABA complex causes a delay in flowering. The ABA-GRC2 complex reacts with a G-protein (section 19.1). The release of a Gα-subunit regulates the K^+-dependent stoma closure and also embryo development. There is, however, yet another signal chain for ABA action involving the release of Ca^{2+} ions via the phosphoinositol pathway with the participation of phospholipase C (Fig. 19.13) and the signal component cyclic ADP ribose (cADPR, Fig. 19.13).

19.7 Ethylene makes fruit ripen

Ethylene is involved in the induction of **senescence**. During senescence, the degradation of leaf material is initiated. Proteins are degraded to amino acids, which, together with certain ions (e.g., Mg^{2+}), are withdrawn from the senescing leaves via the phloem for reutilization. In perennial plants, these substances are stored in the stem or in the roots, and in annual plants

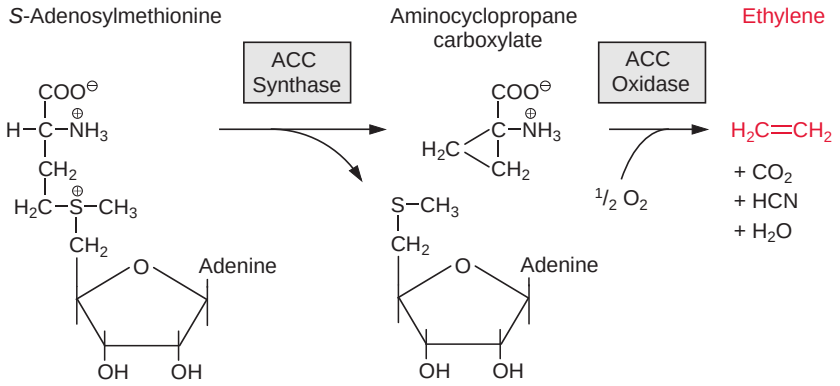

Figure 19.14 Synthesis of ethylene.

they are utilized to enhance the formation of seeds. Ethylene induces **defense reactions** after infection by fungi or when plants are wounded by feeding animals. As an example, the induction of the synthesis of tannins by ethylene in acacia as a response to feeding antelopes has been discussed in section 18.7.

In addition to stimulating the **abscission of fruit**, ethylene has a general function in **fruit ripening**. The ripening of fruit is to be regarded as a special form of senescence. The effect of gaseous ethylene can be demonstrated by placing a ripe apple and a green tomato together in a plastic bag; ethylene produced by the apple accelerates the ripening of the tomato. Bananas are harvested green and transported halfway around the world under conditions that suppress ethylene synthesis (low temperature, CO_2 atmosphere). Before being sold, these bananas are ripened by gassing them with ethylene. Also, tomatoes are often ripened only prior to sale by exposure to ethylene.

***S*-adenosylmethionine** (Fig. 12.10) is a biological methyl group donor as well as the precursor for the synthesis of ethylene (Fig. 19.14). The positive charge of the sulfur atom in *S*-adenosylmethionine enables its cleavage to form a cyclopropane, in a reaction catalyzed by **aminocyclopropane carboxylate synthase**, abbreviated **ACC synthase**. This enzyme limits the rate of ethylene biosynthesis. The fact that *Arabidopsis* contains eight genes for this enzyme illustrates its importance. The amount and stability (half life time 20 min–2 h) of ACC synthase is regulated by MAPK and CDPK phosphorylation (section 19.1). Subsequently, **ACC oxidase** catalyzes the oxidation of the cyclopropane to ethylene with the release of CO_2, HCN, and water. HCN is immediately detoxified by conversion to β-cyanoalanine (reaction not shown).

Genetic engineering has been employed to suppress ethylene synthesis in tomato fruits in two different ways. One possibility is to decrease the activities

of ACC synthase and ACC oxidase by antisense technique (section 22.5). Another alternative is the introduction of a bacterial gene into the plants, which encodes an ACC deaminase. This enzyme degrades the ACC in the tomato fruits so rapidly that consequently the ethylene levels are significantly reduced. The aim of this genetic engineering is to produce tomatoes that delay the ripening process during transport. It may be noted that transgenic tomato plants have also been generated, in which the durability of the harvested fruits is prolonged by an antisense repression of the polygalacturonidase, which is an enzyme that plays a role in lysing the cell wall.

The effect of ethylene is caused by an alteration of gene expression. Since ethylene, like other phytohormones, exerts its effect at very low concentrations (~10^{-9}mol/L), the **ethylene receptor** is expected to have a very high affinity. Like the cytokinin receptor, it consists of a dimer of **histidine receptor kinases**, each containing a histidine residue, which, after autophosphorylation, transfers the phosphate group to histidine or aspartyl residues of target proteins. By the binding of ethylene to the receptor dimer, in which a copper cofactor is involved, the kinase is inactivated and autophosphorylation is prevented. Depending on the phosphorylation state of the ethylene receptor, a signal is transmitted via protein kinase cascades, in which MAPKK and MAPK (section 19.1) participate. This activates signal cascade transcription factors which control the expression of certain genes. It may be noted that histidine kinases occur in plants, yeast, and bacteria, but not in animals.

The signal cascades of the action of ethylene, auxin, cytokinins, brassinosteroids, gibberellins, abscisic acid, and of abiotic stress are interwoven to a network.

19.8 Plants also contain steroid and peptide hormones

Brassinosteroids control plant development

For a long time many steroid hormones with a multitude of effects have been known in animals, but only recently was it discovered that steroid hormones also occur in plants. So-called **brassinosteroids** have essential functions as phytohormones**. Brassinolide** (Fig. 19.15) is the most well-known member of this phytohormone class. In the meantime more than 40 other polyhydroxylated steroids have been identified in plants. Brassinosteroids are synthesized via the isoprenoid biosynthesis pathway with the membrane lipid campesterol (Fig. 15.3) as intermediate. Brassinosteroids are contained

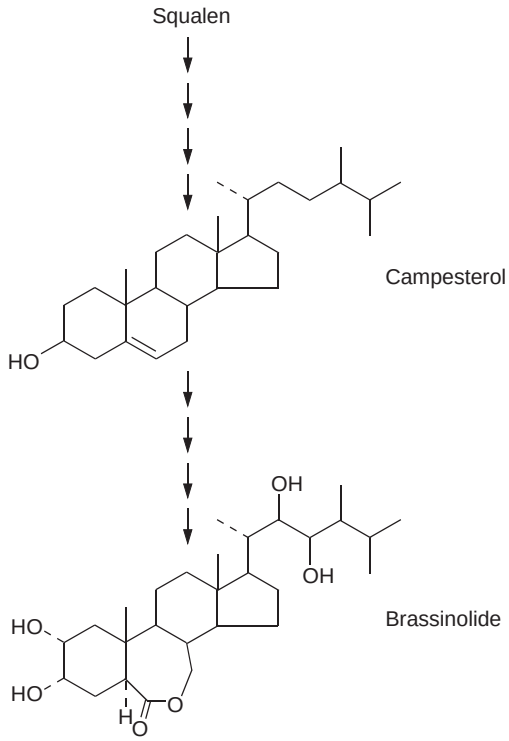

Figure 19.15 Brassinolide is synthesized from the membrane lipid campesterol via a series of synthesis steps involving cyt P_{450}-dependent hydroxylases, a reductase, and others. The synthesis pathway is very similar to the corresponding steroid synthesis pathways in animals.

in all plant organs and regulate the plant development in multiple ways. They stimulate the growth of the shoot, the unfolding of leaves, the differentiation of the xylem, retardation of root growth and the formation of anthocyans.

Brassinosteroids were first isolated from pollen. It was known that pollen contains a growth factor. In 1979 scientists from the US Department of Agriculture isolated from 40 kg of rape pollen collected by bees, 4 mg of a substance that they identified as brassinolide. Later, using very sensitive analysis techniques, it was shown that plants in general contained brassinolide and other brassinosteroids. The function of brassinosteroids as essential phytohormones was clearly established from the study of *Arabidopsis* mutants with developmental defects, such as **dwarf growth**, **reduced apical dominance**, and **lowered fertility**. The search for the defective gene responsible revealed that such mutations affected enzymes of the brassinolide synthesis pathway, which turned out to have very great similarities with

the synthesis pathway of animal steroid hormones. These developmental defects could not be prevented by the addition of "classic" phytohormones, but only by an injection of a nanomolar amount of brassinolide, as contained in plants. These results clearly demonstrated the essential function of brassinosteroids for the growth and development of plants.

In **animal cells**, steroid hormones bind to defined **steroid receptors**, which are present in the cytoplasm. Once activated, the receptor complex is transferred to the nucleus to promote or repress the expression of certain genes. It seems that plant steroids do not function in this way, as plants lack homologues of animal steroid receptors. In plants the steroid hormones associate with receptors bound to the plasma membrane. These receptors belong to the class of leucin rich repeat receptor-like kinases (**LRR-RLK**, section 19.1). Via a signal cascade, not fully resolved and involving several protein kinases and transcription factors, genes are activated which govern, e.g., cell modification, the synthesis of the cytoskeleton and the synthesis and transport of other phytohormones.

Polypeptides function as phytohormones

It is well known that small peptides, such as insulin and glucagon, have an important function in the intercellular communication in animals. Peptide hormones also play a role in plants. There is increasing evidence that plants contain secretory and nonsecretory peptides involved in the regulation of various aspects of plant growth (e.g., growth of callus and roots, organization of the meristem, nodule formation, self-incompatibility and defense reactions).

Systemin induces defense against herbivore attack

Many plants respond to insect attacks by accumulating **proteinase inhibitors**, which are toxic to insects because they impair their digestion of proteins. It was shown in tomato plants that the polypeptide **systemin**, consisting of 18 amino acids, is involved in defense reactions. In response to insect attack, a systemin precursor protein, consisting of 200 amino acids, is synthesized, and then processed by endoproteases to release the active polypeptide. Systemin is perceived by a membrane-bound receptor of very high affinity. A systemin concentration of as low as 10^{-10}mol/L is sufficient for a half saturation of the receptor. The receptor was identified as a receptor-like kinase (**RLK**) (section 19.1), similar to the LRR-RLK that binds brassinoid steroids. The binding of systemin induces a signal transduction chain involving Ca^{2+} calmodulin accumulation, the inactivation of an H^+-P-ATPase, the activation of MAPK protein kinases and of a phospholipase

(section 19.1). The latter catalyzes the release of linolenic acid from membrane lipids, which is a precursor for the synthesis of **jasmonic acid** (section 15.7). **Jasmonic acid** is a key signal in the transcription activation of defense-related genes (e.g., for the synthesis of proteinase inhibitor) (section 19.9). It may be noted that the effect of systemin is species specific. Systemin from tomato also affects potato and pepper, but it has no effect on the closely related tobacco or on other plants. Tobacco produces a systemin-like polypeptide, with a structure similar to the tomato systemin, and has analogous effects. It remains to be elucidated whether systemin-like polypeptide hormones may be involved in defense reactions of other plants.

Phytosulfokines regulate cell proliferation

A factor enhancing the proliferation of the cells was found in media of cell suspension cultures. This factor was isolated and identified as a pentapeptide, named **phytosulfokine** (PSK) containing two tyrosine residues, of which the hydroxyl group is esterified with sulfate:

PSK$_{\alpha}$: Tyr (SO_3H)-Ile-Tyr(SO_3H)-Thr-Gln

The *Arabidopsis* genome has five genes encoding phytosulfokine precursors consisting of about 80 amino acids and an N-terminal secretion signal. Phytosulfokines with identical structures occur in many plants and have, in addition to auxin and cytokinins, an important regulatory effect on the **dedifferentiation** of cells. Plant cells can retain the ability of totipotency, which means that cells can dedifferentiate so that they can reenter the cell cycle to form all the organs of a new plant. A receptor-like protein kinase (**RLK**) has been identified as a receptor for phytosulfokines and is probably connected via signal cascades to transcription factors regulating genes of dedifferentiation and proliferation.

A small protein causes the alkalization of cell culture medium

In the course of the isolation of systemin another peptide of 49 amino acids (deriving from a precursor of 115 amino acids) was identified that caused a rapid alkalization of the media of tobacco cell suspension cultures. This peptide was called **RALF** (rapid alkalization factor). The application of RALF in nanomolar concentrations resulted in a rapid activation of MAPK, the termination of root growth and the enlargement of meristematic cells. Homologues of RALF are found in many plant species. In

Arabidopsis, nine different RALF genes have been identified that are expressed in different organs of the plant. The ubiquity of RALF polypeptides suggests that they play a general role in plants, which remains to be elucidated.

Small cysteine-rich proteins regulate self-incompatibility

Self-incompatibility is a mechanism ensuring that the pollen does not self-fertilize or fertilizes the same or closely related plants. Various plants have different methods for excluding self-fertilization. In *Brassica* species, for example, **S-locus proteins** are involved, including SL glycoproteins (**SLG**), SL receptor kinases (**SRK**) and small proteins (**SCR**) of 74–81 amino acids. The application of only 50×10^{-12}mol of a recombinant SCR protein to a stigma resulted in the inhibition of the hydration of the pollen, which prevents it from being fertilized. It was also shown that SCR proteins interact with an RLK receptor kinase SLK, resulting in an autophosphorylation. Other elements of the signal cascade remain to be elucidated. Characteristic for the small SCR proteins are four disulfide linkages between cysteine residues C1 and C8, C2 and C5, C3 and C6, and C4 and C7.

19.9 Defense reactions are triggered by the interplay of several signals

Plants defend themselves against pathogenic bacteria and fungi by producing **phytoalexins** (section 16.1), and in some cases also by programmed cell death (**hypersensitive reaction**), in order to control an infection. Animals feeding on plants may stimulate the production of defense compounds, which make the plant poisonous or indigestible.

These various defense reactions are initiated by the interplay of several signal components in a network. After an attack by pathogens or as a response to abiotic stress, signal cascades, including the phosphoinositol cascade (section 19.1), are induced, which lead to an increase of the **Ca^{2+}**concentration in the cytosol, which activates the Ca^{2+}-dependent protein kinases (**CDK**). This in turn activates **protein kinase cascades**, which modulate gene expression via transcription factors (section 19.1). Moreover, in an early response, superoxide ($\bullet O_2^-$) and/or H_2O_2 (**r**eactive **o**xygen **s**pecies (**ROS**)) are synthesized by an NADPH oxidase located in the plasma membrane. The ROS represent chemical weapons for a direct attack on the pathogens, but they are also signal components for inducing signal cascades to initiate the production

of other defense compounds. H_2O_2 is involved in the lignification process (section 18.3) and thus plays a role in the solidification of the cell wall, another defense strategy against pathogens.

The formation of nitric oxide (**•NO**), a radical, is a further early response to pathogen attack. It is known as a signal component in animals and plants, and is released by the oxidation of arginine, which is catalyzed by nitric oxide synthase.

$$\text{Arginine} + O_2 + \text{NADPH} \xrightarrow{\textit{Nitric oxide synthase}} \text{Citrulline} + \text{NADP}^+ + \text{NO}$$

Alternatively, NO can be formed from nitrite in a side-reaction of the nitrate reductase (section 10.1).

$$NO_2^- + \text{NAD(P)H} + H^+ \xrightarrow{\textit{Nitrate reductase}} \text{NO} + H_2O + \text{NAD(P)}^+$$

NO is an important messenger in hormonal responses in plants and is involved in the defense against biotic and abiotic stress. NO is an important signal component that regulates, via cGMP and ADP ribose, Ca^{2+} channels to increase the cytoplasmic Ca^{2+} concentration from intracellular stores, and in this way activates signal cascades. In connection with MAPK cascades, it promotes the synthesis of phytoalexins and is involved in the initiation of programmed cell death. In addition to abscisic acid, it induces the opening of stomata (section 8.2).

A precise control of the NO concentration in the cell is needed for it to function as a signal component. The regulation of its synthesis is to a large extent still unknown. A glutathione-dependent formaldehyde dehydrogenase (FALDH) is involved in the control of the cellular NO concentration, by which NO is reversibly bound to glutathione. NO is eliminated by oxidation to nitrate.

Salicylic acid and jasmonic acid are signal molecules in pathogen defense

The biosynthesis of **salicylic acid** (**SA**) is described in section 18.2 and that of **jasmonic acid** (**JA**) in section 15.7. Jasmonic acid and salicylic acid are both involved in signal cascades induced during pathogen attack. SA plays a crucial role in defense responses against biotrophic pathogens (which keep the cell alive), and hemi-biotrophic pathogens (which initially keep the cell alive but kill them at a later stage). Mutants of transgenic tobacco plants,

where the synthesis of salicylic acid had been intercepted, proved to be very vulnerable to infections by biotrophic and hemi-biotrophic pathogens. Enzymes induced by salicylic acid include β1.3 glucanase, which digests the cell wall of fungi, and lipoxygenase, a crucial enzyme in the pathway of the synthesis of jasmonic acid (Figs. 15.29 and 15.30). JA and ethylene are involved in the defense against herbivorous insect and necrotrophic pathogens (which kill cells).

A number of components of the SA signaling cascade which regulate gene expression via transcription factors have by now been identified. Also for JA main signaling components are known, which interact with transcription factors. Both the SA and JA defense pathways contain different components, between which there is, however, positive and negative cross talk. Plant hormone signaling pathways are not isolated pathways but are interconnected with complex regulatory networks involving various defense signaling pathways and developmental processes. A better understanding of phytohormone-mediated plant defense responses is important in designing effective strategies for engineering crops for disease and pest resistance.

JAs are involved in diverse processes such as seed germination, root growth, tuber formation, tendril coiling, fruit ripening, leaf senescence and stomatal opening. Jasmonic acid regulates the **development of pollen** in some plants. *Arabidopsis* mutants, which are unable to synthesize jasmonic acid, cannot produce functioning pollen and therefore are **male-sterile**. The formation of **jasmonic acid** (e.g., induced by systemin) is regulated by a signal cascade involving **Ca^{2+} ions** and **MAP kinases**. Also in the perception of jasmonic acid a MAP kinase cascade regulating transcription factors appears to be involved. Jasmonic acid, its methylester and its precursor 12-oxo-phytodienoic acid (**OPDA**) play a central role in defense reactions. As a response to fungal infection, jasmonic acid induces the synthesis of **phenylammonium lyase** (**PAL**) (Fig. 18.2), the entrance enzyme of phenyl propanoid biosynthesis and **chalcone synthase** (**CHS**) (Fig.18.11), the key enzyme of flavonoid biosynthesis (see Chapter 18). As a response to wounding by herbivores, jasmonic acid causes plants to produce proteinase inhibitors. As a response to mechanical stress (e.g., by wind), jasmonic acid triggers the elevated growth in the thickness of stems or tendrils to make the plants more stable.

In many cases an attack by herbivores initiates defense responses not only in the wounded leaves, but also in more distant parts of a plant (**systemic response**). This requires a long-distance transport of signal substances within the plant. Recent results indicate that **jasmonic acid** and **methyl jasmonate** function as such a **systemic wound signal** in establishing a systemic acquired resistance (**SAR**). Also **methyl salicylate** is responsible for a long-distance signal transfer.

19.10 Light sensors regulate growth and development of plants

Light controls plant development from germination to the formation of flowers in many different ways. Important light sensors are the **phytochromes** which sense red light. Phytochromes are involved when light initiates the germination and greening of the seedling and in the adaptation of the photosynthetic apparatus of the leaves to full sunlight or shade. Five different phytochromes (A–E) have been identified in the model plant *Arabidopsis thaliana* (section 20.1). Plants also have photoreceptors for blue and UV light for their adaptation to the full spectrum of sunlight. So far, three proteins have been identified as blue light receptors; these are **cryptochromes** 1 and 2, each comprising a flavin (Fig. 5.16) and a pterin (Fig. 10.3); and **phototropin**, containing one flavin as a blue light-absorbing pigment.

Phytochromes function as sensors for red light

Since the structure and function of **phytochromes** have been studied extensively in the past, they offer a good example for a detailed discussion on the problems of signal transduction in plants. Phytochromes are soluble **dimeric proteins**. The monomer consists of an apoprotein (molecular mass 120–130 kDa) with six domains (Fig. 19.16A). The first three domains represent the photosensoric part of the protein. These domains are also present in bacterial and fungal phytochromes. The remaining domains 4, 5, and 6 form the regulatory part. Plant phytochromes contain a sequence at the N-terminus of the apoprotein, which is involved in the Pfr → Pr conversion. Domain 6 possesses a kinase which binds ATP and catalyzes an autophosphorylation of the phytochrome. Domain 2 contains an open chain tetrapyrrole that is linked to the protein via a sulfhydryl group of a cysteine residue. It is the chromophore of the holoprotein (Fig. 19.16B). The autocatalytic binding of the tetrapyrrole to the apoprotein results in the formation of a phytochrome

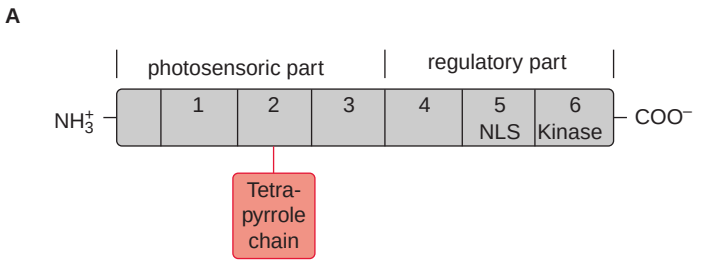

Figure 19.16A Structure of a phytochrome. The apoprotein is composed of 6 domains; domains 1–3 represent the photosensoric part and domains 4–6 the regulatory part. The chromophore, an open tetrapyrrole chain, is linked to domain 2. Domain 6 comprises a Ser/Thr kinase.

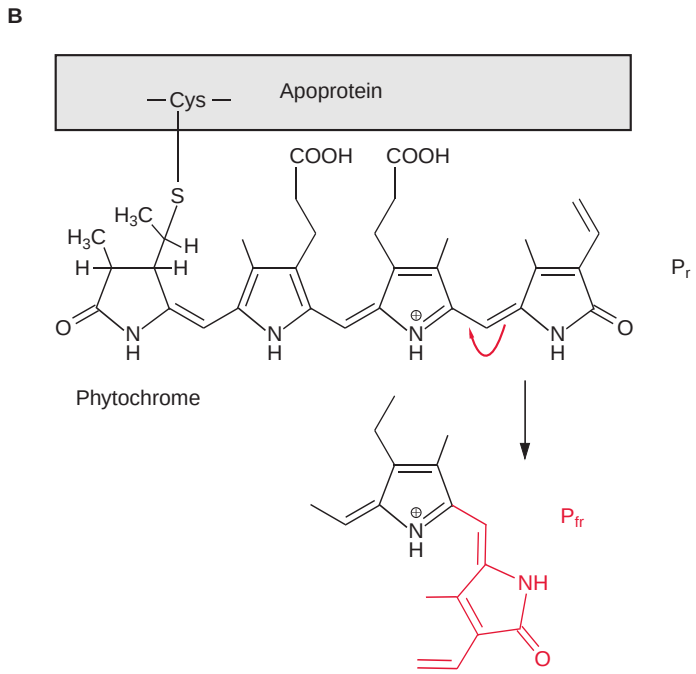

Figure 19.16B The chromophore of a phytochrome consists of an open tetrapyrrole chain, which is linked via a thioether bond to the apoprotein. The absorption of red light results in a *cis-trans*-isomerization of a double bond, causing a change in the position of one pyrrole ring (colored red).

P_r (r = red) with an absorption maximum at about 660 nm (**red light**) (Fig. 19.17). The absorption of this light results in a change in the chromophore; a double bond between the two pyrrole rings changes from the ***trans***- to the ***cis***-configuration (colored red in Fig. 19.16B), which subsequently changes the conformation of the protein. The phytochrome in this new conformation has an absorption maximum at about 730 nm (**far-red light**) named **P_{fr}**, representing the active form of the phytochrome. It reflects the state of illumination. P_{fr} is reconverted to P_r by the absorption of far-red light. Since the light absorption of P_r and P_{fr} overlaps (Fig. 19.17), depending on the color of the irradiated light, a reversible equilibrium between P_r and P_{fr} is attained. Thus, with light of 660 nm, 88% of the total phytochromes are present as P_{fr} and at 720 nm, only 3% is in the P_{fr} form. In bright sunlight, where the red component is stronger than the far-red component, the phytochrome is present primarily as P_{fr} and indicates the state of illumination to the plant.

Whereas the inactive form of phytochrome (P_r) has quite a long lifetime (~100 h), the active form (P_{fr}) is converted within 30 to 60 minutes. P_{fr} can be recovered by a reversal of its formation (Fig. 19.18). In the case of phytochrome A, however, the light absorption can be terminated by conjugation of P_{fr} with **ubiquitin**, which marks it for proteolytic degradation by the **proteasome pathway** (section 21.4).

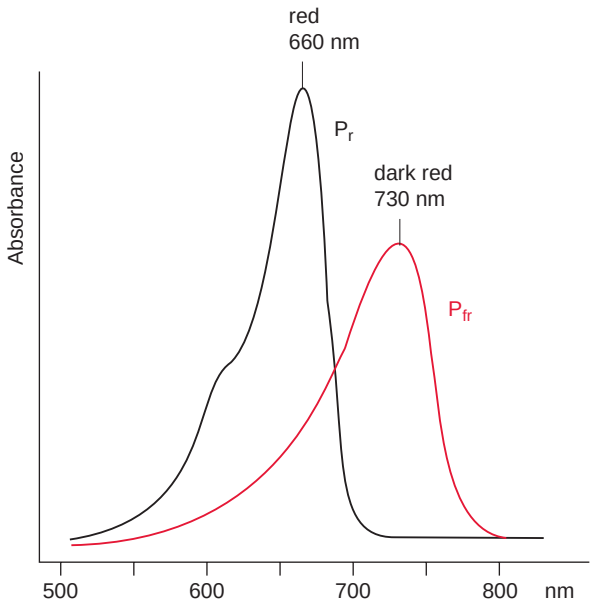

Figure 19.17 Absorption spectra of the two forms of phytochrome A, P_r and P_{fr}.

Phytochromes undergo a photoconversion upon illumination with red and far-red light. In addition to this, phytochromes are transferred between the cytosol and the nucleus. The C-terminal domain 5 (Fig. 19.16A) contains a **nuclear localization signal** (**NLS**) that is responsible for targeting to the nucleus. Under the influence of light the protein kinase of domain 6 causes an autophosphorylation of the protein. This phosphorylation releases the phytochrome from a cytosolic anchor and the NLS domain is uncovered. This allows the migration of the P_{fr} form of phytochrome into the nucleus, where it associates with factors, such as the **phytochrome interacting factor** (**PIF3**) and other transcription factors to affect **gene expression** (Fig. 19.18). It has been shown that phytochrome A affects the transcription of **10% of all genes** in *Arabidopsis*. This effect of phytochromes is modulated by phytohormones, such as cytokinins and brassinosteroids, and the signal cascades of pathogen defense. Light sensors, phytohormones, and defense reactions appear to be interwoven in a **cellular network**.

Phytochrome A, having been most thoroughly investigated, has an absorption maximum at far-red light and is instable in light, whereas the other phytochromes (B–E) are light stable. Phytochrome A often forms homodimers, while the other phytochromes aggregate to heterodimers. The functions of phytochromes B–E have still to be resolved in detail.

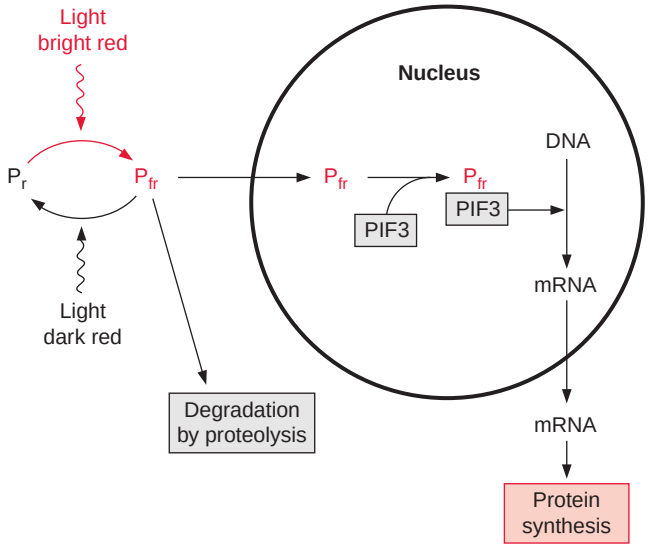

Figure 19.18 Phytochrome A influences gene expression. Phytochrome is converted by irradiation with red light to the active form P_{fr} and is reconverted by far-red light to the inactive P_r. P_{fr} enters the nucleus, where it binds to a transcription factor PIF3. The P_{fr}-PIF3-complex regulates gene expression by binding to promoter regions of the DNA. P_{fr} can also be irreversibly degraded by proteolysis.

Phototropin and cryptochromes are blue light receptors

Light sensors such as phototropin and cryptochrome are present in plant cells in order to use the blue spectrum (320–500 nm) of the sun efficiently. Blue light induces stoma opening, the elongation of the hypocotyls and the chloroplast movement. At low blue light intensity the chloroplasts move to that part of the cell exposed to the light in order to optimize light harvesting, whereas at higher blue light intensity the chloroplasts retreat from the light source to avoid destruction by excessive light.

Phototropin was first isolated in 1997 from pea cotyledons that had been irradiated with blue light, and was found to be ubiquitous in higher plants. The protein structure of phototropin shows similarities to the structure of phytochromes. As in phytochromes the photosensor is located at the N-terminal region which contains a flavine mononucleotide (FMN) (Fig. 5.16) as light absorbent. Moreover, there is a serine/threonine kinase at the C-terminal region, catalyzing the autophosphorylation of the protein. In the dark FMN is associated noncovalently (Fig. 19.19). Upon illumination the FMN is covalently bound within microseconds to a cysteine residue that changes the absorption maximum of the flavine from 447 nm to 390 nm. This induces the kinase at the C-terminal region to catalyze the autophosphorylation of 8 serine residues, converting the phototropin into an active state. In the dark the FMN is released again, the phosphate groups are split off by hydrolysis, presumably by a phosphatase, and the phototropin returns within 10–100 s to the inactive ground state.

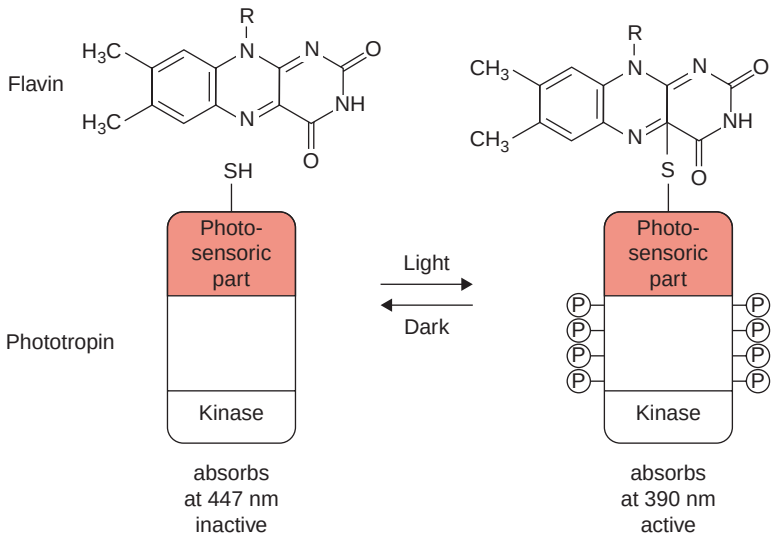

Figure 19.19 Action mode of phototropin. FMN, the chromophore of phototropin, is in the dark noncovalently bound to the protein and absorbs light of 447 nm. Illumination activates FMN to enter a covalent bond with a cysteine residue of the photosensoric part of phototropin. This induces an autophosphorylation of the protein resulting in the activation of phototropin.

Cryptochromes also absorb blue light but are not structurally related to phototropin. They derive from microbial DNA repair enzymes, so-called photolyases. They are flavoproteins influencing many processes in plants, such as hypocotyl and stem elongation, regulation of flowering time and anthocyan accumulation. Details of the interplay of the two blue light receptors, phototropins and cryptochromes, in plant development and metabolism are still largely unknown.

Further reading

Apel, K. Reactive oxygen species: metabolism, oxidative stress, and signal transduction. Annual Review Plant Biology 55, 373–399 (2004).

Badescu, G. O., Napier, R. M. Receptors for auxin: Will it all end in TIRs? Trends in Plant Science 11, 217–223 (2006).

Bari, R., Jones, J. D. G. Role of plant hormones in plant defence responses. Plant Molecular Biology 69, 473–488 (2009).

Batstic, O., Kudla, J. Integration and channelling of calcium signalling through the CBL calcium sensor/CIPK protein kinase network. Planta 219, 915–924 (2004).

Beckers, G. J. M., Spoel, S. H. Fine-tuning plant defense signaling: Salicylate versus jasmonate. Plant Biology 8, 1–10 (2006).

Bonetta, D., McCourt, P. A receptor for gibberellin. Nature 437, 62–628 (2005).

Boudsocq, M., Lauriere, C. Osmotic signalling in plants. Multiple pathways mediated by emerging kinase families. Plant Physiology 138, 1185–1194 (2005).

Callis, J. Auxin action. Nature 435, 436–437 (2005).

Chae, H. S., Kieber, J. J. Eto brute? Role of ACS turnover in regulated ethylene biosynthesis. Trends in Plant Science 10, 291–296 (2005).

Christie, J. M. Phototropin blue-light receptors. Annual Review Plant Biology 58, 21–45 (2007).
Christian, M., Steffens, B., Schenk, D., et al. How does auxin enhance cell elongation? Roles of auxin-binding proteins and potassium channels in growth control. Plant Biology 8, 346–352 (2006).
Christman, A., Moes, D., Himmelbach, A., et al. Integration of abscisic acid signaling into plant responses. Plant Biology 6, 314–325 (2006).
Etheride, N., Hall, B. P., Schaller, G. E. Progress report: Ethylene signaling and responses. Planta 223, 387–391 (2006).
Josse, E. M., Foreman, J., Halliday, KJ. Paths through the phytochrome network. Plant Cell Environment 31, 667–678 (2008).
Kang, B., Grancher, N., Koyffmann, V., et al. Multiple interactions between cryptochrome and phototropin blue-light signaling pathways in *Arabidopsis thaliana*. Planta 227, 1091–1099 (2008).
Kramer, E. M., Bennett, M. J. Auxin transport: a field in flux. Trends in Plant Science 11, 382–386 (2006).
Lamotte, O., Courtois, C., Barnavon, L. Nitric oxide in plants: The biosynthesis and cell signalling properties of a fascinating molecule. Planta 221, 1–4 (2005).
Lange, M. J. P., Lange, T. Gibberellin biosynthesis and the regulation of plant development. Plant Biology 8, 281–290 (2006).
Li, J., Jin, H. Regulation of brassinosteroid signaling. Trends in Plant Science 12, 37–41 (2006).
Liu, X., Yue, Y., Li, B., et al. A G protein-coupled receptor is a plasma membrane receptor for the plant hormone abscisic acid. Science 315, 1712–1716 (2007).
Matsubayashi, Y., Sakagami, Y. Peptide hormones in plants. Annual Review Plant Biology 57, 649–674 (2006).
Müssig, C. Brassinosteroid-promoted growth. Plant Biology 7, 110–117 (2005).
Nakagami, H., Pitzschke, A., Hirt, H. Emerging MAP kinase pathways in plant stress signaling. Trends in Plant Science 10, 339–346 (2005).
Nambara, E., Marion-Poll, A. Abscisic acid biosynthesis and catabolism. Annual Review Plant Biology 56, 165–185 (2005).
Pollmann, S., Müller, A., Weile, E. W. Many roads lead to "Auxin": of nitrilases, synthases, and amidases. Plant Biology 8, 326–333 (2006).
Rockwell, N. C., Su, Y. S., Lagarias, J. C. Phytochrome structure and signaling mechanisms. Annual Review Plant Biology 57, 837–858 (2006).
Sagi, M., Fluhr, R. Production of reactive oxygen species by plant NADPH oxidase. Plant Physiology 141, 336–340 (2006).
Sakakibara, H. Cytokinins: Activity biosynthesis and translocation. Annual Review Plant Biology 57, 431–449 (2006).
Sakomota, T., Morinaka, Y., Ohnishi, T., et al. Erect leaves caused by brassinosteroid deficiency increase biomass production and grain yield in rice. Nature Biotechnology 24, 105–109 (2006).
Shen, Y. Y., Wang, X. F., Wu, F. Q., et al. The Mg-chelatase H subunit is an abscisic acid receptor. Nature 443, 823–826 (2006).
Temple, B. R. S., Jones, A. M. The plant heterotrimeric G-protein complex. Annual Review Plant Biology 58, 249–266 (2007).
Ueguchi-Tanaka, M., Nakajima, M., Motoyuki, A., Matsuoka, M. Gibberellin receptor and its role in gibberellin signaling in plants. Annual Review Plant Biology 58, 183–198 (2007).

Vieten, A., Sauer, M., Brewer, P. B., Friml, J. Molecular and cellular aspects of auxin-transport-mediated development. Trends in Plant Science 12, 160–168 (2007).

Zarate, S. I., Kempema, L. A., Walling, L. L. Silverleaf whitefly induces salicylic acid defenses and suppresses effectual jasmonic acid defenses. Plant Physiology 143, 866–875 (2007).

20

A plant cell has three different genomes

A plant cell contains three genomes: in the **nucleus**, the **mitochondria** and the **plastids**. Table 20.1 lists the size of the three genomes in three plant species and, in comparison, the two genomes in humans. The size of the genomes is given in base pairs (bp). As discussed in Chapter 1, the genetic information of the mitochondria and plastids is located on one or sometimes several circular double strand (ds) DNA, with many copies present in each organelle. During cell division and organelle reproduction, these copies are distributed randomly between the daughter organelles. Each cell contains a large number of plastids and mitochondria, which are also randomly distributed during cell division between both daughter cells. The genetic information of mitochondria and plastids is predominantly maternally inherited from generation to generation, and the large number of inherited gene copies protects against mutations. The structures and functions of the plastid and mitochondrial genomes are discussed in sections 20.6 and 20.7.

Table 20.1: Size of the genome in plants and in humans

	Arabidopsis thaliana	*Zea mays* (maize)	*Vicia faba* (broad bean)	*Homo sapiens* (human)
	Number of nucleotide pairs in a single genome			
Nucleus (haploid chromosome set)	7×10^7	390×10^7	$1{,}450 \times 10^7$	280×10^7
Plastid	156×10^3	136×10^3	120×10^3	
Mitochondrium	370×10^3	570×10^3	290×10^3	17×10^3

20.1 In the nucleus the genetic information is divided among several chromosomes

For almost the whole of their developmental cycle, eukaryotic cells, as they are **diploid**, normally contain two chromosome sets, one set from the mother and the other set from the father. Only the generative cells (e.g., egg, pollen) are **haploid**, that is, they possess just one set of chromosomes. The DNA of the genome is replicated during the interphase of mitosis and generates in this way a quadruple chromosome set. During the anaphase, this set is distributed by the spindle apparatus to two opposite poles of the cell. Thus, after cell division, each daughter cell contains a double chromosome set and is diploid again. **Colchicine**, an alkaloid from the autumn crocus, inhibits the spindle apparatus and thus interrupts the distribution of the chromosomes during the anaphase. In such a case, all the chromosomes of the mother cell can end up in only one of the daughter cells, which then possesses four sets of chromosomes, to render it **tetraploid**. Infrequently this tetraploidy occurs spontaneously due to mitosis malfunction.

Tetraploidy is often stable and is then inherited by the following generations via somatic cells. Hexaploid plants can be generated by crossing tetraploid plants with diploid plants, although this is seldom successful. Tetraploid and hexaploid (polyploid) plants often show a higher growth rate, and this is why many polyploid crop plants are profitable in agriculture. Polyploid plants can also be generated by protoplast fusion, a method that can produce hybrids between two different breeding lines. When very different species are crossed, the resulting diploid hybrids are often sterile due to incompatibilities in their chromosomes. In contrast, polyploid hybrids generally are fertile.

The chromosome content of various plants is listed in Table 20.2. The crucifer ***Arabidopsis thaliana*** (Fig. 20.1), an inconspicuous weed growing at the roadside in central Europe, has only 2×5 chromosomes with altogether just 7×10^7 base pairs (Table 20.1). *Arabidopsis* corresponds in all details to a typical dicot plant and, when grown in a growth chamber, has a lifecycle of only six weeks. The breeding of a defined line of *Arabidopsis thaliana* by the botanist Friedrich Laibach (Frankfurt) in 1943 marked the beginning of the worldwide use of *Arabidopsis* as a model plant for the investigation of the functions of genes and the interplay of the gene products. By now the genome of *Arabidopsis thaliana* has been completely sequenced.

The often much higher number of chromosomes that can be found in other plants is in part the result of a gene combination. Hence, rape seed (*Brassica napus*) with 2×19 chromosomes is a crossing of *Brassica rapa*

Table 20.2: Number of chromosomes

n: Ploidy *m*: Number of chromosomes in the haploid genome	$n \times m$
A. Dicot plants	
Arabidopsis thaliana	2×5
Vicia faba (broad bean)	2×6
Glycine maximum (soybean)	2×20
Brassica napus (rape seed)	2×19
Beta vulgaris (sugar beet)	6×19
Solanum tuberosum (potato)	4×12
Nicotiana tabacum (tobacco)	4×12
B. Monocot plants	
Zea mays (maize)	2×10
Hordeum vulgare (barley)	2×7
Triticum aestivum (wheat)	6×7
Oryza sativa (rice)	2×12

Figure 20.1 *Arabidopsis thaliana*, an inconspicuous small weed, growing in central Europe at the roadsides, from the family *Brassicaceae* (crucifers), has become the most important model plant worldwide, because of its small genome. In the growth chamber with continuous illumination, the time from germination until the formation of mature seed is only six weeks. The plant reaches a height of 30 to 40 cm. Each fruit contains about 20 seeds. (By permission of M.A. Estelle and C.R. Somerville.)

(2 × 10 chromosomes) and *Brassica oleracea* (2 × 9 chromosomes) (Table 20.2). In this case, a diploid genome is the result of crossing. In wheat, on the other hand, the successive crossing of three wild forms resulted in hexaploidy: Crossing of einkorn wheat and goat grass (2 × 7 chromosomes each) resulted in wild emmer wheat (4 × 7 chromosomes), and this crossed with another wild wheat resulted in the wheat (*Triticum aestivum*) with 6 × 7 chromosomes which is cultivated nowadays. Tobacco (*Nicotiana tabacum*) is also a cross between two species (*Nicotiana tomentosiformis* and *N. sylvestris*), each with 2 × 12 chromosomes.

The nuclear genome of broad bean with 14.5×10^9 nucleotide pairs has a 200-fold higher DNA content than *Arabidopsis*. However, this does not mean that the number of protein-encoding genes (structural genes) in the broad bean genome is 200-fold higher than in *Arabidopsis*. Presumably the number of structural genes in both plants does not differ by more than a factor of two to three. The difference in the size of the genome is due to a different number of identical DNA sequences of various sizes arranged in sequence, termed **repetitive DNA**, of which a very large part may contain no encoding function at all. In broad bean, for example, 85% of the DNA represents repetitive sequences. This includes the **tandem repeats**, a large number (sometimes thousands) of identical repeated DNA sequences (of a unit size of 170–180 bp, sometimes also 350 bp). The tandem repeats are spread over the entire chromosome, often arranged as blocks, especially at the beginning and the end of the chromosome, and sometimes also in the interior. This highly repetitive DNA is called **satellite DNA**. This also includes microsatellite DNA, which is discussed in section 20.3. Its sequence is genus or even species specific. In some plants, more than 15% of the total nuclear genome consists of satellite DNA. Perhaps it plays a role in the segregation of species. The sequence of the satellite DNA can be used as a species-specific marker in generating hybrids by protoplast fusion in order to check the outcome of the fusion in cell culture. The polymorphism of satellite DNA is also used for identifying human genomes in criminal cases.

The genes for ribosomal RNAs also occur as repetitive sequences and, together with the genes for some transfer RNAs, are present in the nuclear genome in several thousand copies.

In contrast, structural genes are present in only a few copies, sometimes just one (**single-copy gene**). Structural genes encoding for structurally and functionally related proteins with a high nucleotide identity often form a **gene family**. Such a gene family, for instance, is formed by the genes for the small subunit of the ribulose bisphosphate carboxylase, which exist several times in a slightly modified form in the nuclear genome (e.g., five times in tomato). So far 14 members of the light harvesting complex (LHC) gene family (section 2.4) have been identified in tomato. Zein, which is present

in maize kernels as a storage protein (Chapter 14), is encoded by a gene family of about 100 genes. In *Arabidopsis* almost 40% of the proteins predicted from the genome sequence belong to gene families with more than five members, and 300 genes have been identified that encode P_{450} proteins (see section 18.2).

The DNA sequences of plant nuclear genomes have been analyzed

It was a breakthrough in the year 2000 when the entire nuclear genome of *Arabidopsis thaliana* was completely sequenced (157 Mb). The sequence data revealed that the nuclear genome contains about **26,800 structural genes**, twice as many as in the insect *Drosophila*. A comparison with known DNA sequences from animals showed that about one-third of the *Arabidopsis* genes are plant specific. By now the rice, poplar and moss genome have been sequenced (rice: 490 Mb, ca. 32,000 genes, poplar: 485 Mb ca. 45,600 genes, *Physcomitrella patens*: 511 Mb, ca. 28,000 genes).

The function of many of these genes is not yet known. The elucidation of these functions is a great challenge. One approach to solve this is a comparison of sequence data with identified sequences from microorganisms, animals, and plants, available in data banks, by means of **bioinformatics**. Another way is to eliminate the function of a certain gene by mutation and then investigate its effect on metabolism. A gene function can be eliminated by random mutations (e.g., by Ti-plasmids) (section 22.5) (**T-DNA insertion mutant**). In this case, the mutated gene has to be identified. Alternatively, defined genes can be mutated by the **RNAi technique**, as discussed in section 22.5. All these investigations require an automated evaluation with a very high technical expenditure. The project Arabidopsis 2010 (USA) and the German partner program AFGN (*Arabidopsis* functional genomics network) aim to fully elucidate the function of the *Arabidopsis* genome by the year 2010.

20.2 The DNA of the nuclear genome is transcribed by three specialized RNA polymerases

Of the two DNA strands, only the **template strand** is transcribed (Fig. 20.2). The DNA strand complementary to the template strand is called the **coding strand**. The latter has the same sequence as the transcription product RNA, with the exception that it contains thymine instead of uracil. The DNA of

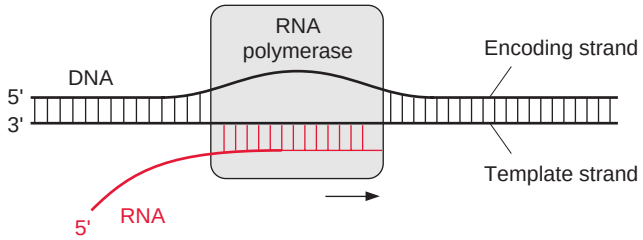

Figure 20.2 The template strand of DNA is transcribed.

Table 20.3: Three RNA polymerases

RNA-polymerase	Transcript	Inhibition by α-amanitin
Type I	Ribosomal RNA (5,8S-, 18S-, 25S-rRNA)	None
Type II	Messenger-RNA-precursors, small RNA (snRNA)	In concentrations of ca. 10^{-8} mol/L
Type III	Transfer-RNA, ribosomal RNA (5S-rRNA)	Only at higher concentrations (10^{-6} mol/L)

the nuclear genome is transcribed by **three specialized RNA polymerases (I, II, and III)** (Table 20.3). The division of labor between the three RNA polymerases, along with many details of the gene structure and principles of gene regulation, are valid for all eukaryotic cells. RNA polymerase II catalyzes the transcription of the structural genes and is strongly inhibited by **α-amanitin** at a concentration as low as 10^{-8} mol/L. α-Amanitin is the deadly poison from the toadstool *Amanita phalloides* (also called death cap). People frequently die from eating this toadstool.

The transcription of structural genes is regulated

In a plant containing about 25,000 to 50,000 structural genes, most of these genes are transcribed only in certain organs and then often only in certain cells. Moreover, many genes are only transcribed at specific times (e.g., the genes for the synthesis of phytoalexins after pathogenic infection) (section 16.1). Therefore the transcription of most structural genes is subject to very complex and specific regulation. The genes for enzymes of metabolism or protein biosynthesis, which proceed in all cells, are transcribed more often. These genes, which every cell needs for such basic functions, independent of its specialization, are called **housekeeping genes**.

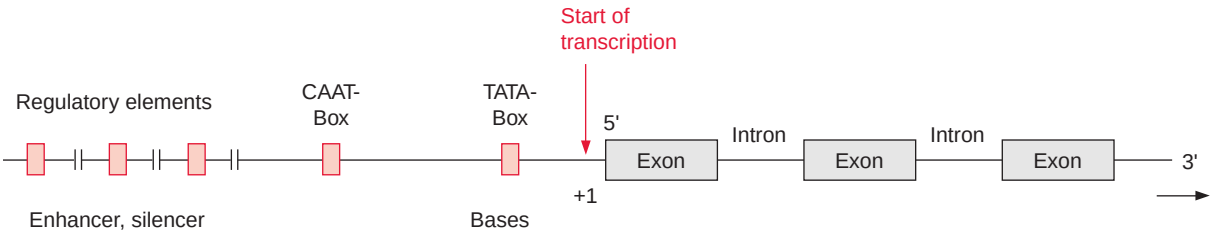

Figure 20.3 Sequence elements of a eukaryotic gene. +1 marks the first nucleotide of the newly synthesized mRNA. Arrow indicates the direction of transcription.

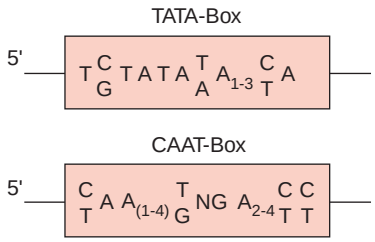

Figure 20.4 Consensus sequences for two promoter elements of the eukaryotic gene (see Fig. 20.3).

Promoter and regulatory sequences regulate the transcription of genes

Figure 20.3 shows the basic design of a structural gene. The section of the DNA on the left of the transcription starting point is termed 5′ or upstream and that to the right is referred to as 3′ or downstream. The encoding region of the gene is distributed among several exons, which are interrupted by introns.

About 25 bp upstream from the transcription start site is situated a **promoter element**, which is the position where RNA polymerase II binds. The sequence of this promoter element can vary greatly between genes and between species, but it can be depicted as a **consensus sequence**. (A consensus sequence is an idealized sequence in which each nucleotide is found in the majority of the sequences. Most of the promoter elements differ in their DNA sequences by only one or two nucleotides from this consensus sequence.) This consensus sequence is named the **TATA box** (Fig. 20.4). Another consensus sequence, the **CAAT box**, is often found about 80 to 110 bp upstream (Fig. 20.4). The housekeeping genes mentioned earlier often contain a C-rich region instead of the CAAT box. Additionally, sometimes more than 1,000 bp upstream, several sequences can be present, which function as **enhancer** or **silencer** (***cis*-regulatory elements**).

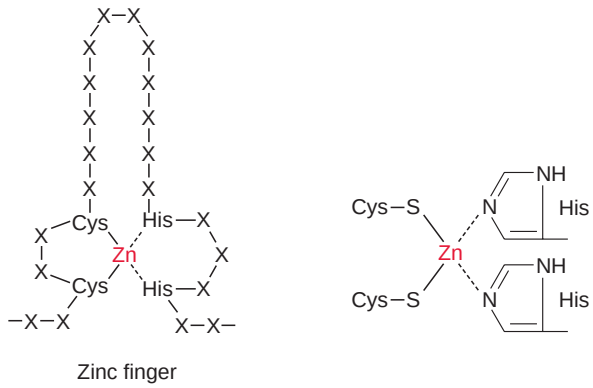

Zinc finger

Figure 20.5 Many transcription factors have the structure of a zinc finger. An amino acid sequence (X = amino acid) comprising 2 cysteine residues separated by 2 to 4 other amino acids, followed by 12 amino acids, 2 histidine residues, which are separated from each other by 3 to 4 amino acids. A zinc ion is bound between the cysteine and the histidine residues. A transcription factor contains 3 to 9 such zinc fingers, and each finger can bind to a sequence of 3 nucleotides on the DNA.

Transcription factors regulate the transcription of a gene

The regulatory elements contain binding sites for **transcription factors** (trans-factors), which are proteins modifying the rate of transcription. It has been estimated that the *Arabidopsis* genome encodes 1,500 factors for the regulation of gene expression. Different transcription factors often have certain structures in common. One type of transcription factor consists of a peptide chain comprising two cysteine residues and, separated from these by 12 amino acids, two histidine residues (Fig. 20.5). The two cysteine residues bind covalently to a zinc atom, which is also coordinatively bound to the imidazole rings of two histidine residues, thus forming a so-called **zinc finger**. Such a finger binds to a nucleotide triplet of a DNA sequence. Zinc finger transcription factors usually possess several (up to nine) fingers and so are able to cling tightly to certain DNA sections.

Another type of transcription factor is a dimer of DNA binding proteins, where each monomer comprises a DNA binding domain and an α-helix with three to nine leucine residues (Fig. 20.6). The hydrophobic leucine residues of the two α-helices are arranged in the dimer in such a way that they are exactly opposite each other like a zipper and both helices are held together by hydrophobic interaction. This typical structure of a transcription factor has been named the **leucine zipper**. The activity of transcription factors is frequently regulated by signal chains linked to the perception of phytohormones or other stimuli (section 19).

Small (sm)RNAs inhibit gene expression by inactivating messenger RNAs

smRNAs, consisting of 21–24 nucleotides regulate the expression of genes that are involved in responses to stress and insufficient supply of nutritients.

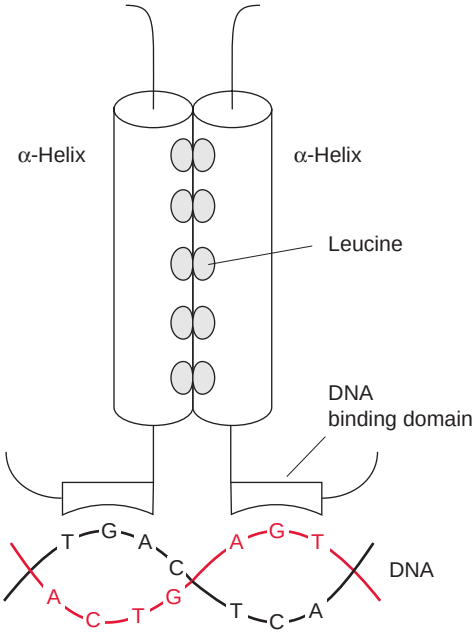

Figure 20.6 A frequent structural motif of transcription factors is the leucine zipper. The factor is a dimer where the two polypeptide chains contain a leucine residue at about every seventh position within an α-helix. The leucine residues, which are all located at one side of the α-helix, hold the two α-helices together due to hydrophobic interactions, similar as in the manner of a zipper. The two DNA binding domains contain basic amino acids, which enable binding to the DNA. Simplified presentation.

Several smRNA types (miRNA, siRNA, nat-siRNA, and pre-miRNA) bind to complementary sequences of target mRNAs to form a double-strand RNA (**dsRNA**). This leads to the degradation of mRNA by RNAse II (**Dicer**) and other RNA degrading enzymes, which ultimately results in an inhibition of translation. In this way smRNAs function as negative regulators that interfere specifically with plant development. This property is utilized in biotechnology to suppress the expression of a certain gene by the so-called RNA interference (**RNAi**) technique. Plants can be made to synthesize a small RNA complementary to a defined mRNA by gene modification. The RNAi technique is also used to identify the function of a certain gene, by inhibiting its expression and evaluating the effects to the plant. In 2006 Andy Fire and Craig Mello (USA) were awarded the Nobel Prize for their basic studies of the RNAi technique.

The transcription of structural genes requires a complex transcription apparatus

RNA polymerase II consists of 8 to 14 subunits, but, on its own, it is unable to start transcription. Transcription factors are required to direct the enzyme to the start position of the gene. The **TATA binding protein**, which recognizes the TATA box and binds to it, has a central function in transcription (Fig. 20.7). The interaction of the TATA binding protein with

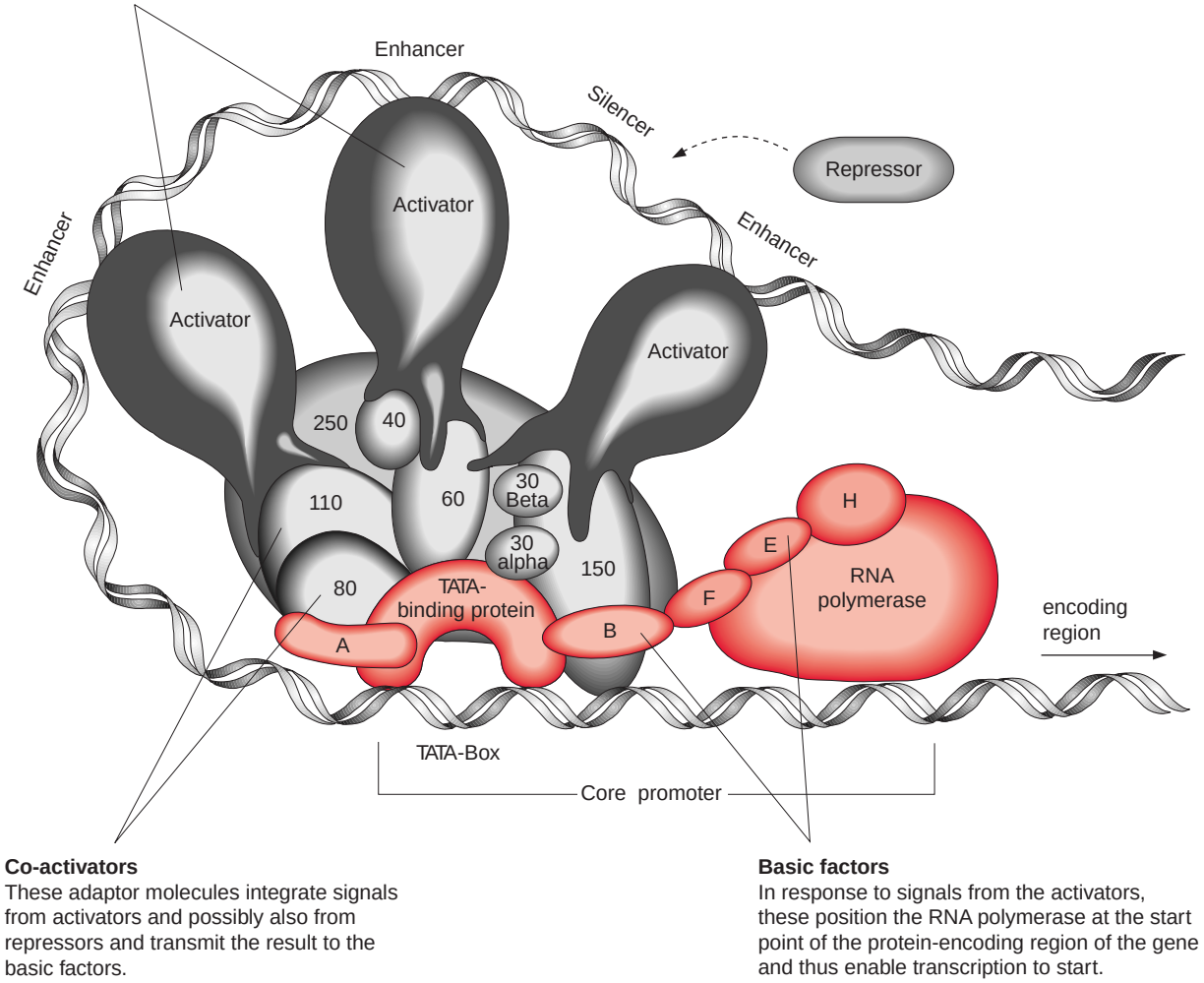

Figure 20.7 Eukaryotic transcription apparatus of mammals, which is thought to be similar to the transcription apparatus of plants. The basal factors (TATA binding protein, proteins A–H, colored red) are indispensable for transcription, but they can neither enhance nor slow down the process. This is brought about by regulatory molecules (*trans*-elements): activators and repressors, the combination of which is different for each gene. They bind to regulatory sequences of the DNA, termed enhancer or silencer (*cis*-elements), which are located far upstream from the transcription start. Activators (and possibly repressors) communicate with the basal factors via co-activators, which form tight complexes with the TATA binding protein. This complex docks first to the core promoter, a control region close to the protein gene. The co-activators are designated according to their molecular weight (given in kDa). (From Tijan, R., Spektrum der Wissenschaft, 4, 1995, with permission.)

RNA polymerase requires a number of additional transcription factors (designated as A, B, F, E, and H in the figure). They are all essential for transcription and are termed **basal factors**.

The transcription apparatus is a complex of many protein components, around which the DNA is wrapped in a loop. In this way *cis*-regulatory elements positioned far upstream or downstream from the encoding gene are able to influence the activity of RNA polymerase. The rate of transcription is determined by transcription factors, either **activators** or **repressors** (summarized as ***trans*-elements**, since they are encoded by other regions of the DNAs) which bind to the upstream regulatory elements (**enhance**r, **silence**r; Fig. 20.3, called ***cis*-elements**, since they are part of the promoter of the encoding gene).

These transcription factors interact through a number of **co-activators** with the TATA binding protein and modulate its function on RNA polymerase. Various combinations of activators and repressors thus lead to activation or inactivation of gene transcription. The scheme of the transcription apparatus shown in Figure 20.7 was derived from investigations with animals but it turned out that the regulation of transcription in plants resembles that of animals.

Knowledge of the promoter and enhancer/silencer sequences is very important for genetic engineering of plants (Chapter 22). It is not always essential for this to know all these boxes and regulatory elements in detail. It can be sufficient for practical purposes if the DNA region is identified that is positioned upstream of the structural gene and influences its transcription in a specific way. In eukaryotic cells, this entire regulatory section is often simply called a promoter. For example, promoter sequences have been identified, which determine that a gene is to be transcribed in a leaf, and there only in the mesophyll cells or the stomata, or in potato tubers, and there only in the storage cells. In such cases, the specificity of gene expression is explained by the effect of cell-specific transcription factors on the corresponding promoters.

The formation of the mature messenger RNA requires processing

The transcription of DNA in the nucleus by RNA polymerase II yields a **primary transcript** (pre-mRNA, Fig. 20.8), which is processed in the nucleus to mature mRNA. During transcription, a GTP is hydrolyzed and a GDP molecule is linked to the 5′-P group of the RNA terminus resulting in a triphosphate bridge (G capping) (Fig. 20.9). Moreover, guanosine and the second ribose (sometimes also the third, not shown in the figure) are methylated using S-adenosylmethionine as a donor (Fig. 12.10). This modified

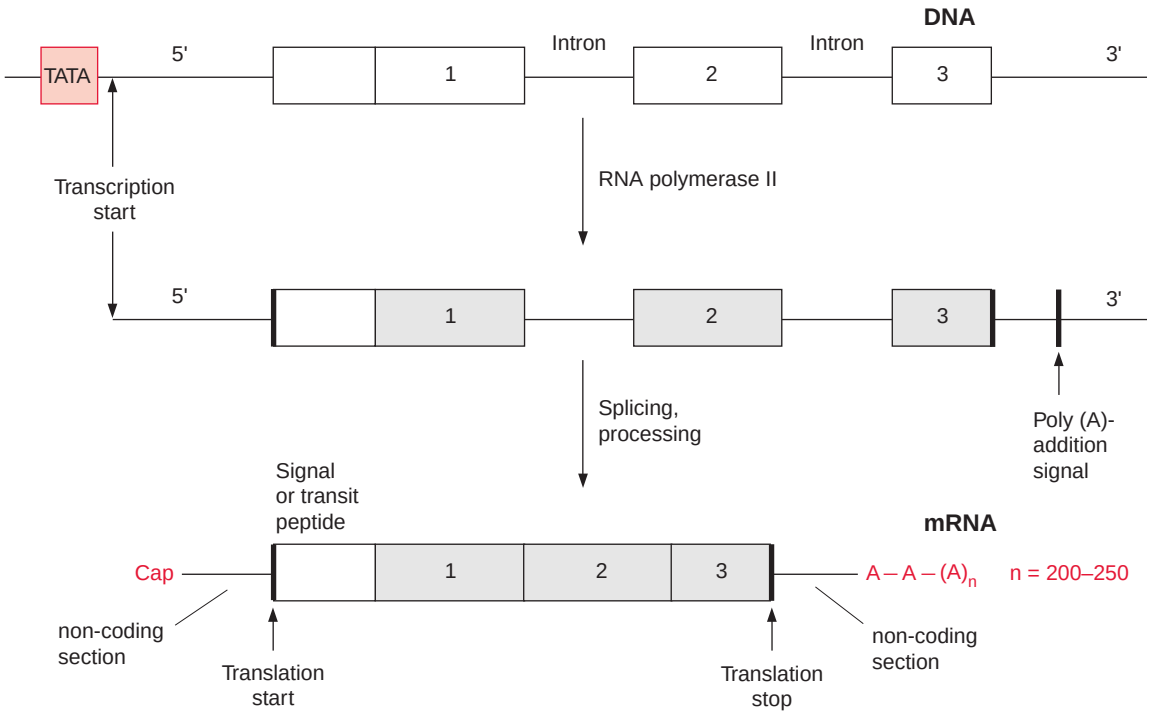

Figure 20.8 Transcription and posttranscriptional processing of a eukaryotic structural gene. The introns are removed from the primary transcript (splicing) (Figs. 20.10 and 20.11). The mature mRNA is formed by the addition of a G-cap sequence (Fig. 20.9) to the 5′ end and a poly (A) sequence to the 3′ end near the poly (A) addition signal (Fig. 20.12).

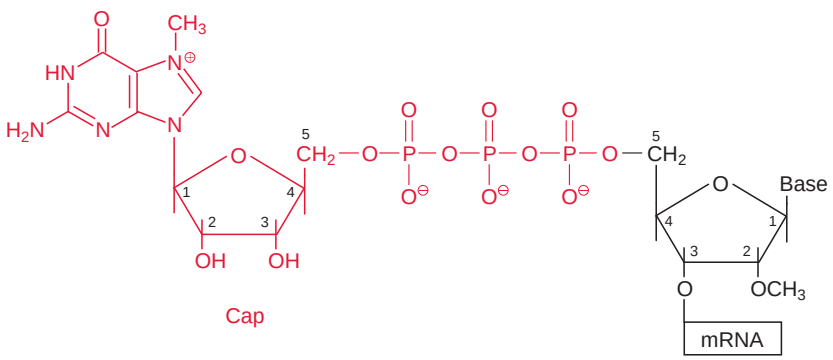

Figure 20.9 The cap sequence consists of a 7′ methyl guanosine triphosphate, which is linked to the 5′ terminal end of the mRNA. The ribose residues of the last two nucleotides of the mRNA are often methylated at the 2′ position.

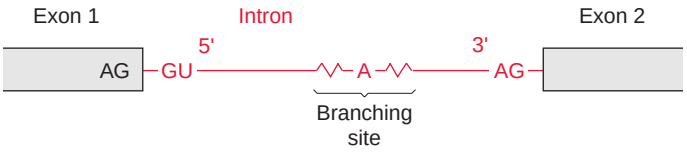

Figure 20.10 The exon-intron border sequence of group I introns is marked by the sequence AG/GU and the end of the intron by the sequence AG. At about 20 to 50 nucleotides upstream of the end of the intron is a consensus adenine nucleotide, which forms the branching site during splicing (see Fig. 20.11).

GTP at the beginning of RNA is called the **5′ cap** and is present only in eukaryotic mRNA. This cap functions as a binding site in the formation of the initiation complex during the start of protein biosynthesis at the ribosomes (section 21.1) and probably also provides protection against degradation by exo-ribonucleases.

The introns are removed during further processing of the pre-mRNA by a process called **splicing**. The size of the introns can vary from 50 to over 10,000 nucleotides. Four types of introns are known. In the introns of group I the border sequences are highly conserved, the last two nucleotides of the exon are in 95% of the cases AG and the first nucleotides of the intron are GU and the last are AG (Fig. 20.10). About 20 to 50 nucleotides upstream from the 3′ end of the intron an adenyl residue is known as the branching site. In the other intron types the border sequences are less conserved.

The excision (**splicing**) of group I introns is catalyzed by **riboprotein complexes**, composed of RNA and proteins. Five different RNAs of 100 to 190 nucleotides, named **snRNA** (sn = small nuclear), are involved in the splicing procedure. Together with proteins and the RNA to be spliced, these snRNA form the **spliceosome** particle (Fig. 20.11). The first step is that the 2′-OH group of the ribose of the nucleotide of the branching site forms a phosphate ester with the phosphate residue, linking the end of exon 1 with the start of the intron and cleaving the ester bond between exon 1 and the intron. This is followed by a second esterification between the 3′-OH group of exon 1 and the phosphate residue at the 5′-OH of exon 2, accompanied by a cleavage of the phosphate ester with the intron. Two transesterification reactions complete the splicing process. The intron remains in the form of a lasso (lariat) and is later degraded by ribonucleases.

As a further step in RNA processing, the 3′ end of the pre-mRNA is cleaved behind a poly(A) addition signal (Fig. 20.12) by an endonuclease, and a **poly(A)-sequence** of up to 250 bp is added at the cleaving site. The resulting mature mRNA is bound to special proteins and leaves the nucleus as a DNA-protein complex.

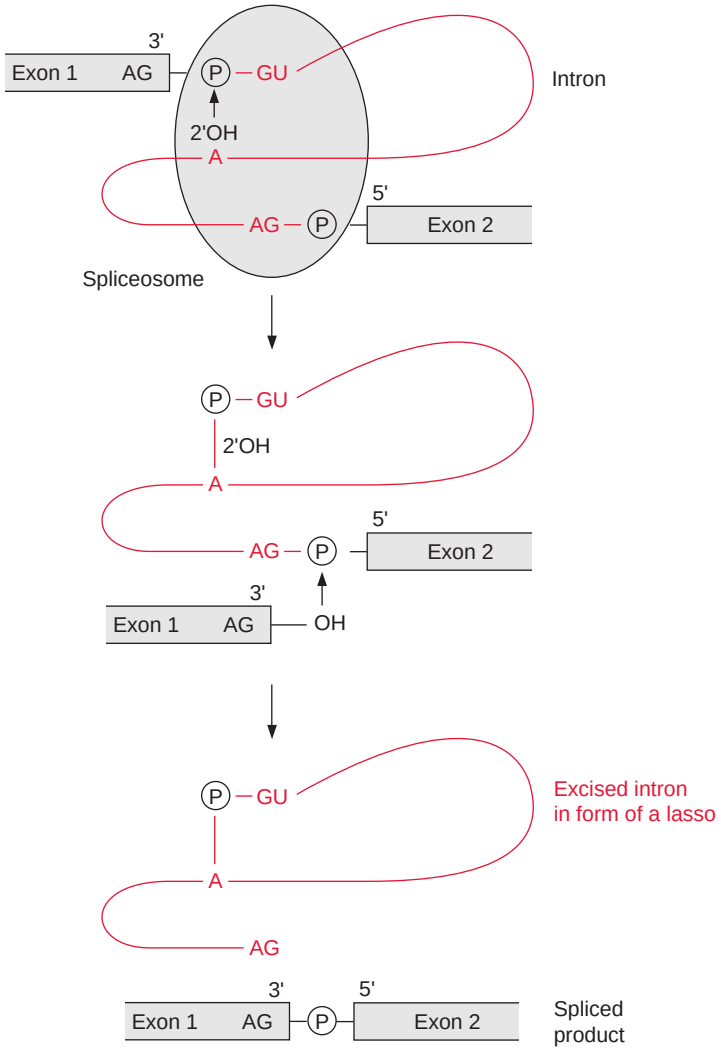

Figure 20.11 In the splicing procedure, several small RNAs and small nuclear (sn) proteins assemble at the splicing site of the RNA to form a spliceosome. The terminal phosphate at the 5′ end of the intron and the 2′-OH group of the adenine nucleotide in the branching site form a new ester bond and subsequently the exon 1/intron junction is cleaved. Then the 3′ end of exon 1 forms a new ester linkage with the phosphate residue at the 5′ end of exon 2, connecting exon 1 and 2 and releasing the intron as a lariat.

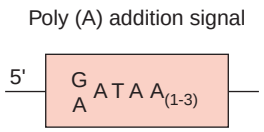

Figure 20.12 Consensus sequence for the poly (A) addition signal.

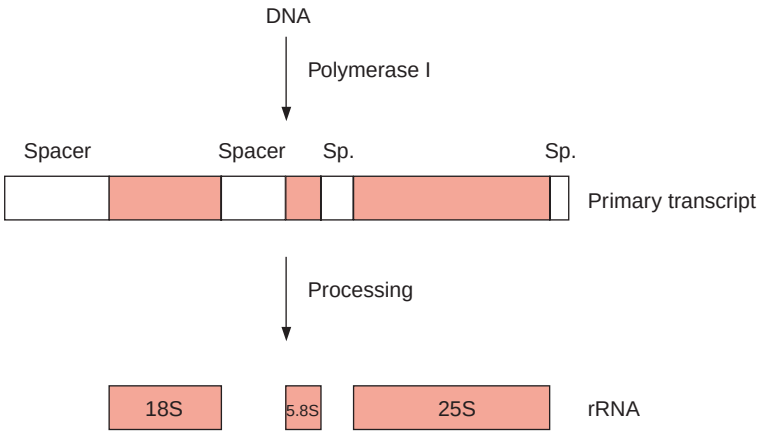

Figure 20.13 rRNA genes are polycistronically transcribed. The intergenic spacers (Sp.) are removed during processing.

rRNA and tRNA are synthesized by RNA polymerase I and III

Eukaryotic ribosomes of plants are made of four different rRNA molecules named 5S-, 5.8S-, 18S-, and 25S-rRNA according to their sedimentation coefficients. The genes for 5S-rRNA are present in many copies, arranged in tandem on certain regions of the chromosomes. The transcription of these genes and also of tRNA genes is catalyzed by **RNA polymerase III**. The three remaining ribosomal RNAs are encoded by a continuous genome sequence, again in tandem and in many copies. These genes are transcribed by **RNA polymerase I**. The primary transcript is subsequently processed after **methylation**, especially of -OH groups of ribose residues, followed by the **cleavage of RNA** to produce mature 18S-, 5.8S-, and 25S-rRNA (Fig. 20.13). The excised RNA sequences between these rRNAs (**intergenetic spacers**) are subsequently degraded. Because of their rapid evolution, comparative sequence analyses of these spacer regions can be used to establish a phylogenetic classification of various plant species within a genus.

20.3 DNA polymorphism yields genetic markers for plant breeding

An organism is defined by the DNA nucleotide sequences of its genome. Differences between the DNA sequences (DNA polymorphisms) exist only between different species, but also to some extent between individuals of

the same species. Between two varieties of a cultivar, in a structural gene often 0.1% to 1% of the nucleotides are altered, mainly in the introns.

Plants usually are selected for breeding purposes by external features (e.g., for their yield or the resistance to certain pests). In the end, these characteristics are all due to differences in the nucleotide sequence of the genome. Selecting plants for breeding would be much easier if it were not necessary to wait until the phenotypes of the next generation were evident, but if instead the corresponding DNA sequences could be analyzed directly. A complete comparative analysis of these genes is not practical, since most of the genes involved in the expression of the phenotypes are not known, and the minute variation (0.1–1 %) of nucleotide sequence of these genes is only detectable with a large analytical expenditure. Other techniques that are easier and less expensive to carry out are available, as will be described in the following.

Individuals of the same species can be differentiated by restriction fragment length polymorphism

It is possible to detect differences in the genes of individuals within a species even without a detailed sequence comparison and to relate these differences empirically to analyzed properties. One of the methods for this is the analysis of restriction fragment length polymorphism (**RFLP**). It is based on the use of bacterial **restriction endonucleases**, which cleave a DNA at a palindromic recognition sequence, known as a **restriction site** (Fig. 20.14). The various restriction endonucleases have specific recognition sites of four to eight base pairs (bp). Since these restriction sites appear at random in DNA, those recognition sequences with 4 bp appear more frequently than those with 8 bp. Therefore it is possible to cleave the genomic DNA of a plant into thousands of defined DNA fragments by using a particular restriction endonuclease (usually enzymes with 6 bp restriction sites). The exchange of a single nucleotide in a DNA may eliminate or newly form a restriction site, resulting in a polymorphism of the restriction fragment length.

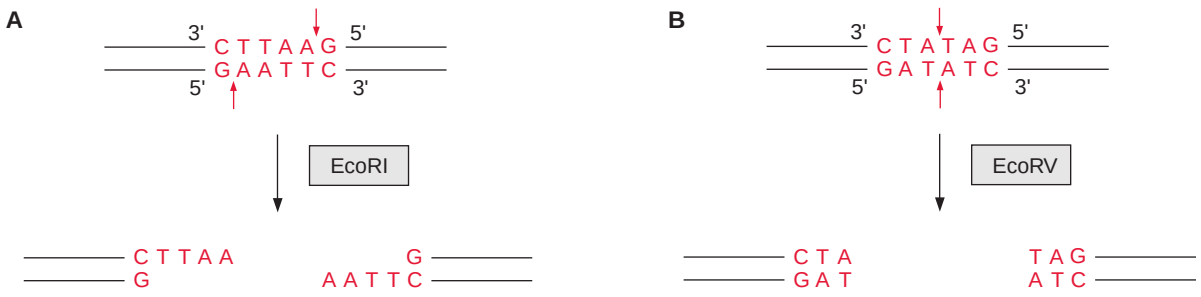

Figure 20.14 Restriction endonucleases of the type II cleave the DNA at restriction sites, which consist of a palindromic recognition sequence. As an example, the restriction sites for two enzymes from *Escherichia coli* strain are shown. A. The restriction endonuclease Eco RI (Fig. 20.14A) causes staggered cuts of the two DNA strands, leaving four nucleotide overhangs of the unpaired strand. These unpaired ends are called sticky ends because they can pair with complementary sticky ends. B. In contrast, the restriction endonuclease Eco RV produces blunt ends.

The digestion of genomic DNA with restriction enzymes results in a multitude of fragments. In order to mark fragments of defined regions of the genome, labeled **DNA probes** are required. Such probes are prepared by the identification of a certain DNA region of a chromosome of about 10 to 20 kbp, located as near as possible to the gene responsible for the trait of interest, or which is even part of that gene. This DNA section is introduced into bacteria (usually *Escherichia coli*) using plasmids or bacteriophages as a vector and is propagated there (see Chapter 22). The plasmids or bacteriophages are isolated from the bacterial suspension; the multiplied DNA sequences are cut out again, isolated, and radioactively labeled or provided with a fluorescence label. Such probes used for this purpose are called **RFLP markers**.

The analysis of DNA restriction fragments by the labeled probes is carried out by the **Southern blot** method, developed by Edwin Southern (Edinburgh) in 1975. The restriction fragments are first separated according to their length by electrophoresis in an agarose gel (the shortest fragment moves the farthest). The separated DNA fragments in the gel are transferred to a nitrocellulose or nylon membrane by placing the membrane on the gel. By covering it with a stack of tissue paper, a buffer solution is drawn through the gel and the membrane, and the diffusive DNA fragments are bound to the membrane. The buffer also causes the dissociation of the DNA fragments into single strands (Fig. 20.15). When a labeled DNA probe is added, it hybridizes to complementary DNA sequences on the membrane. Only those DNA fragments that are complementary to the probe are labeled, and after removal of the nonbound DNA probe molecules by washing, are subsequently identified by autoradiography (in the case of a radioactive probe) or by fluorescence measurement. The position of the band on the blot is then related to its migration and hence its size.

Figure 20.16 explains the principles of RFLP. Figure 20.16A shows in (a) a gene with three restriction sites (R_1, R_2, and R_3). Since the labeled probe binds only to the DNA region between R_1 and R_3, just two noticeable restriction fragments (W and X) will be observed in the autoradiogram. Due to their different lengths, they are separated by gel electrophoresis and detected by hybridization with a probe (Fig. 20.16B (a)). Upon the exchange of one nucleotide (point mutation) (b), the restriction site R_2 is eliminated and therefore only one labeled restriction fragment (Y) is detected, which, because of its larger size, migrates in gel electrophoresis slower than the fragments of (a). When a DNA section is inserted between the restriction sites R_2 and R_3 (c), the corresponding fragment (Z) is longer.

The RFLP represent **genetic markers**, which are inherited according to Mendelian laws and can be employed to characterize a certain variety. Normally several probes are used in parallel measurements. RFLP is also used in plant systematics to establish phylogenetic trees. Moreover, defined

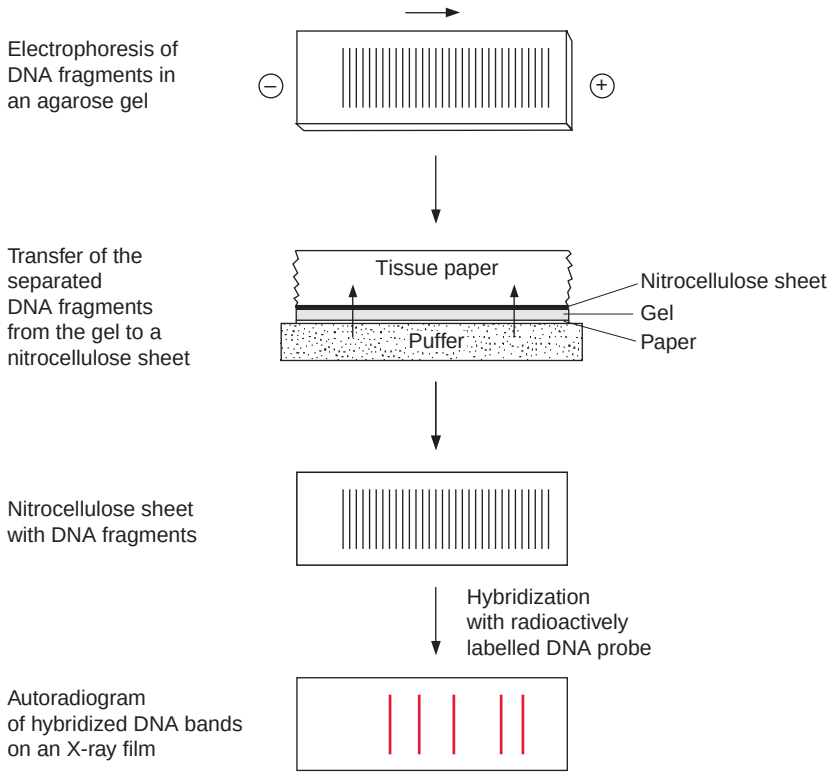

Figure 20.15 The Southern blot procedure.

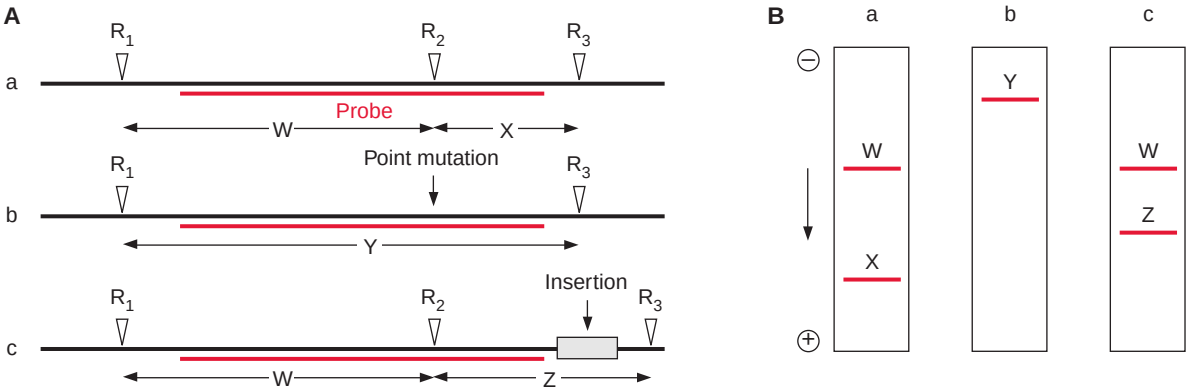

Figure 20.16 The molecular formation of a restriction fragment length polymorphism. A. The restriction sites for the restriction endonuclease in the genotypes a, b, and c are numbered R_1, R_2, and R_3. The probe by which the fragments are identified is marked red. B. (a). The electrophoretic movement of the fragments (W, X) that are labeled by the probe. (b). One restriction site is eliminated by point mutation and only one fragment is formed (Y), which, because of its larger size, migrates more slowly during electrophoresis. (c). Fragment X is enlarged after insertion (Z).

restriction fragments can be used as labeled probes to localize certain genes on the chromosomes. In this way chromosome maps have been established for several plants (e.g., *Arabidopsis*, potato, tomato, and maize).

The RAPD technique is a simple method for investigating DNA polymorphism

An alternative method for analyzing the differences between DNA sequences of individuals or varieties of a species is the amplification of randomly obtained DNA fragments (random amplified polymorphic DNA, **RAPD**). This method, which has been in use only since 1990, is much easier to work with, compared to the RFLP technique, and its application has become widespread in a very short time.

The basis for the RAPD technique is the **polymerase chain reaction** (**PCR**). The method enables selected DNA fragments of a length of up to two to three kbp to be amplified by DNA polymerase (Fig. 20.17). This requires an **oligonucleotide primer** (A), which binds to a complementary sequence of the DNA to be amplified by a special DNA polymerase and indicates the starting point for the synthesis of a DNA daughter strand at the template of the DNA mother strand. A second primer (B) is needed to define the end of the DNA strand that is to be amplified. In the first step, the DNA double strands are separated into single strands by heating to about 95°C. During a subsequent cooling period, the primers hybridize with the DNA single strands and thus enable, in a third step at a medium temperature, the synthesis of DNA. A DNA polymerase originally isolated from the thermophilic bacterium *Thermus aquaticus* which lives in hot springs (**Taq polymerase**) is used, since this enzyme is not affected by the heat treatments. Subsequently, the DNA double strands thus formed are separated again by being heated at 95°C, the primer binds during an ensuing cooling period, and this is followed by another cycle of DNA synthesis by Taq polymerase. The alternating heating and cooling can be continued for 30 to 40 cycles, and the amount of DNA is doubled during each cycle. It should be noted that during the first cycle, the length of the newly formed DNA is only defined at one end. During the second cycle the binding of the primer to the complementary nucleotide sequence of the newly formed DNA strand results in the synthesis of a DNA that is restricted in its length by both primers. With the increasing number of cycles, DNA fragments of uniform length are amplified. Since in the polymerase chain reaction the number of the DNA molecules formed is multiplied exponentially by the number of cycles (e.g., after 25 cycles by the factor 34×10^6) very small DNA samples (in the extreme case a single molecule) can be multiplied *ad libitum*.

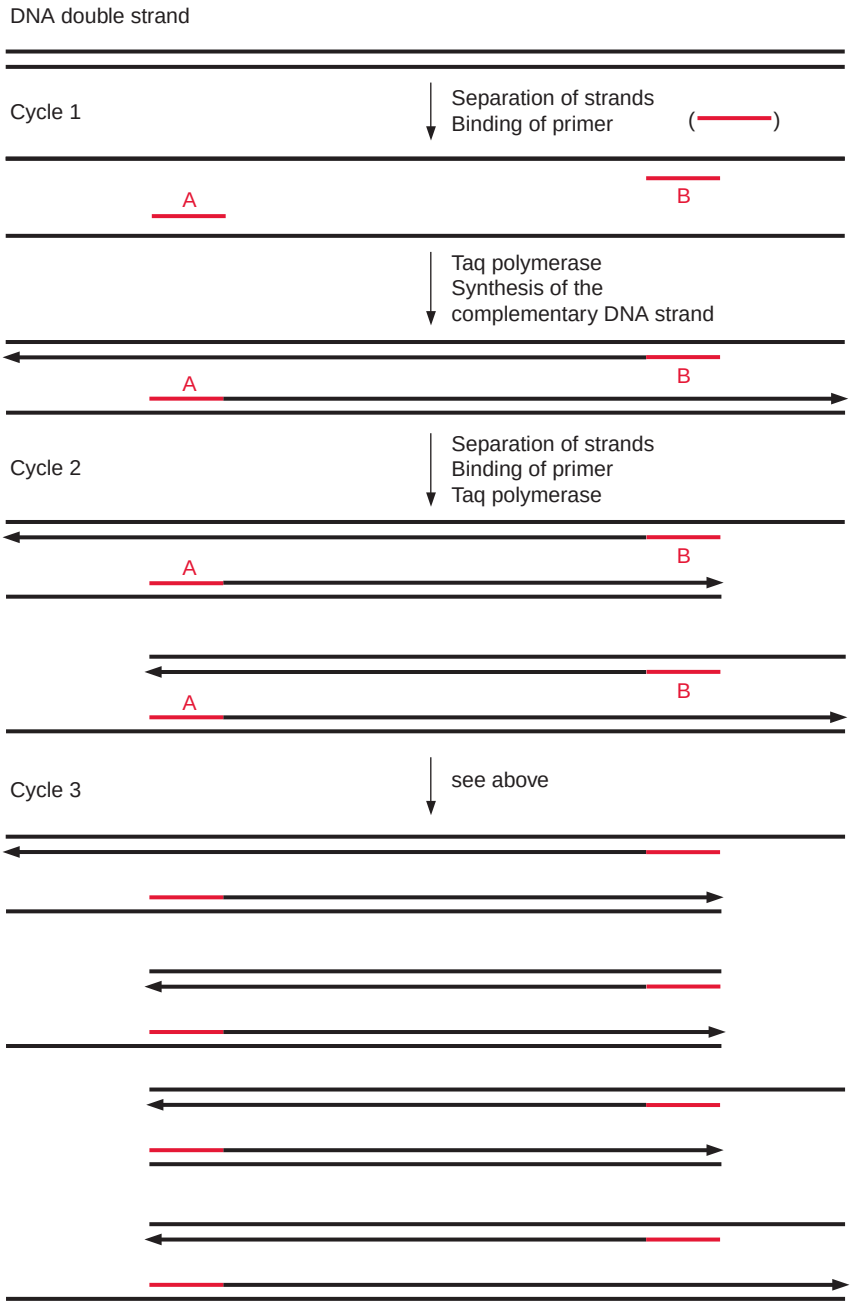

Figure 20.17 Principle of the polymerase chain reaction. A and B are different primers, which bind to complementary DNA sequences, after heat denaturation of the ds DNA. Taq polymerase replicates the DNA between both primers.

In the RAPD technique, genomic DNA and only one oligonucleotide primer consisting typically of 10 nucleotides are required for the polymerase chain reaction. Since the probability of the exact match of 10 complementary nucleotides on the genomic DNA is low, the primer binds at only a few sites of the genomic DNA. Characteristically the DNA polymerases used for this amplification require a distance between the two primers to be no larger than 2,000–3,000 bp. Therefore, only a few sections of the genome are amplified by the polymerase chain reaction and a subsequent selection of the fragments by a probe is not necessary. The amplification produces such high amounts of single DNA fragments that, after being separated by gel electrophoresis and stained with ethidium bromide, the fragments can be detected as fluorescent bands under ultraviolet (UV) light. Point mutations, which eliminate primer binding sites or form new ones, and deletions or insertions, all of which affect the size and number of the PCR products, can change the pattern of the DNA fragments in analogy to the RFLP technique (Fig. 20.16). Changing the primer sequence can generate different DNA fragments. Defined primers of 10 nucleotides are commercially available in many variations. In the RAPD technique, different primers are tried until, by chance, bands of DNA fragments that correlate with a certain trait are obtained. The RAPD technique takes less work than the RFLP technique because it requires neither the preparation of probes nor the time-consuming procedure of a Southern blot. It has the additional advantage that only very small amounts of DNA (e.g., the amount that can be isolated from the embryo of a plant) are required for analysis. Although in most cases it is not possible to define from which gene these fragments derive, the RAPD technique allows differentiation between varieties of a species, and has therefore become an important tool in breeding.

The polymorphism of micro-satellite DNA is used as a genetic marker

Recently **micro-satellite DNA** (section 20.1) has become an important tool for identifying certain plant lines. Micro-satellite DNAs comprise sequences of one to two, sometimes also three to six, nucleotide pairs, which are located in 10 to 50 repetitions at certain sites of the genome, in the region of the intron, or directly before or behind a gene, whereby the number of the repetitions is highly polymorphic. Also, in this method PCR is utilized for detection. Not only is micro-satellite polymorphism used to identify individual humans (e.g., in criminal cases), but also is employed as a genetic marker for plant breeding.

20.4 Transposable DNA elements roam through the genome

In certain maize varieties, a cob may contain some kernels with different pigmentation from the others, indicating that a mutation has changed the pigment synthesis. Snapdragons normally have red flowers, but occasionally have mutated progeny in which parts of the flower no longer accumulate red pigment, resulting in, e.g., white stripes in the flowers. Sometimes the descendants of these defective cells regain the ability to synthesize the red pigment, developing flowers with not only white stripes but also red dots.

Barbara McClintock (USA) studied these phenomena for many years in maize, using the methods of classic genetics. In the genome of maize she found **mobile DNA elements**, which jump into a structural gene and thus inactivate it. Generally, this mobile element does not stay there permanently, but sooner or later jumps into another gene, whereby in most cases the function of the first structural gene is restored. In 1983 Barbara McClintock was awarded the Nobel Prize in Medicine for these important discoveries. Later it became apparent that these transposable elements, which were named **transposons**, are not unique to plants, but also occur in bacteria, fungi, and animals.

Figure 20.18 shows the structure of the transposon Ac (activator) from maize, consisting of double-stranded DNA with 4,600 bp. Both ends contain a 15 bp long inverted repeat sequence (IR_A, IR_B). Inside the transposon is a structural gene that encodes **transposase**, an enzyme catalyzing the transposition of the gene. This enzyme binds to the flanking inverted repeats and catalyzes the transfer of the transposon to another location and its integration into the new location as well as its elimination from there. Sometimes it can happen that the excision of the transposon is imprecise, so that after its translocation the remaining gene may have a slightly modified sequence, which could result in a lasting mutation.

In maize, besides the transposon AC, a transposon DS has been found in which the structural gene for the transposase is defect. Therefore, the transposon DS is mobile only in the presence of the transposase of transposon AC.

A transposon can be regarded as an autonomous unit encoding the proteins required for jumping. There are controversial opinions about the origin and function of the transposons. One explanation is that the transposons are a kind of parasitic DNA, with features comparable to the viruses, which exploit the cell for multiplication. But it is also possible that the transposons offer the cells a selection advantage by increasing the mutation rate in order to enhance adaptation to changed environmental conditions.

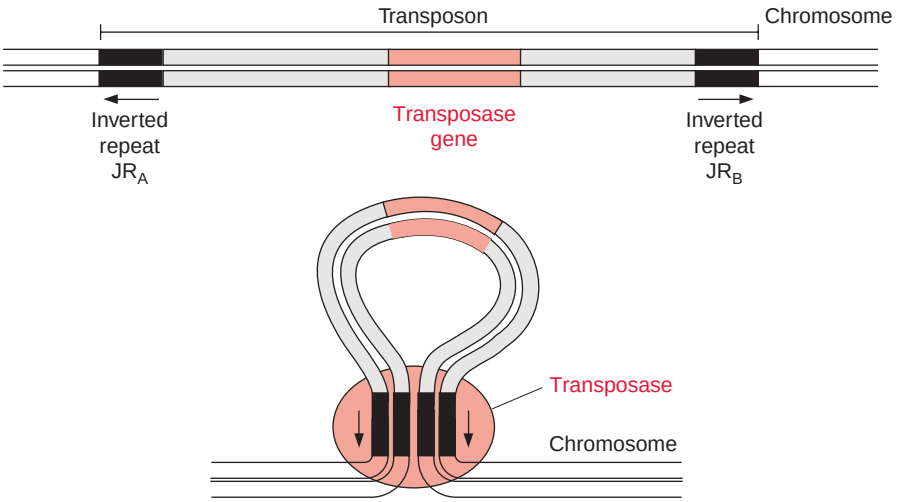

Figure 20.18 A transposon is defined by inverted repeats at both ends. The structural gene for transposase is encoded in the transposon sequence. When a transposon leaves a chromosome by the help of the transposase, the two inverted repeats bind to each other and the remaining gap in the chromosome is closed. In an analogous way the transposon enters the chromosome at another site.

As the transposons can be used for **tagging genes**, they have become an interesting tool in biotechnology. It has already been discussed that the insertion of a transposon in a structural gene results in the loss of the encoding function. For example, when a transposon jumps into a gene for anthocyanin synthesis in snapdragons, the red flower pigment can no longer be synthesized. The transposon inserted in this inactivated gene can be used as a DNA probe (marker) to isolate and characterize a gene of the anthocyanin biosynthesis pathway. The relevant procedures will be discussed in section 22.1.

20.5 Viruses are present in most plant cells

With the exception of meristematic cells, almost all other plant cells are infected by viruses. In most cases, viruses do not kill their host since they depend on the host's metabolism for reproduction. The viruses encode only a few special proteins and use the energy metabolism and the biosynthetic capacity of the host cell to multiply. This often weakens the host plant and lowers the yield of virus-infected cultivars. Infection by some viruses can lead to the destruction of the entire crop. Courgettes and melons are extremely susceptible to the cucumber mosaic virus. In some provinces of Brazil, 75% of the orange trees were destroyed within 12 years by the Tristeza virus.

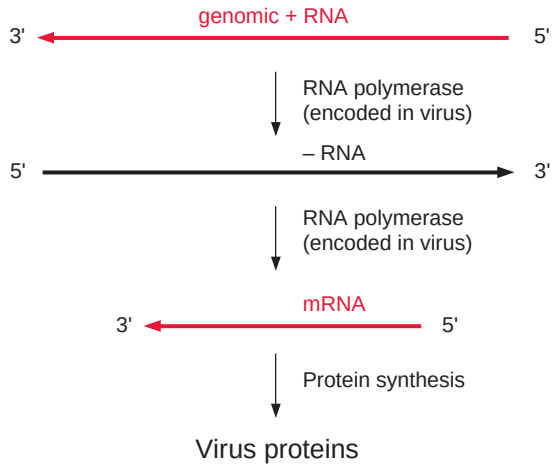

Figure 20.19 The single-stranded genomic RNA of many viruses is first transcribed to a minus strand-RNA, and the latter then to mRNAs, subsequently used for the synthesis of proteins.

The virus genome consists of **RNA** or **DNA** surrounded by a protein coat. The majority of plant virus genomes consist of a single-stranded RNA, called the plus RNA strand. In some viruses (e.g., brome mosaic virus, which infects certain cereals), the plus RNA strand exhibits the characteristics of an mRNA and is therefore translated by the host cell. In other viruses (e.g., the **tobacco mosaic virus** (**TMV**)), the plus RNA strand is first transcribed to a complementary minus RNA strand and the latter then serves as a template for the formation of mRNAs (Fig. 20.19). The translation products of these mRNAs encompass **replicases**, which catalyze the replication of the plus and minus RNAs, **movement proteins** that enable the spreading of the viruses from cell to cell (section 1.1), and **coat proteins** for packing the virus DNA. Normally, a virus infiltrates a cell through wounds, which, for instance, have been caused by insects, such as aphids feeding on the plant (section 13.2). Once viruses have entered the cell, their movement proteins widen the plasmodesmata between single cells to allow virus passage and spreading over the entire symplast (section 1.1).

The retrovirus genome consists also of a single-stranded RNA, but in this case, when the cell has been infected, the RNA is transcribed into DNA by a **reverse transcriptase**. The DNA is integrated in part into the nuclear genome. So far, infections by retroviruses are known only in animals.

The **cauliflower mosaic virus** (**CaMV**), which causes pathogenic changes in leaves of cauliflower and related plants, is somewhat similar to a retrovirus. The genome of the CaMV consists of a double-stranded DNA of about 8 kbp, with gaps in it (Fig. 20.20). When a plant cell is infected, the virus loses its protein coat and the gapped DNA strands are repaired by enzymes of the host. The virus genome acquires a double helical structure and forms

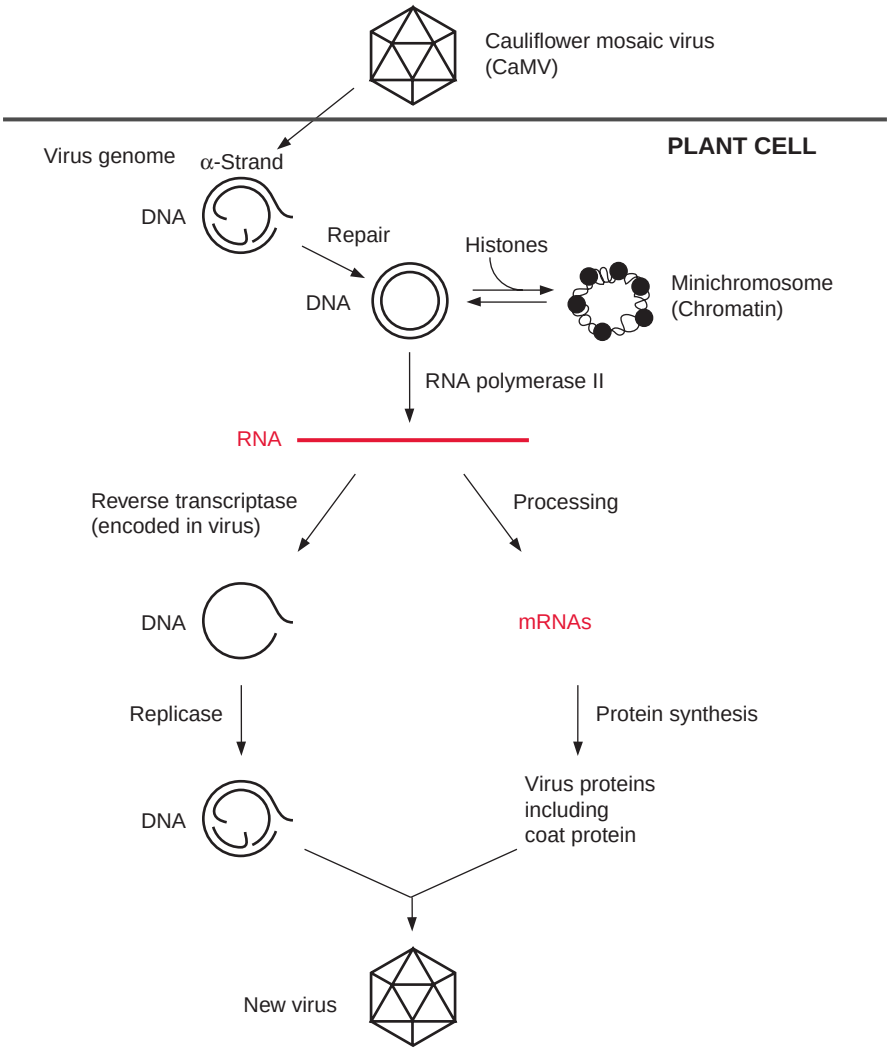

Figure 20.20 Infection of a plant cell by the cauliflower mosaic virus (CaMV).

in the nucleus a chromatin-like aggregate with the histones. This permits the viral genome to stay in the nucleus as a **mini-chromosome**. The viral genome possesses promoter sequences that are similar to those of nuclear genes, such as TATA box and a CAAT box as well as enhancer elements. The virus promoter (35S promoter) is recognized by the RNA polymerase II of the host cell and is transcribed at a high rate. The precursor transcript is subsequently processed into individual mRNAs, which encode the synthesis of six virus proteins, including the coat protein and the reverse

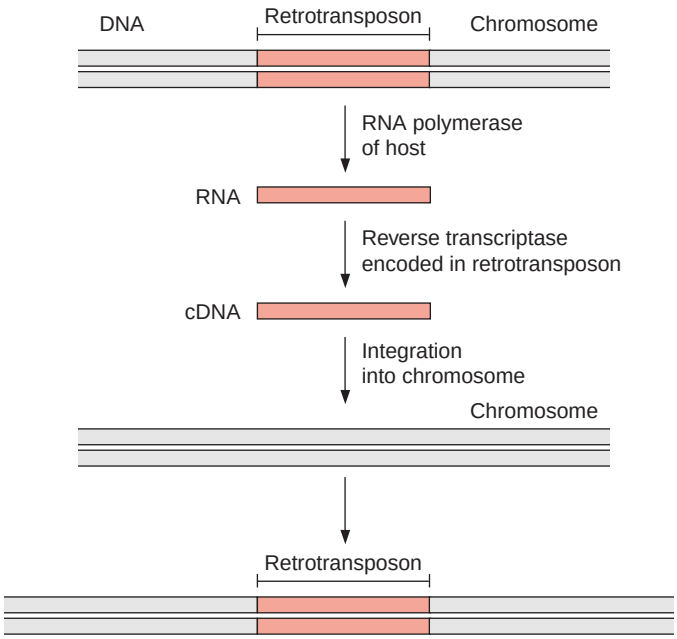

Figure 20.21
Retrotransposons is a DNA sequence that can integrate into a chromosome. Flanking sequences contain the recognition signal for transcription by a host RNA polymerase. The RNA is transcribed into cDNA by a reverse transcriptase encoded in the retrotransposon and integrated into another section of the genome.

transcriptase. The strong CaMV 35S promoter is often used as a promoter for the expression of foreign genes in transgenic plants (Chapter 22).

The transcript synthesized by RNA polymerase II is also reverse transcribed by the virus-encoded reverse transcriptase into DNA and, after synthesis of the complementary strand, packed as double-stranded DNA into a protein coat. This mature virus is now ready to infect other cells.

Retrotransposons are degenerated retroviruses

Besides the transposons there is another class of mobile elements, which are derived from the **retroviruses**. They do not jump out of a gene like the transposons but just multiply. At both ends of the **retrotransposons** sequences are present, which carry signals for the transcription of the retrotransposon DNA by the host RNA polymerase. The retrotransposon RNA does not encode the coat protein, but the reverse transcriptase, which is homologous to the retrovirus enzyme and transcribes the retrotransposon RNA into DNA (Fig. 20.21). This DNA is then inserted into another site of the plant genome. It is assumed that these retrotransposons originate from retroviruses that have lost the ability to synthesize the protein coat. Several different retrotransposons containing all the constituents for their multiplication have been found in *Arabidopsis*, but so far an insertion of a retrotransposon

into a gene of *Arabidopsis* has never been monitored. About 0.1% of the genome of *Arabidopsis* consists of these retrotransposons, suggesting that these actually multiply, albeit at a slow rate.

20.6 Plastids possess a circular genome

Many arguments support the hypothesis that plastids have evolved from prokaryotic endosymbionts (see section 1.3). The circular genome of the plastids is similar to the genome of the prokaryotic cyanobacteria, although much smaller. The DNA of the plastid genome is named **ctDNA** (chloroplast) or **ptDNA** (plastid). In the majority of the plants investigated so far, the **circular plastid genome** has the size of 120 to 160 kbp. Depending on the plant, this is only 0.001% to 0.1% of the size of the nuclear genome (Table 20.1), but the cell contains many copies of the plastid DNA, because each plastid contains many genome copies. In young leaves, the number of ctDNA molecules per chloroplast is about 100, whereas in older leaves, it is between 15 and 20. Furthermore, a cell contains a large number of plastids, a mesophyll cell, for instance 20 to 50. Thus, despite the small size of the plastid genome, the plastid DNA can amount to 5% to 10% of the total cellular DNA.

The first complete analysis of the nucleotide sequence of a plastid genome was carried out in 1986 by the group of Katzuo Shinozaki in Nagoya with chloroplasts from tobacco and by Kanji Ohyama in Kyoto with chloroplasts from the liverwort *Marchantia polymorpha*. Although the two investigated plants are very distantly related, their plastid genomes are rather similar in gene composition and arrangements. Obviously, the plastid genome has changed little during recent evolution. Present analysis of the DNA sequence of plastid genes from many plants supports this notion.

Figure 20.22A shows a complete gene map of the chloroplast genome of tobacco and Figure 20.22B shows schematic representations of the plastid genomes of other plants. The plastid genome of most plants contains so-called **inverted repeats** (IR), which divide the remaining genome into a large or small single copy region. The repeat IR_A and IR_B each encode the genes for the four ribosomal RNAs as well as the genes for some transfer RNAs, and the repeat sizes vary from 20 to 50 kbp. These inverted repeats are not found in the plastid genomes of pea, broad bean, and other legumes (Fig. 20.22C), where the inverted repeats probably have been lost during the course of evolution. On the remainder of the genome (single-copy region), genes are present usually only in a single copy.

Analysis of the ctDNA sequence of tobacco revealed that the genome encodes 122 genes (146 if the genes of each of the two inverted repeats are

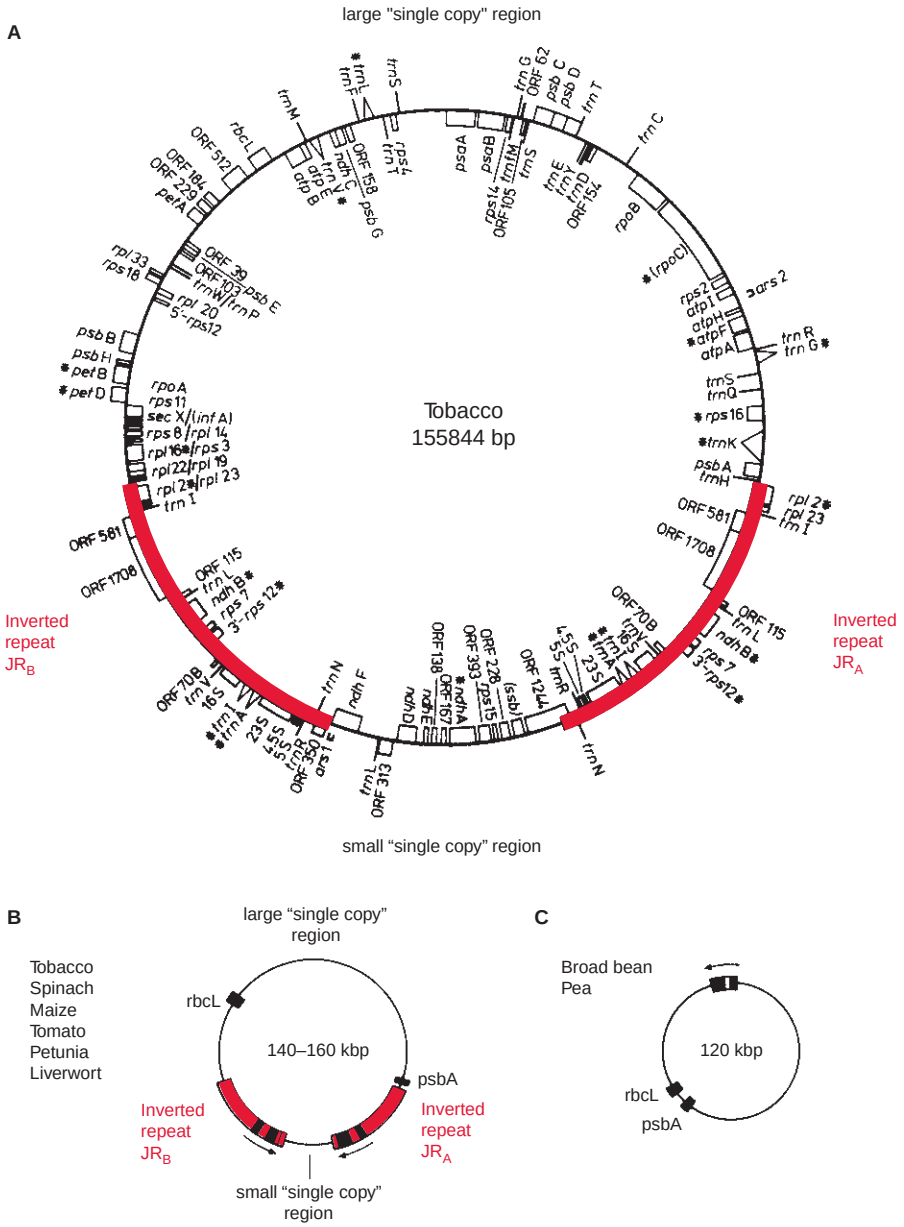

Figure 20.22 A. Gene map of a chloroplast genome of tobacco according to the complete DNA sequence analysis by Shinozaki and collaborators. Some single genes are listed in Table 20.4, where the abbreviations are also explained. B. Basic structure of the chloroplast genes of many plants. C. Broad bean and garden pea do not contain inverted repeats. rbcL encodes the large subunit of RubisCO, psbA: encodes the 32 kDa protein of photosystem II.

counted) (Table 20.4). The gene for the large subunit of ribulose bisphosphate carboxylase/oxygenase (RubisCO, section 6.2) is located in the large single-copy region, whereas the gene for the small subunit is present in the nuclear genome. The single-copy region of the plastid genome also encodes six subunits of F-ATP synthase, whereas the remaining genes of F-ATP

Table 20.4: Some identified genes in the genome of maize chloroplasts (Shinozaki et al.)

Name of the gene	Gene product (protein or RNA)
Photosynthesis apparatus	
rbcL	RubisCO**:** large subunit
atpA, -B, -E	F-ATP-SYNTHASE: subunits α, β, ε,
atpF,-H, -I	F-ATP-SYNTHASE: subunits I, III, IV
psaA, -B, -C	PHOTOSYSTEM I: subunit A1, A2, 9-kDa protein
psbA, -B, -C, -D	PHOTOSYSTEM II: subunit D1, 51 kDa, 44 kDa, D2
psb-E, -F, -G, -H, -I	PHOTOSYSTEM II: subunit Cyt-b_{559}-9 kDa, -4 kDa, G, 10Pi, I-protein
petA, -B, -D	Cyt-b_6/*f*-COMPLEX: Cyt-*f*, Cyt-b_6, subunit IV
ndhA, -B, -C, -D,	NADH-DEHYDROGENASE (ND) subunits 1, 2, 3, 4
ndh-E, -F	NADH-DEHYDROGENASE (ND) subunits ND4L, 5
Protein synthesis	
rDNA	RIBOSOMAL RNAs (16S, 23S, 4,5S, 5S)
trn	Transfer RNAs (30 species)
rps2, -3, -4, -7, -8, -11	30S-RIBOSOMAL PROTEINS (CS) 2, 3, 4, 7, 8, 11
rps -12, -14, -15, -16, -18, -19	30S-RIBOSOMAL PROTEINS (CS) 12, 14, 15, 16, 18, 19
rpl2, -14, -16, -20, -22	50S-RIBOSOMAL PROTEINS (CL) 2, 14, 16, 20, 22
Rpl-23, -33, -36	50S-RIBOSOMAL PROTEINS CL 23, 33, 36
infA	Initiation factor 1
Transcription	
rpoA, -B, -C	RNA polymerase-α, -β, -β'
Ssb	ssDNA binding protein

synthase are encoded in the nucleus. Also encoded in the plastid genome are subunits of photosystem I and II, of the cytochrome-b_6/*f* complex, and of an NADH dehydrogenase (which also occurs in mitochondria, see sections 3.8 and 5.5), and furthermore, proteins of plastid protein synthesis and gene transcription. Some of these plastid structural genes contain introns. In addition, there are putative genes on the genome with so-called open reading frames (ORF), which, like the other genes, are bordered by a start and a stop codon, but where the encoded proteins are not yet known. The plastid genome encodes only a fraction of plastid proteins, as the majority is encoded in the nucleus. It is assumed that many genes of the original endosymbiont have been transferred during evolution to the nucleus, but there also are indications for gene transfer between the plastids and the mitochondria (section 20.7).

All four rRNAs, which are constituents of the plastid ribosome (4.5S-, 5S-, 16S-, and 23S-rRNA) are encoded in the plastid genome. The plastid ribosomes (sedimentation constants 70S) are smaller than the eukaryotic ribosomes (80S) present in the cytosol, but are similar in size to the ribosomes

Figure 20.23 In the plastids of tobacco, all four ribosomal rRNAs and two tRNAs are transcribed as one transcription unit.

of bacteria. As in bacteria, these four rRNAs are encoded in the plastid genome in one transcription unit (polycistronic transcription) (Fig. 20.23). Between the 16S and 23S DNA a large spacer is situated (intergenic spacer), which encodes the sequence for one or two tRNAs. In total, about 30 tRNAs are encoded in the plastid genome. Additional tRNAs needed for transcription in the plastids are encoded in the nucleus.

The transcription apparatus of the plastids resembles that of bacteria

In the plastids **two types of RNA polymerases** are active, of which only one is encoded in the plastid genome and the other in the nucleus:

1. The RNA polymerase encoded in the **plastids** enables the transcription of plastid genes for subunits of the photosynthesis complex. This RNA polymerase is a multienzyme complex resembling that of **bacteria**. In contrast to the RNA polymerase of bacteria, the plastid enzyme is insensitive to **rifampicin**, a synthetic derivative of an antibiotic from *Streptomyces*.
2. The plastid RNA polymerase, which is encoded in the **nucleus**, is derived from the duplication of mitochondrial RNA polymerase. This "imported" RNA polymerase is homologous to RNA polymerases from **bacteriophages**. The nucleus-encoded RNA polymerase transcribes the so-called **housekeeping genes** in the plastids. These are the genes that have general functions in metabolism, such as the synthesis of rRNA or tRNA.

As in bacteria, many plastid genes contain a box 10 bp upstream from the transcription start with the consensus sequence TATAAT and at 35 bp upstream a further promoter site with the consensus sequence TTGACA. Some structural genes are polycistronically transcribed, which means that several are in one transcription unit and are transcribed together as a large primary transcript. Polycistronic transcription often occurs with bacterial genes. In some cases, the primary transcript is subsequently processed by ribonucleases of which many details are still not known (see Figure 20.13)

20.7 The mitochondrial genome of plants varies largely in its size

In contrast to animals, plants possess a very large mitochondrial (mt) genome. In *Arabidopsis* it is 20 times, and in melon 140 times larger than in humans (Table 20.5). The plant mitochondrial genome also encodes more genetic information: the number of encoding genes in a plant mt-genome is about seven times higher than in humans.

The size of the mt-genome varies largely in higher plants, even within a family. *Citrullus lanatus* (330 kbp), *Curcubita pepo* (850 kbp), and *Cucumis melo* (2,400 kbp), listed in Table 20.5, all belong to the family of the *Curcubitaceae* (squash plants). In most plants, however, the size of the plastid genome is relatively constant at 120 to 160 kbp.

The mitochondrial genome in plants often consists of one large circular DNA molecule and several smaller ones. In some mitochondrial genomes, this partitioning may be permanent, but in many cases the fragmentation of the mt-genome seems to be derived from homologous recombination of repetitive elements (e.g., maize contains six such repeats). Figure 20.24 shows how an interaction of two repeats can lead by **homologous recombination** to a fragmentation of a DNA molecule. The 570 kbp mt-genome of maize is present as a **master circle** as well as up to four **subcircles** (Fig. 20.25). The homologous recombination of DNA molecules can also form

Table 20.5: Size of the mitochondrial DNA (mtDNA) in plants in comparison to the mtDNA of humans

Organism	Size of the mtDNA (kbp)
Arabidopsis thaliana	367
Populus trichocarpa (poplar)	803
Vicia faba (broad bean)	290
Zea mays (maize)	570
Oryza sativa (rice)	492
Citrullus lanatus (water melon)	330
Curcubita pepo (pumpkin)	850
Cucumis melo (honey melon)	2,400
Marchantia polymorpha (liverwort)	170
Chlamydomonas reinhardtii (green alga)	15
Homo sapiens (human)	17

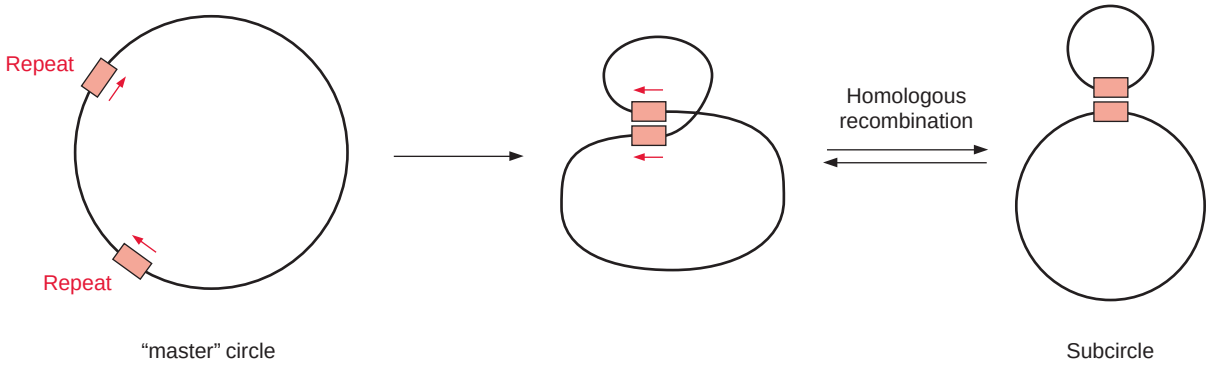

Figure 20.24 From a mitochondrial genome (master circle) two subcircles can be formed by reversible homologous recombination of two repeat sequences.

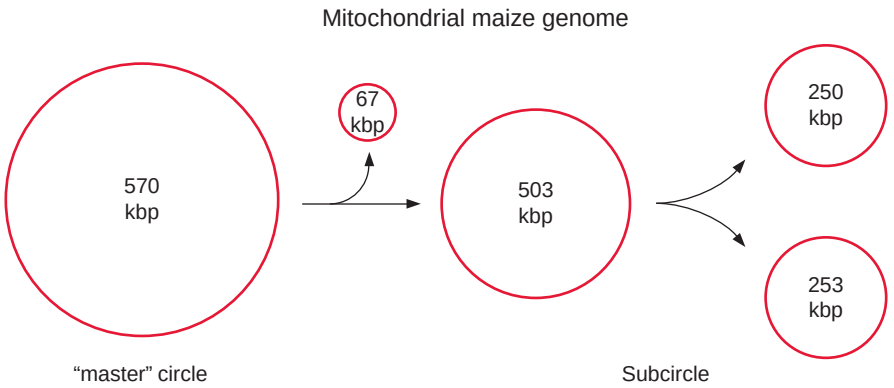

Figure 20.25 Due to homologous recombination, the mitochondrial genome from maize can be present as a continuous large genome as well as in the form of several subcircles. In many mt-genomes of plants only subcircles are observed.

larger units. This may explain the large variability in the size of the mitochondrial genomes in plants.

The number of mitochondria in a plant cell can range between 50 and 2,000, with each mitochondrion containing 1 to 100 genomes.

In animals and in yeast, the mtDNA is normally circular, like the bacterial DNA. Also plant mtDNA is thought to be circular. This is undisputed for the small mtDNA molecules (subcircles, Fig. 20.25), but it remains unclear whether this circular structure also generally applies to the master mtDNA. There are indications that the master genome can also occur as open strands.

Figure 20.26 shows the complete gene map of the mt-genome of *Arabidopsis thaliana*, and Table 20.6 summarizes the genes in the mt-genome of a higher plant. A comparison with the number of genes in the plastid genome (Table 20.4)

Table 20.6: Genes identified in the genome of plant mitochondria

Translation apparatus	5S-, 18S-, 26S-rRNA 10 ribosomal proteins 16 transfer-RNA
NADH-dehydrogenase	9 subunits
Succinate dehydrogenase	1-3″
Cytochrome-*b*/c_1 complex	1″
Cytochrome-*a*/a_3 complex	3″
F-ATP synthase	4″
Cytochrome-*c*-biogenesis	>3 genes
Conserved open reading frame of unknown coding	>10 genes

After Schuster and Brennicke

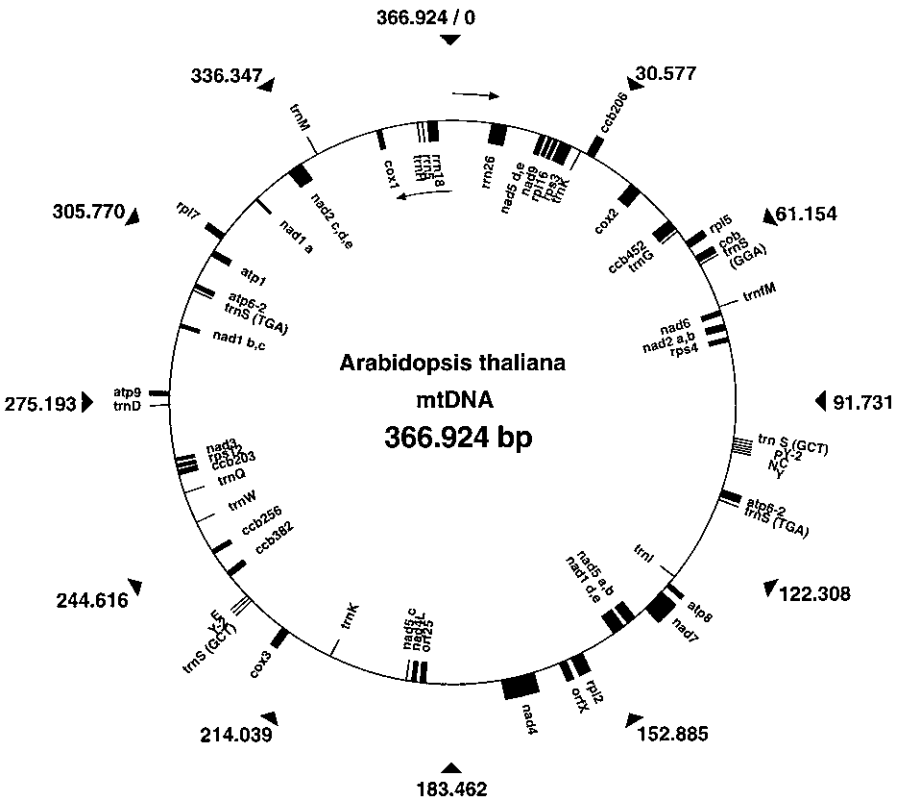

Figure 20.26 Gene map of the mitochondrial genome of *Arabidopsis thaliana* based on the DNA analysis of Unseld et al. (1997). (By kind permission of A. Brennicke.)

shows that the mt-genome of the plant, although usually much larger than the plastid genome, encodes much fewer genes. The relatively small information content of the mt-genome in relation to its size is due to a high content of repetitive sequences, which probably are derived from gene duplication. The mt-genome contains much DNA with no recognizable function, termed **junk DNA**, which has accumulated in the mt-genome during evolution. Some of this junk DNA has its origin in plastid DNA and some in nuclear DNA. The mitochondrial genome, like the nuclear genome, apparently tolerates a large portion of apparently senseless sequences and passes these on to following generations. It is interesting that a large part of mtDNA is transcribed. About 30% of the mt-genome of *Brassica rapa* (218 kbp) is transcribed, as is that of the six times larger genome of *Cucumis melo* (2,400 kbp). Why so many transcripts are synthesized is obscure, considering that in the two mt-genomes mentioned above, the total number of the encoded proteins, tRNAs, and rRNAs amounts only to about 60.

The mitochondrial genome encodes elements of the translation machinery, including three rRNAs, about 16 tRNAs, and about 10 ribosomal proteins. These components of the translation apparatus are involved in the synthesis of various hydrophobic membrane proteins, which are also encoded in the mt-genome, e.g., some subunits of the respiratory chain (section 5.5), of F-ATP synthase (section 4.3), and at least three enzymes of cytochrome-*c* synthesis (section 10.5). About 95% of the mitochondrial proteins, including most subunits for the respiratory chain and F-ATP synthase, as well as several tRNAs, are encoded in the nucleus. Considering that mitochondria have derived from endosymbionts, it must be assumed that the largest part of the genetic information of the endosymbiont genome has been transferred to the nucleus. Such gene transfers occur quite often in plants; the gene content in the mitochondria can vary between the different species. Moreover, genes apparently can pass from the plastids to the mitochondria. Delineated from their nucleotide sequences, several mt tRNA genes seem to originate in the plastid genome.

The promoters of plant mitochondrial genes are heterogeneous. The sequences signaling the start and end of transcription are quite variable, even for the genes within the same mitochondrion. Most likely several mtRNA polymerases are present in plant mitochondria, similarly as in plastids. Mitochondrial transcription factors have not yet been unequivocally characterized. Most of the mitochondrial genes are transcribed monocistronically.

Mitochondrial RNA is corrected after transcription via editing

A comparison of the amino acid sequences of proteins encoded in mitochondria with the corresponding nucleotide sequences of the encoding

genes revealed strange discrepancies: the amino acid sequences did not correspond to the DNA sequences of the genome according to the universal genetic code. At sites of the DNA sequence where, according to the protein sequence a T was to be expected, a C was found, and sometimes vice versa. More detailed studies showed that the transcription of mtDNA yielded an mRNA sequence that would not translate into the "correct" (expected) protein. It was all the more astonishing to discover that this "incorrect" mRNA subsequently is processed in the mitochondria by several replacements of C by U, but sometimes also of U by C, until the correct mRNA is reconstructed as a template for synthesizing the proper protein. This process is called **RNA editing**.

Subsequent editing of the initially incorrect mRNA to the correct, translatable mRNA is not an exception taking place only in some exotic genes, but is the rule for the mitochondrial genes of higher plants. In some mRNAs produced in the mitochondria, 40% of the C is replaced by U in the editing process. Mitochondrial tRNAs are also edited in this way. The question arises whether, by differences in the editing, a structural gene can be translated into different proteins. Now and again mitochondrial proteins were found which had been translated from only partially edited mRNA. Since these proteins normally are nonfunctional, they are probably degraded rapidly.

RNA editing was first shown in the mitochondria of trypanosomes, the unicellular pathogen of sleeping sickness. It also occurs in mitochondria of animals and, in a few cases, has also been found in plastids.

Only since 1989 has RNA editing been known to exist in plant mitochondria. The C-U conversion occurs by desamination, but the mechanisms of other nucleotide exchanges and insertions are still not fully resolved. Many questions are still open. What mechanism is used for RNA editing? Also, the question of the physiological meaning of RNA editing is still unanswered. Is a higher mutation rate of the maternally inherited mt-genome corrected by the editing? From where does the information for the proper nucleotide sequence of the mRNA come? Is this information provided by the nucleus or is it also contained in the mitochondrial genome? It is feasible that the very large mitochondrial genome contains, in addition to the structural genes, single fragments, the transcripts of which are utilized for the correction of the mRNA, as has been observed in the mitochondria from trypanosomes.

Male sterility of plants caused by the mitochondria is an important tool in hybrid breeding

When two selected inbreeding lines are crossed, the resulting **F1 hybrids** are normally larger, are more robust, and produce higher yields of harvest products than the parent plants. This effect, called **hybrid vigor**, was

observed before the rediscovery of the Mendelian laws of inheritance and was first utilized in 1906 for breeding hybrid maize by George Schull in the laboratory at Cold Spring Harbor in the United States. The success of these studies brought about a revolution in agriculture. Based on the results of Schull's research, private seed companies bred maize F_1 hybrids that provided much higher yields than the customary varieties. In 1965, 95% of the maize grown in the Corn Belt of the United States was F_1 hybrids. The use of F_1 hybrids was, to a large extent, responsible for the increase in maize yields per acre by a factor of 3.5 between 1940 and 1980 in the United States. The hybrid technique also brought dramatic yield increases for rice, thus in China the rice harvest was increased from 1975 to 2000 by a factor of 1.8.

F_1 hybrids cannot be further propagated, since according to the Mendelian laws the offspring of the F_2 generation is heterogeneous. Most of the second-generation (F_2) plants have some homozygosity, resulting in yield depression. Each year, therefore, farmers have to purchase new hybrid seed from the seed companies, whereby the seed companies gained a large economical importance. Hybrid breeding has been put to use for the production of many varieties of cultivated species. Taking maize as an example, the following describes the principles and problems of hybrid breeding.

For the production of F_1 hybrid seed (Fig. 20.27), the pollen of a paternal line A is transferred to the pistil of a maternal line B, and only the cobs of B are harvested for seed. These crossings are carried out mostly in the field. Plants of lines A and B are planted in separate, but neighboring rows, so that the pollen is transferred from A to B by the wind. To prevent the pistils of line B from being self- fertilized by the pollen of line B, the plants of line B are emasculated. Since in maize the pollen producing male flowers are separated from the female flowers in a panicle, it is possible to remove only the male flowers by cutting off the panicle. To produce hybrid seeds in this way on a commercial scale, however, requires a great expenditure in manual labor. This method is totally unfeasible on any scale in plants such as rye, where the male and the female parts of the flower are combined.

It was a great step forward in the production of hybrids when maize mutants with sterile pollen were isolated. In these male-sterile plants, the fertility of the pistil was not affected as long as it was fertilized by pollen of other lines. This male sterility is inherited maternally by the genome of the mitochondria. Several male-sterile mutants of maize and other plants are the result of a mutation of mitochondrial genes.

The relationship between the mutation of a mitochondrial gene and the male sterility of a plant has been thoroughly investigated in the maize mutant T (Texas). The mitochondria of this mutant contain a gene designated as **T-urf13**, which encodes a **13 kDa protein**. This gene is probably the

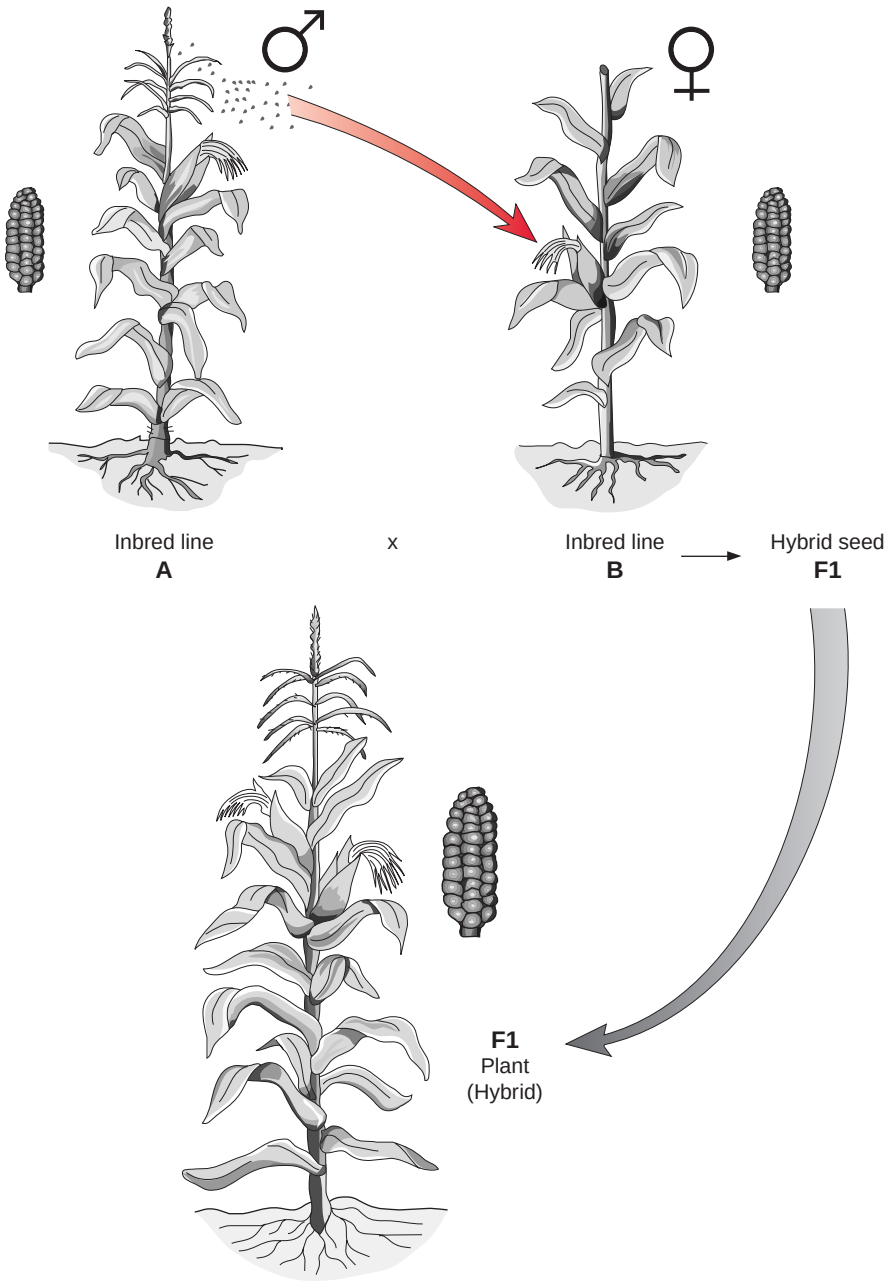

Figure 20.27 Principle of hybrid breeding shown with maize. The lines A and B are inbred lines, which produce a relatively low yield of harvest products. When these lines are crossed, the resulting F_1 progeny is much more robust and produces high yields. The seeds are obtained from line B, which is pollinated by line A. To prevent self-fertilization of B by its own pollen, the male flowers of B are removed by cutting them off the panicle. (From Patricia Nevers, Pflanzenzüchtung aus der Nähe gesehen, Max Planck Institut für Züchtungsforschung, Köln, by permission.)

product of a complex recombination. The 13 kDa protein has no apparent effect on the metabolism of the mitochondria under conditions of vegetative growth, and the mutants are of normal phenotypes. Only the formation of pollen is disturbed by this protein, for reasons not known in all details.

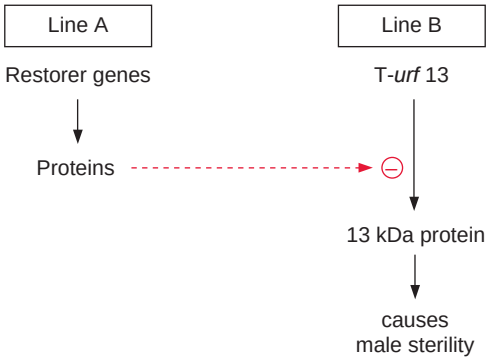

Figure 20.28 A maize mutant T (here designated as line B) contains in the mitochondrial genome a gene named T-urf13. The product of this gene, a 13 kDa protein, prevents the formation of sterile pollen and thus causes male sterility in this mutant. Another maize line (A) contains in its nucleus one or several so-called restorer genes, encoding proteins, which suppress the expression of the T-urf13 gene in the mitochondria. Thus, after a crossing of A with B, the pollen is fertile and the male sterility is abolished.

It is possible that the tapetum cells of the pollen sac, which are involved in pollen production, have an unusual abundance of mitochondria and apparently depend very much on mitochondrial metabolism. Therefore, in these cells a mitochondrial defect, which normally does not affect metabolism, might interfere with pollen production.

The successful use of these male-sterile mutants for seed production is based on a second discovery: maize lines contain so-called **restorer genes** in their nucleus. These encode **pentatricopeptide repeat proteins** (**PRR**) which are grouped into a protein family that is ubiquitous in plants. Structural prediction indicates that these PPR proteins are present in the organelle and bind RNA, causing the degradation of this RNA. In this way PPR represses the expression of the T-urf13 gene in the mitochondria (Fig. 20.28). The crossing of a paternal plant A containing these restorer genes with a male-sterile maternal plant B results in F_1 generation, in which the fertility of the pollen is restored and corn cobs are produced normally.

The crossing of male-sterile T maize lines with lines containing restorer genes enables F_1 hybrids to be produced very efficiently. Unfortunately, however, the 13 kDa protein encoded by the T-urf13 makes a maize plant more sensitive to the toxin of the fungus *Bipolaris maydis T*, the pathogen of the much dreaded fungal disease "southern corn blight," which destroyed a large part of the American maize crop in 1971. The 13 kDa protein reacts with the fungal toxin to form a pore in the inner mitochondrial membrane and thus eliminates mitochondrial ATP production. In order to continue hybrid seed production, it was then necessary to return to the manual removal of the male flowers. Male-sterile lines are now known not only in maize, but also in many other plants, in which the sterility is caused by proteins encoded in the mt-genome, and also other lines that suppress the formation of the inhibiting protein by nuclear encoded proteins. Nowadays these lines are used for the production of fertile F_1 hybrid seeds.

Presumably the reaction of nuclear encoded proteins on the expression of mitochondrial genes such as T-urf13 is a normal reaction of mitochondrial metabolism in plants and therefore, after the production of corresponding mutants, can be used in many ways to generate male sterility.

Today intensive research is being carried out all over the world to find ways of generating male sterility in plants by genetic engineering. Success can be noted. Using a specific promoter, it is possible to express a ribonuclease from the bacterium *Bacillus amyloliquefaciens* exclusively in the tapetum cells of the pollen sac in tobacco and rape seed. This ribonuclease degrades the mRNA formed in tapetum cells, thus preventing the development of pollen. Other parts of the plants are not affected and the plants grow normally. For the generation of a restorer line, the gene of a ribonuclease inhibitor (from the same bacterium) was transferred to the tapetum cells. The great advantage of such a synthetic system is its potential for general application. In this way male sterility can be introduced into species in which this cannot be achieved by manual removal of the stamen, and where male sterility due to mutants is not available. Genetically engineered rape seed hybrids are nowadays grown to a large extent in the United States and Canada. It is to be expected that the generation of male-sterile plants by genetic engineering and the resultant use of hybrid seed might lead to increased harvests of many crops.

Further reading

Arabidopsis genome: A milestone in plant biology. Special Issue Plant Physiology 124, 1449–1865 (2002).

Arabidopsis functional genomics. Special Issues Plant Physiology, *129*, 389–925 (2002).

Baulcombe, D. RNA silencing in plants. Nature 341, 356–363 (2004).

Eckhardt, N. Cytoplasmic male sterility and fertility restoration. Plant Cell 18, 515–517 (2006).

Gutierrez, M. F. J., Ewing, R. M., Cherry, J. M., Green, P. J. Identification of unstable transcripts in Arabidopsis by cDNA microarray analysis: Rapid decay is associated with group of touch- and specific clock-controlled genes. Proceedings of National Academic Society USA 99, 11513–11518 (2002).

Moore, G. Cereal chromosome structure, evolution, and pairing. Annual Review Plant Physiology and Plant Molecular Biology 51, 195–222 (2000).

Ohyama, K., Fukuzuwa, H., Kochi, T., et al. Chloroplast gene organisation deduced from the complete sequence of liverwort *Marchantia polymorpha* chloroplast DNA. Nature 322, 572–574 (1986).

Simamoto, K., Kyozuka, J. Rice as model for comparative genetics in plants. Annual Review Plant Biology 53, 399–420 (2002).

Shinozyki, K., Ohme, M., Wakasugi, T., et al. The complete nucleotide sequence of the chloroplast genome: Its gene organisation and expression. EMBO Journal 9, 2043–2049 (1986).

Takenata, M., van der Merwe, J. A., Verbitskij, D., Neuwirt, J., Zehrmann, A., Brennicke, A. RNA editing in plant mitochondria. In U. Göringer (Ed.), RNA editing. Leiden: Springer Verlag (2007)

The *Arabidopsis* genome initiative. Analysis of genome sequence of the flowering plant *Arabidopsis thaliana. Nature* 408, 796–815 (2000).

The Rice Annotation Project. Curated genome annotation of *Oryza sativa* ssp. *Japonica* and comparative genome analysis with *Arabidopsis thaliana*. Genome Research 17, 175–183 (2007).

Unseld, M., Marienfeld, J. R., Brandt, P., Brennicke, A. The mitochondrial genome of *Arabidopsis thaliana* contains 57 genes on 366.924 nucleotides. Nature Genetics 15, 57–61 (1997).

Vazquez, F. Arabidopsis endogenous small RNAs: Highways and byways. Trends in Plant Science 11, 460–468 (2006).

Willmann, M. R., Poethig, R. S. Conservation and evolution of mRNA regulation programs in plant development. Current Opinion in Plant Biology 10, 503–511 (2007).

21

Protein biosynthesis occurs in three different locations of a cell

During protein biosynthesis, the nucleotide sequence of mRNA is translated into an amino acid sequence. The "interpreters" are **transfer ribonucleic acids** (tRNAs), small RNAs of 75 to 110 ribonucleotides, which have a defined structure with hairpins and loops. One loop exhibits the **anticodon**, which is complementary to the mRNA **codon**. For each amino acid there exists at least one and sometimes several tRNAs. The covalent binding of the amino acid to the corresponding tRNA is catalyzed by its specific **aminoacyl tRNA synthetase**. With the consumption of ATP a mixed anhydride aminoacyl-AMP is synthesized as an intermediate prior to the binding of the amino acid to the 3′ OH of the tRNA (Fig. 21.1).

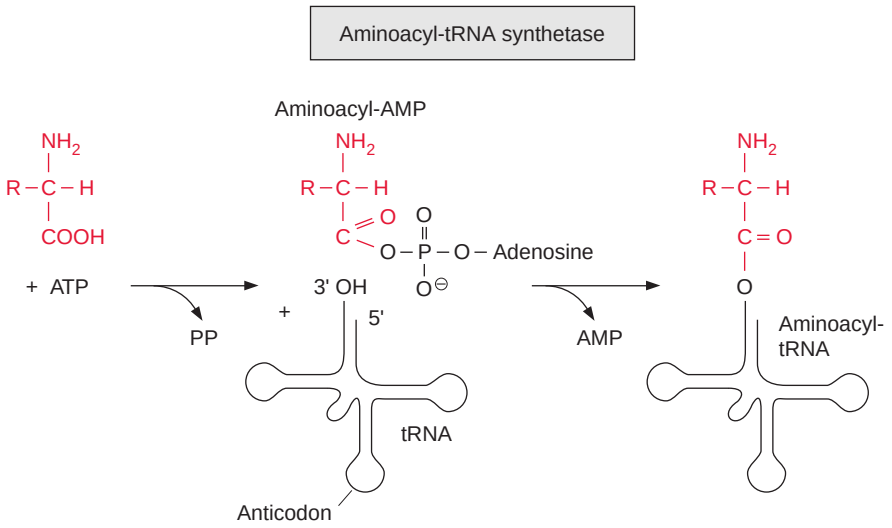

Figure 21.1 tRNA is loaded by aminoacyl-tRNA synthetase with its corresponding amino acid, ATP is used for activation and aminoacyl-AMP is formed as an intermediate.

In a plant cell, protein biosynthesis takes place in three different locations. The translation of the nuclear encoded mRNAs proceeds in the cytosol, and that of the mRNAs encoded in the plastidic or mitochondrial genome takes place in the plastid stroma and mitochondrial matrix, respectively.

21.1 Protein synthesis is catalyzed by ribosomes

Ribosomes are large riboprotein complexes that consist of three to four different rRNA molecules and a large number of proteins. In the intervals between the end of the translation of one mRNA and the start of the translation of another mRNA, the ribosomes dissociate into two subunits. The ribosomes of the cytosol, plastids, and mitochondria are different in size and composition (Table 21.1). The **cytosolic** ribosomes (termed **eukaryotic ribosomes**), with a sedimentation constant of 80S, dissociate into a small subunit of 40S and a large subunit of 60S. In contrast, the **mitochondrial ribosomes**, with a size of about 78S, varying from species to species, and the **plastidic ribosomes** (70S) are smaller. Due to their relationship to the bacterial ribosomes, the mitochondrial and plastidic ribosomes are classified as **prokaryotic ribosomes**. Ribosomes of the bacteria, e.g., *Escherichia coli*, have a sedimentation constant of 70S.

Table 21.1: Composition of the ribosomes in the cytosol, chloroplast stroma, and mitochondrial matrix in plants

	Complete ribosome	Ribosomal subunits	rRNA components	Proteins
Cytosol (eukaryotic ribosome in plants)	80S	Small UE 40S	18S-rRNA	ca. 30
		Large UE 60S	5S-rRNA 5.8S-rRNA 25S-rRNA	ca. 50
Chloroplast (prokaryotic ribosome)	70S	Small UE 30S	16S-rRNA	ca. 24
		Large UE 50S	4.5S-rRNA 5S-rRNA 23S-rRNA	ca. 35
Mitochondrion (prokaryotic ribosome)	78S	Small UE ≈30S	18S-rRNA	ca. 33
		Large UE ≈50S	5S-rRNA 26S-rRNA	ca. 35

At the beginning of translation, the mRNA forms an **initiation complex** with a ribosome. A number of **initiation factors** participate in this process. The eukaryotic translation occurring in the cytosol will be described first. At the beginning of the process, the eukaryotic initiation factor2 (eIF2), together with GTP and a transfer RNA loaded with methionine, form an **initiation-transfer-RNA-complex**. With the participation of other initiation factors, it is then bound to the small 40S subunit of the ribosome. The initiation factor eIF4F, which consists of several protein components (also known as Cap-binding protein), mediates the binding of the initiation-tRNA-complex to the **Cap sequence** of the 5′ end of the mRNA (see Fig. 20.9). For this the consumption of ATP is required. Driven by the hydrolysis of another ATP, the 40S subunit migrates downstream (5′ → 3′) until it finds the AUG start codon. Usually the first AUG triplet on the mRNA is the start codon, but in some mRNAs, the translation starts at a later AUG triplet. The neighboring sequences on the mRNA decide which AUG triplet is recognized as the start codon. The large 60S subunit is then bound to the 40S subunit, accompanied by the dissociation of several initiation factors and GDP. The formation of the initiation complex is now completed and the resulting ribosome is able to translate (Fig. 21.2).

The mitochondrial and plastidic mRNAs have no cap sequence. Plastidic mRNAs have a special ribosome binding site for the initial binding to the small subunit of the ribosome consisting of a purine-rich sequence of about 10 bases. This sequence, called the **Shine-Dalgarno sequence**, binds to the 16S-rRNA of the small ribosome subunit. A Shine-Dalgarno sequence is also found in bacterial mRNAs, but it is not known whether it also plays this role in the mitochondria. In mitochondria, plastids and bacteria, the initiation tRNA is loaded with N-formyl methionine (instead of methionine as in the cytosol). After peptide formation the formyl residue is cleaved from the methionine.

A peptide chain is synthesized

A ribosome, completed by the initiation process, contains two sites where the tRNAs can bind to the mRNA. The **peptidyl site (P)** allows the binding of the initiation tRNA to the AUG start codon (Fig. 21.3). The **aminoacyl (A) site** covers the second codon of the gene. On the other side of site P is the exit **(E) site** where the empty tRNA is released. The **elongation** begins after the corresponding aminoacyl-tRNA occupies the A site by forming base pairs with the second codon. Two **elongation factors** participate in this. The eukaryotic elongation factor (eEF1α) binds GTP and guides the corresponding aminoacyl-tRNA to the A site, during which the GTP is hydrolyzed to GDP and P. The cleavage of the energy-rich anhydride

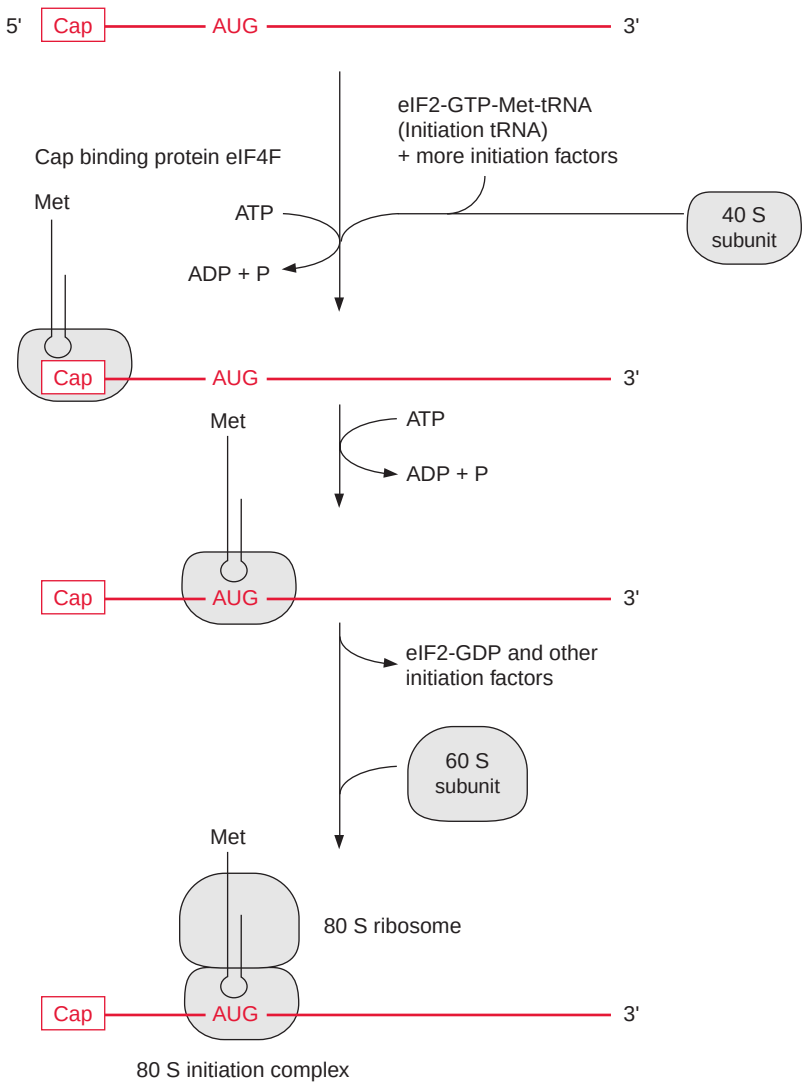

Figure 21.2 Formation of the initiation complex with eukaryotic (80S) ribosomes.

bond in GTP enables the aminoacyl-tRNA to bind to the codon at the A site. Afterwards the GDP, still bound to eEF1α, is exchanged for GTP, as mediated by the elongation factor eEF1$\beta\gamma$. The eEF1α-GTP is now ready for the next cycle.

Subsequently a peptide linkage is formed between the carboxyl group of methionine and the amino group of the amino acid of the tRNA bound to the A site. The **peptidyl transferase**, which, as part of the ribosome, catalyzes this reaction, is a complex enzyme consisting of several ribosomal proteins. The 25S-rRNA has a decisive function in the catalysis. The enzyme

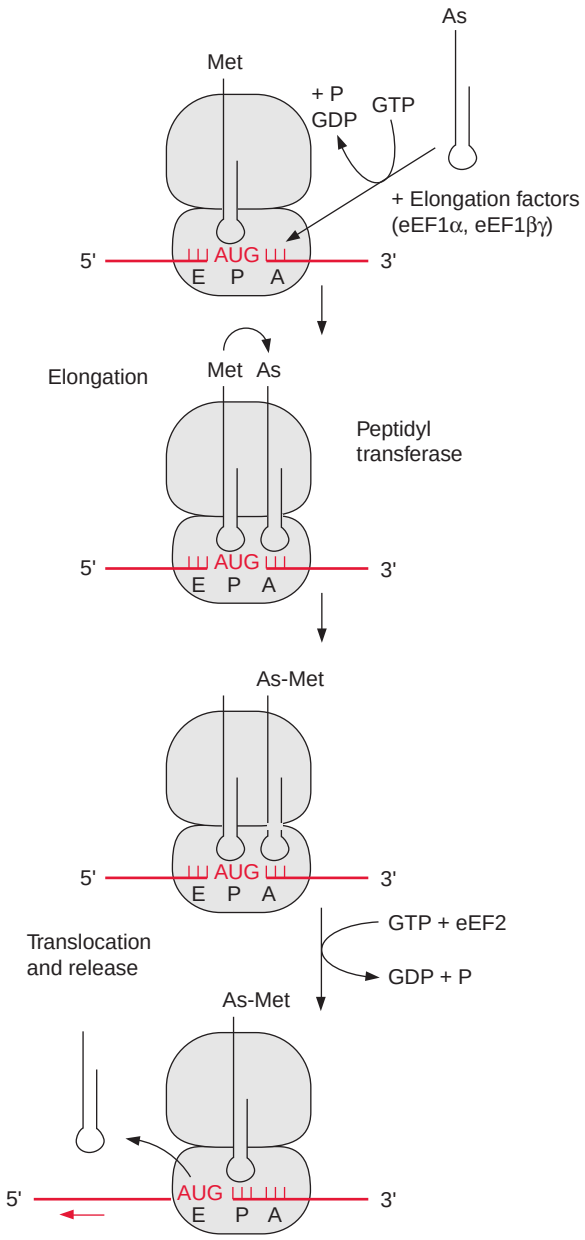

Figure 21.3 Elongation cycle of protein biosynthesis. After binding of the corresponding aminoacyl-tRNA to the A site, a peptide bond is formed by peptidyl transferase. By subsequent translocation, the remaining empty tRNA is moved to the E site and released, while the tRNA loaded with the peptide chain now occupies the P site. By the so-called translocation the ribosome is shifted, making the A side accessible to the next aminoacyl-tRNA. As = amino acid.

facilitates the *N*-nucleophilic attack on the carboxyl group, whereby the peptide bond is formed. This results in the formation of a dipeptide bound to the tRNA at the A site (Fig. 21.4A).

Accompanied by the hydrolysis of one molecule of GTP into GDP and P, the elongation factor eEF2 facilitates the **translocation** of the ribosome

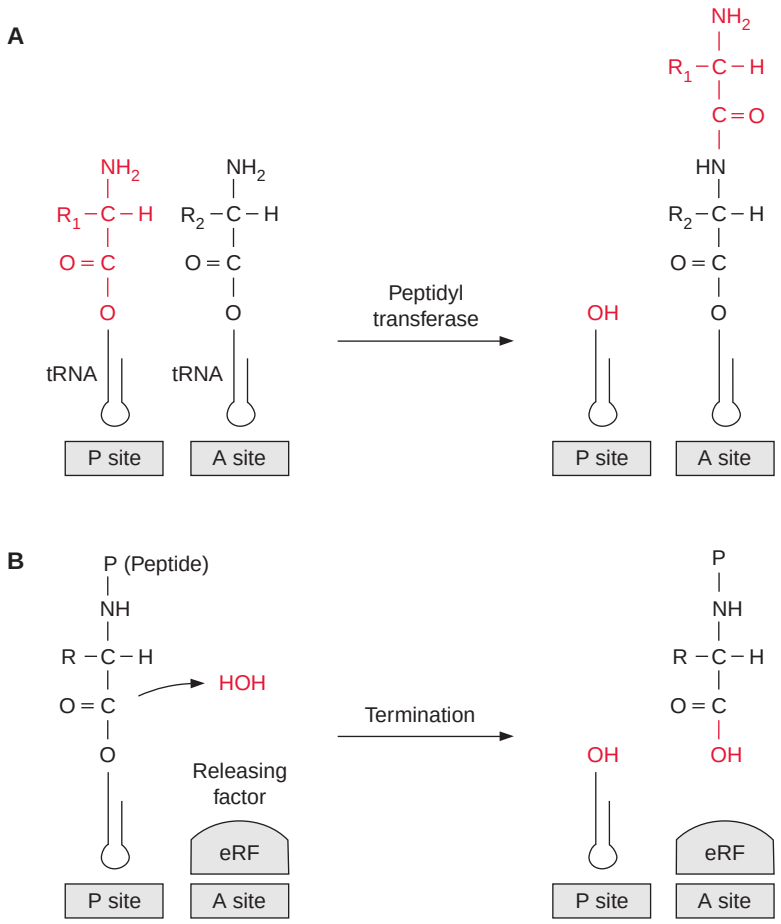

Figure 21.4 A. Formation of a peptide bond by peptidyl transferase. B. Termination of peptide synthesis by the binding of a release factor (eRF) to the stop codon at the A site. The peptide is transferred from the tRNA to an H_2O molecule.

along the mRNA to three nucleotides downstream (Fig. 21.3). In this way the free tRNA arrives at site E, is released, and the tRNA loaded with the dipeptide now occupies the P site. The third aminoacyl-tRNA binds to the vacant site A and a further elongation cycle can begin.

After several elongation cycles, the 5′ end of the mRNA is no longer bound to the ribosome and can start a new initiation complex. An mRNA that is translated simultaneously by several ribosomes is called a **polysome** (Fig. 21.5).

Translation is terminated when the A site finally reaches a **stop codon** (UGA, UAG, or UAA) (Fig. 21.4B). These stop codons bind the **release factor** (eRF) accompanied by hydrolysis of GTP to form GDP and P. Binding of eRF to the stop codon alters the specificity of the peptidyl transferase: a water molecule instead of an amino acid is now the

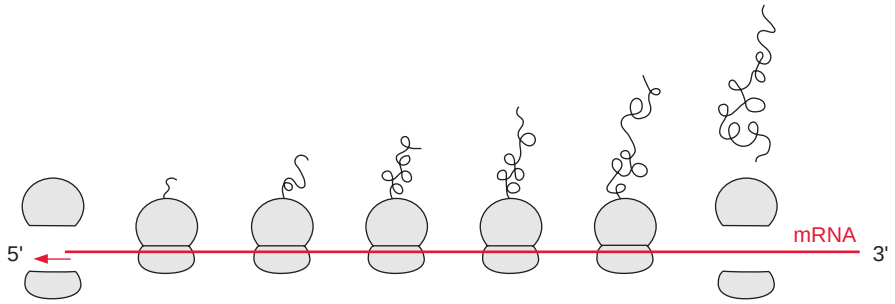

Figure 21.5 Several ribosomes that simultaneously translate the same mRNA are called a polysome.

acceptor for the peptide chain. In this way the protein formed is released from the tRNA.

Specific inhibitors of the translation can be used to decide whether a protein is encoded in the nucleus or the genome of plastids or mitochondria

Elongation, translocation and termination occur in prokaryotic ribosomes in an analogous way as in eukaryotic ribosomes. Only minor alterations are observed, e.g., the termination of the prokaryotic ribosomes does not require GTP. Furthermore, eukaryotic and prokaryotic translation can react differently with certain antibiotics (Fig. 21.6, Table 21.2). **Puromycin**, an analogue of tRNA, is a general inhibitor of protein synthesis, whereas **cycloheximide** inhibits only protein synthesis by **eukaryotic** ribosomes. **Chloramphenicol**, **tetracycline**, and **streptomycin** primarily inhibit protein synthesis by **prokaryotic** ribosomes. These inhibitors can be used to determine whether a certain protein is encoded in the nucleus or in the genome of plastids or mitochondria. A relatively simple method for monitoring protein synthesis is to measure the incorporation of a radioactively labeled amino acid (e.g., ^{35}S-labeled methionine) into proteins. If the incorporation of this amino acid into a protein is inhibited by cycloheximide, this indicates that the protein is encoded in the nucleus. Likewise, inhibition by chloramphenicol shows that the corresponding protein is encoded in the genome of plastids or mitochondria.

The translation is regulated

The synthesis of many proteins is specifically regulated at the level of translation. This regulation may involve protein kinases by which proteins participating in translation are phosphorylated. Since the rate-limiting step of translation is primarily the initiation, this step is especially suited for a

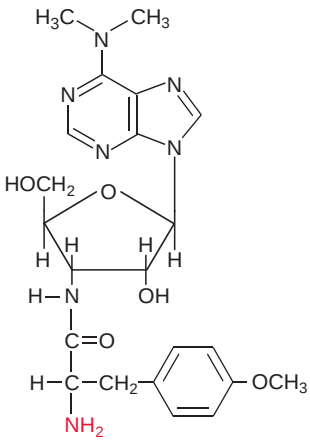

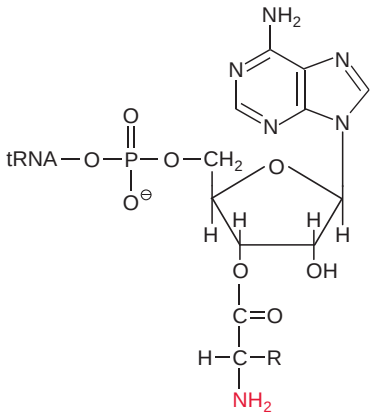

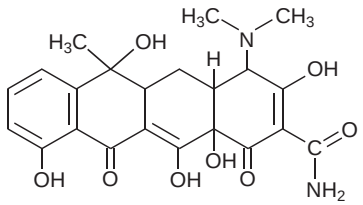

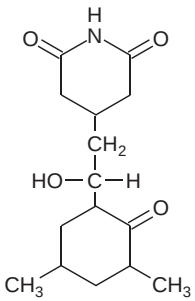

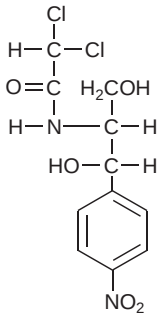

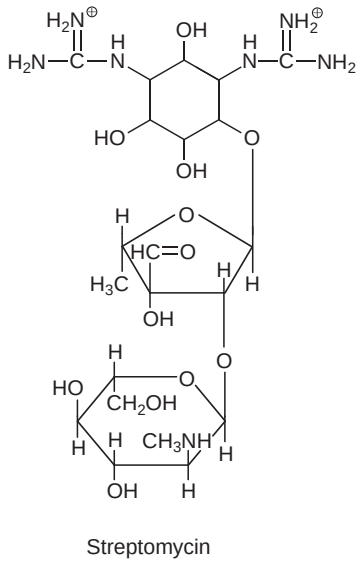

Figure 21.6 Antibiotics as inhibitors of protein synthesis. Their mode of action is described in Table 21.2.

regulation of translation. In animals, the initiation factor eIF2 is inactivated by phosphorylation and initiation is therefore inhibited. Little is known about the regulation of translation in plants.

21.2 Proteins attain their three-dimensional structure by controlled folding

Protein biosynthesis by ribosomes first yields an unfinished (immature) polypeptide. This is converted (if necessary after amino acid sequences, e.g., transit or signal sequences are cleaved off) by specific folding to establish

Table 21.2: Antibiotics as inhibitors of protein synthesis

Antibiotic	Inhibitor action
Puromycin	Binds as an analogue of an aminoacyl-tRNA to the A site and participates in all elongation steps, but prevents the formation of a peptide bond, thus terminating protein synthesis in prokaryotic and eukaryotic ribosomes.
Cycloheximide	Inhibits peptidyl transferase in eukaryotic ribosomes.
Chloramphenicol	Inhibits peptidyl transferase in prokaryotic ribosomes.
Tetracycline	Binds to the 30S subunit and inhibits the binding of aminoacyl-tRNA to prokaryotic ribosomes much more than to eukaryotic ones.
Streptomycin	The interaction with 70S-ribosomes results in an incorrect recognition of mRNA sequences and thus inhibits initiation in prokaryotic ribosomes.

The listed antibiotics are all derived from *Streptomycetae*

the biological active form, the **native protein**. The three-dimensional structure of the native protein normally represents the lowest energy state of the molecule and is determined to a large extent by the amino acid sequence of the molecule.

The folding of a protein is a multistep process

Theoretically there are about 10^{100} possible conformations for a peptide with 100 amino acids, which is a rather small protein of about 11 kDa. Since the reorientation of a single bond requires about 10^{-13} s, it would take the incredibly long time of 10^{87} s to try all possible folding states one after the other. By comparison, the age of the earth is about 1.6 10^{17} s. In reality, a protein attains its native form within seconds or minutes. Apparently the folding of the molecule proceeds in a multistep process. It begins by forming secondary structures such as **α-helices** or **β-sheets**. They consist of 8 to 15 amino acid residues, which are generated or disintegrated within milliseconds (Fig. 21.7). The secondary structures then associate stepwise with increasingly larger domains and in this way also stabilize the regions of the molecule that do not form secondary structures. The driving force in these folding processes is the hydrogen bond interactions between the secondary structures. After further conformational changes, the correct three-dimensional structure of the molecule is attained rapidly by this cooperative folding procedure. In proteins with several subunits, the subunits associate to form a quaternary structure.

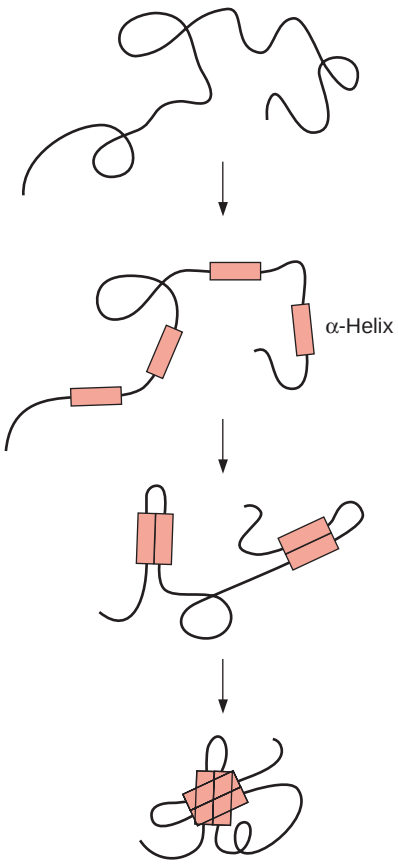

Figure 21.7 Protein folding is a stepwise hierarchic process. First, secondary structures (e.g., α-helices) are formed, which then aggregate successively, until finally, after slight corrections to the folding, the tertiary conformation of the native protein is attained.

Proteins are protected during the folding process

The folding process can be severely disturbed when the secondary structures in the molecule associate incorrectly, or particularly when secondary structures of different molecules associate, resulting in an undesirable aggregation of proteins (hydrophobic collapse). This danger is especially high during protein synthesis, when the incomplete protein is still attached to the ribosome (Fig. 21.5), or during the transport of an unfolded protein through a membrane, when only part of the peptide chain has reached the other side. Moreover, incorrect intermolecular associations are likely to occur when the concentration of a newly synthesized protein is very high, as can be the case in the lumen of the rough endoplasmatic reticulum (Chapter 14). To prevent such incorrect folding, a family of proteins present in the various cell compartments helps newly formed protein

molecules to attain their correct conformation by avoiding incorrect associations. These proteins have been named **chaperones**.

Heat shock proteins protect against heat damage

Chaperones not only have a function during correct folding of proteins but also protect proteins against aggregation when they have been denatured by exposure to high temperatures, thus assisting their reconversion to the native conformation. Bacteria, animal, and plant cells react to a temperature increase of about 10% above the temperature optimum with a very rapid synthesis of so-called **heat shock proteins**, most of which are chaperones. Many plants can survive otherwise lethal high temperatures if they have been pre-exposed to a smaller temperature increase, which had induced the synthesis of heat shock proteins. This phenomenon is called **acquired thermal tolerance**. Investigations with soybean seedlings showed that such tolerance coincides with an increase in the content of heat shock proteins. However, most of these heat shock proteins are constitutively present in the cells, which indicates that heat shock proteins have important functions in the folding of proteins even under normal conditions.

Chaperones bind to unfolded proteins

Since chaperones were initially characterized as heat shock proteins, they are commonly designated by the abbreviation Hsp followed by the molecular mass in kDa.

Chaperones of the **Hsp70 family** have been found in bacteria, mitochondria, chloroplasts, and the cytosol of eukaryotes, as well as in the endoplasmatic reticulum. These are highly conserved proteins. Hsp70 has a binding site for adenine nucleotides, which can be occupied either by ATP or ADP. When occupied by ADP, Hsp70 forms with the chaperone **Hsp40** (also required for the binding of unfolded proteins) a tight complex with unfolded segments of a protein, but not with native proteins (Fig. 21.8). The ADP bound to Hsp70 is subsequently replaced by ATP. The resultant ATP-Hsp70 complex has only a low binding affinity and therefore dissociates from the protein segment. Due to the subsequent hydrolysis of the bound ATP to ADP, Hsp70 is ready to bind once more to an unfolded peptide segment. In this way Hsp70 binds to a protein only for a short time, dissociates from it, and, if necessary, binds to the protein again. This stabilizes an unfolded protein without restricting its folding capacity. The mechanism of the ADP-dependent binding of Hsp70 to unfolded peptides as mediated by Hsp40 has been conserved during evolution. Fifty percent of the amino acids in the sequences of the Hsp70 protein in *E. coli* and in humans are identical.

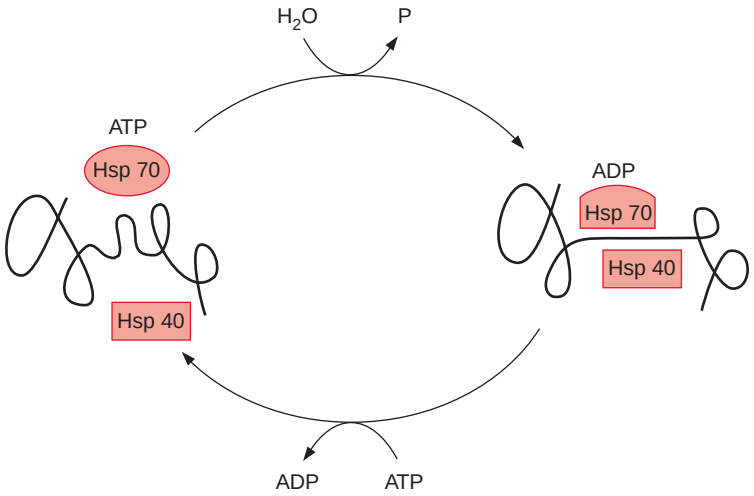

Figure 21.8 The Hsp70 chaperone contains a binding site for ATP and hydrolyzes ATP to ADP. The Hsp70-ADP complex binds tightly with Hsp40 to an unfolded segment of a protein. The ADP bound to Hsp70 is exchanged for ATP. The Hsp70-ATP complex has only a low binding affinity to the protein, which is therefore released. An unfolded protein can be bound to the complex again only after ATP hydrolysis. This simplified scheme does not deal with intermediates involved and also does not represent the real structure of the binding complex.

The proteins of the **Hsp60 family**, present in bacteria, plastids, and mitochondria, also bind to unfolded proteins. They were first identified as the **GroEL factor** in *E. coli* and as RubisCO binding protein in chloroplasts, until it was realized that both proteins are homologous and act as chaperones. A **GroES factor** called **Hsp10** in mitochondria and in chloroplasts is involved in binding the Hsp60 chaperones. In bacteria, 14 GroEL and 7 GroES molecules are assembled to a **superchaperone complex**, forming a large cavity into which an unfolded protein fits (Figs. 21.9, 21.10). The unfolded protein is temporarily bound to Hsp60 molecules of the cavity analogously to the binding to Hsp70 in Figure 21.8. Correct folding to the native protein is aided by several ATP hydrolysis cycles, involving dissociation and rebinding of the protein segments. In this way the unfolded protein can reach the native conformation by avoiding association with other proteins.

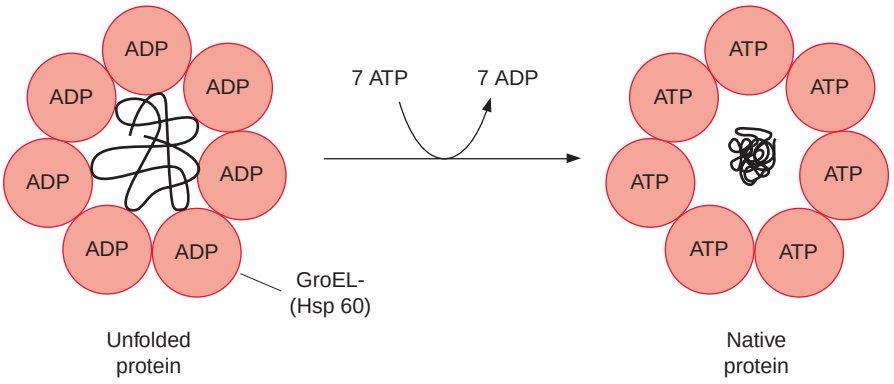

Figure 21.9 Section through the super chaperone complex of prokaryotes consisting of 14 molecules of GroEL (Hsp60) and seven molecules of GroES (Hsp10). The chaperone molecules, paired with ADP, bind unfolded segments of the newly formed protein. Repeated release and binding of the unfolded segments of the protein is driven by ADP/ATP exchange and ATP hydrolysis (see previous figure), until finally the protein is completely correctly folded. The native protein is released because in the end it no longer binds to chaperones due to the lack of unfolded regions.

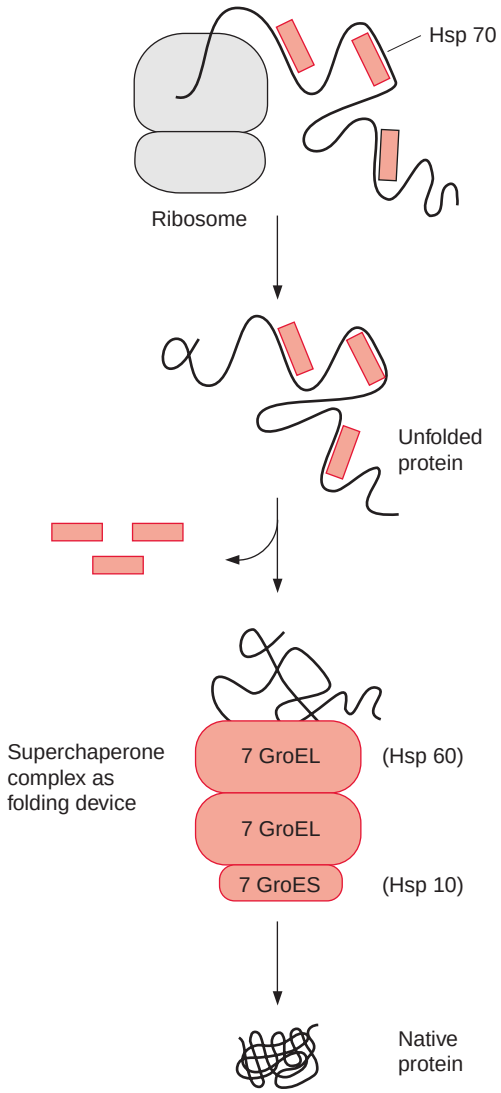

Figure 21.10 The folding of proteins in prokaryotes, plastids, and mitochondria. The unfolded protein is protected by being bound to an Hsp70 chaperone paired with ADP and is then folded to the native protein in the cavity of the super chaperone complex, which consists of GroEL (Hsp60) and GroES (Hsp10). ATP is consumed in this reaction (see Fig. 21.9).

Hsp70 as well as Hsp60 and Hsp10 participate in the protein folding in plastids and mitochondria (Fig. 21.10). Hsp70 protects single segments of the growing peptide chain during protein synthesis, and the super chaperone complex from Hsp60 and Hsp10 finally enables the undisturbed folding of the total protein. The chaperone **Hsp90** is found in very high concentrations in the cytosol of eukaryotes. Hsp90 with co-chaperone (HOP) is regarded as playing a central role in the folding and assembling of cytosolic proteins. Moreover, chaperones named CCT (cytosolic complex T), somewhat

resembling the prokaryotic Hsp60, have been identified in the cytosol of eukaryotes. They act as a folding device by forming oligomeric chaperone complexes, which are probably similar to the Hsp60-Hsp10 super chaperone complex (Fig. 21.10).

Furthermore, there are proteins facilitating other processes, which limit protein folding, such as the formation of disulfide bridges and the *cis-trans* isomerization of the normally non-rotatable prolyl peptide bonds. Since thorough investigation of chaperones began only a few years ago, many questions about their structure and function are still unanswered.

21.3 Nuclear encoded proteins are distributed throughout various cell compartments

The ribosomes present in the cytosol also synthesize proteins destined for cell organelles, such as plastids, mitochondria, peroxisomes, and vacuoles, as well as proteins to be secreted from the cell. To reach their correct location, these proteins must be specifically transported across various membranes.

Proteins destined for the vacuole are transferred through the lumen of the ER (section 14.5). A signal sequence at the N-terminus of the newly synthesized protein binds specifically with a signal recognition particle and the whole complex to a pore protein (receptor) present in the ER membrane and thus directs the protein to the ER lumen. In such a case the ribosome is attached to the ER membrane (rough ER) during protein synthesis and the synthesized protein appears immediately in the ER lumen (Fig. 14.2). This process is called **co-translational protein transport**. These proteins are then transferred from the ER lumen by vesicle transfer across the Golgi apparatus to the vacuole or are exported by secretory vesicles from the cell.

In contrast, protein uptake into plastids, mitochondria, and peroxisomes occurs mainly, if not exclusively, by **post-translational transport**, which means that the proteins are transported across the membrane after completion of protein synthesis and their release from the ribosomes.

Most of the proteins imported into the mitochondria have to cross two membranes

More than 95% of the mitochondrial proteins in a plant are encoded in the nucleus and translated in the cytosol. Our present knowledge about the

import of proteins from the cytosol into the mitochondria derives primarily from studies with yeast. In order to direct proteins from the cytosol to the mitochondria, they have to be provided with a mitochondrial **presequence (transit peptide)** as **targeting signal**. Some proteins destined for the mitochondrial inner membrane or the inter-membrane compartment, as well as all the proteins for the mitochondrial outer membrane, contain internal targeting signals that have not yet been identified. Other proteins of the mitochondrial inner membrane and most of the proteins of the mitochondrial matrix are synthesized in the cytosol as **precursor proteins**, which contain 12 to 70 amino acids at their amino terminus as a **transit peptide**. These targeting presequences have a high content of positively charged amino acids and are able to form α-helices in which one side is positively charged and the other side is hydrophobic. The three-dimensional structure of the amphiphilic α-helices, rather than a certain amino acid sequence, functions as targeting signal. The directing function of this presequence can be demonstrated in an experiment. When a foreign protein, such as the dihydrofolate reductase from mouse, is provided with a targeting presequence for the mitochondrial matrix, this protein is taken up into the mitochondrial matrix.

For the import of proteins into the mitochondrial matrix, both the outer and inner membranes have to be traversed (see Fig. 1.12). This protein import occurs primarily at so-called **translocation sites** where the inner and outer membranes are closely attached to each other (Fig. 21.11). Each membrane provides its own translocation apparatus, which transfers the proteins in the **unfolded state** through the membranes.

The precursor proteins synthesized by the ribosomes associate in the cytosol with chaperones (e.g., Hsp70) in order to prevent premature folding or aggregation of the often hydrophobic precursor proteins. The association with ctHsp70 is accompanied by the hydrolysis of ATP (Fig. 21.8). The transport across the outer membrane is catalyzed by a so-called **TOM complex** (translocase of the outer mitochondrial membrane) consisting of at least eight different proteins. The TOM20 and TOM22 subunits function as receptors for the targeting presequence. An electrostatic interaction between the positively charged side of the α-helix of the presequence and the negative charge on the surface of TOM22 is probably involved in the specific recognition of the targeting signal. TOM22 and TOM20 then mediate the threading of the polypeptide chain into the translocation pore. Another receptor for the transport of proteins is TOM70. This receptor, together with TOM37, mediates the uptake of the ATP-ADP translocator protein and other translocators of the inner membrane, which contain an internal targeting signal instead of a presequence. Probably TOM40 as well as the small subunits TOM5, 6, 7 (not shown in Fig. 21.11) participate in the formation of the translocation pore.

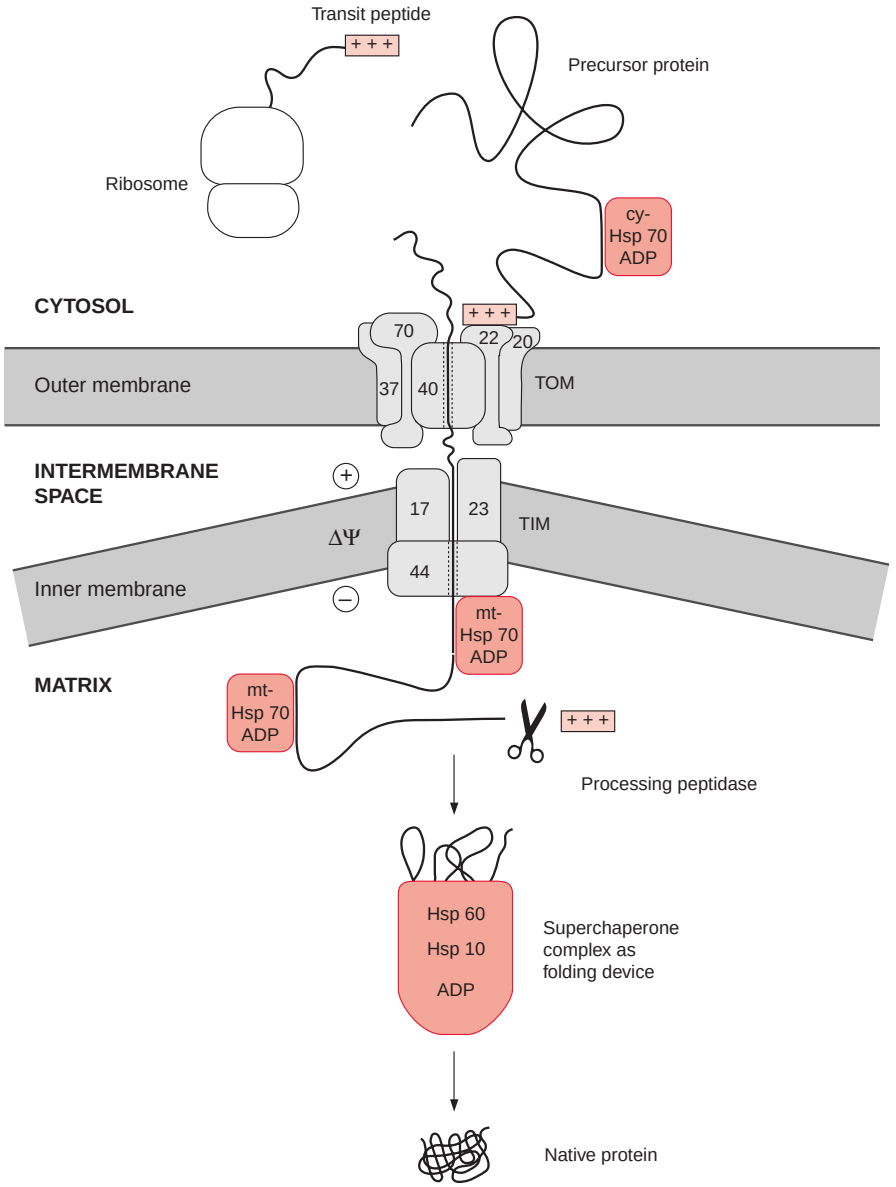

Figure 21.11 Protein import into mitochondria (after Lill and Neupert). The precursor protein synthesized at the cytosolic ribosomes is stabilized in its unfolded conformation by the cytosolic Hsp70 chaperone. A positively charged presequence binds to the receptors TOM20 and TOM22. The presequence threads the precursor protein into the translocation pore of the outer and the inner membranes. Mitochondrial Hsp70 chaperones bind to the peptide chain appearing in the matrix, and thus enable the chain to slide through the translocation pore. The presequence is cut off by a matrix processing peptidase and afterwards the protein attains its native conformation in a super chaperone complex.

The subsequent transport across the inner membrane is catalyzed by the **TIM complex** (translocase of the inner mitochondrial membrane), consisting of the proteins TIM17, 23, 44 and several others not yet identified. A precondition for protein transport across the inner membrane is the presence of a **membrane potential ΔΨ** (section 5.6). Presumably the positively charged presequence is driven through the translocation pore by the negative charge

at the matrix side of the inner membrane. The peptide chain appearing in the matrix is first bound to TIM 44 and is then bound with hydrolysis of ATP (Fig. 21.8) to an mtHsp70 chaperone and also to other chaperones not dealt with here. It is assumed that Brownian movement causes a section of the peptide chain to slip through the translocation pore, which is then immediately bound to the mtHsp70 inside, thus preventing the protein from slipping back. It is postulated that repetitive binding of Hsp70 converts a random movement of the protein chain in the translocation channel into a unidirectional motion. According to this model of a **molecular ratchet**, the ATP required for the reversible binding of mtHsp70 probably is not required for pulling the polypeptide chain through the pore, but, instead, to change its free diffusion across the two translocation pores into unidirectional transport. An alternative hypothesis is also under discussion, according to which the protein entering the pore is pulled into the matrix by ATP-dependent conformational changes of the mtHsp70 bound to the peptide.

When the peptide chain arrives in the matrix, the transit peptide is immediately cleaved off from the protein by a **processing peptidase** (Fig. 21.11). The folding of the matrix protein probably occurs via a super chaperone folding apparatus consisting of the chaperones Hsp60 and Hsp10 (see Figs. 21.9 and 21.10). Proteins destined for the **mitochondrial outer membrane**, after being bound to the receptors of the TOM complex, are directly inserted into the membrane.

In most cases, proteins destined for the **mitochondrial inner membrane**, after transport through the outer membrane, are inserted directly from the inter membrane space into the inner membrane. In some cases, proteins destined for the inner membrane contain a presequence, which first directs them to the matrix space. After this presequence has been cut off by processing peptidases, they are then integrated from the matrix side into the inner membrane via a second targeting sequence.

The import of proteins into chloroplasts requires several translocation complexes

The transport of proteins into the chloroplasts shows parallels but also differences to the transport into mitochondria. Similar to mitochondria most chloroplast proteins are encoded in the nucleus and have to be transferred into the chloroplasts. Transport into the chloroplasts also proceeds **post-translationally**. The precursor proteins synthesized in the cytosol possess a targeting presequence, a **transit peptide** with 30 to 100 amino acid residues at the N-terminus of the protein. As in the mitochondria, the targeting signal probably does not consist of a specific amino acid sequence, but its function is due to the secondary structure of the presequence. The precursor

proteins of the chloroplasts are stabilized by Hsp70 chaperones during their passage through the cytosol.

In order to be imported into the stroma, the protein must cross two membranes (Fig. 21.12). The translocation apparatus of the outer chloroplast envelope membrane contains at least 10 proteins, which, according to their molecular mass (in kDa), are named **TOC** (translocase of the outer chloroplast membrane) and together represent about 30% of the total membrane proteins of the outer envelope membrane. TOC175 functions as receptor and forms with TOC75 the translocation pore for the passage of the unfolded peptide chain. During the transport process further TOC proteins are involved, including those for binding and hydrolysis of GTP. Phosphorylated precursor proteins are recognized by a GTP-TOC34 complex and stimulate its GTPase activity. The change of free energy drives the protein from the resultant GDP-TOC34 complex across the outer membrane. In the intermembrane space the protein is bound to an HSP70. The subsequent transport across the inner envelope membrane involves at least seven **TIC**-(translocase of the inner chloroplast membrane) **proteins**, also named according to their molecular mass. In contrast to mitochondrial protein transport, protein transport into the chloroplast stroma does not require a membrane potential $\Delta\Psi$. Also in the chloroplasts, a unidirectional motion of the unfolded peptide chain through the translocation pore is caused by a repetitive binding of Hsp70 chaperones. According to the model of a molecular ratchet this process is accompanied by the hydrolysis of ATP. After delivering the protein chain to the stroma, the presequence is removed by a processing peptidase of the stroma. The resulting protein is folded to the native conformation, with the aid of an Hsp60-Hsp70-Hsp100 super chaperone complex, and is then released. In this way also the small subunit of RubisCO (section 6.2) is delivered to the stroma, where it is assembled with the large subunit encoded in the chloroplasts.

Those proteins destined for the thylakoid membrane are first delivered to the stroma and then directed by four different mechanisms via internal targeting signals into the thylakoid membrane or lumen (Fig. 21.12). The **SRP** (secretion recognition particle) way inserts proteins (e.g., light harvesting proteins) into the thylakoid membrane. This process, resembling the SRP dependent translocation of proteins into the ER (section 21.3), is driven by a pH gradient and requires GTP. The **TAT** (twin arginine translocation) way transfers proteins into the lumen, facilitated by TAT proteins and driven by a pH gradient. Similar to this the **SEC** (secretion) **way** is facilitated by proteins that are similar to proteins of the secretion pathway (section 1.6) and ATP is required. Some proteins are inserted into the thylakoid membrane spontaneously. In all ways except that of the SRP the presequence with the thylakoid addressing signal is cut off by peptidases.

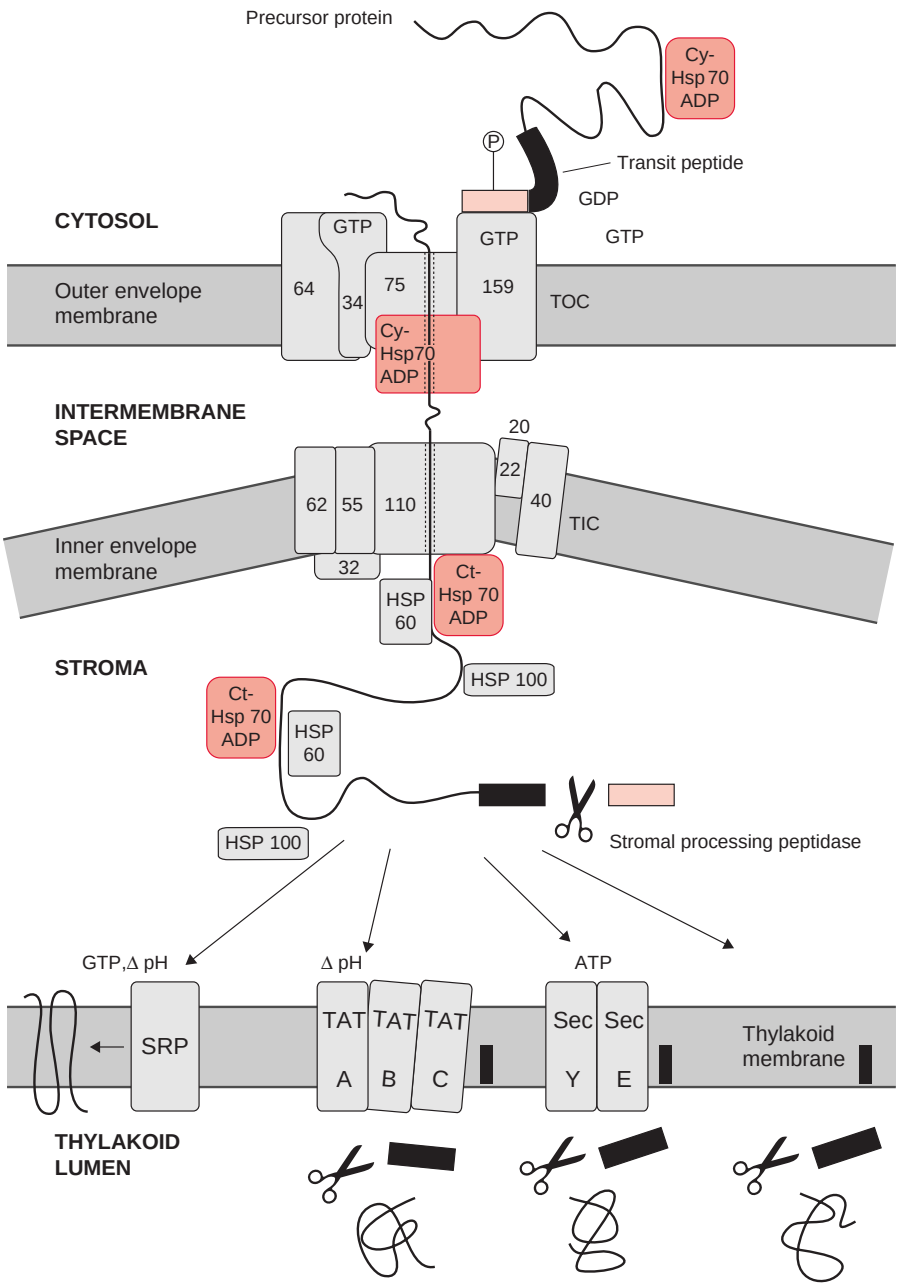

Figure 21.12 Simplified diagram of the protein import into chloroplasts (after Soll, 1995). A protein formed in the cytosol and destined for the thylakoid lumen contains two presequences as targeting signals. The first presequence (colored red) binds to the receptor TOC159 of the translocation apparatus of the outer envelope membrane. The transport of proteins through the translocation pore (TOC75) requires the consumption of GTP. Further TOC proteins are involved in a GDP/GTP exchange, enabling the regeneration of the system. The import requires ATP for the release of the protein from cytosolic (cy) Hsp70 (see Fig. 21.8). The inner translocation pore consists of seven proteins (TIC). The peptide chain appearing in the stroma is bound to several chloroplastic (ct) Hsp70 chaperones and in this way makes it easier for the unfolded chain to slide through the translocation pore. After cleavage of the first presequence (red), the second presequence (black) serves as targeting signal for transport across the thylakoid membrane. Four transport ways are known, facilitated by different proteins and utilizing different energy sources. The second presequence is removed by a membrane-bound thylakoid processing peptidase.

Proteins are imported into peroxisomes in the folded state

The peroxisomes, in contrast to mitochondria and chloroplasts, contain no individual genome. All the peroxisomal proteins are **nuclear-encoded**. Peroxisomes, like mitochondria and chloroplasts, can **multiply by division** and thus are inherited from mother cells. There are also observations that a ***de novo* synthesis** of peroxisomal membranes can take place at the endoplasmatic reticulum. Signal sequences cause some peroxisomal membrane proteins to be incorporated into certain sections of the ER membrane, which are subsequently detached as vesicles regarded as **pre-peroxisomes**. It is postulated that these vesicles fuse to the peroxisomes already present or that they can form new peroxisomes by fusion.

Independent of how the peroxisomes are formed, whether by division or by *de novo* synthesis, it is necessary to import the peroxisomal proteins, which are encoded in the nucleus and synthesized in the cytosol (Fig. 21.13). Two different signal sequences are known as **targeting signals** (peroxisomal targeting signals) PTS1 and PTS2. **PTS1** exhibits at the C-terminus the consensus sequence serine-lysine-leucine (**SKL**) which is not detached after the corresponding protein has been transported into the peroxisomes. **PTS2** consists of a sequence of about nine amino acids near the

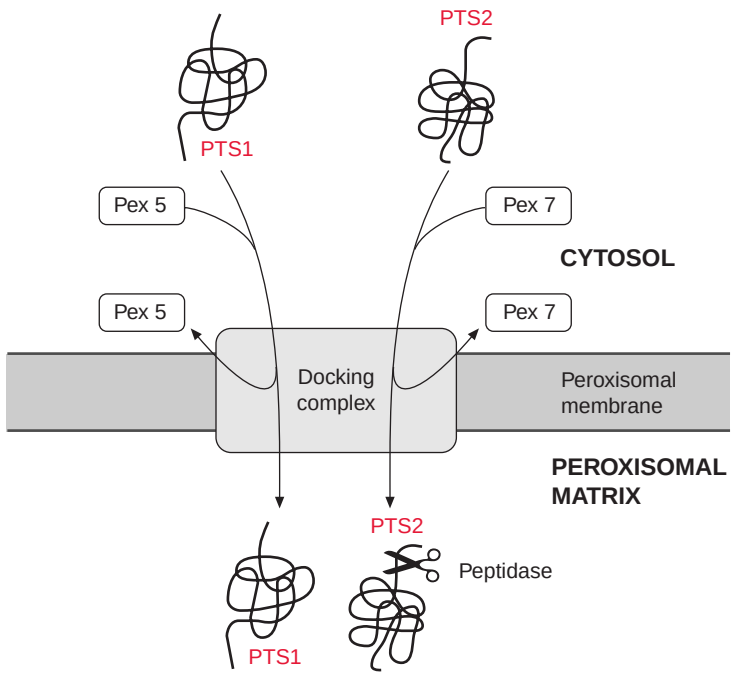

Figure 21.13 Protein import in peroxisomes. The proteins synthesized in the cytosol possess, as target for the import into the peroxisomes, either the signal sequence PTS1 or PTS2. They associate in the cytosol with the relevant soluble receptor proteins Pex5 or Pex7, which conduct them to the docking complex, where the folded proteins are carried through the peroxisomal membrane. After import, a peptidase cleaves off the signal sequence PTS2, whereas the signal sequence PTS1 remains in the mature protein.

N-terminus of certain proteins and is removed after the import of the protein via proteolysis. The proteins targeted by one of the two signals bind to the corresponding **soluble receptor proteins** (Pex5 and Pex7 peroxisomal biogenesis factor), which facilitate the binding to the translocation apparatus (**docking complex**). The docking complex itself consists of several membrane proteins. After dissociation from the receptor proteins, the proteins are transferred upon the consumption of ATP across the membrane into the peroxisomal matrix, in a process not yet fully elucidated. According to present knowledge, the import of proteins into the peroxisomes proceeds in the **folded state** of the proteins, which is in contrast to the import into mitochondria and chloroplasts where protein transport occurs in the unfolded conformation. It seems that protein import into the peroxisomes is entirely different from protein transport into the ER, mitochondria, and plastids.

21.4 Proteins are degraded by proteasomes in a strictly controlled manner

In a eukaryotic cell the protein outfit is regulated not only by its synthesis but also by its degradation. Eukaryotes possess a highly conserved machinery for controlled protein degradation, consisting of a multienzyme complex termed **proteasome**. The outstanding role of this pathway in plants may be illustrated by the fact that more than 5% of all structural genes in *Arabidopsis* participate in this degradation device. In order to be degraded, the corresponding proteins are labeled by covalent attachment of **ubiquitin** molecules. Ubiquitin occurs as a highly conserved protein in all eukaryotes. It has an identical sequence of 76 amino acids in all plants. The C-terminus of the molecule contains a glycine residue, which is the terminal carboxyl group exposed to the outside. Proteins destined for degradation are conjugated to ubiquitin by forming a so-called iso-peptide link between the glycine carboxyl group and the amino group of a lysine residue of the target protein.

The attachment of ubiquitin to a target protein requires the interplay of three different enzymes (Fig. 21.14A). The **ubiquitin-activating enzyme** (**E1**) activates ubiquitin upon the consumption of ATP to form a thioester with an SH-group of the enzyme. The ubiquitin is then transferred to a **ubiquitin-conjugating enzyme** (**E2**). Subsequently the target protein and the ubiquitin attached to E2 react with a specific **ubiquitin-protein ligase** (**E3**) to form the ε-isopeptide linkage bond. More uniquitin molecules can be conjugated, either to lysine residues of the ubiquitin already attached to the target protein or by linkage to other lysine residues of the target protein. In this way target proteins can be labeled with a chain of ubiquitin molecules

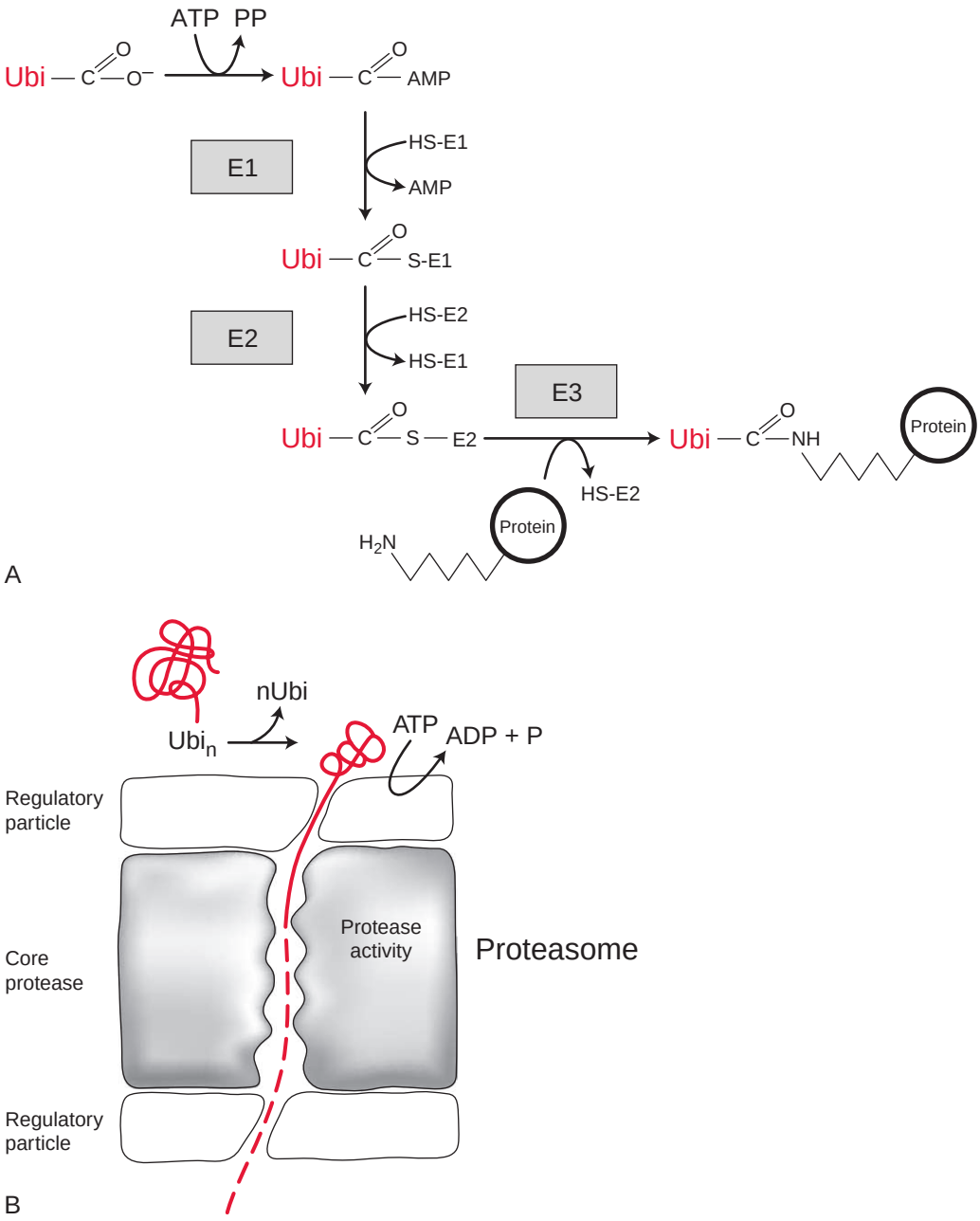

Figure 21.14 Protein degradation by the proteasome pathway. A. A protein destined for degradation (target protein) is tagged by conjugation with ubiquitin (Ubi). Ubiquitin is activated through reaction with ATP by the ubiquitin-activating enzyme (E1) to form via acyl-AMP a thioester link with a cysteine residue of the enzyme. Ubiquitin is then transferred to a cysteine residue of the ubiquitin-conjugating enzyme (E2). Ubiquitin-protein ligase (E3) mediates the transfer of ubiquitin to a lysine residue of a target protein to form an isopeptide bond. By repetition of the process, further ubiquitin molecules can be linked to lysine residues of the existing ubiquitin or to other lysine residues of the target protein. In this way a target protein is often tagged with several ubiquitin molecules. B. Schematic presentation of a proteasome. The multienzyme complex consists of a core protease (CP, 14 subunits) with the shape of a barrel, which is sealed from both sides by regulatory particles of 20 subunits which act as lids. The ubiquitin-tagged protein is bound to RP and the attached ubiquitin molecules are released by hydrolysis. The target protein is unfolded by an ATP-consuming reaction and the resulting polypeptide chain passes the interior of CP, where it is degraded by the proteolytic enzymes.

or by several ubiquitin molecules at various sites. Genome analyses indicated that *Arabidopsis* contains two genes for E1, 24 for E2, and **1,200 genes for E3**. Apparently, the specificity of protein degradation is governed by the various E_3 proteins.

The proteolysis of the labeled target protein is catalyzed by the **proteasome**. This multienzyme complex can be divided into two different particles, a **core protease** (**CP**) consisting of 14 subunits and a **regulatory particle** (**RP**) consisting of 20 subunits. The core protease has a **barrel-like structure**, with the catalytic sites for proteolysis inside it. The openings on both sides are sealed by a regulatory particle (Fig. 21.14B). The regulatory particle recognizes the ubiquitin-labeled target proteins, and catalyzes the hydrolytic cleavage of the ubiquitin molecules, which are thus available for further ubiquitination of proteins. The target protein bound to the RP subunit is unfolded at the expense of ATP, and the peptide chain is allowed to pass through the interior of the barrel, where it is split by the proteolytic activity into peptides of 7 to 9 amino acid residues, which are released from the barrel and further digested by cytosolic peptidases. In organelles proteins are also subjected to a quality control: proteins that carry a defect or are not used anymore are degraded upon the consumption of ATP by a machinery resembling the cytosolic proteasome.

The controlled protein degradation by the proteasome plays a role in the regulatory functions of the phytohormones **gibberellin** and **auxin**. These hormones induce via signal transduction chains the degradation of transcription **repressors** and in this way enhance the expression of genes (sections 19.3 and 19.4). Proteasomes are also involved in the degradation of **activated phytochrome A** (section 19.10).

The ubiquitin-dependent proteasome pathway is not the only way to degrade cellular proteins. During senescence, proteins of the cytoplasm or organelles are surrounded by membranes to form **autophagic vesicles**, which fuse to **lytic vacuoles**, wherein the proteins are subsequently degraded by proteolysis.

Further reading

Baker, A., Sparkes, I. A. Peroxisome protein import: Some answers, more questions. Current Opinion in Plant Biology 8, 640–647 (2005).

Ban, N., Nissen, P., Hansen, J., Moore, P. B., Steitz, T. A. The complete atomic structure of the large ribosomal subunit at 2.4 Å resolution. Science 289, 905–930 (2000).

Bolender, N., Sickmann, A., Wagner, R., Meisinger, C., Pfanner, N. Multiple pathways for sorting mitochondrial precursor proteins. EMBO Reports 9, 42–49 (2008).

Bösl, B., Grimminger, V., Walter, S. The molecular chaperone Hsp104—a molecular machine for protein disaggregation. Journal Structural Biology 156, 139–148 (2006).

Cech, T. R. The ribosome is a ribozyme. Science 289, 878–879 (2000).

Gutensohn, M., Fan, E., Frielingsdorf, S., et al. Structure and function of protein transport machineries in chloroplasts. Journal of Plant Physiology 163, 333–347 (2006).

Hörmann, F., Soll, J., Bölter, B. The chloroplast protein import machinery: A review. Methods Molecular Biology 390, 179–194 (2007).

Kotak, S., Larkindale, J., Lee, U., von Koskull-Döring, P., Vierling, E., Scharf, K. D. Complexity of the heat stress response in plants. Current Opinion Plant Biology 10, 310–316 (2007).

Léon, S., Goodman, J. M., Subramani, S. Uniqueness of the mechanism of protein import into the peroxisome matrix: Transport of folded, co-factor-bound and oligomeric proteins by shuttling receptors. Biochimica Biophysica Acta 1763, 1552–1564 (2006).

López-Juez, E. Plastid biogenesis, between light and shadows. Journal Experimental Botany 58, 11–26 (2007).

Millar, A. H., Whelan, J., Small, I. Recent surprises in protein targeting to mitochondria and plastids. Current Opinion Plant Biology 9, 610–615 (2006).

Mullen, R. T., Trelease, R. N. The ER-peroxisome connection in plants: Development of the "ER-semi-autonomous peroxisome maturation and replication" model for plant peroxisome biogenesis. Biochimica Biophysica Acta 1763, 1655–1668 (2006).

Perry, A. J., Rimmer, K. A., Mertens, H. D., Waller, R. F., Mulhern, T. D., Lithgow, T., Gooley, P. R. Structure, topology and function of the translocase of the outer membrane of mitochondria. Plant Physiology Biochemistry 46, 265–274 (2008).

Sakamoto, W. Protein degradation machineries in plastids. Annual Review Plant Biology 57, 5999–6006 (2006).

Sangster, T. A., Queitsch, C. The HSP90 chaperone complex, an emerging force in plant development and phenotypic plasticity. Current Opinion Plant Biology 8, 86–92 (2005).

Schünemann, D. Mechanisms of protein import into thylakoids of chloroplasts. Biological Chemistry 388, 907–915 (2007).

Smalle, J., Vierstra, R. D. The ubiquitin 26 S proteasome proteolytic pathway. Annual Review Plant Biology 55, 555–590 (2004).

Young, J. C., Agashe, V. R., Siegers, K., Hartl, F. U. Pathways of chaperone-mediated protein folding in the cytosol. Nature 5, 781–791 (2004).

22

Biotechnology alters plants to meet requirements of agriculture, nutrition and industry

Recent years have witnessed spectacular developments in plant biotechnology. In 1984 the group of Jeff Schell and Marc van Montagu in Cologne and Gent, and the group of Robert Horsch and collaborators of the Monsanto Company in St. Louis, Missouri (USA), simultaneously published procedures for the transfer of foreign DNA into the genome of plants utilizing the Ti plasmids of ***Agrobacterium tumefaciens*** (new nomenclature: ***Rhizobium radiobacter***). This method has made it possible to alter the protein complement of a plant specifically to meet special requirements: for example, to render plants resistant to pests or herbicides, to achieve a qualitative or quantitative improvement of the productivity of crop plants, and to adapt plants to the production of defined sustainable raw materials for the chemical industry.

Hardly any other discovery in botany has had such far-reaching consequences in such a short time, when one considers that in 2009 the biotech crop area reached 134 million hectare (about 7% of the global crop area). The main crops altered by genetic engineering using *Agrobacterium tumefaciens* are soy beans, cotton, maize and rape seed. These numbers demonstrate that the results of basic research on an exotic theme, namely, the gall formation in a plant, has led to a technique that brought about a revolution in agriculture.

The following sections will describe how a plant can be altered by genetic engineering. From the abundance of established procedures, only the principles of some major methods can be outlined here. For the sake of brevity, details or complications in methods will be omitted. Some practical examples will show how genetic engineering can be used to alter crop plants.

22.1 A gene is isolated

Let us consider the case where a transgenic plant A is to be generated, which synthesizes a foreign protein (e.g., a protein from plant B). For this, the gene encoding the corresponding protein first has to be isolated from plant B. Since a plant contains between 25,000 and 50,000 structural genes, it will be difficult to isolate a single gene from this very large number.

A gene library is required for the isolation of a gene

To isolate a particular gene from the great number of genes existing in the plant genome, it is advantageous to make these genes available in the form of a gene DNA library. Two different kinds of gene libraries can be prepared.

To prepare a **genomic DNA library**, the total genome of the organism is cleaved by restriction endonucleases (section 20.3) into fragments of about 15 to several 100 kbp. Digestion of the genome in this way results in a very large number of DNA fragments, which frequently contain only parts of genes. These fragments are inserted into a vector (e.g., a plasmid or a bacteriophage) and then each fragment is amplified by cloning, usually in bacteria.

To prepare a **cDNA library**, the mRNA molecules present in a specific plant tissue are first isolated and then transcribed into corresponding cDNAs by **reverse transcriptase** (see section 20.5). The mRNA is isolated from a tissue in which the corresponding gene is expressed at high levels. The cDNAs are inserted into a vector and amplified by cloning. In contrast to the fragments of the genomic library, the resulting cDNAs contain no introns and can therefore, after transformation, be expressed in prokaryotes to synthesize the foreign proteins. Since a cDNA contains no promoter regions, such an expression requires a prokaryotic promoter to be added to the cDNA.

To prepare a cDNA library from leaf tissue, for example, the total RNA is isolated from the leaves, of which the mRNA may amount to only 2%. To separate the mRNA from the bulk of the other RNA species (rRNAs and tRNAs), one makes use of the fact that eukaryotic mRNA contains a **poly(A) tail** at the 3′ terminus (see Fig. 20.8). This allows mRNA to be separated from the other RNAs by affinity chromatography. The column material consists of solid particles of cellulose or another matrix to which a poly-deoxythymidine oligonucleotide (poly-dT) is linked. When an RNA mixture extracted from leaves is applied to the column, the poly-(A) tails of the mRNA hybridizes to the poly-(dT) of the column, whereas other RNAs do not bind and run through (Fig. 22.1). With an appropriate buffer, the bound mRNA is eluted from the column.

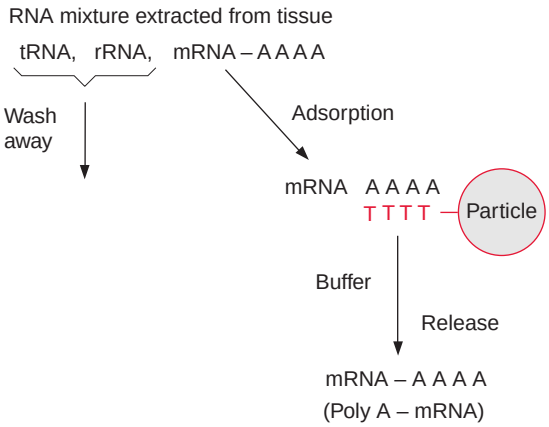

Figure 22.1 Separation of mRNA from an RNA mixture by binding to poly-(dT) sequences that are linked to a matrix.

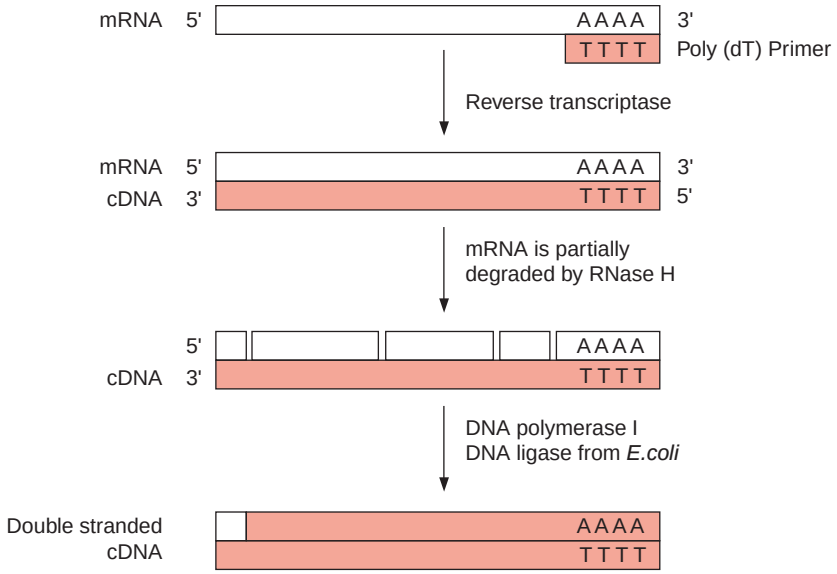

Figure 22.2 Transcription of mRNA to double-stranded cDNA.

The poly-A enriched RNA preparation is then used to synthesize by reverse transcriptase a cDNA strand complementary to the mRNA. The reverse transcriptase starts its synthesis at a poly-(dT) primer (Fig. 22.2). Subsequently, the mRNA is hydrolyzed by a ribonuclease either completely or, as shown in the figure, only partly. The latter method has the advantage that the mRNA fragments can serve as primers for the synthesis of the second cDNA strand by DNA polymerase. DNA polymerase I replaces

mRNA fragments successively by DNA fragments and these are linked to each other by DNA ligase. A short RNA section remains, which is not replaced at the end of the second cDNA strand, but this is of minor importance, since in most cases the mRNA at the 5′ terminus does not encode protein sequence (see Fig. 20.8).

The double-stranded (ds) cDNA molecules thus formed from the mRNA molecules are amplified by cloning. **Plasmids or bacteriophages** can be used as **cloning vectors**. Nowadays a large variety of made-to-measure phages and plasmids are commercially available for many special purposes. A distinction is made between vectors that amplify only DNA and **expression vectors** by which the proteins encoded by the amplified genes can be synthesized.

A gene library can be kept in phages

Figure 22.3 shows the insertion of cDNA into the DNA of a **λ phage**. In the example shown here, the phage DNA possesses a cleavage site for the restriction endonuclease *Eco*RI (section 20.3). The cDNA double strand is first methylated by an *Eco*RI methylase at its own *Eco*RI restriction sites in order to protect this restriction site within the cDNA. DNA ligase is then used to link chemically synthesized double-stranded oligonucleotides with an inbuilt restriction site (in this case for *Eco*RI) to both ends of the double-stranded cDNA. These oligonucleotides are called **linkers**. The restriction endonuclease *Eco*RI cleaves this linker as well as the λ phage DNA and thus generates **sticky ends** at which the complementary nucleotides of the cDNA and the phage DNA can anneal by base pairing. The DNA strands are then linked by DNA ligase, and in this way the cDNA is inserted into the phage vector.

The phage DNA with the inserted cDNA is packed *in vitro* into a **phage protein coat** (Fig. 22.4), using a packing extract from phage-infected bacteria. In this way one obtains a gene library, in which the cDNA from many different mRNAs of the leaf tissue are packed in phages. After infecting bacteria they can be amplified *ad libitum*, whereby each packed cDNA is one individual clone harboring one plant gene.

The bacteria are infected by mixing them with the phages. At first bacteria grow on the agar plates to produce a bacterial lawn, and then the phages, which have been priorly propagated in bacteria, are added on top. After incubation, the infected and lysed bacterial colonies appear on the agar plate as clear spots within the bacterial lawn and are called **plaques**. These plaques contain newly formed phages, which can be multiplied further. It is customary to plate a typical cDNA gene library on about 10 to 20 agar plates of ca. 20 cm diameter. Ideally, each of these plaques contains only one clone. From

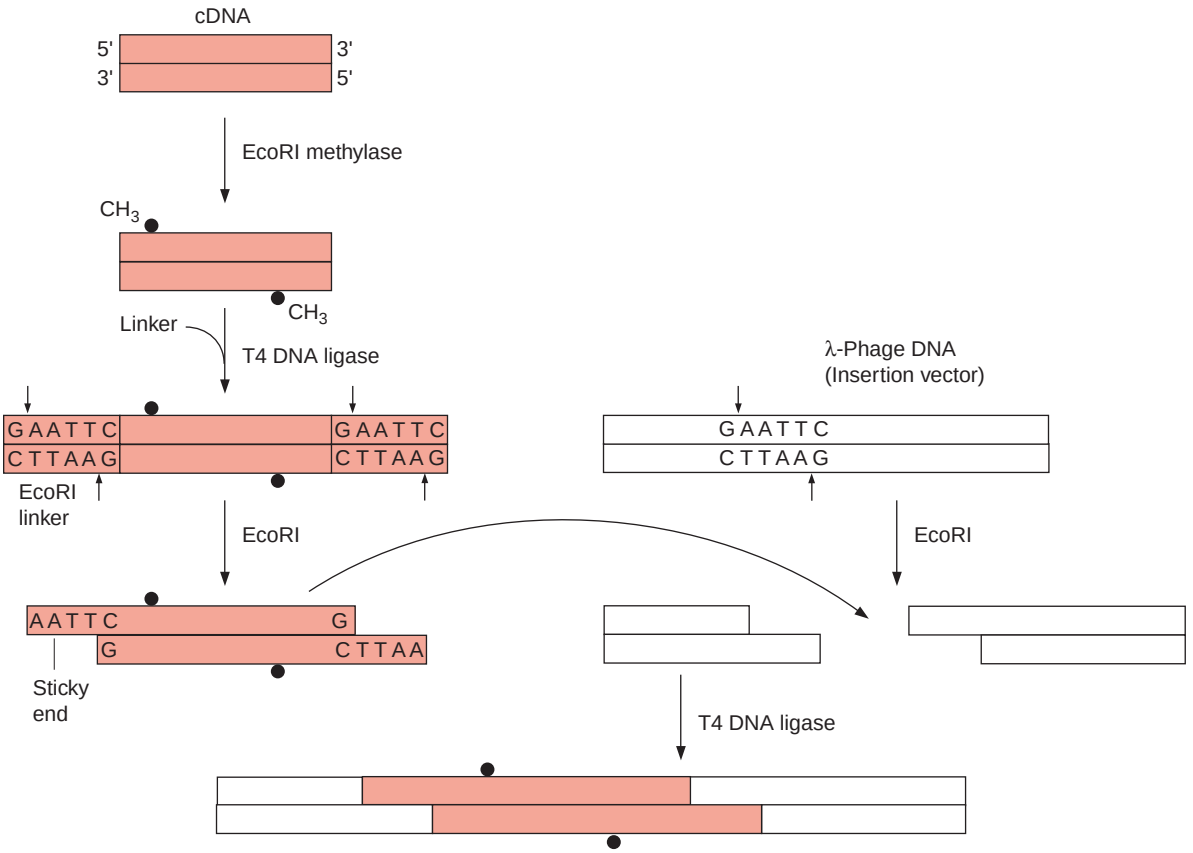

Figure 22.3 Insertion of cDNA into a λ-phage insertion vector.

these plaques, the phage clone containing the cDNA of the desired gene is selected, using specific probes as will be described later.

A gene library can also be propagated in plasmids

cDNA cloning into plasmids is carried out similarly to that described via restriction. To clone a cDNA gene library into plasmids, cDNA is inserted into plasmids via a restriction cleavage site in more or less the same way as in the insertion into phage DNA (Fig. 22.5). The plasmids are then transferred into *E. coli* cells. The transfer can be brought about by treating the cells with $CaCl_2$ to make their membrane more permeable (competent) to the plasmid. The cells are then mixed with plasmid DNA and exposed to a short heat shock. In order to select the transformed bacterial cells from

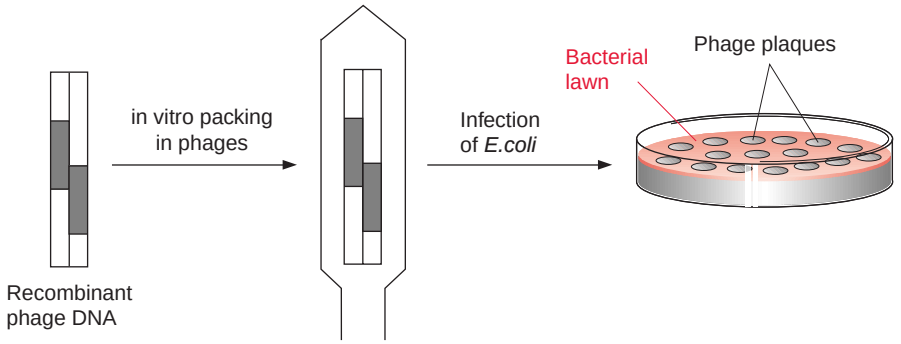

Figure 22.4 A recombinant phage DNA is packed into a virus particle. *E. coli* cells are infected with the phage and plated on agar plates. Infected colonies lyse after phage propagation and show transparent spots (plaques) in the bacterial lawn.

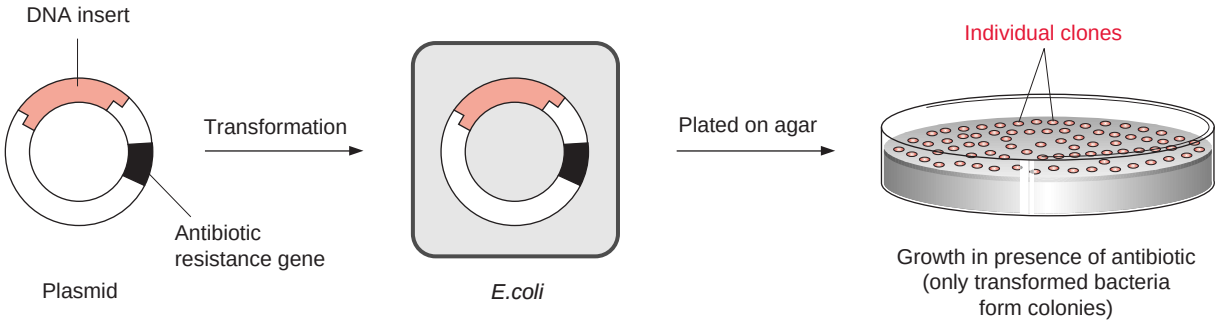

Figure 22.5 cDNA can be propagated via a plasmid vector in *E. coli.* An antibiotic resistance gene on the plasmid enables the selection of the transformed cells.

the large majority of untransformed cells, the plasmid vector of the transformed cells is provided with a marker. The plasmid vector contains an **antibiotic resistance gene**, which renders the bacteria resistant to growing on a certain antibiotic, such as ampicillin or tetracycline. When the corresponding antibiotic is added to the culture medium, only cells containing the plasmid survive and grow, whereas the other nontransformed cells die. After plating on an agar culture medium, bacterial colonies develop which and can be recognized as spots.

In order to verify that a plasmid actually contains an inserted DNA sequence (**insert**), the blue/white screen can be used. Specific vectors which encode the enzyme β-galactosidase were designed (Fig. 22.6). This enzyme hydrolyzes the colorless compound X-Gal into an insoluble blue product. When X-Gal is added to the agar culture medium, all the clones that do not contain a DNA insert, and therefore contain an intact β-galactosidase

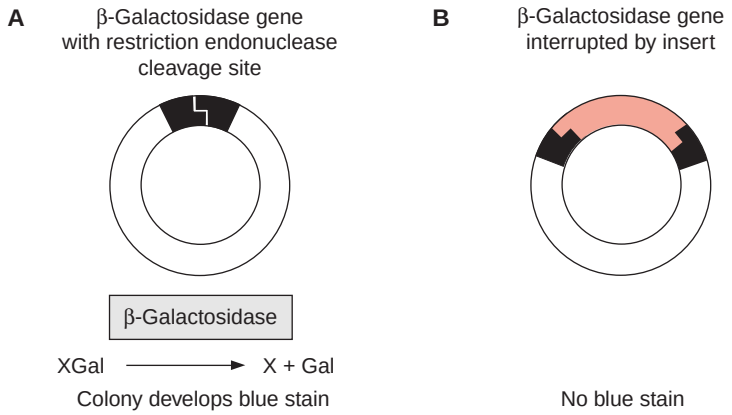

Figure 22.6 To check whether the plasmid of a bacterial colony carries a DNA insert, a blue/white selection is carried out. In colonies with the intact gene (i.e., no insert), the colorless chemical X-Gal (5-bromo-4-chloro-3-indolyl-β-D-galactopyranoside) is hydrolyzed by the corresponding β-galactosidase into galactose and an indoxyl derivative, which oxidizes to form a blue colored dimer. This results in blue staining of the colony. When the β-galactosidase gene is disrupted by a DNA insert, the enzyme can no longer be expressed and the corresponding colonies remain white as the X-Gal is not hydrolyzed. X = 5-Brom-4-chlor 3-indol.

gene, form blue colonies. If a DNA fragment is inserted into the cleavage site of the β-galactosidase gene, this gene is interrupted and no longer able to encode a functional β-galactosidase. Therefore the corresponding colonies are not stained blue but remain white (blue/white selection).

A gene library is screened for a certain gene

Specific probes that correspond to the gene of interest are employed to screen the bacterial colonies or phage plaques. A blot is made by placing a nylon or nitrocellulose membrane on top of the bacterial colonies or phage plaques (Fig. 22.7). Some of the phages of the plaques or the bacterial clone will bind to the blotting membrane, although most of them remain on the agar plate. After special treatment to lyse bacteria or phages the DNA of the bacteria or phages is fixed to the membrane. Two kinds of probes can be used to screen the DNA or protein bound to the blotting membrane derived from the phages or bacteria:

1. Specific DNA probes to label the DNA of the desired clone by hybridization and
2. Specific antibodies to identify the desired protein expressed as gene product of the clone (Western blot).

A clone is identified by antibodies which specifically detect the gene product

Antibodies against a certain protein are often used to identify the corresponding gene (e.g., by **Western blot**). This method is only applicable when approximately 1 mg of the protein of the gene of interest is purified beforehand in order

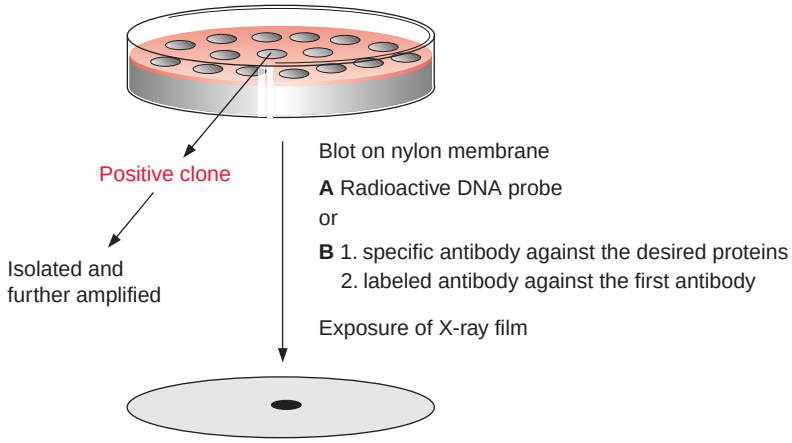

Figure 22.7 For screening the gene library, a blot is prepared by placing a nylon or nitrocellulose membrane on the agar plate. A labeled probe (A, DNA probe or antibody) identifies the gene or the protein of interest as a dark spot on the X-ray film, caused by radioactivity or by chemoluminescent light. The corresponding clone is identified on the agar plate by comparing the positions and can be picked with a toothpick for further propagation.

to obtain **polyclonal antibodies** by immunization of animals. Furthermore, the cDNA library must be inserted in an appropriate expression vector, so that transcription and translation of the foreign proteins can occur in *E. coli*. The vector contains a promoter sequence, which controls initiation of transcription of the inserted gene, and often also a sequence for termination of the transcription at its end.

In practice, bacteria bound to the blotting membrane are disrupted by alkali treatment and the released bacterial proteins are fixed to the membrane (Fig. 22.7). When phages are used as vectors, cell disruption is not required, since the phages themselves lyse the bacterial cell and thus liberate the cellular proteins, which are then fixed to the blotting membrane. Afterwards, antibodies are added, which bind specifically to the corresponding protein, but are washed off from all other parts of the membrane. Usually a second antibody, which recognizes the first antibody, is used to detect the first bound antibody (Fig. 22.8). Formerly the second antibody was labeled with radioactive ^{125}iodine. Nowadays more often the **ECL-technique** (enhanced luminescence) is employed. This entails a peroxidase from radish being attached to the second antibody. This peroxidase catalyzes the oxidation of added luminol (3-aminophthalic acid hydrazide) with H_2O_2 as oxidant. This reaction is accompanied by the emission of blue luminescent light, which can be detected after about 1 hour exposure to an X-ray film. Using a luminescence enhancer, the intensity of this chemoluminescence can be increased by a factor of 1,000. A positive colony can be recognized as a dark spot in the autoradiography (Fig. 22.7). The position of the positive clone on the agar plate can be identified from the position of the spot on the blotting membrane. After the first screening, due to a high density of the plated bacteria an apparently positive clone may actually contain several clones. For this

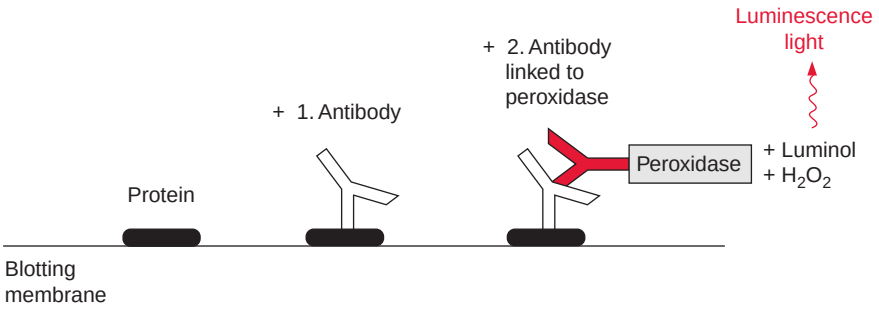

Figure 22.8 A primary antibody bound to a protein is recognized by a second antibody, to which a peroxidase is linked. The peroxidase catalyzes the oxidation of luminol by H_2O_2 resulting in the emission of luminescent light, which is detected by, e.g., exposure to an X-ray film.

reason, the colony, picked up from the positive region with a toothpick, is diluted and plated again on an agar plate. By repeating the screening procedure described above (**rescreening**), finally single pure clones are obtained. Positive phage plaques are also regrown in bacteria and plated again in order to obtain pure clones.

A clone can also be identified by DNA probes

In this procedure, the phages or bacteria present on the blotting membrane are first lysed and the proteins are removed. The remaining DNA is then denatured to obtain single strands, which are tightly bound to the membrane. Complementary DNA sequences, which are radioactively labeled by ^{32}P-labeled deoxynucleotides or by digoxigenin-labeled dUTP (DIG11αdUTP), are used as probes. These probes bind to complementary DNA sequences present on the blotting membrane by hybridization. The identification of the positive clones proceeds via autoradiography or with digoxigenin antibodies that have been conjugated with a chemiluminescence dye.

Chemically synthesized oligonucleotides of about 20 bases are also employed as DNA probes. These probes are radioactively labeled at the 5′ end by ^{32}P-phosphate and are used particularly when only low quantities of the purified proteins are available, and which are not sufficient for the generation of antibodies. For the synthesis of oligonucleotides with automatic synthesizers some sequence information of the gene of interest is needed, either from homologous genes of other species or a partial amino acid sequence of the corresponding protein. With very low amounts of protein, it is possible to determine part of the N-terminal amino acid sequence of the protein by micro-sequencing. From such a partial amino acid sequence, the corresponding DNA sequence can be deduced according to the universal genetic code. The corresponding oligonucleotide probes are subsequently produced by chemical synthesis using automatic synthesizers. However, the

Figure 22.9 A degenerated oligonucleotide comprises a mixture of oligonucleotides to cover all the possible sequences of the universal genetic code encoding a given amino acid sequence.

degeneracy of the genetic code implies that amino acids are often encoded by more than one nucleotide triplet (Fig. 22.9). This is taken into account during the design of oligonucleotides. When, for example, the third base of the triplet encoding lysine can be either an A or a G, a mixture of both nucleotides is added to the synthesizer during the reaction with the third nucleotide of this triplet. In order to introduce the third nucleotide of the triplet encoding alanine triplet, a mixture of all four nucleotides is added to the synthesizer. The synthesized "degenerate" oligonucleotide shown in Figure 22.9 is thus, in fact, a mixture of 48 different oligonucleotides, only one of which contains the correct sequence of the desired gene.

When the protein encoded by the desired gene could not be purified, a corresponding gene section from related organisms can be sometimes used as a homologous probe. Domains with specific amino acid sequences are often conserved in enzymes or other proteins (e.g., translocators) even from distantly related plants, and are encoded by correspondingly similar gene sequences.

After the DNA for the desired protein has been successfully isolated, usually the next step is to determine the complete nucleotide sequence, mostly by automatic analyzers, which will not be described here.

Genes encoding unknown proteins can be functionally assigned by complementation

In some cases it has been possible to isolate the cDNA encoding an unknown protein. One method for identifying the function of the gene is by the complementation of **deficiency mutants** of bacteria or yeast. To do so, the plasmids from a cDNA library are transformed into bacteria or yeast mutants (Fig. 22.10). Plasmids that can be amplified in *E. coli* as well as in yeast are available as cloning vectors and can be used to express the encoded protein. Several plant translocators, including the sucrose translocator involved in phloem loading (section 13.1), have been identified by complementation. To identify the gene of the sucrose translocator, a yeast deficiency mutant was employed that had lost the ability to take up sucrose and therefore could no longer use sucrose as a nutritional source. This mutant was transformed with plasmids from a plant cDNA library, where the plasmid DNA was provided with a yeast promoter in order to express

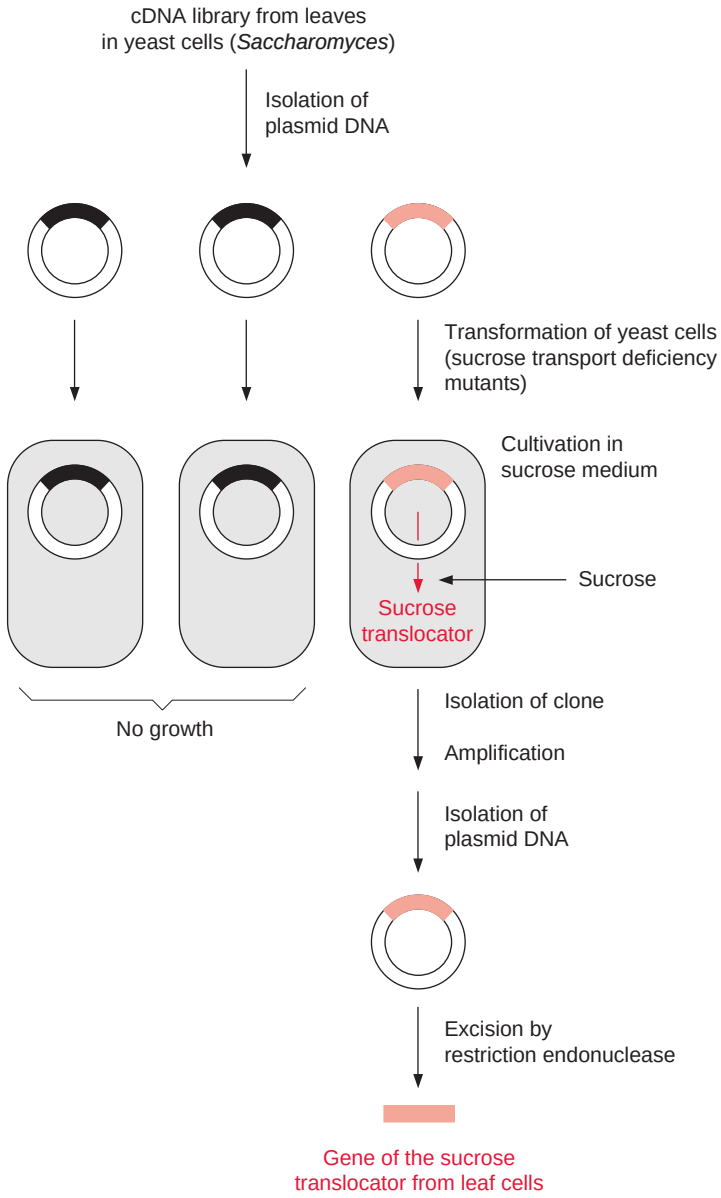

Figure 22.10 Identification of a plant gene by complementation of a yeast mutant deficient in sucrose uptake.

the inserted DNA within the yeast cell. After plating the transformed yeast cells on a culture medium with sucrose as the only carbon source, a yeast clone was found that grew on the sucrose cultivation medium. This indicated that transformation with the corresponding plasmid from the plant cDNA library had generated yeast cells that produced the plant sucrose

translocator and incorporated it into their cell membrane. After this positive yeast clone had been amplified, plasmid cDNA was isolated and sequenced. The cDNA sequence yielded the amino acid sequence of the previously unknown sucrose translocator.

Genes can be identified with the help of transposons or T-DNA

Another possibility for identifying genes, aside from the function of their gene products, is to use **transposons**. Transposons are DNA sequences that can "jump" within the genome of a plant, which sometimes results in a recognizable elimination of a gene function (section 20.4). This could, for example, be the loss of the ability to synthesize a flower pigment. In such a case, a gene probe based on the known transposon sequence is used to identify by DNA hybridization the region of the genome in which the transposon has been inserted. By using the cloning and screening procedures already mentioned, it is possible to identify a gene, in our example a gene for the enzyme of flower pigment synthesis, and to determine the amino acid sequence of the corresponding enzyme by DNA sequence analysis. Labeling a gene with an inserted transposon is called **gene tagging**.

An alternative method, which has superseded the transposon technique of tracking genes, is the T-DNA insertion technique, which will be described in the next section in detail. Inserting T-DNA into the genome causes random mutations (**T-DNA-insertion mutants**). The gene locus into which the T-DNA has "jumped" is identified by using a gene probe and is subsequently sequenced. The complete sequence of the mutated gene is then identified, usually by comparing the relevant gene region with a database of the known sequence of T-DNA insertion mutants. For instance, the firm Syngenta provides a data bank with the sequences of about 100,000 T-DNA insertion mutants of *Arabidopsis*.

22.2 Agrobacteria can transform plant cells

Gram-negative soil bacteria of the species ***Agrobacterium tumefaciens*** (new nomenclature: *Rhizobium radiobacter*) induce a tumor growth at wounding sites in various plants, often on the stem, which can lead to the formation of **crown galls**. The tumor tissue from these galls continues to grow as a callus in cell culture. As described in sections 19.3 and 19.5, mature differentiated plant cells, which normally no longer divide, can be stimulated to unrestricted growth by the addition of the phytohormones **auxin** and **cytokinin**. In this way a tumor in the form of a callus can be obtained from a differentiated

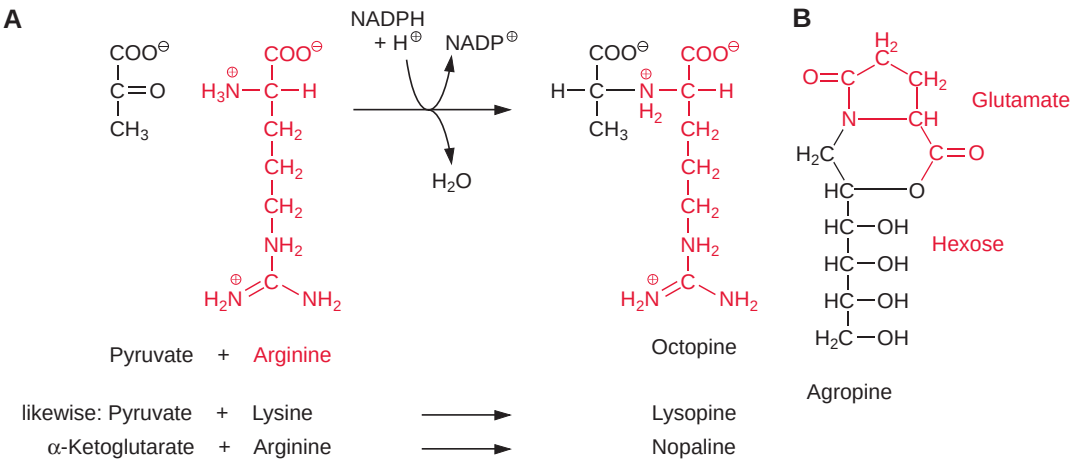

Figure 22.11 Opines are synthesized from amino acids and ketoacids (A) or amino acid and a hexose (B).

plant cell. The gall produced by the *Agrobacterium* is formed in basically the same way. The bacteria force the wounded plants to produce high concentrations of auxin and cytokinin, resulting in a proliferation of the plant tissue and leading to tumor growth. Since the capacity for increased cytokinin and auxin synthesis is inherited after cell division by all the succeeding cells, a callus culture of crown gall tissue can be multiplied without adding phytohormones.

The crown gall tumor cells have acquired yet another ability: they can produce a variety of products named **opines** by condensating amino acids and α-ketoacids or amino acids and sugars. These opines are synthesized in such high amounts that they are excreted from the crown galls. Figure 22.11 shows **octopine**, **lysopine**, **nopaline**, and **agropine** as examples of opines. Each *Agrobacterium* strain induces the synthesis of only a single opine. The synthesis of the first three opines mentioned proceeds via condensation to form a Schiff base and a subsequent reduction by NADPH. The opines are so stable that they cannot be metabolized by most soil bacteria. *Agrobacterium tumefaciens* strains have specialized in utilizing these opines. Normally, a particular opine can be catabolized only by that bacterial strain which has induced its synthesis in the plant. In such a way the wounded plants are forced to produce a special nutrient that can be consumed only by the corresponding *Agrobacterium*.

The conversion of differentiated plant cells to opine-producing tumor cells occurs without the *Agrobacteria* entering those cells. This reprogramming of plant cells is caused by the transfer of functional genes from the bacteria to the genome of the wounded plant cells. The *Agrobacteria* have

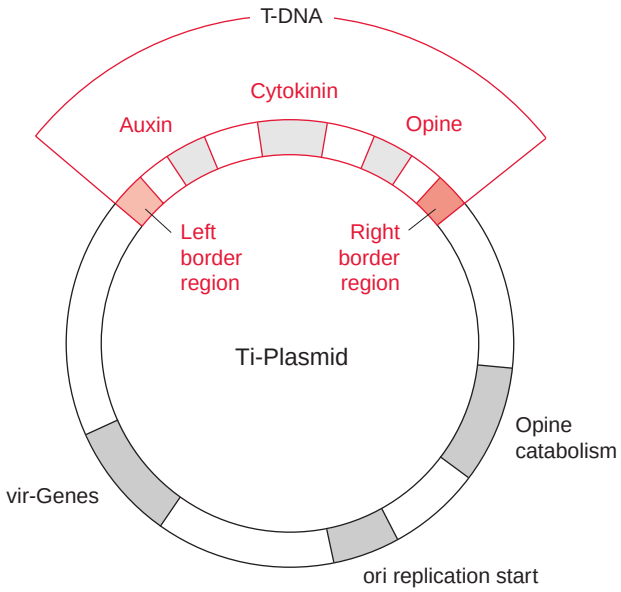

Figure 22.12 Schematic presentation of a Ti-plasmid (not to scale). The T-DNA that is transferred to the plant genome, representing about 7% to 13% of the Ti-plasmid, is defined by its left and right border sequences. The T-DNA contains genes encoding enzymes for the synthesis of the phytohormones cytokinin and auxin, and of a specific opine. The T-DNA is transcribed and translated only in the plant cell. The remaining part of the plasmid is transcribed and translated in the bacterium and encodes several *vir* genes as well as a single or several genes for opine catabolism. The *ori* region represents the replication start. (After Glick and Pasternak.)

acquired the ability to transform plants in order to use them as a production site for their nutrient. Jeff Schell named this novel parasitism **genetic colonization**.

The Ti plasmid contains the genetic information for tumor formation

The phytopathogenic function of *A. tumefaciens* is encoded in a tumor-inducing **Ti plasmid** with a size of about 200 kbp (Fig. 22.12). Strains of *A. tumefaciens* containing no Ti plasmids are unable to induce the formation of crown galls.

Plants are infected by bacteria at wounds frequently occurring at the stem base. After being wounded, plants excrete phenolic compounds as a defense against pathogens (Chapter 18). These phenols are used by the agrobacteria for the chemotactic localization of the wounded plant cells and the subsequent initiation of infection. Phenols stimulate the expression of about 11 virulence genes (**vir genes**) located on the Ti plasmid. These vir genes encode virulence proteins which enable the transfer of the bacterial tumor-inducing genes to the plant genome. From a 12 to 25 kbp long section of the Ti plasmid, named **T-DNA** (T, transfer), a single strand is excised by a **vir nuclease**. The cleavage sites are defined by **border sequences** present at both ends of the T-DNA. The transfer of the single strand T-DNA from the bacterium to the plant cell nucleus (Fig. 22.13) proceeds

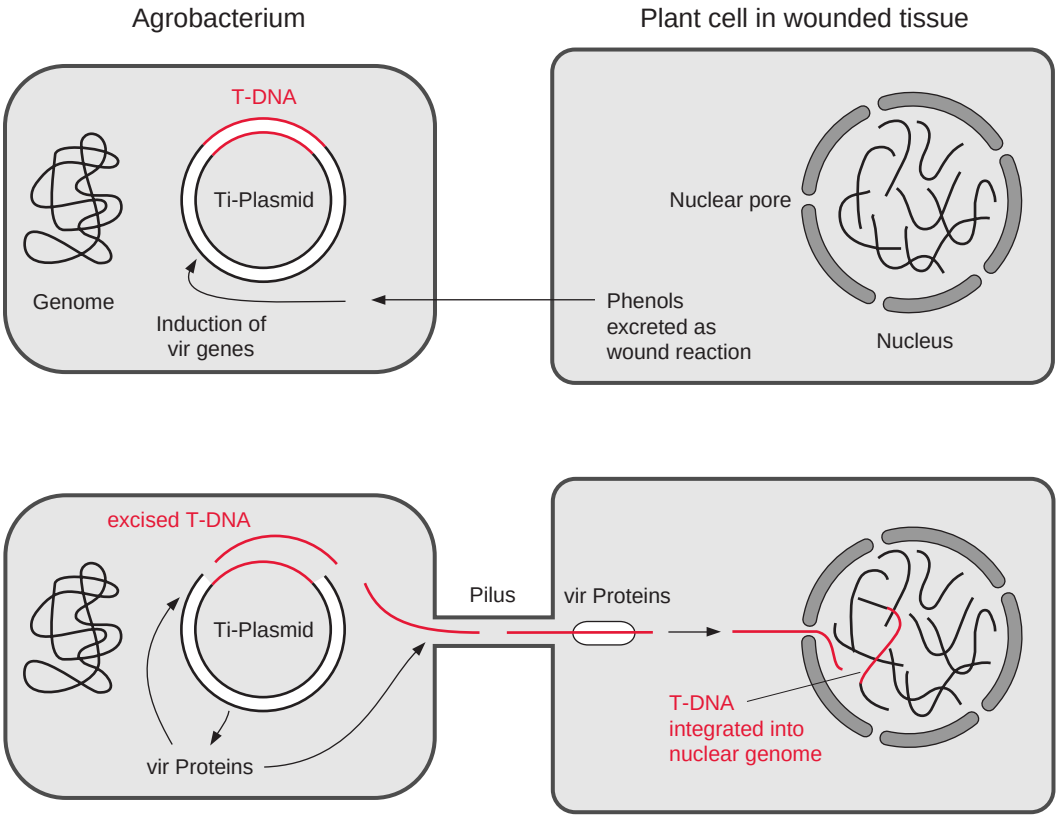

Figure 22.13 *Agrobacteria* transform plant cells to force them to produce opines, which are nutrients of the bacteria. Wounded plant tissues induce the expression of virulence genes, which are localized on the Ti-plasmid of the *Agrobacterium*. The virulence proteins cause a single-stranded DNA segment known as T-DNA to be excised from the plasmid, transferred to the plant cell, and integrated into the nuclear genome.

in analogy to the conjugation, which is a bacterial sexual reproduction process. To connect the bacterium to the plant cell, vir proteins form a **pilus**, a threadlike structure through which the T-DNA is conducted. After being transferred into the plant cell, the T-DNA strand migrates further into the nucleus. Vir-encoded proteins protect the T-DNA from being attacked en route by DNA-degrading plant enzymes and also facilitate the transport through the nuclear pores to the nucleus. The right border region of the T-DNA has an important function in its integration into the plant nuclear genome. The T-DNA is integrated randomly into chromosomes and, when inserted in a gene, can eliminate the function of this gene. This can be used to identify a gene by gene tagging in an analogous way as the gene tagging by the transposons described at the end of section 22.1.

The T-DNA integrated in the nuclear genome has the properties of a eukaryotic gene and is inherited in a Mendelian fashion. It is replicated by the plant cell as if it were its own DNA and, since it contains eukaryotic promoters, is also transcribed. The resultant mRNA corresponds to a eukaryotic mRNA and is translated as such. The T-DNA encodes cytokinin synthase, a key enzyme for the synthesis of the cytokinin **zeatin** (Fig. 19.11), as well as two enzymes for the synthesis of the auxin **indoleacetic acid** (**IAA**). This bacterial IAA synthesis proceeds in a different manner than plant IAA biosynthesis (Fig. 19.7), but details of this pathway will not be considered here. Moreover, the T-DNA encodes one or two enzymes, varying from strain to strain, for the synthesis of a special opine.

The enzymes required for catabolism of the corresponding opine are encoded in that part of the Ti plasmid that remains in the bacterium. Thus, in parallel to the transformation of the plant cell, the enzymes for opine degradation are synthesized by the bacteria.

22.3 Ti-Plasmids are used as transformation vectors

Its ability to transform plants has made *A. tumefaciens* an excellent tool for integrating foreign genes in their functional state in a plant genome. It was necessary, however, to modify Ti-plasmids before they could be used as vectors (Fig. 22.14). The genes for auxin and cytokinin synthesis were removed to prevent tumor growth in the transformed plants. Since synthesis of an opine is unnecessary for a transgenic plant and would be a burden on its metabolism, the genes for opine synthesis were also removed. Thus the T-DNA is defined only by the two border sequences. In order to insert a foreign gene between these two border sequences, it was necessary to incorporate a DNA sequence containing cleavage sites for several restriction endonucleases (known as a **polylinker sequence** or a multicloning site) within the T-DNA region of the Ti-plasmid. The Ti-plasmid could then be cleaved in the T-DNA region by a certain restriction endonuclease. A foreign DNA sequence, excised by the same restriction endonuclease, can be inserted in this cleavage site (see Fig. 22.3). Since the polylinker sequence contains cleavage sites for several restriction endonucleases, several DNA molecules can be inserted sequentially into the T-DNA. In Figure 22.14, a promoter, enabling the expression of the inserted DNA in the host cell, is located to the left of the cleavage site.

In modern transformation systems, vectors derived from the Ti-plasmid no longer contain any vir genes and are therefore unable to transform a

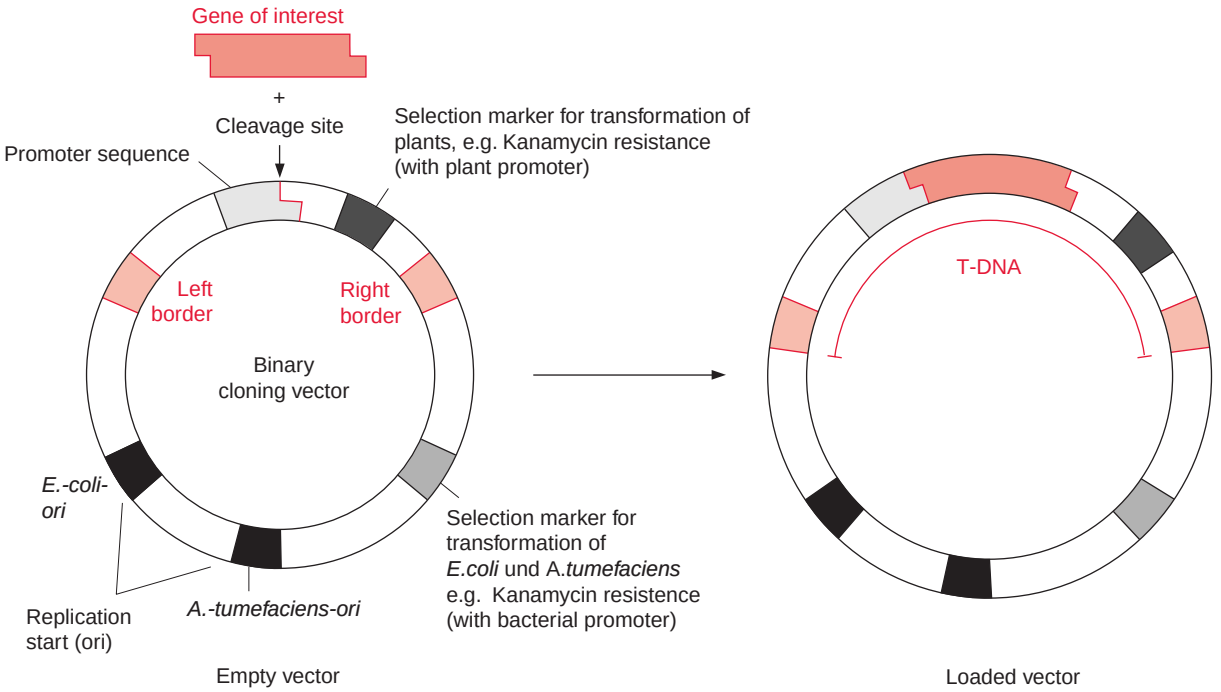

Figure 22.14 T-DNA binary cloning vector with a gene of interest is constructed for the transformation of plant cells.

plant cell on their own. For transformation they require the assistance of a second so-called **helper plasmid**, which contains the vir genes, but no T-DNA and is therefore unable to transform a plant on its own. Those *A. tumefaciens* strains used nowadays in biotechnological applications possess the helper plasmid (Fig. 22.15). The vector used for the transformation is referred to as **binary cloning vector**. A large variety of such has been designed for special applications and is available commercially.

In order to transform a plant, a sufficient amount of vector-DNA, containing the gene to be transferred, has to be isolated. It proved to be advantageous to first amplify the vectors by cloning them in *E. coli* (Fig. 22.15). Since *E. coli* does not recognize the replication start site of the natural Ti-plasmid (***A. tumefaciens-ori***), a second replication start (***E. coli-ori***) is introduced into the plasmid.

The plasmid is provided with a selection marker in order to select those *E. coli* cells that have been transformed by the Ti-plasmid. For this a gene encoding **neomycin phosphotransferase** is frequently used. This enzyme degrades the antibiotic **kanamycin**, thus rendering the cell resistant to this

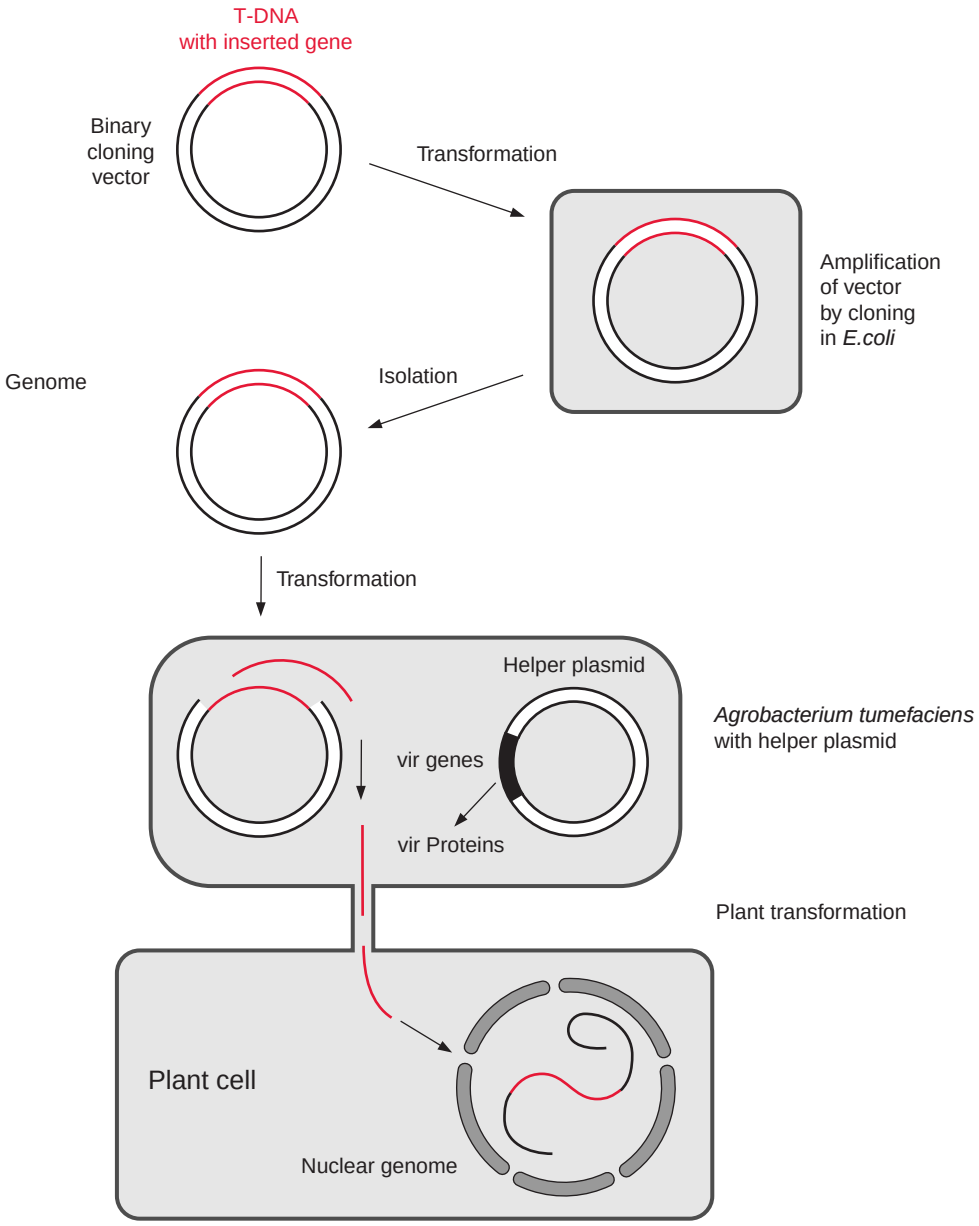

Figure 22.15 Plant transformations are performed with a binary cloning system. After bacterial transformation, the T-DNA vector contains the DNA insert and is propagated in *E. coli*, the plasmid is isolated, and transferred into *Agrobacterium*. A helper plasmid, already present in *Agrobacterium*, encodes the virulence proteins required for the transformation of plant cells.

antibiotic. The kanamycin resistance gene is linked to a bacterial promoter and therefore its expression is limited to *E. coli* cells. When kanamycin is added to the culture medium of the bacteria, only the transformed bacteria survive, since they are protected against the antibiotic due to the resistance gene on the vector. Thus, the Ti-plasmid can be propagated efficiently by cloning in *E. coli*.

A new plant is regenerated after the transformation of a leaf cell

After transformation, the few transformed plant cells are selected from the large number of nontransformed cells by another selection marker provided by the T-DNA vector. In most cases the kanamycin resistance gene described previously is also used for this purpose, but in this specific case provided with a plant promoter. Since kanamycin is very seldom used in medicine the use of a kanamycin resistance gene in generating transgenic plants appears to be advantageous.

It was mentioned earlier that *A. tumefaciens* attacks plants at wounded areas. Leaf discs therefore, with their cut edges, are good targets for a transformation with *A. tumefaciens* (Fig. 22.16). The leaf discs are immersed in a suspension of *A. tumefaciens* cells that comprise the binary and helper vectors. After a short time, the discs are transferred to a culture medium containing agarose, which, besides nutrients, contains the phytohormones **cytokinin** and **auxin** which induce cells of the leaf disc to grow to a callus. The addition of the antibiotics, e.g., kanamycin, only allows the growth of transformed cells. The cut edges of the leaf discs are the site where the calli of the transformed cells develop. When the concentrations of cytokinin and auxin are appropriate, these calli can be propagated in tissue culture. In this way transformed plant cells can be kept and propagated in tissue culture for very long periods of time. If required, new plants can be regenerated from these tissue cultures.

To regenerate new plants, cells of the callus culture are transferred to a culture medium containing more cytokinin than auxin, and this hormonal imbalance induces the callus to develop shoots. Root growth is then stimulated by transferring the shoots to a culture medium containing more auxin than cytokinin. After plantlets with roots were grown to an appropriate size, they can be transplanted to soil, where in most cases they develop into normal plants, capable of reproduction by flowering and seed production.

The pioneer work of Jeff Schell, Marc van Montagu, Patricia Zambryski, Robert Horsch, and several others has developed the *A. tumefaciens* transformation system to a very easy method for transferring foreign genes to cells of higher plants. Nowadays it is often possible for even students to

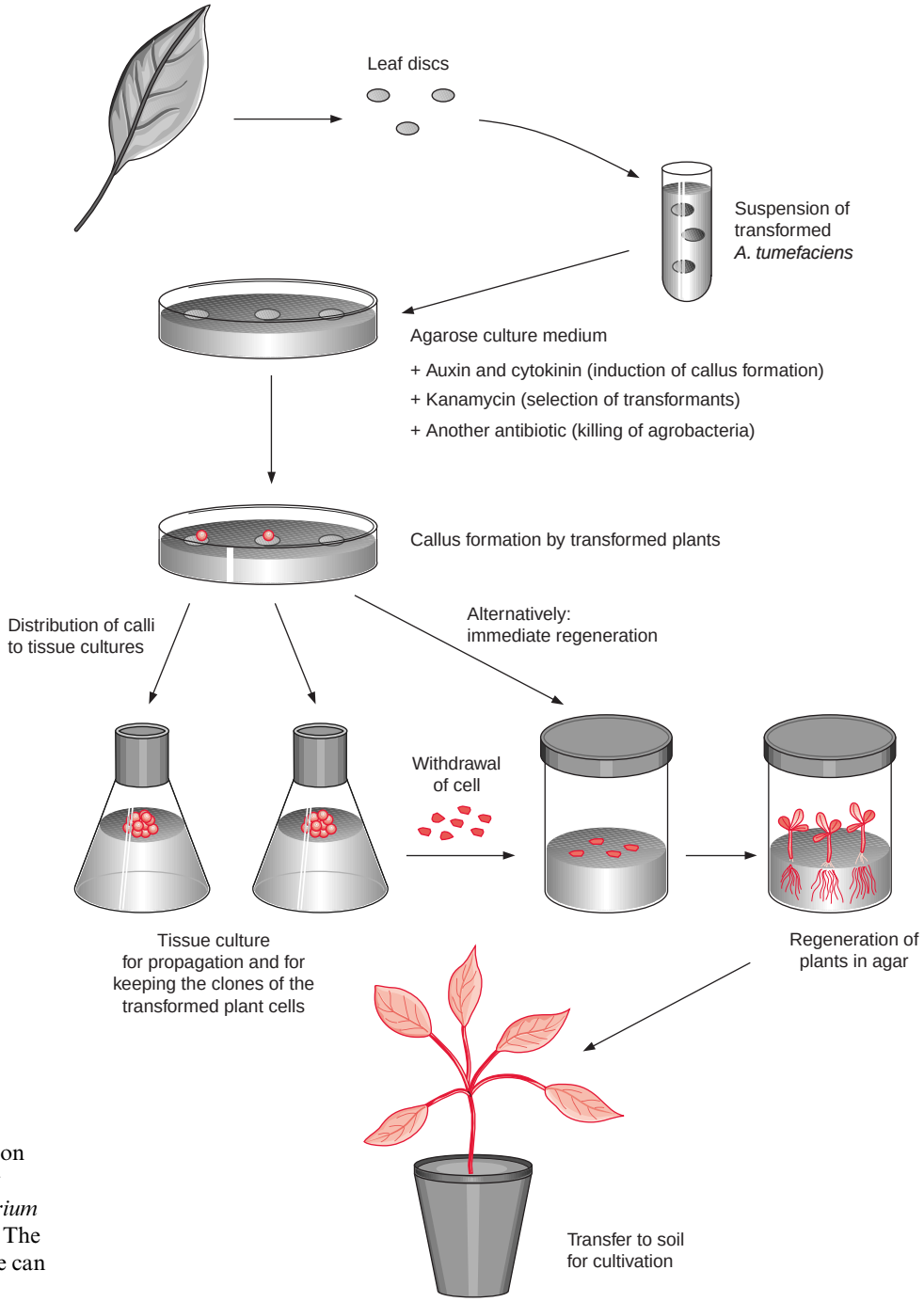

Figure 22.16 Generation of a transgenic plant by means of an *Agrobacterium* transformation system. The step of the tissue culture can be omitted. See text.

produce several hundred different transgenic tobacco plants with no great difficulty.

Using this method, well over 100 different plant species have been transformed successfully. Initially, it was very difficult or even impossible to transform monocot plants with the *Agrobacterium* system. Recently, this transformation method has been improved to such an extent, that it can now also be successfully applied to transform several monocots, such as rice. A successful adaption of the method is the **agroinjection** in which the agrobacteria suspension is injected into the stigma of flowers. This method has been used for altering the gene expression in tomato fruits. An alternative way to transform plant cells is a physical gene transfer, the most successful being the bombardment of plant cells by **microprojectiles**.

Plants can be transformed by a modified shotgun

Transformation by bombardment of plant cells with microprojectiles was developed in 1985. The microprojectiles are small spheres of tungsten or gold with a diameter of 1 to 4 μm, which are coated with DNA. A **gene gun** (similar to a shotgun) is used to shoot the pellets into plant cells (Fig. 22.17). Initially, gunpowder was used as propellant, but nowadays the microprojectiles are often accelerated by compressed air, helium, or other gases. The target materials include calli, embryonic tissues, and leaves. In order to penetrate the cell wall of the epidermis and mesophyll cells, the velocity of the projectiles must be very high and can reach about 1,500 km/h in a vacuum chamber. The cells in the center of the line of fire may be destroyed and killed during such a strong bombardment, but, because the projectiles are so small, the cells nearer the periphery survive. The DNA transferred to the cells by these projectiles can be integrated not only into the nuclear genome, but also into the genome of mitochondria and chloroplasts. Therefore, this method allows the transformation of mitochondria and chloroplasts. In some plants, the gene gun works especially well. Thus, by bombardment of embryonic callus cells of sugarcane, routinely up to 10 to 20 different transformed plant lines can be obtained with one shot.

Protoplasts can be transformed by the uptake of DNA

The transformation of protoplasts is another way to transfer foreign genetic information into a plant cell. Protoplasts can be obtained from plant tissues by digestion of the cell walls (section 1.1). Protoplasts are able to take up foreign DNA in the presence of $CaCl_2$ and polyethylene glycol, and often integrate the DNA into their genomes. This transformation resembles that of bacteria by plasmids. During protoplast transformation, the gene to be transferred

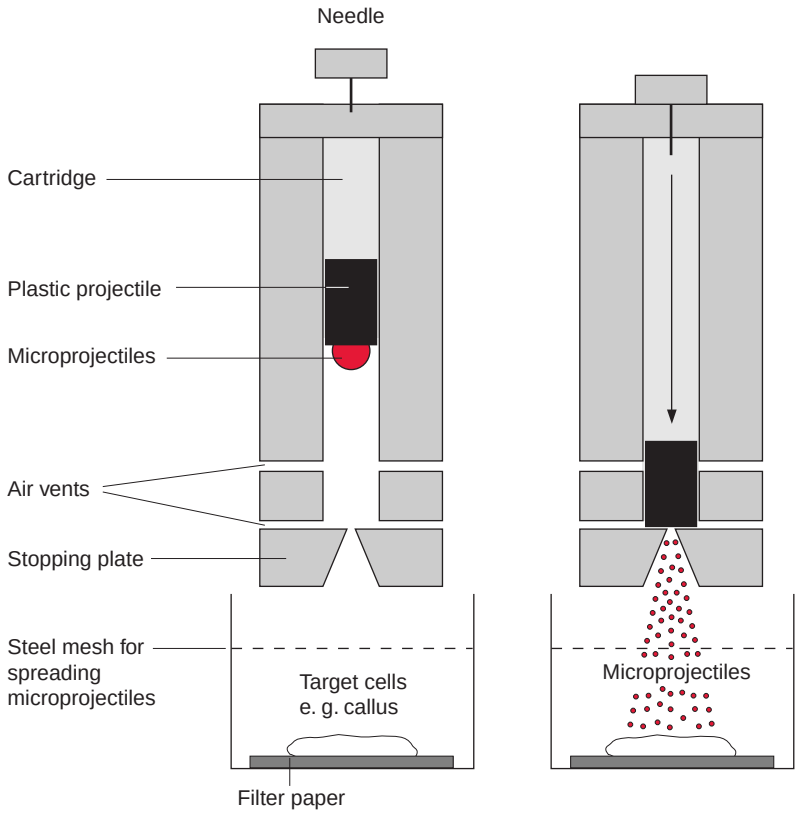

Figure 22.17 Transformation of a plant by a gene gun. Gold or tungsten spheres are coated with a thin DNA layer by a deposit of $CaCl_2$. The spheres are inserted in front of a plastic projectile into the barrel of the gun. The gun and the target cells are in an evacuated chamber. When the gun is fired, the plastic projectile is driven to the stopping plate, by which the microprojectiles are driven through holes and shot at a high velocity into the cells of the plant tissue. The DNA carried in this way into the plant cells contains an antibiotic resistance gene (e.g., for kanamycin resistance) as well as the gene of interest. Transformed cells can be selected by this marker in the same way as for cells transformed with *A. tumefaciens*. The transformed cells are propagated via callus tissue culture and plants can be regenerated. (After Hess, Biotechnologie der Pflanze, Verlag Ulmer, Stuttgart, 1992.)

is linked with a selection marker encoding resistance to an antibiotic. After the antibiotic has been added, only the transformed protoplasts survive. In principle, the protoplasts of all plants can be transformed in this way, since there is no host specificity involved, as in the case of transformation by *A. tumefaciens*. However, the use of this method is applied successfully to only some plant species, e.g., rice and maize, where it has been possible to regenerate

intact fertile plants from protoplasts. In fact it is the regeneration of plant which limits the application of this method.

Plastid transformation to generate transgenic plants is advantageous for the environment

Recently, the **transformation of chloroplasts** has gained importance. Transgenic plants obtained by transformation of the nuclear genome (e.g., by the Ti-plasmid) could pass their genetic information via pollen to cultivars in neighboring fields or in some cases also to related wild plants. This can lead to undesirable cross-breeding (e.g., causing the generation of herbicide-resistant weeds in the neighborhood of herbicide-resistant cultivars). This problem can be avoided when the genetic transformations are performed in the plastid genome of the plant. Since in most cases the plastid genome is **maternally inherited**, the genetic alteration will not spread to other plants via pollen transfer (pollination).

The **gene gun** is usually used for the transformation of chloroplasts. The foreign DNA that is to be integrated into the plastid genome is provided at both ends with sequences, which are identical to sequences in the plastid genome (Fig. 22.18). After the foreign DNA has entered the plastids, it can be integrated into the plastid genome by **homologous recombination** at a site defined by the sequences at both ends. Whereas in the plant nuclear genome homologous recombinations are rare events, these occur frequently in the plastid genome. In this way random mutations are avoided, which occur when Ti-plasmids are used for transformation of the nuclear genome. A drawback of plastid transformation is, however, that plant cells contain many plastids, each with 10 to 100 genomes. By repetitive selection and regeneration, it is possible to achieve transgenic lines in which practically all the plastid genomes have integrated the foreign DNA (**transplastome plants**). Plants in which each cell contains many hundred copies of a foreign gene can be cultivated. This has the advantage that these transformed plants can produce large amounts of foreign proteins (up to 46% of the soluble protein), which might be relevant when the plants are to be used for the synthesis of defense compounds or pharmaceuticals.

Another advantage of the plastid transformation is that plastid genes can be transcribed **polycistronically**. While the DNA present in the nucleus usually is transcribed to monocistronic mRNAs, which are then translated into only one protein, most of the plastid genes are transcribed to polycistronic mRNAs, which encode several proteins and afterwards are processed to single translatable mRNAs. This property of the plastid transcription allows the integration of several foreign genes (e.g., for a synthesis pathway) in one step into the plastid genome. It should be noted, however, that in

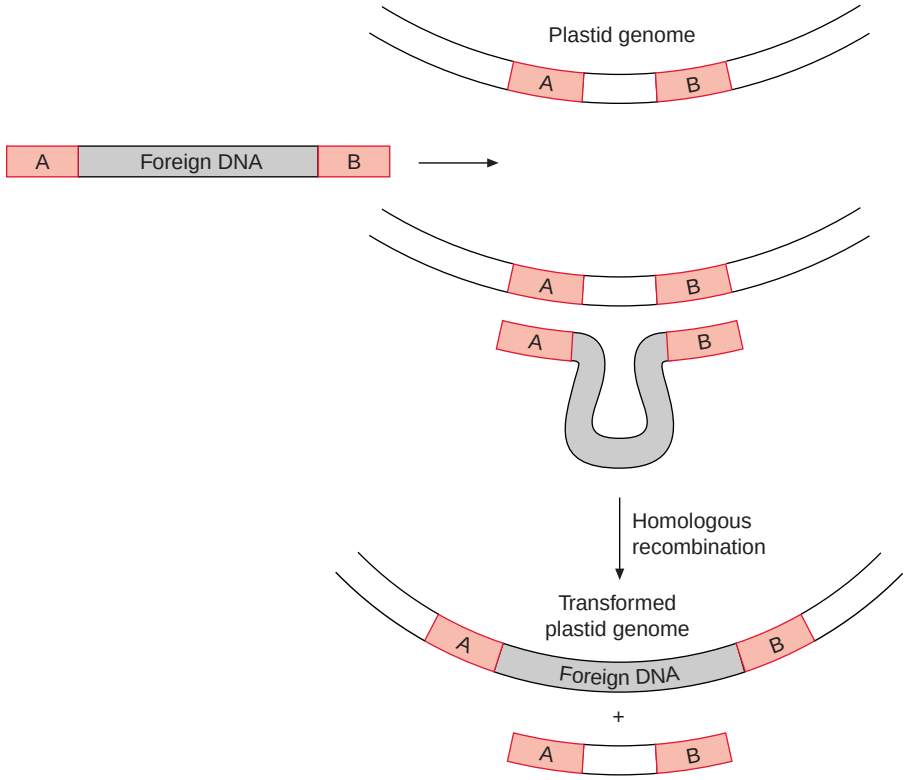

Figure 22.18
Transformation of the plastid genome. The gene of interest is flanked with DNA sequences which are analogous to sequences on the plastid genome (A and B). With the aid of a gene gun, the foreign DNA is shot into the plastids. The foreign DNA is integrated into the plastid genome by homologous recombination.

certain cases this can also be achieved by the transformation of the nuclear genome. Another advantage of the plastid transformation is that proteins with a **disulfide bridge** can be formed in the plastids, which is not possible in the cytosol. As described earlier, chloroplast enzymes are regulated by the oxidation of adjacent -SH groups (Fig. 6.25). Because of this ability the plastid compartment is well suited to produce, after genetic transformation, animal proteins, such as antibodies or oral vaccines, where disulfide bridges are responsible for the correct folding. The expression of genes originating from bacteria, e.g., Bt toxin (section 22.6), is made easy since bacteria and chloroplasts employ the same triplet codons. Transplastome tobacco plants have been generated. The plastid transformation of other crop plants is still a big challenge, as it would allow generating transformants which harmonize with the environment, as they cannot spread their foreign genes to other plants by pollen.

22.4 Selected promoters enable the defined expression of a foreign gene

Any foreign gene transferred to a plant can be expressed only when it has been provided with a suitable promoter (section 20.2). The selection of the promoter determines where, when, how much, and under what conditions gene expression takes place. Usually promoters are already included in the commercially available vectors (see Fig. 22.14).

The **CaMV-35S promoter** from the cauliflower mosaic virus (section 20.5) is often used to reach high expression levels of an inserted foreign gene in all parts of the plants. This promoter comprises transcription enhancers that enable a particularly high transcription rate in different tissues of very many plants. The ***nos* promoter** from the Ti-plasmid of *A. tumefaciens*, normally regulating the gene for nopaline synthesis, is also often used as a nonspecific promoter in transgenic plants.

The DNA sequences of specific plant promoters are identified by the analysis of plant genes obtained from a genomic gene library (section 22.1). A promoter for specific gene expression in the potato tuber, for instance, has been identified by analysis of the DNA sequence of the gene for patatin, the storage protein of the potato (Chapter 14).

A **reporter gene** can be used to determine whether an isolated promoter sequence is tissue specific. Such reporter genes encode proteins that are easily detected in a plant, for instance, the **green fluorescent protein** (GFP) from the jellyfish *Aequorea victoria*, which can be seen directly by confocal microscopy in intact leaves. Frequently, the gene for the **β-glucuronidase (GUS)** enzyme from *E. coli* also is used as a reporter gene (Fig. 22.19). This enzyme resembles β-galactosidase (mentioned in section 22.1) and does not occur in plants. It hydrolyzes a synthetic X-glucuronide which releases a blue hydrolysis product, easily identifiable under the microscope. When a potato plant is transformed with the GUS reporter gene fused to the patatin promoter, after addition of X-glucuronide, a deep blue color develops only in cuts of the tubers, but not in other tissues of the plant. Thus, the patatin promoter acts as an organ-specific promoter. Many promoters have been isolated that are active only in certain organs or tissues, such

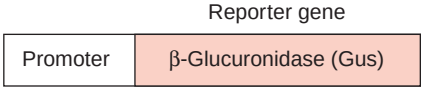

Figure 22.19 The function of a promoter can be determined by linking it to a reporter gene. In the example shown, the reporter gene encodes the enzyme β-glucuronidase (Gus) from *E. coli*. X-Glucuronide is hydrolyzed by this enzyme and a blue-stained product is released analogously to the β-galactosidase reaction (see Fig. 22.6).

as leaves, roots, phloem, flowers, or seed. Moreover, promoters have been isolated that control the expression of gene products only under certain environmental conditions, such as light, high temperatures, water stress, or pathogenic infection. Frequently, promoters are also active in heterologous plant species, although the extent of expression by a certain promoter can vary between different plant species.

Gene products are directed to certain subcellular compartments by targeting sequences

In transgenic plants, the expression of a foreign gene can be restricted to certain tissue or cell types by the use of defined promoters. Furthermore, a protein encoded by a foreign gene can be directed to a particular subcellular destination (e.g., the chloroplast stroma or the vacuolar compartment) by the presence of additional amino acid. Such amino acids can be **presequences or transit peptides**, which serve as **targeting signals** for transfer via the various subcellular membrane transport systems (sections 14.5, 21.3). Many targeting sequences are now available, which can be used in gene technology to direct a foreign protein to a defined subcellular compartment, such as the vacuolar compartment or the chloroplast stroma.

22.5 Genes can be turned off via plant transformation

In addition to producing transgenic plants with new properties by the transfer and expression of foreign genes, it is of great interest to decrease or even eliminate certain properties by inhibiting the expression of the corresponding gene, for instance the activity of a translocator or of an enzyme. Turning off a gene is also an important way to identify its function by investigating the consequences of the missing gene on plant metabolism.

Homologous recombinations frequently occur in prokaryotic genomes (including the mitochondrial and plastid genomes) as well as in the nuclear genome of animals. This property is utilized in animals to eliminate the function of a defined gene by generating a so-called "**knock-out**" mutant. To eliminate the function of a gene of interest, a section of this knock-out mutant has to be isolated and cloned. Thereafter its sequence is altered by genetic techniques, and then subsequently reintroduced into the nucleus, where it can replace the unaltered gene by homologous recombination and

the function of the gene is eliminated in the organism. In plants, however, this technique is usually not applicable, since in the nuclear genome of plants homologous recombinations are rare. Therefore alternative methods are required in plants. A decrease in the expression of a gene can be achieved by inactivating the encoding mRNA by the synthesis of a complementary RNA, called **antisense RNA** (Fig. 22.20). Normally, mRNA occurs as a single strand, but in the presence of an antisense RNA strand, it can form a double-stranded RNA. Double-stranded RNA is unstable and degrades rapidly by ribonucleases. Therefore mRNA loses the ability to encode protein synthesis when the corresponding antisense RNA is present.

To synthesize the antisense RNA, the corresponding gene is first isolated according to the methods already described and then inserted as cDNA in **reverse orientation** in a vector, able to transform the plant of interest. As the orientation is reversed in this inserted gene (the promoter is positioned at the wrong side), the RNA polymerase transcribes the antisense RNA. This **antisense technique** has become a very important tool in plant genetic engineering particularly when decreased expression levels of a defined gene are required. Unfortunately this method does not always lead to the desired results. In many cases, it turned out to be impossible to decrease the synthesis of a protein (e.g., an enzyme or a translocator) by more than 90%. In some cases the activity of the remaining protein could be even enhanced by enzyme regulation, counteracting the intended elimination of gene function. The antisense technique is particularly problematic when the corresponding gene is part of a multi-gene family.

A very effective new technique for eliminating the expression of a defined gene is the **RNAi-technique** (RNA-mediated-interference) (see section 20.2). In this method, a double-stranded RNA (**dsRNA**) is prepared from a small RNA section (up to 30 nucleotides) of the mRNA to be inactivated. It was found that the presence of such dsRNA inhibits very effectively the translation of the respective mRNA and causes it to be degraded by the cell's nucleases (RNase II, section 20.2). Therefore it is possible to eliminate the expression of a certain gene by transforming a plant with DNA encoding both strands of the dsRNA. Since the RNAi technique appears to have advantages over the antisense technique it is widely used.

For many plants, the transformation by *A. tumefaciens* is a simple way to eliminate gene functions at random (see section 20.1). Plants take up the T-DNA of the Ti-plasmids and integrate them randomly into the genome. When the T-DNA is integrated into a gene, this gene is mutated (**T-DNA insertion mutant**) and therefore loses its function. The mutant can be subsequently identified by a probe for the employed T-DNA.

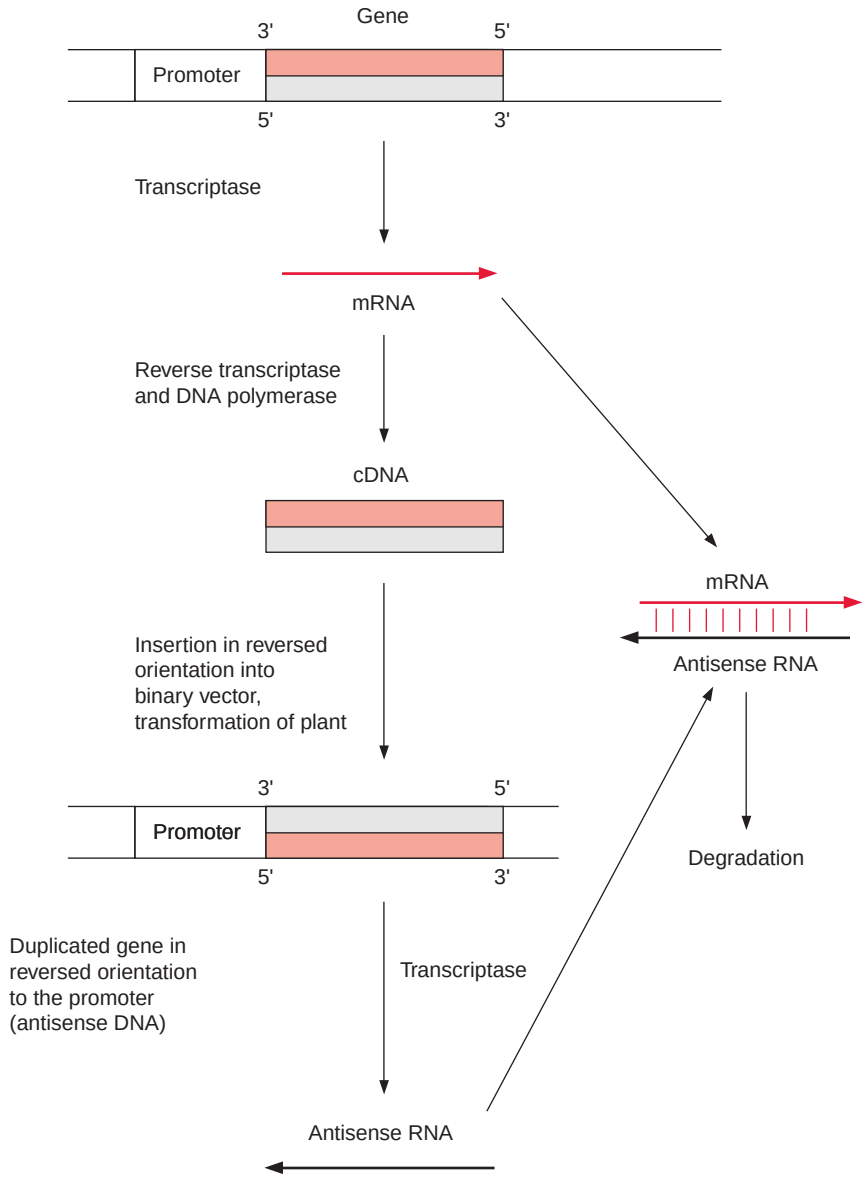

Figure 22.20 The level of gene expression can be lowered by antisense RNA. The mRNA synthesized by transcription of a gene is reverse transcribed to form into a double-stranded cDNA (see Fig. 22.2) and then inserted in opposite orientation into a plant transformation vector (Fig. 22.14). The transformed plant contains in its genome the normal gene which transcribed into sense mRNA and a duplicated gene in opposite orientation, from which the promoter causes transcription of the originally non-encoding DNA strand resulting in antisense RNA. Transcription of both genes results in the formation of an mRNA double-strand due to base pairing. ds RNA is unstable and is therefore degraded.

22.6 Plant genetic engineering can be used for many different purposes

The method of genetic engineering via the *Agrobacterium* system has produced revolutionary results in basic as well as in applied plant science. In

basic science, it has led in a very short time to the identification and characterization of very many new proteins, such as enzymes and translocators. When investigating the function of a protein in a plant, it is now common to increase or decrease the expression of the protein by molecular genetic transformation (see previous sections). From the effects of these changes on the phenotype or others, conclusions can be drawn about the role of the corresponding protein in metabolism.

In agriculture, plant genetic engineering has been utilized in many ways to augment protection against pests, to increase the qualitative and quantitative yield of crop plants, and to produce sustainable raw materials for industrial purposes. By now many genetically altered (transgenic) cultivars are grown worldwide, especially in North and South America and in China. The exception is Europe, where until now only one single transgenic species of a cultivated plant (a BT maize, see below) is grown, due to lack of public acceptance. Of the worldwide cultivated transgenic plants by far the largest part was developed with the aim of improving pest and weed management, by generating resistance to insects, viruses and herbicides. In order to increase the harvest yield, genetically engineered male-sterile plants (e.g., of rape seed (canola)) have been generated for producing hybrids. Transformants were also produced to improve the quality of the harvest (e.g., to improve storage properties of tomatoes (section 19.5)) or the production of customized fats in rape (section 20.7).

Plants are protected against some insects by the BT protein

Field crops are in great danger of being attacked by insects. Some examples may illustrate this:

1. The Colorado beetle, originating in North America, can cause complete defoliation of potato fields.
2. The larvae of the corn borer, penetrating maize shoots, causes large crop damage by feeding inside the shoots.
3. In a similar way, the cotton borer prevents the formation of cotton flowers by feeding inside shoots.

It has been estimated that about one-sixth of the global plant food production is lost due to insect pests. In order to avoid serious crop losses, the farmer very often has no option but to use chemical pest protection. In former times, chlorinated hydrocarbons such as DDT or Aldrin were used as a very potent means of protection against insects. Since these compounds degrade only very slowly and therefore accumulate in the food chain, they cause damage to the environment and are now restricted in

their use or even forbidden by law in many countries. Nowadays, mostly organophosphorous compounds are used as insecticides, which, as phosphoesterase inhibitors, impair the nerve function at the site of the synapses. These compounds are readily degraded, but unfortunately destroy not only pests, but also useful insects such as bees, and are poisonous for humans. The threat to humans lies not so much in the pesticide residues in consumed plant material, but primarily to the people applying the insecticides.

For more than 30 years, preparations from *Bacillus thuringensis* have been used as alternative biological insecticides. These bacteria form toxic peptides (**BT proteins**) that bind to receptors in the intestine of certain insects, thus impairing the uptake of food. This inactivation of the intestinal function causes the insect to starve to death. More than 100 bacterial strains are known, which form different BT proteins with a relatively specific toxicity towards certain insects. Toxicological investigations have shown that BT proteins are not harmful to humans. For many years now, bacterial suspensions containing the BT protein have been used as a biological spray to protect crops from insects. They are admitted for the production of so-called "organic" products. Unfortunately, these preparations are relatively expensive and are easily washed off the leaves by rain. Spraying also has the disadvantage that it does not reach larvae which are already inside plant shoots (e.g., the corn borer and cotton borer).

The genes for various BT proteins have been cloned and used to transform a number of plants. Although transgenic plants produce only very low amounts of the toxic BT protein (0.1% of total protein), it is more than enough to deter insects from eating the plant. The BT protein is decomposed in soil and is degraded in the human digestive tract just like all other proteins. On this basis, insect-resistant transformed varieties of, e.g., maize and cotton are grown worldwide on a large scale. In certain countries more genetically modified cotton is grown than traditional varieties. Traditional cotton varieties, due to very high pest infestation, have to be sprayed with pesticides between 2 and12 times, and in single cases up to 30 times, which is a great hazard for the entire insect population. The cultivation of insect-resistant transformed varieties has resulted in a substantial reduction in the use of pesticides, easing threats to the entire fauna spectrum. The use of such transgenic plants thus may contribute to preserving the environment.

The insertion by genetic engineering of foreign genes encoding **proteinase inhibitors** is an alternative way to protect plants from insect pests (see section 14.4). After wounding (e.g., by insect attack or by fungal infection), the formation of proteinase inhibitors, which inhibit specific proteinases of animals and microorganisms, is induced in many plants. Insects feeding on these plants consume the inhibitor, whereby their digestive processes are disrupted with the result that the insect pest starves to death. The synthesis

of the inhibitors is not restricted to the wound site, but often occurs in large parts of the plant and thereby protects them from further attacks. The introduction of suitable foreign genes in transgenic potato, lucerne (alfalfa), and tobacco plants enabled a high expression of proteinase inhibitors in these plants, protecting them efficiently from being eaten by insects. This strategy has the advantage that the proteinase inhibitors are not specific to certain insect groups. These proteinase inhibitors are contained naturally in many of our foods, sometimes in relatively high concentrations, but they are destroyed by cooking.

The expression of an **amylase inhibitor** in pea seeds, which prevents storage losses caused by the larvae of the pea beetle (section 14.4), is another example of how genetic engineering of plants offers protection from insect damage.

Plants can be protected against viruses by gene technology

Virus diseases can result in catastrophic harvest losses. Many crop plants are threatened by viruses. Infection with the **cucumber mosaic virus** can lead to the total destruction of pumpkin, cucumber, melon, and courgette crops. In sugar beet, losses of up to 60% are caused by the viral disease **rhizomania**. In contrast to fungal or animal pests, viruses cannot be directly combated by the use of chemicals. Traditional procedures, such as decreasing the propagation of the viruses by crop rotation, are not always successful. Another way to control virus infections has been to attack the virus-transferring insects, especially aphids, with pesticides.

It has long been known that after infection with a weak pathogenic strain of a certain virus, a plant may be protected against infection by a more aggressive strain. This phenomenon has been applied successfully in the biological plant protection of squash plants. It was presumed that a single molecular constituent of the viruses caused this protective function, and this has been verified by molecular biology: the introduction of the **coat protein** gene of the tobacco mosaic virus into the genome of tobacco plants makes them resistant to this virus. This has been confirmed for many other viruses: if a gene for a coat protein of a particular plant virus is expressed sufficiently in a plant, the plant usually becomes resistant to infection by this pathogen. This principle has already been used several times with success to generate virus-resistant plants by genetic engineering. In the United States, a virus-resistant squash variety generated in this way has been licensed for cultivation. In Hawaii, where the cultivation of papayas had broken down completely due to virus infection, the utilization of virus-resistant papaya varieties made this valuable crop possible again.

The generation of fungus-resistant plants is still at an early stage

The use of gene technology to generate resistance to fungal infections in plants is still at an early stage. An attempt is being made to utilize the natural protective mechanisms of plants. Some plants protect themselves against fungi by attacking the cell wall of the fungi. The cell walls of most fungi contain chitin, an N-acetyl-D-glucosamine polymer, which does not occur in plants. Some plants express **chitinases** in their seeds, which lyse the cell wall of fungi. This protective function has been transferred to other plants. Plant cultivars have been generated by transformation which contains a chitinase gene from beans, thereby gaining an increased resistance against certain fungi. Another strategy lies in the expression of enzymes for the synthesis of fungicide phytoalexins (e.g., stilbenes) (see section 18.4). However, it may still take some time until fungus-resistant plants are ready for cultivation.

Nonselective herbicides can be used as a selective herbicide by the generation of herbicide-resistant plants

The importance of herbicides for plant protection has been discussed in section 3.6, and examples of the effects of various herbicides have been given in sections 3.6, 10.4, and 15.3. The most economically successful herbicide is **glyphosate** (trade name Round Up, Monsanto) (Fig. 10.18), which inhibits specifically the synthesis of aromatic amino acids at the EPSP synthase of the shikimate pathway (Fig. 10.19). Animals are not affected by glyphosate since they lack the shikimate pathway. Glyphosate is from its structure a simple compound and therefore degraded rapidly by soil bacteria. Therefore it can be applied only by spraying the leaves. As a nonselective herbicide, glyphosate even destroys many of the very persistent weeds. For example, it is widely used to clear vegetation from railway tracks, to control the weeds on the grounds of fruit and wine plantations, and to kill weeds before crops are planted. In order to apply this powerful herbicide as a selective **post-emergence herbicide**, glyphosate-resistant transformants have been generated for a number of crop plants by means of genetic engineering. To generate glyphosate resistance in plants, the bacterial EPSP synthase was isolated, which is less sensitive to glyphosate than the plant enzyme. Transgenic plants that express the bacterial EPSP synthase activity therefore acquired protection against the herbicide. Glyphosate-resistant cotton, rape seed, and soybean are now available to the farmer. In a similar way, crop plants have been made resistant to the herbicide glufosinate (trade name Basta, Bayer, Crop Science) (Fig. 10.7) by the expression of bacterial detoxifying enzymes in transgenic plants. Herbicide-resistant

cultivars of soybean, maize, rape and cotton, also in combination with insect resistance by Bt protein, represent the large majority of the transgenic crop plants grown worldwide today.

Plant genetic engineering is used for the improvement of the yield and quality of crop products

The application of genetic engineering for generating resistance against pests or herbicides requires usually that only one additional gene is transferred into the plant. To alter the quality or the yield of harvest products, however, it is often necessary to transfer several genes which is more difficult.

A promising way to increase crop yields is the generation of **hybrids** from genetically engineered male-sterile plants, as described in section 20.7. Another strategy for the improvement of crop yield is to alter the partitioning of biomass between the harvestable and nonharvestable organs of the plants. An improvement of the tuber yield has been observed in transgenic potato plants (section 13.3), but these results have yet to be confirmed by field trials.

Genetic engineering is now being utilized in multiple ways to improve the quality and in particular the health value of food and fodder. Examples of this are the formation of highly unsaturated fatty acids in rape seed oil (section 15.5), the generation of rice containing provitamin A (golden rice, section 17.6), or the increase of the methionine content in soy beans (section 14.3), as discussed earlier.

Genetic engineering is used to produce renewable resources for industry

Genetic engineering is a method with a great promise for the production of plants as renewable resources for industry. Transgenic plants which produce customized fats, with short chain fatty acids for the detergent and cosmetic industries, and with high erucic acid content for the production of synthetic materials, were discussed in section 15.5. Transgenic potatoes which contain only the branched starch amylopectine (section 9.1) (AMFLORA, BASF) are grown as raw material for industry, e.g., for the production of glues. Transgenic potatoes which produce starch consisting only of long-chain α-amylose would be an interesting supplier of raw material for the production of plastics. Amylose ethers have polymer properties similar to those of polyethylenes, but with the advantage that they are biodegradable (i.e., can be degraded by microorganisms).

Transgenic plants, especially plastidic transformants (transplastomes), are well suited for the production of peptides and proteins, such as human

serum albumin or interferon. Progress is being made in the attempts to use plants for the production of human monoclonal antibodies (e.g., for curing intestinal cancer). Antibodies against bacteria causing caries have been produced in plants, and it is feasible that they could be added to toothpaste. To make such a project economically viable, it would be necessary to produce very large amounts of antibody proteins at low cost. Plants would be suitable for this purpose. There also has been success in using transgenic plants for the production of oral vaccines. The fodder plant lucerne (*Medicago sativa*) was transformed to produce an oral vaccine against foot and mouth disease. Oral vaccines for hepatitis B virus have been produced in potatoes and lupines, and a vaccine for rabies has been produced in tomatoes. Although these experiments are still at an initial experimental phase, they open up the possibility of vaccination by ingesting plant material (e.g., fodder for animals or fruit for humans).

Genetic engineering provides a chance for increasing the protection of crop plants against environmental stress

In the preceding chapters, various mechanisms have been described by which a plant protects itself against environmental stresses, such as heat (section 21.2), cold (sections 3.10 and 15.1), drought and soil salinity (Chapter 8 and section 10.4), xenobiotics, heavy metal pollution (section 12.2), and oxygen radical production (sections 3.9 and 3.10). Genetic engineering opens up the prospect of increasing the resistance of cultivated plants to these stresses by overexpression of enzymes involved in the stress responses. Thus, an increase of the number of double bonds in the fatty acids of membrane lipids through genetic engineering has improved the cold tolerance of tobacco (section 15.1). The generation of plants accumulating heavy metals, such as mercury and cadmium, in order to detoxify polluted soils (section 12.2), may have a great future.

With the growth of the world's population, the availability of sufficient arable land becomes an increasing problem. Large areas of the world can no longer be utilized for agriculture, because of the high salt content of the soil, often caused by inadequate irrigation management. In 1990, 20% of the total area used worldwide for agriculture (including 50% of the artificially irrigated land) has been classified as salt stressed. Investigations are in progress to develop salt-tolerant plants by increasing the synthesis of osmotically compatible compounds, such as mannitol, betaine, or proline (section 10.4), but also by increasing the expression of enzymes, which eliminate reactive oxygen species (**ROS**) (sections 3.9 and 3.10). ROS cause serious damages during drought and salt stress. Results obtained so far are promising, although it may still take considerable time until these efforts can be put into general

practice. So far one drought-resistant wheat variety is in the licensing phase. If plant genetic engineering were to succeed in generating salt-resistant crop plants, this would be a very important contribution in securing the world's food supply.

The introduction of transgenic cultivars requires a risk analysis

At present, plant genetic engineering, on the one hand, raises sometimes exaggerated expectations and, on the other hand, induces fear in parts of the population. Responsible application of plant genetic engineering requires that for each plant licensed for cultivation, a risk analysis be made according to strict scientific criteria as to whether the corresponding plant represents a hazard to the environment. Among other criteria, it has to be examined whether crossing between the released transgenic and wild plants is possible, and what are the potential consequences for the environment. For example, crossing can occur between transgenic rape seed and other *Brassicaceae* such as wild mustard. This could be prevented by generating chloroplast transformants (section 22.5). Moreover, transgenic plants themselves could grow in the wild. In this way herbicide-resistant weeds may develop from herbicide-resistant cultivars. However, it also should be noted that in the conventional application of herbicides, herbicide-resistant weeds have evolved, namely, by natural selection (see section 10.4). Experiments in the laboratory as well as controlled field tests are required for such risk analyses. It is beyond the scope of this book to deal with the criteria set by legislation to evaluate the risk entailed by the release of a transgenic cultivar. It is expected that, when used responsibly, plant genetic engineering may contribute to the improvement of crop production, an increase of the health benefit of foods, and the provision of sustainable raw materials for industry. If plant protection based on plant genetic engineering were simply to have the result that "**fewer chemicals are put on the field**," then this would be an improvement for the environment.

Further reading

Are there hazards to the consumer when eating food from genetically modified plants? Report InterAcademy Panel Initiative on Genetically Modified Organisms, Berlin (2006). http://www.akademienunion.de/publikationen/

Bates, S. I., Zhao, J.-Z., Roush, R. T., Shelton, A. M. Insect resistance management in GM crops: Past, present and future. Nature Biotechnology 23, 57–62 (2005).

Blumwald, E. Engineering salt tolerance in plants. Biotechnology Genetic Engineering Reviews 20, 261–275 (2003).

Bock, R. Plastid biotechnology: Prospects for herbicide and insect resistance, metabolic engineering and molecular farming. Current Opinion Biotechnology 18, 100–106 (2007).

Chilton, M. D. *Agrobacterium*. A memoir. Plant Physiology 125, 9–14 (2001).
Daniell, H. Production of biopharmaceuticals and vaccines in plants via the chloroplast genome. Biotechnology Journal 1, 1071–1079 (2006).
Datta, K., Baisakh, N., Oliva, N., Torrizo, L., Abrigo, E., Tan, J., Rai, M., Rehana, S., Al-Babili, S., Beyer, P., Potrykus, I., Datta, S. K. Bioengineered "golden" indica rice cultivars with beta-carotene metabolism in the endosperm with hygromycin and mannose selection systems. Plant Biotechnology Journal 1, 81–90 (2003).
De Block, M., Herrera-Estrella, L., Van Montagu, M., Schell, J. Expression of foreign genes in regenerated plants and their progeny. EMBO Journal 3, 1681–1689 (1984).
Genetically modified insect resistant crops with regard to developing countries. Report InterAcademy Panel Initiative on Genetically Modified Organisms, Berlin (2007). http://www.akademienunion.de/publikationen/
Global review of commercialised transgenic crops. International Service for the Acquisition of Agri-Biotech Applications (ISAAA) 41 (2009). http://www.isaaa.org/
GM Science Review: An open review of the science relevant to GM crops and food based on the interest and concern of the public. The Royal Society (London) First Report July 2003, Second Report (2004). http://royalsociety.org/
Hellens, R., Mullineaux, P., Klee, H. A guide to *Agrobacterium* binary Ti vectors. Trends in Plant Science 5, 446–451 (2000).
High, S. M., Cohen, M. B., Shu, Q. Y., Altosar, I. Achieving successful employment of *Bt* rice. Trends in Plant Science 9, 286–292 (2004).
Horsch, R. B., Fraley, R. T., Rogers, S. G., Sanders, P. R., Lloyd, A., Hoffman, N. Inheritance of functional foreign genes in plants. Science 223, 496–498 (1984).
Lu, X. M., Yin, W. B., Hu, Z. M. Chloroplast transformation. Methods Molecular Biology 318, 285–303 (2006).
Ma, J. K., Drake, P. M., Christou, P. The production of recombinant pharmaceutical proteins in plants. Nature Reviews Genetics 4, 794–805 (2003).
Maliga, P. Plastid transformation higher plants. Annual Review Plant Biology 55, 289–313 (2004).
Mansoor, S., Amin, I., Hussain, M., Zafar, Y., Briddon, R. W. Engineering novel traits in plants through RNA interference. Trends in Plant Science 11, 559–565 (2006).
Orzaez, D., Mirbel, S., Wieland, W. H., Granell, A. Agroinjection of tomato fruits. A tool for rapid functional analysis of transgenes directly in fruit. Plant Physiology 140, 3–11 (2006).
Renneberg, R. Biotechnology for Beginners. 2. Auflage. Elsevier Academic Press, Amsterdam, Boston (2006).
Sandermann, H. Plant biotechnology: Ecological case studies on herbicide resistance. Trends in Plant Science 11, 324–328 (2006).
Schillberg, S., Fischer, R., Emans, N. "Molecular farming" of antibodies in plants. Naturwissenschaften 90, 145–155 (2003).
Straughan, R. Moral and ethical issues in plant biotechnology. Current Opinion in Plant Biology 3, 163–165 (2000).
Vinocur, B., Altmann, A. Recent advances in engineering plant tolerance to abiotic stress: Achievements and limitations. Current Opinion Biotechnology 16, 123–132 (2005).
Ward, D. V., Zupan, J. R., Zambryski, P. C. *Agrobacterium* VirE2 gets the VIPI treatment in plant nuclear import. Trends in Plant Science 7, 1–3 (2002).

Index